frontiers | Research Topics

Nutraceuticals modulation for oxidative stress in disease and health

Edited by
Siti Fatimah Ibrahim, Ahmad Nazrun Shuid and Kok Yong Chin

Published in
Frontiers in Pharmacology

ISSN 1664-8714
ISBN 978-2-8325-2294-3
DOI 10.3389/978-2-8325-2294-3

About Frontiers

Frontiers is more than just an open access publisher of scholarly articles: it is a pioneering approach to the world of academia, radically improving the way scholarly research is managed. The grand vision of Frontiers is a world where all people have an equal opportunity to seek, share and generate knowledge. Frontiers provides immediate and permanent online open access to all its publications, but this alone is not enough to realize our grand goals.

Frontiers journal series

The Frontiers journal series is a multi-tier and interdisciplinary set of open-access, online journals, promising a paradigm shift from the current review, selection and dissemination processes in academic publishing. All Frontiers journals are driven by researchers for researchers; therefore, they constitute a service to the scholarly community. At the same time, the *Frontiers journal series* operates on a revolutionary invention, the tiered publishing system, initially addressing specific communities of scholars, and gradually climbing up to broader public understanding, thus serving the interests of the lay society, too.

Dedication to quality

Each Frontiers article is a landmark of the highest quality, thanks to genuinely collaborative interactions between authors and review editors, who include some of the world's best academicians. Research must be certified by peers before entering a stream of knowledge that may eventually reach the public - and shape society; therefore, Frontiers only applies the most rigorous and unbiased reviews. Frontiers revolutionizes research publishing by freely delivering the most outstanding research, evaluated with no bias from both the academic and social point of view. By applying the most advanced information technologies, Frontiers is catapulting scholarly publishing into a new generation.

What are Frontiers Research Topics?

Frontiers Research Topics are very popular trademarks of the *Frontiers journals series*: they are collections of at least ten articles, all centered on a particular subject. With their unique mix of varied contributions from Original Research to Review Articles, Frontiers Research Topics unify the most influential researchers, the latest key findings and historical advances in a hot research area.

Find out more on how to host your own Frontiers Research Topic or contribute to one as an author by contacting the Frontiers editorial office: frontiersin.org/about/contact

Nutraceuticals modulation for oxidative stress in disease and health

Topic editors
Siti Fatimah Ibrahim — National University of Malaysia, Malaysia
Ahmad Nazrun Shuid — MARA University of Technology, Malaysia
Kok Yong Chin — National University of Malaysia, Malaysia

Topic Coordinator
Farah Hanan Fathihah Binti Jaffar — University of Malaya, Malaysia

Citation
Ibrahim, S. F., Shuid, A. N., Chin, K. Y., eds. (2023). *Nutraceuticals modulation for oxidative stress in disease and health*. Lausanne: Frontiers Media SA.
doi: 10.3389/978-2-8325-2294-3

Table of contents

frontiers | Frontiers in Pharmacology

TYPE Editorial
PUBLISHED 14 April 2023
DOI 10.3389/fphar.2023.1199293

OPEN ACCESS

EDITED BY
Javier Echeverria,
University of Santiago, Chile

REVIEWED BY
Luca Rastrelli,
University of Salerno, Italy

*CORRESPONDENCE
Siti Fatimah Ibrahim,
timi@ukm.edu.my

RECEIVED 03 April 2023
ACCEPTED 11 April 2023
PUBLISHED 14 April 2023

CITATION
Chin K-Y, Shuid AN and Ibrahim SF (2023), Editorial: Nutraceuticals modulation for oxidative stress in disease and health. *Front. Pharmacol.* 14:1199293. doi: 10.3389/fphar.2023.1199293

Editorial: Nutraceuticals modulation for oxidative stress in disease and health

Kok-Yong Chin[1], Ahmad Nazrun Shuid[2] and Siti Fatimah Ibrahim[3]*

[1]Department of Pharmacology, Faculty of Medicine, Universiti Kebangsaan Malaysia, Cheras, Malaysia, [2]Department of Pharmacology, Faculty of Medicine, Universiti Teknologi MARA, Sungai Buloh, Malaysia, [3]Department of Physiology, Faculty of Medicine, Universiti Kebangsaan Malaysia, Cheras, Malaysia

KEYWORDS

antioxidants, free radicals, natural products, reactive oxygen species, redox status

Editorial on the Research Topic
Nutraceuticals modulation for oxidative stress in disease and health

Oxygen is an essential component of life because it is used in aerobic respiration to generate energy from glucose. Reactive oxygen species (ROS) are produced as by-products of cellular respiration. The enzymatic and non-enzymatic antioxidants in the cells maintain the ROS at low levels, whereby they play a physiological role in cellular signalling, differentiation, autophagy and metabolic adaptation (Sena and Chandel, 2012). When the cellular antioxidant capacity is overwhelmed by ROS, a phenomenon known as oxidative stress occurs. The excess ROS could damage macromolecules important to sustain life, such as lipids, nucleic acids and protein (Caliri et al., 2021). The accumulated damage can lead to cellular senescence or dysfunction, causing organ damage and various degenerative diseases and even cancers (Liguori et al., 2018). Oxidative stress can be triggered by many factors in the modern environment, including pollutants, radiation, smoking, alcohol, psychosocial stress, and unhealthy diets (Birch-Machin and Bowman, 2016; Kerahrodi and Michal, 2020).

Since complete avoidance of factors triggering oxidative stress is not feasible, enhancing the cellular antioxidant system could be an alternative to tackle this problem. Consumption of natural products such as fruits and vegetables has been associated with various health-beneficial effects (Angelino et al., 2019; Wang et al., 2021). Natural products are rich in hydrophilic (such as flavonoids, lignans, phenolic acids, and stilbenes) and lipophilic antioxidants (such as carotenoids and tocochromanols) (Xu et al., 2017), which possess health-enhancing effects. These natural antioxidants can scavenge free radicals, terminate the lipid peroxidation chain, and modulate the cellular antioxidant response. They are also used in combination as in the case of traditional Chinese and other folk medicines to enhance the health effects. Nutraceuticals, which are substances derived from natural products used to prevent or manage chronic diseases, have been receiving attention (Nasri et al., 2014).

In response to the increasing evidence of nutraceuticals in modulating oxidative stress in health and diseases, this Research Topic gathers high-quality papers on the topic. The researchers adopted several approaches to tackle the issue, i.e., using single bioactive compounds or crude extract, traditional Chinese medicine formulation or reviews of previous literature.

Herbs used in traditional medicine are major sources of nutraceuticals, and a topic of active investigation. Using menthol derived from peppermint, Matouk et al. reported attenuation of histopathological and enzymatic changes in the liver caused by sepsis with treatment. These beneficial effects were mediated by the anti-inflammatory, antioxidant and anti-apoptotic

properties of menthol. Using the aqueous extract of *Labisia Pumila* (Blume) Fern.-Vill. Var. Alata, Ibrahim et al. reported that the extract promoted the healing of burn wounds. The effects of leaf extract were more potent because it promoted better histomorphometric features and hydroxyproline production in the wound. Nurul Akmal et al. found that methanolic extract of *Piper sarmentosum* prevented lesions and the increase of inflammation and oxidative stress of gastric mucosa in rats subjected to water-immersion restrain stress. Mumtazah Razak et al. compared the antioxidant potential of subcritical water extract of soil and soilless-grown gingers. They found that soil-grown variety yielded higher amounts of extract and antioxidant activities *ex vivo*. In rats, subcritical water extract of soil-grown ginger suppressed inflammation and the product of oxidative stress, while increasing the activity of catalase. Fungi are a major source of bioactive compounds with antioxidant activities. Tang et al. demonstrated that the extract of *Penicillium oxalicum* isolated from *Ligusticum chuanxiong* Hort protected *Caenorhabditis elegans* from thermal, UV and oxidative stress by upregulating antioxidant enzyme and heat-shock protein expression. The extract could also protect against DNA scission in plasmid and lymphocytes.

Two studies demonstrated the antioxidant potential of traditional Chinese medicine formulation in managing health. Lee et al. found that the spleen-tonifying formula, KI Essence extract, promoted the survival of neurons and neurite growth through antioxidant effects and ERK phosphorylation *in vitro*. In animals, the formulation prevented hypomyelination, oxidative stress and inflammation in the brain of maternal immune activation offspring, probably through modulation of gut microbiota. Sun et al. reported that topical application of *Scutellaria baicalensis* Georgi (SBG) improved the skin condition, collagen production and redox status. Through *in vitro* studies, they showed that SBG antagonises REV-ERBα to upregulate BMAL1, thus achieving protection against skin ageing.

The Research Topic also includes three reviews that summarise the health effects of phytoestrogens, herbs and traditional Chinese medicines with antioxidant effects. Jayusman et al. reviewed the potential of phytoestrogens in preserving bone and periodontal health derived from preclinical studies. Although the evidence on periodontal bone loss is limited, they concluded that phytoestrogens could effectively prevent bone resorption and enhance bone formation, thus preventing osteoporosis and alveolar bone loss. In a systematic review, Othman et al. reported that *P. sarmentosum* exerted beneficial effects against diabetes and hypertension from preclinical studies. Meta-analysis of the hypertensive effects showed that *P. sarmentosum* extract induced substantial reduction in systolic, diastolic and mean arterial pressure *in vivo* models. The review of Huang et al. summarized the effects of several traditional Chinese medicine components and formulations with antioxidant, anti-inflammatory, neuroprotective properties, which could potentially be used to manage spinal cord injury with an underlying oxidative stress pathology.

Overall, nutraceuticals hold great promise in preventing and managing chronic diseases through their antioxidant properties. They could complement lifestyle interventions to prevent the progression of the diseases to the stage wherein standard pharmaceuticals are required. However, to adopt them in a clinical setting, more safety and efficacy data in properly planned randomised controlled trials in humans would be required. Standardising the extraction and formulation is also critical in ensuring the effectiveness of the nutraceuticals.

Author contributions

All authors listed have made a substantial, direct, and intellectual contribution to the work and approved it for publication.

Acknowledgments

The authors thank Universiti Kebangsaan Malaysia and Universiti Teknologi MARA for support.

Conflict of interest

The authors declare that the research was conducted in the absence of any commercial or financial relationships that could be construed as a potential conflict of interest.

Publisher's note

References

Angelino, D., Godos, J., Ghelfi, F., Tieri, M., Titta, L., Lafranconi, A., et al. (2019). Fruit and vegetable consumption and health outcomes: An umbrella review of observational studies. *Int. J. Food Sci. Nutr.* 70 (6), 652–667. doi:10.1080/09637486.2019.1571021

Birch-Machin, M. A., and Bowman, A. (2016). Oxidative stress and ageing. *Br. J. Dermatology* 175 (S2), 26–29. doi:10.1111/bjd.14906

Caliri, A. W., Tommasi, S., and Besaratinia, A. (2021). Relationships among smoking, oxidative stress, inflammation, macromolecular damage, and cancer. *Mutat. Research/Reviews Mutat. Res.* 787, 108365. doi:10.1016/j.mrrev.2021.108365

Kerahrodi, J. G., and Michal, M. (2020). The fear-defense system, emotions, and oxidative stress. *Redox Biol.* 37, 101588. doi:10.1016/j.redox.2020.101588

Liguori, I., Russo, G., Curcio, F., Bulli, G., Aran, L., Della-Morte, D., et al. (2018). Oxidative stress, aging, and diseases. *Clin. Interv. Aging* 13, 757–772. doi:10.2147/CIA.S158513

Nasri, H., Baradaran, A., Shirzad, H., and Rafieian-Kopaei, M. (2014). New concepts in nutraceuticals as alternative for pharmaceuticals. *Int. J. Prev. Med.* 5 (12), 1487–1499.

Sena, L. A., and Chandel, N. S. (2012). Physiological roles of mitochondrial reactive oxygen species. *Mol. Cell* 48 (2), 158–167. doi:10.1016/j.molcel.2012.09.025

Wang, D. D., Li, Y., Bhupathiraju, S. N., Rosner, B. A., Sun, Q., Giovannucci, E. L., et al. (2021). Fruit and vegetable intake and mortality: Results from 2 prospective cohort studies of US men and women and a meta-analysis of 26 cohort studies. *Circulation* 143 (17), 1642–1654. doi:10.1161/CIRCULATIONAHA.120.048996

Xu, D. P., Li, Y., Meng, X., Zhou, T., Zhou, Y., Zheng, J., et al. (2017). Natural antioxidants in foods and medicinal plants: Extraction, assessment and resources. *Int. J. Mol. Sci.* 18 (1), 96. doi:10.3390/ijms18010096

frontiers | Frontiers in Pharmacology

TYPE Original Research
PUBLISHED 25 August 2022
DOI 10.3389/fphar.2022.964255

OPEN ACCESS

EDITED BY
Ahmad Nazrun Shuid,
MARA University of Technology,
Malaysia

REVIEWED BY
Raquel Romay-Tallon,
University of Illinois at Chicago,
United States
Putri Ayu Jayusman,
Universiti Kebangsaan Malaysia,
Malaysia
Norasikin Ab Azis,
Universiti Teknologi MARA, Malaysia

*CORRESPONDENCE
Sung-Hui Tseng,
m003089010@tmu.edu.tw

SPECIALTY SECTION
This article was submitted to Ethnopharmacology, a section of the journal Frontiers in Pharmacology

RECEIVED 08 June 2022
ACCEPTED 05 August 2022
PUBLISHED 25 August 2022

CITATION
Lee GA, Zhao H-W, Chang Y-W, Lee C-J, Yang Y-CSH, Wu Y-C, Lin W-L, Liu Y-R, Ning D-S and Tseng S-H (2022), KI Essence extract (a spleen-tonifying formula) promotes neurite outgrowth, alleviates oxidative stress and hypomyelination, and modulates microbiome in maternal immune activation offspring.
Front. Pharmacol. 13:964255.
doi: 10.3389/fphar.2022.964255

KI Essence extract (a spleen-tonifying formula) promotes neurite outgrowth, alleviates oxidative stress and hypomyelination, and modulates microbiome in maternal immune activation offspring

Gilbert Aaron Lee[1,2,3], Hong-Wei Zhao[4], Yu-Wei Chang[1], Chia-Jung Lee[5,6], Yu-Chen S. H. Yang[7], Ying-Chieh Wu[1], Wan-Li Lin[1], Yun-Ru Liu[7], De-Shan Ning[4] and Sung-Hui Tseng[8,9]*

[1]Department of Medical Research, Taipei Medical University Hospital, Taipei, Taiwan, [2]Department of Microbiology and Immunology, School of Medicine, College of Medicine, Taipei Medical University, Taipei, Taiwan, [3]Child Development Research Center, Taipei Medical University Hospital,, Taipei, Taiwan, [4]Infinitus (China) Company Ltd, Guangzhou, Guangdong, China, [5]PhD Program for Clinical Drug Discovery of Herbal Medicine, College of Pharmacy, Taipei Medical University, Taipei, Taiwan, [6]Graduate Institute of Pharmacognosy Science, College of Pharmacy, Taipei Medical University, Taipei, Taiwan, [7]Joint Biobank, Office of Human Research, Taipei Medical University, Taipei, Taiwan, [8]Department of Physical Medicine and Rehabilitation, School of Medicine, College of Medicine, Taipei Medical University, Taipei, Taiwan, [9]Department of Physical Medicine and Rehabilitation, Taipei Medical University Hospital, Taipei, Taiwan

Mushrooms and Chinese traditional herbs have bioactive nutraceuticals with multiple therapeutic functions, including antioxidant and antibacterial activities and microbiome modulation properties. Mushroom-derived bioactive compounds are used in medicines for the treatment of neurological disorders with abnormal brain–gut–microbiome axis. This study examined the effects of KI Essence extract, a spleen-tonifying formula, on neurite growth, antioxidant activity, hypomyelination modulation, and the microbiome profile in lipopolysaccharide (LPS)-induced maternal immune activation (MIA) offspring. The KI Essence extract induced PC12 cell neurite growth by increasing extracellular signal–regulated kinase (ERK) phosphorylation, promoting 2,2′-diphenyl-1-picrylhydrazyl radical scavenging activity, reducing the level of tert-butylhydroperoxide–induced lipid peroxidation in brain homogenates, protecting PC12 cells from H_2O_2-induced cell death (through the inhibition of ERK phosphorylation), alleviating hypomyelination, and downregulating interleukin-1β through LPS-activated microglia production; moreover, the numbers of Enterobacteriaceae, Actinobacteria, Peptostreptococcaceae, Erysipelotrichaceae, and *Bifidobacterium* bacteria in MIA offspring increased. In summary, the KI Essence extract promotes neurite outgrowth, alleviates oxidative stress and hypomyelination, and modulates microbiota dysbiosis in MIA offspring.

KEYWORDS

mushroom, maternal immune activation, myelination, microbiota, oxidative stress, spleen-tonifying formula

Introduction

Neurodevelopmental diseases are characterized by an abnormal brain–gut–microbiome axis. The etiopathophysiology of mental disorders involve impaired neurite outgrowth, altered myelination, oxidative stress, and microbial dysbiosis (Graciarena et al., 2018; Nguyen et al., 2018; Xu et al., 2019; Pangrazzi et al., 2020b). Clinical evidence has demonstrated that patients with autism spectrum disorder (ASD) exhibit oxidative stress–related responses, including increases in reactive oxygen species (ROS) and lipid peroxidation levels (Chauhan and Chauhan, 2006; Yui et al., 2020). ROS-induced peroxidation products such as malondialdehyde (MDA), a lipid peroxidation product, can damage cellular components and exacerbate neurodevelopmental disease status (Pangrazzi et al., 2020b; Yui et al., 2020). Oxidative stress also leads to the downregulation of myelin-related gene expression in human oligodendrocytes and of myelin basic protein (MBP) expression levels in the rat brain (Maas et al., 2017). Thus, alleviating oxidative damage is a promising treatment strategy for neurodevelopmental diseases.

Mushrooms and traditional Chinese herbal medicines are considered nutraceuticals that can alleviate the symptoms of neurodevelopmental diseases (Bang et al., 2017). Numerous edible mushrooms, including *Sarcodon scabrosus*, *Ganoderma lucidum*, *Grifola frondosa*, *Hericium erinaceusm*, and *Pleurotus giganteus*, can promote neurite outgrowth in PC12 cells through the extracellular signal–regulated kinase [ERK] signaling pathway (Sabaratnam et al., 2013). The *Tremella fuciformis* extract promotes neurite outgrowth in PC12h cells (Kim et al., 2007). Edible mushrooms (e.g., *Lentinula edodes, Flammulina velutipes*, and *T. fuciformis*) contain bioactive compounds and polysaccharides and thus exhibits antioxidant activity (Li et al., 2014; Yuan et al., 2019; Diallo et al., 2020). The traditional Chinese herbal extract exhibits potent antioxidant activity (Matkowski et al., 2013). In particular, *Lycium barbarum*, *Cassia obtusifolia*, *Euryale ferox*, *Ziziphus jujuba*, and *Prunus mume* extracts exhibit antioxidant activity (Lee et al., 2002; Pi and Lee, 2017; Lu et al., 2019; Wu et al., 2019; Rajaei et al., 2021). The *Crataegus pinnatifida* extract contains maslinic acid, which has been noted to promote synaptogenesis and axon growth through Akt/GSK-3β activation in a cerebral ischemia model (Qian et al., 2015). The medicinal mushroom *Poria cocos* is one of the most commonly used Chinese herbal medicines for autism spectrum disorder (ASD) treatment; studies have verified its anti-inflammatory activity and spleen-tonifying effects (Rios, 2011; Bang et al., 2017; Nie et al., 2020). However, further research is warranted to clarify how the aforementioned mushrooms and traditional Chinese herbal medicines regulate the signaling pathways involved in neuritogenesis and antioxidant responses.

Mitogen-activated protein kinase (MAPK) signaling pathways are involved in the regulation of neuritogenesis and oxidative responses. Specifically, nerve growth factor (NGF) activates ERK 1/2 to promote neuritogenesis (Wang et al., 2011). Oxidative stress also causes the activation of intracellular signaling pathways, including ERK1/2 and p38 MAPK pathways (Rezatabar et al., 2019). The inhibition of these MAPK pathways can protect cells from oxidative stress–induced apoptosis (Rezatabar et al., 2019). Thus, targeting MAPK signaling can inhibit both neuritogenesis and oxidative response–induced cell death.

An increasing number of studies have suggested that gut microbial dysbiosis and oxidative stress play integral roles in neurodevelopmental diseases (Nitschke et al., 2020; Svoboda, 2020). Gut microbiota regulates host physiology, nutrition, and brain function (Vuong and Hsiao, 2017). Dysbiosis is associated with altered integrity of the intestinal barrier and gut inflammation in a maternal immune activation (MIA) model that is known to have features of ASD (Hughes et al., 2018; Li et al., 2021). Microbiota-derived metabolites are correlated with behavioral abnormalities and neuropathology in ASD (Peralta-Marzal et al., 2021), suggesting that gut dysbiosis is associated with ASD pathophysiology.

In traditional Chinese medicine, neurological disorder treatment mainly involves tonifying the spleen and invigorating the brain (Greenwood, 2017). Mushrooms contain bioactive ingredients that modulate gut microbiota and increase spleen Qi (Greenwood, 2017; Ma et al., 2021; Vamanu et al., 2021). KI Essence is a commercial product that contains mushrooms and traditional Chinese herbal extracts; its ingredients have spleen-tonifying effects and can modulate the gut microbiome (Xu et al., 2015; Xu et al., 2021; Zou et al., 2021). MIA elicits oxidative and inflammatory responses during pregnancy, which lead to the development of an abnormal brain–gut–microbiota axis in offspring (Simoes et al., 2018; Lee et al., 2021). In this study, we assessed the potential of the KI Essence extract for neurite outgrowth promotion, oxidative stress alleviation, and maternal infection–induced abnormal brain–gut–microbiota profile modulation in a MIA animal model.

Materials and mehthods

KI Essence extract preparation

The KI Essence extract examined in this study was obtained from Infinitus (Guangzhou, Guangdong, China).

The raw materials of this extract, including fresh and dry materials, were *Lentinula edodes* (Berk.) Pegler, *Flammulina velutipes* (Curtis) Singer, *Wolfiporia extensa* (Peck) Ginns, *Tremella fuciformis* Berk, *Crataegus pinnatifida* Bunge [Rosaceae], *Lycium barbarum* L. [Solanaceae], *Senna obtusifolia* (L.) [Fabaceae], *Euryale ferox Salisb* [Nymphaeaceae], *Ziziphus jujube* Mill. [Rhamnaceae], *Prunus mume* (Siebold) Siebold & Zucc. [Rosaceae], and *Ostreae gigas*. The weight percentages of each raw material used in the KI Essence extract preparation are presented in Supplementary Table S1. In total, 100 g of raw materials were extracted twice with 1.2 and 1 L of 95°C distilled water for 1.5 and 1 h, respectively. Next, the extract was concentrated in vacuo to obtain a final yield of 24%.

High-performance liquid chromatography fingerprint analysis

The KI Essence extract (10 mg) was dissolved in H_2O to obtain a high-performance liquid chromatography (HPLC) sample solution (10 mg/ml). HPLC fingerprint analysis was conducted using a Waters HPLC system (Milford, MA, United States) comprising a Waters 600 pump system, Waters 2996 Photodiode Array Detector, Waters 717 plus Autosampler, and Sugai U-620 Column Oven (Wakayama City, Japan). A Cosmosil 5C18-MS-II reversed-phase column (5 μm, 4.6 mm × 250 mm; Nacalai Tesque, Japan) equipped with a LiChrospher RP-18 end-capped guard column (5 μm, 4.0 mm × 10 mm; Merck, Germany) was used for the stationary phase. The gradient eluents consisted of eluents A (H_2O:KH_2PO_4:10% H_3PO_4 = 1,000 g: 2.72 g:1 ml), B (acetonitrile), and C (H_2O), with the following profile: 0–25 min, 80%–100% A and 0%–20% B; 25–45 min, 65%–80% A and 20%–35% B; 45–60 min, 0%–65% A, 35%–80% B, and 0%–20% C; 60–65 min, 10%–80% B and 20%–90% C; and 65–70 min, 0%–100% A, 0%–10% B, and 0%–90% C. The applied flow rate was 1 ml/min, and the column temperature was maintained at 35°C. The relevant data are presented in Supplementary Figure S1. The following components of the KI Essence extract were detected: cytosine, cytidine, hypoxanthine, uridine, guanosine, adenosine, and maslinic acid.

High-performance liquid chromatography analysis of marker substances in KI essence extract

We used a Hitachi HPLC system, consisting of a Chromaster 5110 pump system, Chromaster 5430 Photodiode Array Detector, Chromaster 5210 plus Autosampler (Hitachi, Japan), and Super CO-150 column oven. A LiChrospher RP-18 reversed-phase column (5 μm, 4.6 mm × 250 mm; Merck) equipped with a LiChrospher RP-18 end-capped guard column (5 μm, 4 mm × 10 mm; Merck) was used as the stationary phase. The mobile phase included 0.05% trifluoroacetic acid (CH_3CN gradient elution: 0 min, 95:5; 50 min, 0:100). The flow rate was 1 ml/min, and the column temperature was maintained at 40°C. The ultraviolet detection wavelength of maslinic acid was 215 nm. Because of the poor water solubility of maslinic acid, 0.1 g of the KI Essence extract was extracted using 10 ml of 50% methanol through ultrasonic oscillation at 25°C for 20 min to obtain total maslinic acid. The sample was subsequently filtered through a 0.45-μm syringe filter, and a 5-μl aliquot was directly injected into the HPLC system. Maslinic acid standard (Sigma) was used to identify the target peak and amounts of maslinic acid in KI Essence extract. The concentration range of the maslinic acid calibration curve was 10–500 μg/ml. Maslinic acid content in the KI Essence extract was found to be 11.3 ± 0.7 mg/g.

Phenol–sulfuric acid method for measuring total carbohydrates

We mixed 100 μl of 10 mg/ml KI Essence extract with 800 μL of 95% ethanol with thorough stirring. This mixture was allowed to stand for 30 min and then centrifuged, and the supernatant was discarded. The obtained pellet was washed with 500 μl of 80% ethanol and centrifuged to remove the solvent. The aforementioned steps were repeated three times. Thereafter, the precipitate was dissolved uniformly in 2 ml of 2 M sulfuric acid. Subsequently, 200 μl of phenol and 100 μl of sulfuric acid were added into an Eppendorf vial with the dissolved precipitate. After the solution was reacted for 15 min in a 100°C water bath, glucose (0, 12.5, 25, 50, and 100 μg/ml) was used as a standard for preparing a calibration curve, and optical density (OD) at 480 nm was interpolated to calculate the content of condensed tannins relative to that of glucose (Masuko et al., 2005). The KI Essence commercial product used here contained 70 mg/g of carbohydrates (including monosaccharides, disaccharides, oligosaccharides, and polysaccharides).

Cell culture

PC12 cells, obtained from American Type Culture Collection (USA; ATCC CRL-1721), were maintained in RPMI 1640 medium (Gibco-Life Technologies, United States) supplemented with nutrient mixture F-12 (Gibco-Life Technologies), 5% fetal bovine serum (FBS), 10% horse serum, and penicillin–streptomycin. The cells were maintained in an incubator at 37°C under atmospheric conditions (CO_2:air = 5%:95%).

PC12 cell viability and neurite outgrowth assay

PC12 cells were seeded in six-well culture plates (Corning, NY, United States) coated with 0.1 mg/ml poly-L-lysine at a density of 0.7×10^6 cells per well in culture medium for 1 day. The cultured PC12 cells were then transferred to low-serum medium (containing 1% horse serum with 0.5% FBS) and cultured for 24 h. Subsequently, these cells were stimulated with 50 ng/ml NGF for 2 days in the low-serum medium with various concentrations of the KI Essence extract. The viability of differentiated PC12 cells was assessed through cell counting kit-8 (CCK-8) assays (Dojindo, Japan). OD at 450 nm, which was measured using a spectrophotometer (Thermo Fisher Scientific, USA), was used to estimate cell viability. In the experiments for counting the neurite-bearing PC12 cells, the cells were photographed using a digital camera under a phase-contrast microscope. The images of five randomly selected fields were obtained for each dish, and a mean of 10–20 PC12 cells per field were observed. The percentage of neurite-bearing cells per field was calculated using the following equation: (number of neurite-bearing cells/total number of cells) × 100. Finally, the results from all the fields were tallied and divided by the total number of fields (n = 5) to obtain the percentage of neurite-bearing cells per condition (Wiatrak et al., 2020).

Viability of H_2O_2-induced differentiated PC12 cell death assay

PC12 cells were seeded in 96-well culture plates (Corning, United States) coated with 0.1 mg/ml poly-L-lysine at a density of 10,000 cells/well in a culture medium for 1 day. The cultured PC12 cells were then transferred to low-serum medium containing 50 ng/ml NGF and cultured for 2 days. Subsequently, the differentiated PC12 cells were stimulated with 200 μM H_2O_2 and various concentrations of the KI Essence extract (0, 0.5, and 1 mg/ml) for 1 day, after which a CCK-8 viability assay was performed (Dojindo).

Western blotting

We seeded 1×10^6 PC12 cells in 6-cm tissue culture dishes, with overnight incubation. The cultured PC12 cells were then transferred to low-serum medium (containing 1% horse serum with 0.5% FBS) and cultured for 24 h. The PC12 cells were stimulated with 50 ng/ml NGF and the KI Essence extract for 0, 0.5, or 1 h. In another set of experiments, 1×10^6 NGF–induced differentiated PC12 cells were treated with 200 μM H_2O_2 and the KI Essence extract for 0, 0.5, or 1 h. Subsequently, cell lysates were prepared using a PRO-PREP protein extraction solution (iNtRON Biotechnology, Korea) containing 2 mM Na_3VO_4. The cell lysates were immunoblotted using primary antibodies against p-ERK1/2, p-p38, and β-Actin (Cell Signaling Technology, USA) and horseradish peroxidase–conjugated goat antirabbit or antimouse immunoglobin G (GoalBio, Taiwan). All data were acquired using a ChemiDoc Touch Imaging System (Bio-Rad, USA).

2,2′-diphenyl-1-picrylhydrazyl scavenging assay

We added a 100-μL aliquot of 500 μM 2,2′-diphenyl-1-picrylhydrazyl (DPPH)–ethanol solution to each well of a 96-well plate, followed by the addition of 100 μl of the KI Essence extract at various concentrations. Butylated hydroxytoluene was used as a standard antioxidant compound. The plates were incubated for 30 min in the dark, and absorbance was measured at 530 nm on an enzyme-linked immunosorbent assay (ELISA) microplate reader (Thermo Fisher Scientific). Moreover, 300-μl aliquots of ethanol were used as blanks, and the following equation was used to calculate the DPPH radical scavenging rate (%): $[1 - (S_T/E_C)] \times 100$, where S_T and E_C are the OD at 530 nm of the sample and control, respectively.

Antiperoxidation effects of KI Essence extract through malondialdehyde assay

Lipid peroxidation levels in brain homogenates were determined by measuring MDA levels. In brief, brain samples from C57BL/6 mice were first homogenized in ice-cold phosphate-buffered saline (PBS) at a concentration of 25% (w/v). The protein levels in the homogenized tissues were quantified using a protein assay dye (Bio-Rad). The brain homogenates (200 μg/ml) were incubated with 50 mM tert-butyl hydroperoxide (t-BHP; Sigma) and various concentrations of the KI Essence extract for 1 h at 37°C. The MDA levels in the sample were measured using an MDA assay kit (Abcam, USA) according to the manufacturer's instructions.

Lipopolysaccharide-induced maternal immune activation rat model and oral KI Essence extract treatment

Eight-week-old female Wistar rats (BioLASCO, Taiwan) were mated overnight with male rats; the presence of a vaginal plug was used to confirm the success of mating. Each pregnant rat was allowed to raise its own litter in an individual cage. Subsequently, 500 μg/kg lipopolysaccharide (LPS; from

Escherichia coli O127:B8; Sigma) or PBS was injected intraperitoneally into the pregnant rats on gestation day 9.5. The 5-week-old male offspring of the rats were treated orally with H_2O or the KI Essence extract (40 mg/kg) for 2 weeks. Thereafter, their stool and brain were collected for microbiota analysis and immunohistochemistry assay, respectively. The experiments were conducted in accordance with the guidelines of the International Council for Laboratory Animal Science for the care and use of laboratory animals in experiments. Moreover, all animal procedures were approved by the Animal Care and Use Committee of Taipei Medical University (LAC-2019-0198).

16S rRNA gene and next-generation sequencing

The detailed procedure for performing 16S rRNA gene sequencing and next-generation sequencing has been provided elsewhere (Lee et al., 2021). The rats were allowed to defecate freely in clean cages, and DNA was extracted from fresh stool samples by using the QIAamp Fast DNA Stool Mini Kit (Qiagen, Germany). Library preparation was performed using an Illumina MiSeq system in accordance with the protocol for 16S rRNA gene amplicons. The universal primers 341F and 805R were used to amplify the V3–V4 region of bacterial 16S rRNA genes. Demultiplexed, paired reads were removed using Cutadapt (version 1.12). The filtered reads were processed using the DADA2 package (version 1.14.1) in R (version 3.6.1) (Callahan et al., 2016a; Callahan et al., 2016b); however, the rarefying procedure was not performed. V3–V4 sequence variants in the samples were inferred using the DADA2 package, and the frequency of each sequence variant in each sample was obtained. Taxonomy assignment was conducted using the SILVA database (version 138) (Quast et al., 2013), with a minimum bootstrap confidence of 80. The multiple sequence alignment of variants and the preparation of a phylogenetic tree were performed using DECIPHER (version 2.14.0) and phangorn (version 2.5.5), respectively (Schliep, 2011). The taxonomy assignment, count table, and phylogenetic tree were applied in a phyloseq object, and community analysis was conducted using phyloseq (version 1.30.0) (Mcmurdie and Holmes, 2013). Alpha diversity indices were calculated to estimate the richness function of the phyloseq package. Statistical analyses were conducted using the Wilcoxon–Mann–Whitney test ($\alpha = 0.05$). UniFrac distances were calculated using the GUniFrac package (version 1.1) to assess community dissimilarity among the groups examined in the present study (Chen et al., 2012). Principal coordinate analysis ordination was applied for UniFrac distances, and the adonis and betadisper functions from the vegan package (version 2.4) for R were used to analyze the dissimilarity of composition among the examined groups and the homogeneity of their dispersion, respectively.

Immunohistochemistry

The rats were anaesthetized with Zoletil (40 mg/kg) and Xylazine (10 mg/kg), then transcardially perfused with PBS and 4% paraformaldehyde. Their whole brains were fixed with 4% paraformaldehyde for 3 days, and 2-mm coronal slices were embedded in paraffin blocks. These blocks were sliced into 5-μm-thick sections, which were then deparaffinized, rehydrated, and subjected to an antigen retrieval process. Subsequently, the sections were stained with horseradish peroxidase–conjugated MBP antibody (Abcam), followed by staining with 3,3′-diaminobenzidine and hematoxylin, using a Chemicon IHC Select system (Millipore, USA). The sections were observed through microscopy (Olympus/Bx43, Japan), and the MBP-positive area were calculated using the tissue analysis software program HistoQuest (Tissue Gnostics, Austria).

Interleukin-1β production in lipopolysaccharide-stimulated microglia assay

Enriched glial cultures (microglia and astrocytes) were prepared from the brains of newborn C57BL/6 mice (National Laboratory Animal Center, Taiwan) that were collected on postnatal day 1. In brief, cerebral cortical cells were cultured in Dulbecco's Modified Eagle Medium/Nutrient Mixture F-12 containing 10% FBS and 1% penicillin–streptomycin for 14 days to enable their differentiation into glial cells. Microglia were detached by shaking the culture flasks containing the cells at 160 rpm for 5 h. The suspended microglia were collected and seeded in 96-well culture plates coated with poly-D-lysine at 5×10^4 cells per well for 1 day. The purity of these isolated cells was measured through staining with CD11b antibody (Biolegend, USA), and these cells were analyzed through flow cytometry. The obtained microglia were stimulated using 250 ng/ml LPS in different concentrations of KI Essence extract for 24 h. The interleukin (IL)-1β content of the culture supernatant was analyzed using a ELISA MAX Deluxe Set Mouse IL-1β kit (Biolegend).

Statistical analysis

For neurite-bearing cell, MDA content, western blot, MBP^+ area, IL-1β production data analyses, one-way

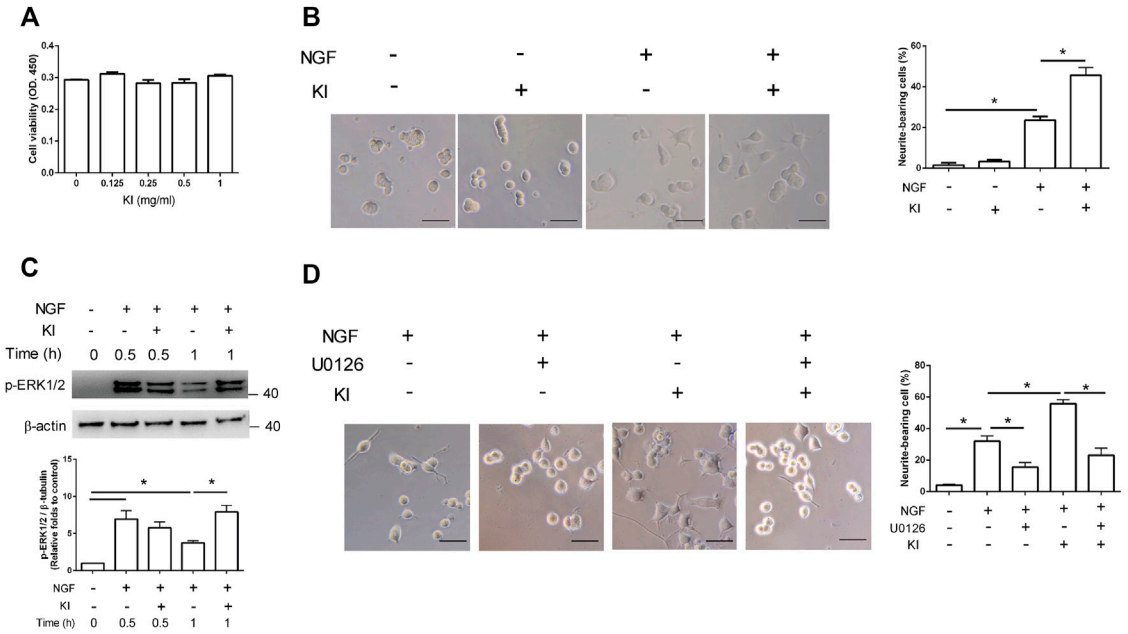

FIGURE 1
PC12 cell neurite growth induction through extracellular signal–regulated kinase (ERK)1/2 phosphorylation after KI Essence extract treatment. **(A)** KI Essence extract treatment did not affect the viability of PC12 cells. PC12 cells were pretreated with low-serum medium for 1 day and then with various concentrations of the KI Essence extract and nerve growth factor (NGF; 50 ng/ml) for 48 h. PC12 cell viability was determined using cell counting kit-8 (CCK-8) assay. **(B)** Phase-contrast images of cells on day 2 after treatment with NGF in presence or absence of the KI Essence extract (0.25 mg/ml; scale bar: 50 μm). PC12 cells were cotreated with the KI Essence extract and NGF for 2 days, and percentages of neurite-bearing cells on day 2 was assessed. The data are expressed as means ± standard errors of means (SEMs) for (n = 3; $^*p < 0.05$). **(C)** PC12 cells treated with 0.25 mg/ml KI Essence extract for various durations (0, 0.5, and 1 h). Phosphorylation levels of ERK (p-ERK) 1/2 and β-tubulin were analyzed through Western blotting. Quantitation of p-ERK1/2 to β-tubulin is presented in the bar graph (n = 3; $^*p < 0.05$). **(D)** PC12 cells were treated with the KI Essence extract (0.25 mg/ml) and NGF for 2 days in the presence or absence of 10 μM U0126. Phase-contrast images of neurite-bearing cells on day 2 are shown (scale bar: 50 μm). The data are expressed means ± SEMs (n = 3). Quantitation of percentage of neurite-bearing cells is presented in the bar graph $^*p < 0.05$).

ANOVA was performed using Prism (GraphPad, USA); in the analysis results, error bars represent the standard errors of the mean. The microbiota enrichment analysis of the groups was conducted using the linear discriminant analysis (LDA) effect size (LEfSe) method. Data were compared using the Kruskal–Wallis and Wilcoxon tests; differences were considered significant when $p \leq 0.05$ and logarithmic LDA score ≥ 2 (Segata et al., 2011).

Results

Effects of KI Essence extract on neurite outgrowth in PC12 cells

Our phenol–sulfuric acid analysis revealed that the KI Essence extract used in this present study contained 70 mg/g carbohydrates (including monosaccharides, disaccharides, oligosaccharides, and polysaccharides; data not shown). The key components of the KI Essence extract include several edible mushrooms, and nucleotides are major components of many edible mushrooms (Ranogajec et al., 2010). As shown in Supplementary Figure S1, several nucleotides were detected in the KI Essence extract, which included cytosine, cytidine, hypoxanthine, uridine, guanosine, and adenosine. Maslinic acid was also detected using HPLC finger printing and HPLC analyses (Supplementary Figures S1,S2).

We first used the CCK-8 assay to assess whether the KI Essence extract affected PC12 cell viability. The results indicated that treatment with the KI Essence extract at various concentrations did not affect the OD at 450 nm, indicating that this extract did not affect the differentiated PC12 cell viability (Figure 1A). Subsequently, we examined whether the KI Essence extract affected the neuritogenesis of PC12 cells. After 48 h of NGF stimulation, the percentage of neurite-bearing cells increased significantly to 21.5% ± 1.8% in PC12 cells treated with 50 ng/ml NGF compared with the negative control (5% ± 0.5%; Figure 1B). Furthermore, the KI Essence extract increased the percentage of neurite-bearing cells in a dose-dependent manner under NGF stimulation (Figure 1B and Supplementary Figure

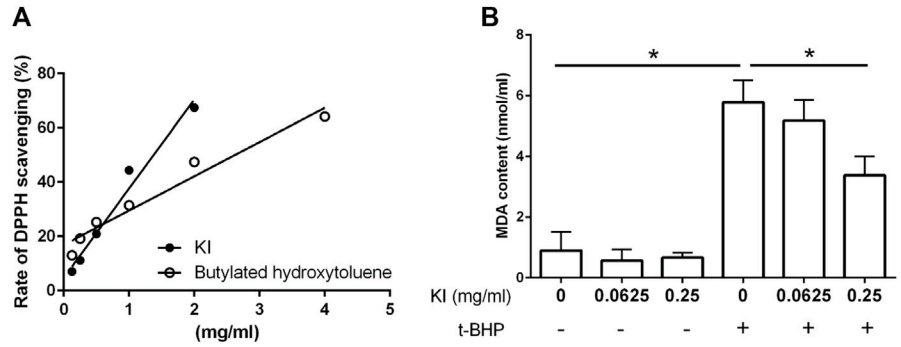

FIGURE 2
Characterization of KI Essence extract in radical scavenging and anti-lipid peroxidation properties. **(A)** 2,2′-diphenyl-1-picrylhydrazyl (DPPH) scavenging property of the KI Essence extract and butylated hydroxytoluene. 500 μM DPPH were tested at various concentrations of the KI Essence extract and butylated hydroxytoluene. **(B)** Effects of the KI Essence extract on tert-butyl hydroperoxide (t-BHP)-induced lipid peroxidation in brain homogenates. Brain homogenates were incubated with various concentrations of the KI Essence extract (0, 0.0625, and 0.25 mg/ml) with (+) or without (–) t-BHP stimulation for 1 h. Malondialdehyde (MDA) contents are presented in the bar graph. The results are presented as means ± standard errors of means (n = 3; $^*p < 0.05$).

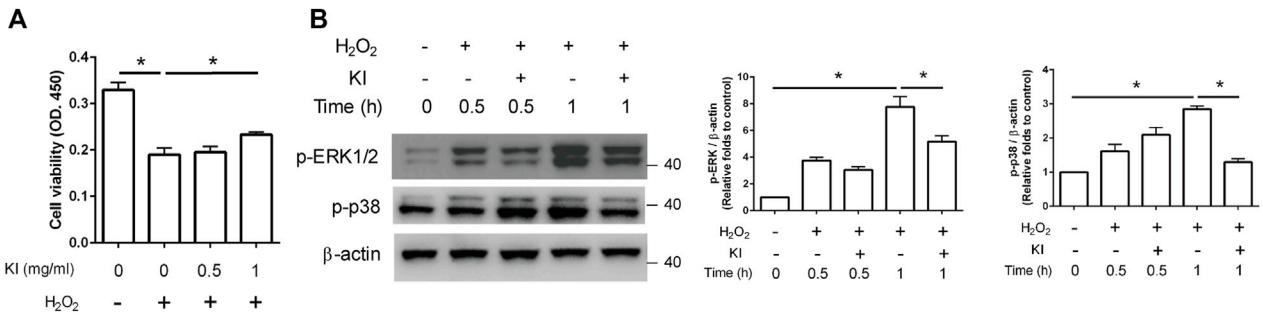

FIGURE 3
Protective effect of KI Essence extract treatment on PC12 cells against H_2O_2-induced cell death through inhibition of ERK phosphorylation. **(A)** PC12 cells were treated with 200 μM H_2O_2 and various concentrations of the KI Essence extract for 1 day. Viability of PC12 cells was measured using CCK-8 assay. The results are presented as means ± standard errors of means (SEMs; n = 3; $^*p < 0.05$). **(B)** PC12 cells treated with 1 mg/ml KI Essence extract for various durations (0, 0.5, and 1 h) in the presence of 200 μM H_2O_2. Levels of p-ERK1/2, p-p38, and β-Actin were analyzed through Western blotting. Quantitation of p-ERK1/2 and p-p38 to β-Actin is presented in the bar graph. The results are presented as means ± SEMs (n = 3; $^*p < 0.05$).

S3). However, treatment with only the KI Essence extract did not induce neurite outgrowth in PC12 cells. To assess whether KI Essence extract treatment enhanced NGF-induced ERK signaling pathways in PC12 cells, we examined the phosphorylation level of ERK (i.e., p-ERK1/2 level) in PC12 cells. The results indicated that the KI Essence extract enhanced p-ERK1/2 expression in NGF-stimulated PC12 cells (Figure 1C). We next assessed whether the KI Essence extract promoted neurite outgrowth under NGF stimulation through MEK1 and MEK2 activation. Our results indicated that U0126, which inhibits MEK1 and MEK2, abolished the KI Essence extract–induced neurite outgrowth effect in PC12 cells under NGF stimulation (Figure 1D, column 4 vs. 5). Therefore, the KI Essence extract enhanced neurite growth in PC12 cells through ERK1/2 phosphorylation.

Characterization of radical scavenging and anti-lipid peroxidation properties of KI Essence extract

The radical scavenging property of the KI Essence extract was determined using a DPPH chemical test. As illustrated in Figure 2A, the DPPH radicals were inhibited by KI Essence extract in a dose-dependent manner; it was found to be better than butylated hydroxytoluene, a standard antioxidant

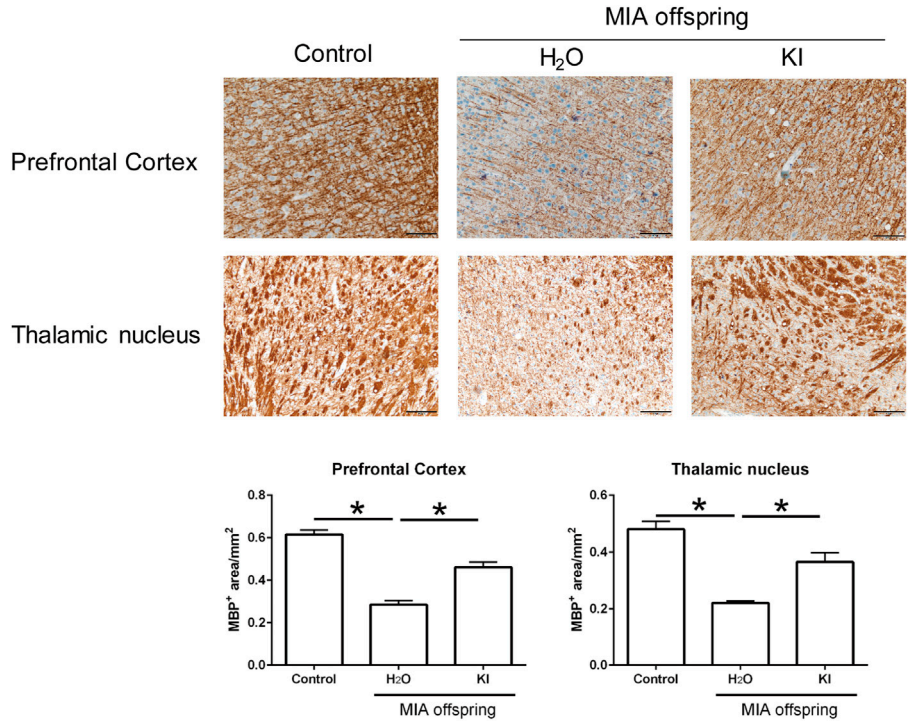

FIGURE 4
Amelioration of hypomyelination in maternal immune activation (MIA) offspring after oral KI Essence extract treatment. Myelin basic protein (MBP) expression levels in the prefrontal cortex and thalamic nucleus of control group, H_2O-treated MIA offspring, and KI Essence extract–treated MIA offspring were detected through immunohistochemical staining. Quantification of MBP^+ area in the prefrontal cortex and thalamic nucleus is presented in the bar graph $^*p < 0.05$; $n = 3$ for each group). All data are presented as means ± standard errors of means (scale bar: 100 μm).

compound (Olugbami et al., 2014). Because oxidative stress is a key inducer of central nervous system developmental diseases, we evaluated the effects of the KI Essence extract on t-BHP-induced lipid peroxidation in mouse brain homogenates. The KI Essence extract exerted a considerable, dose-dependent inhibitory effect on MDA production in the homogenates (Figure 2B).

Effects of KI Essence extract on H_2O_2-induced cell death of differentiated PC12 cells

The viability of H_2O_2-treated PC12 cells was considerably (62.5%) lower than that of control cells (Figure 3A, column 1 vs. 2). The viability of KI Essence extract–treated cells was higher than that of untreated cells, indicating that KI Essence extract treatment reduced the toxic effect of H_2O_2 stimulation (Figure 3A, column 2 vs. 4). We then assessed whether the KI Essence extract affected H_2O_2-induced ERK1/2 and p38 signaling pathways in differentiated PC12 cells. The results revealed that H_2O_2 treatment significantly upregulated ERK1/2 and p38 phosphorylation after 1 h of stimulation. By contrast, KI Essence extract treatment ameliorated ERK1/2 and p38 phosphorylation (Figure 3B). Therefore, the KI Essence extract protected differentiated PC12 cells from H_2O_2-induced oxidative stress and ameliorated H_2O_2-induced ERK1/2 and p38 phosphorylation.

Effects of oral KI Essence extract treatment on myelination in maternal immune activation offspring

Maternal LPS stimulation causes oxidative stress and hypomyelination in the prefrontal cortex and thalamus nucleus of MIA offspring (Wischhof et al., 2015; Simoes et al., 2018). In this study, to evaluate the effects of KI Essence extract treatment on the *in vivo* modulation of myelination in the rat brain, we examined myelination levels in MIA offspring brains after oral KI Essence extract treatment. Immunohistochemical staining revealed that the MBP^+ area was smaller in the prefrontal cortex and thalamic nucleus of the MIA offspring (H_2O treatment) than in the control rats; nevertheless, oral KI Essence extract treatment alleviated the loss of the MBP^+ area in the MIA offspring (Figure 4). These results indicated that oral

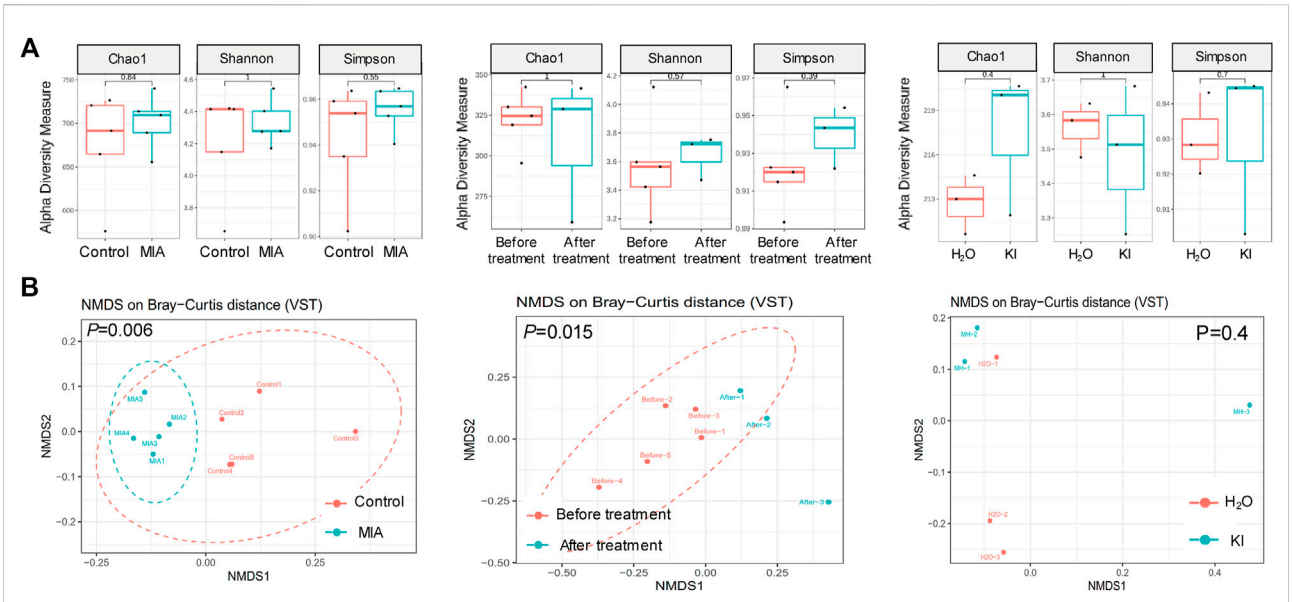

FIGURE 5
Modulation of fecal microbiome distribution in maternal immune activation (MIA) offspring after oral KI Essence extract treatment. Fecal microbiome profiling of male MIA offspring was performed through high-throughput 16S rRNA gene sequencing. **(A)** Alpha diversity of fecal microbiota and **(B)** principal coordinate analysis plots (as obtained through nonmetric multidimensional scaling with Bray–Curtis distance analysis) for control and MIA rats before and after H_2O and KI Essence extract treatment. Permutational multivariate analysis of variance (vegan::adonis, 1000 permutations) revealed a significant difference in beta diversity, which was quantified using a betadisper (vegan::betadisper, 1000 permutations). Adonis and betadisper indices yielded *p* values of <0.05 and >0.05, respectively. *n* = 5 for control and MIA group; *n* = 5 for before treatment group; *n* = 3 for after treatment, H_2O, and KI Essence extract treatment group.

KI Essence extract treatment alleviated hypomyelination in MIA offspring.

Effects of oral KI Essence extract treatment on microbiome profile in maternal immune activation offspring

Mushrooms contain bioactive ingredients that can modulate gut microbiota (Ma et al., 2021; Vamanu et al., 2021). LPS-induced MIA offspring exhibit a microbiome profile similar to that of humans with ASD (Lee et al., 2021). Therefore, we examined the effects of KI Essence extract treatment on the modulation of the microbiome profile in the examined MIA offspring. The alpha diversity of the fecal microbiota in the MIA offspring was similar to that of the control offspring (Figure 5A, left panel). Nonmetric multidimensional scaling (NMDS) was performed using the Bray–Curtis distance method, and the results indicated that the fecal microbiome profile of the MIA offspring was significantly different from that of the control offspring (Figure 5B, left panel). As presented in Figure 6A, significant differences were found in the abundance of microbial species between the control and MIA offspring. Compared with the MIA offspring, the control offspring had significantly higher LDA scores for Firmicutes, Proteobacteria, and Actinobacteriota bacteria at the phylum level. NMDS with Bray–Curtis distance analysis was subsequently performed, and the results indicated that after 2 weeks of oral KI Essence extract treatment, the fecal microbiome profile of the MIA offspring was significantly different from that of the MIA offspring (Figure 5B, middle panel); however, the differences in alpha diversity were nonsignificant (Figure 5A, middle panel). By contrast, the oral KI Essence extract–treated MIA offspring did not differ significantly from the H_2O-treated male MIA offspring in terms of the beta diversity of their microbiota (Figure 5B, right panel). At the phylum level, the LDA scores for Firmicutes, Proteobacteria, and Actinobacteriota bacteria in the MIA offspring were higher after oral KI Essence extract treatment than before treatment (Figure 6B); these scores were also higher than those of the H_2O-treated MIA offspring (Figure 6C). Similarly, at the family level, the LDA scores for Peptostreptococcaceae, Enterobacteriaceae, Erysipelotrichaceae, Lactobacillaceae, and Bifidobacteriaceae bacteria in the MIA offspring were higher after oral KI Essence extract treatment than before treatment (Figure 6B); these scores were also higher than those of the H_2O-MIA offspring (Figure 6C). In summary, oral KI Essence extract treatment could modulate the dysbiotic microbiome profile of the MIA offspring.

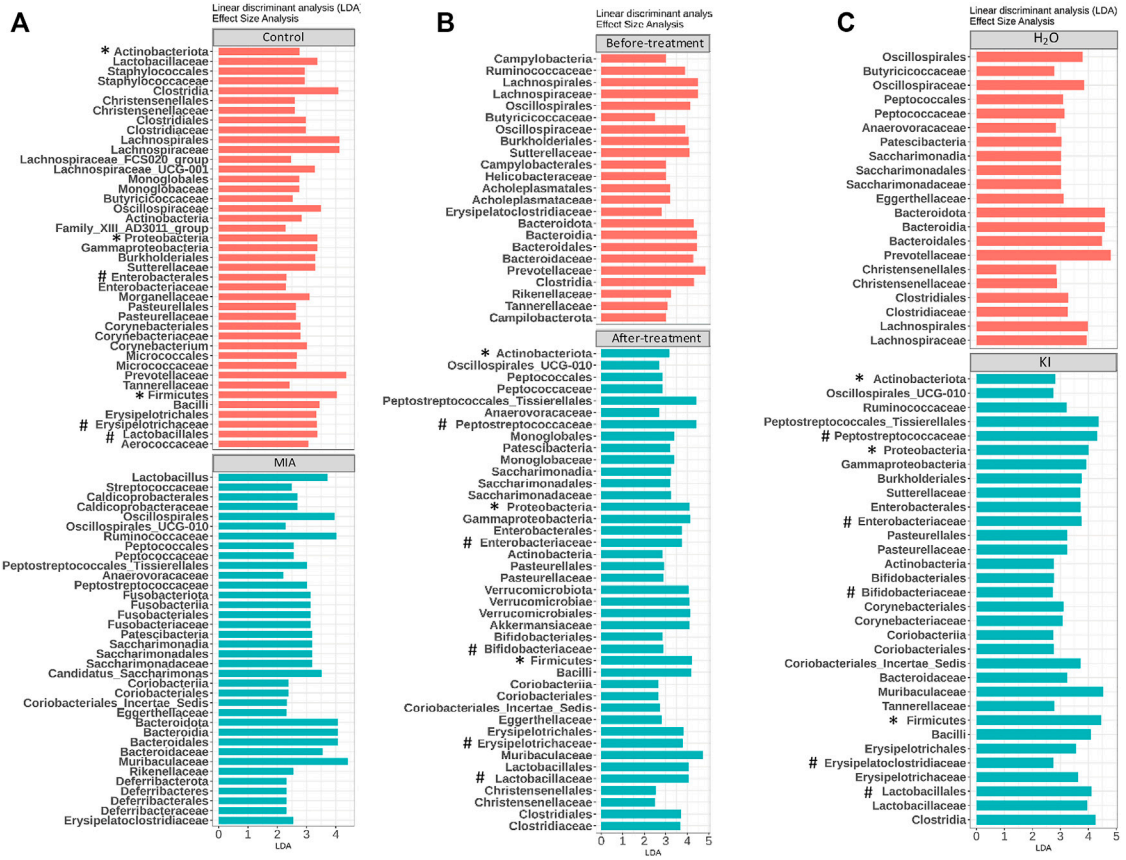

FIGURE 6
Modulation of microbiome profile in maternal immune activation (MIA) offspring after oral KI Essence extract treatment. Linear discriminant analyses (LDAs) for comparing **(A)** gut microbiota effect sizes of control and MIA offspring, **(B)** gut microbiota effect sizes of MIA offspring before and after KI Essence extract treatment, and **(C)** gut microbiota effect sizes of MIA offspring after H_2O and KI Essence extract (KI) treatment. Significant biomarkers are defined as taxa with LDA score (log_{10}) ≥ 2. * and # indicated that abundance of bacterial species at the phylum and family levels was significantly different, respectively. *n* = 5 for control and MIA group; *n* = 5 for before treatment group; *n* = 3 for after treatment, H_2O, and KI Essence extract treatment group.

Effects of KI Essence extract treatment on lipopolysaccharide-stimulated microglia

During the gestational stage, elevated IL-1β levels are associated with hypomyelination in LPS-induced MIA offspring (Rousset et al., 2006; Simoes et al., 2018; Chamera et al., 2020). LPS stimulation prompts IL-1β production in microglia (Kim et al., 2006). In this study, we observed that KI Essence extract treatment inhibited IL-1β production in LPS-activated microglia (Figure 7).

Discussion

In the present study, we observed that the extract of the spleen-tonifying formula KI Essence promoted neuritogenesis activity, alleviated hypomyelination, and modulated the microbiome profile in MIA offspring. Supplementary Figure S4 presents a schematic of the workflow for the present study. Our results were as follows: 1) KI Essence extract treatment enhanced p-ERK expression to promote NGF-induced neuritogenesis and inhibited p-ERK expression to protect differentiated PC12 cells from H_2O_2-induced cell death. 2) The KI Essence extract demonstrated DPPH radical inhibition and reduced the peroxidation response in rat brain homogenates. 3) Oral KI Essence extract treatment alleviated prenatal LPS-induced hypomyelination in the prefrontal cortex and thalamic nucleus of the MIA offspring and increased the abundance of Peptostreptococcaceae, Enterobacteriaceae, Erysipelotrichaceae, Bifidobacteriaceae, and Lactobacillales bacteria in the offspring. This is the first study to demonstrate that treatment with a spleen-tonifying formula can promote neurite growth, alleviate oxidative stress, and alter the brain–gut–microbiota axis in MIA offspring.

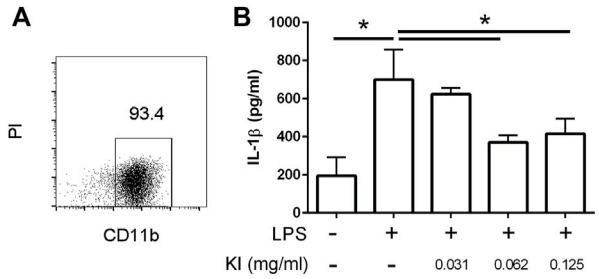

FIGURE 7
Inhibitory effect of KI Essence treatment on interleukin (IL)-1β production from lipopolysaccharide (LPS)-induced microglia activation. **(A)** Percentage of CD11b$^+$ cells in enriched microglia cell culture. PI: propidium iodide. **(B)** Microglia treated with KI Essence (0, 0.031, 0.062, 0.125 mg/ml) in the presence of 250 ng/ml LPS for 24 h. Amount of IL-1β in culture supernatant was determined through enzyme-linked immunosorbent assay ($n = 3$; $^*p < 0.05$).

Mushroom and traditional Chinese herbal extracts contain polysaccharides and nucleotides that can induce neuronal differentiation and promote antioxidant activity (Sabaratnam et al., 2013; Kozarski et al., 2015; Cor et al., 2018). Our three-dimensional HPLC fingerprint analysis revealed the presence of guanosine, uridine, and maslinic acid in the examined KI Essence extract (Supplementary Figure S1). Guanosine exhibits antioxidant activity and protects DNA from the oxidative damage induced by ROS (Gudkov et al., 2006). Uridine has been noted to enhance neurite outgrowth in NGF-differentiated PC12 cells (Pooler et al., 2005). Maslinic acid promotes synaptogenesis and axon growth (Qian et al., 2015). In the present study, the examined KI Essence extract increased ERK1/2 phosphorylation to promote neurite outgrowth in differentiated PC12 cells under NGF stimulation. We also observed that KI Essence extract treatment ameliorated the phosphorylation level of ERK1/2 in H_2O_2-treated PC12 cells. These contrasting effects on ERK phosphorylation in PC12 cells are attributable to the different components in KI Essence: maslinic acid and uridine in KI Essence may promote neurite outgrowth by upregulating ERK phosphorylation. Polysaccharides and guanosine in KI Essence can ameliorate H_2O_2-induced oxidative stress and thus inhibit H_2O_2-induced ERK phosphorylation. Our data indicated that p-p38 expression slightly increased after 30-min treatment with both KI Essence extract and H_2O_2, but it decreased after 60 min of this treatment. This finding suggests that KI Essence components enhance p-p38 expression after 30 min of KI Essence extract treatment in the presence of H_2O_2 stimulation. We also noted that although H_2O_2 stimulation caused the p-p38 expression signal to peak after 1 h of treatment, the KI Essence extract exhibited antioxidant activity to ameliorate the effects of H_2O_2 stimulation on p-p38 expression. Thus, our results demonstrate that KI Essence can promote neurite outgrowth and antioxidant activity.

Prenatal LPS stimulation causes oxidative stress (including ROS generation and peroxisomal dysfunction), inflammation, and hypomyelination in MIA offspring (Arsenault et al., 2014; Maas et al., 2017). (Yui et al., 2020) also reported that lipid peroxidation levels are higher in patients with ASD than in healthy controls. Oxidative stress inhibits oligodendrocyte maturation by inhibiting differentiation-related gene expression; thus, lipid peroxidation stress may affect the maturation of oligodendrocytes (French et al., 2009; Chew et al., 2020). LPS-activated microglia cause oligodendrocyte progenitor cell death, reducing the number of mature myelinating oligodendrocytes (Pang et al., 2010). The elevated levels of the inflammatory cytokine IL-1β during the gestational stage is associated with hypomyelination in LPS-induced MIA offspring with ASD-like behavior (Rousset et al., 2006; Simoes et al., 2018; Chamera et al., 2020). In the present study, the examined KI Essence extract demonstrated DPPH radical scavenging activity, ameliorated lipid peroxidation in rat brain homogenates, and inhibited IL-1β production in LPS-activated microglia. These findings suggest that oral KI Essence extract treatment inhibits prenatal LPS-induced oxidative stress and microglia activation in MIA offspring, thereby alleviating hypomyelination in the prefrontal cortex and thalamic nucleus of the offspring.

Microbial dysbiosis is correlated with behavioral abnormalities and neuropathology (Vuong and Hsiao, 2017). Mushrooms are functional foods containing various biologically active compounds that can mitigate microbial dysbiosis (Cheung et al., 2020; Vamanu et al., 2021). Gut microbiota transplantation (primarily with a mixture of bifidobacteria, streptococci, and lactobacilli) is a therapeutic method used to alter microbiome profiles and improve neurobehavioral symptoms (Kang et al., 2017; Fattorusso et al., 2019; Chen et al., 2020; Abuaish et al., 2021). In this study, the low abundance of Enterobacteriaceae, Actinobacteria, Peptostreptococcaceae, and Erysipelotrichaceae that was observed in the LPS-induced MIA rat offspring is consistent with the microbiome profile in humans with ASD (Rosenfeld, 2015; Liu et al., 2019; Xu et al., 2019). Patients with ASD exhibit a low abundance of Bifidobacteriaceae family bacteria (phylum Actinobacteriota) (Finegold et al., 2010; Xu et al., 2019). We observed that oral KI Essence extract treatment increased the number of Enterobacteriaceae, Actinobacteria, Peptostreptococcaceae, Erysipelotrichaceae, and *Bifidobacterium* bacteria in the MIA offspring. Current psychopharmacological treatments include psychotropic medications and dietary supplements with antioxidant activity (Aishworiya et al., 2022). The intake of supplements with antioxidant activity leads to the reduction of ROS levels and the upregulation of genes involved in detoxification and neuroprotection in the central nervous system (Pangrazzi et al., 2020a). Our results suggest that KI Essence has the potential to serve as an ancillary treatment for alleviating oxidative stress and dysbiosis.

Conclusion

The KI Essence extract was noted to have dual effects in an NGF-differentiated PC12 cell model: neurite outgrowth and antioxidant properties promotion through ERK1/2 signaling pathway activation and inhibition, respectively. Because of its antioxidant and radical scavenging properties, this extract could also alleviate MIA-induced oxidative stress and prevent myelin loss in MIA offspring. Oral KI Essence extract treatment increased the deficits in the microbial species, including those from Enterobacteriaceae, Actinobacteria, Peptostreptococcaceae, Erysipelotrichaceae, and *Bifidobacterium*; this result is similar to that observed in patients with ASD.

This study highlights the relationship among the microbiome, immune system, and central nervous system, which is crucial in the etiopathophysiology of mental disorders. Furthermore, KI Essence extract treatment can alter abnormal brain–gut–microbiota axis phenotypes. Nevertheless, three issues as limitations of this study remain unresolved. First, DPPH is a chemical test and may not accurately measure the radical scavenging effects of KI Essence extracts. Second, the single dose study was used in the study. Several doses should have been used to get a more accurate conclusion. Third, whether KI Essence can alleviate mental disorder symptoms, such as social behavior deficit, and whether different oral doses of KI Essence have varied effects on MIA offspring warrant further research.

Data availability statement

The original contributions presented in the study are included in the article/Supplementary Material, further inquiries can be directed to the corresponding author.

Ethics statement

The animal study was reviewed and approved by The Animal Care and Use Committee of Taipei Medical University.

Author contributions

Conceptualization, GAL and S-HT; Methodology, GAL and Y-CY; Software, GAL; Validation, GAL; Formal Analysis: C-JL, H-WZ, Y-WC, Y-RL, and Y-CY; Investigation, Y-WC, GAL, Y-CW, W-LL; Resources, D-SN, H-WZ, and C-JL.; Data Curation, GAL; Writing (Original draft preparation), GAL; Writing (Review and editing), GAL; Visualization, GAL; Supervision, S-HT; Project administration, S-HT; Funding acquisition, S-HT. All authors have read and agreed to the published version of the manuscript.

Funding

This research was funded by Taipei Medical University (grant no. TMU A00000952) and Taipei Medical University Hospital (grant nos. 110TMU-TMUH-09, 109TMUH-SP-03, 111TMU-TMUH-05-2, 111TMU-TMUH-05-1, 111TMUH-MOST-12), MOST 111-2314-B-038-097-MY3 and TMU110-AE2-I03-1.

Acknowledgments

This manuscript was edited by Wallace Academic Editing. We would like to acknowledge the support provided by Core Laboratory of Human Microbiome and Laboratory Animal Center, Taipei Medical University. We also acknowledge the HPLC fingerprint analysis support provided by Herbiotek Co., Ltd.

Conflict of interest

Authors H-WZ and D-SN were employed by the company Infinitus.

The remaining authors declare that the research was conducted in the absence of any commercial or financial relationships that could be construed as a potential conflict of interest.

Publisher's note

Supplementary material

The Supplementary Material for this article can be found online at: https://www.frontiersin.org/articles/10.3389/fphar.2022.964255/full#supplementary-material

References

Abuaish, S., Al-Otaibi, N. M., Abujamel, T. S., Alzahrani, S. A., Alotaibi, S. M., Alshawakir, Y. A., et al. (2021). Fecal transplant and Bifidobacterium treatments modulate gut Clostridium bacteria and rescue social impairment and hippocampal BDNF expression in a rodent model of autism. *Brain Sci.* 11, 1038. doi:10.3390/brainsci11081038

Aishworiya, R., Valica, T., Hagerman, R., and Restrepo, B. (2022). An update on psychopharmacological treatment of autism spectrum disorder. *Neurotherapeutics* 19, 248–262. doi:10.1007/s13311-022-01183-1

Arsenault, D., St-Amour, I., Cisbani, G., Rousseau, L. S., and Cicchetti, F. (2014). The different effects of LPS and poly I:C prenatal immune challenges on the behavior, development and inflammatory responses in pregnant mice and their offspring. *Brain Behav. Immun.* 38, 77–90. doi:10.1016/j.bbi.2013.12.016

Bang, M., Lee, S. H., Cho, S.-H., Yu, S.-A., Kim, K., Lu, H. Y., et al. (2017). Herbal medicine treatment for children with autism spectrum disorder: A systematic review. *Evid. Based. Complement. Altern. Med.* 2017, 8614680. doi:10.1155/2017/8614680

Callahan, B. J., Mcmurdie, P. J., Rosen, M. J., Han, A. W., Johnson, A. J., and Holmes, S. P. (2016a). DADA2: High-resolution sample inference from Illumina amplicon data. *Nat. Methods* 13, 581–583. doi:10.1038/nmeth.3869

Callahan, B. J., Sankaran, K., Fukuyama, J. A., Mcmurdie, P. J., and Holmes, S. P. (2016b). Bioconductor workflow for microbiome data analysis: From raw reads to community analyses. *F1000Res.* 5, 1492. doi:10.12688/f1000research.8986.2

Chamera, K., Kotarska, K., Szuster-Gluszczak, M., Trojan, E., Skorkowska, A., Pomierny, B., et al. (2020). The prenatal challenge with lipopolysaccharide and polyinosinic:polycytidylic acid disrupts cx3cl1-cx3cr1 and cd200-cd200r signalling in the brains of male rat offspring: a link to schizophrenia-like behaviours. *J. Neuroinflammation* 17, 247. doi:10.1186/s12974-020-01923-0

Chauhan, A., and Chauhan, V. (2006). Oxidative stress in autism. *Pathophysiology* 13, 171–181. doi:10.1016/j.pathophys.2006.05.007

Chen, J., Bittinger, K., Charlson, E. S., Hoffmann, C., Lewis, J., Wu, G. D., et al. (2012). Associating microbiome composition with environmental covariates using generalized UniFrac distances. *Bioinformatics* 28, 2106–2113. doi:10.1093/bioinformatics/bts342

Chen, K., Fu, Y., Wang, Y., Liao, L., Xu, H., Zhang, A., et al. (2020). Therapeutic effects of the *in vitro* cultured human gut microbiota as transplants on altering gut microbiota and improving symptoms associated with autism spectrum disorder. *Microb. Ecol.* 80, 475–486. doi:10.1007/s00248-020-01494-w

Cheung, M. K., Yue, G. G. L., Chiu, P. W. Y., and Lau, C. B. S. (2020). A review of the effects of natural compounds, medicinal plants, and mushrooms on the gut microbiota in colitis and cancer. *Front. Pharmacol.* 11, 744. doi:10.3389/fphar.2020.00744

Chew, H., Solomon, V. A., and Fonteh, A. N. (2020). Involvement of lipids in alzheimer's disease pathology and potential therapies. *Front. Physiol.* 11, 598. doi:10.3389/fphys.2020.00598

Cor, D., Knez, Z., and Knez Hrncic, M. (2018). Antitumour, antimicrobial, antioxidant and antiacetylcholinesterase effect of Ganoderma lucidum terpenoids and polysaccharides: A review. *Molecules* 23, E649. doi:10.3390/molecules23030649

Diallo, I., Boudard, F., Morel, S., Vitou, M., Guzman, C., Saint, N., et al. (2020). Antioxidant and anti-inflammatory potential of shiitake culinary-medicinal mushroom, lentinus edodes (agaricomycetes), sporophores from various culture conditions. *Int. J. Med. Mushrooms* 22, 535–546. doi:10.1615/IntJMedMushrooms.2020034864

Fattorusso, A., Di Genova, L., Dell'isola, G. B., Mencaroni, E., and Esposito, S. (2019). Autism Spectrum Disorders and the Gut Microbiota, *Nutrients* 11, 521. doi:10.3390/nu11030521

Finegold, S. M., Dowd, S. E., Gontcharova, V., Liu, C., Henley, K. E., Wolcott, R. D., et al. (2010). Pyrosequencing study of fecal microflora of autistic and control children. *Anaerobe* 16, 444–453. doi:10.1016/j.anaerobe.2010.06.008

French, H. M., Reid, M., Mamontov, P., Simmons, R. A., and Grinspan, J. B. (2009). Oxidative stress disrupts oligodendrocyte maturation. *J. Neurosci. Res.* 87, 3076–3087. doi:10.1002/jnr.22139

Graciarena, M., Seiffe, A., Nait-Oumesmar, B., and Depino, A. M. (2018). Hypomyelination and oligodendroglial alterations in a mouse model of autism spectrum disorder. *Front. Cell. Neurosci.* 12, 517. doi:10.3389/fncel.2018.00517

Greenwood, M. T. (2017). Dysbiosis, spleen Qi, phlegm, and complex difficulties. *Med. Acupunct.* 29, 128–137. doi:10.1089/acu.2017.1226

Gudkov, S. V., Shtarkman, I. N., Smirnova, V. S., Chernikov, A. V., and Bruskov, V. I. (2006). Guanosine and inosine display antioxidant activity, protect DNA *in vitro* from oxidative damage induced by reactive oxygen species, and serve as radioprotectors in mice. *Radiat. Res.* 165, 538–545. doi:10.1667/RR3552.1

Hughes, H. K., Rose, D., and Ashwood, P. (2018). The gut microbiota and dysbiosis in autism spectrum disorders. *Curr. Neurol. Neurosci. Rep.* 18, 81. doi:10.1007/s11910-018-0887-6

Kang, D. W., Adams, J. B., Gregory, A. C., Borody, T., Chittick, L., Fasano, A., et al. (2017). Microbiota transfer therapy alters gut ecosystem and improves gastrointestinal and autism symptoms: an open-label study. *Microbiome* 5, 10. doi:10.1186/s40168-016-0225-7

Kim, J. H., Ha, H. C., Lee, M. S., Kang, J. I., Kim, H. S., Lee, S. Y., et al. (2007). Effect of Tremella fuciformis on the neurite outgrowth of PC12h cells and the improvement of memory in rats. *Biol. Pharm. Bull.* 30, 708–714. doi:10.1248/bpb.30.708

Kim, Y. J., Hwang, S. Y., Oh, E. S., Oh, S., and Han, I. O. (2006). IL-1beta, an immediate early protein secreted by activated microglia, induces iNOS/NO in C6 astrocytoma cells through p38 MAPK and NF-kappaB pathways. *J. Neurosci. Res.* 84, 1037–1046. doi:10.1002/jnr.21011

Kozarski, M., Klaus, A., Jakovljevic, D., Todorovic, N., Vunduk, J., Petrovic, P., et al. (2015). Antioxidants of edible mushrooms. *Molecules* 20, 19489–19525. doi:10.3390/molecules201019489

Lee, G. A., Lin, Y. K., Lai, J. H., Lo, Y. C., Yang, Y. S. H., Ye, S. Y., et al. (2021). Maternal immune activation causes social behavior deficits and hypomyelination in male rat offspring with an autism-like microbiota profile. *Brain Sci.* 11, 1085. doi:10.3390/brainsci11081085

Lee, S. E., Ju, E. M., and Kim, J. H. (2002). Antioxidant activity of extracts from Euryale ferox seed. *Exp. Mol. Med.* 34, 100–106. doi:10.1038/emm.2002.15

Li, H., Lee, H. S., Kim, S. H., Moon, B., and Lee, C. (2014). Antioxidant and anti-inflammatory activities of methanol extracts of Tremella fuciformis and its major phenolic acids. *J. Food Sci.* 79, C460–C468. doi:10.1111/1750-3841.12393

Li, W., Chen, M., Feng, X., Song, M., Shao, M., Yang, Y., et al. (2021). Maternal immune activation alters adult behavior, intestinal integrity, gut microbiota and the gut inflammation. *Brain Behav.* 11, e02133. doi:10.1002/brb3.2133

Liu, S., Li, E., Sun, Z., Fu, D., Duan, G., Jiang, M., et al. (2019). Altered gut microbiota and short chain fatty acids in Chinese children with autism spectrum disorder. *Sci. Rep.* 9, 287. doi:10.1038/s41598-018-36430-z

Lu, Y., Guo, S., Zhang, F., Yan, H., Qian, D. W., Wang, H. Q., et al. (2019). Comparison of functional components and antioxidant activity of Lycium barbarum L. Fruits from different regions in China. *Molecules* 24, E2228. doi:10.3390/molecules24122228

Ma, G., Du, H., Hu, Q., Yang, W., Pei, F., and Xiao, H. (2021). Health benefits of edible mushroom polysaccharides and associated gut microbiota regulation. *Crit. Rev. Food Sci. Nutr.*, 1–18. doi:10.1080/10408398.2021.1903385

Maas, D. A., Valles, A., and Martens, G. J. M. (2017). Oxidative stress, prefrontal cortex hypomyelination and cognitive symptoms in schizophrenia. *Transl. Psychiatry* 7, e1171. doi:10.1038/tp.2017.138

Masuko, T., Minami, A., Iwasaki, N., Majima, T., Nishimura, S., and Lee, Y. C. (2005). Carbohydrate analysis by a phenol-sulfuric acid method in microplate format. *Anal. Biochem.* 339, 69–72. doi:10.1016/j.ab.2004.12.001

Matkowski, A., Jamiolkowska-Kozlowska, W., and Nawrot, I. (2013). Chinese medicinal herbs as source of antioxidant compounds--where tradition meets the future. *Curr. Med. Chem.* 20, 984–1004. doi:10.2174/0929867311320080003

Mcmurdie, P. J., and Holmes, S. (2013). phyloseq: an R package for reproducible interactive analysis and graphics of microbiome census data. *PLoS One* 8, e61217. doi:10.1371/journal.pone.0061217

Nguyen, H. T. N., Kato, H., Masuda, K., Yamaza, H., Hirofuji, Y., Sato, H., et al. (2018). Impaired neurite development associated with mitochondrial dysfunction in dopaminergic neurons differentiated from exfoliated deciduous tooth-derived pulp stem cells of children with autism spectrum disorder. *Biochem. Biophys. Rep.* 16, 24–31. doi:10.1016/j.bbrep.2018.09.004

Nie, A., Chao, Y., Zhang, X., Jia, W., Zhou, Z., and Zhu, C. (2020). Phytochemistry and pharmacological activities of Wolfiporia cocos (F.A. Wolf) ryvarden & gilb. *Front. Pharmacol.* 11, 505249. doi:10.3389/fphar.2020.505249

Nitschke, A., Deonandan, R., and Konkle, A. T. (2020). The link between autism spectrum disorder and gut microbiota: A scoping review. *Autism* 24, 1328–1344. doi:10.1177/1362361320913364

Olugbami, J. O., Gbadegesin, M. A., and Odunola, O. A. (2014). *In vitro* evaluation of the antioxidant potential, phenolic and flavonoid contents of the stem bark ethanol extract of Anogeissus leiocarpus. *Afr. J. Med. Med. Sci.* 43, 101–109.

Pang, Y., Campbell, L., Zheng, B., Fan, L., Cai, Z., and Rhodes, P. (2010). Lipopolysaccharide-activated microglia induce death of oligodendrocyte

progenitor cells and impede their development. *Neuroscience* 166, 464–475. doi:10.1016/j.neuroscience.2009.12.040

Pangrazzi, L., Balasco, L., and Bozzi, Y. (2020a). Natural Antioxidants: A Novel Therapeutic Approach to Autism Spectrum Disorders? *Antioxidants (Basel)* 9, 1186. doi:10.3390/antiox9121186

Pangrazzi, L., Balasco, L., and Bozzi, Y. (2020b). Oxidative stress and immune system dysfunction in autism spectrum disorders. *Int. J. Mol. Sci.* 21, E3293. doi:10.3390/ijms21093293

Peralta-Marzal, L. N., Prince, N., Bajic, D., Roussin, L., Naudon, L., Rabot, S., et al. (2021). The impact of gut microbiota-derived metabolites in autism spectrum disorders. *Int. J. Mol. Sci.* 22, 10052. doi:10.3390/ijms221810052

Pi, K., and Lee, K. (2017). Prunus mume extract exerts antioxidant activities and suppressive effect of melanogenesis under the stimulation by alpha-melanocyte stimulating hormone in B16-F10 melanoma cells. *Biosci. Biotechnol. Biochem.* 81, 1883–1890. doi:10.1080/09168451.2017.1365591

Pooler, A. M., Guez, D. H., Benedictus, R., and Wurtman, R. J. (2005). Uridine enhances neurite outgrowth in nerve growth factor-differentiated PC12 [corrected]. *Neuroscience* 134, 207–214. doi:10.1016/j.neuroscience.2005.03.050

Qian, Y., Huang, M., Guan, T., Chen, L., Cao, L., Han, X. J., et al. (2015). Maslinic acid promotes synaptogenesis and axon growth via Akt/GSK-3β activation in cerebral ischemia model. *Eur. J. Pharmacol.* 764, 298–305. doi:10.1016/j.ejphar.2015.07.028

Quast, C., Pruesse, E., Yilmaz, P., Gerken, J., Schweer, T., Yarza, P., et al. (2013). The SILVA ribosomal RNA gene database project: Improved data processing and web-based tools. *Nucleic Acids Res.* 41, D590–D596. doi:10.1093/nar/gks1219

Rajaei, A., Salarbashi, D., Asrari, N., Fazly Bazzaz, B. S., Aboutorabzade, S. M., and Shaddel, R. (2021). Antioxidant, antimicrobial, and cytotoxic activities of extracts from the seed and pulp of Jujube (Ziziphus jujuba) grown in Iran. *Food Sci. Nutr.* 9, 682–691. doi:10.1002/fsn3.2031

Ranogajec, A., Beluhan, S., and Smit, Z. (2010). Analysis of nucleosides and monophosphate nucleotides from mushrooms with reversed-phase HPLC. *J. Sep. Sci.* 33, 1024–1033. doi:10.1002/jssc.200900516

Rezatabar, S., Karimian, A., Rameshknia, V., Parsian, H., Majidinia, M., Kopi, T. A., et al. (2019). RAS/MAPK signaling functions in oxidative stress, DNA damage response and cancer progression. *J. Cell. Physiol.* 234, 14951–14965. doi:10.1002/jcp.28334

Rios, J. L. (2011). Chemical constituents and pharmacological properties of Poria cocos. *Planta Med.* 77, 681–691. doi:10.1055/s-0030-1270823

Rosenfeld, C. S. (2015). Microbiome disturbances and autism spectrum disorders. *Drug Metab. Dispos.* 43, 1557–1571. doi:10.1124/dmd.115.063826

Rousset, C. I., Chalon, S., Cantagrel, S., Bodard, S., Andres, C., Gressens, P., et al. (2006). Maternal exposure to LPS induces hypomyelination in the internal capsule and programmed cell death in the deep gray matter in newborn rats. *Pediatr. Res.* 59, 428–433. doi:10.1203/01.pdr.0000199905.08848.55

Sabaratnam, V., Kah-Hui, W., Naidu, M., and Rosie David, P. (2013). Neuronal health - can culinary and medicinal mushrooms help? *J. Tradit. Complement. Med.* 3, 62–68. doi:10.4103/2225-4110.106549

Schliep, K. P. (2011). phangorn: phylogenetic analysis in R. *Bioinformatics* 27, 592–593. doi:10.1093/bioinformatics/btq706

Segata, N., Izard, J., Waldron, L., Gevers, D., Miropolsky, L., Garrett, W. S., et al. (2011). Metagenomic biomarker discovery and explanation. *Genome Biol.* 12, R60. doi:10.1186/gb-2011-12-6-r60

Simoes, L. R., Sangiogo, G., Tashiro, M. H., Generoso, J. S., Faller, C. J., Dominguini, D., et al. (2018). Maternal immune activation induced by lipopolysaccharide triggers immune response in pregnant mother and fetus, and induces behavioral impairment in adult rats. *J. Psychiatr. Res.* 100, 71–83. doi:10.1016/j.jpsychires.2018.02.007

Svoboda, E. (2020). Could the gut microbiome be linked to autism? *Nature* 577, S14-S15–S15. doi:10.1038/d41586-020-00198-y

Vamanu, E., Dinu, L. D., Pelinescu, D. R., and Gatea, F. (2021). Therapeutic properties of edible mushrooms and herbal teas in gut microbiota modulation. *Microorganisms* 9, 1262. doi:10.3390/microorganisms9061262

Vuong, H. E., and Hsiao, E. Y. (2017). Emerging roles for the gut microbiome in autism spectrum disorder. *Biol. Psychiatry* 81, 411–423. doi:10.1016/j.biopsych.2016.08.024

Wang, X., Wang, Z., Yao, Y., Li, J., Zhang, X., Li, C., et al. (2011). Essential role of ERK activation in neurite outgrowth induced by alpha-lipoic acid. *Biochim. Biophys. Acta* 1813, 827–838. doi:10.1016/j.bbamcr.2011.01.027

Wiatrak, B., Kubis-Kubiak, A., Piwowar, A., and Barg, E. (2020). PC12 cell line: Cell types, coating of culture vessels, differentiation and other culture conditions. *Cells* 9, 958. doi:10.3390/cells9040958

Wischhof, L., Irrsack, E., Osorio, C., and Koch, M. (2015). Prenatal LPS-exposure--a neurodevelopmental rat model of schizophrenia--differentially affects cognitive functions, myelination and parvalbumin expression in male and female offspring. *Prog. Neuropsychopharmacol. Biol. Psychiatry* 57, 17–30. doi:10.1016/j.pnpbp.2014.10.004

Wu, D.-T., Liu, W., Han, Q.-H., Wang, P., Xiang, X.-R., Ding, Y., et al. (2019). Extraction optimization, structural characterization, and antioxidant activities of polysaccharides from Cassia seed (Cassia obtusifolia). *Molecules* 24, 2817. doi:10.3390/molecules24152817

Xu, M., Xu, X., Li, J., and Li, F. (2019). Association between gut microbiota and autism spectrum disorder: A systematic review and meta-analysis. *Front. Psychiatry* 10, 473. doi:10.3389/fpsyt.2019.00473

Xu, X., Yang, J., Ning, Z., and Zhang, X. (2015). Lentinula edodes-derived polysaccharide rejuvenates mice in terms of immune responses and gut microbiota. *Food Funct.* 6, 2653–2663. doi:10.1039/c5fo00689a

Xu, Y., Xie, L., Zhang, Z., Zhang, W., Tang, J., He, X., et al. (2021). Tremella fuciformis polysaccharides inhibited colonic inflammation in dextran sulfate sodium-treated mice via Foxp3+ T cells, gut microbiota, and bacterial metabolites. *Front. Immunol.* 12, 648162. doi:10.3389/fimmu.2021.648162

Yuan, F., Gao, Z., Liu, W., Li, H., Zhang, Y., Feng, Y., et al. (2019). Characterization, antioxidant, anti-aging and organ protective effects of sulfated polysaccharides from Flammulina velutipes. *Molecules* 24, E3517. doi:10.3390/molecules24193517

Yui, K., Imataka, G., Sasaki, H., and Shiroki, R. (2020). The role of lipid peroxidation in individuals with autism spectrum disorders. *Metab. Brain Dis.* 35, 1101–1108. doi:10.1007/s11011-020-00585-4

Zou, Y. T., Zhou, J., Wu, C. Y., Zhang, W., Shen, H., Xu, J. D., et al. (2021). Protective effects of Poria cocos and its components against cisplatin-induced intestinal injury. *J. Ethnopharmacol.* 269, 113722. doi:10.1016/j.jep.2020.113722

frontiers | Frontiers in Pharmacology

TYPE Systematic Review
PUBLISHED 25 August 2022
DOI 10.3389/fphar.2022.976247

OPEN ACCESS

EDITED BY
Ahmad Nazrun Shuid,
MARA University of Technology, Malaysia

REVIEWED BY
Aminu Mohammed,
Ahmadu Bello University, Nigeria
Maizura Mohd Zainudin,
International Islamic University Malaysia, Malaysia
Nurul Alimah Abdul Nasir,
University Teknologi MARA, Malaysia
Ahmad Naqib Shuid,
Universiti Sains Malaysia, Malaysia

*CORRESPONDENCE
Azizah Ugusman,
dr.azizah@ppukm.ukm.edu.my
Adila A. Hamid,
adilahamid@ppukm.ukm.edu.my

SPECIALTY SECTION
This article was submitted to Ethnopharmacology, a section of the journal Frontiers in Pharmacology

RECEIVED 23 June 2022
ACCEPTED 20 July 2022
PUBLISHED 25 August 2022

CITATION
Othman NS, Che Roos NA, Aminuddin A, Murthy JK, A. Hamid A and Ugusman A (2022), Effects of *Piper sarmentosum* Roxb. on hypertension and diabetes mellitus: A systematic review and meta-analysis. *Front. Pharmacol.* 13:976247. doi: 10.3389/fphar.2022.976247

Effects of *Piper sarmentosum* Roxb. on hypertension and diabetes mellitus: A systematic review and meta-analysis

Nur Syakirah Othman[1], Nur Aishah Che Roos[2], Amilia Aminuddin[1], Jaya Kumar Murthy[1], Adila A. Hamid[1]* and Azizah Ugusman[1]*

[1]Department of Physiology, Faculty of Medicine, Universiti Kebangsaan Malaysia, Kuala Lumpur, Malaysia, [2]Faculty of Medicine and Defence Health, National Defence University of Malaysia, Kuala Lumpur, Malaysia

Hypertension and diabetes mellitus are among the most prevalent diseases affecting people from all walks of life. Medicinal herbs have garnered interest as potential agents for the prevention and treatment of diabetes mellitus and hypertension due to their multiple beneficial effects. *Piper sarmentosum* Roxb. (PS) is an edible medicinal plant that has been traditionally used in Asia for treating hypertension and diabetes mellitus. This review is aimed to provide comprehensive information from the literature on the effects of PS on hypertension and diabetes mellitus. A computerized database search was performed on Scopus, PubMed and Web of Science databases with the following set of keywords: Piper sarmentosum AND diabetes mellitus OR diabetic OR diabetes OR hyperglyc*emia OR blood glucose OR HbA1c OR glycated h*emoglobin OR h*emoglobin A1c OR hyperten* OR blood pressure. A total of 47 articles were screened and 14 articles published between the years 1998 until 2021 were included for data extraction, comprising of six articles on antihypertensive and eight articles on antidiabetic effects of PS. These studies consist of two *in vitro* studies and eleven *in vivo* animal studies. Meta-analysis of three studies on hypertension showed that PS versus no treatment significantly lowered the systolic blood pressure with mean difference (MD) −39.84 mmHg (95% confidence interval (CI) −45.05, −34.62; $p < 0.01$), diastolic blood pressure with MD −26.68 mmHg (95% CI −31.48, −21.88; $p < 0.01$), and mean arterial pressure with MD −30.56 mmHg (95% CI −34.49, −26.63; $p < 0.01$). Most of the studies revealed positive effects of PS against hypertension and diabetes mellitus, suggesting the potential of PS as a natural source of antidiabetic and antihypertensive agents.

KEYWORDS

antihypertensive, hypertension, *Piper sarmentosum*, diabetes mellitus, antidiabetic

1 Introduction

Hypertension and diabetes mellitus are among the most common non-communicable diseases and cardiovascular risk factors worldwide. Diabetic patients have a two to three-fold rise in hypertension prevalence compared to non-diabetics (Wan et al., 2018). Hypertension coexists in about 40–60% of type 2 diabetic patients (Tatsumi and Ohkubo, 2017). Hypertension may also precede the onset of diabetes, with more than 50% of adults having both hypertension and diabetes at the time of diagnosis (Nibouche and Biad, 2016). Diabetes mellitus and hypertension often coexist and share common pathways contributing to metabolic syndrome. Metabolic syndrome is associated with a greater risk for cardiovascular diseases (CVD) including heart attack and stroke (Isomaa et al., 2001; Tune et al., 2017).

The development of hypertension in diabetic patients is contributed by multiple factors such as insulin resistance, hyperglycemia, oxidative stress, and inflammation. Insulin resistance leads to the development of hyperinsulinemia. The anti-natriuretic activity of insulin increases sodium and water reabsorption from the renal tubules, leading to volume overload and elevation of blood pressure. Moreover, the body's extracellular fluid volume rises because fluid move from the tissues into the vasculature following hyperglycemia-induced hyperosmolarity (Kawasoe et al., 2017). Hyperinsulinemia also activates the sympathetic nervous system and renin-angiotensin system (RAS), leading to an increase in blood pressure (Ohishi, 2018). Besides, hyperinsulinemia leads to vascular smooth muscle cell proliferation and increased vascular stiffness that predispose to hypertension (Shiny et al., 2016; Tsimihodimos et al., 2018). Furthermore, hyperglycemia triggers oxidative stress and inflammatory processes in the vascular wall that cause endothelial dysfunction, impaired vasodilatation and eventually hypertension (Wong et al., 2013; Oguntibeju, 2019; Sun et al., 2020).

On the other hand, hypertensive patients also have an increased risk of developing diabetes mellitus (Zhang et al., 2020). Hypertension is characterized by endothelial dysfunction, which might link hypertension with diabetes (Emdin et al., 2015). Numerous studies have reported that decreased endothelium-dependent vasodilatation in hypertension leads to decreased capillary recruitment that restricts insulin delivery to the metabolically active, insulin-sensitive muscle tissues (Bonadonna et al., 1998; Serné et al., 1999; Meigs et al., 2004). Besides, the altered endothelial permeability impairs insulin delivery to the interstitial space (Meigs et al., 2004). The interstitial insulin level is a rate-limiting step for insulin effectiveness (Miles et al., 1995).

Hypertension and diabetes mellitus share not only common pathophysiologic pathways but also common complications involving the macro- and microvascular disorders. Macrovascular complications include stroke, coronary artery disease and peripheral vascular disease, while microvascular complications include retinopathy, nephropathy and neuropathy (Yamazaki et al., 2018). Since the development of hypertension in patients with diabetes is marked by a significant risk of macro- and microvascular complications, efforts should be made to delay or ideally prevent the increase in blood pressure. Hence, a therapy that can help with glycemic and blood pressure control will be of significant clinical value.

Piper sarmentosum Roxb. (PS) is a herbaceous plant that is widely cultivated in Southeast Asia, Northeast India and China (Mathew et al., 2004). It is a terrestrial creeping herb that belongs to the family of Piperaceae, with an average height of 20 cm and easily grows in shady areas (Mohd Zainudin et al., 2013). PS leaves are light to dark green in colour (Chaveerach et al., 2006), and the fruits are obovoid in shape and sweet to taste (Figure 1). PS are also known as "Kaduk" or "Sirih duduk" in Malaysia; "Cha plu" in Thailand; "Karuk", "Mengkadak" or "Sirih tanah" in Indonesia; "La lot" in Vietnam; "Phak i leut" in Laos and "Jia ju", "Xi ye qing wei teng" or "Qing ju" in China (Ismail et al., 2018).

Historically, PS has long been used as a culinary plant as well as a traditional medicine to treat hypertension, joint aches (Subramaniam et al., 2003), cough, pleurisy, fever (Farhana Syed Ab Rahman 2016), and indigestion (Hussain et al., 2012). Pharmacologically, PS possesses antiatherosclerosis (Amran et al., 2010; Amran et al., 2011), anticarcinogenic (Zainal Ariffin et al., 2009), anti-inflammatory (Ridtitid et al., 2007; Zakaria et al., 2010), antiplatelet aggregation (Han, 1995), antiangiogenic (Hussain et al., 2015) and antituberculosis (Hussain et al., 2008) effects. PS also protects against glucocorticoid-induced osteoporosis (Mohamad Asri et al., 2016) and paracetamol-induced oxidative liver injury (Nur Azlina et al., 2014). Several studies have reported that PS has a high antioxidative activity (Subramaniam et al., 2003; Hafizah et al., 2010; Ugusman et al., 2010; Mohd Zainudin et al., 2015). Interestingly, PS also has antidiabetic (Peungvicha et al., 1998; Azlina et al., 2009; Luangpirom et al., 2014) and antihypertensive effects (Hussan et al., 2013; Alwi et al., 2018; Fauzy et al., 2019).

Previous studies demonstrated that different parts of PS contain various phytochemical compounds. The methanolic extract of PS leaves contains carotenes, tannin, vitamin C, vitamin E, xanthophylls, and phenolics (Chanwitheesuk et al., 2005), while the roots and stems of PS contain piplartine, langkamide and 3,4,5-trimethoxycinnamic acid (Bokesch et al., 2011). Besides, the aqueous extract of PS leaves contains flavonoids, phenolic and ascorbic acids (Sumazian et al., 2010). Meanwhile, three amides; 3-(3′,4′,5′-trimethoxyphenylpropanoyl) pyrrolidine, 3-(4′-methoxyphenylpropanoyl) pyrrole and N-(3-phenylpropanoyl) pyrrole, and a sterol; β-sitosterol have been successfully isolated from the hexane and ethyl acetate extracts of aerial parts of PS (Atiax et al., 2011).

The aqueous extract of PS leaves up to 2000 mg/kg/day does not cause subacute toxicity effects; hence it is safe for

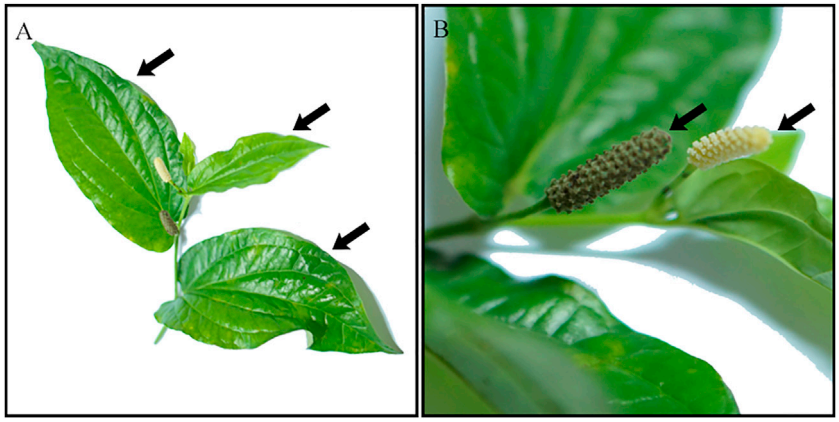

FIGURE 1
Piper sarmentosum Roxb. Leaves **(A)** and fruit **(B)**.

consumption (Mohd Zainudin et al., 2013). Recently, the consumption of herbal products for complementary and alternative medicine has been rapidly increasing. Previous studies have suggested that antioxidants could be beneficial for managing diabetes mellitus and hypertension (Sabadashka et al., 2021; Tain and Hsu 2022). An earlier systematic review has confirmed the antioxidative effect of PS (Ismail et al., 2018). However, no systematic review and meta-analysis have been conducted to explore the effect of PS on hypertension and diabetes. Thus, we aimed to systemically review the available literature on the effects of PS on diabetes mellitus and hypertension to better understand the herb's medicinal potential to support its scientific use further.

2 Methodology

2.1 Search strategy

The review was reported according to the Preferred Reporting Items for Systematic Reviews and Meta-Analyses (PRISMA) guideline. The relevant studies were identified from three main databases: Scopus, PubMed and Web of Science (WoS) from their respective inception dates to March 2022. The last search was performed on 26th March 2022. The following set of keywords was used: Piper sarmentosum AND (diabetes mellitus OR diabetic OR diabetes OR hyperglyc*emia OR blood glucose OR HbA1c OR glycated h*emoglobin OR h*emoglobin A1c OR hyperten* OR blood pressure). Articles that could be missing during the database search were searched from the reference list of the review articles retrieved from the initial search and added to the selected articles list (Thent and Das, 2015). The protocol of this review was registered at the International Platform of Registered Systematic Review and Meta-analysis Protocols (INPLASY registration number: 202240020) (Othman et al., 2022).

2.2 Eligibility and exclusion criteria

Only full-length original research articles published in the English language were included. Any clinical (randomized controlled trial) and preclinical (*in vitro*, *in vivo*, and *ex vivo*) studies that reported the effects of PS on hypertension and diabetes models, regardless of the route of administration, formulation, dose and duration of intervention were included. However, any observational studies and studies using combined preparation of PS with other herbs were excluded. Review articles, news, book chapters, conference proceedings, editorial letters, and case studies were also excluded from this review.

2.3 Study selection and data extraction

The literature search and articles screening were performed according to the population, interventions, compare, outcome and study design (PICOS) framework, as follows:

1) Population (P): Adult patients with established hypertension and/or diabetes and preclinical models of hypertension and diabetes, regardless of animal species, were included.
2) Intervention (I): Studies that used PS as an intervention in the experimental group were included.
3) Comparison (C): The comparator groups received either no intervention or were treated with relevant conventional drug.
4) Outcome (O): Changes in blood pressure, blood glucose or glycosylated hemoglobin ($HbA1_C$).

5) Study design (S): Clinical (randomized controlled trial) and preclinical (*in vitro*, *in vivo*, *ex vivo*) studies.

The articles were primarily screened through the articles' type, language, title and abstracts related to the effect of PS on hypertension and diabetes. Duplicates were removed from each database. The secondary screening involved the removal of articles based on the inclusion and exclusion criteria set for this study. Any similar studies were removed to avoid selection bias. The retrieved articles were reviewed independently by two authors (NO. and AU). Any disagreements were resolved by seeking a third reviewer's opinion (NR).

Study characteristics including study design, animal model used, plant source, the part of plant used, type of extraction and phytochemical used were extracted. Primary outcomes such as systolic blood pressure (SBP), diastolic blood pressure (DBP), mean arterial pressure (MAP), and blood glucose level were extracted. Other parameters such as nitric oxide (NO), endothelial nitric oxide synthase (eNOS), asymmetric dimethylarginine (ADMA), endothelin-1 (ET-1) and malondialdehyde (MDA) levels, α-glucosidase and α-amylase activities, insulin and urine glucose levels, body and organ weights, and histological analysis of the target organs were also extracted where available. For studies with more than one interventional arms, data from only the relevant arms were considered, e.g. hypertensive rats receiving PS versus hypertensive rats receiving positive control or no treatment. In case of missing or incomplete information, the respective author was contacted by email and the missing data were requested if necessary.

2.4 Risk of bias assessment

Two reviewers analyzed the risk of bias independently (NO and AU). Any disagreement was resolved through discussion with the third reviewer (NR). Cochrane risk of bias (RoB) tool was used to assess the risk of bias in randomized clinical trials (Higgins et al., 2019). Meanwhile, animal studies were assessed using the Systematic Review Center for Laboratory Animal Experimentation (SYRCLE) risk of bias tool. The main components of this item were as follows: 1) Selection bias: random sequence generation, baseline characteristics, allocation concealment; 2) Detection bias: random housing, blinding, random outcome assessment; 3) Attrition bias: incomplete outcome data; 4) Reporting bias: selective reporting; and 5) Other bias (Hooijmans et al., 2014). For *in vitro* studies, a customized risk of bias tool based on the Joanna Briggs Institute (JBI) checklist for non-randomized experimental studies were used (JBI, 2020). The customized RoB tool comprises of three domains as follows: 1) Reporting quality: source of plant, amount of plant/extract/sample used; 2) Performance bias: reliable tools and/or reagents used to measure outcome; and 3) Detection bias: standard/appropriate control used, multiple measurements of outcome performed. Each domain was evaluated as being a high, moderate, low or unclear risk of bias.

2.5 Statistical analysis

The meta-analysis was performed using the Review Manager (RevMan) 5.4 software (The Cochrane Collaboration, 2020). The mean difference (MD) together with its 95% confidence intervals (CI) was used in reporting the effect size of PS on blood pressure (BP). The heterogeneity between studies was evaluated using 1) the Chi-squared test with a p-value of less than 0.10 denoted statistical significance and 2) the Higgin's I^2 statistic (Higgins et al., 2003). An I^2 value of less than 25% was regarded as low heterogeneity, 30%–50% was regarded as moderate heterogeneity, and any value above 75% as high heterogeneity. Due to the small number of studies available for meta-analysis, a fixed-effect (FE) model was used. A p-value of less than 0.05 indicated statistical significance. Sensitivity analysis was conducted by only including studies using a similar PS dose (500 mg/kg) for evaluation of result's robustness. No subgroup analysis was performed due to the limited number of studies available for meta-analysis. A funnel plot was not reported as less than ten studies were included in the meta-analysis.

3 Results

3.1 Studies selected

Initially, a total of 76 potential articles were identified in Scopus ($n = 37$), PubMed ($n = 12$) and Web of Science ($n = 27$). An additional article was retrieved from the list of references cited in the review articles ($n = 1$). Subsequently, 30 articles were removed due to duplication. After reviewing the titles and abstracts, 33 articles were excluded. The full text of the remaining 27 articles were read thoroughly and 13 articles were further excluded as they did not fulfil the inclusion criteria. Finally, 14 studies published between the years 1998–2021 were selected for inclusion in this review, comprising of six articles on antihypertensive and eight articles on antidiabetic effects of PS. A flowchart of the article selection process is shown in Figure 2.

3.2 Risk of bias

The risk of bias assessment for the animal studies included in this review is presented in Figure 3. Selection risk and detection of bias was low for all studies. Attrition bias was either low risk

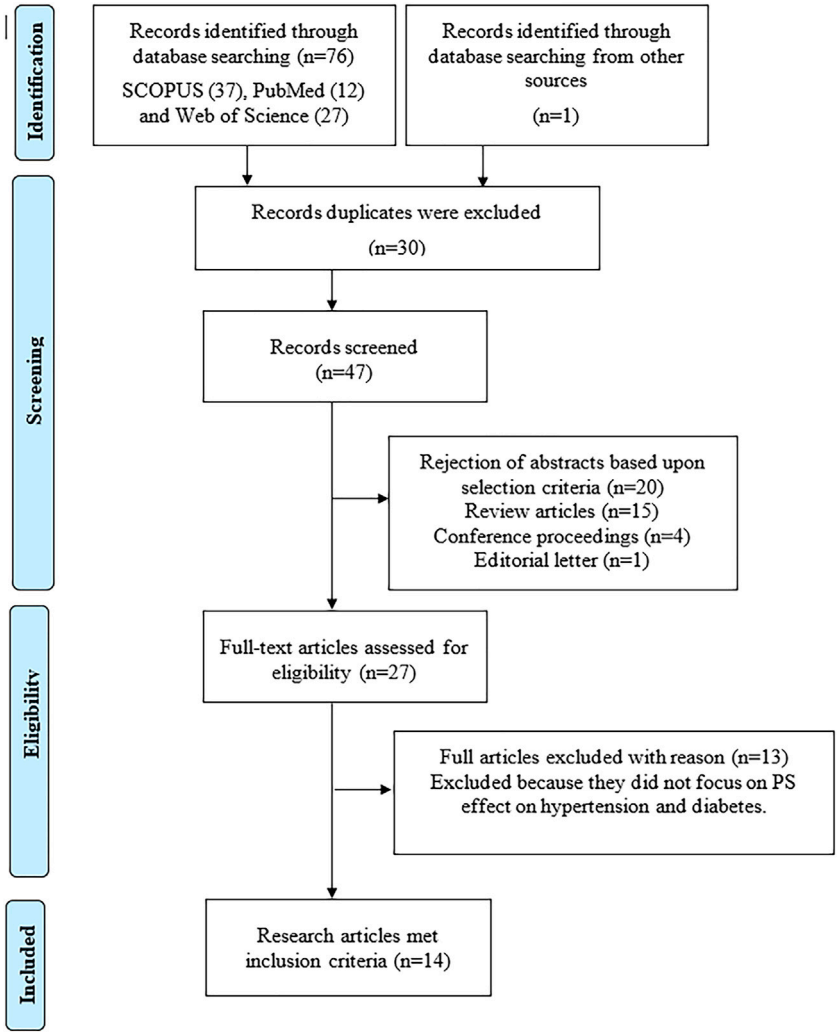

FIGURE 2
The selection process of the articles according to the Preferred Reporting Items for Systematic Reviews and Meta-Analyses (PRISMA) guideline.

(n = 10) or unclear (n = 2) in the included studies. Selection reporting risk of bias was unclear in two of the studies and the remainder (n = 10) was low risk. Other bias was unclear in one of the studies and low for the remainder (n = 11). The JBI critical appraisal checklist summary for reporting *in vitro* studies is shown in Figure 4. Reporting quality bias was low for all studies. Performance and detection bias was either low risk (n = 1) or unclear (n = 1).

3.3 Study design characteristics

The characteristics of the selected studies are described in Tables 1, 2. All the included studies were preclinical studies, with no clinical trial done previously. As for the preclinical studies, 12 studies involved animal models (Peungvicha et al., 1998; Thent et al., 2012a; Thent et al., 2012b; Hussan et al., 2013; Luangpirom et al., 2014; Mohd Zainudin et al., 2015; Thent and Das, 2015; Alwi et al., 2018; Mohd Zainudin et al., 2019; Fauzy et al., 2019; Ugusman et al., 2020; Firdaus Azmi et al., 2021) and the remaining two studies were *in vitro* chemical assay studies (Wongsa et al., 2012; Sallehuddin et al., 2020). For studies related to the effect of PS on hypertension, the animal models of hypertension used were spontaneous hypertensive rats (SHR) (Mohd Zainudin et al., 2015; Fauzy et al., 2019; Mohd Zainudin et al., 2019), dexamethasone-induced hypertensive rats (Ugusman et al., 2020; Firdaus Azmi et al., 2021) and N^{ω}-nitro-L-arginine methyl ester hydrochloride (L-NAME)-induced hypertensive rats (Alwi et al., 2018). Meanwhile, induction of diabetes in all the studies were done through streptozotocin (STZ) injection.

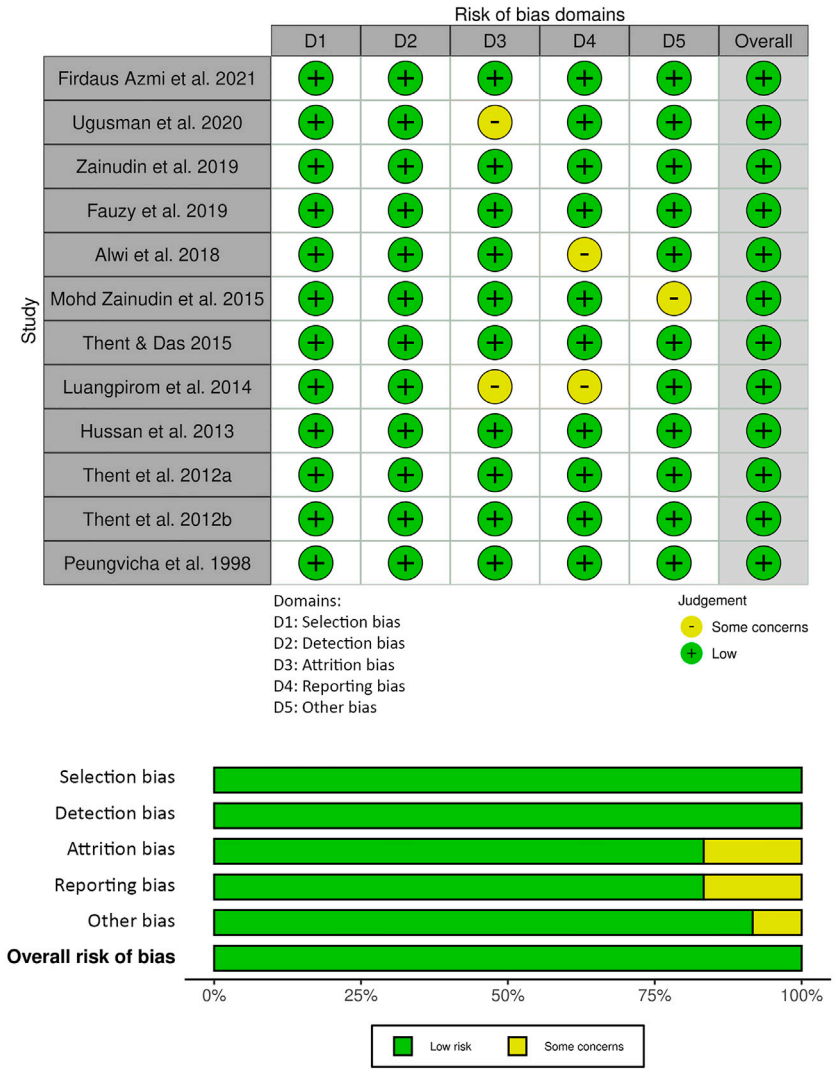

FIGURE 3
Systematic Review Center for Laboratory Animal Experimentation (SYRCLE) risk of bias summary: review authors' judgements about each risk of bias item for each included study.

The quality control and chemical analysis of PS extracts in the selected studies were summarized in Table 3. The origins of PS were from two main countries: Malaysia (Thent et al., 2012a; Thent et al., 2012b; Hussan et al., 2013; Mohd Zainudin et al., 2015; Thent and Das, 2015; Alwi et al., 2018; Fauzy et al., 2019; Mohd Zainudin et al., 2019; Sallehuddin et al., 2020; Ugusman et al., 2020; Firdaus Azmi et al., 2021) and Thailand (Peungvicha et al., 1998; Wongsa et al., 2012; Luangpirom et al., 2014). Most of the studies used the leaves of PS (Thent et al., 2012a, 2012b; Wongsa et al., 2012; Hussan et al., 2013; Luangpirom et al., 2014; Mohd Zainudin et al., 2015; Alwi et al., 2018; Fauzy et al., 2019; Mohd Zainudin et al., 2019; Sallehuddin et al., 2020; Ugusman et al., 2020; Firdaus Azmi et al., 2021) and only one study used all parts of PS (Peungvicha et al., 1998). Different types of PS extract were used, including ethanol extract (Thent and Das 2015; Sallehuddin et al., 2020), aqueous extract (Peungvicha et al., 1998; Thent et al., 2012a; Thent et al., 2012b; Wongsa et al., 2012; Hussan et al., 2013; Luangpirom et al., 2014; Mohd Zainudin et al., 2015; Alwi et al., 2018; Fauzy et al., 2019; Mohd Zainudin et al., 2019; Ugusman et al., 2020; Firdaus Azmi et al., 2021) and methanol-soluble and -insoluble fractions of aqueous extract of PS (Peungvicha et al., 1998). Among the active compounds found in the phytochemical analyses of the PS extracts were rutin, vitexin (Ugusman et al., 2020; Firdaus Azmi et al., 2021), catechin, naringin (Sallehuddin et al., 2020), caffeic acid and p-coumaric acid (Wongsa et al., 2012).

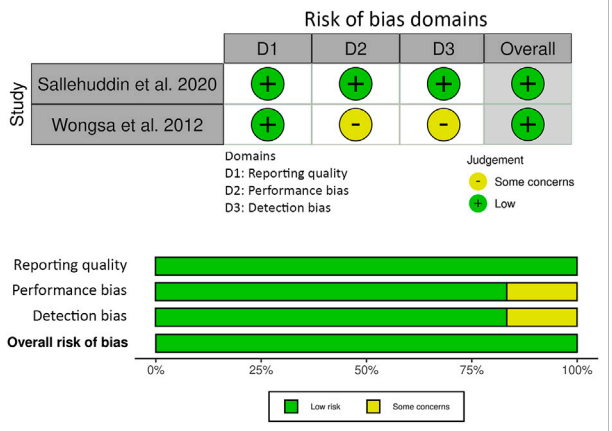

FIGURE 4
The Joanna Briggs Institute (JBI) critical appraisal checklist summary for reporting *in vitro* studies.

3.4 Effect of *Piper sarmentosum* Roxb. on hypertension

There were six *in vivo* animal studies that focused on the effect of PS on hypertension (Mohd Zainudin et al., 2015; Alwi et al., 2018; Fauzy et al., 2019; Mohd Zainudin et al., 2019; Ugusman et al., 2020; Firdaus Azmi et al., 2021). Systolic blood pressure (SBP), diastolic blood pressure (DBP), mean arterial pressure (MAP) and nitric oxide (NO) levels were the most common parameters measured. All six studies showed that treatment with PS caused a marked reduction in the SBP, DBP and MAP of hypertensive rat models. A study by Fauzy et al. (2019) demonstrated that PS increased NO and reduced ET-1 levels in the mesenteric artery of SHR. Mohd Zainudin et al. (2015) showed that PS possessed an antihypertensive effect by reducing MDA and increasing serum NO levels in SHR. These findings were further supported by three other studies which demonstrated that the BP-lowering effect of PS was associated with increased NO levels in L-NAME-induced hypertensive rats (Alwi et al., 2018), dexamethasone-induced hypertensive rats (Ugusman et al., 2020; Firdaus Azmi et al., 2021) and SHR (Mohd Zainudin et al., 2019). Ugusman et al. (2020) found that PS increased vascular NO production by increasing eNOS mRNA expression, eNOS protein and eNOS activity in dexamethasone-induced hypertensive rats. Meanwhile, Mohd Zainudin et al. (2015) demonstrated that PS significantly decreased plasma ADMA levels in SHR. However, none of the studies investigated the effect of PS on target organ damage in hypertension.

3.5 Effect of *Piper sarmentosum* Roxb. on diabetes mellitus

Out of the 14 studies, eight studies assessed the effect of PS on diabetes mellitus. The effects of PS on diabetes were evaluated in two *in vitro* studies (Wongsa et al., 2012; Sallehuddin et al., 2020) and six *in vivo* studies (Peungvicha et al., 1998; Thent et al., 2012a; Thent et al., 2012b; Hussan et al., 2013; Luangpirom et al., 2014; Thent and Das, 2015). The *in vitro* studies involved screening of antidiabetic activity of PS using α-glucosidase and α-amylase inhibition assays. Wongsa et al. (2012) showed that PS had α-glucosidase but not α-amylase inhibitory activity. In contrast, another *in vitro* study revealed that PS had no α-glucosidase inhibitory activity (Sallehuddin et al., 2020). As for *in vivo* study, it was first reported that administration of 0.125 g/kg PS for 7 days significantly decreased blood glucose levels in both normal and diabetic rats (Peungvicha et al., 1998). Subsequently, Thent et al. (2012b) showed that PS increased the body weight and reduced fasting blood glucose and urine glucose levels in STZ-induced diabetic rats. Meanwhile, Luangpirom et al. (2014) found that diabetic rats treated with PS improved pancreatic islet function and increased serum insulin, leading to reduced fasting blood glucose.

3.5.1 *Piper sarmentosum* Roxb.'s effect on diabetic complications/target organ and tissue damage

PS were also beneficial in attenuating the degenerative changes of the target organs in diabetes such as the heart, aorta, kidney, and liver. Light microscopic observation showed that PS reduced the degenerative changes in the myocardium and aortic tissues of diabetic rats as evidenced by lack of connective tissue deposit in the myocardium, reduced tunica media thickness, reduced tunica intima to tunica media ratio and less disruption of elastic fibre in the tunica media layer of the aorta (Thent et al., 2012a). Electron microscopic analysis further supported the findings as PS supplementation restored the ultrastructural integrity of the heart and aorta of diabetic rats (Thent et al., 2012b). As for the liver, PS increased the liver weight and reversed the diabetes-induced degenerative changes in the liver tissues as evidenced by the absence of nuclear deformation in the hepatocytes, less hyperemic areas in the sinusoids and less necrosis and vacuolization in the liver (Thent and Das, 2015). Interestingly, Hussan et al. (2013) demonstrated that PS prevented further progression of diabetic nephropathy in STZ-induced rats as evidenced by less contracted glomeruli, mild inflammatory cells infiltration, reduced urinary space size and absence of glomerular membrane thickening.

3.6 Meta-analysis

Only three studies were included in our meta-analysis, all of which provided data for the pooling of effects of PS on blood pressure parameters. No suitable data on glycemic parameters was available from the included studies, hence no meta-analysis was performed to explore the effects of PS on diabetes. The corresponding author (Luangpirom et al., 2014) was contacted to enquire for more details of the data, but no response was received.

TABLE 1 Characteristics of selected studies on the effects of *Piper sarmentosum* Roxb. on hypertension.

Study design	Plant source	Plant part	Type of extract	Phyto-chemical(s)	Results	Outcomes	References
In vivo animal study. Thirty male Sprague Dawley rats (8 weeks old) were divided into five groups (n = 6) including control (normal saline), PS (500 mg/kg/day orally), dexamethasone (20 μg/kg/day subcutaneously to induce hypertension), dexamethasone + PS and dexamethasone + captopril (40 mg/kg/day orally as positive control). Treatments were administered for 28 days. The systolic blood pressure (SBP), diastolic blood pressure (DBP) and mean arterial pressure (MAP) of the rats were measured using tail-cuff method.	Selangor and Penang, Malaysia	Leaf	Aqueous	Rutin Vitexin	PS decreased SBP at day 14 (132.72 ± 3.07 mmHg vs. 109.28 ± 2.95 mmHg, $p < 0.001$) and day 28 (143.06 ± 3.65 mmHg vs. 105.22 ± 2.89 mmHg, $p < 0.001$), DBP at day 14 (105.28 ± 2.58 mmHg vs. 86.56 ± 5.31 mmHg, $p < 0.05$) and day 28 (104.61 ± 2.32 mmHg vs. 82.83 ± 3.49 mmHg, $p < 0.001$), and MAP at day 14 (114.43 ± 2.3 mmHg vs. 94.13 ± 4.41 mmHg, $p < 0.05$) and day 28 (117.43 ± 2.06 mmHg vs. 90.30 ± 2.53 mmHg, $p < 0.001$) and these effects were comparable to captopril.	PS extract quantified to rutin and vitexin has antihypertensive effect.	Firdaus Azmi et al. (2021)
In vivo animal study. Thirty male Sprague Dawley rats (8–12 weeks) were divided into five groups (n = 6) including control (normal saline), PS (500 mg/kg/day orally), dexamethasone (20 μg/kg/day subcutaneously to induce hypertension), dexamethasone + PS and dexamethasone + captopril (40 mg/kg/day orally as positive control). Treatments were administered for 28 days. The SBP, DBP and MAP of the rats were measured using tail-cuff method. The rat's thoracic aorta was analyzed for endothelial nitric oxide synthase (eNOS) mRNA expression, protein and activity while the serum was analyzed for nitric oxide (NO) level.	Penang, Malaysia	Leaf	Aqueous	Rutin Vitexin	- PS decreased SBP at day 14 (136 ± 2.0 mmHg vs. 111 ± 2.8 mmHg, $p < 0.001$) and day 28 (146 ± 2.7 mmHg vs. 107 ± 2.9 mmHg, $p < 0.001$), DBP at day 14 (105 ± 2.5 mmHg vs. 82 ± 5.1 mmHg, $p < 0.01$) and day 28 (104 ± 3.1 mmHg vs. 79 ± 1.7 mmHg, $p < 0.01$), and MAP at day 14 (114.43 ± 2.2 mmHg vs. 92 ± 3.7 mmHg, $p < 0.001$) and day 28 (118 ± 2.5 mmHg vs. 88 ± 1.4 mmHg, $p < 0.001$) and these effects were comparable to captopril. - Treatment of dexamethasone-induced hypertensive rats with PS increased the NO level (31.0 ± 5.18 μM vs. 56.8 ± 6.22 μM, $p < 0.05$), eNOS mRNA expression by 1.4 folds ($p < 0.01$), eNOS protein (10.17 ± 1.54 pg/mg protein vs. 40.17 ± 9.51 pg/mg protein, $p < 0.01$), and eNOS activity (1.1 ± 0.073 μM nitrite/min/mg protein vs. 1.4 ± 0.109 μM nitrite/min/mg protein, $p < 0.05$).	PS demonstrates antihypertensive effect by enhancing eNOS activity and production of NO.	Ugusman et al. (2020)
In vivo animal study. Twenty-four spontaneous hypertensive rats (SHR) were divided into four groups (n = 6) including hypertensive control (distilled water), PS (500 mg/kg/day), perindopril (3 mg/kg/day), and combined PS (500 mg/kg/day) + perindopril (1.5 mg/kg/day).	Kuantan, Pahang, Malaysia	Leaf	Aqueous		- PS decreased SBP ($p < 0.05$) and DBP ($p < 0.05$) of SHR. The reduction in DBP was greater than SBP ($p < 0.05$). However, PS was not as potent as perindopril in reducing blood pressure. - There was a reduction in plasma ADMA level ($p < 0.05$) and an increase in	PS reduces blood pressure by increasing the clearance of ADMA and production of NO.	Mohd Zainudin et al. (2019)

(Continued on following page)

TABLE 1 (*Continued*) Characteristics of selected studies on the effects of *Piper sarmentosum* Roxb. on hypertension.

Study design	Plant source	Plant part	Type of extract	Phyto-chemical(s)	Results	Outcomes	References
All treatments were given orally for 28 days. SBP and DBP were measured using tail-cuff method. Serum NO and plasma asymmetric dimethylarginine (ADMA) levels were also determined.					serum NO level ($p < 0.05$) in SHR following PS treatment.		
In vivo animal study. Twenty-four SHR (11 weeks) were divided into four groups ($n = 6$): hypertension control (distilled water), PS (500 mg/kg/day), perindopril (3 mg/kg/day), and combined PS (500 mg/kg/day) + perindopril (1.5 mg/kg/day). All treatments were given orally for 28 days. SBP, DBP and MAP were measured using tail-cuff method. Rats mesenteric arteries were analyzed for NO and endothelin-1 (ET-1) levels.	Kuantan, Pahang, Malaysia	Leaf	Aqueous		- SHR showed reductions in SBP ($p < 0.05$), DBP ($p < 0.05$) and MAP ($p < 0.05$) with PS treatment. However, PS showed no superior effect in reducing blood pressure compared to perindopril. - PS increased mesenteric artery NO level ($p < 0.05$) and reduced ET-1 level ($p < 0.05$) in SHR.	PS decreases blood pressure by reducing ET-1 level and increasing NO level in the resistance artery.	Fauzy et al. (2019)
In vivo animal study. Thirty-six Wistar rats (6–8 weeks) were divided into six groups ($n = 6$): control (normal saline), PS (500 mg/kg/day), L-NAME (100 mg/L) to induce hypertension) and three groups of combined L-NAME and different doses of PS (125, 250 and 500 mg/kg/day). Treatments were administered orally for 4 weeks. SBP, DBP and MAP were measured using tail-cuff method. Serum NO and malondialdehyde (MDA) levels were quantitated.	Selayang, Selangor, Malaysia	Leaf	Aqueous		- Treatment with three doses of PS (125, 250 and 500 mg/kg/day) lowered the SBP (172.3 ± 5.06 mmHg vs. 126.0 ± 5.2, 127.83 ± 3.79 and 129.67 ± 3.74 mmHg, $p < 0.001$), DBP (127.5 ± 3.93 mmHg vs. 84.5 ± 4.38, 90.0 ± 2.44, and 86.3 ± 4.19 mmHg, $p < 0.05$), and MAP (142.0 ± 4.49 mmHg vs. 97.0 ± 3.44, 101.2 ± 1.86 and 100.5 ± 2.71 mmHg, $p < 0.05$). - There were decreased serum MDA (65.59 ± 5.46 nmol/g protein vs. 22.70 ± 3.63, 16.57 ± 4.64, and 25.15 ± 11.39 nmol/g protein, $p < 0.001$) and increased serum NO level (4.5 ± 1.92 μM vs. 56.33 ± 9.15, 80.88 ± 8.55 μM, and 75.02 ± 8.46 μM, $p < 0.001$).	Antihypertensive effect of PS is mediated by increased NO and reduced oxidative stress.	Alwi et al. (2018)
In vivo animal study. Six normotensive Wistar rats served as negative control group, while thirty-two SHR (10 weeks) were divided into four groups (n = 6 for positive control, n = 8 for three treatment groups): hypertensive control, and SHR treated with three different doses of PS (0.5, 1, 2 mg/kg/day) orally for 28 days. The blood pressure, serum NO, MDA and total cholesterol levels were measured.	Kuantan, Pahang, Malaysia	Leaf	Aqueous		- PS reduced SBP ($p < 0.05$), DBP ($p < 0.05$) and MAP ($p < 0.05$). - PS increased serum NO ($p < 0.05$) and decreased MDA ($p < 0.05$) levels.	PS attenuates hypertension by increasing NO level and decreasing oxidative stress.	Mohd Zainudin et al. (2015)

ADMA, plasma asymmetric dimethylarginine; eNOS, endothelial nitric oxide synthase; ET, Endothelin-1; DBP, diastolic blood pressure; MAP, mean arterial pressure; L-NAME, N^{ω}-nitro-L-arginine methyl ester hydrochloride; MDA , malondialdehyde; NO, nitric oxide; PS, *Piper sarmentosum* Roxb.; SBP, systolic blood pressure; SHR, spontaneous hypertensive rats.

TABLE 2 Characteristics of selected studies on the effects of *Piper sarmentosum* Roxb. on diabetes mellitus.

Study design	Plant source	Plant parts	Type of extract	Phyto-chemical(s)	Results	Outcomes	References
In vitro study. Antidiabetic activity was measured using α-glucosidase inhibitory activity.	Selangor, Malaysia	Leaf	Ethanol	Catechin. Naringin	PS at 1,000 μg/ml did not inhibit α-glucosidase activity.	PS has no antidiabetic activity.	Sallehuddin et al. (2020)
In vitro study. Antidiabetic activity was evaluated by α-glucosidase and α-amylase inhibitory activity.	Chiangrai province, Thailand	Leaf	Aqueous	Caffeic acid p-Coumaric acid.	PS showed α-glucosidase inhibitory activity but did not show inhibition against α -amylase activity.	PS has antidiabetic effect by inhibiting α-glucosidase activity.	Wongsa et al. (2012)
In vivo animal study. Twenty-four male, Sprague Dawley rats were divided into four groups (n = 6) including non-diabetic control, non-diabetic treated with PS (0.125 g/kg/day), untreated diabetic (induced with single intramuscular injection of 50 mg/kg STZ) and diabetic treated with PS (0.125 g/kg/day). Treatment with PS was started 4 weeks after STZ injection, for a total of 28 days via intragastric tube. SBP was measured using tail-cuff method. The rat's liver was collected for morphological analysis.	Negeri Sembilan, Malaysia	Leaf	Aqueous		-PS decreased the SBP of streptozotocin-induced diabetic rats ($p < 0.05$). -Compared to untreated diabetic rats, treatment with PS increased the liver weight (6.03 ± 0.39 g vs. 10.23 ± 0.27 g, $p < 0.05$) and reversed the diabetes-induced degenerative changes in the liver tissues as evidenced by absence of nuclear deformation in the of hepatocytes, less hyperemic areas in the sinusoids and less necrosis and vacuolization in the liver.	PS has a positive effect on diabetes and its complications.	Thent and Das (2015)
In vivo animal study. Fifty adult male mice (ICR strain, 8-week-old) were randomly divided into five groups (n = 6 for References group and n = 11 for diabetic groups) including non-diabetic control, untreated diabetic (induced with intraperitoneal injection of 6 mg/100 g BW STZ), diabetic treated with glibenclamide (1 mg/100 g BW/day orally as positive control), diabetic treated with PS_1 (60 mg/100 g BW/day orally) and diabetic treated with PS_2 (100 mg/100 g BW). Treatments were administered for 21 days. Fasting blood glucose (FBG) level was measured by glucometer via blood from the tail artery. Plasma was analysed for insulin levels. Pancreas was also assessed histologically.	Khon Kaen Province, Thailand	Leaf	Aqueous		Compared with untreated diabetic rats, diabetic rats treated with PS had: - Greater change in FBG (+46.01% vs. -32.75%). - Higher insulin level (14.19 ± 2.95 IU/L vs. 21.36 ± 2.53 IU/L, $p < 0.05$). - Increase in size and decrease in number of dead cells in the pancreatic islets. - PS was as potent as glibenclamide in increasing insulin level.	PS has hypoglycemic activities by increasing insulin secretion and improving pancreatic islet function.	Luangpirom et al. (2014)
In vivo animal study. Eighteen male Sprague Dawley rats were randomly	Selangor, Malaysia	Leaf	Aqueous		- PS did not have significant effect on the body weight, kidney	Antihyperglycemic activity of PS prevents	Hussan et al. (2013)

(Continued on following page)

TABLE 2 (*Continued*) Characteristics of selected studies on the effects of *Piper sarmentosum* Roxb. on diabetes mellitus.

Study design	Plant source	Plant parts	Type of extract	Phyto-chemical(s)	Results	Outcomes	References
divided into three groups (n = 6) including nondiabetic control, untreated diabetic (induced with single intramuscular injection of 50 mg/kg STZ) and diabetic treated with PS (0.125 g/kg/day orally). Treatment with PS was started 10 days following STZ induction and continued for 28 days. Body weight and kidney weight index were recorded. FBG was measured using glucometer from the tail vein. Kidneys were collected for histomorphometric and histological analysis.					weight index and FBG of diabetic rats. - PS attenuated the histological changes in the diabetic rat's kidney as evidenced by less contracted glomeruli, mild inflammatory cells infiltration, reduced urinary space size and absence of glomerular membrane thickening.	further progression of diabetic nephropathy.	
In vivo animal study. Twenty-four male Sprague Dawley rats were randomly divided into four groups (n = 6) including nondiabetic control (normal saline), nondiabetic treated with PS (0.125 g/kg/day orally), untreated diabetic (induced with single intramuscular injection of 50 mg/kg STZ) and diabetic treated with PS (0.125 g/kg/day orally). Treatments were administered for 28 days. The rat's cardiac and aortic tissues were collected for histological analysis.	Negeri Sembilan, Malaysia	Leaf	Aqueous		Treatment of diabetic mice with PS caused less degenerative changes in the myocardium and aortic tissues as evidenced by lack of connective tissue deposit in the myocardium, reduced tunica media thickness, reduced tunica intima to tunica media ratio and less disruption of elastic fibre in the tunica media layer of the aorta.	PS has beneficial effect on diabetes by reducing degenerative changes in the myocardium and aorta.	Thent et al. (2012a)
In vivo animal study Thirty-two male Sprague Dawley rats were randomly divided into four groups (n = 8) including nondiabetic control (normal saline), nondiabetic treated with PS (0.125 g/kg/day orally), untreated diabetic (induced with single intramuscular injection of 50 mg/kg STZ) and diabetic treated with PS (0.125 g/kg/day orally). Treatments were started 28 days following diabetes induction for 28 days continuously. The body weight was recorded. Urine and blood glucose levels were measured by Combur test and glucometer, respectively. The rat's left ventricular cardiac tissue and proximal aorta were analyzed under the electron microscope.	Negeri Sembilan, Malaysia	Leaf	Aqueous		Compared to untreated diabetic rats, PS supplementation to diabetic rats caused: - Higher body weight (178 ± 10.91 g vs. 231 ± 13.52 g, $p < 0.05$). - Lower FBG level (31.9 ± 1.72 mmol/L vs. 23.2 ± 2.24 mmol/L, $p < 0.05$). - Lower urine glucose level. - Less irregular arrays of myofibrils within the cardiac sarcomere. - Less disrupted cardiac muscle fibres. - Intact cardiac mitochondria with reduced mitochondrial size and cytoplasmic spaces. - Less disruption of the elastic lamina, decreased proliferation of smooth muscle cells and presence of the endothelial cells in the proximal aorta.	PS has antidiabetic effect and restores ultrastructural integrity of the diabetic cardiovascular tissues.	Thent et al. (2012b)

(Continued on following page)

TABLE 2 (*Continued*) Characteristics of selected studies on the effects of *Piper sarmentosum* Roxb. on diabetes mellitus.

Study design	Plant source	Plant parts	Type of extract	Phyto-chemical(s)	Results	Outcomes	References
In vivo animal study. Male Wistar rats (5 weeks old) were divided into five groups (n = 6–8) including nondiabetic control, untreated diabetic (induced with single intraperitoneal injection of 75 mg/kg STZ), diabetic treated with glibenclamide (5 mg/kg orally), diabetic treated with PS_1 (0.125 g/kg orally) and diabetic treated with PS_2 (0.250 g/kg orally). Treatments were administered for 7 days. Fasting plasma glucose level and oral glucose tolerance test (OGTT) were determined.	Bangkok, Thailand	Whole plant	Aqueous, methanol soluble fraction and methanol insoluble fraction of aqueous extract.		- Single dose of PS did not reduce the blood glucose but repeated administration of 0.125 g/kg PS for 7 days produced significant decrease in the plasma glucose of diabetic rats. - Hypoglycemic effect of the methanol soluble fraction of PS aqueous extract was more potent than the aqueous extract.	PS has hypoglycemic effect.	Peungvicha et al. (1998)

FBG, fasting blood glucose; OGTT, oral glucose tolerance test; PS, *Piper sarmentosum* Roxb.; SBP, systolic blood pressure; STZ, streptozotocin.

TABLE 3 Quality control and chemical analysis of *Piper sarmentosum* Roxb. extracts in the selected studies.

Study	Source	Concentration (%)	Quality control reported? (Yes/No)	Chemical analysis reported? (Yes/No)
Firdaus Azmi et al. (2021)	Selangor and Penang, Malaysia	10	Yes- Standardization based on active compounds	Yes-UPLC
Ugusman et al. (2020)	Penang, Malaysia	10	Yes-Standardization based on active compounds	Yes-HPLC
Mohd Zainudin et al. (2019)	Kuantan, Pahang, Malaysia	10	Yes-FRAP and DPPH radical scavenging assays	Yes-HPLC
Fauzy et al. (2019)	Kuantan, Pahang, Malaysia	10	No	No
Alwi et al. (2018)	Selayang, Selangor, Malaysia	10	Yes-Protocol citation	No
Mohd Zainudin et al. (2015)	Kuantan, Pahang, Malaysia	10	Yes- DPPH radical and superoxide scavenging assays	No
Sallehuddin et al. (2020)	Selangor, Malaysia	10	Yes- DPPH radical scavenging assay	Yes-HPLC
Wongsa et al. (2012)	Chiangrai province, Thailand	5	Yes- TPC, DPPH radical scavenging and antioxidant protection factor assays	Yes-HPLC
Thent and Das (2015)	Negeri Sembilan, Malaysia	5	Yes-Protocol citation	No
Luangpirom et al. (2014)	Khon Kaen Province, Thailand	20	Yes-Protocol citation	No
Hussan et al. (2013)	Selangor, Malaysia	10	Yes-Protocol citation	No
Thent et al. (2012a)	Negeri Sembilan, Malaysia	5	Yes-Protocol citation	No
Thent et al. (2012b)	Negeri Sembilan, Malaysia	5	Yes-Protocol citation	No
Peungvicha et al. (1998)	Bangkok, Thailand	30	No	No

DPPH, 2,2-diphenyl-1-picrylhydrazyl, FRAP, Ferric-reducing antioxidant power activity; HPLC, high performance liquid chromatography; UPLC, ultra performance liquid chromatography; TPC, total phenolic content.

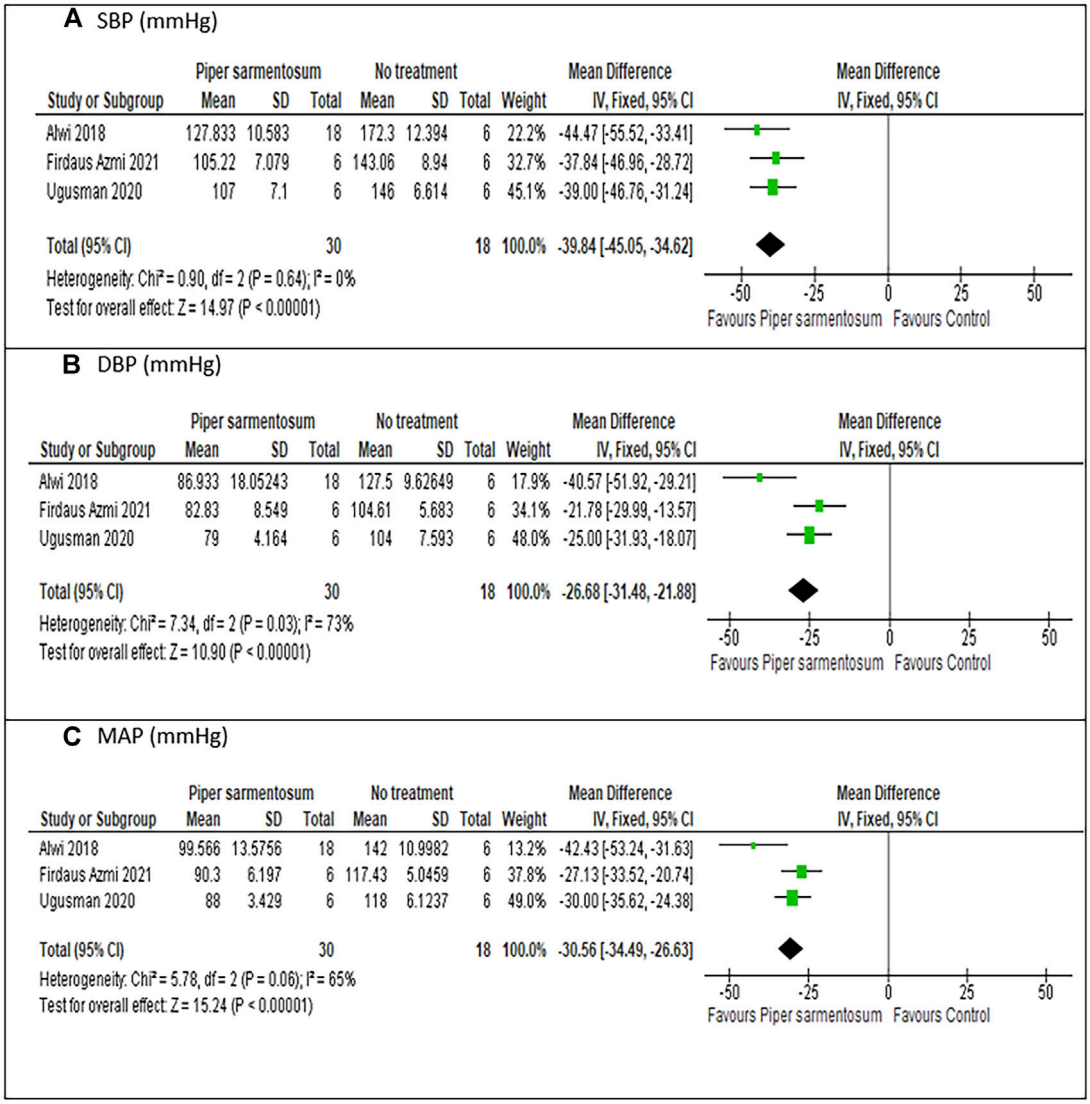

FIGURE 5
Meta-analysis of the effects of *Piper sarmentosum* Roxb. versus control on blood pressure: **(A)** SBP, Systolic blood pressure; **(B)** DBP, diastolic blood pressure, **(C)** MAP, mean arterial pressure.

3.6.1 Effects of *Piper sarmentosum* Roxb. versus no treatment on hypertension

Meta-analysis of three studies (Alwi et al., 2018; Ugusman et al., 2020; Firdaus Azmi et al., 2021) on the effect of PS versus no treatment have shown a statistically significant reduction in SBP with MD −39.84 mmHg (95% CI −45.05, −34.62; $p < 0.01$; Figure 5A) and no heterogeneity was observed. Similarly, pooling of results from three studies have shown that treatment with PS significantly reduced DBP and MAP with MD values of −26.68 mmHg (95% CI −31.48, −21.88; $p < 0.01$; Figure 5B), and -30.56 mmHg (95% CI −34.49, − 26.63; $p < 0.01$; Figure 5C) respectively, albeit the heterogeneity observed were substantial. A sensitivity analysis was performed to assess the robustness of PS effect on BP parameters. When limited to PS dose of 500 mg/kg, a comparable pooled effect size, direction, magnitude and statistical significance were obtained with MD −39.28 mmHg (95% CI −44.61, −33.95; $p < 0.01$; Figure 6A), −26.84 mmHg (95% CI −31.63, −22.05; $p < 0.01$; Figure 6B) and −29.74 mmHg (95% CI −33.82, −25.66; $p < 0.01$; Figure 6C) for SBP, DBP, and MAP respectively.

3.6.2 Effects of *Piper sarmentosum* Roxb. versus positive control on hypertension

Meta-analysis of three studies (Alwi et al., 2018; Ugusman et al., 2020; Firdaus Azmi et al., 2021) on the effect of PS versus captopril, a positive control, indicated no significant difference in SBP (MD = 2.20 mmHg, 95% CI −3.75, 8.15; $p = 0.47$; Figure 7A), DBP (MD =

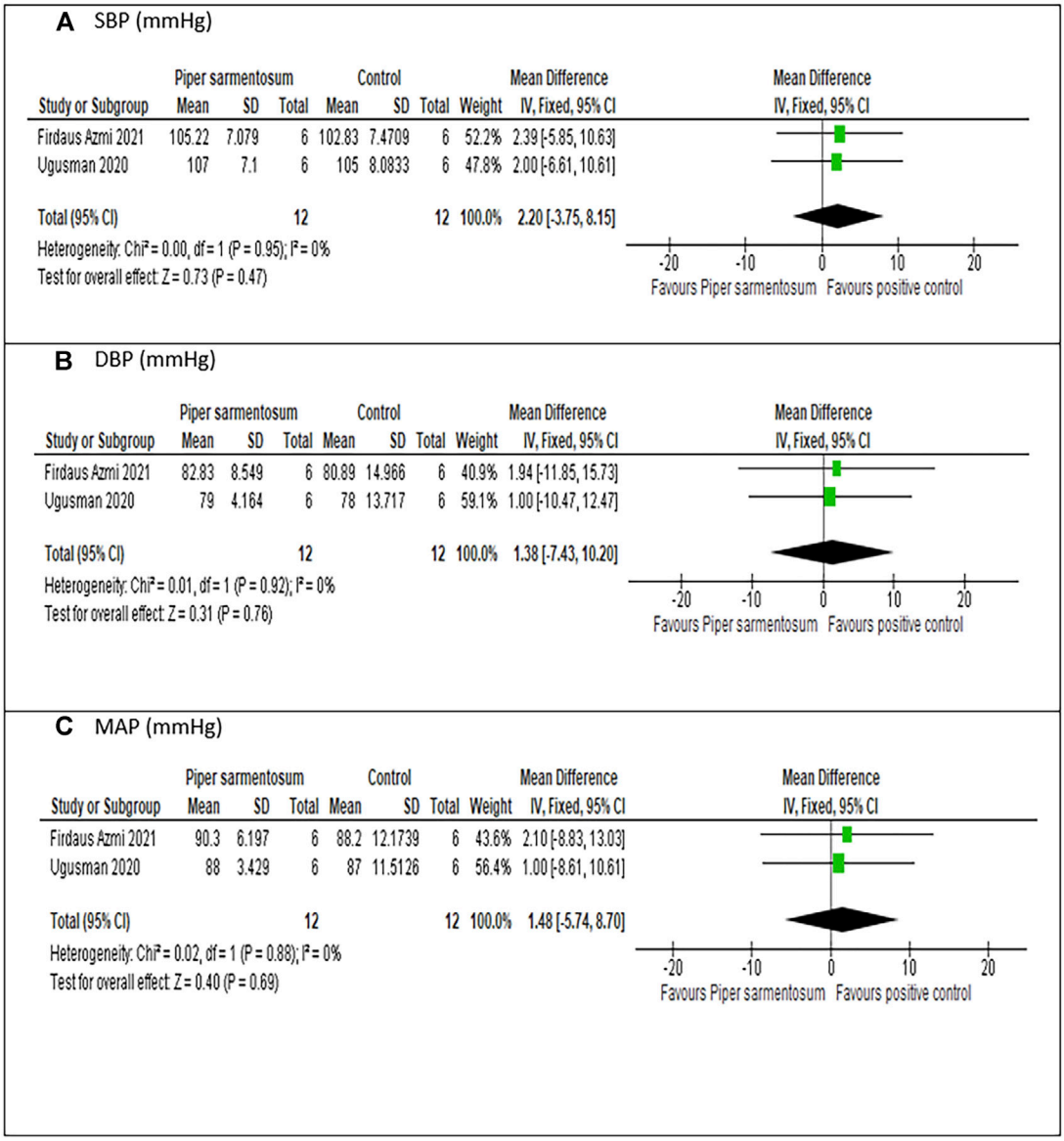

FIGURE 6
Meta-analysis of the effects of *Piper sarmentosum* Roxb. versus positive control on blood pressure: **(A)** SBP, Systolic blood pressure; **(B)** DBP, diastolic blood pressure, **(C)** MAP, mean arterial pressure.

1.38 mmHg, 95% CI −7.43, 10.20; p = 0.76; Figure 7B) and MAP (MD = 1.48 mmHg, 95% CI −5.74, 8.70; p = 0.69; Figure 7C). No heterogeneity was observed.

4 Discussion

The present systematic review and meta-analysis suggests that PS has beneficial effects on BP and glycemic control in hypertensive and diabetic animal models.

4.1 Effects of *Piper sarmentosum* Roxb. on hypertension

PS has demonstrated its antihypertensive effect in various hypertensive animal models including SHR (Mohd Zainudin et al., 2015; Fauzy et al., 2019; Mohd Zainudin et al., 2019), dexamethasone-induced hypertensive rats (Ugusman et al., 2020; Firdaus Azmi et al., 2021) and L-NAME-induced hypertensive rats (Alwi et al., 2018). Our meta-analysis has shown that PS supplementation resulted in significantly reduced SBP, DBP, and

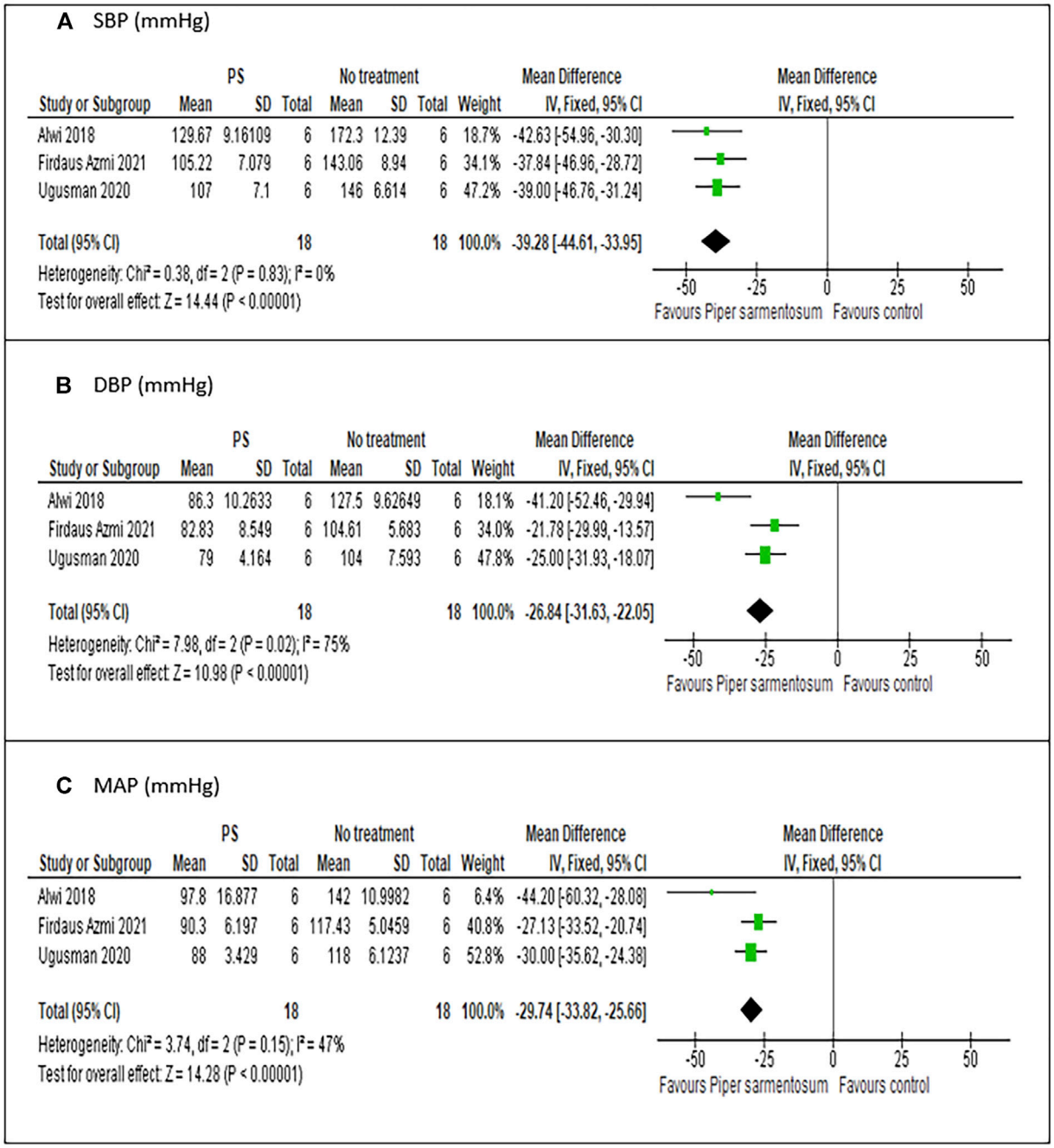

FIGURE 7
Sensitivity analysis of the effects of 500 mg/kg *Piper sarmentosum* Roxb. versus control on blood pressure: **(A)** SBP, Systolic blood pressure; **(B)** DBP, diastolic blood pressure, **(C)** MAP, mean arterial pressure.

MAP by 39.84, 26.688, and 30.56 mmHg, respectively, in hypertensive rat models. The significant reduction is only observed when the groups of hypertensive animals receiving PS were compared to hypertensive rats that do not receive any intervention. No significant difference was observed in BP parameters when the groups of hypertensive animals receiving PS were compared to the groups of animals receiving positive control. A positive control is used in the included studies to control for variability of the experiments as well as for unbiased and objective observation of the effects of studied intervention on BP (Torday and Baluška, 2019). Although the mechanism involved may be different, the analysis has shown evidence

that PS has similar effects, if not equal, to captopril in reducing BP parameters.

SHR exhibits many features of human essential hypertension, including increased blood pressure and total peripheral resistance. These features are preceded by oxidative stress, which leads to endothelial dysfunction (Fauzy et al., 2019). MDA, a lipid peroxidation product, is a marker of oxidative stress damage. PS administration to SHR caused a significant reduction in MDA level (Mohd Zainudin et al., 2015), suggesting that the antihypertensive effect of PS was attributed to its antioxidative activity. A previous study also demonstrated that PS reduced oxidative stress by decreasing MDA in endothelial cells (Hafizah et al., 2010). Interestingly, another study showed that PS enhanced the expression of the antioxidant enzymes; superoxide dismutase (SOD), catalase (CAT) and glutathione peroxidase in hydrogen peroxide-induced endothelial cells (Ugusman et al., 2011).

A healthy endothelium releases a plethora of vasoactive factors that contribute to maintaining vascular homeostasis. Endothelial vasoactive mediators such as NO and ET-1 can either decrease or increase the vascular tone, respectively. The imbalance between endothelium-derived vasodilators and vasoconstrictors leads to endothelial dysfunction, which is a precursor of hypertension (Rubanyi, 1993). Endothelial dysfunction occurs when there is reduced NO synthesis, decreased NO bioavailability, or NO antagonism by endothelium-derived vasoconstrictors such as ET-1 (Mordi et al., 2016). The majority of vascular NO is synthesized by eNOS. Meanwhile, decreased bioavailability of NO can be attributed to reactive oxygen species (ROS) that converts NO to peroxynitrite (Mordi et al., 2016).

Dexamethasone-induced hypertensive rats showed reduced eNOS mRNA expression, protein, activity, and serum NO level (Ugusman et al., 2020). Several studies have reported that dexamethasone results in overproduction of ROS that decreases NO bioavailability, which in turn leads to hypertension (de Gennaro Colonna et al., 2002; Rojas et al., 2006; Dubey et al., 2017). Dexamethasone also increases the level of angiotensin-converting enzyme, which is responsible for increasing blood pressure (Fishel et al., 1995). Meanwhile, chronic blockade of NO synthesis by L-NAME is a well-known model of experimental hypertension. It is well established that administration of L-NAME inhibits NO synthesis, causes endothelial dysfunction and vasoconstriction, and thus leads to hypertension (Alwi et al., 2018).

Supplementation of PS successfully reduced the blood pressure of dexamethasone-induced and L-NAME-induced hypertensive rats. This could be attributed to the positive effect of PS on NO production (Alwi et al., 2018; Ugusman et al., 2020; Firdaus Azmi et al., 2021). PS treatment in dexamethasone-induced hypertensive rats increased the eNOS mRNA level, protein level and activity and NO level (Ugusman et al., 2020). Upregulation of eNOS mRNA expression causes more eNOS protein to be synthesized, leading to increased eNOS activity and NO generation. These findings were congruent with a previous study whereby PS increased NO production in hydrogen peroxide-induced endothelial cells by increasing eNOS mRNA expression, protein level and activity (Ugusman et al., 2010). Owing to the antioxidative activity of PS, PS may increase the bioavailability of NO (Mohd Zainudin et al., 2019), as an antioxidant protects NO from the breakdown by ROS (d'Unienville et al., 2021). In SHR, oral administration of a potent antioxidant, lazaroid, improves NO bioavailability and reduces blood pressure (Sorriento et al., 2018).

Competitive inhibitor of eNOS such as ADMA lowers NO synthesis (Hsu and Tain, 2021). Decreased NO also gives rise to unabated ET-1 actions that contribute to vasoconstriction, thereby increasing blood pressure (Böger and Ron, 2005). SHR showed increased ADMA level, which was attenuated by PS supplementation (Mohd Zainudin et al., 2019). Decreased ADMA level is associated with its effective degradation by dimethylarginine dimethylaminohydrolase (DDAH). A previous study reported that PS stimulated DDAH activity in tumor necrosis factor-α-induced endothelial cells, which in turn reduced ADMA level and enhanced NO production (Sundar et al., 2019). Apart from stimulating NO production, PS also reduced ET-1 level in the mesenteric artery of SHR (Fauzy et al., 2019). This observation indicates that PS possesses an anti-vasoconstrictor effect, which contributes to its antihypertensive action.

Even though all the studies reviewed showed positive effects of PS on hypertension, all the studies are animal studies with no clinical trials performed on hypertensive patients. Besides, none of the studies investigated the effect of PS on the renin-angiotensin system, which is an important system that regulates blood pressure. Only two studies on the effect of PS on hypertension that identified the active compounds present in their PS extracts, in which the extracts contain rutin and vitexin (Ugusman et al., 2020; Firdaus Azmi et al., 2021). Oral administration of rutin lowers the blood pressure of L-NAME-induced hypertensive rats (Ganga Raju et al., 2019). Other studies involving phytochemical analysis of PS showed that PS also contains piperine, myricetin and quercetin (Firdaus Azmi et al., 2021). Piperine reduces the blood pressure of L-NAME-induced hypertensive rats (Kumar et al., 2010). Myricetin has also been reported to lower the blood pressure of deoxycorticosterone acetate-salt-hypertensive rats (Borde et al., 2011), whereas quercetin lowers the blood pressure of SHR (Galindo et al., 2012).

4.2 Effects of *Piper sarmentosum* Roxb. on diabetes mellitus

Hyperglycemia is the hallmark of diabetes secondary to either insufficient insulin secretion, resistance to the action of insulin, or both. Induction of diabetes in laboratory animals using chemical ablation of pancreatic β-cells is the most common experimental model. Alloxan and STZ are the most popular

diabetogenic chemicals in diabetes research. However, STZ has notable advantages over alloxan due to its rapid onset, the long half-life, low toxicity and cost-effectiveness (Wszola et al., 2021). STZ is a toxic glucose analogue that is preferentially accumulated in the pancreatic β-cells via the GLUT2 glucose transporters in the plasma membrane.

Following its uptake into beta-cells, STZ triggers oxidative stress, eventually causing the pancreatic β-cells to undergo necrotic cell death, resulting in hypoinsulinemia and hyperglycemia (Choudhari et al., 2017). Additionally, GLUT2 transporters are not only expressed in pancreatic β-cells, but also in the epithelial cells of the kidneys and hepatocytes (Sędzikowska and Szablewski, 2021; Yang et al., 2022). Thus, administration of STZ may result in nephro- and hepatotoxicity along with its potential to damage pancreatic β-cells (Wszola et al., 2021). All six animal studies that investigated the effects of PS on diabetes used a single, high dose of STZ injection (up to 75 mg/kg) to induce pancreatic β-cells damage and diabetes in rats, which mimics type 1 diabetes. None of the studies incorporates the rodent models of type 2 diabetes with underlying insulin resistance, obesity and pancreatic dysfunction, such as the Zucker diabetic fatty rat and db/db mouse (Schwarzer, 2016).

PS supplementation reduced the fasting blood glucose levels (Peungvicha et al., 1998) and urine glucose levels (Thent et al., 2012b) of STZ-induced diabetic rats. One of the mechanisms of the glucose-lowering effect of PS is through improved pancreatic islet function and increased serum insulin (Luangpirom et al., 2014). However, in one study, PS did not cause any significant reduction in the diabetic rats' fasting blood glucose levels (Hussan et al., 2013). The authors only used fasting blood glucose to measure the rats' glycemic status without other supporting tests such as the oral glucose tolerance test and HbA1c, thus making the glycemic status assessment less accurate (Bur et al., 2003). Besides, a reduction in body weight was observed in rats following diabetes induction with STZ (Thent et al., 2012b; Hussan et al., 2013). In response to hypoinsulinemia, the body starts burning fat and muscle for energy, causing a reduction in overall body weight (Eleazu et al., 2013). However, the body weights of the diabetic rats were restored with PS supplementation (Thent et al., 2012b). Since PS has been shown to improve pancreatic islet function and increase serum insulin (Thent et al., 2012b; Luangpirom et al., 2014), this might contribute to the improved body weight of the diabetic rats.

PS also exhibits an α-glucosidase inhibitory effect, but not an α-amylase inhibitory effect (Wongsa et al., 2012). In contrast, another *in vitro* study showed that PS did not possess any α-glucosidase inhibitory effect (Sallehuddin et al., 2020). Alpha-glucosidase and α-amylase inhibitory effects are commonly used to screen the antidiabetic action of natural products (Kittiwisut et al., 2021). Alpha-glucosidase inhibitors act by inhibiting the enzyme α-glucosidase, such as glucoamylase, sucrase, maltase, and isomaltase at the brush border of the intestinal epithelium. This action will block the absorption of carbohydrates in the small intestine, hence reducing postprandial hyperglycemia (Malunga et al., 2016). Meanwhile, α-amylase inhibitors prevent the hydrolysis of α-(1–4)-d-glucosidic linkages in starch, thus reducing carbohydrate digestion and absorption in the gastrointestinal tract and lowering blood glucose (Gong et al., 2020). Most plant-based natural products were effective against either α-amylase or α-glucosidase, with just a few exceptions being effective against both enzymes (Poovitha and Parani, 2016). Besides, α-amylase or α-glucosidase inhibitory assays serve as screening tools for the extract's antidiabetic activity, in which the results should be further supported by *in vivo* study findings.

Among the target organs of diabetic complications are the kidney, liver, heart and blood vessels (Wei et al., 2022). PS has been proven to attenuate the damaging effects of diabetes in the kidney, liver, heart and aorta (Thent et al., 2012a; Thent et al., 2012b; Hussan et al., 2013; Thent and Das 2015). Significant alterations in the liver weight, histology and oxidative stress markers are linked to STZ-induced diabetes (Rodríguez et al., 2018; Yazdi et al., 2019). Treatment with PS also increased the liver weight and reversed diabetes-induced degenerative changes in the liver tissues; an effect attributed to its antioxidative action (Thent and Das, 2015). Inflammation in response to intermittent or chronic hyperglycemia is involved in the initiation and progression of diabetic nephropathy (Amorim et al., 2019; Donate-Correa et al., 2021). Diabetic rats have increased kidney weight due to renal hypertrophy, with histological changes of diabetic nephropathy such as contracted glomeruli with widened urinary spaces, marked inflammatory cell infiltration in the renal cortex and medulla, and glomerular membrane thickening (Hussan et al., 2013). Even though treatment with PS did not change the kidney weight, it attenuated the histological changes in the diabetic rat's kidney as evidenced by less contracted glomeruli, mild inflammatory cells infiltration, reduced urinary space size and absence of glomerular membrane thickening. This could be due to the anti-inflammatory effect of PS (Hussan et al., 2013). Furthermore, PS supplementation reduced the degenerative changes and restored the ultrastructural integrity of the heart and aorta of diabetic rats under light and electron microscopic analyses (Thent et al., 2012a; Thent et al., 2012b). Overall, PS attenuates the complications of diabetes in the kidney, liver, heart and blood vessels through its antioxidative, anti-inflammatory and glucose-lowering effects.

Even though most of the studies reviewed showed positive effects of PS on diabetes, all studies are preclinical studies with no clinical trials performed on diabetic patients. Besides, none of the studies used type 2 diabetes model, which is more common in the society. Only two studies on the effect of PS on diabetes that identified the active compounds present in their PS extracts, in which the extracts contain catechin, naringin (Sallehuddin et al., 2020), caffeic acid and p-coumaric acid (Wongsa et al., 2012). Treatment with catechin lowers blood glucose levels and increases the activity of antioxidant enzymes such as SOD, CAT and glutathione-S-transferase in diabetic rats (Gong et al., 2020). In another study, naringin administration decreased the plasma glucose of diabetic rats as measured

using OGTT (Ahmed et al., 2012). Caffeic acid reduces fasting blood glucose when given to alloxan-induced diabetic rats (Oršolić et al., 2021), whereas p-coumaric acid improves glycemic status and increases plasma insulin level in STZ-induced diabetic rats (Amalan and Vijayakumar, 2015).

4.3 Strength and limitation of the study

To the best of our knowledge, this is the first systematic review and meta-analysis investigating the effects of PS on hypertension and diabetes. The systematic literature search ensures all relevant articles were identified whilst at the same time minimizes selection bias. In addition, the meta-analyses performed enables objective evaluation of the effect of PS on BP parameters. However, the current review is not without its limitation. The small number of included studies may have influenced the effect estimates generated in our meta-analysis. Therefore, interpretation of results should be made with caution. Moreover, the various approach used in reporting the results did not allow us to objectively report the effect of PS on glycemic control. Nevertheless, most of the studies reported uniform effects of PS on diabetes mellitus.

5 Conclusion

Overall, PS showed promising antihypertensive and antidiabetic effects. However, all the studies reviewed are preclinical studies with no randomized clinical trials conducted to investigate the antihypertensive and antidiabetic effects of PS in human subjects. Therefore, further clinical studies are recommended to validate the antihypertensive and antidiabetic activities of PS to prepare evidence-based formulations.

Data availability statement

The original contributions presented in the study are included in the article/Supplementary Material, further inquiries can be directed to the corresponding authors.

Author contributions

AU, JM, AA, and AAH. contributed to conception and design; AU, NR, and NO contributed to data acquisition; AU, NC, and NO were involved in analysis, interpretation and drafting the manuscript; AU, NC, JM, AA, and AAH revise the manuscript critically for important intellectual content. The version to be published has received final approval from all authors.

Funding

This study was funded by Faculty of Medicine, Universiti Kebangsaan Malaysia (Grant code: FF-2020-042) and Ministry of Higher Education Malaysia Fundamental Research Grant Scheme (FRGS/1/2019/SKK08/UKM/02/8).

Acknowledgments

We would like to thank Associate Prof. Dr. Siti Fatimah Ibrahim for her technical assistance.

Conflict of interest

The authors declare that the research was conducted in the absence of any commercial or financial relationships that could be construed as a potential conflict of interest.

Publisher's note

References

Ahmed, O. M., Mahmoud, A. M., Abdel-Moneim, A., and Ashour, M. B. (2012). Antidiabetic effects of hesperidin and naringin in type 2 diabetic rats. *Diabetol. Croat.* 41 (2), 53–67.

Alwi, N. A. N. M., Zakaria, Z., Karim, A. A. H., Nordin, N. A. M. M., and Ugusman, A. (2018). Antihypertensive effect of *Piper sarmentosum* in L-NAME-induced hypertensive rats. *Sains Malays.* 47 (10), 2421–2428. doi:10.17576/jsm-2018-4710-18

Amalan, V., and Vijayakumar, N. (2015). Antihyperglycemic effect of P-coumaric acid on streptozotocin induced diabetic rats. *Indian J. Appl. Res.* 5 (1), 1–4.

Amorim, R. G., Guedes, G. D. S., Vasconcelos, S. M. D. L., and Santos, J. C. D. F. (2019). Kidney disease in diabetes mellitus: cross-linking between hyperglycemia, redox imbalance and inflammation. *Arq. Bras. Cardiol.* 112 (5), 577–587. doi:10.5935/abc.20190077

Amran, A. A., Zakaria, Z., Othman, F., Das, S., Raj, S., and Nordin, N. A. M. M. (2010). Aqueous extract of *Piper sarmentosum* decreases atherosclerotic lesions in high cholesterolemic experimental rabbits. *Lipids Health Dis.* 9 (44), 44–46. doi:10.1186/1476-511X-9-44

Amran, A. A., Zakaria, Z., Othman, F., Das, S., Al-Mekhlafi, H. M., and Nordin, N. A. M. (2011). Changes in the vascular cell adhesion molecule-1, intercellular adhesion molecule-1 and C-reactive protein following administration of aqueous extract of *Piper sarmentosum* on experimental rabbits fed with cholesterol diet. *Lipids Health Dis.* 10 (2), 2–8. doi:10.1186/1476-511X-10-2

Atiax, E., Ahmad, F., Sirat, H. M., and Arbain, D. (2011). Antibacterial activity and cytotoxicity screening of sumatran kaduk (*Piper sarmentosum* Roxb). *Iran. J. Pharmacol. Ther.* 10 (1), 1–5.

Azlina, A. A., Farihah, S., Qodriyah, M. S., and Nur Azlina, M. F. (2009). Effects of *Piper sarmentosum* (kaduk) water extract on adiponectin and blood glucose levels in ovariectomy-induced obese rats. *Res. J. Med. Plant* 3 (3), 109–115. doi:10.3923/rjmp.2009.109.115

Böger, R. H., and Ron, E. S. (2005). L-Arginine improves vascular function by overcoming deleterious effects of ADMA, a novel cardiovascular risk factor. *Altern. Med. Rev.* 10 (1), 14–23.

Bokesch, H. R., Gardella, R. S., Rabe, D. C., Bottaro, D. P., Linehan, W. M., McMahon, J. B., et al. (2011). A new hypoxia inducible factor-2 inhibitory pyrrolinone alkaloid from roots and stems of *Piper sarmentosum*. *Chem. Pharm. Bull.* 59 (9), 1178–1179. doi:10.1248/cpb.59.1178

Bonadonna, R. C., Saccomani, M. P., del Prato, S., Bonora, E., DeFronzo, R. A., and Cobelli, C. (1998). Role of tissue-specific blood flow and tissue recruitment in insulin- mediated glucose uptake of human skeletal muscle. *Circulation* 98, 234–241. doi:10.1161/01.cir.98.3.234

Borde, P., Mohan, M., and Kasture, S. (2011). Effect of myricetin on deoxycorticosterone acetate (DOCA)-salt-hypertensive rats. *Nat. Prod. Res.* 25 (16), 1549–1559. doi:10.1080/14786410903335190

Bur, A., Herkner, H., Woisetschläger, C., Vlcek, M., Derhaschnig, U., and Hirschl, M. M. (2003). Is fasting blood glucose a reliable parameter for screening for diabetes in hypertension? *Am. J. Hypertens.* 16 (4), 297–301. doi:10.1016/S0895-7061(02)03273-9

Chanwitheesuk, A., Teerawutgulrag, A., and Rakariyatham, N. (2005). Screening of antioxidant activity and antioxidant compounds of some edible plants of Thailand. *Food Chem.* 92 (3), 491–497. doi:10.1016/j.foodchem.2004.07.035

Chaveerach, A., Mokkamul, P., Sudmoon, R., and Tanee, T. (2006). Ethnobotany of the genus piper (Piperaceae) in Thailand. *Ethnobot. Res. App.* 4, 223–231. doi:10.17348/era.4.0.223-231

Choudhari, V. P., Gore, K. P., and Pawar, A. T. (2017). Antidiabetic, antihyperlipidemic activities and herb-drug interaction of a polyherbal formulation in streptozotocin induced diabetic rats. *J. Ayurveda Integr. Med.* 8 (4), 218–225. doi:10.1016/j.jaim.2016.11.002

d'Unienville, N. M. A., Blake, H. T., Coates, A. M., Hill, A. M., Nelson, M. J., and Buckley, J. D. (2021). Effect of food sources of nitrate, polyphenols, L-arginine and L-citrulline on endurance exercise performance: a systematic review and meta-analysis of randomised controlled trials. *J. Int. Soc. Sports Nutr.* 18 (76), 76–28. doi:10.1186/s12970-021-00472-y

de Gennaro Colonna, V., Rossoni, G., Rigamonti, A. E., Bonomo, S., Manfredi, B., Berti, F., et al. (2002). Enalapril and quinapril improve endothelial vasodilator function and aortic eNOS gene expression in L-NAME-treated rats. *Eur. J. Pharmacol.* 450 (1), 61–66. doi:10.1016/S0014-2999(02)02046-0

Donate-Correa, J., Ferri, C. M., Sánchez-Quintana, F., Pérez-Castro, A., González-Luis, A., Martín-Núñez, E., et al. (2021). Inflammatory cytokines in diabetic kidney disease: pathophysiologic and therapeutic implications. *Front. Med.* 22 (7), 628289–9. doi:10.3389/fmed.2020.628289

Dubey, H., Singh, A., Patole, A. M., and Tenpe, C. R. (2017). Antihypertensive effect of allicin in dexamethasone-induced hypertensive rats. *Integr. Med. Res.* 6 (1), 60–65. doi:10.1016/j.imr.2016.12.002

Eleazu, C. O., Iroaganachi, M., Okafor, P. N., Ijeh, I. I., and Eleazu, K. C. (2013). Ameliorative potentials of ginger (Z. Officinale roscoe) on relative organ weights in streptozotocin induced diabetic rats. *Int. J. Biomed. Sci.* 9 (2), 82–90.

Emdin, C. A., Anderson, S. G., Woodward, M., and Rahimi, K. (2015). Usual blood pressure and risk of new-onset diabetes evidence from 4.1 million adults and a meta-analysis of prospective studies. *J. Am. Coll. Cardiol.* 66 (14), 1552–1562. doi:10.1016/j.jacc.2015.07.059

Farhana Syed Ab Rahman, S. (2016). *Piper sarmentosum* Roxb: a mini review of ethnobotany, phytochemistry and Pharmacology. *J. Anal. Pharm. Res.* 2 (5), 12–14. doi:10.15406/japlr.2016.02.00031

Fauzy, F. H., Zainudin, M. M., Ismawi, H. R., and Elshami, T. F. T. (2019). *Piper sarmentosum* leaves aqueous extract attenuates vascular endothelial dysfunction in spontaneously hypertensive rats. *Evid. Based Complement. Altern. Med.*, 2019, 7198592–7198598. doi:10.1155/2019/7198592

Firdaus Azmi, M., Aminuddin, A., Azdina Jamal, J., Hamid, A. A., and Ugusman, A. (2021). Quantified *Piper sarmentosum* Roxb. Leaves aqueous leaf extract and its antihypertensive effect in dexamethasone-induced hypertensive rats. *Sains Malays.* 50 (1), 171–179. doi:10.17576/jsm-2021-5001-17

Fishel, R. S., Eisenberg, S., Shai, S. Y., Redden, R. A., Bernstein, K. E., and Berk, B. C. (1995). Glucocorticoids induce angiotensin-converting enzyme expression in vascular smooth muscle. *Hypertension* 25 (3), 343–349. doi:10.1161/01.HYP.25.3.343

Galindo, P., Rodriguez-Gómez, I., González-Manzano, S., Dueñas, M., Jiménez, R., Menéndez, C., et al. (2012). Glucuronidated quercetin lowers blood pressure in spontaneously hypertensive rats via deconjugation. *PLoS ONE* 7 (3), e32673–8. doi:10.1371/journal.pone.0032673

Ganga Raju, M., Prem Prasad, G., and Suvarchala Reddy, N. (2019). Antihypertensive effect of rutin: pharmacological and computational approach. *Asian J. Pharm. Clin. Res.* 12 (8), 87–92. doi:10.22159/ajpcr.2019.v12i18.34118

Gong, L., Feng, D., Wang, T., Ren, Y., Liu, Y., and Wang, J. (2020). Inhibitors of α-amylase and α-glucosidase: potential linkage for whole cereal foods on prevention of hyperglycemia. *Food Sci. Nutr.* 8 (12), 6320–6337. doi:10.1002/fsn3.1987

Hafizah, A. H., Zaiton, Z., Zulkhairi, A., Mohd Ilham, A., Nor Anita, M. M. N., and Zaleha, A. M. (2010). *Piper sarmentosum* as an antioxidant on oxidative stress in human umbilical vein endothelial cells induced by hydrogen peroxide. *J. Zhejiang Univ. Sci. B* 11 (5), 357–365. doi:10.1631/jzus.B0900397

Han, G. (1995). PAF receptor antagonistic principles from Chinese traditional drugs. *Prog. Nat. Sci.* 5, 299–306.

Higgins, J. P. T., Thompson, S. G., Deeks, J. J., and Altman, D. G. (2003). Measuring inconsistency in meta-analyses. *BMJ* 327 (7414), 557–560. doi:10.1136/bmj.327.7414.557

Higgins, J., Savović, J., Page, M. J., and Sterne, J. A. C. (2019). RoB 2: A revised Cochrane risk-of-bias tool for randomized trials - cribsheet. BMJ. Available at: https://methods.cochrane.org/bias/resources/rob-2-revised-cochrane-risk-bias-tool-randomized-trials (Accessed May 10, 2020).

Hooijmans, C. R., Rovers, M. M., de Vries, R. B. M., Leenaars, M., Ritskes-Hoitinga, M., and Langendam, M. W. (2014). SYRCLE's risk of bias tool for animal studies. *BMC Med. Res. Methodol.* 14 (1), 43–49. doi:10.1186/1471-2288-14-43

Hsu, C. N., and Tain, Y. L. (2021). Asymmetric dimethylarginine (ADMA) in pediatric renal diseases: from pathophysiological phenomenon to clinical biomarker and beyond. *Children* 8 (10), 837–914. doi:10.3390/children8100837

Hussain, K., Ismail, Z., Sadikun, A., and Ibrahim, P. (2008). Analysis of proteins, polysaccharides, glycosaponins contents of *Piper sarmentosum* Roxb and anti-TB evaluation for bio-enhancing/interaction effects of leaf extracts with isoniazid (INH). *Nat. Prod. Radiance* 7 (5), 402–408.

Hussain, K., Hashmi, F. K., Latif, A., Ismail, Z., and Sadikun, A. (2012). A review of the literature and latest advances in research of *Piper sarmentosum*. *Pharm. Biol.* 50 (8), 1045–1052. doi:10.3109/13880209.2011.654229

Hussain, K., Ismail, Z., Sadikun, A., Ibrahim, P., and Malik, A. (2015). In vitro antiangiogenesis activity of standardized extracts of *Piper sarmentosum* Roxb. *J. Ris. Kim.* 1 (2), 146–150. doi:10.25077/jrk.v1i2.50

Hussan, F., Bt Mat Zin, N. N., Zullkefli, M. R., Choon, Y. S., Bt Abdullah, N. A., and Lin, T. S. (2013). *Piper sarmentosum* water extract attenuates diabetic complications in streptozotocin induced sprague-dawley rats. *Sains Malays* 42 (11), 1605–1612.

Ismail, S. M., Hui, C. K., Aminuddin, A., and Ugusman, A. (2018). *Piper sarmentosum* as an antioxidant: a systematic review. *Sains Malays.* 47 (10), 2359–2368. doi:10.17576/jsm-2018-4710-12

Isomaa, B., Almgren, P., Tuomi, T., Forsén, B., Lahti, K., Nissén, M., et al. (2001). Cardiovascular morbidity and mortality associated with the metabolic syndrome. *Diabetes Care* 2424 (4), 683683–689689. doi:10.2337/diacare.24.4.683

JBI (2020). Critical appraisal tools. Joanna Briggs Institute (JBI). Available at: https://jbi.global/critical-appraisal-tools (Accessed March 15, 2022).

Kawasoe, S., Maruguchi, Y., Kajiya, S., Uenomachi, H., Miyata, M., Kawasoe, M., et al. (2017). Mechanism of the blood pressure-lowering effect of sodium-glucose cotransporter 2 inhibitors in obese patients with type 2 diabetes. *BMC Pharmacol. Toxicol.* 18 (1), 23–10. doi:10.1186/s40360-017-0125-x

Kittiwisut, S., Amnuoypol, S., Pathompak, P., and Setharaksa, S. (2021). α-Glucosidase and α-amylase inhibitory effects with anti-oxidative activity of tetracera loureiri (finet & gagnep.) pierre ex craib leaf extracts. *Pharm. Sci. Asia* 48 (2), 175–184. doi:10.29090/psa.2021.02.19.125

Kumar, S., Saravana Kumar, M., and Raja, B. (2010). Efficacy of piperine, an alkaloidal constituent of pepper on nitric oxide, antioxidants and lipid peroxidation markers in L-NAME induced hypertensive rats. *Int. J. Res. Pharm. Sci.* 1 (3), 300–307. doi:10.1002/cbf.1331

Luangpirom, A., Kourchampa, W., and Somsapt, P. (2014). Evaluation of hypoglycemic properties and fertility effect of *Piper sarmentosum* Roxb. Aqueous leaf extract in streptozotocin induced diabetic mice. *Int. J. Phytomedicine* 6 (3). doi:10.5138/ijpm.v6i3.1496

Malunga, L. N., Eck, P., and Beta, T. (2016). Inhibition of intestinal α -glucosidase and glucose absorption by feruloylated arabinoxylan mono- and oligosaccharides from corn bran and wheat aleurone. *J. Nutr. Metab.* 21, 1932532–1932539. doi:10.1155/2016/1932532

Mathew, S. P., Mohandas, A., and Nair, G. M. (2004). *Piper sarmentosum* Roxb - an addition to the flora of andaman islands. *Curr. Sci.* 41, 147–156.

Meigs, J. B., Hu, F. B., Rifai, N., and Manson, J. A. E. (2004). Biomarkers of endothelial dysfunction and risk of type 2 diabetes mellitus. *J. Am. Med. Assoc.* 291 (16), 1978–1986. doi:10.1001/jama.291.16.1978

Miles, P. D. G., Levisetti, M., Reichart, D., Khoursheed, M., Moossa, A. R., and Olefsky, J. M. (1995). Kinetics of insulin action in vivo: identification of rate-limiting steps. *Diabetes* 44 (8), 947–953. doi:10.2337/diab.44.8.947

Mohamad Asri, S. F., Mohd Ramli, E. S., Soelaiman, I. N., Mat Noh, M. A., Abdul Rashid, A. H., and Suhaimi, F. (2016). *Piper sarmentosum* effects on 11β-hydroxysteroid dehydrogenase type 1 enzyme in serum and bone in rat model of glucocorticoid-induced osteoporosis. *Molecules* 21 (11), 15233–E1610. doi:10.3390/molecules21111523

Mohd Zainudin, M., Zakaria, Z., Megat Mohd Nordin, N. A., and Othman, F. (2013). Does oral ingestion of *Piper sarmentosum* cause toxicity in experimental animals? *Evid. Based Complement. Altern. Med.* 2013, 705950–705959. doi:10.1155/2013/705950

Mohd Zainudin, M., Zakaria, Z., and Megat Mohd Nordin, N. A. (2015). The use of *Piper sarmentosum* leaves aqueous extract (Kadukmy™) as antihypertensive agent in spontaneous hypertensive rats. *BMC Complement. Altern. Med.* 15 (54), 54–10. doi:10.1186/s12906-015-0565-z

Mohd Zainudin, M., Hashim Fauzy, F., Razak Tariq, A., Elshami, T., Zainudin, M. M., Tft, E., et al. (2019). Factors regulating nitric oxide production in spontaneously hypertensive rats treated with *Piper sarmentosum* aqueous extract. *IMJM* 18 (3), 1–7. doi:10.31436/imjm.v18i3.199

Mordi, I., Mordi, N., Delles, C., and Tzemos, N. (2016). Endothelial dysfunction in human essential hypertension. *J. Hypertens.* 34 (8), 1464–1472. doi:10.1097/HJH.0000000000000965

Nibouche, W. N., and Biad, A. (2016). Arterial hypertension at the time of diagnosis of type 2 diabetes in adults. *Ann. Cardiol. Angeiol.* 65 (3), 152–158. doi:10.1016/j.ancard.2016.04.017

Nur Azlina, M. F., Qodriyah, H. M. S., Hamizah, A. H., and Kamisah, Y. (2014). Kesan ekstrak metanol *Piper sarmentosum* terhadap kecederaan oksidatif hepar tikus aruhan parasetamol. *Sains Malays* 43 (3), 415–421.

Oguntibeju, O. O. (2019). Type 2 diabetes mellitus, oxidative stress and inflammation: examining the links. *Int. J. Physiol. Pathophysiol. Pharmacol.* 11 (3), 45–63.

Ohishi, M. (2018). Hypertension with diabetes mellitus: physiology and pathology. *Hypertens. Res.* 41 (6), 389–393. doi:10.1038/s41440-018-0034-4

Oršolić, N., Sirovina, D., Odeh, D., Gajski, G., Balta, V., Šver, L., et al. (2021). Efficacy of caffeic acid on diabetes and its complications in the mouse. *Molecules* 26 (11), 3262–3325. doi:10.3390/molecules26113262

Othman, N. S., Che Roos, N. A., Hamid, A. A., Aminuddin, A., Kumar, J., and Ugusman, A. (2022). Effects of *Piper sarmentosum* on diabetes mellitus and hypertension: a systematic review. *Inplasy Protoc.*, 1–3. doi:10.37766/inplasy2022.4.0020

Peungvicha, P., Thirawarapan, S., Temsiririrkkul, R., Watanabe, H., Kumar Prasain, J., and Kadota, S. (1998). Hypoglycemic effect of the water extract of *Piper sarmentosum* in rats. *J. Ethnopharmacol.* 60 (1), 27–32. doi:10.1016/S0378-8741(97)00127-X

Poovitha, S., and Parani, M. (2016). In vitro and in vivo α-amylase and α-glucosidase inhibiting activities of the protein extracts from two varieties of bitter gourd. *BMC Complement. Altern. Med.* 16 (1), 185–189. doi:10.1186/s12906-016-1085-1

Ridtitid, W., Ruangsang, P., Reanmongkol, W., and Wongnawa, M. (2007). Studies of the anti-inflammatory and antipyretic activities of the methanolic extract of *Piper sarmentosum* Roxb. Leaves in rats. *Songklanakarin J. Sci. Technol.* 29 (6), 1519–1526.

Rodríguez, V., Plavnik, L., and Tolosa de Talamoni, N. (2018). Naringin attenuates liver damage in streptozotocin-induced diabetic rats. *Biomed. Pharmacother.* 105, 95–102. doi:10.1016/j.biopha.2018.05.120

Rojas, A., Figueroa, H., Re, L., and Morales, M. A. (2006). Oxidative stress at the vascular wall. Mechanistic and pharmacological aspects. *Arch. Med. Res.* 37 (4), 436–448. doi:10.1016/j.arcmed.2005.11.012

Rubanyi, G. M. (1993). The role of endothelium in cardiovascular homeostasis and diseases. *J. Cardiovasc. Pharmacol.* 22 (4), S1–S14. doi:10.1097/00005344-199322004-00002

Sabadashka, M., Hertsyk, D., Strugała-Danak, P., Dudek, A., Kanyuka, O., Kucharska, A. Z., et al. (2021). Anti-diabetic and antioxidant activities of red wine concentrate enriched with polyphenol compounds under experimental diabetes in rats. *Antioxidants* 10 (9), 1399–1424. doi:10.3390/antiox10091399

Sallehuddin, N. A., Abdul-Hamid, A., Salleh, S. Z., Abdul-Majid, N., Halim, H. H., Ramli, N. S., et al. (2020). Ergogenic, anti-diabetic and antioxidant attributes of selected Malaysian herbs: Characterisation of flavonoids and correlation of functional activities. *Int. Food Res. J.* 27 (1), 197–207.

Schwarzer, M. (2016). "Models to investigate cardiac metabolism," in *The scientist's guide to cardiac metabolism* (Cambridge: Academic Press), 103–122. doi:10.1016/b978-0-12-802394-5.00008-x

Sędzikowska, A., and Szablewski, L. (2021). Human glucose transporters in renal glucose homeostasis. *Int. J. Mol. Sci.* 22 (24), 13522–13617. doi:10.3390/ijms222413522

Serné, E. H., Stehouwer, C. D. A., ter Maaten, J. C., ter Wee, P. M., Rauwerda, J. A., Donker, A. J. M., et al. (1999). Microvascular function relates to insulin sensitivity and blood pressure in normal subjects. *Circulation* 99 (7), 896–902. doi:10.1161/01.CIR.99.7.896

Shiny, A., Regin, B., Mohan, V., and Balasubramanyam, M. (2016). Coordinated augmentation of NFAT and NOD signaling mediates proliferative VSMC phenotype switch under hyperinsulinemia. *Atherosclerosis* 246, 257–266. doi:10.1016/j.atherosclerosis.2016.01.006

Sorriento, D., De Luca, N., Trimarco, B., and Iaccarino, G. (2018). The antioxidant therapy: new insights in the treatment of hypertension. *Front. Physiol.* 9, 258–311. doi:10.3389/fphys.2018.00258

Subramaniam, V., Adenan, M. I., Ahmad, A. R., and Sahdan, R. (2003). Natural antioxidants: *Piper sarmentosum* (kadok) and Morinda elliptica (mengkudu). *Malays. J. Nutr.* 9 (1), 41–51.

Sumazian, Y., Syahida, A., Hakiman, M., and Maziah, M. (2010). Antioxidant activities, flavonoids, ascorbic acid and phenolic contents of Malaysian vegetables. *J. Med. Plant Res.* 4 (10), 881–890. doi:10.5897/JMPR10.011

Sun, H. J., Wu, Z. Y., Nie, X. W., and Bian, J. S. (2020). Role of endothelial dysfunction in cardiovascular diseases: the link between inflammation and hydrogen sulfide. *Front. Pharmacol.* 10, 1568–1615. doi:10.3389/fphar.2019.01568

Sundar, U. M., Ugusman, A., Chua, H. K., Latip, J., and Aminuddin, A. (2019). *Piper sarmentosum* promotes endothelial nitric oxide production by reducing asymmetric dimethylarginine in tumor necrosis factor-A-induced human umbilical vein endothelial cells. *Front. Pharmacol.* 10, 1033–1039. doi:10.3389/fphar.2019.01033

Tain, Y. L., and Hsu, C. N. (2022). Oxidative stress-induced hypertension of developmental origins: preventive aspects of antioxidant therapy. *Antioxidants* 11 (3), 511–520. doi:10.3390/antiox11030511

Tatsumi, Y., and Ohkubo, T. (2017). Hypertension with diabetes mellitus: significance from an epidemiological perspective for Japanese. *Hypertens. Res.* 40 (9), 795–806. doi:10.1038/hr.2017.67

The Cochrane Collaboration (2020). *Cochrane's Collaboration Review Manager (RevMan)*. Version 5.4 [Computer program].

Thent, Z. C., and Das, S. (2015). *Piper sarmentosum* maintains blood pressure and morphological integrity of liver in type 1 diabetic rats. *Int. J. Pharma Med. Biol. Sci.* 4 (1), 24–28.

Thent, Z. C., Lin, T. S., Das, S., and Zakaria, Z. (2012a). Histological changes in the heart and the proximal aorta in experimental diabetic rats fed with *Piper sarmentosum*. *Afr. J. Tradit. Complement. Altern. Med.* 9 (3), 396–404. doi:10.4314/ajtcam.v9i3.15

Thent, Z. C., Seong Lin, T., Das, S., and Zakaria, Z. (2012b). Effect of *Piper sarmentosum* extract on the cardiovascular system of diabetic sprague-dawley rats: electron microscopic study. *Evid. Based. Complement. Altern. Med.* 2012, 628750–628759. doi:10.1155/2012/628750

Torday, J. S., and Baluška, F. (2019). Why control an experiment?: from empiricism, via consciousness, toward implicate order. *EMBO Rep.* 20 (10), e49110–4. doi:10.15252/embr.201949110

Tsimihodimos, V., Gonzalez-Villalpando, C., Meigs, J. B., and Ferrannini, E. (2018). Hypertension and diabetes mellitus coprediction and time trajectories. *Hypertension* 71 (3), 422–428. doi:10.1161/HYPERTENSIONAHA.117.10546

Tune, J. D., Goodwill, A. G., Sassoon, D. J., and Mather, K. J. (2017). Cardiovascular consequences of metabolic syndrome. *Transl. Res.* 183, 57–70. doi:10.1016/j.trsl.2017.01.001

Ugusman, A., Zakaria, Z., Hui, C. K., and Nordin, N. A. M. M. (2010). *Piper sarmentosum* increases nitric oxide production in oxidative stress: a study on human umbilical vein endothelial cells. *Clinics* 65 (7), 709–714. doi:10.1590/S1807-59322010000700010

Ugusman, A., Zakaria, Z., Hui, C. K., and Megat Mohd Nordin, N. A. (2011). *Piper sarmentosum* inhibits ICAM-1 and Nox4 gene expression in oxidative stress-induced human umbilical vein endothelial cells. *BMC Complement. Altern. Med.* 11 (1), 31–39. doi:10.1186/1472-6882-11-31

Ugusman, A., Md Fadze, N., Hamid, A. A., Asmawi, Z., and Aminuddin, A. (2020). *Piper sarmentosum* attenuates dexamethasone-induced hypertension by

stimulating endothelial nitric oxide synthase. *JRP* 24 (1), 1–9. doi:10.35333/jrp.2020.122

Wan, E. Y. F., Yu, E. Y. T., Chin, W. Y., Fung, C. S. C., Fong, D. Y. T., Choi, E. P. H., et al. (2018). Effect of achieved systolic blood pressure on cardiovascular outcomes in patients with type 2 diabetes: a population-based retrospective cohort study. *Diabetes Care* 41 (6), 1134–1141. doi:10.2337/dc17-2443

Wei, J., Tian, J., Tang, C., Fang, X., Miao, R., Wu, H., et al. (2022). The influence of different types of diabetes on vascular complications. *J. Diabetes Res.* 2022, 3448618–3448712. doi:10.1155/2022/3448618

Wong, W. T., Tian, X. Y., and Huang, Y. (2013). Endothelial dysfunction in diabetes and hypertension: cross talk in RAS, BMP4, and ROS-dependent COX-2-derived prostanoids. *J. Cardiovasc. Pharmacol.* 61 (3), 204–214. doi:10.1097/FJC.0b013e31827fe46e

Wongsa, P., Chaiwarit, J., and Zamaludien, A. (2012). In vitro screening of phenolic compounds, potential inhibition against α-amylase and α-glucosidase of culinary herbs in Thailand. *Food Chem.* 131 (3), 964–971. doi:10.1016/j.foodchem.2011.09.088

Wszola, M., Klak, M., Kosowska, A., Tymicki, G., Berman, A., Adamiok-Ostrowska, A., et al. (2021). Streptozotocin-induced diabetes in a mouse model (Balb/c) is not an effective model for research on transplantation procedures in the treatment of type 1 diabetes. *Biomedicines* 9 (12), 1790–1818. doi:10.3390/biomedicines9121790

Yamazaki, D., Hitomi, H., and Nishiyama, A. (2018). Hypertension with diabetes mellitus complications. *Hypertens. Res.* 41, 147–156. doi:10.1038/s41440-017-0008-y

Yang, M., Chen, Y., Vagionitis, S., Körtvely, E., Ueffing, M., Schmachtenberg, O., et al. (2022). Expression of glucose transporter-2 in murine retina: Evidence for glucose transport from horizontal cells to photoreceptor synapses. *J. Neurochem.* 160 (2), 283–296. doi:10.1111/jnc.15533

Yazdi, H. B., Hojati, V., Shiravi, A., Hosseinian, S., Vaezi, G., and Hadjzadeh, M. A. R. (2019). Liver dysfunction and oxidative stress in streptozotocin-induced diabetic rats: Protective role of artemisia turanica. *J. Pharmacopuncture* 22 (2), 109–114. doi:10.3831/KPI.2019.22.014

Zainal Ariffin, S. H., Wan Omar, W. H. H., Safian, M. F., Ariffin, Z. Z., Senafi, S., and Megat Abdul Wahab, R. (2009). Intrinsic anticarcinogenic effects of *Piper sarmentosum* ethanolic extract on a human hepatoma cell line. *Cancer Cell Int.* 9 (6), 6–9. doi:10.1186/1475-2867-9-6

Zakaria, Z. A., Patahuddin, H., Mohamad, A. S., Israf, D. A., and Sulaiman, M. R. (2010). In vivo anti-nociceptive and anti-inflammatory activities of the aqueous extract of the leaves of *Piper sarmentosum*. *J. Ethnopharmacol.* 128 (1), 42–48. doi:10.1016/j.jep.2009.12.021

Zhang, Y., Nie, J., Zhang, Y., Li, J., Liang, M., Wang, G., et al. (2020). Degree of blood pressure control and incident diabetes mellitus in Chinese adults with hypertension. *J. Am. Heart Assoc.* 9 (16), e017015–31. doi:10.1161/JAHA.120.017015

frontiers | Frontiers in Pharmacology

TYPE Original Research
PUBLISHED 30 August 2022
DOI 10.3389/fphar.2022.983716

OPEN ACCESS

EDITED BY
Ahmad Nazrun Shuid,
MARA University of Technology, Malaysia

REVIEWED BY
Carlos L. Cespedes-Acuña,
Universidad del Bío-Bío, Chile
Yuan Wei,
Jiangsu University, China

*CORRESPONDENCE
Zizhong Tang,
14126@sicau.edu.cn
Hui Chen,
chen62hui@163.com

†These authors have contributed equally to this work and share first authorship

SPECIALTY SECTION
This article was submitted to Ethnopharmacology, a section of the journal Frontiers in Pharmacology

RECEIVED 01 July 2022
ACCEPTED 05 August 2022
PUBLISHED 30 August 2022

CITATION
Tang Z, Qin Y, Wang Y, Lin W, Wang Q, Shen N, Xiao Y, Chen H, Chen H, Bu T, Li Q, Yao H, Feng S and Ding C (2022), The endophytic fungus Penicillium oxalicum isolated from Ligusticum chuanxiong Hort possesses DNA damage-protecting potential and increases stress resistance properties in Caenorhabditis elegans.
Front. Pharmacol. 13:983716.
doi: 10.3389/fphar.2022.983716

The endophytic fungus *Penicillium oxalicum* isolated from *Ligusticum chuanxiong* Hort possesses DNA damage-protecting potential and increases stress resistance properties in *Caenorhabditis elegans*

Zizhong Tang[1*†], Yihan Qin[1†], Yueyu Wang[1], Wenjie Lin[1], Qing Wang[1], Nayu Shen[1], Yirong Xiao[2], Hong Chen[3], Hui Chen[1*], Tongliang Bu[1], Qingfeng Li[1], Huipeng Yao[1], Shiling Feng[1] and Chunbang Ding[1]

[1]College of Life Sciences, Sichuan Agricultural University, Ya'an, China, [2]Sichuan Agricultural University Hospital, Sichuan Agricultural University, Ya'an, China, [3]College of Food Science, Sichuan Agricultural University, Ya'an, China

The chemical composition and antioxidant activity of extracts (POE) of *Penicillium oxalate* isolated from *Ligusticum chuanxiong* Hort have been investigated. However, the biological activity of POE is limited, and its antioxidant, stress resistance and DNA protection effects *in vivo* are unclear. The current study aims to explore the beneficial effects of POE on DNA damage protection in pBR322 plasmid and lymphocytes and stress resistance in *Caenorhabditis elegans*. The results showed that POE increased the survival rate of *C. elegans* under 35°C, UV and H_2O_2 stress, attenuated ROS and MDA accumulation, and enhanced the activity of some important enzymes (SOD, CTA, and GSH-PX). In addition, the POE-mediated stress resistance involved the upregulation of the expression of the *sod-3*, *sod-5*, *gst-4*, *ctl-1*, *ctl-2*, *daf-16*, *hsp-16.1*, *hsp-16.2*, and *hsf-1* genes and acted dependently on *daf-16* and *hsf-1* rather than *skn-1*. Moreover, POE also reduced lipofuscin levels, but did not prolong the lifespan or damage the growth, reproduction and locomotion of *C. elegans*. Furthermore, POE showed a protective effect against DNA scission in the pBR322 plasmid and lymphocytes. These results suggested that *P. oxalate* extracts have significant anti-stress and DNA protection potential and could be

Abbreviations: Res, resveratrol; VE, vitamin E; MDA, malondialdehyde; SOD, superoxide dismutase; CAT, catalase; GSH-Px, glutathione peroxidase; ROS, reactive oxygen species; POE, *Penicillium oxalate* extract.

potential drug candidates in the pharmaceutical field, thus greatly broadening the understanding of the biological effects of the endophytic fungus *P. oxalate*.

KEYWORDS

endophytic fungi, *Penicillium oxalicum*, antioxidant, oxidative stress resistant, *Caenorhabditis elegans*, DNA damage protection

1 Introduction

There is increasing evidence that reactive oxygen species (ROS, e. g., O_2– and OH) and free radical-meditated reactions damage DNA, lipids and proteins (Dubois et al., 2018), eventually leading to various diseases. For example, DNA damage affects normal physiological metabolism and blocks some metabolic pathways, leading to ageing, cancer, atherosclerosis, coronary heart ailment, diabetes, Alzheimer's disease and other neurodegenerative disorders (Xu et al., 2005). Currently, antioxidants have various degrees of anti-inflammatory, antiatherosclerotic, antitumor, antimutagenic, anticarcinogenic, antibacterial or antiviral effects (Aruoma, 1998) and are considered highly effective in treating ROS-mediated pathologies. Many synthetic antioxidant compounds, such as butylated hydroxyanisole and butyl hydroxytoluene, are useful, but they are cytotoxic and are suspected to be potential causes of health damage (Conning and Phillips, 1986). Accordingly, finding efficient and safe antioxidants from natural resources to prevent and reduce the occurrence of related diseases is urgently warranted (Denis et al., 2013).

Currently, endophytic fungi isolated from medicinal plants have received greater attention due to their great potential to produce bioactive compounds with a variety of biological properties (Strobel, 2003; Strobel et al., 2004). Previous studies have suggested that endophytic fungus extracts contain bioactive substances with antibacterial, antioxidant and other bioactivities (da Silva et al., 2020), such as *Lasiodiplodia venezuelensis* isolated from *Syzygium samarangense* L (Budiono et al., 2019) and *Cercospora* sp. PM018 was isolated from *Lal-bisalyakarani* (Mookherjee et al., 2020), and could be a potential antioxidant resource for the treatment of related diseases. Moreover, *in vitro* fermentation culture of endophytic fungi has the advantages of high yield, a short fermentation period, high production efficiency, and sustainable production of target bioactive ingredients (Ludwig-Müller, 2015). Hence, the efficacy and potential usefulness of endophytic fungus extracts have led to a number of studies with the aim of detecting their antioxidant activity. However, there have been few studies on the oxidative stress resistance of endophytic fungus extracts *in vivo* models (Tiwari et al., 2014) and most studies have only confirmed the antioxidant activity of endophytic fungal extracts *in vitro* (Huang et al., 2007; Li et al., 2015). Fortunately, *C. elegans*, a powerful tool, is commonly used to test various physiological processes, the mechanisms of some diseases and the biological activity of natural products due to its advantages of small body size, ease of handling and many mutant strains (Wang et al., 2014). For instance, previous studies frequently used *C. elegans* as a model to explore the antioxidant, anti-stress and anti-ageing capacities of different plant extracts (Duangjan et al., 2021). In addition, as far as we know, DNA damage is associated with ROS imbalance, and excess free radicals can damage DNA strands leading to the occurrence of various diseases (Thanan et al., 2014). Nevertheless, an extensive survey of the literature revealed very few reports corroborating the protective potential against DNA damage of endophytic fungus extracts (Kaur et al., 2020).

In previous studies by our group, an extract of *Penicillium oxalate* (POE) isolated *Ligusticum chuanxiong* Hort was reported to have antioxidant capacity (Tang et al., 2021), but its antioxidant and oxidative stress resistance properties in animal models and DNA damage protection effects are lacking. Therefore, the purpose of this study was to enrich the biological effects of the endophytic fungus *Penicillium oxalicum*, such as anti-stress and DNA damage protection properties. Our present findings could accelerate the utilization of POE in the field of therapeutics by virtue of its DNA damage protection, antioxidant activity and increased stress resistance potential in *C. elegans*.

2 Materials and methods

2.1 Materials

The endophytic fungus *P. oxalate* was isolated from the roots of *L. chuanxiong* Hort and stored in the "Fermentation Engineering Laboratory" (College of Life Sciences, Sichuan Agricultural University, Ya'an, China).

The activated endophytic fungus *p. oxalate* was inoculated in PDA medium and cultured on a shaker for approximately 1 week at 28°C. Subsequently, vacuum-filtered fermentation broth was extracted with ethyl acetate and concentrated with a rotary evaporator to obtain the *P. oxalate* extract (POE).

2.2 *Caenorhabditis elegans* strains and culture conditions

The strains N2 (wild type), CF1038 [*daf-16* (mu86)I] (WBStrain00004840), EU1 [*skn-1* (zu67) IV/nT1 (IV; V)] (WBStrain00007249), PS3551 [*hsf-1* (sy441)I] (WBStrain00030901) and *Escherichia coli* OP50 (*E. coli* OP50)

were obtained from the Caenorhabditis Genetics Center United States. Worms were cultured at 20°C in solid nematode growth medium (NGM) and seeded with inactivated *E. coli* OP50 as a food source. The worms were age synchronized based on the bleaching method as follows: eggs were obtained by bleaching adults using lysis solution 3.5 ml of M9 buffer, 0.5 ml of NaClO (5%) and 1 ml of NaOH (5 mol/L). Unless otherwise stated, all eggs were incubated on NGM plates containing *E. coli* OP50 and different concentrations of POE.

2.3 Acute toxicity assay

Toxicity tests in liquid medium were performed according to a previous method with modifications (Moliner et al., 2018). In brief, synchronized L4 worms were placed in M9 buffer in a 96-well microplate with different concentrations (1–100 μg/ml) of POE at 20°C for 24 h. At least 100 worms per condition were evaluated per treatment and M9 was used as a negative control. Subsequently, the survival rate (%) was calculated after 24 h.

Survival rate% = (Number of alive worms× 100)/Total number of worms.

2.4 Stress resistance assay

Before exposure to the corresponding stressors, the age-synchronized L1 larvae worms were treated or not treated with POE (25, 50, 75 μg/ml) for 3 days at 20°C. Subsequently, the late L4 larvae or young adult were washed twice with sterile water and exposed to various stresses until all individuals died. The worms were considered dead when they did not respond to platinum wire stimulus. All trials were repeated three times. Resveratrol (Res, 22.5 μg/ml) was used as a positive control (Zhuang et al., 2016).

2.4.1 Ultraviolet-B stress assay

To evaluate resistance to UV irradiation, the POE-treated worms were exposed to UV irradiation (120 mJ cm^{-2}) for 4 h. The number of surviving worms was counted every 24 h (Wang et al., 2018).

2.4.2 H_2O_2-induced oxidative stress assay

This assay was performed as described previously (Saul et al., 2008). Briefly, the POE-treated worms were transferred to fresh NGM containing 2 mM H_2O_2 to determine the effects of POE on oxidative stress. The survival rate of the worms was observed every 30 min.

2.4.3 Heat shock assay

The heat shock assay using *C. elegans* was performed according to Lin et al. (2019). The POE-treated worms were moved from a comfortable cultivation environment (20°C) to a 35°C mediated stress environment. Subsequently, the number of surviving worms was monitored every hour to determine their heat stress resistance.

2.5 Intracellular malondialdehyde content, and superoxide dismutase, catalase, and glutathione peroxidase activities

The POE (25, 50, 75 μg/ml)-treated worms (L4 stage) were treated with and without H_2O_2 (2 mM) for 1 h. Next, worm bodies were lysed by ultrasound equipment and supernatant was obtained after centrifugation. The MDA and protein content, SOD, CAT, and GSH-Px activity were determined according to the commercial assay kits (Nanjing Jiancheng Biotechnology Institute, China). Final results were normalized to protein levels (Xiao et al., 2014).

2.6 Reactive oxygen species accumulation assay

Estimation of endogenous ROS levels was based on the method described by Prasanth et al. (2019). Briefly, the worms were treated with different concentrations of POE (25.50 and 75 μg/ml) for 3 days and exposed to oxidative stress (2 mM H_2O_2) for 1 h. Then, the worms were washed thoroughly with M9 buffer and incubated with 5 μg/ml 2′,7′-dichloro-fluorescein diacetate (DCFH-DA) for 20 min, followed by another wash to remove the excess DCFH-DA. Furthermore, the worms were transferred with a drop of sodium azide (0.5%) onto a glass slide. Fluorescent imaging was performed on 10 worms using an Olympus FV1200 confocal microscope (Tianjin Leike Optical Instruments Co., Ltd.). The relative fluorescence was measured and calculated using ImageJ software.

2.7 Lipofuscin accumulation and body length assay

The lipofuscin level was measured after 5 days of POE treatment. Then the worms were randomly selected and washed with M9 buffer three times and then anesthetized with 0.5% NaN_3 as described in previous study (Onken and Driscoll, 2010). At least 10 worms were selected for imaging using a fluorescence microscope (CX23, Olympus, Tokyo, Japan) at wavelength with excitation/emission (360/420 nm) filters. The fluorescence intensity and the body size of the worms were measured using ImageJ software.

2.8 Longevity assay

The N2 worms were used for lifespan analysis under normal conditions as described in previous study (Duangjan et al.,

2019a). In brief, synchronized L4 larval worms were placed on NGM plates with POE. Then, live worms were counted and transferred to fresh NGM plates containing POE every day until all individuals died. The L4 worms were defined as a starting time point (d 0) for lifespan assay. The assay was performed with approximately 100 worms in each group and the results are expressed as the survival rate%.

2.9 Fertility assay

The fertility assay was performed as described in a previous study (Lin et al., 2020). In brief, reproductive capacity was evaluated by three indexes: brood size, progeny number and hatchability (the ratio of progeny number to brood size number). The parents of the worms were transferred daily to fresh NGM containing 50 μg/ml POE during the progeny production period. Then, the eggs on the old NGM were counted daily. Moreover, the old NGM was kept at 20°C for 24 h to detect viable eggs. The experiment was performed with at least 10 worms per group.

2.10 Movement assays

The body movement assay was performed as described previously (Herndon et al., 2002). The age-synchronized L1 larvae worms were treated and the motility of worms was evaluated on Days 3, 7, and 10. Then, worms were transferred to fresh plates for 1-min of free movement. Subsequently, the motility behaviour of worms was observed using a stereomicroscope and was classified into classes A, B, and C: the highly mobile worms, which we designated class A, moved spontaneously and smoothly; members of class B did not move unless prodded, and they left tracks that were nonsinusoidal; and class C worms did not move forward or backwards, but oscillated their nose or tails in response to touch.

2.11 Expression levels of gene assays

The worms were treated with or without 50 μg/ml POE for 72 h from eggs and then incubated with 2 mM H_2O_2 for 1 h. Total RNA was extracted using the TRIzol Total RNA Extraction Kit (Tiangen, Beijing, China) and synthesized into cDNA using the FastKing RT Kit (TSINGKE Biotech Co., Ltd., Beijing, China). Subsequently, quantitative reverse transcription polymerase chain reaction (qRT–PCR) was performed using SuperReal PreMix Plus (SYBR Green) and a real-time PCR detection system (Bio-Rad, Laboratories, Hercules, CA, United States). The expression of mRNA was analysed using the comparative $2^{-\Delta\Delta Ct}$ method and *act-1* was the internal control gene. The primers used for qRT–PCR in this study are listed in Supplementary Table S1.

2.12 Determination of DNA damage protective activity

2.12.1 DNA nicking assay for hydroxyl radical scavenging activity

The potential of POE to protect the supercoiled pBR322 plasmid from the destructive effect of free radicals caused by the Fenton reagent was estimated using the DNA nicking assay as described by Jeong et al.(2009). Five microlitres of PBS (10 mM), 2 μl of plasmid DNA (0.5 μg), POE (5 μl, 25, 50, and 75 μg/ml), 2 μl of $FeSO_4$(1 mM) and 2 μl of H_2O_2(1 mM) were mixed. The reaction mixture was incubated for 30 min at 37°C. After incubation, 2 μl of loading buffer were added to stop the reaction and the DNA was analysed with 1% agarose gel electrophoresis for 30 min under 120 V. Subsequently, the different forms of DNA, i.e., Supercoiled (SC) and open circular (OC) DNA were visualized and semi-quantitative analysis to calculate the double helix percentage under the gel documentation system (Gel Doc XR, Bio-Rad, United States). The positive control was 500 μM vitamin E (VE) (Liu et al., 2022).

$$\text{Double helix rate } (\%) = A_0/(A_0 + A_1) \times 100\%$$

where A_0 is the grey value of the double helix conformation, and A_1 is the grey value of the open-loop conformation.

2.12.2 Cytochalasin blocked micronucleus assay in lymphocytes

In this assay, lymphocytes were cultured by adding 500 μl of whole blood with 9 ml of RPM11640, 10% foetal bovine serum, penicillin (100 units/ml), streptomycin (100 μg/ml) and phytohemagglutinin (5 μg/ml). Then, the cells were exposed to H_2O_2 (250 μM) to induce DNA damage. Simultaneously, POE at different concentrations (25 50 and 75 μg/ml) was added to the cultures for 72 h in 5% CO_2 at 37°C. At 44 h, cytochalasin-B (3 μg/ml) was added to the cultures to block cytokinesis. At 72 h, the cultures were collected and treated (Carvalho-Silva et al., 2016). Coded slides were stained for 30 min with Giemsa and observed under a microscope. MN and other nuclear abnormalities were scored in 500 well spread cells of each culture (Fenech et al., 1999).

2.13 Statistical analysis

Survival curves were drawn to determine significant differences using log-rank (Mantel-Cox) tests (GraphPad

TABLE 1 Effects of POE on the viability of *C. elegans*: The results are presented as mean of viability ± SEM%.

Concentration (μg/ml)	Survival rate (%)	*p*-value
Control	92 ± 1	
100	93 ± 4	>0.05
80	94 ± 5	>0.05
60	95 ± 3	>0.05
40	93 ± 3	>0.05
20	91 ± 4	>0.05
10	93 ± 5	>0.05

Not significance differences between treatment and control groups found ($p > 0.05$).

Software, CA, United States) (*$p < 0.05$, **$p < 0.01$, and ***$p < 0.001$). Other statistical calculations used one-way ANOVA followed by LSD and Duncan tests (SPSS software, version 20). All data are expressed as the mean ± SD ($n = 3$), and different letters in columns indicate that the values are significantly different ($p < 0.05$).

3 Results

3.1 Effect of *P. oxalate* extract on acute toxicity in *C. elegans*

The acute toxicity of POE was initially assessed by studying the effect of POE on the viability of *C. elegans*. The results showed that, compared with the control group, the viability of the worms was not affected after 24 h of POE treatment at concentrations ranging from 10 to 100 μg/ml (Table 1). Worms exposed to maximum dose extracts also maintained a survival rate of 93% ± 4%, while the viability rates of the control group were 92% ± 1% (Table 1). Thus, POE did not produce acute toxicity to the model organism at the tested concentrations.

3.2 Effect of *P. oxalate* extract on stress in *C. elegans*

To comprehensively evaluate the stress resistance of POE, we measured the lifespan of worms under conditions of ultraviolet radiation, H_2O_2 and 35°C.

First, we found that the treatment in the presence of POE (50 μg/ml) promoted right shift in the worm survival curve under UV radiation when compared with the controls (Figure 1A), and the mean lifespan of worms treated with UV radiation was increased by 6.4%, 14.0%, and 6.9% in the 25, 50, and 75 μg/ml treatment groups, respectively, compared with the control group (Supplementary Table S2), although the difference was only significant in the group treated with 50 μg/ml POE (Supplementary Table S2; $p < 0.05$). Furthermore, there was no significant difference in the maximum lifespan between the treatment group (50 μg/ml) and the control group, but the mean and median lifespans were increased significantly (Supplementary Table S2; $p < 0.05$). Second, in the H_2O_2-

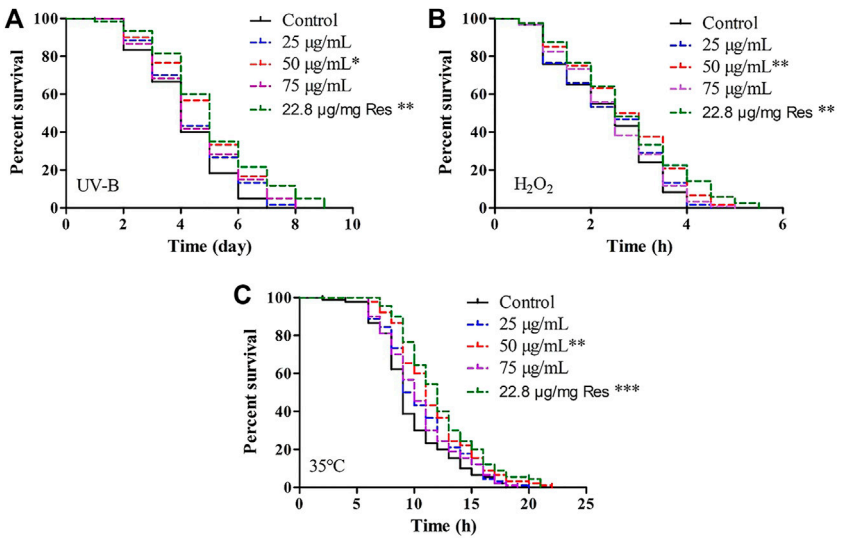

FIGURE 1
The effect of POE on stress resistance in *C. elegans*. **(A)** Survival curve of worms under UV irradiation-induced stress. **(B)** Survival curve of worms under H_2O_2-induced stress. **(C)** Survival curve of worms under 35°C-induced stress. Three independent biological replicates were performed. Differences compared to control group were considered significant at $p < 0.05$ (*), $p < 0.01$ (**) and $p < 0.001$ (***).

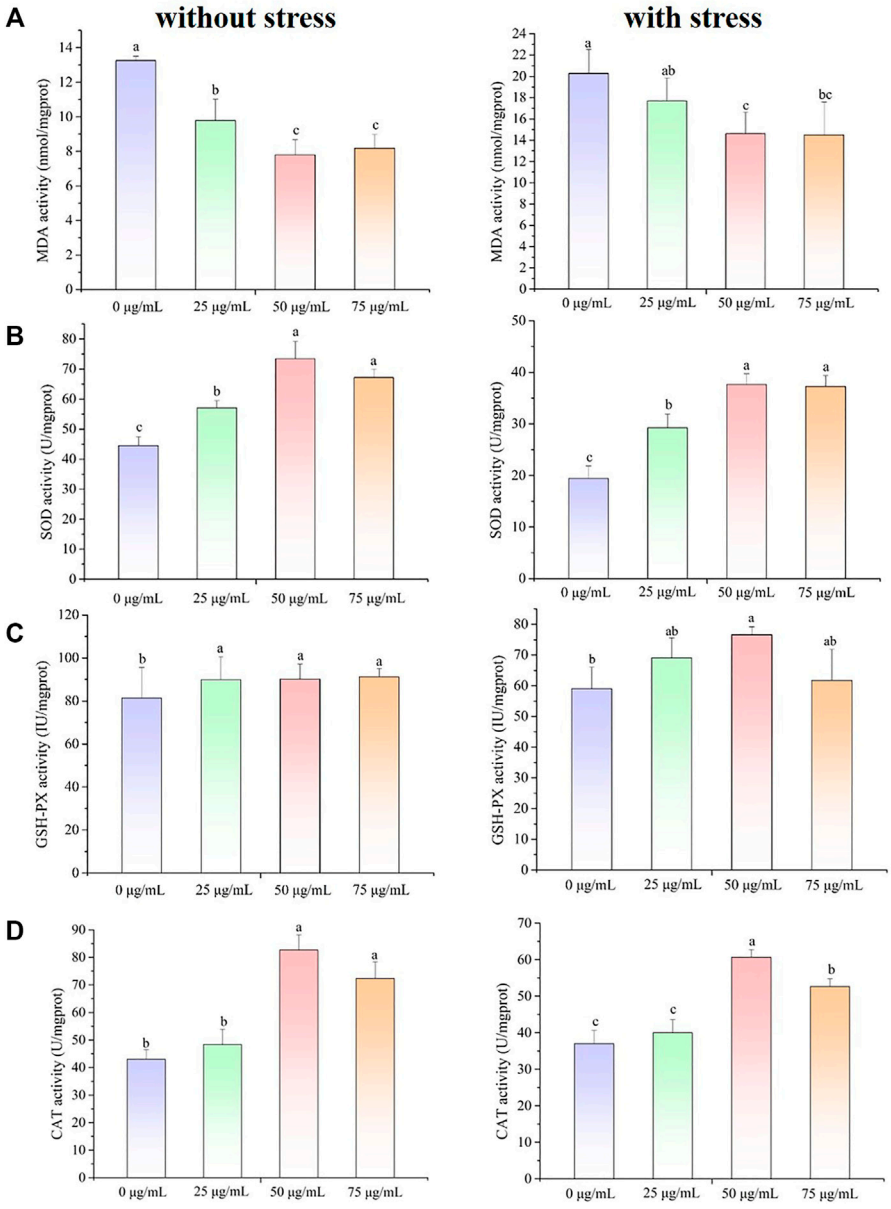

FIGURE 2
The effect of POE on the antioxidant defense system in *C. elegans* under normal and H_2O_2-induced oxidative stress conditions. **(A)** The MDA content. **(B)** The SOD activity. **(C)** The GSH-Px activity. **(D)** The CAT activity. Bars with no letters in common are significantly different ($p < 0.05$).

induced oxidative stress assay, a similar protective effect was observed in the 50 μg/ml POE treatment groups and was comparable to that with resveratrol (Figure 1B). There was no statistically significant difference in survival rate between the treatment groups (25 and 75 μg/ml) and the control group (Figure 1B). However, pretreatment with 50 μg/ml POE significantly improved the mean lifespan, median lifespan and maximum lifespan of worms under H_2O_2-induced oxidative stress (Supplementary Table S2; $p < 0.05$). Last, a similar result was also observed: the survival rate of POE (50 μg/ml) pretreated worms was higher than that of the control group under thermal stress conditions, although the effect was not as good as that in the resveratrol treatment group (Figure 1C; Supplementary Table S2). As expected, the 50 μg/ml POE treatment group exhibited the highest mean and maximum survival times, which were 11.2 ± 0.41 h and 20.50 ± 2.65 h, respectively (Supplementary Table S2; $p < 0.05$).

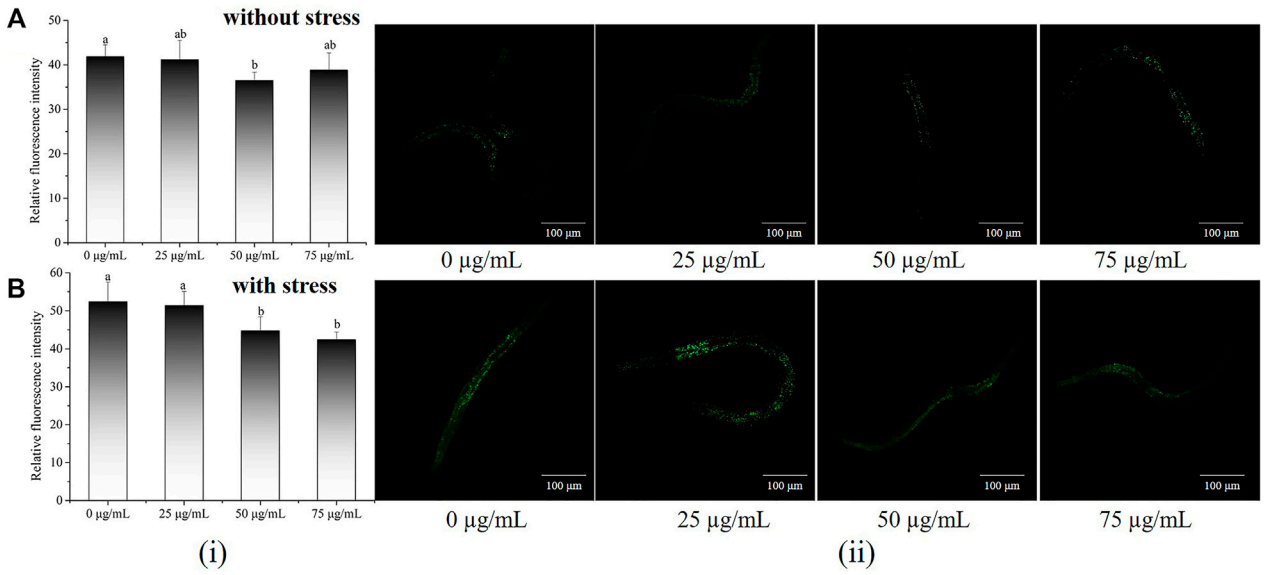

FIGURE 3
The effect of POE on intracellular levels of ROS in *C. elegans*. **(A)** Accumulation of ROS in *C. elegans* under normal conditions. **(B)** Accumulation of ROS in *C. elegans* under H_2O_2-induced oxidative stress. (i): Relative fluorescence intensity of worms was quantified using ImageJ software. (ii): Representative image of worms which was treated with POE in both conditions. Bars with no letters in common are significantly different ($p < 0.05$).

These results indicated that supplementation with POE has the potential to resist UV- and H_2O_2-mediated oxidative stress and 35°C-mediated heat stress in the *C. elegans* model.

3.3 Effect of *P. oxalate* extract on malondialdehyde content and antioxidant enzyme activity in *C. elegans*

To elucidate the antioxidant and oxidative resistance properties of the POE *in vivo*, the MDA content and SOD and GSH-Px activities of POE-treated *C. elegans* were determined in H_2O_2-treated *C. elegans*, and the corresponding indexes were also determined under normal conditions. As shown in Figure 2A, the MDA content was decreased under both conditions compared to the control, indicating that POE was able to alleviate lipid peroxidation in *C. elegans* under normal and pressure conditions. Furthermore, since SOD and GSH-Px are the main ROS scavenging enzymes in the antioxidant defence system of *C. elegans*, we further measured the activities of antioxidant enzymes. As expected, compared with the control group, the SOD activity of *C. elegans* treated with POE was significantly increased under H_2O_2-induced oxidative stress conditions (Figure 2B; $p < 0.05$). A similar result was also observed in the absence of stress (Figure 2B). For GSH-Px and CAT activity, the enzyme activity in the POE treated group was significantly increased with and without pressure, compared with the control group (Figures 2C,D; $p < 0.05$). It was obvious that POE showed an excellent *in vivo* antioxidant capacity to activate the antioxidant defence system of *C. elegans*.

3.4 Effect of *P. oxalate* extract on Reactive oxygen species accumulation in *C. elegans*

To further delve into the antioxidant potential of POE, the ROS levels of *C. elegans* were assessed under normal or stressful conditions. As shown in Figures 3A,B, higher ROS levels were found in worms with or without POE treatment under oxidative stress than in the absence of oxidative stress, indicating that H_2O_2 caused the accumulation of ROS in worms. Furthermore, POE treatment resulted in a decrease in ROS levels compared to the controls regardless of the conditions (Figure 3), which was directly proportional to the reduction in fluorescence. The ROS levels were significantly decreased in the 50 and 75 μg/ml POE-treated groups under oxidative stress and in the 50 μg/ml POE-treated group under normal conditions compared to controls (Figures 3A,B; $p < 0.05$). It was obvious that POE showed a significant antioxidant capacity and could scavenge intracellular ROS to a certain extent, which was consistent with reducing MDA and enhancing the activities of SOD and GSH-P_X.

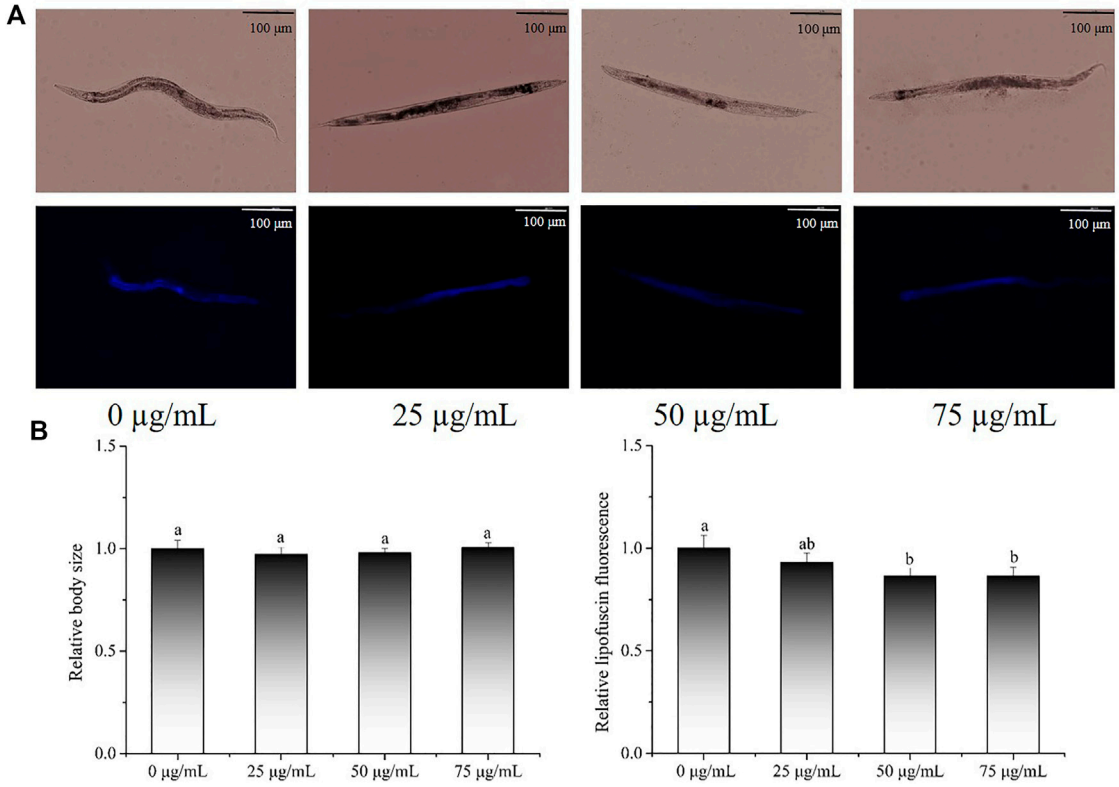

FIGURE 4
The effect of POE on lipofuscin accumulation and body size in *C. elegans*. **(A)** Representative images of fluorescence and bright field micrographs are shown, the scale bar was 100 μm; **(B)** body length and lipofuscin was measured and quantitated by ImageJ. Bars with no letters in common are significantly different ($p < 0.05$).

3.5 Effects of *P. oxalate* extract on body length and lipofuscin accumulation in *C. elegans*

Lipofuscin, a marker of ageing, is commonly used to assess the health status of *C. elegans*. The body length and lipofuscin levels in *C. elegans* were also evaluated and representative images are presented in Figure 4A. In terms of body size (Figure 4B), there was no significant change between the POE treatment groups and the control group ($p > 0.05$), indicating that POE did not affect the body size of the worms. Relative fluorescence quantitative analysis showed that 50 and 75 μg/ml POE significantly reduced the accumulation of lipofuscin by 13.63% and 13.61%, respectively, in comparison with the control group (Figure 4B; $p < 0.05$).

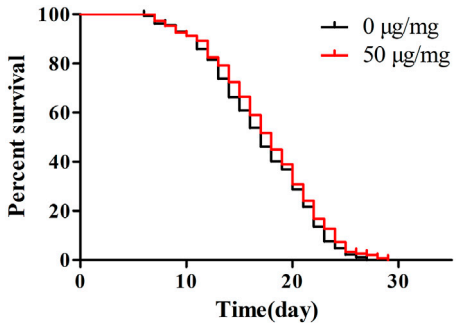

FIGURE 5
The effect of POE on lifespan of *C. elegans*. Results of lifespan experiments were analysed using the Kaplan-Meier survival model, and for significance by means of a long rank pairwise comparison test between the control and treatment groups. Differences compared to control group were considered significant at $p < 0.05$ (*), $p < 0.01$ (**) and $p < 0.001$ (***).

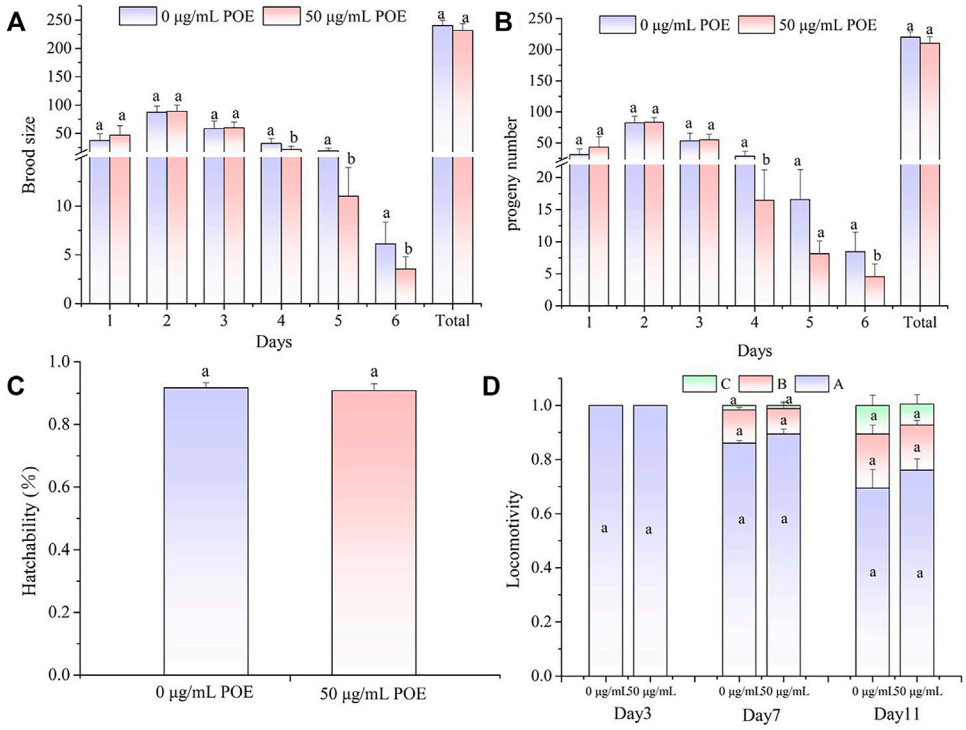

FIGURE 6
The effect of POE on reproduction and movement in *C. elegans*. **(A)** Brood size; **(B)** Progeny number; **(C)** Hatchability; **(D)** The three levels of locomotivity were measured and the individuals were classified according to the movement: A-free movement, B-movement after prodding, C-weak movement after prodding. Data were expressed as the mean ± SD (n = 3). Bars with different letters indicated statistical significance ($p < 0.05$).

3.6 Effect of *P. oxalate* extract on the lifespan of *C. elegans*

Next, we evaluated whether POE (50 μg/ml) could prolong the lifespan of worms. This concentration was chosen as the treatment dose because it was found to be more beneficial for reducing lipofuscin accumulation and enhancing stress tolerance. However, there was no significant difference in survival curves between the treatment and control groups (Figure 5; $p > 0.05$ by the log-rank test), indicating that although POE can alleviate the accumulation of age pigments, it is not sufficient to prolong the lifespan of worms.

3.7 Effect of *P. oxalate* extract on the fertility and movement of *C. elegans*

Fertility and movement assays were performed to examine whether POE had some side effects on the physiological function of this dose (50 μg/ml). Analyses of fertility showed that the size of the brood and progeny number from Day 4 were slightly decreased after POE treatment, but there were no differences in total brood size, total progeny number or total hatchability in worms treated with POE when compared with the controls (Figures 6A–C).

In addition, we found that, as the worms aged, their motility gradually declined, and B-class and C-class locomotion began to appear in the middle and middle-late stages of the life cycle (Figure 6D). However, the movement assay did not show significant differences in locomotion ability between the POE-treated group and control group in the different stages of the life cycle (Figure 6D).

Considered together, these results showed that POE had no obvious effects on the reproductive and motor systems of *C. elegans*.

3.8 *P. oxalate* extract enhanced stress resistance in *C. elegans* by activating oxidative stress-inducible genes that might not be associated with *skn-1* but might be dependent on *daf-16* and *hsf-1*

The antistress ability of POE has been proved, but the underlying molecular mechanisms require further study. Since POE can enhance antioxidant enzyme activity and reduce ROS

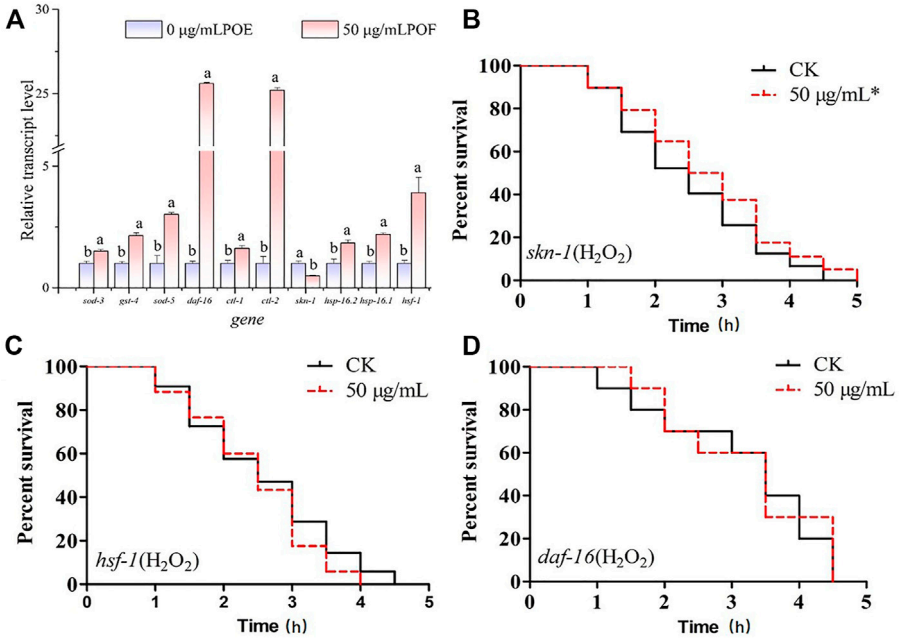

FIGURE 7
The molecular mechanism of POE in the antioxidant stress. **(A)** The expression of stress-related genes in *C. elegans* under H_2O_2-induced oxidative stress conditions. **(B)** The survival curve of *skn-1* mutant worms under H_2O_2-induced oxidative stress. **(C)** The survival curve of *hsf-1* mutant worms under H_2O_2-induced oxidative stress. **(D)** The survival curve of *daf-16* mutant worms under H_2O_2-induced oxidative stress. Data were expressed as the mean ± SD (n = 3). Bars with different letters indicated statistical significance ($p < 0.05$). * Significant p-value <0.05 by the log-rank test.

accumulation, we further investigated the relative expression levels of oxidative stress-inducible genes (*sod-3*, *sod-5*, *gst-4*, *ctl-1*, and *ctl-2*) using RT–qPCR. As indicated in Figure 7, the relative expression levels of various oxidative stress-inducible genes of in the POE-treated group were significantly higher than that of the control group, especially *ctl-2* (exhibiting a 25.2-fold increase). Moreover, it was observed that the relative expression levels of *daf-16* (25.59-fold), *hsf-1* (4.21-fold), *hsp-16.1* (2.19-fold) and *hsp-16.2* (1.82-fold) were upregulated significantly ($p < 0.05$) compared to the control group. However, the relative expression levels of *skn-1* were decreased 0.48 times. In addition, to further confirm the underlying molecular mechanisms, the *daf-16*, *skn-1*, and *hsf-1* mutants were used to evaluate the effects of POE on lifespan in *C. elegans* mutants under H_2O_2-induced oxidative stress. We found that the survival rate of POE-treated *skn-1* mutants was significantly increased compared to that of the control group (Figure 7B, $p < 0.05$), confirming that POE might act independently of *skn-1*. However, the *daf-16* and *hsf-1* mutants did not show a protective effect of POE on worm lifespan (Figures 7C,D; $p > 0.05$), indicating that *daf-16* and *hsf-1* might be necessary for POE to improve stress resistance.

3.9 Effect of *P. oxalate* extract on DNA damage protective activity

3.9.1 DNA nicking assay for hydroxyl radical scavenging activity

The protective effect of POE on hydroxyl radical-induced DNA oxidative damage is shown in Figure 8. The plasmid DNA corresponding to the prominent faster moving band was the supercoiled form (SC DNA) (Figure 8A, **Lane 1**). After the addition of Fe^{2+} and H_2O_2, the supercoiled circular DNA completely converted into the open circular or linear forms (OC DNA) referred to as the slowest moving line (Figure 8A, **Lane 2**) and the DNA double helix percentage was 13% (Figure 8B), suggesting that the hydroxyl radicals generated by the Fenton reaction damaged the original structure of DNA and led to DNA nicking. However, when different concentrations of POE were added, part of the OC DNA reverted to SC DNA (Figure 8A, **Lanes 3–5**) and their DNA double helix percentages were 44%, 55%, and 57%, respectively (Figure 8B), indicating that POE can effectively relieve hydroxyl radical-induced DNA damage.

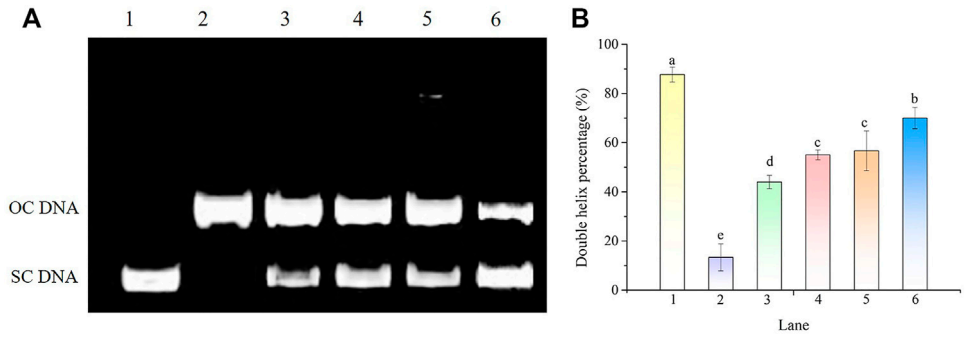

FIGURE 8
The DNA protective effect of POE against ●OH generated by Fenton's reagent. **(A)** Electrophoretogram. Lanes 1 and 2 were the normal DNA treated with and without 1 mM $FeSO_4$ and 1 mM H_2O_2, respectively. Lanes 3–6 were treated with various concentrations of POE (25, 50, and 75 μg/ml) and VE (500 μM). **(B)** Double helix percentage. Bars with different letters indicated statistical significance ($p < 0.05$).

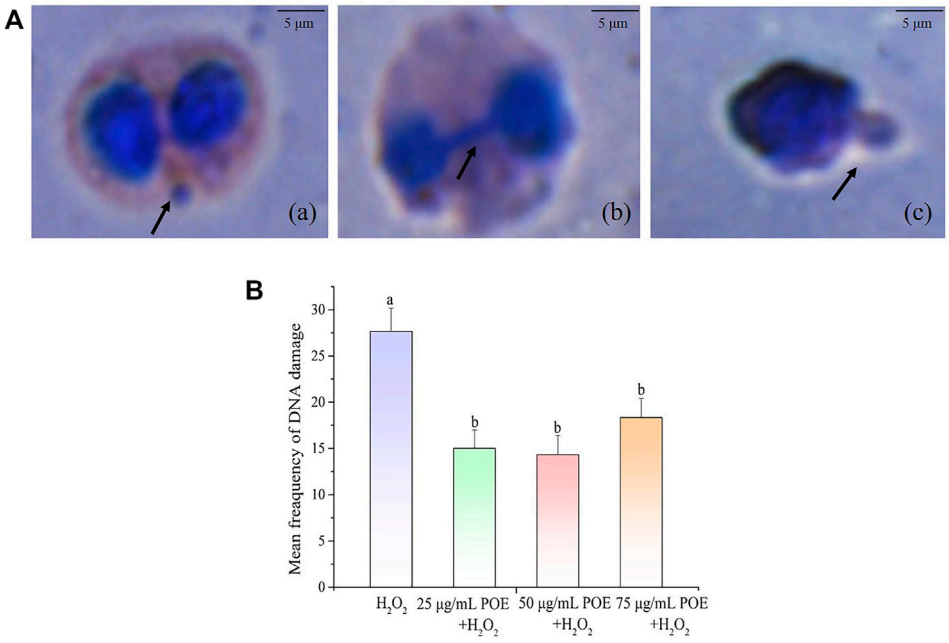

FIGURE 9
The effect of POE on DNA damage protection in lymphocyte. **(A)** Various forms of DNA damage seen as (a) MN, (b) nucleoplasmic ridge and (c) nuclear bud on cells treated with H_2O_2, the scale bar was 5 μm. **(B)** The mean frequency of DNA damage in human lymphocytes exposed to H_2O_2 (250 μM), H_2O_2 (250 μM) + POE (25, 50, and 75 μg/ml). Data were expressed as the mean ± SD ($n = 3$). Bars with different letters indicated statistical significance ($p < 0.05$).

3.9.2 Cytochalasin blocked micronucleus assay in lymphocytes

The DNA damage protection of POE was also investigated using the CBMN assay (Figure 9). As shown in Figure 9A, the forms of DNA damage were MN, nuclear buds and nucleoplasmic bridges and the mean frequency of DNA damage in the 25, 50, and 75 μg/ml treatment groups was 15 ± 2, 14.3 ± 2 and 18 ± 2, respectively, exhibiting a significant decrease in micronucleus frequency compared with the controls (27.7 ± 2.5) (Figure 9B; $p < 0.05$). The current study revealed that POE was able to improve the protection against DNA damage in lymphocytes.

4 Discussion

Endophytic fungi can produce medicinal ingredients with the same or similar functions as the host plant by long-term mutualism with host plants (Aly et al., 2011). *L. chuanxiong* Hort (Umbelliferae), a medicinal and edible plant, is commonly used for the promotion of good body health, anti-inflammation, antioxidation, neuron protection and blood vessel elasticity (Yuan et al., 2020). It has also been reported that the endophytic fungus *L. chuanxiong* can produce abundant secondary metabolites that might be applied for various purposes (Li et al., 2020; Cao et al., 2021). In our earlier study, *P. oxalate* isolated from *L. chuanxiong* exhibited strong antioxidant activity in chemical-based assays and *P. oxalate* extracts (POE) contained rich polyphenols such as ferulic acid, hesperidin and chlorogenic acid (Tang et al., 2021). In the present study, the biological activities of POE were further studied with regard to DNA damage protection effects and stress resistance properties.

Oxidative stress is closely related to the pathogenesis of various diseases such as cancer and neurological diseases (Xie et al., 2013). According to our results, we first found that POE could improve tolerance against oxidative stress (UV, 35°C and H_2O_2-induced) in *C. elegans* and the protection was not given in a concentration-dependent manner. In fact, only treatment with POE at 50 μg/ml significantly improved the worm's ability to respond to various stressors, while 75 μg/ml POE showed no effect.

The reason for this finding could be that POE has been proven to contain complex chemical components, while some compounds, such as caffeic acid, exhibit a hormetic response, eventually producing a deleterious effect when its content increases to greater than certain levels (Pietsch et al., 2011; Gutierrez-Zetina et al., 2021). Therefore, we hypothesized that POE concentrations of 50–75 μg/ml could represent the inflection point from which the beneficial effects induced by the POE in *C. elegans* would begin to decline. Furthermore, some authors have also observed that the survival of oxidative stress-induced *C. elegans* was significantly improved with increasing extract concentrations within a certain level, but decreased at higher concentrations (Dueñas et al., 2013; Duangjan et al., 2019b), which is consistent with our results. Notably, moderate-dose POE was found to enhance the mean lifespan of *C. elegans* under H_2O_2-mediated oxidative stress (increased by 17.12%), comparable to resveratrol (positive control) and some crude extracts such as polysaccharides (Lin et al., 2020). Moreover, ferulic acid, hesperidin, chlorogenic acid and other polyphenols with antioxidant activity have been reported (Gülçin, 2012; Li and Schluesener, 2017), while their content is very low in POE. However, some researchers have attributed the biological effect of the extract to the synergic and additive action among multiple chemicals (Vayndorf et al., 2013; Wang et al., 2018). Therefore, we proposed that the outstanding stress resistance activity of POE might be attributed to the interactions among various compounds of endophytic fungi instead of single secondary metabolites. However, it is inevitable that the study also had some limitations, such as lack of studies on biological effects of other single components of POE, requiringes further study in the future.

It is widely believed that compounds exert their biological effects not only because of their role as conventional antioxidants but also because of their ability to modulate the expression of related genes and act simultaneously on complex signalling pathways (Mansuri et al., 2014). In *C. elegans*, the *daf-16* gene encodes the transcription factor DAF-16, which is considered to be a crucial regulator in the insulin/IGF-1 signalling pathway and regulates stress-related gene expression in cells (Sen et al., 2020). Thus, extracts can increase the ability to prevent or repair stress damage in *C. elegans* by activating the daf-16 transcription factor and reducing IIS pathway activity (Ayuda-Durán et al., 2019). Moreover, *sod-3,4*, *ctl-1*, *ctl-2*, and *gst-4* are target genes of DAF-16, which encode proteins responsible for antioxidant defences (Murphy et al., 2003). In our study, the survival curve of the *daf-16* mutant showed no significant change after POE treatment, suggesting that the observed overexpression of these genes following treatment with POE could be related to the increase in the expression of DAF-16 (Gutierrez-Zetina et al., 2021). Therefore, POE improved the stress resistance of *C. elegans* by activating the daf-16 transcription factor, further promoting the expression of downstream target genes. Moreover, some antioxidant enzymes can reduce or eliminate excess free radicals in the body through biochemical reactions to maintain body stability. For example, superoxide dismutase-3 (SOD-3) catalyses the conversion of superoxide radicals to hydrogen peroxide and diatomic oxygen (Moreno-arriola et al., 2014). Thus, the overexpression of these target genes in *C. elegans* can also explain the decreased ROS level in the present study. In addition to DAF-16 signalling, SKN-1 is also an important regulator of oxidative stress resistance, mobilizing a conservative phase 2 detoxification response and promoting the activation of multiple genes in *C. elegans* (Tullet et al., 2008). However, there was no significant change in the expression of the *skn-1* gene in worms treated with POE, and POE treatment significantly increased the longevity of the *skn-1* mutant, indicating that it might not be conducive to POE-mediated resistance. In addition, another important gene was *hsf-1*. This gene encodes the thermal shock transcription factor HSF-1 which regulates the expression of various molecular chaperones (HSP-16.1 and HSP-16.2) to defend against thermal or oxidative stress (Hsu et al., 2003; Hsu et al., 2003; Kumsta et al., 2017). In the present study, overexpression of *hsf-1*, *hsp-16.1*, and *hsp-16.2* and the lack of effect of POE on the longevity of *hsf-1* mutants provide evidence that the HSF-1 pathway might be necessary for the antistress properties of POE. Accordingly, we hypothesized that the mechanism by which POE improves the stress resistance of *C. elegans* is that

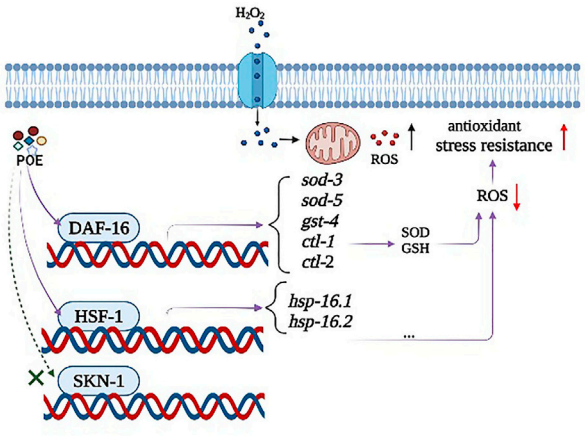

FIGURE 10
A possible model of the mechanism of action of POE-mediated stress resistance in *C. elegans*. POE alleviates the accumulation of ROS by activating the antioxidant defense system, and ultimately improves the anti-stress ability of *C. elegans*. The observed effects were mediated, at least in part, by the two master regulators DAF-16 and HSF-1 signaling pathways rather than SKN-1.

POE activates daf-16 to activate oxidative stress-inducible genes (*sod-3*, *sod-5*, *gst-4*, *ctl-1*, and *ctl-2*) and hsf-1 to promote the expression of downstream heat stress-inducible genes (*hsp-16.1* and *hsp-16.2*), rather than *skn-1* under stress conditions (Figure 10).

In general, an increase in lifespan is often accompanied by an increase in stress resistance in *C. elegans* (Murphy et al., 2003). Lipofuscin is an autofluorescent compound that accumulates gradually with the ageing of *C. elegans* (Clokey and Jacobson, 1986). However, our results showed that POE decreased lipofuscin levels in worms, while it did not extend life, indicating that POE showed some health benefits, but they were not sufficient to prolong the lifespan of worms because the lifespan is affected by multiple factors. Thus, the enhanced antistress ability of worms treated with POE found in the present study is not in line with lifespan extension, consistent with the observations of Duangjan et al. (2021) working. Moreover, lifespan analysis was used to evaluate the long-term toxicity of extracts (Romero-Márquez et al., 2022). Thus, the results also showed that POE has no long-term toxicity to worms. Ideally, there should be no harm to health indicators while showing some beneficial biological effects. However, some studies have measured only one or two indicators to evaluate the side effects of extracts on worms (Moliner et al., 2020; Duangjan et al., 2021). Therefore, this study comprehensively evaluated from four perspectives: long-term and short-term acute toxicity, reproduction, locomotion and growth. It demonstrated that POE has a beneficial effect on enhancing stress resistance without adverse effects.

There is a considerable amount of evidence revealing a correlation between DNA lesions and the occurrence of chronic and degenerative illness (Thanan et al., 2014); for example, DNA strand breaks caused by hydroxyl radical-induced persistent oxidative damage are suspected to be a major cause of carcinogenesis (Powell et al., 2005; Chandrasekara and Shahidi, 2011). In our study, the DNA damage protection capacity of POE was evaluated on pBR322 plasmid DNA when treated with Fenton's reagent. The hydroxyl radical generated by the Fenton reactant can attack DNA and cause a dramatic scission of the supercoiled (SC) DNA strand to open circular (OC) strands (Qian et al., 2008). Under such conditions, POE can may interfere with the reaction of $Fe^{2+}$with H_2O_2 or directly quench hydroxyl radicals by providing an electron due to its high antioxidant potential and further protect the supercoiled plasmid DNA against hydroxyl radicals (Chandrasekara and Shahidi, 2011). Moreover, a significant reduction in CBMN was observed in H_2O_2 treated lymphocytes when exposed to POE, which again demonstrated its antioxidant and DNA damage protection effects. This result is in line with previous studies in which *Aspergillus fumigatus* (Kaur et al., 2021) and *P. oxalicum* (Kaur et al., 2020) extracts showed DNA damage protection. Abundant phenolic compounds, viz; hesperetin, ferulic acid, alternariol and apigenin have been found in POE in our previous studies (Tang et al., 2021), which might be responsible for its biological effects. For example, hesperidin not only showed strong free radical scavenging ability *in vitro* (Wilmsen et al., 2005), but it also provided strong cellular antioxidant protection to alleviate oxidative stress and DNA damage (Sahu et al., 2013). Therefore, although the underlying mechanisms of DNA damage protection are not fully understood, the protective ability of POE could be related to the abundant secondary metabolites of *P. oxalate*.

5 Conclusion

In this study, the antioxidant activity and stress resistance of POE were investigated in *C. elegans*, and the protection activity against DNA damage of POE was evaluated by the pBR322 plasmid and lymphocytes. Our study revealed that POE might effectively counteract UV, 35°C and H_2O_2-induced oxidative stress without compromising the growth, reproduction and locomotion of *C. elegans*. The partial oxidative resistance properties of POE can be attributed to diminished intracellular ROS, as well as elevated activity of antioxidant enzymes (SOD CAT and GSH-P_X). The possible mechanism by which POE enhances stress resistance in *C. elegans* is mediated by activating the DAF-16 and HSF-1 pathways and promoting the overexpression of stress response genes. In addition, we found that POE had a

protective effect against Fenton reaction produced DNA nicking and H_2O_2-induced DNA damage in lymphocytes. In summary, this study is the first to report the antistress effects and DNA damage protection potential of endophytic fungus *P. oxalate* extracts, which could be a potential resource for treating oxidative stress and DNA damage diseases. However, the underlying mechanisms of the biological effects and more *in vivo* interventions with complex model organisms are needed to support the therapeutic potential of POE in the future.

Data availability statement

The original contributions presented in the study are included in the article/Supplementary Material, further inquiries can be directed to the corresponding authors.

Author contributions

ZT and YQ conceived and designed the experiments, performed the experiments, and prepared figures and/or tables. YW, WL, QW, NS, YX, HoC, TB, and QL performed the experiments, prepared figures and/or tables. HuC conceived and designed the experiments, drafted the work, approved the final draft. HY, SF, and CD analyzed the data, drafted the work. TB and HoC analyzed the data, revised it critically for important content.

Acknowledgments

We gratefully acknowledge financial support for this work from Enzyme Resources Sharing and Service Platform of Sichuan Province (Platform project number. 2020JDPT0018).

Conflict of interest

The authors declare that the research was conducted in the absence of any commercial or financial relationships that could be construed as a potential conflict of interest.

Publisher's note

All claims expressed in this article are solely those of the authors and do not necessarily represent those of their affiliated organizations, or those of the publisher, the editors and the reviewers. Any product that may be evaluated in this article, or claim that may be made by its manufacturer, is not guaranteed or endorsed by the publisher.

Supplementary material

The Supplementary Material for this article can be found online at: https://www.frontiersin.org/articles/10.3389/fphar.2022.983716/full#supplementary-material

References

Aly, A. H., Debbab, A., and Proksch, P. (2011). Fungal endophytes: Unique plant inhabitants with great promises. *Appl. Microbiol. Biotechnol.* 90, 1829–1845. doi:10.1007/s00253-011-3270-y

Aruoma, O. I. (1998). Free radicals, oxidative stress, and antioxidants in human health and disease. *J. Am. Oil Chem. Soc.* 75, 199–212. doi:10.1007/s11746-998-0032-9

Ayuda-Durán, B., González-Manzano, S., Miranda-Vizuete, A., Dueñas, M., Santos-Buelga, C., and González-Paramás, A. M. (2019). Epicatechin modulates stress-resistance in C. Elegans via insulin/IGF-1 signaling pathway. *PLoS ONE* 14, e0199483–26. doi:10.1371/journal.pone.0199483

Budiono, B., Elfita, E., Muharni, M., Yohandini, H., and Widjajanti, H. (2019). Antioxidant activity of Syzygium samarangense L. and their endophytic fungi. *Molekul* 14, 48–55. doi:10.20884/1.jm.2019.14.1.503

Cao, Y. M., Guo, D. Le, Jin, M. Y., Tan, L., Yang, T. L., Deng, F., et al. (2021). Two new nor-sesquiterpenoids from Fusarium tricinctum, an endophytic fungus isolated from Ligusticum chuanxiong. *Nat. Prod. Res.* 35, 3535–3539. doi:10.1080/14786419.2020.1712385

Carvalho-Silva, R., Pereira, A. C. F., Santos Alves, R. P. Dos, Guecheva, T. N., Henriques, J. A. P., Brendel, M., et al. (2016). DNA protection against oxidative damage using the hydroalcoholic extract of garcinia mangostana and alpha-mangostin. *Evid. Based. Complement. Altern. Med.* 2016, 3430405. doi:10.1155/2016/3430405

Chandrasekara, A., and Shahidi, F. (2011). Antiproliferative potential and DNA scission inhibitory activity of phenolics from whole millet grains. *J. Funct. Foods* 3, 159–170. doi:10.1016/j.jff.2011.03.008

Clokey, G. V., and Jacobson, L. A. (1986). The autofluorescent "lipofuscin granules" in the intestinal cells of *Caenorhabditis elegans* are secondary lysosomes. *Mech. Ageing Dev.* 35, 79–94. doi:10.1016/0047-6374(86)90068-0

Conning, D. M., and Phillips, J. C. (1986). Comparative metabolism of BHA, BHT and other phenolic antioxidants and its toxicological relevance. *Food Chem. Toxicol.* 24, 1145–1148. doi:10.1016/0278-6915(86)90300-5

da Silva, M. H. R., Cueva-Yesquén, L. G., Júnior, S. B., Garcia, V. L., Sartoratto, A., de Angelis, D. de F., et al. (2020). Endophytic fungi from passiflora incarnata: An antioxidant compound source. *Arch. Microbiol.* 202, 2779–2789. doi:10.1007/s00203-020-02001-y

Denis, M. C., Furtos, A., Dudonné, S., Montoudis, A., Garofalo, C., Desjardins, Y., et al. (2013). Apple peel polyphenols and their beneficial actions on oxidative stress and inflammation. *PLoS ONE* 8, e53725. doi:10.1371/journal.pone.0053725

Duangjan, C., Rangsinth, P., Gu, X., Wink, M., and Tencomnao, T. (2019a). Lifespan extending and oxidative stress resistance properties of a leaf extracts from *anacardium occidentale* L. In caenorhabditis elegans. *Oxidative Med. Cell. Longev.* 2019, 16. doi:10.1155/2019/9012396

Duangjan, C., Rangsinth, P., Gu, X., Zhang, S., Wink, M., and Tencomnao, T. (2019b). Glochidion zeylanicum leaf extracts exhibit lifespan extending and oxidative stress resistance properties in *Caenorhabditis elegans* via DAF-16/FoxO and SKN-1/Nrf-2 signaling pathways. *Phytomedicine* 64, 153061. doi:10.1016/j.phymed.2019.153061

Duangjan, C., Rangsinth, P., Zhang, S., Gu, X., Wink, M., and Tencomnao, T. (2021). Vitis vinifera leaf extract protects against glutamate-induced oxidative toxicity in HT22 hippocampal neuronal cells and increases stress resistance properties in Caenorhabditis elegans. *Front. Nutr.* 8, 634100–634115. doi:10.3389/fnut.2021.634100

Dubois, C., Lecomte, C., Ruys, S. P., Kuzmic, M., Della-Vedova, C., Dubourg, N., et al. (2018). Precoce and opposite response of proteasome activity after acute or chronic exposure of *C. elegans* to γ-radiation. *Sci. Rep.* 8, 11349. doi:10.1038/s41598-018-29033-1

Dueñas, M., Surco-Laos, F., González-Manzano, S., González-Paramás, A. M., Gómez-Orte, E., Cabello, J., et al. (2013). Deglycosylation is a key step in biotransformation and lifespan effects of quercetin-3-O-glucoside in *Caenorhabditis elegans*. *Pharmacol. Res.* 76, 41–48. doi:10.1016/j.phrs.2013.07.001

Fenech, M., Crott, J., Turner, J., and Brown, S. (1999). Necrosis, apoptosis, cytostasis and DNA damage in human lymphocytes measured simultaneously within the cytokinesis-block micronucleus assay: Description of the method and results for hydrogen peroxide. *Mutagenesis* 14, 605–612. doi:10.1093/mutage/14.6.605

Gülçin, I. (2012). Antioxidant activity of food constituents: An overview. *Arch. Toxicol.* 86, 345–391. doi:10.1007/s00204-011-0774-2

Gutierrez-Zetina, S. M., González-Manzano, S., Ayuda-Durán, B., Santos-Buelga, C., and González-Paramás, A. M. (2021). Caffeic and dihydrocaffeic acids promote longevity and increase stress resistance in caenorhabditis elegans by modulating expression of stress-related genes. *Molecules* 26, 1517. doi:10.3390/molecules26061517

Herndon, L. A., Schmeissner, P. J., Dudaronek, J. M., Brown, P. A., Listner, K. M., Sakano, Y., et al. (2002). Stochastic and genetic factors influence tissue-specific decline in ageing *C. elegans*. *Nature* 419, 808–814. doi:10.1038/nature01135

Hsu, A., Murphy, C. T., and Kenyon, C. (2003). Regulation of aging and age-related disease by DAF-16 and heat-shock factor. *Science* 300, 1142–1145. doi:10.1126/science.1083701

Huang, W. Y., Cai, Y. Z., Xing, J., Corke, H., and Sun, M. (2007). A potential antioxidant resource: Endophytic fungi from medicinal plants. *Econ. Bot.* 61, 14–30. doi:10.1663/0013-0001(2007)61[14:APAREF]2.0.CO;2

Jeong, J. B., Park, J. H., Lee, H. K., Ju, S. Y., Hong, S. C., Lee, J. R., et al. (2009). Protective effect of the extracts from Cnidium officinale against oxidative damage induced by hydrogen peroxide via antioxidant effect. *Food Chem. Toxicol.* 47, 525–529. doi:10.1016/j.fct.2008.11.039

Kaur, N., Arora, D. S., Kaur, S., Kumar, A., and Kaur, S. (2021). Antiproliferative and oxidative damage protection activities of endophytic fungi Aspergillus fumigatus and Chaetomium globosum from moringa oleifera lam. *Appl. Biochem. Biotechnol.* 193, 3570–3585. doi:10.1007/s12010-021-03625-6

Kaur, R., Kaur, J., Kaur, M., Kalotra, V., Chadha, P., Kaur, A., et al. (2020). An endophytic Penicillium oxalicum isolated from Citrus limon possesses antioxidant and genoprotective potential. *J. Appl. Microbiol.* 128, 1400–1413. doi:10.1111/jam.14553

Kumsta, C., Chang, J. T., Schmalz, J., and Hansen, M. (2017). Hormetic heat stress and HSF-1 induce autophagy to improve survival and proteostasis in C. Elegans. *Nat. Commun.* 8, 14337. doi:10.1038/ncomms14337

Li, C., and Schluesener, H. (2017). Health-promoting effects of the citrus flavanone hesperidin. *Crit. Rev. Food Sci. Nutr.* 57, 613–631. doi:10.1080/10408398.2014.906382

Li, S., Chen, J. F., Qin, L. L., Li, X. H., Cao, Z. X., Gu, Y. C., et al. (2020). Two new sesquiterpenes produced by the endophytic fungus Aspergillus fumigatus from Ligusticum wallichii. *J. Asian Nat. Prod. Res.* 22, 138–143. doi:10.1080/10286020.2018.1540606

Li, Y. L., Xin, X. M., Chang, Z. Y., Shi, R. J., Miao, Z. M., Ding, J., et al. (2015). The endophytic fungi of salvia miltiorrhiza bge.f. alba are a potential source of natural antioxidants. *Bot. Stud.* 56, 5. doi:10.1186/s40529-015-0086-6

Lin, C., Su, Z., Luo, J., Jiang, L., Shen, S., Zheng, W., et al. (2020). Polysaccharide extracted from the leaves of Cyclocarya paliurus (Batal.) Iljinskaja enhanced stress resistance in *Caenorhabditis elegans* via skn-1 and hsf-1. *Int. J. Biol. Macromol.* 143, 243–254. doi:10.1016/j.ijbiomac.2019.12.023

Lin, C., Zhang, X., Xiao, J., Zhong, Q., Kuang, Y., Cao, Y., et al. (2019). Effects on longevity extension and mechanism of action of carnosic acid in: *Caenorhabditis elegans*. *Food Funct.* 10, 1398–1410. doi:10.1039/c8fo02371a

Liu, Q., Zhang, T., Hong, Y., Li, Y., Li, W., Gao, C., et al. (2022). Composition, antioxidant activity and DNA damage protection effect of bound phenolics from ottelia acuminata. *Sci. Technol. food industry* 43, 7. doi:10.13386/j.issn1002-0306.2021070217

Ludwig-Müller, J. (2015). Plants and endophytes: Equal partners in secondary metabolite production? *Biotechnol. Lett.* 37, 1325–1334. doi:10.1007/s10529-015-1814-4

Mansuri, M. L., Parihar, P., Solanki, I., and Parihar, M. S. (2014). Flavonoids in modulation of cell survival signalling pathways. *Genes Nutr.* 9, 400. doi:10.1007/s12263-014-0400-z

Moliner, C., Barros, L., Dias, M. I., López, V., Langa, E., Ferreira, I. C. F. R., et al. (2018). Edible flowers of tagetes erecta l. As functional ingredients: Phenolic composition, antioxidant and protective effects on caenorhabditis elegans. *Nutrients* 10, E2002. doi:10.3390/nu10122002

Moliner, C., López, V., Barros, L., Dias, M. I., Ferreira, I. C. F. R., Langa, E., et al. (2020). Rosemary flowers as edible plant foods: Phenolic composition and antioxidant properties in caenorhabditis elegans. *Antioxidants* 9, E811–11. doi:10.3390/antiox9090811

Mookherjee, A., Mitra, M., Kutty, N. N., Mitra, A., and Maiti, M. K. (2020). Characterization of endo-metabolome exhibiting antimicrobial and antioxidant activities from endophytic fungus Cercospora sp. PM018. *South Afr. J. Bot.* 134, 264–272. doi:10.1016/j.sajb.2020.01.040

Moreno-arriola, E., Cárdenas-rodríguez, N., Coballase-urrutia, E., Pedraza-chaverri, J., Carmona-aparicio, L., and Ortega-cuellar, D. (2014). *Caenorhabditis elegans* : A useful model for studying metabolic disorders in which oxidative stress is a contributing factor. *Oxid. Med. Cell Longev.* 2014, 705253. doi:10.1155/2014/705253

Murphy, C. T., McCarroll, S. A., Bargmann, C. I., Fraser, A., Kamath, R. S., Ahringer, J., et al. (2003). Genes that act downstream of DAF-16 to influence the lifespan of *Caenorhabditis elegans*. *Nature* 424, 277–283. doi:10.1038/nature01789

Onken, B., and Driscoll, M. (2010). Metformin induces a dietary restriction-like state and the oxidative stress response to extend *C. elegans* healthspan via AMPK, LKB1, and SKN-1. *PLoS ONE* 5, e8758. doi:10.1371/journal.pone.0008758

Pietsch, K., Saul, N., Chakrabarti, S., Stürzenbaum, S. R., Menzel, R., and Steinberg, C. E. W. (2011). Hormetins, antioxidants and prooxidants: Defining quercetin-caffeic acid- and rosmarinic acid-mediated life extension in *C. elegans*. *Biogerontology* 12, 329–347. doi:10.1007/s10522-011-9334-7

Powell, C. L., Swenberg, J. A., and Rusyn, I. (2005). Expression of base excision DNA repair genes as a biomarker of oxidative DNA damage. *Cancer Lett.* 229, 1–11. doi:10.1016/j.canlet.2004.12.002

Prasanth, M. I., Brimson, J. M., Chuchawankul, S., Sukprasansap, M., and Tencomnao, T. (2019). Antiaging, stress resistance, and neuroprotective efficacies of cleistocalyx nervosum var. paniala fruit extracts using caenorhabditis elegans model. *Oxid. Med. Cell. Longev.* 2019, 7024785. doi:10.1155/2019/7024785

Qian, Z. J., Jung, W. K., Byun, H. G., and Kim, S. K. (2008). Protective effect of an antioxidative peptide purified from gastrointestinal digests of oyster, *Crassostrea gigas* against free radical induced DNA damage. *Bioresour. Technol.* 99, 3365–3371. doi:10.1016/j.biortech.2007.08.018

Romero-Márquez, J. M., Navarro-Hortal, M. D., Jiménez-Trigo, V., Vera-Ramírez, L., Forbes-Hernández, T. J., Esteban-Muñoz, A., et al. (2022). An oleuropein rich-olive (Olea europaea L.) leaf extract reduces β-amyloid and tau proteotoxicity through regulation of oxidative- and heat shock-stress responses in *Caenorhabditis elegans*. *Food Chem. Toxicol.* 162, 112914. doi:10.1016/j.fct.2022.112914

Sahu, B. D., Kuncha, M., Sindhura, G. J., and Sistla, R. (2013). Hesperidin attenuates cisplatin-induced acute renal injury by decreasing oxidative stress, inflammation and DNA damage. *Phytomedicine* 20, 453–460. doi:10.1016/j.phymed.2012.12.001

Saul, N., Pietsch, K., Menzel, R., and Steinberg, C. E. W. (2008). Quercetin-mediated longevity in *Caenorhabditis elegans*: Is DAF-16 involved? *Mech. Ageing Dev.* 129, 611–613. doi:10.1016/j.mad.2008.07.001

Sen, I., Zhou, X., Chernobrovkin, A., Puerta-Cavanzo, N., Kanno, T., Salignon, J., et al. (2020). DAF-16/FOXO requires Protein Phosphatase 4 to initiate transcription of stress resistance and longevity promoting genes. *Nat. Commun.* 11, 138. doi:10.1038/s41467-019-13931-7

Strobel, G. A. (2003). Endophytes as sources of bioactive products. *Microbes Infect.* 5, 535–544. doi:10.1016/S1286-4579(03)00073-X

Strobel, G., Daisy, B., Castillo, U., and Harper, J. (2004). Natural products from endophytic microorganisms. *J. Nat. Prod.* 67, 257–268. doi:10.1021/np030397v

Tang, Z., Qin, Y., Chen, W., Zhao, Z., Lin, W., Xiao, Y., et al. (2021). Diversity, chemical constituents, and biological activities of endophytic fungi isolated from Ligusticum chuanxiong Hort. *Front. Microbiol.* 12, 771000–771014. doi:10.3389/fmicb.2021.771000

Thanan, R., Oikawa, S., Hiraku, Y., Ohnishi, S., Ma, N., Pinlaor, S., et al. (2014). Oxidative stress and its significant roles in neurodegenerative diseases and cancer. *Int. J. Mol. Sci.* 16, 193–217. doi:10.3390/ijms16010193

Tiwari, S., Singh, S., Pandey, P., Saikia, S. K., Negi, A. S., Gupta, S. K., et al. (2014). Isolation, structure determination, and antiaging effects of 2, 3-pentanediol from endophytic fungus of Curcuma amada and docking studies. *Protoplasma* 251, 1089–1098. doi:10.1007/s00709-014-0617-0

Tullet, J. M. A., Hertweck, M., An, J. H., Baker, J., Hwang, J. Y., Liu, S., et al. (2008). Direct inhibition of the longevity-promoting factor SKN-1 by insulin-like signaling in *C. elegans*. *Cell* 132, 1025–1038. doi:10.1016/j.cell.2008.01.030

Vayndorf, E. M., Lee, S. S., and Liu, R. H. (2013). Whole apple extracts increase lifespan, healthspan and resistance to stress in *Caenorhabditis elegans*. *J. Funct. Foods* 5, 1236–1243. doi:10.1016/j.jff.2013.04.006

Wang, H., Liu, J., Li, T., and Liu, R. H. (2018). Blueberry extract promotes longevity and stress tolerance via DAF-16 in *Caenorhabditis elegans*. *Food Funct.* 9, 5273–5282. doi:10.1039/c8fo01680a

Wang, Q., Yang, F., Guo, W., Zhang, J., Xiao, L., Li, H., et al. (2014). *Caenorhabditis elegans* in Chinese medicinal studies: Making the case for aging and neurodegeneration. *Rejuvenation Res.* 17, 205–208. doi:10.1089/rej.2013.1512

Wilmsen, P. K., Spada, D. S., and Salvador, M. (2005). Antioxidant activity of the flavonoid hesperidin in chemical and biological systems. *J. Agric. Food Chem.* 53, 4757–4761. doi:10.1021/jf0502000

Xiao, L., Li, H., Zhang, J., Yang, F., Huang, A., Deng, J., et al. (2014). Salidroside protects caenorhabditis elegans neurons from polyglutamine-mediated toxicity by reducing oxidative stress. *Molecules* 19, 7757–7769. doi:10.3390/molecules19067757

Xie, H., Hou, S., Jiang, J., Sekutowicz, M., Kelly, J., and Bacskai, B. J. (2013). Rapid cell death is preceded by amyloid plaque-mediated oxidative stress. *Proc. Natl. Acad. Sci. U. S. A.* 110, 7904–7909. doi:10.1073/pnas.1217938110

Xu, W., Chi, L., Xu, R., Ke, Y., Luo, C., Cai, J., et al. (2005). Increased production of reactive oxygen species contributes to motor neuron death in a compression mouse model of spinal cord injury. *Spinal Cord.* 43, 204–213. doi:10.1038/sj.sc.3101674

Yuan, X., Han, B., Feng, Z. M., Jiang, J. S., Yang, Y. N., and Zhang, P. C. (2020). Chemical constituents of Ligusticum chuanxiong and their anti-inflammation and hepatoprotective activities. *Bioorg. Chem.* 101, 104016. doi:10.1016/j.bioorg.2020.104016

Zhuang, S., Huang, B., Zeng, Y., Liu, M., Jiahui, X. U., and Liu, J. (2016). Influence of resveratrol on oxidative stress level and mitochondrial function of vitrified-thawed mature oocytes in mice. *China Med. Her.* 11, 27–30.

frontiers | Frontiers in Pharmacology

TYPE Original Research
PUBLISHED 30 August 2022
DOI 10.3389/fphar.2022.952337

OPEN ACCESS

EDITED BY
Kok Yong Chin,
National University of Malaysia, Malaysia

REVIEWED BY
Tina Didari,
Tehran University of Medical Sciences, Iran
Busra Dincer,
Erzincan Binali Yıldırım University Erzincan, Turkey

*CORRESPONDENCE
Al-Shaimaa F. Ahmed,
Shaimaa.faissal@minia.edu.eg

†These authors share first authorship

SPECIALTY SECTION
This article was submitted to Ethnopharmacology, a section of the journal Frontiers in Pharmacology

RECEIVED 25 May 2022
ACCEPTED 01 August 2022
PUBLISHED 30 August 2022

CITATION
Matouk AI, El-Daly M, Habib HA, Senousy S, Naguib Abdel Hafez SM, Kasem AW, Almalki WH, Alzahrani A, Alshehri A and Ahmed A-SF (2022), Protective effects of menthol against sepsis-induced hepatic injury: Role of mediators of hepatic inflammation, apoptosis, and regeneration. *Front. Pharmacol.* 13:952337. doi: 10.3389/fphar.2022.952337

Protective effects of menthol against sepsis-induced hepatic injury: Role of mediators of hepatic inflammation, apoptosis, and regeneration

Asmaa I. Matouk[1], Mahmoud El-Daly[1†], Heba A. Habib[1], Shaymaa Senousy[1], Sara Mohamed Naguib Abdel Hafez[2], AlShaimaa W. Kasem[3], Waleed Hassan Almalki[4], Abdulaziz Alzahrani[5], Ahmed Alshehri[5] and Al-Shaimaa F. Ahmed[1*]

[1]Department of Pharmacology and Toxicology, Faculty of Pharmacy, Minia University, Minya, Egypt, [2]Department of Pathology, Faculty of Medicine, Minia University, Minya, Egypt, [3]Department of Histology and Cell Biology, Faculty of Medicine, Minia University, Minya, Egypt, [4]Department of Pharmacology and Toxicology, Umm Al-Qura University, Makkah, Saudi Arabia, [5]Department of Pharmacology and Toxicology, College of Clinical Pharmacy, AlBaha University, Al Bahah, Saudi Arabia, [6]Department of Pharmacology and Toxicology, Faculty of Pharmacy, Northern Border University, Rafha, Saudi Arabia

Liver dysfunction in sepsis is a major complication that amplifies multiple organ failure and increases the risk of death. Inflammation and oxidative stress are the main mediators in the pathophysiology of sepsis. Therefore, we investigated the role of menthol, a natural antioxidant, against sepsis-induced liver injury in female Wistar rats. Sepsis was induced by cecal ligation and puncture (CLP). Menthol (100 mg/kg) was given intragastric 2 h after CLP. Blood samples and liver tissues were collected 24 h after surgery. Menthol significantly ($p < 0.05$) attenuated the sepsis-induced elevation in serum liver enzymes and improved the hepatic histopathological changes. Menthol treatment significantly ($p < 0.05$) decreased hepatic levels of tumor necrosis factor-alpha, malondialdehyde, total nitrite, and cleaved caspase-3. It restored the hepatic levels of superoxide dismutase and reduced glutathione. Additionally, menthol significantly ($p < 0.05$) increased hepatic levels of B-cell lymphoma 2 (Bcl-2); an anti-apoptotic factor, and proliferating cell nuclear antigen (PCNA), a biomarker of regeneration and survival. Our results showed the therapeutic potential of menthol against liver injury induced by sepsis.

KEYWORDS

clp, hepatoprotection, tNF-alpha, PCNA, apoptosis

1 Introduction

Sepsis is a global health issue and a leading cause of death, especially in patients with low immunity, including children, the elderly, immunocompromised individuals, and intensive care unit patients (Fleischmann et al., 2016; Rudd et al., 2017; Dou et al., 2019a). Sepsis is a condition of life-threatening organ dysfunction mainly due to the host's immune response to infections (Seymour et al., 2016). Sepsis induces damage to many organs, including the lungs, heart, and liver. However, the liver is more vulnerable and often affected earlier by sepsis (Saini et al., 2022). Hepatic dysfunction during sepsis incidence ranges from 34% to 46% and is considered a powerful predictor of sepsis-related mortality. The risk of death due to sepsis-induced hepatic failure is 54%–68% (Strnad et al., 2017; Woznica et al., 2018), which is higher than the death rate due to sepsis-induced lung dysfunction (Yan and Li, 2014). The liver is a key component of the primary defense line against infection. Early in sepsis, Kupffer cells play an essential role in the removal of bacteria and endotoxins through the release of proinflammatory cytokines such as interleukin (IL)-1β, IL-6, IL-18, and tumor necrosis factor-alpha (TNF-α) (Traeger et al., 2010). Although these cytokines help eradicate the pathogens, they also provoke liver damage and stimulate the release of other inflammatory mediators in a process known as a cytokine storm. This eventually leads to a systemic inflammatory response and multiple organ damage (Lelubre and Vincent, 2018; Woznica et al., 2018). Sepsis leads to a profound reduction in hepatic functions, including the dysregulation of carbohydrate, lipid, and protein metabolism, decreased synthesis and release of bile and coagulation factors, impaired defense against pathogens, increased production of inflammatory mediators, and the amplification of other organs' failure (Srivastava and Gimson, 2013; Yan and Li, 2014; Strnad et al., 2017). Understanding the underlying mechanisms of hepatic dysfunction in sepsis is still a challenge. The pathogenesis of sepsis-induced liver injury involves many factors, including bacterial toxins, septic shock induced-hypotension, hepatic hypoperfusion (Spapen, 2008; Henrion, 2012), impairment of the endothelial function of hepatic microvasculature (La Mura et al., 2013), production of reactive oxygen species (ROS), and proinflammatory cytokines (Strnad et al., 2017). Increased ROS production and inflammation remain the hallmarks of hepatic damage in sepsis. Thus, efforts to control sepsis-induced liver injury focused on drugs with antioxidant and anti-inflammatory effects to prevent multiple organ damage and decrease mortality (Ahmed et al., 2020; Al-Kadi et al., 2020).

Menthol, the main component of *Mentha arvensis L. (Lamiaceae) and Mentha piperita L.* essential oil, is a naturally occurring monoterpene widely employed in different pharmaceutical formulations as a flavoring agent and an oral care product. Menthol has multiple biological activities, including antinociceptive (Pergolizzi et al., 2018), antispasmodic (Amato et al., 2014), local anesthetic (Galeotti et al., 2001), antibacterial, and antifungal effects (Sabzghabaee et al., 2011). Accumulating evidence showed that menthol modulates the production of TNF-α and interleukins, decreases ROS generation, and enhances the antioxidant enzyme activity in different animal models (Janbaz and Gilani, 2002; Rozza et al., 2014; Bastaki et al., 2018; Rozza et al., 2021). The anti-inflammatory and antioxidant effects of menthol proved protective against paracetamol- and carbon tetrachloride (CCl_4)-induced hepatic toxicity (Janbaz and Gilani, 2002), acetic acid-induced colitis (Bastaki et al., 2018), gastric ulceration (Rozza et al., 2013; Rozza et al., 2014), Parkinson's disease (Du et al., 2020), skin wounds (Rozza et al., 2021), and Freund adjuvant-induced peripheral inflammation (Hilfiger et al., 2021). Menthol, a natural product with minimal side effects, is available at low costs and possesses hepatoprotective effects. However, whether or not menthol can alleviate sepsis-induced liver injury has not yet been studied. Hence, this study aimed to explore the therapeutic potential and possible protective mechanisms of menthol against sepsis-induced hepatic dysfunction.

2 Materials and methods

2.1 Animals and drugs

Female Wistar rats (8–10 weeks old) weighing (200–220 g) were obtained from El-Nahda University Animal House (Beni-Suef, Egypt) for this study. Rats were housed under specific pathogen-free conditions on a 12-hrs light-dark cycle with free access to regular rat chow (El-Nasr Company, Abou Zaabal, Cairo, Egypt) and tap water. Rats were left for 1 week as an acclimatization period prior to the experiment. All experimental procedures were approved by The Commission on the Ethics of Scientific Research, Faculty of Pharmacy, Minia University, Egypt (ES02/2020). Menthol was purchased from (Sigma-Aldrich Inc., United States).

2.2 Induction of sepsis

Cecal ligation and puncture (CLP), a precise and commonly used sepsis model, was used to induce sepsis as previously prescribed (Nemzek et al., 2008; Ahmed et al., 2020). Rats were anesthetized with ketamine (50 mg/kg) and xylazine (10 mg/kg). A longitudinal abdominal incision was made in the lower left quadrant of the body to expose the cecum. 0.3-mm silk surgical suture thread was used to ligate the cecum just below the ileo-cecal valve, and the ligated part was punctured

twice with an 18-gauge needle to ensure the same degree of severity of sepsis in all groups. The percentage of the ligated portion (75%) was kept constant in all groups. Finally, the cecum was gently returned to its place in the abdominal cavity, and the incision was sutured. All animals received normal saline [3 ml/100 g, subcutaneous (S.C.)] to help for resuscitation after surgery. After the surgical procedure, the rats exhibited symptoms of illness, including piloerection, diarrhea, and malaise according to Morton and Griffiths (Morton and Griffiths, 1985). In addition, similar to our previous studies (Ibrahim et al., 2020a; Al-Kadi et al., 2020; Al-Kadi et al., 2021), ischemia and inflammation in the ligated cecum confirmed the induction of sepsis in CLP rats (Supplementary Figure S1).

2.3 Survival study

Female Wistar rats (200–220 g) were randomly assigned to four groups (n = 10, each): sham group, the rats were exposed to all the surgical procedures for the induction of sepsis, except for the ligation and puncture steps. They were given vehicle (1 ml water/kg, I. G) 2 hours after surgery; sham-menthol group, the rats of this group are sham rats that received intragastric (I.G.) menthol (100 mg/kg) dissolved in water (L ml/kg); sepsis group, the rats of this group were exposed to CLP then received the vehicle (1 ml water/kg, I. G) 2 h after CLP surgery; and sepsis-menthol group, the rats of this group were exposed to CLP then received menthol (100 mg/kg, I. G) 2 h after the surgery. All rats were monitored for 7 days to assess the mortality rate. The sample size for the survival analysis was determined according to previous studies in our lab (Ibrahim et al., 2020a; Al-Kadi et al., 2021) and by others (Chen et al., 2021).

2.4 Experimental groups

Thirty female rats were randomly divided into four groups: Group 1 (sham group, n = 6), Group 2 (sham-menthol, n = 6), Group 3 (sepsis group, n = 12), and Group 4 (sepsis-menthol, n = 6). All animals received either vehicle (Group 1 and 3) or menthol (100 mg/kg, I. G; Group 2 and 4) 2 h after surgery to ensure the complete recovery from anesthesia and allow I.G. administration. The time of the drug intervention was chosen based on our preliminary study and previous reports (Aksoy et al., 2014; Ibrahim et al., 2020a; Al-Kadi et al., 2020; Al-Kadi et al., 2021). Our preliminary studies showed the best survival results in the CLP septic rats that received 100 mg/kg menthol (Supplementary Figure S2). Furthermore, this dose was in the range previously reported to have anti-inflammatory, antioxidant, and anti-apoptotic effects in other models (Janbaz and Gilani, 2002; Ghasemi-Pirbaluti et al., 2017; Hilfiger et al., 2021).

Rats of all groups were sacrificed 24 h after surgery and blood samples were then collected by cardiac puncture. A segment of the medial lobe from each animal's liver was fixed in 10% buffered formalin solution for 24 h, and prepared for histopathological and immunohistochemical examination. Other liver samples were flash-frozen in liquid nitrogen and stored at -80°C for further assessments.

2.5 Assessment of hepatic function

For early detection of hepatic dysfunction, serum levels of Glutamic–Pyruvic Transaminase (GPT; ALT) (EC2.6.1.2) and Glutamic–Oxaloacetic Transaminase (GOT; AST) (EC2.6.1.1) were determined by colorimetric assay kits (Diamond Diagnostics, Cairo, Egypt) based on the method of Reitman and Frankel as per the manufacturer's instructions (Reitman and Frankel, 1957). The measuring range of ALT and AST were up to 94 and 89 U/L, respectively. For quantitation of AST, the samples were diluted ten times, then the results were multiplied by 10.

2.6 Assessment of hepatic histopathological changes

Specimens from formalin-fixed liver tissues were processed for routine paraffin embedding. Sections (5-μm-thickness) were stained with haematoxylin and eosin (H&E). A CCD digital camera adapted to BX51 microscope (Olympus, Japan) was used to capture images at ×400 magnification. ImageJ software was used for semi-quantitative analysis. The parameters used to assess histopathological changes included dilated central veins, sinusoidal congestion, hepatocyte necrosis, and hepatocyte fatty changes (Jensen, 2008). All histopathological assessments were done by a histopathologist blind to the treatment.

2.7 Assessment of hepatic oxidative stress and antioxidant enzyme activity

To assess the liver's oxidative stress, levels of malondialdehyde (MDA), a product of lipid peroxidation and an index of oxidative stress, were calorimetrically measured based on the Buege method (Buege and Aust, 1978). Levels of total nitrite were determined calorimetrically based on the Griess assay method previously prescribed (Moorcroft et al., 2001). To assess the antioxidant enzyme activity, hepatic reduced glutathione (GSH) levels were determined by colorimetric measurement of 5-thio-2-nitrobenzoic acid, which is produced after the reduction of Ellman's reagent (5,5-dithio-bis-2-nitrobenzoic acid) by the sulfahydryl (–SH) group of GSH (Beutler et al., 1963). Hepatic superoxide dismutase (SOD)

levels were determined according to a previously described method (Marklund and Marklund, 1974) by measuring the amount of SOD enzyme that inhibits the autoxidation of pyrogallol by 50%.

2.8 Immunohistochemical determination of hepatic tumor necrosis factor-alpha, cleaved caspase-3, B-cell lymphoma 2, and proliferating cell nuclear antigen

Liver sections (5-μm-thick) were obtained from representative formalin-fixed, paraffin-embedded blocks and transferred to adhesive slides. After the deparaffinization and dehydration of the sections, endogenous peroxidase activity was blocked by incubation with hydrogen peroxide. Microwave treatment in sodium citrate buffer, pH 6, was used for antigen retrieval. Tissue sections were then incubated with rabbit anti-cleaved caspase-3 (catalog number A19664, ABclonal, MA, United States), mouse anti-proliferating cell nuclear antigen (PCNA) (catalog number A9909, ABclonal, MA, United States), rabbit anti-B-cell lymphoma 2 (Bcl-2) (catalog number A19693, ABclonal, MA, United States), or rabbit anti-TNF-α (catalog number A11534, ABclonal, MA, United States). A negative control experiment was done using the same steps but without the addition of the primary antibody to ensure the reaction specificity. Sections were then incubated with a biotinylated secondary antibody for 30 min at room temperature. An avidin-biotin complex immunoperoxidase system was used to visualize the reaction using 3,3′-diaminobenzidine (DAB) as a chromogen. Sections were counterstained using hematoxylin, then dehydrated, cleared, and mounted with distyrene, plasticizer, and xylene (DPX). The mean surface area fractions of anti-cleaved caspase-3, PCNA, Bcl-2, and TNF-α immuno-positive cells were measured using ImageJ software (version 1.51 k, Wayne Rasband, National Institutes of Health, United States) by a pathologist blind to the experimental groups.

2.9 Statistical analysis of data

All statistical analyses were performed using GraphPad Prism (version 7.0; San Diego, CA, United States). Values were expressed as mean ± S.E.M. Shapiro-Wilk normality test was used to test the normality of the data. All data followed a normal distribution. One-way analysis of variance (ANOVA) test was used to test the significance of the results. Tukey's post hoc test was used for multiple comparisons. Survival analysis was performed using the Log-rank (Mantel-Cox) test. The results were considered statistically significant if the probability (p)-values were <0.05. Correlation analysis was carried out by calculating the Pearson correlation coefficient (r). If r <|0.3|, the correlation is considered weak. If r is between |0.3| and |0.7|, this indicates a moderate correlation. If r >|0.7|, this indicates a strong correlation.

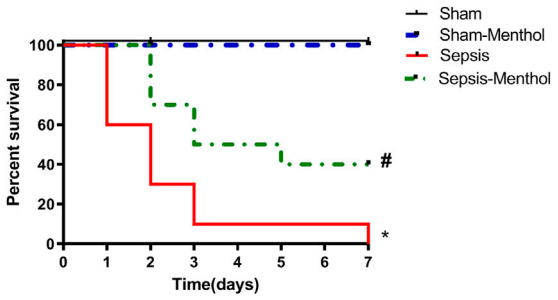

FIGURE 1
Effect of menthol on CLP-induced mortality. Induction of sepsis by CLP model resulted in 0% survival at the end of the 7th day. Treatment with menthol (100 mg/kg, I. G) 2 h after CLP improved the survival by 40% at the end of the 7th day. The sham group and sham-menthol (100 mg/kg, I. G) group had no mortality throughout the study. Data are presented as a percentage of survival of rats (n = 10 per group). * significant difference from the sham group at p ˂0.05. # significant difference from the sepsis group at p ˂0.05.

3 Results

3.1 Menthol improved survival in septic rats

Sepsis induction by CLP resulted in 40%, 70%, and 90% mortality by the end of the first, second-, and third-day post-surgery, respectively. On the other hand, administration of menthol (100 mg/kg, I. G) 2 h post CLP resulted in the survival of 100% of rats after the first day, 70% after the second day, and 50% after the third day. All rats in the sham and sham-menthol groups survived the entire seven-day study period. Survival analysis illustrated a significant difference (p < 0.05) between the sham group and the sepsis group, as well as between the menthol-treated septic rats and the untreated septic rats (Figure 1).

3.2 Menthol attenuated sepsis-induced hepatic injury

The serum levels of the cytoplasmic liver enzymes, ALT (Figure 2A) and AST (Figure 2B), were significantly (p ˂0.05) elevated in the untreated sepsis group when compared with sham group. Treating CLP rats with menthol significantly (p ˂0.05) attenuated the sepsis-induced elevation in serum AST and ALT levels. As shown in Figure 2, tissue sections from the sham group

10.3389/fphar.2022.952337

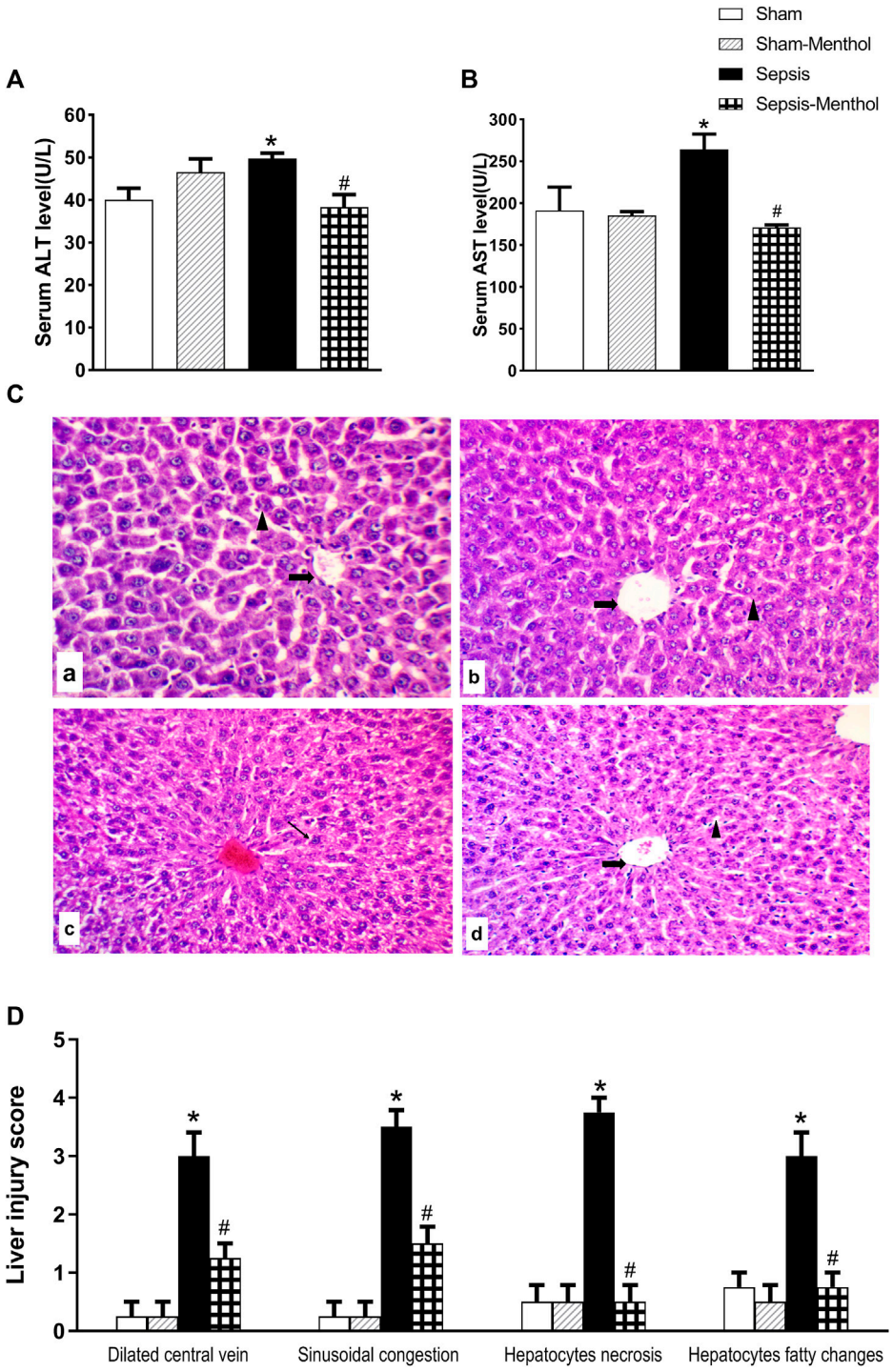

FIGURE 2
The effect of menthol (100 mg/kg, I.G) on serum levels of ALT (Figure 2A) and AST (Figure 2B) in CLP septic rats. Figure 2C: Photomicrographs showing liver sections from all groups (n = 6, each) examined by H&E-stained (200x). The sham groups [sham and sham-menthol; **(A)** and **(B)**] showed normal liver cells (arrow head) with normal central vein (arrow). The liver tissue from the sepsis group **(C)** showed disrupted hepatic cells architecture (arrow head) with dilated central veins (arrow). Liver tissues from the menthol-treated septic rats **(D)** showed normal liver cells. Figure 2D: Scoring the histopathological changes; 0: absent, 1: <25%, 2: >25% and <50%, 3: >50% and <75% and 4: >75% of the entire section showed histopathological alterations. Data represented as a mean score of each group for each observed histopathological alteration. * significant difference from the sham group at p ˂0.05. # significant difference from the sepsis group at p ˂0.05.

TABLE 1 The effect of menthol (100 mg/kg, I.G.) treatment on hepatic oxidative stress and antioxidant enzyme levels in CLP sepsis model.

Groups	Amount of MDA (nmol/g tissue)	Amount of total nitrite (nmol/g tissue)	SOD activity (U/mg tissue)	GSH (nmol/g tissue)
Sham	0.29 ± 0.09	1.92 ± 0.44	1.64 ± 0.02	10.45 ± 1.03
Sham-Menthol	0.32 ± 0.08	1.87 ± 0.17	2.01 ± 0.70	10.98 ± 1.12
Sepsis	0.75 ± 0.12*	3.22 ± 0.92 *	0.25 ± 0.02*	4.49 ± 1.28*
Sepsis-Menthol	0.49 ± 0.15#	1.71 ± 0.41#	1.33 ± 0.22#	12.18 ± 1.05#

Data was analyzed by ANOVA test, followed by Tukey-Kramer for multiple comparison. Data represent the mean ± SEM of 6 observations; * significant difference from the sham group at p <0.05. # significant difference from the sepsis group at p <0.05.

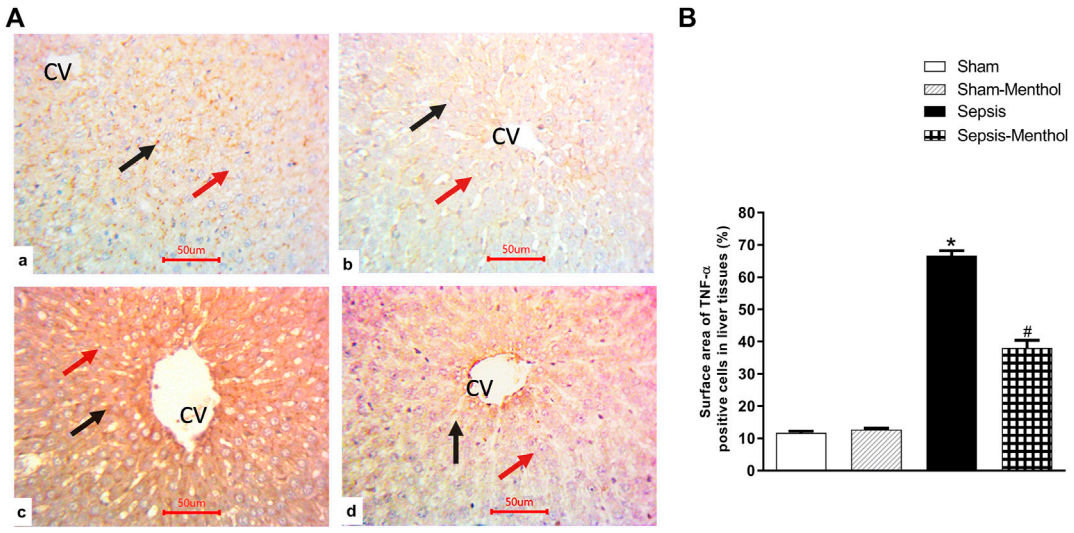

FIGURE 3
The effect of menthol (100 mg/kg, I.G) on hepatic TNF-α in CLP sepsis model; **(A)**; Representative photomicrographs showing TNF-α immunoreactivity in liver tissue, **(B)**; Bar charts showing semi-quantitative analysis of data in A from sections of the sham, sham-menthol, sepsis, and sepsis-menthol groups. * significant difference from the sham group at p <0.05. # significant difference from the sepsis group at p <0.05. Data represented as mean ± S.E (n = 6).

and the sham-menthol group exhibited normal histology. However, the sepsis group showed a dilated and congested central vein, surrounded by polygonal-shaped hepatocytes which were separated by congested sinusoidal spaces. Furthermore, perivascular focal necrosis, apoptotic bodies, and moderate fatty changes of peripheral hepatocytes were observed (Figure 2C). The sepsis-menthol group showed a mildly dilated and congested central vein, as well as mild fatty changes in the peripheral hepatocytes. Less inflammation and apoptosis were observed in menthol-treated septic rats. Scores of dilation and congestion of the central vein and sinusoids, as well as necrosis and fatty changes of hepatocytes were significantly (p <0.05) higher compared to the sham groups. Thus, indicating sepsis-induced deterioration of liver tissues. These changes were significantly (p <0.05) mitigated by menthol (Figure 2D).

3.3 Menthol decreased hepatic oxidative stress in septic rats

Compared with sham-operated rats, liver samples obtained from septic rats showed a significant ($p < 0.05$) elevation in the level of MDA, a biomarker of oxidative stress and lipid peroxidation, as well as the total nitrites (Table 1). The untreated sepsis group showed a significant ($p < 0.05$) reduction in the hepatic antioxidant defense markers, SOD and GSH (Table 1), when compared with the sham-operated rats. Treatment with menthol after CLP surgery significantly ($p < 0.05$) decreased MDA and total nitrite levels. Furthermore, menthol significantly ($p < 0.05$) attenuated the sepsis-induced reduction in hepatic SOD and GSH levels (Table 1).

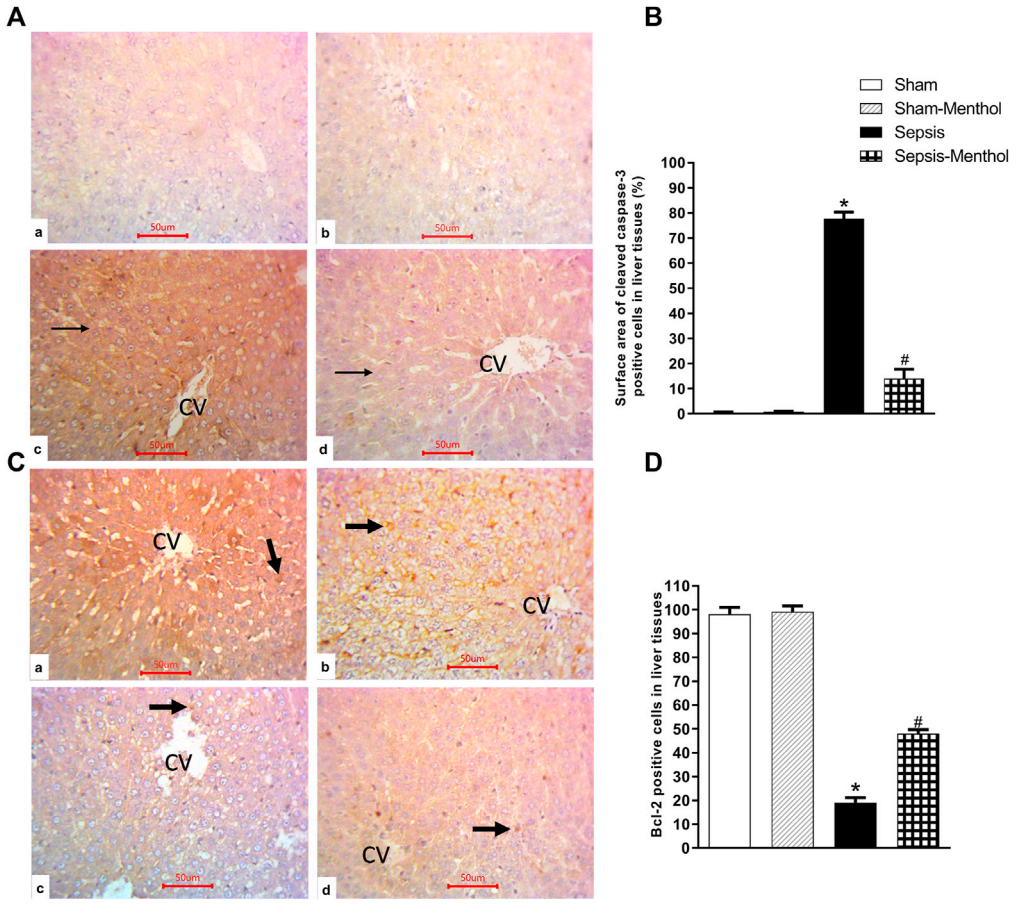

FIGURE 4
The effect of menthol (100 mg/kg, I.G) on hepatic cleaved caspase-3 and Bcl-2 levels in CLP sepsis model. **(A)**; Representative photomicrographs showing cleaved caspase-3 immunoreactivity in liver tissues. **(B)**; Bar charts showing semi-quantitative analysis of data in A from tissue sections of the sham, sham-menthol, sepsis, and sepsis-menthol groups. **(C)** Representative photomicrographs showing Bcl-2 immunoreactivity in liver tissues. **(D)** Bar charts showing semi-quantitative analysis of data in C from tissue sections of the sham, sham-menthol, sepsis, and sepsis-menthol groups * significant difference from the sham group at p <0.05. # significant difference from the sepsis group at p <0.05. Data represented as mean ± S.E (n = 6).

3.4 Menthol attenuated sepsis-induced hepatic inflammation and apoptosis

Immunohistochemical data revealed a significant ($p < 0.05$) increase in the hepatic expression of the inflammatory mediator TNF-α in the untreated sepsis group (Figure 3). Additionally, untreated septic rats exhibited a significant ($p < 0.05$) upregulation of the apoptotic factor cleaved caspase-3, accompanied by a significant ($p < 0.05$) reduction in the expression of the anti-apoptotic factor Bcl-2 (Figure 4). In contrast, menthol treatment significantly ($p < 0.05$) abrogated the sepsis-induced elevation in hepatic TNF-α levels (Figure 3). Compared to the untreated sepsis group, menthol exhibited remarkable anti-apoptotic activity reflected by a significant ($p < 0.05$) decline in hepatic cleaved caspase-3 expression (Figure 4B) and enhanced expression of Bcl-2 in treated septic rats (Figure 4D).

3.5 Menthol promoted hepatocellular regeneration in septic rats

Hepatic levels of PCNA, an index of cell proliferation and regeneration, were significantly ($p < 0.05$) decreased in the sepsis group (Figure 5). This finding aligns with the observed elevation in hepatic apoptosis in these animals (Figure 4). Menthol administration significantly ($p < 0.05$) attenuated the sepsis-induced decline in PCNA expression (Figure 5).

3.6 Analysis of correlation between different parameters

A strong positive correlation was found between the liver injury score and the inflammatory marker, TNF-α., and the

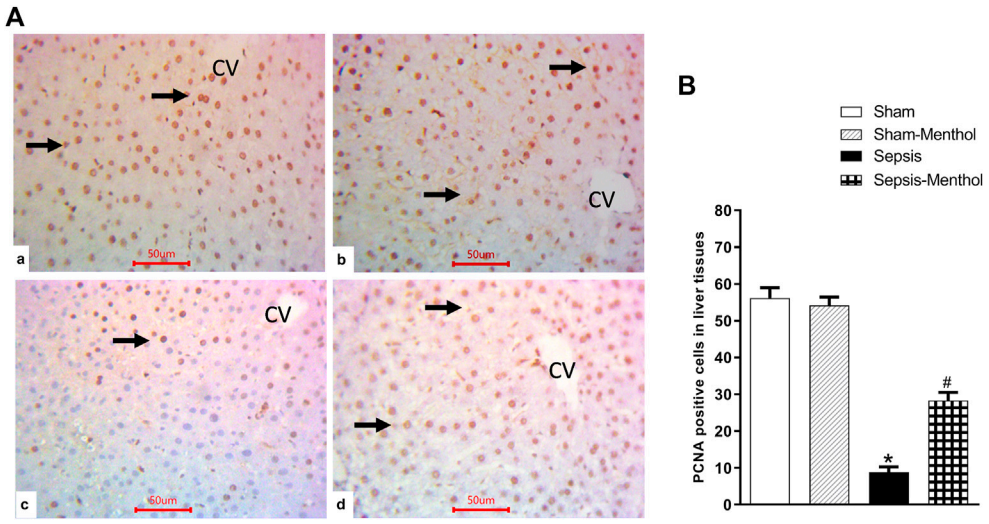

FIGURE 5
The effect of menthol (100 mg/kg, I.G) on hepatic PCNA levels in CLP sepsis model **(A)**; Representative photomicrographs showing PCNA immunoreactivity in liver tissues. **(B)**; Bar charts showing semi-quantitative analysis of the data from all groups. * significant difference from the sham group at p ˂0.05. # significant difference from the sepsis group at p ˂0.05. Data represented as mean ± S.E (n = 6).

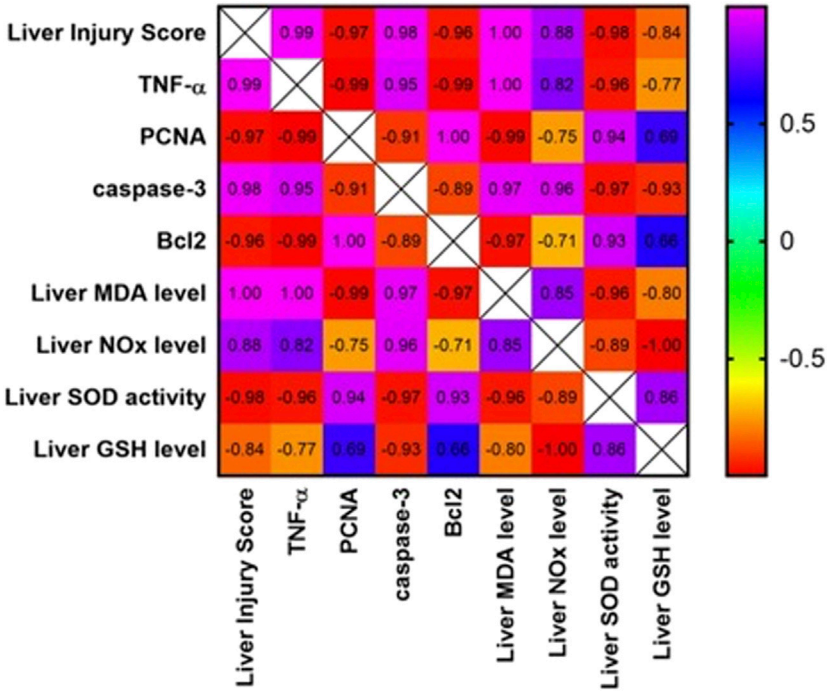

FIGURE 6
Correlation matrix for different parameters included in the study. Pearson correlation coefficient (r) was used to measure the correlation. If r is between |0.3| and |0.7|, a moderate correlation is indicated. If r >|0.7|, a strong correlation is indicated. If r<|0.3|, a weak correlation is indicated. Positive values indicate a positive correlation, while negative values indicate a negative correlation. The color of the scale bar to the right ranges from violet to red, indicating r values from +1 to -1. The graph is colored according to the scale. TNF-α: tumor necrosis factor-alpha; PCNA: proliferating cell nuclear antigen; Bcl-2: B-cell lymphoma 2.

apoptotic marker, cleaved caspase-3 (Figure 6). In contrast, the liver injury score was negatively correlated with the hepatocellular regeneration marker, PCNA, and the anti-apoptotic marker, Bcl-2. Furthermore, hepatic TNF-α and cleaved caspase-3 were positively correlated with each other and negatively correlated with the liver expression of Bcl-2 and PCNA.

4 Discussion

Sepsis is a life-threatening condition resulting from an unregulated host response to an infection. Sepsis causes damage and failure of many organs, including the heart, kidney, and liver. Despite sepsis induced lung injury is highly common than sepsis-induced hepatic injury, the latter is associated with a higher mortality rate (Yan and Li, 2014; Strnad et al., 2017; Woznica et al., 2018). Sepsis-induced hepatic dysfunction directly contributes to the poor prognosis and increased risk of death in septic patients (Yan and Li, 2014; Strnad et al., 2017; Woznica et al., 2018). The pathophysiology of sepsis-induced hepatic failure is extremely complex. However, a systemic hyperinflammatory response associated with increased oxidative stress contributes to the hepatic dysfunction (Liu et al., 2017). Here, we investigated, for the first time, the hepatoprotective effects of menthol, a powerful antioxidant and natural anti-inflammatory agent, in the CLP-induced sepsis model. Menthol (100 mg/kg, I. G) administration after CLP surgery decreased hepatic oxidative stress, inflammation, and apoptosis and enhanced hepatocellular regeneration.

In our current study, which is consistent with previous studies (Ahmed et al., 2020; Al-Kadi et al., 2020), the induction of sepsis by CLP resulted in severe hepatic injury manifested as fatty changes, infiltration of inflammatory cells, apoptotic and necrotic hepatocyte death, as well as the dilation and congestion of the central vein. Damage to the liver tissues was confirmed by the elevation in serum levels of hepatic transaminases (ALT and AST). These cytoplasmic enzymes are typically localized in the cytoplasm of hepatocytes, with minimal presence in the serum; however, hepatic injury increases their serum levels. Therefore, they are commonly used as surrogates of hepatic function, indicating the magnitude of hepatocellular injury (McGill, 2016). Their levels were markedly elevated in the early phase of sepsis due to sepsis-induced hypotension and hepatic hypoperfusion (Fuhrmann et al., 2009; Fuhrmann et al., 2010; Dou et al., 2019b). Treatment of CLP rats with menthol 2 h after surgery prevented the elevation of serum hepatic transaminases, which was supported by the preserved histopathology in this group. Menthol abrogated the sepsis-induced dilation and congestion of the central hepatic veins and decreased the necrosis and fatty changes of hepatocytes, suggesting a possible hepatoprotective effect against the CLP sepsis model. Notably, the hepatoprotective effects of menthol were previously reported against paracetamol- and CCl_4-induced hepatic injury (Janbaz and Gilani, 2002).

The increased oxidative stress significantly contributes to the hepatic dysfunction induced by sepsis (Moradi et al., 2021). There are many sources of ROS production during sepsis, including the exaggerated release of inflammatory mediators, neutrophil infiltration, and mitochondrial dysfunction (Zhang et al., 2018). In this study, the sepsis group showed increased hepatic MDA levels. Oxidation of polyunsaturated phospholipids of the cell membrane under increased oxidative stress results in the formation of MDA. Thus, it is used as a standard marker of increased oxidative stress (Petronilho et al., 2015; Zhou et al., 2020). The sepsis group also showed elevated total nitrite levels, indicating high tissue levels of the vasodilator mediator, nitric oxide (NO). Elevated NO mediates the sepsis-induced hypotension, and when combined with ROS, contributes to the formation of peroxynitrite, a potent oxidizing agent that causes cellular damage (Iwakiri and Kim, 2015). The current results align with the previous studies indicating that sepsis-induced ROS production parallels a decrease in hepatic antioxidant defense markers, such as GSH and SOD (Giustina et al., 2019; Larrouyet-Sarto et al., 2020). It is worth mentioning, that our study lacks the measurement of other important antioxidative stress parameters such catalase and glutathione peroxidase enzyme activities. However, results from our previous work (Ahmed et al., 2020; Ibrahim et al., 2020a; Al-Kadi et al., 2020; Al-Kadi et al., 2021; Senousy et al., 2022), in line with others (Chen et al., 2012; Yang et al., 2018; Giustina et al., 2019; Ibrahim et al., 2020b; Larrouyet-Sarto et al., 2020; Aboyoussef et al., 2021), showed that either enzyme alone or GSH is a good surrogate of the antioxidant capacity of the tissue, while the levels of MDA directly reflect tissue oxidative damage. Akin to its established antioxidant effects (Rozza et al., 2014; Bastaki et al., 2018), menthol ameliorated the sepsis-induced elevation in hepatic ROS and total nitrite levels, while preserving the hepatic antioxidant GSH and SOD levels. These effects were positively correlated with the observed menthol-induced improvement in hepatic functions and histopathology. Previous studies discussing menthol inhibition of neutrophil infiltration (Rozza et al., 2014), and the subsequent attenuation of ROS production, may explain the observed antioxidant effects of menthol.

Evidence supports crosstalk between oxidative stress and the initiation and progression of inflammation (Aziz et al., 2013; Pandey et al., 2015). Our data, in line with previous reports (Vandewalle et al., 2019; Ahmed et al., 2020; Al-Kadi et al., 2020), showed elevated hepatic TNF-α in the untreated septic rats, which positively correlated with increased hepatic oxidative stress and decreased antioxidant capacity. TNF-α enhances the expression of inducible nitric oxide synthase (iNOS) leading to a massive release of NO (Ozaki et al., 2010), the stimulation of ROS production, the expression of inflammatory cytokines such as IL-

6, the activation of neutrophil infiltration, and ultimately hepatic damage (Bozza et al., 2007; Vandewalle et al., 2019). Bacteremia and subsequent endotoxemia directly stimulate the release of inflammatory cytokines, including TNF-α, IL-1β, IL-6, IL-12, and IL-18 in sepsis (Traeger et al., 2010). Our results showed downregulated hepatic TNF-α and decreased oxidative stress in the menthol-treated septic rats, supporting the immunomodulatory and anti-inflammatory effects reported by others (Rozza et al., 2014; Zaia et al., 2016). Accumulating evidence shows that the activation of the transient receptor potential melanin-8 (TRPM8) mediates the menthol-induced cooling sensation and analgesic effects (Bautista et al., 2007; Ordas et al., 2019). Interestingly, the activation of TRPM8 reduced the release of TNF-α and increased the anti-inflammatory cytokine IL-10 (Khalil et al., 2016; Wang et al., 2017; Khalil et al., 2018; Ordas et al., 2019), which further supports the anti-inflammatory effects observed with menthol in this study. Unfortunately, the current results cannot determine whether the activation of TRPM8 mediates the hepatoprotective effects of menthol. Thus, it would be of interest to design future studies to further explore the role of TRPM8 and its potential significance in novel anti-sepsis modalities.

Sepsis induces hepatocellular apoptosis leading to organ damage and dysfunction (Jaeschke et al., 2000; Gao et al., 2018). As a result, attenuation of apoptosis would counteract the sepsis-induced hepatocellular damage (Yoon and Gores, 2002). Tissue infiltration by neutrophils and macrophages contributes to the proapoptotic signaling by elevating the levels of cytokines (e.g., TNF-α), NO, and ROS (Zhang et al., 2014). Cleaved caspase-3, a hallmark of apoptosis, is activated by several cell death signals to execute the apoptotic changes (Mazumder et al., 2008). Our results showed increased hepatic expression of cleaved caspase-3, positively correlated with sepsis-induced liver injury. To add to that, the liver of septic rats revealed low expression of the anti-apoptotic marker, Bcl-2. The increased hepatocellular apoptosis observed in septic rats is coherent with previous studies (Wesche-Soldato et al., 2007; Su et al., 2020). As reported by other studies (Rozza et al., 2014), menthol exhibited remarkable anti-apoptotic effects; it nearly eliminated the sepsis-induced elevation in hepatic cleaved caspase-3 and upregulated the anti-apoptotic marker, Bcl-2. The anti-apoptotic, anti-inflammatory, and antioxidant effects of menthol support the observed protection against sepsis-induced hepatotoxicity.

There is a correlation between hepatocellular regeneration and the levels of PCNA, a nuclear factor involved in cell proliferation and DNA replication (Hall et al., 1990; Moldovan et al., 2007). Increased PCNA levels indicate hepatocyte regeneration and recovery from hepatic damage (Li et al., 2016). In addition, PCNA protects against apoptotic cell death by binding to and inactivating procaspases (Witko-Sarsat et al., 2010). In sepsis, increased hepatic inflammation and apoptosis decrease the gene expressions of PCNA, as shown in this study and other studies (Abcejo et al., 2011). The decreased hepatic PCNA levels in septic rats correlated with liver injury, inflammation, and apoptosis. Interestingly, menthol upregulated the hepatic expression of PCNA in CLP septic rats. This effect was positively correlated to the menthol-induced enhancement of hepatic antioxidant activity and decreased apoptotic and inflammatory effects, suggesting a potential role in the enhancement of hepatocellular regeneration.

In conclusion, we investigated, for the first time, the hepatoprotective effects of menthol in an experimental CLP model of sepsis. The antioxidant, anti-inflammatory, and anti-apoptotic effects of menthol contributed to its hepatoprotection. In addition, menthol may induce the expression of PCNA, thus, promoting compensatory liver regeneration. Together, these effects suggest that menthol is a promising therapy that limits liver injury in septic patients. Indeed, the lack of *in vitro* studies that further explore the hepatoprotective effects of menthol in sepsis, the need to investigate the possible involvement of the menthol receptor (TRPM8) in preventing sepsis-associated complications and the elucidation of the main signaling pathways mediating the antioxidant effects of menthol are considered limitations of the present study that should be addressed in future studies.

Data availability statement

The raw data supporting the conclusions of this article will be made available by the authors, without undue reservation.

Ethics statement

The animal study was reviewed and approved by The Commission on the Ethics of Scientific Research, Faculty of Pharmacy, Minia University, Egypt (ES02/2020).

Author contributions

AA, ME, MA, SS, and HH: Design and execution of experiments, sample collection, data handling, and manuscript writing. WA and AS: Histopathology and the immunohistochemistry studies and revision and approval of manuscript. AK and AA: Experiment design, manuscript writing, revision, and approval, and funding source.

Funding

This work was funded by the Deanship of Scientific Research at Umm Al-Qura University, Makkah, Saudi Arabia by Grant code (22UQU4310387DSR16).

Acknowledgments

The authors would like to thank the Deanship of Scientific Research at Umm Al-Qura University for supporting this work by Grant code (22UQU4310387DSR16). The authors would also like to thank Amr A. Kamel (Faculty of Pharmacy, Minia University) for technical assistance.

Conflict of interest

The authors declare that the research was conducted in the absence of any commercial or financial relationships that could be construed as a potential conflict of interest.

Publisher's note

All claims expressed in this article are solely those of the authors and do not necessarily represent those of their affiliated organizations, or those of the publisher, the editors and the reviewers. Any product that may be evaluated in this article, or claim that may be made by its manufacturer, is not guaranteed or endorsed by the publisher.

Supplementary material

The Supplementary Material for this article can be found online at: https://www.frontiersin.org/articles/10.3389/fphar.2022.952337/full#supplementary-material

References

Abcejo, A., Andrejko, K. M., Ochroch, E. A., Raj, N. R., and Deutschman, C. S. (2011). Impaired hepatocellular regeneration in murine sepsis is dependent on regulatory protein levels. *Shock* 36 (5), 471–477. doi:10.1097/SHK.0b013e31822d60ff

Aboyoussef, A. M., Mohammad, M. K., Abo-Saif, A. A., and Messiha, B. A. S. (2021). Granisetron attenuates liver injury and inflammation in a rat model of cecal ligation and puncture-induced sepsis. *J. Pharmacol. Sci.* 147 (4), 358–366. doi:10.1016/j.jphs.2021.08.005

Ahmed, A-S. F., Bayoumi, A., Eltahir, H. M., Abdel Hafez, S., and Abouzied, M. M. (2020). Amelioration of Sepsis-induced liver and lung injury by a superoxide dismutase mimetic; role of TNF-ڇ± and Caspase-3. *J. Adv. Biomed. Pharm. Sci.* 3 (1), 31–39. doi:10.21608/jabps.2019.19876.1061

Aksoy, A., Toker, A., Celik, M., Aksoy, M., Halıcı, Z., and Aksoy, H. (2014). The effect of progesterone on systemic inflammation and oxidative stress in the rat model of sepsis. *Indian J. Pharmacol.* 46, 622–626. doi:10.4103/0253-7613.144922

Al-Kadi, A., Ahmed, A-S., El-Tahawy, N. F. G., Khalifa, M. M. A., and El-Daly, M. (2020). Silymarin protects against sepsis-induced acute liver and kidney injury via anti-inflammatory and antioxidant mechanisms in the rat. *J. Adv. Biomed. Pharm. Sci.* 3 (4), 190–197. doi:10.21608/jabps.2020.37074.1091

Al-Kadi, A., El-Daly, M., El-Tahawy, N. F., Khalifa, M., and Ahmed, A-S. (2021). Angiotensin aldosterone inhibitors improve survival and ameliorate kidney injury induced by sepsis through suppression of inflammation and apoptosis. *Fundam. Clin. Pharmacol.* 36, 286–295. doi:10.1111/fcp.12718

Amato, A., Liotta, R., and Mule, F. (2014). Effects of menthol on circular smooth muscle of human colon: Analysis of the mechanism of action. *Eur. J. Pharmacol.* 740, 295–301. doi:10.1016/j.ejphar.2014.07.018

Aziz, M., Jacob, A., Yang, W. L., Matsuda, A., and Wang, P. (2013). Current trends in inflammatory and immunomodulatory mediators in sepsis. *J. Leukoc. Biol.* 93 (3), 329–342. doi:10.1189/jlb.0912437

Bastaki, S. M., Adeghate, E., Amir, N., Ojha, S., and Oz, M. (2018). Menthol inhibits oxidative stress and inflammation in acetic acid-induced colitis in rat colonic mucosa. *Am. J. Transl. Res.* 10 (12), 4210–4222.

Bautista, D. M., Siemens, J., Glazer, J. M., Tsuruda, P. R., Basbaum, A. I., Stucky, C. L., et al. (2007). The menthol receptor TRPM8 is the principal detector of environmental cold. *Nature* 448 (7150), 204–208. doi:10.1038/nature05910

Beutler, E., Duron, O., and Kelly, B. M. (1963). Improved method for the determination of blood glutathione. *J. Lab. Clin. Med.* 61, 882–888.

Bozza, F. A., Salluh, J. I., Japiassu, A. M., Soares, M., Assis, E. F., Gomes, R. N., et al. (2007). Cytokine profiles as markers of disease severity in sepsis: A multiplex analysis. *Crit. Care* 11 (2), R49. doi:10.1186/cc5783

Buege, J. A., and Aust, S. D. (1978). Microsomal lipid peroxidation. *Methods Enzymol.* 52, 302–310. doi:10.1016/s0076-6879(78)52032-6

Chen, H., Zhu, W., Feng, J., and Li, S. (2012). Protective effect of diallyl trisulfide on liver in rats with sepsis and the mechanism. *J. Huazhong Univ. Sci. Technol. Med. Sci.* 32 (5), 657–662. doi:10.1007/s11596-012-1013-7

Chen, R., Xie, Y., Zhong, X., Chen, F., Gong, Y., Wang, N., et al. (2021). MSCs derived from amniotic fluid and umbilical cord require different administration schemes and exert different curative effects on different tissues in rats with CLP-induced sepsis. *Stem Cell Res. Ther.* 12 (1), 164. doi:10.1186/s13287-021-02218-8

Dou, J., Zhou, Y., Cui, Y., Chen, M., Wang, C., and Zhang, Y. (2019). AST-to-platelet ratio index as potential early-warning biomarker for sepsis-associated liver injury in children: A database study. *Front. Pediatr.* 7 (331), 00331. doi:10.3389/fped.2019.00331

Dou, J., Zhou, Y., Cui, Y., Chen, M., Wang, C., and Zhang, Y. (2019). AST-to-platelet ratio index as potential early-warning biomarker for sepsis-associated liver injury in children: A database study. *Front. Pediatr.* 7, 331. doi:10.3389/fped.2019.00331

Du, J., Liu, D., Zhang, X., Zhou, A., Su, Y., dewei, H., et al. (2020). Menthol protects dopaminergic neurons against inflammation-mediated damage in lipopolysaccharide (LPS)-Evoked model of Parkinson's disease. *Int. Immunopharmacol.* 85, 106679. doi:10.1016/j.intimp.2020.106679

Fleischmann, C., Scherag, A., Adhikari, N. K., Hartog, C. S., Tsaganos, T., Schlattmann, P., et al. (2016). Assessment of global incidence and mortality of hospital-treated sepsis. Current estimates and limitations. *Am. J. Respir. Crit. Care Med.* 193 (3), 259–272. doi:10.1164/rccm.201504-0781OC

Fuhrmann, V., Jager, B., Zubkova, A., and Drolz, A. (2010). Hypoxic hepatitis - epidemiology, pathophysiology and clinical management. *Wien. Klin. Wochenschr.* 122 (5-6), 129–139. doi:10.1007/s00508-010-1357-6

Fuhrmann, V., Kneidinger, N., Herkner, H., Heinz, G., Nikfardjam, M., Bojic, A., et al. (2009). Hypoxic hepatitis: Underlying conditions and risk factors for mortality in critically ill patients. *Intensive Care Med.* 35 (8), 1397–1405. doi:10.1007/s00134-009-1508-2

Galeotti, N., Ghelardini, C., Mannelli, L., Mazzanti, G., Baghiroli, L., and Bartolini, A. (2001). Local anaesthetic activity of (+)- and (-)-menthol. *Planta Med.* 67 (2), 174–176. doi:10.1055/s-2001-11515

Gao, X., Yan, X., Yin, Y., Lin, X., Zhang, Q., Xia, Y., et al. (2018). Therapeutic targeting of apoptosis inhibitor of macrophage/cd5l in sepsis. *Am. J. Respir. Cell Mol. Biol.* 60 (3), 323–334. doi:10.1165/rcmb.2018-0272OC

Ghasemi-Pirbaluti, M., Motaghi, E., and Bozorgi, H. (2017). The effect of menthol on acute experimental colitis in rats. *Eur. J. Pharmacol.* 805, 101–107. doi:10.1016/j.ejphar.2017.03.003

Giustina, A. D., Danielski, L. G., Novochadlo, M. M., Goldim, M. P. S., Joaquim, L., Metzker, K. L. L., et al. (2019). Vitamin B6 reduces oxidative stress in lungs and liver in experimental sepsis. *An. Acad. Bras. Cienc.* 91 (4), e20190434. doi:10.1590/0001-3765201920190434

Hall, P. A., Levison, D. A., Woods, A. L., Yu, C. C., Kellock, D. B., Watkins, J. A., et al. (1990). Proliferating cell nuclear antigen (PCNA) immunolocalization in paraffin sections: An index of cell proliferation with evidence of deregulated expression in some neoplasms. *J. Pathol.* 162 (4), 285–294. doi:10.1002/path.1711620403

Henrion, J. (2012). Hypoxic hepatitis. *Liver Int.* 32 (7), 1039–1052. doi:10.1111/j.1478-3231.2011.02655.x

Hilfiger, L., Triaux, Z., Marcic, C., Héberlé, E., Emhemmed, F., Darbon, P., et al. (2021). Anti-hyperalgesic properties of menthol and pulegone. *Front. Pharmacol.* 12, 753873. doi:10.3389/fphar.2021.753873

Ibrahim, Y. F., Fadl, R. R., Ibrahim, S., Gayyed, M. F., Bayoumi, A., and Refaie, M. (2020). Protective effect of febuxostat in sepsis-induced liver and kidney injuries after cecal ligation and puncture with the impact of xanthine oxidase, interleukin 1β, and c-Jun N-terminal kinases. *Hum. Exp. Toxicol.* 39 (7), 906–919. doi:10.1177/0960327120905957

Ibrahim, Y. F., Moussa, R. A., Bayoumi, A. M. A., and Ahmed, A-S. F. (2020). Tocilizumab attenuates acute lung and kidney injuries and improves survival in a rat model of sepsis via down-regulation of NF-κB/JNK: A possible role of P-glycoprotein. *Inflammopharmacology* 28 (1), 215–230. doi:10.1007/s10787-019-00628-y

Iwakiri, Y., and Kim, M. Y. (2015). Nitric oxide in liver diseases. *Trends Pharmacol. Sci.* 36 (8), 524–536. doi:10.1016/j.tips.2015.05.001

Jaeschke, H., Farhood, A., Cai, S. X., Tseng, B. Y., and Bajt, M. L. (2000). Protection against TNF-induced liver parenchymal cell apoptosis during endotoxemia by a novel caspase inhibitor in mice. *Toxicol. Appl. Pharmacol.* 169 (1), 77–83. doi:10.1006/taap.2000.9035

Janbaz, K. H., and Gilani, A. H. (2002). Menthol prevents liver damage induced by paracetamol and CCl4. *Pak. J. Biol. Sci.*5. 1101–1103. doi:10.3923/pjbs.2002.1101.1103

Jensen, K. (2008). Theory and practice of histological techniques, 6th edition. *J. Neuropathol. Exp. Neurol.* 67 (6), 6332. doi:10.1097/nen.0b013e31817e2933

Khalil, M., Alliger, K., Weidinger, C., Yerinde, C., Wirtz, S., Becker, C., et al. (2018). Functional role of transient receptor potential channels in immune cells and epithelia. *Front. Immunol.* 9, 174. doi:10.3389/fimmu.2018.00174

Khalil, M., Babes, A., Lakra, R., Forsch, S., Reeh, P. W., Wirtz, S., et al. (2016). Transient receptor potential melastatin 8 ion channel in macrophages modulates colitis through a balance-shift in TNF-alpha and interleukin-10 production. *Mucosal Immunol.* 9 (6), 1500–1513. doi:10.1038/mi.2016.16

La Mura, V., Pasarin, M., Meireles, C. Z., Miquel, R., Rodriguez-Vilarrupla, A., Hide, D., et al. (2013). Effects of simvastatin administration on rodents with lipopolysaccharide-induced liver microvascular dysfunction. *Hepatology* 57 (3), 1172–1181. doi:10.1002/hep.26127

Larrouyet-Sarto, M. L., Tamura, A. S., Alves, V. S., Santana, P. T., Ciarlini-Magalhaes, R., Rangel, T. P., et al. (2020). P2X7 receptor deletion attenuates oxidative stress and liver damage in sepsis. *Purinergic Signal.* 16 (4), 561–572. doi:10.1007/s11302-020-09746-7

Lelubre, C., and Vincent, J. L. (2018). Mechanisms and treatment of organ failure in sepsis. *Nat. Rev. Nephrol.* 14 (7), 417–427. doi:10.1038/s41581-018-0005-7

Li, X., Fan, X., Li, D., Zeng, X., Zeng, H., Wang, Y., et al. (2016). Schisandra sphenanthera extract facilitates liver regeneration after partial hepatectomy in mice. *Drug Metab. Dispos.* 44 (5), 647–652. doi:10.1124/dmd.115.068288

Liu, X., Yang, X., Han, L., Ye, F., Liu, M., Fan, W., et al. (2017). Pterostilbene alleviates polymicrobial sepsis-induced liver injury: Possible role of SIRT1 signaling. *Int. Immunopharmacol.* 49, 50–59. doi:10.1016/j.intimp.2017.05.022

Marklund, S., and Marklund, G. (1974). Involvement of the superoxide anion radical in the autoxidation of pyrogallol and a convenient assay for superoxide dismutase. *Eur. J. Biochem.* 47 (3), 469–474. doi:10.1111/j.1432-1033.1974.tb03714.x

Mazumder, S., Plesca, D., and Almasan, A. (2008). Caspase-3 activation is a critical determinant of genotoxic stress-induced apoptosis. *Methods Mol. Biol.* 414, 13–21. doi:10.1007/978-1-59745-339-4_2

McGill, M. R. (2016). The past and present of serum aminotransferases and the future of liver injury biomarkers. *EXCLI J.* 15, 817–828. doi:10.17179/excli2016-800

Moldovan, G. L., Pfander, B., and Jentsch, S. (2007). PCNA, the maestro of the replication fork. *Cell* 129 (4), 665–679. doi:10.1016/j.cell.2007.05.003

Moorcroft, M. J., Davis, J., and Compton, R. G. (2001). Detection and determination of nitrate and nitrite: A review. *Talanta* 54 (5), 785–803. doi:10.1016/s0039-9140(01)00323-x

Moradi, M., Goodarzi, N., Faramarzi, A., Cheraghi, H., Hashemian, A. H., and Jalili, C. (2021). Melatonin protects rats testes against bleomycin, etoposide, and cisplatin-induced toxicity via mitigating nitro-oxidative stress and apoptosis. *Biomed. Pharmacother. = Biomedecine Pharmacother.* 138, 111481. doi:10.1016/j.biopha.2021.111481

Morton, D. B., and Griffiths, P. (1985). Guidelines on the recognition of pain, distress and discomfort in experimental animals and an hypothesis for assessment. *Vet. Rec.* 116 (16), 431–436. doi:10.1136/vr.116.16.431

Nemzek, J. A., Hugunin, K. M., and Opp, M. R. (2008). Modeling sepsis in the laboratory: Merging sound science with animal well-being. *Comp. Med.* 58 (2), 120–128.

Ordas, P., Hernandez-Ortego, P., Vara, H., Fernandez-Pena, C., Reimundez, A., Morenilla-Palao, C., et al. (2019). Expression of the cold thermoreceptor TRPM8 in rodent brain thermoregulatory circuits. *J. Comp. Neurol.* 529 (1), 234–256. doi:10.1002/cne.24694

Ozaki, T., Habara, K., Matsui, K., Kaibori, M., Kwon, A. H., Ito, S., et al. (2010). Dexamethasone inhibits the induction of iNOS gene expression through destabilization of its mRNA in proinflammatory cytokine-stimulated hepatocytes. *Shock* 33 (1), 64–69. doi:10.1097/SHK.0b013e3181a7fd74

Pandey, S., Kawai, T., and Akira, S. (2015). Microbial sensing by Toll-like receptors and intracellular nucleic acid sensors. *Cold Spring Harb. Perspect. Biol.* 7 (1), a016246. doi:10.1101/cshperspect.a016246

Pergolizzi, J. V., Jr., Taylor, R., Jr., LeQuang, J. A., and Raffa, R. B. (2018). The role and mechanism of action of menthol in topical analgesic products. *J. Clin. Pharm. Ther.* 43 (3), 313–319. doi:10.1111/jcpt.12679

Petronilho, F., Florentino, D., Danielski, L. G., Vieira, L. C., Martins, M. M., Vieira, A., et al. (2015). Alpha-lipoic acid attenuates oxidative damage in organs after sepsis. *Inflammation* 39 (1), 357–365. doi:10.1007/s10753-015-0256-4

Reitman, S., and Frankel, S. (1957). A colorimetric method for the determination of serum glutamic oxalacetic and glutamic pyruvic transaminases. *Am. J. Clin. Pathol.* 28 (1), 56–63. doi:10.1093/ajcp/28.1.56

Rozza, A., Hiruma-Lima, C., Takahira, R., Padovani, C., and Pellizzon, C. (2013). Effect of menthol in experimentally induced ulcers: Pathways of gastroprotection. *Chem. Biol. Interact.* 206, 272–278. doi:10.1016/j.cbi.2013.10.003

Rozza, A. L., Beserra, F. P., Vieira, A. J., Oliveira de Souza, E., Hussni, C. A., Martinez, E. R. M., et al. (2021). The use of menthol in skin wound healing-anti-inflammatory potential, antioxidant defense system stimulation and increased epithelialization. *Pharmaceutics* 13 (11), 1902. doi:10.3390/pharmaceutics13111902

Rozza, A. L., Meira de Faria, F., Souza Brito, A. R., and Pellizzon, C. H. (2014). The gastroprotective effect of menthol: Involvement of anti-apoptotic, antioxidant and anti-inflammatory activities. *PLOS ONE* 9 (1), e86686. doi:10.1371/journal.pone.0086686

Rudd, K. E., Johnson, S. C., Agesa, K. M., Shackelford, K. A., Tsoi, D., Kievlan, D. R., et al. (2017). Global, regional, and national sepsis incidence and mortality, 1990-2017: Analysis for the global burden of disease study. *Lancet* 395 (10219), 200–211. doi:10.1016/S0140-6736(19)32989-7

Sabzghabaee, A. M., Nili, F., Ghannadi, A., Eizadi-Mood, N., and Anvari, M. (2011). Role of menthol in treatment of candidial napkin dermatitis. *World J. Pediatr.* 7 (2), 167–170. doi:10.1007/s12519-011-0253-0

Saini, K., Bolia, R., and Bhat, N. K. (2022). Incidence, predictors and outcome of sepsis-associated liver injury in children: A prospective observational study. *Eur. J. Pediatr.* 181 (4), 1699–1707. doi:10.1007/s00431-022-04374-2

Senousy, S. R., El-Daly, M., Ibrahim, A. R. N., Khalifa, M. M. A., and Ahmed, A. F. (2022). Effect of celecoxib and infliximab against multiple organ damage induced by sepsis in rats: A comparative study. *Biomedicines* 10 (7), 1613. doi:10.3390/biomedicines10071613

Seymour, C. W., Liu, V. X., Iwashyna, T. J., Brunkhorst, F. M., Rea, T. D., Scherag, A., et al. (2016). Assessment of clinical criteria for sepsis: For the third international consensus definitions for sepsis and septic shock (Sepsis-3). *JAMA* 315 (8), 762–774. doi:10.1001/jama.2016.0288

Spapen, H. (2008). Liver perfusion in sepsis, septic shock, and multiorgan failure. *Anat. Rec.* 291 (6), 714–720. doi:10.1002/ar.20646

Srivastava, B., and Gimson, A. (2013). Hepatic changes in systemic infection. *Best. Pract. Res. Clin. Gastroenterol.* 27 (4), 485–495. doi:10.1016/j.bpg.2013.06.011

Strnad, P., Tacke, F., Koch, A., and Trautwein, C. (2017). Liver - guardian, modifier and target of sepsis. *Nat. Rev. Gastroenterol. Hepatol.* 14 (1), 55–66. doi:10.1038/nrgastro.2016.168

Su, H., Ma, Z., Guo, A., Wu, H., and Yang, X. (2020). Salvianolic acid B protects against sepsis-induced liver injury via activation of SIRT1/PGC-1α signaling. *Exp. Ther. Med.* 20 (3), 2675–2683. doi:10.3892/etm.2020.9020

Traeger, T., Mikulcak, M., Eipel, C., Abshagen, K., Diedrich, S., Heidecke, C. D., et al. (2010). Kupffer cell depletion reduces hepatic inflammation and apoptosis but decreases survival in abdominal sepsis. *Eur. J. Gastroenterol. Hepatol.* 22 (9), 1039–1049. doi:10.1097/MEG.0b013e32833847db

Vandewalle, J., Steeland, S., Van Ryckeghem, S., Eggermont, M., Van Wonterghem, E., Vandenbroucke, R. E., et al. (2019). A study of cecal ligation and puncture-induced sepsis in tissue-specific tumor necrosis factor receptor 1-deficient mice. *Front. Immunol.* 10, 2574. doi:10.3389/fimmu.2019.02574

Wang, X. P., Yu, X., Yan, X. J., Lei, F., Chai, Y. S., Jiang, J. F., et al. (2017). TRPM8 in the negative regulation of TNFα expression during cold stress. *Sci. Rep.* 7, 45155. doi:10.1038/srep45155

Wesche-Soldato, D. E., Chung, C. S., Gregory, S. H., Salazar-Mather, T. P., Ayala, C. A., and Ayala, A. (2007). CD8+ T cells promote inflammation and apoptosis in the liver after sepsis: Role of fas-FasL. *Am. J. Pathol.* 171 (1), 87–96. doi:10.2353/ajpath.2007.061099

Witko-Sarsat, V., Mocek, J., Bouayad, D., Tamassia, N., Ribeil, J. A., Candalh, C., et al. (2010). Proliferating cell nuclear antigen acts as a cytoplasmic platform controlling human neutrophil survival. *J. Exp. Med.* 207 (12), 2631–2645. doi:10.1084/jem.20092241

Woznica, E. A., Inglot, M., Woznica, R. K., and Lysenko, L. (2018). Liver dysfunction in sepsis. *Adv. Clin. Exp. Med.* 27 (4), 547–551. doi:10.17219/acem/68363

Yan, J., and Li, S. (2014). The role of the liver in sepsis. *Int. Rev. Immunol.* 33 (6), 498–510. doi:10.3109/08830185.2014.889129

Yang, J-x., Li, Y-l., and Shi, N-c. (2018). Attenuation of sepsis-induced rat liver injury by epigallocatechin gallate via suppression of oxidative stress-related inflammation. *Trop. J. Pharm. Res.* 16, 2877. doi:10.4314/tjpr.v16i12.11

Yoon, J. H., and Gores, G. J. (2002). Death receptor-mediated apoptosis and the liver. *J. Hepatol.* 37 (3), 400–410. doi:10.1016/s0168-8278(02)00209-x

Zaia, M. G., Cagnazzo, T., Feitosa, K. A., Soares, E. G., Faccioli, L. H., Allegretti, S. M., et al. (2016). Anti-inflammatory properties of menthol and menthone in schistosoma mansoni infection. *Front. Pharmacol.* 7, 170. doi:10.3389/fphar.2016.00170

Zhang, H., Feng, Y. W., and Yao, Y. M. (2018). Potential therapy strategy: Targeting mitochondrial dysfunction in sepsis. *Mil. Med. Res.* 5 (1), 41. doi:10.1186/s40779-018-0187-0

Zhang, H., Wang, W., Fang, H., Yang, Y., Li, X., He, J., et al. (2014). GSK-3β inhibition attenuates CLP-induced liver injury by reducing inflammation and hepatic cell apoptosis. *Mediat. Inflamm.* 2014, 629507. doi:10.1155/2014/629507

Zhou, Y. X., Han, W. W., Song, D. D., Li, Z. P., Ding, H. J., Zhou, T., et al. (2020). Effect of miR-10a on sepsis-induced liver injury in rats through TGF-β1/Smad signaling pathway. *Eur. Rev. Med. Pharmacol. Sci.* 24 (2), 862–869. doi:10.26355/eurrev_202001_20070

frontiers | Frontiers in Pharmacology

TYPE Original Research
PUBLISHED 30 September 2022
DOI 10.3389/fphar.2022.991917

OPEN ACCESS

EDITED BY
Ahmad Nazrun Shuid,
MARA University of Technology,
Malaysia

REVIEWED BY
Andrzej T Slominski,
University of Alabama at Birmingham,
United States
Siti Norsyafika Kamarudin,
Universiti Teknologi MARA, Malaysia

*CORRESPONDENCE
Dong Dong,
dongdong1983jd@163.com
Baojian Wu,
bj.wu@hotmail.com

†These authors have contributed equally to this work

SPECIALTY SECTION
This article was submitted to Ethnopharmacology, a section of the journal Frontiers in Pharmacology

RECEIVED 12 July 2022
ACCEPTED 12 September 2022
PUBLISHED 30 September 2022

CITATION
Sun G, Dang Y, Lin Y, Zeng W, Wu Z, Zhang X, Dong D and Wu B (2022), Scutellaria baicalensis Georgi regulates REV-ERBα/BMAL1 to protect against skin aging in mice.
Front. Pharmacol. 13:991917.
doi: 10.3389/fphar.2022.991917

Scutellaria baicalensis Georgi regulates REV-ERBα/BMAL1 to protect against skin aging in mice

Guanghui Sun[1†], Yongkang Dang[2†], Yanke Lin[2], Wanying Zeng[2], Zongjian Wu[2], Xingwang Zhang[1], Dong Dong[3*] and Baojian Wu[2*]

[1]College of Pharmacy, Jinan University, Guangzhou, China, [2]Institute of Molecular Rhythm and Metabolism, Guangzhou University of Chinese Medicine, Guangzhou, China, [3]School of Medicine, Jinan University, Guangzhou, China

Scutellaria baicalensis Georgi (SBG) is a traditional Chinese medicine widely used to treat disorders such as hypertension, dysentery and hemorrhaging. Here, we aimed to assess the pharmacological effects of SBG on skin aging and to investigate the underlying mechanisms. Mice with skin aging were established by treatment with D-galactose and ultraviolet-B. SBG (topical application) showed a protective effect on skin aging in mice, as evidenced by less formation of skin wrinkles, higher levels of SOD (superoxide dismutase) and HYP (hydroxyproline) as well as a lower level of MDA (malondialdehyde). In the meantime, skin MMP-1 and p53 expression were lower, epidermis was thinner and collagen amount was higher in SBG-treated mice. Anti-skin aging effects of SBG were also confirmed in NIH3T3 and HaCaT cells, as well as in mouse primary dermal fibroblasts and human primary epidermal keratinocytes. Furthermore, we found that loss of *Rev-erbα* (a known repressor of Bmal1) up-regulated skin BMAL1 (a clock component and a known anti-aging factor) and ameliorated skin aging in mice. Moreover, SBG dose-dependently increased the expression of BMAL1 in the skin of aged mice and in senescent NIT3H3 cells. In addition, based on a combination of Gal4 chimeric, luciferase reporter and expression assays, SBG was identified as an antagonist of REV-ERBα and thus an inducer of BMAL1 expression. In conclusion, SBG antagonizes REV-ERBα to up-regulate BMAL1 and to protect against skin aging in mice.

KEYWORDS

scutellaria baicalensis georgi, skin aging, REV-erbα, BMAL1, photoaging

Abbreviations:: Bmal1, brain and muscle ARNT–like one; CCGs, clock–controlled genes; Clock, circadian locomotor output cycles kaput; Crys, cryptochromes; D–gal, D–galactose; HYP, hydroxyproline; MDA, malondialdehyde; NR1D1, nuclear receptor subfamily one group D member one; Pers, periods; qPCR, quantitative polymerase chain reaction; ROS, reactive oxygen species; SA–β–gal, senescence–associated–β–galactosidase; SBG, Scutellaria baicalensis Georgi; SOD, superoxide dismutase; UV, ultraviolet.

Introduction

Scutellaria baicalensis Georgi (SBG, also known as *Huangqin* in Chinese), a traditional Chinese medicine, possesses various pharmacological effects such as anti-inflammatory, antiviral, anticancer, anti-oxidant and antibacterial activities. SBG is widely used to treat diarrhea, hypertension, dysentery and hemorrhaging (Liao et al., 2021). Many types of chemicals are found in SBG, including flavones, phenylethanoids, amino acids, sterols and essential oils (Zhao et al., 2016). Of note, flavones (e.g., baicalin, baicalein, wogonin and oroxylin A) are thought to be a major class of active ingredients of SBG as they show the health-promoting effects (such as anti-inflammation, antivirus, anticancer, anti-oxidation and anti-bacteria) typically observed for SBG (Brown, 1980; Li et al., 2004). It is interesting to note that SBG has great potential to manage the skin diseases caused by sunlight irradiation (Brown, 1980). The underlying mechanisms may involve scavenging of free radicals and attenuation of lipid oxidation (Gabrielska et al., 1997). However, it remains unknown whether SBG can protect against skin aging.

Skin aging is classified into intrinsic (chronological) and extrinsic aging, and the latter is also referred to as premature skin aging or photoaging (Bocheva et al., 2019). Intrinsic aging is an unpreventable spontaneous process, whereas extrinsic aging caused by exogenous factors (e.g., ultraviolet/UV light, cigarette smoking and pollution) is preventable (Fisher et al., 2002; Bernhard et al., 2007). UV radiation is a major cause of photoaging, and can be divided into three bands [i.e., UVA (315–400 nm), UVB (280–315 nm) and UVC (100–280 nm)]. Of note, UVB is the predominant form that causes injuries to living organisms (Slominski et al., 2018a; Frommeyer et al., 2022). UV radiation not only induces skin pathology, but also exert systemic effects, including activation of hypothalamic-pituitary-adrenal axis, opioidogenic effects, and immunosuppression. Thus, UV radiation has therapeutic applications in management of various diseases such as addiction, autoimmune and mood disorders (Slominski et al., 2018a). Although skin aging is regarded as a cosmetic problem, it can result in disfigurement and skin diseases (such as skin cancers) and has profound psychological consequences (Watson et al., 2016; Narayanan et al., 2010). There are two major classes of agents for management of skin aging, namely, antioxidants and cell regulators. However, these medications (e.g., retinoid) are concerned with the lack of effectiveness and/or adverse effects (Krutmann et al., 2021; Mukherjee et al., 2006). Therefore, it is of value to search for more effective and safer therapeutic agents.

BMAL1 (Brain and muscle ARNT-like protein 1) is a transcription factor and a core component of circadian clock system, which generates and maintains circadian rhythms in most aspects of physiology and behaviors (Gekakis et al., 1998; Hogenesch et al., 1998; Bunger et al., 2000). *Bmal1* and other clock genes work cooperatively to drive circadian gene expression using a negative feedback mechanism (Chen et al., 2009; Duong et al., 2011). BMAL1 forms a heterodimer with CLOCK (circadian locomotor output cycles kaput) to activate the transcription of *Pers* (periods) and *Crys* (cryptochromes) as well as many other clock-controlled genes (CCGs) (Langmesser et al., 2008). Once reaching a critical level, PER and CRY proteins in turn inhibit the activity of the BMAL1/CLOCK dimer, bringing down the levels of CCGs (Böger, 2014). As PER and CRY proteins are reduced due to degradation, a new cycle of BMAL1/CLOCK-driven transcription can begin (Duong et al., 2011). In addition to regulating circadian rhythms, BMAL1 plays a role in the development and progression of many types of diseases such as cancers (Jung et al., 2013), obesity (Hemmeryckx et al., 2011), and neurodegenerative disorders (Vieira et al., 2020). Notably, *Bmal1* is also involved in aging (Khapre et al., 2011). *Bmal1*-deficient mice have reduced lifespan and are prone to premature aging (exemplified by sarcopenia, cataracts, reduced subcutaneous fat, decreased organ size and impaired hair growth) (Kondratov et al., 2006). *Bmal1* regulates aging *via* modulation of the expression of major antioxidant enzymes including SOD, peroxiredoxines and glutathione peroxidase (Kondratov et al., 2009).

REV-ERBα (also known as NR1D1, nuclear receptor subfamily one group D member 1) is a nuclear receptor that participates in regulation of circadian rhythms *via* inhibiting BMAL1 expression (Yin and Lazar, 2005). REV-ERBα functions as a transcriptional repressor that inhibits the transcription of target genes (e.g., *Bmal1*) by binding to a response element (called RevRE) in the promoters and recruiting the corepressors nuclear corepressor one and histone deacetylase 3 (Liu et al., 2008; Yin et al., 2010). REV-ERBα has been also implicated in regulation of a variety of diseases including inflammatory diseases (e.g., fulminant hepatitis, pulmonary inflammation, and colitis) (Wang et al., 2020), metabolic disorders (Delezie et al., 2012) and cancers (Wang et al., 2015). SR8278 (a synthetic compound) is identified as an antagonist of REV-ERBα and widely used to probe the function of REV-ERBα (Kojetin et al., 2011; Pardee et al., 2011). Notably, we recently found that REV-ERBα restrains *Propionibacterium acnes*-induced skin inflammation through inhibiting the NF-κB/NLRP3 axis to protect against acne vulgaris (Li et al., 2022). However, it remains elusive whether and how REV-ERBα regulates skin aging.

In the present study, we aimed to assess the pharmacological effects of SBG on skin aging and to investigate the underlying mechanisms. Anti-skin aging effects of SBG were evaluated using mouse and cell models

of aging (induced by D-galactose and/or ultraviolet-B). Skin aging was assessed by analyzing SOD, HYP, MDA, ROS and MMP-1/p53 and by measuring epidermal thickness and collagen content. The role of REV-ERBα/BMAL1 in regulating skin aging was assessed using gene knockout mice. Antagonism of REV-ERBα was determined using Gal4 chimeric assay. We for the first time demonstrated that SBG antagonizes REV-ERBα to up-regulate BMAL1 (a skin aging-inhibiting factor) and to protect against skin aging in mice.

Materials and methods

Materials

SBG was purchased from Biopurify Phytochemicals (Chengdu, China). D-galactose (D-gal) was purchased from Aladdin (Shanghai, China). Vitamin C was obtained from Yuanye Biotechnology (Shanghai, China). Biochemical kits for SOD, MDA, ROS and HYP were purchased from Jiancheng Bioengineering Institute (Nanjing, Jiangsu, China). Staining kit for senescence-associated-β-galactosidase (SA-β-gal) was obtained from Beyotime Biotechnology (Shanghai, China). Antibodies against GAPDH, MMP-1, p53, BMAL1, REV-ERBα, BHMT and NLRP3 were purchased from Abcam (Cambridge, United Kingdom).

Preparation of SBG extract

SBG was extracted for 90 min by refluxing in 80% ethanol (3:20, *w*/*v*), and filtered with filter paper. The filtrate was concentrated and freeze-dried. The dry residue (SBG extract) was stored at -20°C. The extraction yield was 23.3%, and the main active ingredients of SBG are shown in Supplementary Table S1. For animal experiments, SBG extract was mixed with a homemade cream containing stearic acid, triethanolamine, and propylene glycol.

Animals

C57BL/6 mice (10 weeks old) weighing 18–22 g were obtained from HFK Bioscience (Beijing, China). *Rev-erbα*$^{-/-}$ mice (on a C57BL/6 background) have been established and validated in our laboratory (Wang et al., 2018). All mice were maintained on a 12 h light/12 h dark cycle, with free access to food and water. Mice were individually placed in the cages to prevent offensive behaviors from other mice, that may cause injuries to the skin. Mice from the same litter (with hair growth in the anagen phase) were used for experiments. Note that we used male mice to assess the therapeutic effect of SBG on skin aging, without considering factors such as hormone-induced wrinkling of skin. Protocols for animal experiments were approved by the Institutional Animal Care and Use Committee of Guangzhou University of Chinese Medicine (Appr. Date: 2021–05-17; IACUC Issue No: ZYD-2021–112).

LC-MS/MS analysis

The main active constituents (i.e., wogonoside, baicalein, baicalin and wogonin) in SBG extract were quantified using a Shimadzu LCMS-8045 triple quadrupole liquid chromatograph mass spectrometer (LC-MS) equipped with Shimadzu-Nexera XR high-performance liquid chromatography (HPLC). The mobile phases consisted of acetonitrile (A) and water (B). Flow rate was set at 0.3 ml/min. Gradient elution program was 40% B (0–1 min), 40–10% B (1–3 min), 10% B (3–4 min) and 10–40% B (4–5 min). Mass spectrometer was operated at positive ion scan mode. The mass transition ion pairs and contents of main active constituents are provided in Supplementary Table S1

Mouse model of skin aging and drug treatment

To induce skin aging, mice were injected subcutaneously with 250 mg/kg D-gal daily in the back neck and irradiated on the back daily with 120 mJ/cm^2 UVB for 6 weeks as previously described (Zhang et al., 2020). The source of radiation was a narrow band UVB bulb (Philips model PL-9 9W/01/2P) emitting photons with wavelengths between 306 and 316 nm, with a peak at 312 nm. The distance from the UVB lamp (KN-4003BL, Kernel Medical Equipment, Xuzhou, China) to the mouse back was 25 cm. Control mice were injected subcutaneously with vehicle (saline). To assess the effects of SBG on skin aging, SBG extract (25, 100 or 400 mg/kg), vitamin C (40 mg/kg) or vehicle was applied topically (once daily after UVB exposure) on the skin of mouse models for 4 weeks from the third week. Mice were sacrificed to collect skin samples, followed by qPCR, Western blotting and biochemical analyses (SOD, MDA and HYP).

Isolation of mouse primary dermal fibroblasts

Mouse primary dermal fibroblasts were isolated from newborn mice as previously described (Terao et al., 2014). The newborn mice were sacrificed by rapid cervical dislocation. Trunk skin was peeled off and incubated with 4 mg/ml dispase overnight at 4 °C. On the next day, the dermis was separated from the epidermis using forceps, and incubated with 0.25% trypsin for 10 min. After filtration, cells were centrifuged at 200 g for 10 min, resuspended in Dulbecco's modified Eagle's medium (DMEM) supplemented with 10% fetal bovine serum (FBS) and incubated at 37°C and 5% CO_2.

TABLE 1 Primers used for qPCR assays.

Gene	Forward (5–3′)	Reverse (5–3′)
mp53	GTCACAGCACATGACGGAGG	TCTTCCAGATGCTCGGGATAC
mMmp-1	CTTCTTCTTGTTGAGCTGGACTC	CTGTGGAGGTCACTGTAGACT
mBhmt	TTAGAACGCTTAAATGCCGGAG	GATGAAGCTGACGAACTGCCT
mNlrp3	ATTACCCGCCCGAGAAAGG	TCGCAGCAAAGATCCACACAG
mRev-erbα	TTTTTCGCCGGAGCATCCAA	ATCTCGGCAAGCATCCGTTG
mBmal1	CTCCAGGAGGCAAGAAGATTC	ATAGTCCAGTGGAAGGAATG
mGapdh	CAAGGAGTAAGAAACCCTGGA	CGAGTTGGGATAGGGCCTCT
hp53	TTGGCTCTGACTGTACCACCAT	CAGTGTGATGATGGTGAGGATG
hMMP-1	TCGGGGCTTTGATGTACCCT	ACACGCTTTTGGGGTTTGTG
hGAPDH	CATGAGAAGTATGACAACAGCCT	TAGTCCTTCCACGATACCAAAGT

m, mouse; h, human.

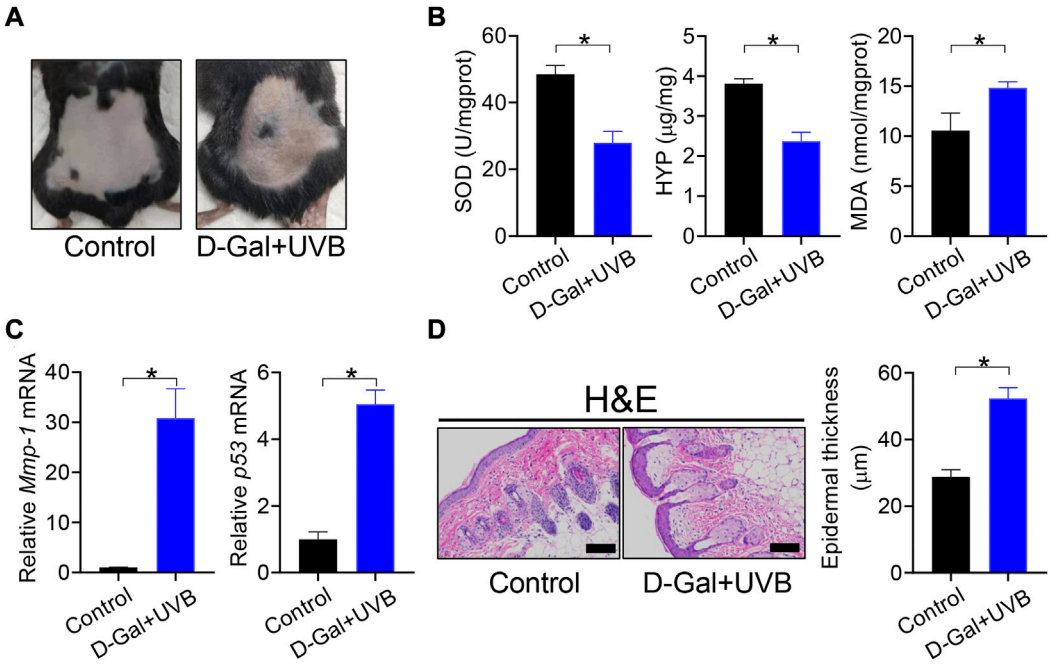

FIGURE 1
Establishment of mice with skin aging. **(A)** Surface examination of dorsal skin derived from D-gal/UVB-treated and control mice. **(B)** Skin SOD activity and HYP/MDA levels in D-gal/UVB-treated and control mice. Data are mean ± SD ($n = 7$). *$p < 0.05$ (*t*-test). **(C)** mRNA expression of *Mmp-1* and *p53* in the skin of D-gal/UVB-treated and control mice. Data are mean ± SD ($n = 7$). *$p < 0.05$ (*t*-test). **(D)** H&E staining (left panel) and epidermal thickness (right panel) of skin derived from D-gal/UVB-treated and control mice. Scale bar = 100 μm.

Cell culture and treatment

NIH3T3, HaCaT and Primary adult human epidermal keratinocytes (HEKa) cells were obtained from the American Type Culture Collection (Rockville, MD). NIH3T3, HaCaT and HEKa were maintained in DMEM supplemented with 10% FBS, 100 U/ml penicillin and 100 mg/ml streptomycin. To induce NIH3T3 cell senescence, 8 g/L D-gal was added to the culture medium for 96 h. To induce cell senescence of HaCaT, mouse primary dermal fibroblasts and HEKa, cells were subjected to UVB irradiation (100 mJ/cm^2) with a thin layer of PBS (phosphate-buffered saline) using a UVB lamp (KN-4003BL, Kernel Medical Equipment, Xuzhou, China). Cells were then treated with SBG or vehicle. On next day, cells were collected for qPCR and Western blotting.

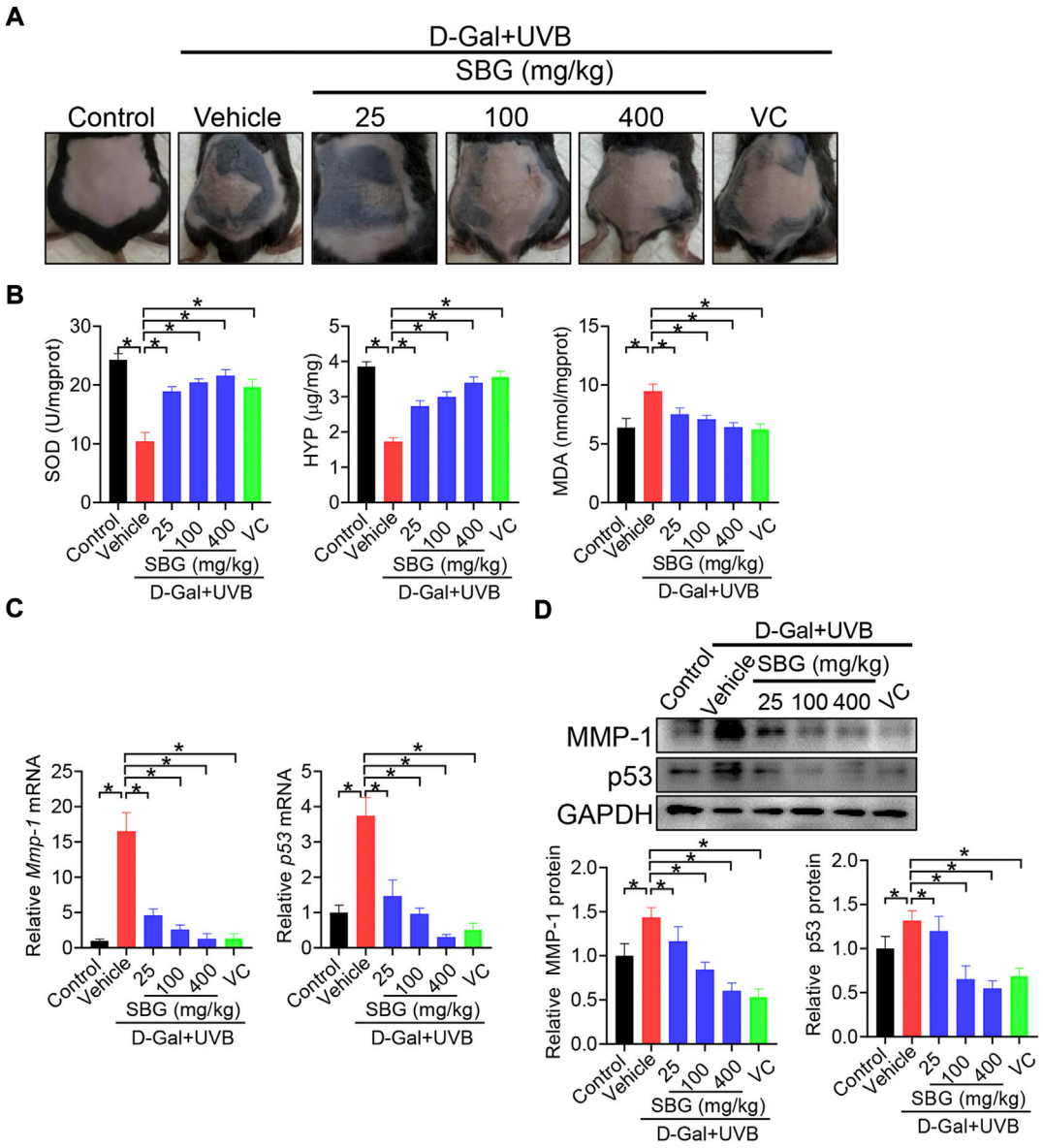

FIGURE 2
SBG protects against skin aging induced by D-gal/UVB in mice. **(A)** Surface examination of dorsal skin derived from D-gal/UVB-treated and control mice. **(B)** Skin SOD activity and HYP/MDA levels in D-gal/UVB-treated and control mice. **(C)** mRNA expression of *Mmp-1* and *p53* in the skin of D-gal/UVB-treated and control mice. **(D)** Protein expression (top panel) and quantification (bottom panel) of MMP-1/p53 in the skin of D-gal/UVB-treated and control mice. In panels B–D, data are mean ± SD ($n = 7$). *$p < 0.05$ (one-way ANOVA and Bonferroni post hoc test). VC, vitamin.

Gal4 co-transfection assay

Gal4 co-transfectionthe assay was performed as previously described (Zhang et al., 2018). In brief, HEK293 cells were co-transfected with pGal4-Rev-erbα-LBD plasmid (200 ng), pGL-4.35-Luc reporter (100 ng, a Gal4-reponsive luciferase reporter) and pRL-TK vector (10 ng) using jetPRIME (Polyplus Transfection, Illkirch, France). On next day, cells were treated with SBG or SR8278 or vehicle. 24 h later, luciferase activities were measured using the Dual-Luciferase Reporter Assay system and GloMax 20/20 luminometer (Promega Madison, WI).

Luciferase reporter assays

Luciferase reporter assays were performed as previously described (Chen et al., 2020). In brief, NIH3T3 cells were cultured in DMEM medium (containing 10% FBS, 1%

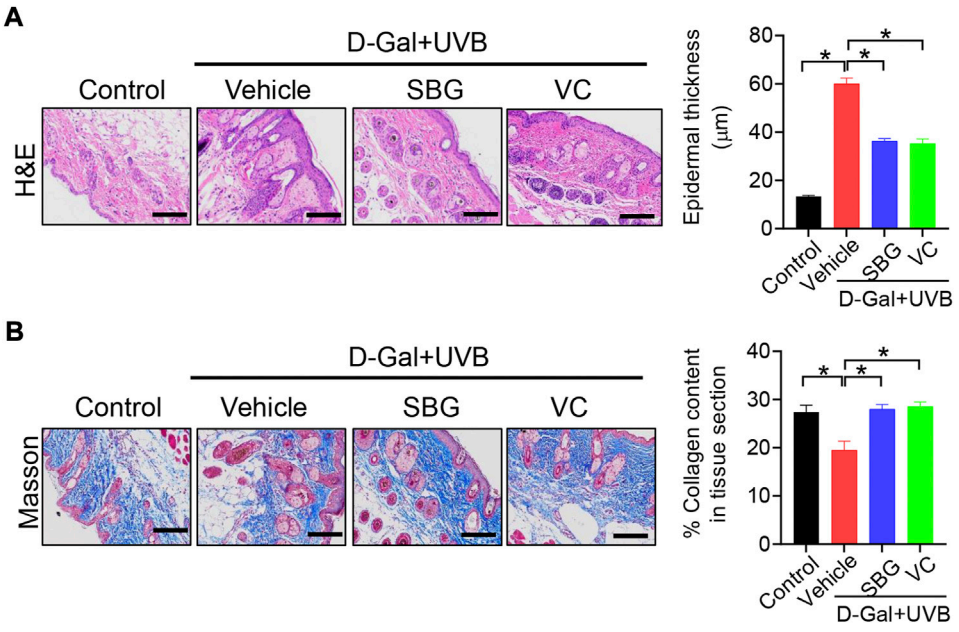

FIGURE 3
Effects of SBG on epidermal thickness and collagen content in aging mice. **(A)** H&E staining (left panel) and epidermal thickness (right panel) of skin derived from D-gal/UVB-treated and control mice. Scale bar = 100 μm. **(B)** Masson staining of the skin derived from D-gal/UVB-treated and control mice. The right panel shows collagen content in the skin. Data are mean ± SD (n = 7). *p < 0.05 (one-way ANOVA and Bonferroni post hoc test). Scale bar = 100 μm.

penicillin-streptomycin) and transfected with 250 ng of Bmal1 luciferase reporter plasmid and 50 ng of pRL-TK using jetPRIME (Polyplus Transfection, Illkirch, France). On next day, SBG or SR8278 or vehicle was added to the culture medium for 24 h. Cells were harvested and lysed with passive lysis buffer. Luciferase activities were detected using the Dual-Luciferase Reporter Assay system and GloMax 20/20 luminometer (Promega, Madison, WI).

H&E and masson staining

Skin samples were fixed in 10% formalin, embedded in paraffin, and cut to 4 μm-thick sections. The sections were subjected to H&E (hematoxylin and eosin) and Masson staining. The images were captured using an optical microscope (Olympus, Tokyo, Japan).

Measurement of intracellular ROS

Cells were treated with 2′7′-dichlorodihydrofluorescein diacetate (10 μM) at 37°C for 1 h. Fluorescence intensity was determined at excitation (485 nm) and emission (530 nm) wavelengths using a Synergy HT Multi-Mode Microplate Reader (BioTek, Winooski, VT).

MTT assay

MTT assays were performed to determine cell viability as previously described (Kumar et al., 2018). Briefly, cells were incubated with MTT [3-(4,5-dimethylthiazol-2-yl)-2,5 diphenyl tetrazolium bromide, 0.5 mg/ml] for 4 h, and the formazan crystals were dissolved in 100 μl DMSO. The absorbance was determined at 570 nm using a Synergy HT Multi-Mode Microplate Reader (BioTek, Winooski, VT).

SA-β-gal assay

SA-β-gal activity was measured using a SA-β-gal staining kit according to the manufacturer's instructions (Beyotime, Shanghai, China). Briefly, cells were fixed in a fixing solution for 15 min, washed with PBS and incubated with senescence detection solution at 37°C. On next day, the number of SA-β-gal-positive cells were determined by counting blue-stained cells using an Eclipse ci-L microscope (Nikon, Tokyo, Japan).

Real-time luminescence monitoring

Real-time luminescence monitoring was performed as previously described (Hirota et al., 2008; du Pré et al., 2017). In brief,

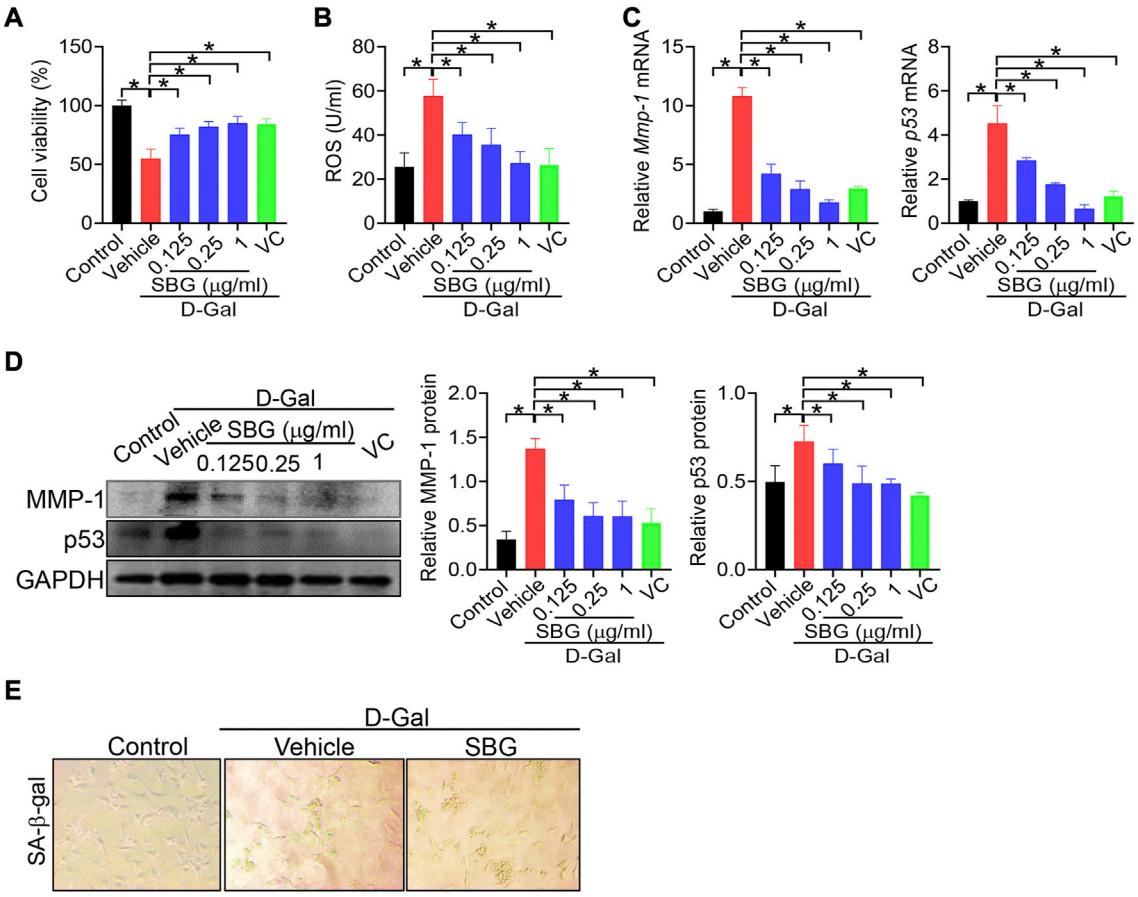

FIGURE 4
SBG attenuates D-gal-induced senescence in NIH3T3 cells. **(A)** Effects of SBG on the viability of D-gal-treated NIH3T3 cells. **(B)** Effects of SBG on ROS accumulation in D-gal-treated NIH3T3 cells. **(C)** Effects of SBG on *Mmp-1* (left panel) and *p53* (right panel) mRNA expression in D-gal-treated NIH3T3 cells. **(D)** Effects of SBG on protein expression of MMP-1 and p53 in D-gal-treated NIH3T3 cells. **(E)** Representative images showing SA-β-Gal activity in SBG-treated senescent NIH3T3 cells. In panels A–D, data are mean ± SD ($n = 3$). *$p < 0.05$ (one-way ANOVA and Bonferroni post hoc test).

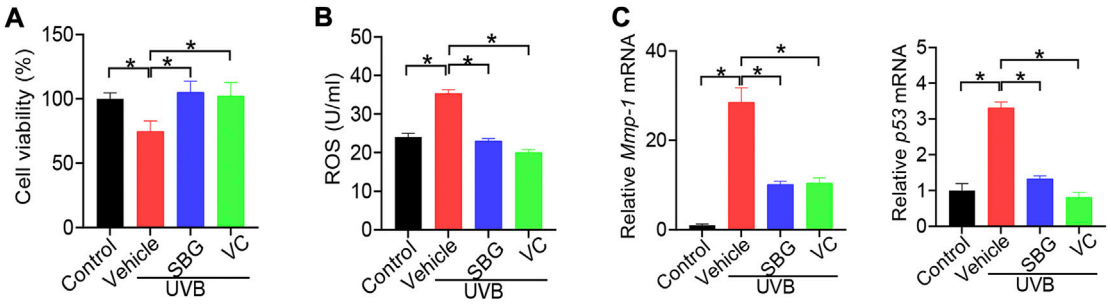

FIGURE 5
SBG attenuates UVB-induced senescence in HaCaT cells. **(A)** Effects of SBG on the viability of UVB-treated HaCaT cells. **(B)** Effects of SBG on ROS accumulation in UVB-treated HaCaT cells. **(C)** Effects of SBG on the mRNA expression of *Mmp-1* and *p53* in UVB-treated HeCaT cells. Data are mean ± SD ($n = 3$). *$p < 0.05$ (one-way ANOVA and Bonferroni post hoc test).

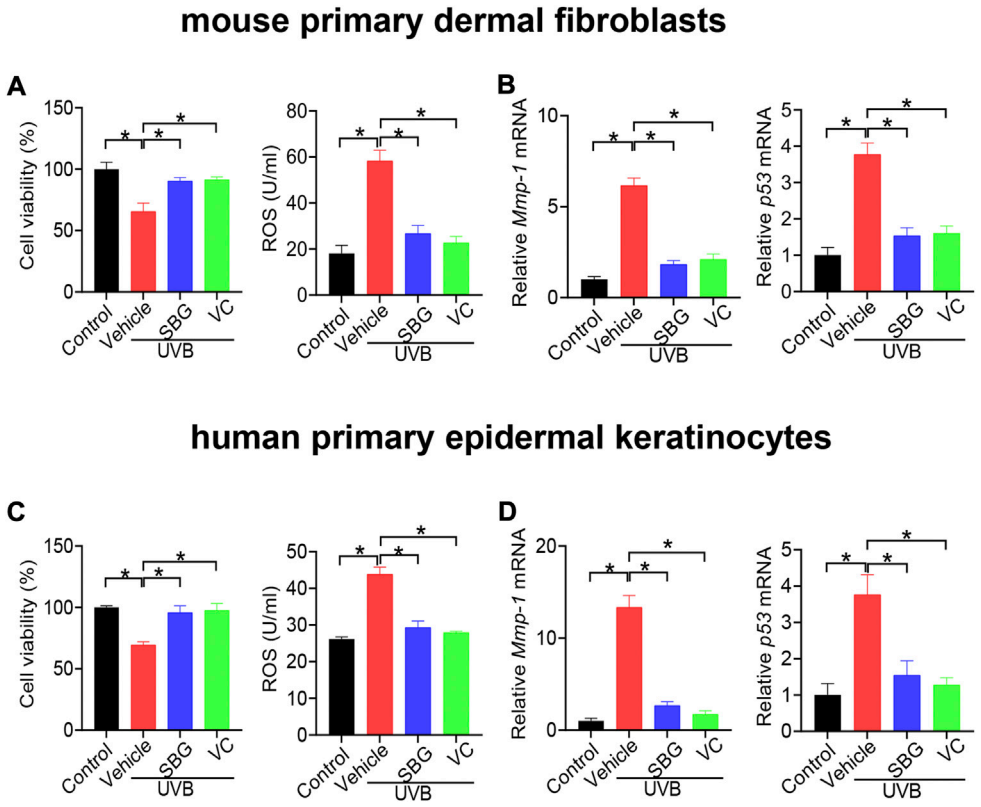

FIGURE 6
SBG attenuates UVB-induced senescence in mouse primary dermal fibroblasts and HEKa cells. **(A)** Effects of SBG on cell viability and ROS accumulation for UVB-treated mouse primary dermal fibroblasts. **(B)** Effects of SBG on mRNA expression of *Mmp-1* and *p53* in UVB-treated mouse primary dermal fibroblasts. **(C)** Effects of SBG on cell viability and ROS accumulation for UVB-treated HEKa cells. **(D)** Effects of SBG on mRNA expression of *Mmp-1* and *p53* in UVB-treated HEKa cells. Data are mean ± SD ($n = 3$). *$p < 0.05$ (one-way ANOVA and Bonferroni post hoc test).

NIH3T3 cells stably overexpressed with *Bmal1-dLuc* were seeded into a 35 mm dish and maintained in DMEM containing 10% FBS. On next day, cells were incubated with a recording medium containing 1 μg/ml SBG or vehicle. Luminescence data (counts/s) were collected by using Lumicycle 32 (Actimetrics, Wilmette, IL).

Western blotting

Protein samples were subjected to 10% sodium dodecyl sulfate-polyacrylamide gel electrophoresis (SDS-PAGE), and transferred to PVDF membranes. The membranes were blocked with 5% skim milk, and sequentially incubated with primary and secondary antibodies. Protein bands were visualized by using enhanced chemiluminescence and Omega Lum G imaging system (Aplegen, Pleasanton, CA), and quantified with Fluorchem 5500 software (Fisher Scientific, Fair Lawn, NJ). GAPDH was used as a loading control.

qPCR (quantitative polymerase chain reaction)

RNA was extracted using RNAiso Plus reagent (Takara, Shiga, Japan) and transcribed to cDNA using PrimeScript RT Master Mix (Vazyme, Jiangsu, China). qPCR reactions were performed using the SYBR Premix Ex Taq (Vazyme, Jiangsu, China). Amplification procedures consisted of an initial denaturation at 95°C for 5 min, 40 cycles of denaturation at 95°C for 15 s, annealing at 60°C for 30 s, and extension at 72°C for 30 s. Mouse *Gapdh* was used as an internal control. Gene expression was determined using the $2^{-\Delta\Delta CT}$ method. Primers are provided in Table 1.

Statistical analysis

Data are presented as means ± SD (standard deviation). Comparisons between two groups were analyzed using Student's t-test. One-way ANOVA followed by Bonferroni post hoc test

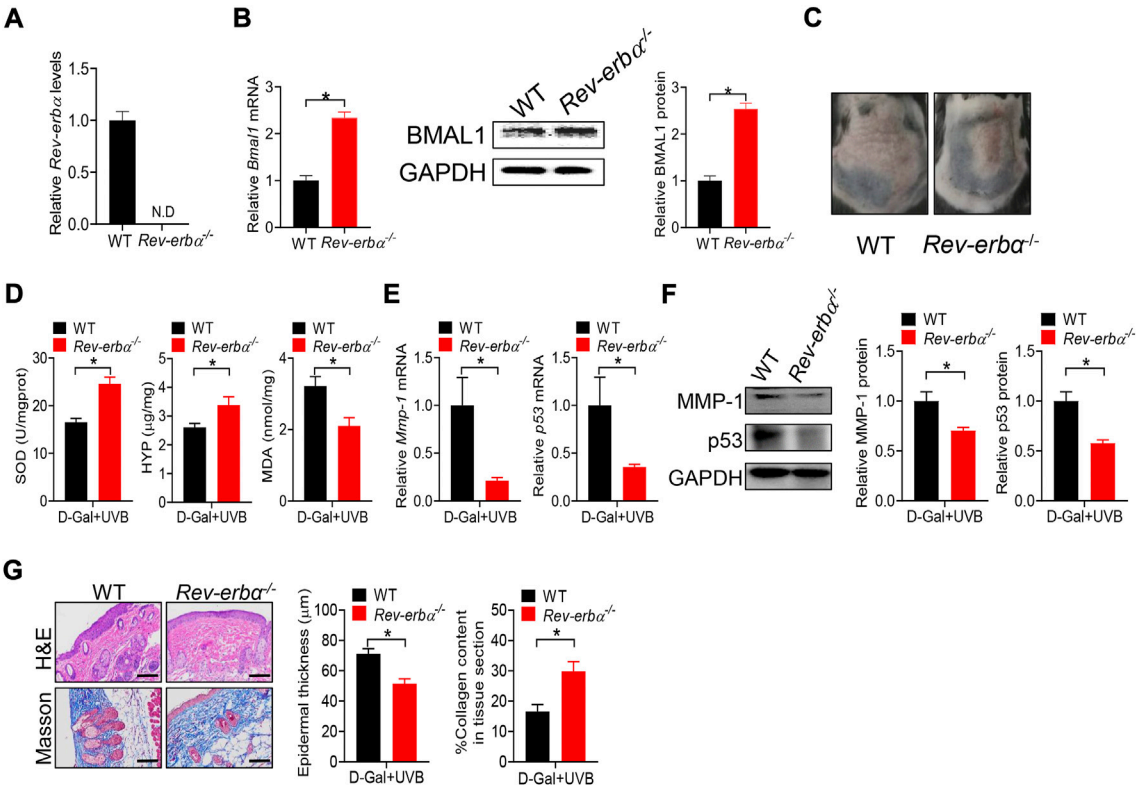

FIGURE 7
Loss of *Rev-erbα* up-regulates skin BMAL1 and ameliorates skin aging in mice. **(A)** mRNA expression of *Rev-erbα* in skin derived from *Rev-erbα*$^{-/-}$ and wild-type (WT) mice. **(B)** mRNA (left panel) and protein (right panel) expression of BMAL1 in skin derived from *Rev-erbα*$^{-/-}$ and WT mice. **(C)** Surface examination of dorsal skin derived from *Rev-erbα*$^{-/-}$ and WT mice treated with D-gal/UVB. **(D)** Skin SOD activity and HYP/MDA levels in skin derived from *Rev-erbα*$^{-/-}$ and WT mice treated with D-gal/UVB. **(E)** mRNA expression of *Mmp-1* and *p53* in the skin derived from *Rev-erbα*$^{-/-}$ and WT mice treated with D-gal/UVB. **(F)** Protein expression of MMP-1/p53 in skin derived from *Rev-erbα*$^{-/-}$ and WT mice treated with D-gal/UVB. **(G)** H&E and Masson staining showing epidermal thickness and collagen content in skin derived from *Rev-erbα*$^{-/-}$ and WT mice treated with D-gal/UVB. In panels A–B, data are mean ± SD (n = 3). In panels C–G, data are mean ± SD (n = 7). *p < 0.05 (t-test).

was performed to compare means of more than two groups. The level of significance was set at $p < 0.05$ (*).

RESULTS

SBG protects against skin aging induced by D-gal/UVB in mice

Mice with skin aging were established by treatment with D-gal/UVB as previously described (du Pré et al., 2017). As expected, D-gal/UVB-treated mice showed skin aging-like symptoms such as roughness, stiffness, and lack of elasticity (Figure 1A). These mice had lower levels of SOD activity and HYP and a higher level of MDA in the skin as compared to normal mice (Figure 1B). We also observed marked increases in the expression of *Mmp-1* and *p53* (two genes closely associated with skin aging) in the skin of D-gal/UVB-treated mice (Figure 1C). In addition, the epidermis (D-gal/UVB-exposed region) was thicker in aging mice than in control mice according to H&E staining (Figure 1D). These data indicated successful construction of mice with skin aging.

We next assessed the effects of SBG (topical application) on skin aging in mice. Like vitamin C (a known anti-aging agent and used as a positive control), SBG reduced the wrinkle formation in the skin of D-gal/UVB-treated mice (Figure 2A). Further, SBG dose-dependently increased the SOD activity and HYP level, and decreased the MDA level in the skin of aging mice (Figure 2B). Moreover, SBG reduced the mRNAs and proteins of both MMP-1 and p53 in the skin of aging mice in a dose-dependent manner (Figure 2C/D). In addition, compared to vehicle-treated aging mice, SBG-treated mice had thinner D-gal/UVB-exposed epidermis, and a higher amount of collagen (Figure 3A/B). Taken together, these findings clearly indicated a protective effect of SBG on skin aging in mice.

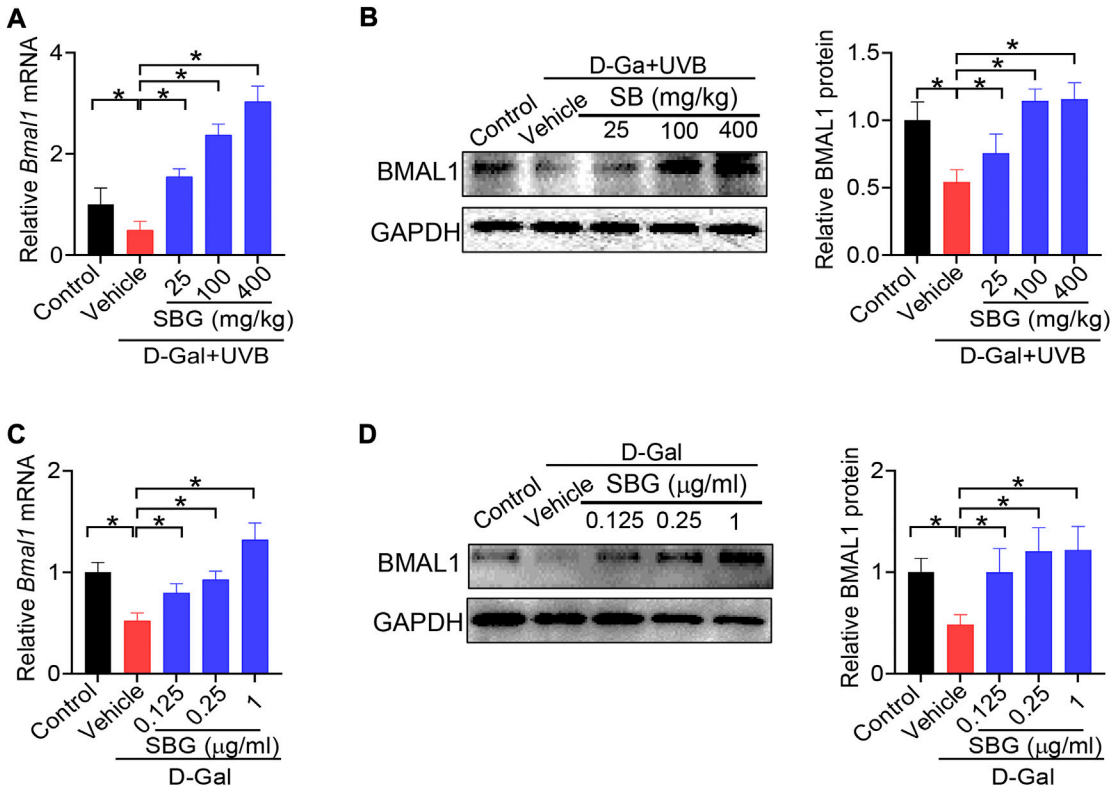

FIGURE 8
SBG up-regulates the clock gene *Bmal1* in mouse and cell models of aging. **(A)** Effects of SBG on *Bmal1* mRNA in the skin of D-gal/UVB-treated mice. **(B)** Effects of SBG on BMAL1 protein in the skin of D-gal/UVB-treated mice. **(C)** Effects of SBG on *Bmal1* mRNA in D-gal-treated NIH3T3 cells. **(D)** Effects of SBG on BMAL1 protein in D-gal-treated NIH3T3 cells. Data are mean ± SD ($n = 7$). *$p < 0.05$ (one-way ANOVA and Bonferroni post hoc test).

SBG attenuates D-gal- and UVB-induced cell senescence

We next investigated whether SBG can affect cell senescence using NIH3T3 and HaCaT cells. NIH3T3 cells were exposed to 8 g/L D-gal for 96 h to induce cell senescence as previously described (Gao et al., 2014). As expected, D-gal treatment of NIH3T3 cells resulted in senescence as evidenced by a decrease in cell viability, and elevations in ROS level and MMP-1/p53 expression, as well as an increase in senescence-associated β-galactosidase (SA-β-gal, a senescence-specific marker) activity (Figure 4). We found that SBG dose-dependently increased the cell viability and decreased the ROS level in D-gal-treated NIH3T3 cells (Figure 4A/B). Furthermore, SBG down-regulated the mRNA levels of both *Mmp-1* and *p53* in a dose-dependent fashion in D-gal-treated cells (Figure 4C). In line with the mRNA changes, MMP-1 and p53 proteins were reduced by SBG in the aged cells (Figure 4D). Moreover, SBG-treated senescent cells had a lower activity of SA-β-gal (Figure 4E).

We additionally examined the effects of SBG on senescene of HaCaT, mouse primary dermal fibroblasts and HEKa cells induced by UVB. SBG increased the cell viability and decreased the ROS level and MMP-1/p53 expression in the senescent cells (Figures 5, 6). These similar effects were also observed for vitamin C (Figures 5, 6). Altogether, these findings supported that SBG had a protective effect on skin aging.

Loss of *Rev-erbα* up-regulates skin BMAL1 and ameliorates skin aging in mice

Deficiency of *Bmal1* has been previously shown to promote premature aging in mice, identifying *Bmal1* as a key regulator of aging (Kondratov et al., 2006). *Bmal1* regulates aging *via* modulation of the expression of antioxidant enzymes including SOD, peroxiredoxines and glutathione peroxidase (Kondratov et al., 2009). *Bmal1* is a target gene of REV-ERBα, which functions as a transcriptional repressor (Crumbley and Burris, 2011). Loss of *Rev-erbα* leads to up-regulation of BMAL1 (Burris, 2008). Thus, we hypothesized that *Rev-erbα* may promote skin aging considering that *Bmal1* has a protective role. To test this

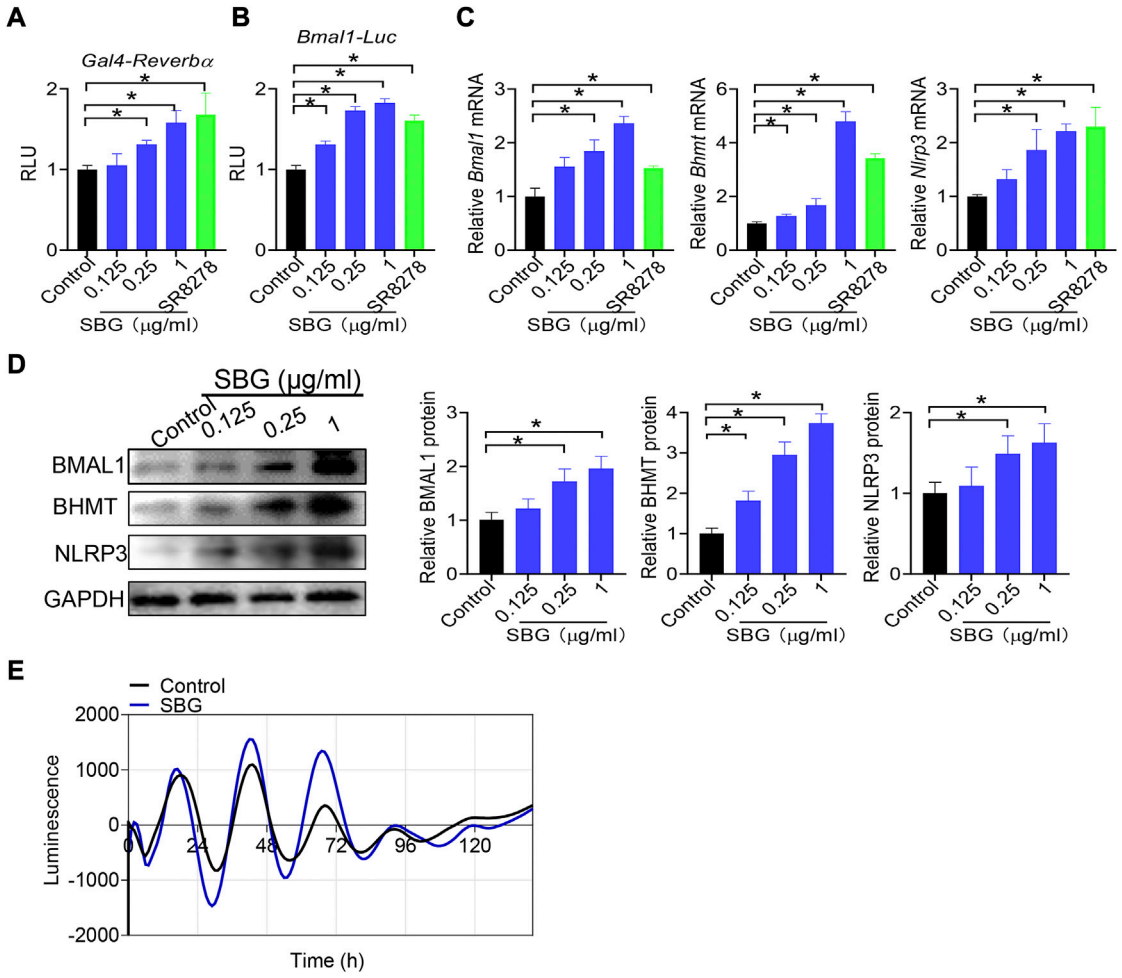

FIGURE 9
SBG antagonizes REV-ERBα to induce BMAL1 expression. **(A)** Dose-dependent effects of SBG on Gal4 luciferase activity. HEK293 cells were co-transfected with pGal4-*Rev-erbα*-LBD and pGL4.35-Luc plasmids for 24 h, followed by treatment with SBG or vehicle for 24 h. **(B)** Effects of SBG on *Bmal1-Luc* reporter activity. **(C)** Effects of SBG on the mRNA expression of *Bmal1, Bhmt and Nlrp3* in NIH3T3 cells treated with SBG or vehicle. **(D)** Effects of SBG on the protein expression of BMAL1, BHMT and NLRP3 in NIH3T3 cells treated with SBG or vehicle. **(E)** Bioluminescent recordings of *Bmal1-dLuc*-overexpressed NIH3T3 cells after SBG treatment. In panels A–B, data are mean ± SD (n = 6). In panels C–D, data are mean ± SD (n = 3). *p < 0.05 (one-way ANOVA and Bonferroni post hoc test).

hypothesis, we generated and tested a mouse line with deletion of *Rev-erbα* gene (*Rev-erbα*$^{-/-}$ mice). *Rev-erbα*$^{-/-}$ mice were validated by qPCR, and showed the absence of wild-type *Rev-erbα* transcript in the skin (Figure 7A). As expected, BMAL1 mRNA and protein were up-regulated in the skin of *Rev-erbα*$^{-/-}$ mice (Figure 7B). *Rev-erbα*$^{-/-}$ and control mice were subjected to induction of skin aging by D-gal/UVB. We found that loss of *Rev-erbα* ameliorated skin aging as evidenced by less formation of skin wrinkles, higher levels of SOD and HYP as well as a lower level of MDA (Figure 7C/D). In the meantime, skin MMP-1 and p53 expression were lower, epidermis was thinner and collagen amount was higher in *Rev-erbα*$^{-/-}$ mice (Figures 7E–G). Taken together, *Rev-erbα* ablation up-regulated skin BMAL1 and ameliorated skin aging in mice. Our findings supported a critical role of REV-ERBα/BMAL1 in regulation of skin aging.

SBG up-regulates the clock gene *Bmal1* in mouse and cell models of aging

Because *Bmal1* and its upstream regulator *Rev-erbα* are involved in skin aging, we wondered whether *Bmal1* has a role in protection of skin aging by SBG. We found that SBG dose-dependently increased the BMAL1 mRNA and protein in the skin of D-gal/UVB-treated mice (Figure 8A/B). Likewise, SBG led to increases in the mRNA and protein of BMAL1 in D-gal-treated NIT3H3 cells (Figure 8C/D). Therefore, the protective

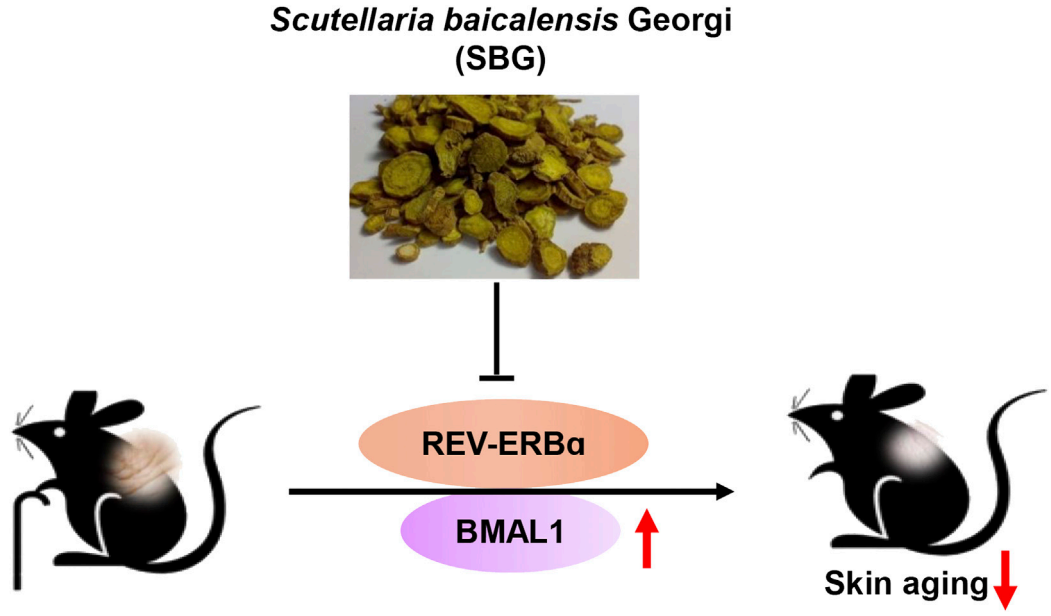

FIGURE 10
Schematic diagram showing the proposed mechanism for anti-skin aging effect of SBG.

effects of SBG on skin aging can be attributed to enhanced BMAL1 expression.

SBG antagonizes REV-ERBα to induce BMAL1 expression

Bmal1 expression is directly regulated by REV-ERBα, a nuclear receptor whose activity can be modified by small molecules (Kojetin and Burris, 2014). We next tested whether SBG modulates *Bmal1* expression *via* REV-ERBα. We first assessed the activity of SBG in HEK293 cells expressing a chimeric receptor (i.e., the DNA-binding domain of Gal4 is fused to the LBD of *Rev-erbα*) and a Gal4-responsive luciferase reporter (Figure 9A). SBG dose-dependently inhibited the repressor activities of REV-ERBα in the Gal4 chimeric assay (Figure 9A), suggesting SBG as a REV-ERBα antagonist. Furthermore, like SR8278, SBG dose-dependently enhanced the promoter activity of *Bmal1* (−2000/+100 bp) in a luciferase reporter assay (Figure 9B). Moreover, SBG increased the mRNA and protein expression of BHMT and NLRP3 (i.e., two known targets of REV-ERBα) in addition to BMAL1 in NIH3T3 cells in a dose-dependent fashion (Figure 9C/D). In addition, SBG increased the circadian amplitude of *Bmal1* gene according to cell-based circadian assay with NIH3T3 cells expressing *Bmal1*-dLuc reporter (Figure 9E). Taken together, these findings indicated that SBG antagonized REV-ERBα to induce BMAL1 expression.

DISCUSSION

In this study, we have identified SBG as a novel anti-skin aging agent. Compared with synthetic agents such as retinoid (Mukherjee et al., 2006), SBG is more advantageous in practical applications because it is a herbal medicine without safety concern. More importantly, we have uncovered that SBG protects against skin aging in mice by antagonizing REV-ERBα and increasing skin expression of BMAL1, an aging-inhibiting factor (Figure 10). The evidence for antagonism of REV-ERBα by SBG is strong. First, SBG dose-dependently inhibited the repressor activities of REV-ERBα in the Gal4 chimeric assay. Second, like SR8278 (a known REV-ERBα antagonist), SBG dose-dependently enhanced the promoter activity of *Bmal1* in a luciferase reporter assay. Third, SBG increased the expression of BMAL1, BHMT and NLRP3 (three known targets of REV-ERBα and repressed by REV-ERBα) in NIH3T3 cells. Fourth, SBG increased the circadian amplitude of *Bmal1* gene according to circadian assays with NIH3T3 cells expressing *Bmal1*-dLuc reporter (Figure 9). It is noteworthy that herbal extract instead of purified active compounds was used in current study. This will affect reproducibility because different sources of SBG and slight changes in extraction can lead to different composition of active compounds.

Our finding that REV-ERBα/BMAL1 (as core clock components) regulate skin aging supports the notion that skin pathophysiology is under the control of circadian clock. In fact,

circadian clock has been implicated in regulation of several other types of skin diseases such as skin cancer, infections and sunburn (Duan et al., 2021). Because among clock components BMAL1 has a direct effect on skin aging, it likely acts to connect this skin disorder to circadian clock. Supporting this, *Bmal1* was markedly down-regulated in the skin of aged mice (Figure 8). We have identified REV-ERBα as a potential target for prevention and treatment of skin aging. Compared with other targets such as BMAL1, REV-ERBα is more advantageous because it is a ligand-responsive receptor whose activity can be modified by small molecules. We found that SBG is a novel REV-ERBα antagonist. However, it remains unknown which constituents in this herbal medicine are responsible for the antagonistic action. We reasoned that baicalein (a known active constituent) may have a contribution as it can induce the expression of *Bmal1*, a direct target of REV-ERBα, and shows a protective effect on skin damage (Nomura et al., 2018).

This study has unraveled that SBG promotes BMAL1 expression to protect against skin aging in mice. BMAL1 functions as an anti-aging factor by up-regulating major antioxidant enzymes such as SOD, peroxiredoxines and glutathione peroxidase (Kondratov et al., 2009; Töbelmann and Dittmar, 2021). It is noteworthy that there is a possibility that other mechanisms are also involved in the protection of skin aging by SBG considering that herbal medicines usually contain hundreds of chemical constituents. The potential mechanisms include inactivation of MAPK/AP-1 and NF-κB signaling pathways, activation of TGF-β/Smad pathway, and modulation of cyclooxygenase (COX), hypoxia-Inducible factor (HIF)-1 and inducible nitric oxide synthase (iNOS) (Domaszewska-Szostek et al., 2021; Chi and Kim, 2005; Gu et al., 2020). However, whether these mechanisms have a contribution to the SBG effect on skin aging awaits further investigations.

Mouse models of skin aging were established in current study by treatment with D-gal/UVB as previously described (Jiayi et al., 2019; Zhang et al., 2020; Cao et al., 2022). Chronic injection of D-gal, a reducing sugar, results in oxidative stress including reductions of antioxidant enzymes, inflammation and apoptosis, mimicking a natural aging process (Shen et al., 2002; Shan et al., 2009; Chen et al., 2018). UVB is the most harmful constituent of UV radiation. Chronic UVB exposure can cause excessive ROS production, abnormal elastin deposition, and impairment of collagen fibers (Starcher et al., 1999; Heck et al., 2003; Lee et al., 2021). D-gal and UVB co-treatment induces a large-scale burst of free radicals, leading to the oxidative damage in the skin and skin aging-like symptoms such as wrinkling, sagging, dryness, and erythema (Zhang et al., 2020). This animal model has been widely used to elucidate cellular and molecular changes that may have a causal role in skin aging, and to screen anti-aging drugs (Jiayi et al., 2019; Zhang et al., 2020; Cao et al., 2022).

Anti-aging effects of SBG were assessed here by measuring SOD activity, MDA/HYP levels, and MMP-1/p53 expression. SOD is a major free radical scavenger in the body, and functions to remove superoxide anions (Li et al., 2020; Park et al., 2008). MDA is a final product of oxidation, and its content can directly reflect the level of lipid peroxidation (Gil et al., 2002; Zhang et al., 2014). SOD activity and MDA level can be used as indicators of the level of organism aging which is associated with oxidative stress and ROS production (Yi et al., 2019). HYP is the most abundant amino acid in collagen, and its level indirectly reflects the total collagen content (Li and Wu, 2018; Li et al., 2016). MMP-1 is a collagenase that plays an important role in degradation of dermal collagen during skin aging (Sapna et al., 2014). Thus, HYP and MMP-1 can be used as markers of skin aging process. *P53* is a tumor suppressor gene that induces cell senescence by promoting the expression of growth suppressive genes (Bond et al., 1996; Luo et al., 2004), and is also regarded as a marker of skin aging. In fact, measurements of SOD activity, MDA/HYP levels, and MMP-1/p53 expression have been widely performed to assess aging and to screen anti-aging agents (Jiayi et al., 2019; Park et al., 2008; Hwang et al., 2012).

An important part of the skin response to stress is its ability for melatonin synthesis and subsequent metabolism (Slominski et al., 2017; Slominski et al., 2018b). Melatonin is indispensable for physiological skin functions and has a protective role against photoaging (Skobowiat, et al., 2018; Bocheva et al., 2022). However, whether SBG affects skin melatonin remains unknown. Like vitamin C, vitamin D exerts a variety of antiaging and photoprotective effects on the skin (Bocheva et al., 2021; Slominski et al., 2020). However, whether the anti-skin aging effect of SBG is comparable to that of vitamin D was unaddressed. It is noteworthy that UV radiation not only induces skin pathology, but also exert systemic effects, including activation of hypothalamic-pituitary-adrenal axis, opioidogenic effects, and immunosuppression. Thus, UV radiation has therapeutic applications in management of various diseases such as addiction, autoimmune and mood disorders (Slominski et al., 2018a).

In summary, SBG displays a pharmacological effect on skin aging based on mouse and cell models of aging. Mechanistically, SBG protects against skin aging in mice by antagonizing REV-ERBα and increasing skin expression of BMAL1, an aging-inhibiting factor.

Data availability statement

The original contributions presented in the study are included in the article/Supplementary Material, further inquiries can be directed to the corresponding authors.

Ethics statement

The animal study was reviewed and approved by Institutional Animal Care and Use Committee of Guangzhou University of Chinese Medicine

Author contributions

BW, DD, and GS designed the study; GS, YD, YL, WZ, ZW performed experiments; GS, YD, and YL and XZ collected and analyzed data; BW, DD, GS, and YL wrote the manuscript. All data were generated in-house, and no paper mill was used. All authors agree to be accountable for all aspects of work ensuring integrity and accuracy.

Funding

This work was supported by the National Natural Science Foundation of China (No. 81722049 & 82003839) and Natural Science Foundation of Guangdong Province (No. 2019A1515110892 & 2021A1515012189).

Conflict of interest

The authors declare that the research was conducted in the absence of any commercial or financial relationships that could be construed as a potential conflict of interest.

Publisher's note

All claims expressed in this article are solely those of the authors and do not necessarily represent those of their affiliated organizations, or those of the publisher, the editors and the reviewers. Any product that may be evaluated in this article, or claim that may be made by its manufacturer, is not guaranteed or endorsed by the publisher.

Supplementary material

The Supplementary Material for this article can be found online at: https://www.frontiersin.org/articles/10.3389/fphar.2022.991917/full#supplementary-material

References

Bernhard, D., Moser, C., Backovic, A., and Wick, G. (2007). Cigarette smoke–anaging accelerator? *Exp. Gerontol.* 42 (3), 160–165. doi:10.1016/j.exger.2006.09.016

Bocheva, G., Slominski, R. M., Janjetovic, Z., Kim, T. K., Böhm, M., Steinbrink, K., et al. (2022). Protective role of melatonin and its metabolites in skin aging. *Int. J. Mol. Sci.* 23 (3), 1238. doi:10.3390/ijms23031238

Bocheva, G., Slominski, R. M., and Slominski, A. T. (2019). Neuroendocrine aspects of skin aging. *Int. J. Mol. Sci.* 20 (11), 2798. doi:10.3390/ijms20112798

Bocheva, G., Slominski, R. M., and Slominski, A. T. (2021). The impact of vitamin D on skin aging. *Int. J. Mol. Sci.* 22 (16), 9097. doi:10.3390/ijms22169097

Böger, R. (2014). [Circadian clocks and energy metabolism]. *Dtsch. Med. Wochenschr.* 139 (24), 1320. doi:10.1055/s-0034-1370115

Bond, J., Haughton, M., Blaydes, J., Gire, V., Wynford-Thomas, D., and Wyllie, F. (1996). Evidence that transcriptional activation by p53 plays a direct role in the induction of cellular senescence. *Oncogene* 13 (10), 2097–2104.

Brown, J. P. (1980). A review of the genetic effects of naturally occurring flavonoids, anthraquinones and related compounds. *Mutat. Res.* 75 (3), 243–277. doi:10.1016/0165-1110(80)90029-9

Bunger, M. K., Wilsbacher, L. D., Moran, S. M., Clendenin, C., Radcliffe, L. A., Hogenesch, J. B., et al. (2000). Mop3 is an essential component of the master circadian pacemaker in mammals. *Cell* 103 (7), 1009–1017. doi:10.1016/s0092-8674(00)00205-1

Burris, T. P. (2008). Nuclear hormone receptors for heme: REV-ERBalpha and REV-ERBbeta are ligand-regulated components of the mammalian clock. *Mol. Endocrinol.* 22 (7), 1509–1520. doi:10.1210/me.2007-0519

Cao, C., Xiao, Z., Tong, H., Liu, Y., Wu, Y., and Ge, C. (2022). Oral intake of chicken bone collagen peptides anti-skin aging in mice by regulating collagen degradation and synthesis, inhibiting inflammation and activating lysosomes. *Nutrients* 14 (8), 1622. doi:10.3390/nu14081622

Chen, M., Zhou, C., Xu, H., Zhang, T., and Wu, B. (2020). Chronopharmacological targeting of Rev-erbα by puerarin alleviates hyperhomocysteinemia in mice. *Biomed. Pharmacother. = Biomedecine Pharmacother.* 125, 109936. doi:10.1016/j.biopha.2020.109936

Chen, P., Chen, F., and Zhou, B. (2018). Antioxidative, anti-inflammatory and anti-apoptotic effects of ellagic acid in liver and brain of rats treated by D-galactose. *Sci. Rep.* 8 (1), 1465. doi:10.1038/s41598-018-19732-0

Chen, R., Schirmer, A., Lee, Y., Lee, H., Kumar, V., Yoo, S. H., et al. (2009). Rhythmic PER abundance defines a critical nodal point for negative feedback within the circadian clock mechanism. *Mol. Cell* 36 (3), 417–430. doi:10.1016/j.molcel.2009.10.012

Chi, Y. S., and Kim, H. P. (2005). Suppression of cyclooxygenase-2 expression of skin fibroblasts by wogonin, a plant flavone from Scutellaria radix. *Prostagl. Leukot. Essent. Fat. Acids* 72 (1), 59–66. doi:10.1016/j.plefa.2004.04.009

Crumbley, C., and Burris, T. P. (2011). Direct regulation of CLOCK expression by REV-ERB. *PloS one* 6 (3), e17290. doi:10.1371/journal.pone.0017290

Delezie, J., Dumont, S., Dardente, H., Oudart, H., Gréchez-Cassiau, A., Klosen, P., et al. (2012). The nuclear receptor REV-ERBα is required for the daily balance of carbohydrate and lipid metabolism. *FASEB* 26 (8), 3321–3335. doi:10.1096/fj.12-208751

Domaszewska-Szostek, A., Puzianowska-Kuźnicka, M., and Kuryłowicz, A. (2021). Flavonoids in skin senescence prevention and treatment. *Int. J. Mol. Sci.* 22 (13), 6814. doi:10.3390/ijms22136814

du Pré, B. C., Dierickx, P., Crnko, S., Doevendans, P. A., Vos, M. A., Geijsen, N., et al. (2017). Neonatal rat cardiomyocytes as an *in vitro* model for circadian rhythms in the heart. *J. Mol. Cell. Cardiol.* 112, 58–63. doi:10.1016/j.yjmcc.2017.08.009

Duan, J., Greenberg, E. N., Karri, S. S., and Andersen, B. (2021). The circadian clock and diseases of the skin. *FEBS Lett.* 595 (19), 2413–2436. doi:10.1002/1873-3468.14192

Duong, H. A., Robles, M. S., Knutti, D., and Weitz, C. J. (2011). A molecular mechanism for circadian clock negative feedback. *Science* 332 (6036), 1436–1439. doi:10.1126/science.1196766

Fisher, G. J., Kang, S., Varani, J., Bata-Csorgo, Z., Wan, Y., Datta, S., et al. (2002). Mechanisms of photo aging and chronological skin aging. *Arch. Dermatol.* 138 (11), 1462–1470. doi:10.1001/archderm.138.11.1462

Frommeyer, T. C., Gilbert, M. M., Brittain, G. V., Wu, T., Nguyen, T. Q., Rohan, C. A., et al. (2022). UVB-induced microvesicle particle release and its effects on the cutaneous microenvironment. *Front. Immunol.* 13, 880850. doi:10.3389/fimmu.2022.880850

Gabrielska, J., Oszmiański, J., Zyłka, R., and Komorowska, M. (1997). Antioxidant activity of flavones from Scutellaria baicalensis in lecithin liposomes. *Z. fur Naturforsch. C* 52 (11-12), 817–823. doi:10.1515/znc-1997-11-1215

Gao, B., Li, K., Wei, Y. Y., Zhang, J., Li, J., Zhang, L., et al. (2014). Zinc finger protein 637 protects cells against oxidative stress-induced premature senescence by mTERT-mediated telomerase activity and telomere maintenance. *Cell Death Dis.* 5 (7), e1334. doi:10.1038/cddis.2014.298

Gekakis, N., Staknis, D., Nguyen, H. B., Davis, F. C., Wilsbacher, L. D., King, D. P., et al. (1998). Role of the CLOCK protein in the mammalian circadian mechanism. *Science* 280 (5369), 1564–1569. doi:10.1126/science.280.5369.1564

Gil, P., Fariñas, F., Casado, A., and López-Fernández, E. (2002). Malondialdehyde: A possible marker of ageing. *Gerontology* 48 (4), 209–214. doi:10.1159/000058352

Gu, Y., Han, J., Jiang, C., and Zhang, Y. (2020). Biomarkers, oxidative stress and autophagy in skin aging. *Ageing Res. Rev.* 59, 101036. doi:10.1016/j.arr.2020.101036

Heck, D. E., Vetrano, A. M., Mariano, T. M., and Laskin, J. D. (2003). UVB light stimulates production of reactive oxygen species: Unexpected role for catalase. *J. Biol. Chem.* 278 (25), 22432–22436. doi:10.1074/jbc.C300048200

Hemmeryckx, B., Himmelreich, U., Hoylaerts, M. F., and Lijnen, H. R. (2011). Impact of clock gene Bmal1 deficiency on nutritionally induced obesity in mice. *Obes. (Silver Spring, Md.)* 19 (3), 659–661. doi:10.1038/oby.2010.266

Hirota, T., Lewis, W. G., Liu, A. C., Lee, J. W., Schultz, P. G., and Kay, S. A. (2008). A chemical biology approach reveals period shortening of the mammalian circadian clock by specific inhibition of GSK-3beta. *Proc. Natl. Acad. Sci. U. S. A.* 105 (52), 20746–20751. doi:10.1073/pnas.0811410106

Hogenesch, J. B., Gu, Y. Z., Jain, S., and Bradfield, C. A. (1998). The basic-helix-loop-helix-PAS orphan MOP3 forms transcriptionally active complexes with circadian and hypoxia factors. *Proc. Natl. Acad. Sci. U. S. A.* 95 (10), 5474–5479. doi:10.1073/pnas.95.10.5474

Hwang, I. S., Kim, J. E., Choi, S. I., Lee, H. R., Lee, Y. J., Jang, M. J., et al. (2012). UV radiation-induced skin aging in hairless mice is effectively prevented by oral intake of sea buckthorn (Hippophae rhamnoides L.) fruit blend for 6 weeks through MMP suppression and increase of SOD activity. *Int. J. Mol. Med.* 30 (2), 392–400. doi:10.3892/ijmm.2012.1011

Jiayi, M. A., Yan, G. U. O., Juan, Y. E., and Wenyu, M. A. (2019). Protective effect of lycium ruthenicum procyanidin on mice skin aging model. *Chin. General Pract.* 22 (15), 1851.

Jung, C. H., Kim, E. M., Park, J. K., Hwang, S. G., Moon, S. K., Kim, W. J., et al. (2013). Bmal1 suppresses cancer cell invasion by blocking the phosphoinositide 3-kinase-Akt-MMP-2 signaling pathway. *Oncol. Rep.* 29 (6), 2109–2113. doi:10.3892/or.2013.2381

Khapre, R. V., Kondratova, A. A., Susova, O., and Kondratov, R. V. (2011). Circadian clock protein BMAL1 regulates cellular senescence *in vivo*. *Cell cycleGeorget. Tex.)* 10 (23), 4162–4169. doi:10.4161/cc.10.23.18381

Kojetin, D. J., and Burris, T. P. (2014). REV-ERB and ROR nuclear receptors as drug targets. *Nat. Rev. Drug Discov.* 13 (3), 197–216. doi:10.1038/nrd4100

Kondratov, R. V., Kondratova, A. A., Gorbacheva, V. Y., Vykhovanets, O. V., and Antoch, M. P. (2006). Early aging and age-related pathologies in mice deficient in BMAL1, the core componentof the circadian clock. *Genes Dev.* 20 (14), 1868–1873. doi:10.1101/gad.1432206

Kondratov, R. V., Vykhovanets, O., Kondratova, A. A., and Antoch, M. P. (2009). Antioxidant N-acetyl-L-cysteine ameliorates symptoms of premature aging associated with the deficiency of the circadian protein BMAL1. *Aging* 1 (12), 979–987. doi:10.18632/aging.100113

Kojetin, D., Wang, Y., Kamenecka, T. M., and Burris, T. P. (2011). Identification of SR8278, asynthetic antagonist of the nuclear hemereceptor REV-ERB. *ACS Chem. Biol.* 6 (2), 131–136. doi:10.1021/cb1002575

Krutmann, J., Schalka, S., Watson, R., Wei, L., and Morita, A. (2021). Daily photo protection to prevent photo aging. *Photodermatol. Photoimmunol. Photomed.* 37 (6), 482–489. doi:10.1111/phpp.12688

Kumar, P., Nagarajan, A., and Uchil, P. D. (2018). Analysis of cell viability by the MTT assay. *Cold Spring Harb. Protoc.* 2018 (6). doi:10.1101/pdb.Prot095505

Langmesser, S., Tallone, T., Bordon, A., Rusconi, S., and Albrecht, U. (2008). Interaction of circadian clock proteins PER2 and CRY with BMAL1 and CLOCK. *BMC Mol. Biol.* 9, 41. doi:10.1186/1471-2199-9-41

Lee, J. J., Ng, S. C., Ni, Y. T., Liu, J. S., Chen, C. J., Padma, V. V., et al. (2021). Protective effects of galangin against H_2O_2/UVB-induced dermal fibroblast collagen degradation via hsa-microRNA-4535-mediated TGFβ/Smad signaling. *Aging* 13 (23), 25342–25364. doi:10.18632/aging.203750

Li, C. W., Wang, Q., Li, J., Hu, M., Shi, S. J., Li, Z. W., et al. (2016). Silver nanoparticles/chitosan oligosaccharide/poly(vinyl alcohol) nanofiber promotes wound healing by activating TGFβ1/Smad signaling pathway. *Int. J. Nanomedicine* 11, 373–386. doi:10.2147/IJN.S91975

Li, F., Lin, L., He, Y., Sun, G., Dong, D., and Wu, B. (2022). BMAL1 regulates Propionibacterium acnes-induced skin inflammation via REV-ERBα in mice. *Int. J. Biol. Sci.* 18 (6), 2597–2608. doi:10.7150/ijbs.71719

Li, H. B., Jiang, Y., and Chen, F. (2004). Separation methods used for Scutellaria baicalensis active components. *J. Chromatogr. B Anal. Technol. Biomed. Life Sci.* 812 (1-2), 277–290. doi:10.1016/j.jchromb.2004.06.045

Li, P., and Wu, G. (2018). Roles of dietary glycine, proline, and hydroxyproline in collagen synthesis and animal growth. *Amino acids* 50 (1), 29–38. doi:10.1007/s00726-017-2490-6

Li, W., Wang, S., Li, J., Wang, X., Cui, L., Chen, J., et al. (2020). Antioxidative enzyme activities in the Rhodeinae sinensis Gunther and Macrobrachium nipponense and multi-endpoint assessment under tonalide exposure. *Ecotoxicol. Environ. Saf.* 199, 110751. doi:10.1016/j.ecoenv.2020.110751

Liao, H., Ye, J., Gao, L., and Liu, Y. (2021). The main bioactive compounds of Scutellaria baicalensis Georgi. For alleviation of inflammatory cytokines: A comprehensive review. *Biomed. Pharmacother. = Biomedecine Pharmacother.* 133, 110917. doi:10.1016/j.biopha.2020.110917

Liu, A. C., Tran, H. G., Zhang, E. E., Priest, A. A., Welsh, D. K., and Kay, S. A. (2008). Redundant function of REV-ERBalpha and beta and non-essential role for Bmal1 cycling in transcriptional regulation of intracellular circadian rhythms. *PLoS Genet.* 4 (2), e1000023. doi:10.1371/journal.pgen.1000023

Luo, J., Li, M., Tang, Y., Laszkowska, M., Roeder, R. G., and Gu, W. (2004). Acetylation of p53 augments its site-specific DNA binding both *in vitro* and *in vivo*. *Proc. Natl. Acad. Sci. U. S. A.* 101 (8), 2259–2264. doi:10.1073/pnas.0308762101

Mukherjee, S., Date, A., Patravale, V., Korting, H. C., Roeder, A., and Weindl, G. (2006). Retinoids in the treatment of skin aging: An overview of clinical efficacy and safety. *Clin. Interv. Aging* 1 (4), 327–348. doi:10.2147/ciia.2006.1.4.327

Narayanan, D. L., Saladi, R. N., and Fox, J. L. (2010). Ultraviolet radiation and skin cancer. *Int. J. Dermatol.* 49 (9), 978–986. doi:10.1111/j.1365-4632.2010.04474.x

Nomura, K., Hirai, T., Nakashima, K. I., and Inoue, M. (2018). "Baicalein regulates FGF21 expression through RORα-mediated transcriptional activity," in Proceedings for Annual Meeting of The Japanese Pharmacological Society WCP2018 (The 18th World Congress of Basic and Clinical Pharmacology) (Japanese Pharmacological Society), PO2–12.

Pardee, K., Necakov, A. S., and Krause, H. (2011). Nuclear receptors: Small molecule sensors that coordinate growth, metabolism and reproduction. *Subcell. Biochem.* 52, 123–153. doi:10.1007/978-90-481-9069-0_6

Park, S. H., Cho, D. M., Choi, B. D., Choi, Y. J., and Choi, J. H. (2008). Antioxidative effects of skinned mugwort (Artemisia vulgaris L.) extracts on UV-irradiated hairless mouse skin. *J. Korean Soc. Food Sci. Nutr.* 37 (1), 20–26. doi:10.3746/jkfn.2008.37.1.20

Sapna, G., Gokul, S., and Bagri-Manjrekar, K. (2014). Matrix metalloproteinases and periodontal diseases. *Oral Dis.* 20 (6), 538–550. doi:10.1111/odi.12159

Shan, Q., Lu, J., Zheng, Y., Li, J., Zhou, Z., Hu, B., et al. (2009). Purple sweet potato color ameliorates cognition deficits and attenuates oxidative damage and inflammation in aging mouse brain induced by d-galactose. *J. Biomed. Biotechnol.* 2009, 564737. doi:10.1155/2009/564737

Shen, Y. X., Xu, S. Y., Wei, W., Sun, X. X., Yang, J., Liu, L. H., et al. (2002). Melatonin reduces memory changes and neural oxidative damage in mice treated with D-galactose. *J. Pineal Res.* 32 (3), 173–178. doi:10.1034/j.1600-079x.2002.1o850.x

Skobowiat, C., Brożyna, A. A., Janjetovic, Z., Jeayeng, S., Oak, A., Kim, T. K., et al. (2018). Melatonin and its derivatives counteract the ultraviolet B radiation-induced damage in human and porcine skin *ex vivo*. *J. Pineal Res.* 65 (2), e12501. doi:10.1111/jpi.12501

Slominski, A. T., Chaiprasongsuk, A., Janjetovic, Z., Kim, T. K., Stefan, J., Slominski, R. M., et al. (2020). Photoprotective properties of vitamin D and lumisterol hydroxyderivatives. *Cell biochem. Biophys.* 78 (2), 165–180. doi:10.1007/s12013-020-00913-6

Slominski, A. T., Hardeland, R., Zmijewski, M. A., Slominski, R. M., Reiter, R. J., and Paus, R. (2018b). Melatonin: A cutaneous perspective on its production, metabolism, and functions. *J. Invest. Dermatol.* 138 (3), 490–499. doi:10.1016/j.jid.2017.10.025

Slominski, A. T., Zmijewski, M. A., Plonka, P. M., Szaflarski, J. P., and Paus, R. (2018a). How UV light touches the brain and endocrine system through skin, and why. *Endocrinology* 159 (5), 1992–2007. doi:10.1210/en.2017-03230

Slominski, A. T., Zmijewski, M. A., Semak, I., Kim, T. K., Janjetovic, Z., Slominski, R. M., et al. (2017). Melatonin, mitochondria, and the skin. *Cell. Mol. Life Sci.* 74 (21), 3913–3925. doi:10.1007/s00018-017-2617-7

Starcher, B., Pierce, R., and Hinek, A. (1999). UVB irradiation stimulates deposition of new elastic fibers by modified epithelial cells surrounding the hair follicles and sebaceous glands in mice. *J. Invest. Dermatol.* 112 (4), 450–455. doi:10.1046/j.1523-1747.1999.00553.x

Terao, M., Tani, M., Itoi, S., Yoshimura, T., Hamasaki, T., Murota, H., et al. (2014). 11β-hydroxysteroid dehydrogenase 1 specific inhibitor increased dermal collagen content and promotes fibroblast proliferation. *PloS one* 9 (3), e93051. doi:10.1371/journal.pone.0093051

Töbelmann, D., and Dittmar, M. (2021). Diurnal relationship between core clock gene BMAL1, antioxidant SOD1 and oxidative RNA/DNA damage in young and older healthy women. *Exp. Gerontol.* 151, 111422. doi:10.1016/j.exger.2021.111422

Vieira, E., Mirizio, G. G., Barin, G. R., de Andrade, R. V., Nimer, N., and La Sala, L. (2020). Clock genes, inflammation and the immune system-implications for diabetes, obesity and neurodegenerative diseases. *Int. J. Mol. Sci.* 21 (24), 9743. doi:10.3390/ijms21249743

Wang, S., Li, F., Lin, Y., and Wu, B. (2020). Targeting REV-ERBα for therapeutic purposes: Promises and challenges. *Theranostics* 10 (9), 4168–4182. doi:10.7150/thno.43834

Wang, S., Lin, Y., Yuan, X., Li, F., Guo, L., and Wu, B. (2018). REV-ERBα integrates colon clock with experimental colitis through regulation of NF-κB/NLRP3 axis. *Nat. Commun.* 9 (1), 4246–4312. doi:10.1038/s41467-018-06568-5

Wang, Y., Kojetin, D., and Burris, T. P. (2015). Anti-proliferative actions of a synthetic REV-ERBα/β agonist in breast cancer cells. *Biochem. Pharmacol.* 96 (4), 315–322. doi:10.1016/j.bcp.2015.06.010

Watson, M., Holman, D. M., and Maguire-Eisen, M. (2016). Ultraviolet radiation exposure and its impact on skin cancer risk. *Semin. Oncol. Nurs.* 32 (3), 241–254. doi:10.1016/j.soncn.2016.05.005

Yi, R., Zhang, J., Sun, P., Qian, Y., and Zhao, X. (2019). Protective effects of kuding tea (Ilex kudingcha C. J. Tseng) polyphenols on UVB-induced skin aging in SKH1 hairless mice. *Mol. (Basel, Switz.* 24 (6), 1016. doi:10.3390/molecules24061016

Yin, L., and Lazar, M. A. (2005). The orphan nuclear receptor Rev-erbalpha recruits the N-CoR/histone deacetylase 3 corepressor to regulate the circadian Bmal1 gene. *Mol. Endocrinol.* 19 (6), 1452–1459. doi:10.1210/me.2005-0057

Yin, L., Wu, N., and Lazar, M. A. (2010). Nuclear receptor rev-erbalpha: A heme receptor that coordinates circadian rhythm and metabolism. *Nucl. Recept. Signal.* 8, e001. doi:10.1621/nrs.08001

Zhang, S., Dong, Z., Peng, Z., and Lu, F. (2014). Anti-aging effect of adipose-derived stem cells in a mouse model of skin aging induced by D-galactose. *PloS one* 9 (5), e97573. doi:10.1371/journal.pone.0097573

Zhang, T., Zhao, M., Lu, D., Wang, S., Yu, F., Guo, L., et al. (2018). REV-ERBα regulates CYP7A1 through repression of liver receptor homolog-1. *Drug Metab. Dispos.* 46 (3), 248–258. doi:10.1124/dmd.117.078105

Zhang, Z., Zhu, H., Zheng, Y., Zhang, L., Wang, X., Luo, Z., et al. (2020). The effects and mechanism of collagen peptide and elastin peptide on skin aging induced by D-galactose combined with ultraviolet radiation. *J. Photochem. Photobiol. B* 210, 111964. doi:10.1016/j.jphotobiol.2020.111964

Zhao, Q., Chen, X. Y., and Martin, C. (2016). Scutellaria baicalensis, the golden herb from the garden of Chinese medicinal plants. *Sci. Bull.* 61 (18), 1391–1398. doi:10.1007/s11434-016-1136-5

frontiers | Frontiers in Pharmacology

TYPE Review
PUBLISHED 05 October 2022
DOI 10.3389/fphar.2022.976757

OPEN ACCESS

EDITED BY
Kok Yong Chin,
National University of Malaysia, Malaysia

REVIEWED BY
Ginpreet Kaur,
SVKM's Narsee Monjee Institute of Management Studies, India
Rita De Cássia Avellaneda Guimarães,
Universidade Federal de Mato Grosso do Sul, Brazil
Ruben F. Gonzalez-Laredo,
Durango Institute of Technology, Mexico

*CORRESPONDENCE
Jianbang Tang,
85945915@qq.com

SPECIALTY SECTION
This article was submitted to Ethnopharmacology, a section of the journal Frontiers in Pharmacology

RECEIVED 27 June 2022
ACCEPTED 20 September 2022
PUBLISHED 05 October 2022

CITATION
Huang Z, Wang J, Li C, Zheng W, He J, Wu Z and Tang J (2022), Application of natural antioxidants from traditional Chinese medicine in the treatment of spinal cord injury.
Front. Pharmacol. 13:976757.
doi: 10.3389/fphar.2022.976757

Application of natural antioxidants from traditional Chinese medicine in the treatment of spinal cord injury

Zhihua Huang[1], Jingyi Wang[2], Chun Li[1], Weihong Zheng[3], Junyuan He[3], Ziguang Wu[1] and Jianbang Tang[3]*

[1]Zhongshan Hospital of Traditional Chinese Medicine Affiliated to Guangzhou University of Chinese Medicine, Zhongshan, China, [2]Faculty of Chinese Medicine, Macau University of Science and Technology, Macau, China, [3]Zhongshan Hospital of Traditional Chinese Medicine, Zhongshan, China

Spinal cord injury (SCI) is a devastating central nervous system disease, caused by physical traumas. With the characteristic of high disability rate, catastrophic dysfunction, and enormous burden on the patient's family, SCI has become a tough neurological problem without efficient treatments. Contemporarily, the pathophysiology of SCI comprises complicated and underlying mechanisms, in which oxidative stress (OS) may play a critical role in contributing to a cascade of secondary injuries. OS substantively leads to ion imbalance, lipid peroxidation, inflammatory cell infiltration, mitochondrial disorder, and neuronal dysfunction. Hence, seeking the therapeutic intervention of alleviating OS and appropriate antioxidants is an essential clinical strategy. Previous studies have reported that traditional Chinese medicine (TCM) has antioxidant, anti-inflammatory, antiapoptotic and neuroprotective effects on alleviating SCI. Notably, the antioxidant effects of some metabolites and compounds of TCM have obtained numerous verifications, suggesting a potential therapeutic strategy for SCI. This review aims at investigating the mechanisms of OS in SCI and highlighting some TCM with antioxidant capacity used in the treatment of SCI.

KEYWORDS

spinal cord injury, traditional Chinese medicine, oxidative strees, natural medicine, antioxidants

1 Introduction

Spinal cord injury (SCI) is a neurological injury disease caused by trauma or intraspinal lesions, which often leads to partial or complete loss of sensory and motor functions below the injury segment (Eckert and Martin, 2017). The damage to neuronal structure and function has the irreversible property, leaving SCI patients usually presented with a poor prognosis and a high rate of disability. The severe and long-term physical injury will not only reduce the patients' quality of life but also result in consequences of serious economic burden on their families (Eli et al., 2021).

The spinal cord contains gray matter and white matter that include nerve cell bodies, along with the ascending tracts and descending tracts. According to the classification of

the external physical impact and internal impacts, SCI can be divided into traumatic and non-traumatic spinal cord injury. The former is induced by trauma, such as acute stretch, acute distraction, compression, and axonal shearing (Eckert and Martin, 2017), which is mainly discussed in this review. The latter is often caused by compression of tumors and congenital diseases (Gedde et al., 2019). Degrees of disability can vary from slight sensory abnormality and motor dysfunction to severe paralysis, based on various locations and the traumatic extent of SCI.

The pathophysiological changes of SCI are very complex, so the mechanism of SCI is not well defined. But previous studies have found that oxidative stress (OS) caused by excessive reactive oxygen species (ROS) could aggravate the damage of neurons. Thus, our paper focused on the mechanisms of OS affecting SCI and discussed the etiology of OS from the perspective of traditional Chinese medicine (TCM) theory for SCI patients. Additionally, we highlighted some metabolites and compounds of TCM with antioxidant capacity used in the treatment of SCI, providing the potential treatment therapy of SCI *via* using the natural antioxidants derived from TCM.

2 Materials and methods

In this review, an electronic search of published articles published between 2000 and 2021 was conducted from Web of Science, PubMed, Science Direct, Google Scholar, and China National Knowledge Infrastructure (CNKI), with the use of the following keywords: "spinal cord injury, oxidative stress, and traditional Chinese medicine or herbal medicine or Chinese herbal medicine".

Besides, to ensure the accurate scientific nomenclature for plants in our paper, all names and information on the source species were obtained and validated from Kewscience (http://mpns.kew.org/mpns-portal/) and pharmacopeia of the People's Republic of China.

3 The pathophysiology of spinal cord injury

The pathophysiology of SCI is complicated, which contains acute phase, subacute phase and chronic phase (Supplementary Figure S1). The primary occurrence of SCI results from the initial trauma immediately, including acute stretch, acute distraction, compression, and axonal shearing (Katoh et al., 2019). The primary injury initiated by trauma will progressively cause the secondary injury, and further leads to the lesion of adjacent, uninjured tissue (Anjum et al., 2020). The pathophysiology of secondary injury mainly includes damage to neuronal fiber, blood-spinal cord barrier (BSCB) destruction, excessive free radical production (von Leden et al., 2017), ion imbalances (Garcia et al., 2018), inflammation (Zrzavy et al., 2021) neural cell necrosis and apoptosis (Wang et al., 2019), demyelination (Fan et al., 2018), Among the pathological processes of secondary injury, oxidative stress plays an indispensable and critical role in contributing to a poor microenvironment development, which is considered a hallmark of the secondary injury of SCI (Savikj et al., 2019).

3.1 The association between oxidative stress and spinal cord injury

The essence of the OS reaction is the imbalance between oxidative free radicals and antioxidants. Oxidative free radicals include ROS and reactive nitrogen species (RNS) (Fatima et al., 2015). ROS contains superoxide, singlet oxygen, hydroxyl radical, and hydrogen peroxide, mainly generated by the mitochondria and microglia. RNS are also involved in the pathological mechanism of SCI, including nitric oxide (NO) and peroxynitrite (PON). Excessive generation of NO can induce neuronal apoptosis *via* cytotoxic effects (Cadenas, 2018) and PON are the key initiator of the lipids peroxidation (LP), as well protein nitration in the SCI (Hall et al., 2016) (Figure 1).

3.1.1 Oxidative stress causes the damage of biological macromolecules in spinal cord injury

Notably, the spinal cord is very vulnerable to oxidative damage because it contains overabundant polyunsaturated fatty acids that are particularly susceptible to ROS peroxidation (Anjum et al., 2020). Therefore, LP easily occurs after the trauma, which progressively includes three chemical phases, namely initiation, propagation, and termination (Hall et al., 2016). To begin with, highly reactive oxygen radical with the function of electron-snatching, such as -OH, -NO2, or -CO3, has a reaction with the polyunsaturated fatty acid composition of the membrane, such as arachidonic acid, eicosapentaenoic acid, and linoleic acid, causing the damage of membrane integrity. These types of radicals can be considered to have the characteristic called "electrophilic," which snatches the electron from polyunsaturated fatty acid, leading to quenching of the original radicals whereas the polyunsaturated fatty acid (L), turns to a lipid radical (L•). As for the stage of propagation, L• sets off a chain reaction of constantly producing lipid peroxyl radicals (LOO•) and lipid hydroperoxides (LOOH). When the peroxidizable substrate is depleted or the reaction of lipid radical and another radical or radical scavenger produces other end products, including three carbon-containing malondialdehyde (MDA) and 4-hydroxynonenal (4-HNE) (Hamann and Shi, 2009; Hall et al., 2010), LP greets its termination (Hall et al., 2016). As essential components of membranes, LP can lead to cellular dysfunction, eventually resulting in cell death.

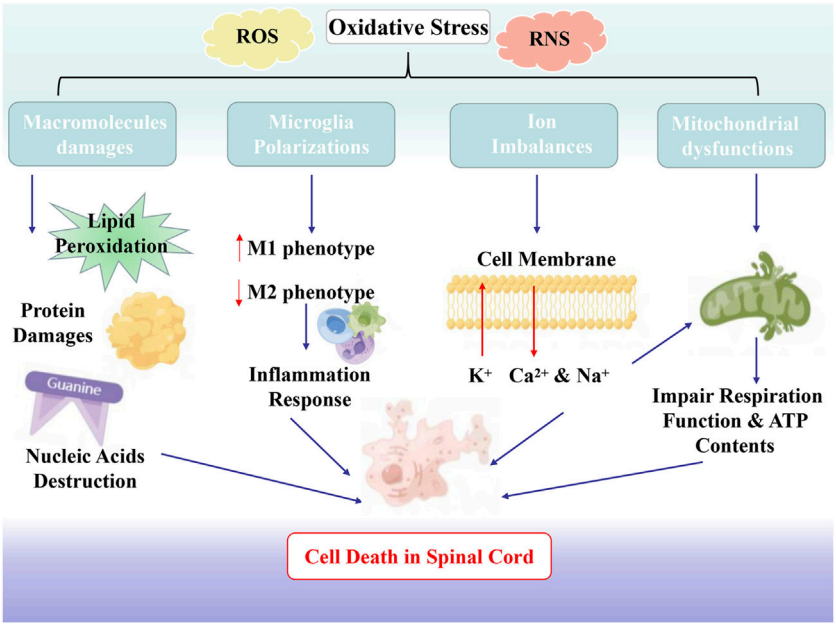

FIGURE 1
The Association Between Oxidative Stress and SCI. Oxidative stress substantively leads to ion imbalance, lipid peroxidation, inflammatory cell infiltration, mitochondrial disorder, and neuronal dysfunction.

In addition to lipids, proteins are also easy to be damaged by OS, and the damaging effects of OS on proteins are also fundamental factors of the continuous deterioration of SCI. Protein oxidation mainly includes breakage of the polypeptide chain, modification of amino-acid side chains, and protein degradation, as well as the conversed derivatives from protein, which are sensitive to proteolysis (Hawkins and Davies, 2019). The products of LP, MDA, and 4-HNE can compromise the structural and functional integrity of cellular proteins by undergoing a carbonyl ammonia cross-linking reaction to form covalent compounds (Wu et al., 2017). Besides, PON can trigger an exacerbated overload of intracellular Ca^{2+} overload, activating the cysteine protease calpain, which ultimately results in the damage of several cellular targets (Xiong et al., 2007).

Finally, the destructive effects of OS on nucleic acid substances are also not negligible factors. It is well documented that guanine is the most oxidation prone-nucleobase (Singh et al., 2019). When structured in the G-quadruplex entity, guanine can respond particularly towards OS (Singh et al., 2019), principally reflected in the generation of 8-oxoguanine *via* the initiation of 8-oxoguanine glycosylases (Every and Russu, 2013). Overproduced PON can also react with guanine to form 8-nitroguanine (8-NO(2)-G), resulting in the exchange of G and T bases to cause mutagenic damage (Piao et al., 2011). The consequences of base modification are mutations and genomic instability. Currently, the expression of certain microRNAs has been proven to be altered *via* OS. Excessive ROS generation can enhance the expression of miR-200c by negatively regulating the expression of Fas-associated phosphatase-1 (FAP-1), thereby inducing apoptosis (Yu et al., 2015).

3.1.2 Oxidative stress and microglia polarization in spinal cord injury

Microglia, polarized into two phenotypes: pro-inflammatory (M1) phenotype and anti-inflammatory (M2) phenotype, have great significance to the pathophysiological evolution of SCI (Fan et al., 2018). During acute trauma, microglia in the spinal cord tissue are primarily polarized to the M1 phenotype (Kroner et al., 2014). The polarized M1 has close correlations with the release of TNF-α, IL-6, IL-1β, ROS, NO, glutamate, and superoxide, which can trigger inflammation and OS, further initiating cascades of neurotoxic damage of SCI and contributing to apoptosis and necrosis (Anwar et al., 2016; Tang and Le, 2016). On the contrary, M2 phenotype plays critical role in antagonizing the pro-inflammatory responses and promoting neurodegeneration, accompanied by the release of several neurotrophic factors, anti-inflammatory cytokines (IL-4, IL-10, IL-13), and transforming growth factor beta (TGF-β) (Anwar et al., 2016; Tang and Le, 2016). Meanwhile, M2 phenotype can generate Arg1 that competes with iNOS for the arginine substrate and

downregulate NO production, thereby reducing the collateral damage of OS to neuronal tissues (Yang et al., 2016). The homeostasis of the local microenvironment depends on the balance between M1 and M2. Therefore, inhibiting M1 or promoting the polarization of M2 may be an effective therapeutic strategy to promote functional recovery after SCI.

3.1.3 Oxidative stress and ion imbalances in spinal cord injury

The imbalance of Na^+, K^+, and Ca^{2+} ions caused by OS is a vital mechanism for triggering necrotic cell death and apoptosis. OS significantly aggravates the influx of Ca^{2+} and Na^+, as well as the decrease of intracellular K^+ concentrations *via* destroying cell membrane structure, which could disturb ionic homeostasis and leads to necrotic cell death and apoptosis (Vanzulli and Butt, 2015). As an indispensable participator of synaptic transmission, Ca^{2+} plays a critical role in responding to the injuries of the CNS. Ca^{2+}-pump ATPase in plasma and endoplasmic reticulum membrane is highly sensitive to OS. LP caused by OS can interfere with the transportation of Ca^{2+} and increase the intracellular Ca^{2+} concentrations *via* inhibiting the activation of Ca^{2+}-pump ATPase. At the same time, the inhibition of Na+/K + -pump ATPase caused by OS can increase the accumulation of Na+and further promote the accumulation of Ca^{2+} in cells (Lowry et al., 2020). With the influx of Na^+ and the alterations of change of osmotic pressure, cytotoxic cellular edema occurs, further promoting intracellular phospholipase activity and intracellular acidosis (Piao et al., 2011).

3.1.4 Oxidative stress and mitochondrial dysfunctions in spinal cord injury

Mitochondrial dysfunction is an important section of the cascade of traumatic cell death after SCI. Following the exacerbation of injury, there is a loss of homeostasis of mitochondria, together with the imbalance of synaptic homeostasis. As energy reservoirs, mitochondria can regulate cytosolic Ca^{2+} ion levels (Turtle et al., 2019). After trauma, the mitochondrial damage is mediated by the elevated Ca^{2+} levels in SCI. Elevated cytosolic Ca^{2+} levels can activate NADH dehydrogenase, increase ATP generation and promote ROS production. The surfeit of Ca^{2+} further disturbs the proton gradient and results in cell swelling or death by opening the mitochondrial permeability transition pores (mPTPs) (Cao et al., 2013). Besides, three PON forms (ONOO−, ONOOCO2, and ONOOH) can deplete stores of mitochondrial antioxidants, leading to protein nitration (Valdez et al., 2000). Excessive PON ulteriorly induced 4-HNE, 3-nitrotyrosine (3-NT), and protein carbonyl content in mitochondrial proteins, further aggravating mitochondrial dysfunction (Sullivan et al., 2007). An extremely low concentration of 4-HNE could significantly impair the respiration function of mitochondria (Xiao et al., 2017). Moreover, NO has been also shown to exist in mitochondria stemming from a NO synthase isoform. Because the neurons are particularly sensitive to energy, preventing the lack of energy prone to cause neurodegeneration is crucial. However, widespread damage to mitochondria can finally and easily cause neuronal death owing to the insufficient energy provided for cell survival (Golpich et al., 2017). Hence, mitochondria are highly regarded as the potential vital target for SCI pharmacological treatment. During the first 6 h after SCI, promoting mitochondrial fusion may even be used as a potential method of improving spinal cord function (Cao et al., 2013).

4 Mechanism of oxidative stress in the aetiology of traditional Chinese medicine for spinal cord injury

Therefore, alleviating OS is a critical step in therapeutic intervention in SCI. Seeking the appropriate antioxidant therapy to prevent OS after the injury has become a top priority. With its natural antioxidant capacity, TCM has recently become a novel and promising supplementary treatment. The TCM theory holds that the pathogenesis of SCI is characterized by blood stasis and deficiency of qi. In the theory of TCM, qi is regarded as a very delicate substance with strong vitality. Constituting the human body and maintaining human life activities, the concept of qi is consistent with the adenosine triphosphate (ATP) that is mainly produced in the mitochondrion (Wong and Ko, 2013; Yong et al., 2020). Moreover, Some TCM with the “Qi-invigorating” action has a close link to the safeguarding of mitochondrial function (Kang et al., 2020; Tian et al., 2021). Mitochondrial dysfunction induced by OS resembles the deficiency of qi. The function of qi lies in the power to promote blood flow. When the power of push is insufficient, flowing blood will generate the pathological product, blood stasis. The blockade of blood stasis obstructs the transportation and absorption of nutrients in channels and collaterals, leading to the body not being nurtured, which is consistent with the neurodegeneration caused by the lack of energy owing to the mitochondrial dysfunction induced by OS. The equivalence between qi deficiency and mitochondrial dysfunction provides a modern microbiology perspective for TCM to understand the pathological mechanism. Thus, TCM can treat SCI by supplementing qi, activating blood circulation, and removing blood stasis. Additionally, from the modern perspective, as natural antioxidants, TCM intervenes in SCI by attenuating OS and preventing mitochondrial dysfunction. The overlap of the two theories makes the feasibility of auxiliary treatment of SCI with TCM.

5 Therapeutic intervention with traditional Chinese medicine

Attracting a great quantity of attention, TCM has been considered a promising supplementary treatment in recent years. Active herbal extracts, metabolites (Tables 1, 2), traditional botanical drugs (Table 3), and formulas (Table 4) all have shown their effectiveness, playing vital roles in the prevention and treatment of SCI, especially as natural antioxidants.

5.1 Therapeutic intervention with active herbal extracts and metabolites

5.1.1 Quercetin

Quercetin ($C_{15}H_{10}O_7$), is abundant in a variety of plants, fruits, and vegetables, such as onion annd broccoli, as well as *Bupleurum chinense* DC [Apiaceae; Bupleuri Radix] and *Morus alba* L. [Moraceae; Mori Folium], which is one of the major flavonoids that are part of human diets. It plays a role in the prevention of various diseases such as cancer and cardiovascular diseases (Reyes-Farias and Carrasco-Pozo, 2019).

In recent years, it has been revealed that quercetin could protect the injured spinal cord by decreasing oxidative. Aged rats with quercetin (20 mg/kg/d intraperitoneally for 10 days) had a decreased level of MDA and reversed the major degenerative changes, restraining OS (Firgany and Sarhan, 2020). The underlying mechanism may be related to the regulation of p38 mitogen-activated protein kinase (MAPK) and activating transcription factor 2 (ATF2) pathway, thus quercetin antagonized OS. Even compared to the specific p38MAPK inhibitor SB203580, quercetin has stronger effects on enhancing SOD activity and inhibiting MDA in SCI rats. Immunohistochemistry consequences revealed that after quercetin administration (0.2 mg/kg/d intraperitoneally for 14 days), the postoperatively elevated rate of iNOS-positive cells was significantly decreased (Song et al., 2013).

5.1.2 Gastrodin

Gastrodin ($C_{13}H_{18}O_7$) is a phenolic glycoside compound extracted from *Gastrodia elata* Blume [Orchidaceae; Gastrodiae rhizome]. Studies have indicated that gastrodin has various pharmacological effects, such as antihypertensive, lipid-lowering, and anticoagulant, which also beneficial functions in the protection of neurons, by inhibiting OS, regulating immune inflammation, and regulating ion channels (Liu et al., 2018).

Recently, gastrodin has emerged as a potential treatment for SCI. Administration of gastrodin (100 or 200 mg/kg/d intraperitoneally for 5 days) could enhance expressions of nuclear factor (erythroid-derived 2)-like 2 (Nrf2), modified subunit of γ-glutamylcysteine ligase (GCLm), and catalytic subunit of γ-glutamylcysteine ligase (GCLc), and subsequently improve the OS and recovery of locomotor function, as illustrated by the accumulation of Basso-Beattie-Bresnahan (BBB) scores (Du et al., 2016). Similarly, the spinal cord ischemia-reperfusion injury model by blocking the abdominal aorta under the renal artery and intervening with gastrodin showed an increase in SOD, glutathione peroxidase (GSH-Px), and total antioxidant capacity (T-AOC), as well as the decrease in ROS and MDA. Simultaneously, the reduction of mitochondrial swelling (MSD) also confirmed the effects of gastrodin (100 mg/kg/d intraperitoneally for 1 day) on protecting spinal cord ischemia-reperfusion injury by promoting the antioxidant capacity of spinal cord mitochondria and inhibiting the inflammatory response to the injury (Fang et al., 2016).

5.1.3 Asiatic acid

Asiatic acid (AA, $C_{30}H_{48}O_5$) is a naturally occurring pentacyclic triterpenoid, which is found mainly in the *Centella asiatica* (L.) Urb. [Apiaceae; Centeliae herba]. It has been reported that AA has broad-spectrum anticancer abilities.

Current research has shown that AA can be used to protect damaged spinal cord by reducing OS. AA treatment (75 mg/kg/d intraperitoneally for 1 day) significantly increased BBB scores and inclined plane test scores that were reduced by acute SCI. In addition, AA suppressed myeloperoxidase activity and reduced the levels of pro-inflammatory cytokines, ROS, and MDA, while increasing superoxide dismutase activity and glutathione production (Gurcan et al., 2017). Additionally, intragastric injection with AA (30 mg/kg or 75 mg/kg) was demonstrated that could lead to the downregulation of ROS, MDA, and tumor necrosis factor-alpha, while upregulating superoxide dismutase activity and glutathione production, which may be related to the inhibition of NLRP3 inflammasome pathway and the activation of Nrf2 and HO-1 (Jiang et al., 2016).

5.1.4 Tetramethylpyrazine

Tetramethylpyrazine (TMP, $C_8H_{12}N_2$), a natural alkaloid which is isolated from the Chinese botanical drug *Ligusticum chuanxiong* Hort. [Apiaceae; Chuanxiong Rhizoma], has been found to have antioxidant and anti-inflammatory effects (AlKreathy et al., 2020).

Previous study reported the TMP treatment (30 mg/kg, intraperitoneally 30 min before occlusion) decreased the expression level of proinflammatory cytokines TNF-α and IL-1β, and inhibited the activation of NF-κB in spinal cord ischemia rats (Fan et al., 2011). Recently, TMP and monosialotetrahexosylganglioside (GM1) have been effectively used in the treatment of SCI. It is well documented that Selenium nanoparticles (SeNPs) have excellent antioxidant activity. As a novel multi-functionalized SeNPs, SeNPs@GM1/TMP, being loaded with TMP/GM1 and decorated with polysaccharide-protein complex (PTW)/PG-6 peptide, showed a strong protective effect against apoptosis after SCI. SeNPs@GM1/

TABLE 1 Therapeutic intervention with active herbal extracts and metabolites.

	Active herbal extracts and metabolites				
Name	**Source**	**Molecular formula**	**Molecular structure**	**Mechanisms**	**Effects on SCI**
Quercetin	*Bupleurum chinense* DC [Apiaceae; Bupleuri Radix] and *Morus alba* L. [Moraceae; Mori Folium]	$C_{15}H_{10}O_7$	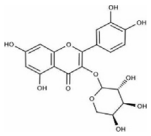	Decreases MDA and iNOS-positive cells, activates ATF2 pathway and suppresses NF-κB and STAT1 pathway	Decreases necroptosis, antioxidant properties
Gastrodin	*Gastrodia elata* Blume [Orchidaceae; Gastrodiae rhizome]	$C_{13}H_{18}O_7$	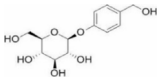	Enhances expressions of Nrf2 and modifies subunit of GCLm and GCLc, decreases ROS and MDA	Recovery of locomotor function and antioxidant properties
Asiatic acid	*Centella asiatica* (L.) Urb. [Apiaceae; Centeliae herba]	$C_{30}H_{48}O_5$	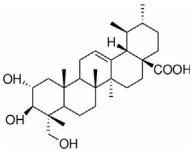	Suppresses myeloperoxidase activity, reduces ROS and MDA and blocks NF-kB/STAT3/ERK pathway	Increases BBB scores and inclined plane test scores, antioxidant effects
Tetramethylpyrazine	*Ligusticum chuanxiong* Hort. [Apiaceae; Chuanxiong Rhizoma]	$C_8H_{12}N_2$	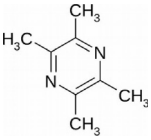	Reduces ROS production and inhibits p53/MAPK pathways	Prevents mitochondria dysfunction, antioxidant effects
Schisandrin B	*Schisandra chinensis* (Turcz) Baill. [Schisandraceae; Schisandrae Chinensis Fructus]	$C_{23}H_{28}O_7$	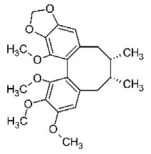	Increases SOD expression and decreases MDA expression	Improves the inclined plate test scores, antioxidant properties
Rosmarinic acid	*Perilla frutescens* (L.) Britton. [Lamiaceae; Perillae Fructus]	$C_{18}H_{16}O_8$	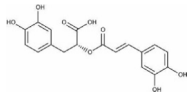	Decreased ROS and activates Nrf2 and HO-1 pathway	Mitigates cytotoxicity and inflammatory injury, antioxidant properties
Allicin	*Allium sativum* L. [Amaryllidaceae; Allii Sativi Bulbus]	$C_6H_{10}OS_2$	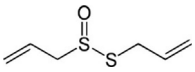	Increases Nrf2 nuclear translocation, inhibits ROS and LP. Inhibit lipid peroxidation by quenching free radicals	Accelerates recovery of motor functions, antioxidant properties
Resveratrol	*Polygonum cuspidatum* Sieb. et Zucc. [Polygonaceae; Polygoni Cuspidati Rhizoma et Radix]	$C_{14}H_{12}O_3$	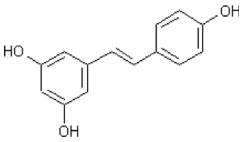	Inhibits the iNOS/p38MAPK pathway and activates Nrf2/HO-1 pathway	Strong antioxidant effects
Crocin	*Crocus sativus L.* [Iridaceae; Croci Stigma]	$C_{44}H_{64}O_{24}$	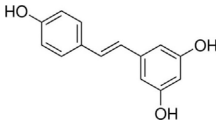	Enhances the expression level of neurotrophic factors in epidermal neural crest stem cells	Promotes spinal cord regeneration
Tetrandrine	*Stephania tetrandra S.Moore* [Menispermaceae; Stephaniae Tetrandrae Radix]	CHNO	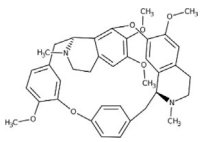	Reduces the production of pro-inflammatory factors and regulates PI3K/AKT/NF-κB pathway	Repairs the integrity of the blood-spinal cord barrier

(Continued on following page)

TABLE 1 (*Continued*) Therapeutic intervention with active herbal extracts and metabolites.

	Active herbal extracts and metabolites				
Name	**Source**	**Molecular formula**	**Molecular structure**	**Mechanisms**	**Effects on SCI**
Lycopene	Tomatoes, watermelons, and pink grapefruits	$C_{40}H_{56}$	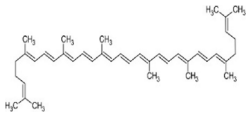	Inhibits MDA and LP	Strong antioxidant effects
Curcumin	*Curcuma longa L.* [Zingiberaceae; Curcumae Longae Rhizoma]	$C_{21}H_{20}O_6$	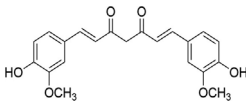	Enhances ability of lymphocytes to resist oxidative stress, increases the SOD content and protects the integrity of mitochondrial membranes	Improves mitochondrial dysfunction and strong antioxidant effects

TMP (0.3, 0.6 and 1.2 μM) attenuated ROS overproduction *via* inhibiting p53 and MAPK in concentration dependent, thus preventing mitochondria dysfunction (Rao et al., 2019).

5.1.5 Schisandrin B

Schisandrin B (Sch B, $C_{23}H_{28}O_7$), a dibenzocyclooctadiene lignan, is one of the most abundant active dibenzocyclooctadiene derivatives found in the *Schisandra chinensis* (Turcz.) Baill. [Schisandraceae; Schisandrae Chinensis Fructus]. Several studies had shown that Sch B has anti-fibrosis effects (Cuiqiong et al., 2020) and has a protective effect on myocardial injury (Zhang et al., 2017).

Currently, Xin et al. (2017) found that Sch B (50 mg/kg/day orally for 5 days) reduced the inflammatory response and inhibited OS in SCI model rats. ELISA kits showed that Sch B significantly increased SOD expression and decreased MDA expression levels compared with the untreated SCI group, which may be related to the inhibition of the P53 signaling pathway. Besides, Sch B improved the maximum angle of inclined plate test, behavioral examination scores, and inhibited spinal cord water content in rats with SCI.

5.1.6 Rosmarinic acid

Rosmarinic acid (RA, $C_{18}H_{16}O_8$) exists in *Perilla frutescens (L.)* Britton. [Lamiaceae; Perillae Fructus]. RA was proved with multiple biological activities, including, anti-inflammatory, neuroprotective, and antiangiogenic abilities (Colica et al., 2018).

In the animal experiment conducted by Ma et al. (2020), they found that RA notably upregulated the activities of CAT, SOD and GSH-Px and downregulated the MDA levels, indicating the attenuation of SCI-induced oxidative damage. Among the three groups designed in their study, the highest content administration of RA (40 mg/kg) showed significantly highest levels of SOD, CAT and GSH-Px than groups with 20 mg/kg and 10 mg/kg RA ($p < 0.05$). Besides, Treatment with RA could remarkably increase Nrf2 and HO-1 levels to ameliorate the increase in oxidative injury and apoptosis induced by H_2O_2. Meanwhile, the activation of the Nrf2/HO-1 pathway further amplified the inhibition of the NF-κB pathway, mitigating LPS-induced cytotoxicity and inflammatory injury.

5.1.7 Allicin

Allicin ($C_6H_{10}OS_2$), a thioester of sulfenic acid, is a natural antioxidant found in *Allium sativum* L. [Amaryllidaceae; Allii Sativi Bulbus]. Studies have shown that allicin has a good effect on a variety of diseases, such as bone diseases (Ding et al., 2016; Yang et al., 2020; Li et al., 2021) and neurodegenerative diseases (Zhang et al., 2018).

It is noteworthy that allicin played an important therapeutic role in SCI by inhibiting OS. SCI rats administrated with allicin showed better histological outcomes and accelerating recovery of motor functions, which may be related that allicin increased Nrf2 nuclear translocation in SCI rats (Lv et al., 2015). Additionally, the protective effects of allicin on antioxidation in SCI rats were dependent on the elevated production of NADH and inhibited levels of ROS (Wang and Ren, 2016). In the SCI model induced by glutamate, allicin was also shown to attenuate the release of lactate dehydrogenase (LDH), and inhibit OS by the mediation of heat shock protein 70 (HSP70)/inducible nitric oxide synthase (iNOS) pathway (Wang and Ren, 2016). Collectively, allicin may serve as a new therapeutic strategy for spinal cord injury (Liu et al., 2015).

5.1.8 Resveratrol

Resveratrol ($C_{14}H_{12}O_3$) is a kind of natural non-flavonoid polyphenol found in many vegetables and fruits, mainly in grapes and *Polygonum cuspidatum* Sieb. et Zucc. [Polygonaceae; Polygoni Cuspidati Rhizoma et Radix]. Numerous studies have shown that resveratrol can serve as a good antioxidant, improving overall health by inhibiting OS (Wang et al., 2013; Chen et al., 2020; Recalde et al., 2020).

In the animal experiment conducted by Fu et al., resveratrol (10 mg/kg intraperitoneally) functioned as a strong antioxidant

TABLE 2 The specific data of references cited in Section 5.1

Active herbal extracts and monomers	Study type	Experimental subjects	Dose	Duration	Controls
Quercetin	Preclinical trial	40 male rats aged 18 months	*In vivo*: 20 mg/g/d, i.p	10 days	1 ml distilled water both intraperitoneally and subcutaneously
	Preclinical trial	240 adult male Sprague–Dawley rats	*In vivo*: 0.2 mg/kg/d, i.p	14 days	Methylprednisolone 30 mg/kg/d, i.p
Gastrodin	Preclinical trial	60 male Sprang-Dawley rats	*In vivo*: 100 or 200 mg/kg/d, i.p	5 days	Intraperitoneally treated with vehicle
	Preclinical trial	36 New Zealand white rabbits	*In vivo*: 100 mg/kg/d	1 day	Perfuse normal saline 100 mg/kg
Asiatic acid	Preclinical trial	32 adult male Sprague-Dawley rats	*In vivo*: 75 mg/kg	1 day	Vehicle
	Preclinical trial	150 Sprague-Dawley rats	*In vivo*: 30 mg/kg/d or 30 mg/kg/d intragastric injection	3 days	Intragastric injection of vehicle 1 h after SCI
Tetramethylpyrazine	Preclinical trial	Adrenal phaeochromocytoma PC12 cells	*In vitro*: 0.3, 0.6, and 1.2 μM	10, 30, 60, and 120 min	Saline
	Preclinical trial	30 Sprague-Dawley rats	*In vivo*: 30 mg/kg, i.p	30 min before occlusion	Normal saline
Schisandrin B	Preclinical trial	40 adult male Sprague-Dawley rats	*In vivo*: 50 mg/kg, orally	5 days	Physiological saline (0.1 ml/100 g, i.p
Rosmarinic acid	Preclinical trial	60 adult female Sprague-Dawley rats	*In vivo*: 10, 20, and 40 mg/kg, i.p	28 days	Normal saline, i.p
Carnosic acid	Preclinical trial	Adult (8 weeks old) male CF-1 mice	*In vivo*: 0.3, 1.0, and 3.0 mg/kg, i.p	2 days	Saline
	Preclinical trial	Adult (8 weeks old) male CF-1 mice	*In vivo*: 1.0 mg/kg, i.p	2 days	Sulforaphane 5.0 mg/kg
Allicin	Preclinical trial	90 female Sprague-Dawley rats	*In vivo*: 2, 10, and 50 mg/kg/d, i.p	21 days	0.9% NaCl daily
	Preclinical trial	40 adult BALB/c mice	*In vivo*: 1, 5, and 10 mg/kg/d, i.p	7 days	2 ml sterile saline
Resveratrol	Preclinical trial	35 Male Sprague–Dawley rats	*In vivo*: 10 mg/kg, i.p	36 h	1 ml of saline, i.p
	Preclinical trial	42 male Sprague-Dawley rats	*In vivo*:100 mg/kg	48 h	Quercetin 200 mg/kg i.p
Crocin	Preclinical trial	Epidermal neural crest stem cells	*In vitro*: 12.5, 50, 100, 200, 500, 1,000, 1,500, 2,000, and 2,500 μM	72 h	1 mM valproic acid
	Preclinical trial	25 Female Wistar rats	*In vivo*: 150 mg/kg/d, i.p	14 days	Vehicle
Tetrandrine	Preclinical trial	Spinal cord astrocytes	*In vitro*: 0.1, 1, 10, and 20 mM	24 h	PI3K inhibitor LY294002 and NF-κB inhibitor PDTC
	Preclinical trial	48 healthy adult male or female New Zealand white rabbits	*In vivo*: 22.5 mg/kg, i.p	Before Ischemia reperfusion injury	Saline
Lycopene	Preclinical trial	30 adult male SD rats	*In vivo*: 5,10,20 mg/kg/d, i.p	7 days	Saline
Curcumin	Preclinical trial	40 male Wistar rats	*In vivo*: 200 mg/kg, i.p	Immediately after the trauma	1 ml of rice bran oil and 30 mg/kg methylprednisolone sodium succinate
	Preclinical trial	39 male Sprague-Dawley rats	*In vivo*: 40 mg/kg/d, i.p	6 days	Saline

to protect the ischemia-damaged spinal cord by inhibiting the iNOS/p38MAPK signaling (Fu et al., 2018). Moreover, resveratrol (100 mg/kg intraperitoneally) was found that it had a good preventive effect on secondary injury caused by SCI (Çiftçi et al., 2016).

5.1.9 Crocin

Crocin ($C_{44}H_{64}O_{24}$), belonging to apocarotenoid glycosides, is the main colorant and bioactive ingredient in *Crocus sativus* L. [Iridaceae; Croci Stigma]. Studies have shown that crocin has attracted much attention in the field

TABLE 3 Therapeutic intervention with Chinese herbs.

	Chinese herbs				
Name	**Species and source**	**Components**	**Picture**	**Effects in TCM theory**	**Antioxidant mechanisms**
Salvia miltiorrhiza Bunge	Lamiaceae; Salviae Miltiorrhizae Radix et Rhizome	Hydrophilic depside derivatives (e.g., danishes, salvianolic acids A–C, E–G, caffeic acid, and ferulic acid) and lipophilic diterpenoids (e.g., tanshinones I, IIA, andIIB, tanshinoneA, and tanshindiols A and B)		Promotes blood circulation, removes blood stasis, and reduces pain	Improves SOD, decreases the MDA, inhibits MAPK pathways, and preserves CAT activities
Cistanche deserticola Ma	Orobanchaceae; Cistanches herba	Total glycosides (TGs, phenylethanoid glycosides, and other glycosides) and oligosaccharides		Tonifies yang qi and blood, and moistens the intestines	Reduces p53, IL-6, and TNF-α, decreases MDA, increases SOD, GSH-Px, and CAT, facilitates Nrf-2 nuclear translocation

TABLE 4 Therapeutic intervention with traditional formulas.

Name	**Effects in TCM theory**	**Mechanisms**
JisuiKang	Removes blood stasis and dredge meridians, reconciles qi and blood	(1) Protects the microstructure of neurons, such as mitochondria, dendritic spine, and endoplasmic reticulum (2) Inhibits the expression of the Nogo receptor (NgR) in neurons and reduces the activation of the NgR/RhoA/ROCK signal pathway (3) Inhibits the expression of NOS and the content of NO and MDA while improving the activity of SOD
Xuefuzhuyu Decoction	Promotes blood circulation and dissolves stasis	(1) Reduces the content of MDA in the spinal cord and promotes the relief of spinal cord edema (2) Improve the content of SOD

of food and cosmetics. It can be used to produce functional products and as an anti-aging cosmetic agent for the skin (Fagot et al., 2018). Despite being used in dermatology, the results of Abdulkareem Aljumaily et al. (2021) verified that it can be used as a heart-protective agent for patients with cancers.

In recent years, crocin also has been found to have a significant effect on SCI. A recent investigation demonstrated that crocin may have therapeutic effects on SCI by enhancing the expression level of neurotrophic factors in epidermal neural crest stem cells (Baharvand et al., 2020). SCI rats treated with crocin (150 mg/kg/d intraperitoneally for 2 weeks) presented a notably reduced level of calcitonin gene-related peptide than the control group (Karami et al., 2013). In a word, crocin can greatly promote spinal cord regeneration and is an effective drug for treating SCI (Terraf et al., 2017).

5.1.10 Tetrandrine

Tetrandrine (CHNO) is an alkaloid, which mainly exists in the dry roots of *Stephania tetrandra* S. Moore [Menispermaceae; Stephaniae Tetrandrae Radix]. In recent years, studies have investigated that it can lessen lung damage, having a potential role in the treatment of asthma (Lin et al., 2019; Lin et al., 2020).

As for the aspect of tetrandrine treating SCI, scholars found tetrandrine was capable to protect damaged spinal cord astrocytes in rats and diminished the accumulation of IL-1β, IL-6, and TNF-α, which may be related to PI3K/AKT/NF-κB signaling pathway (Bao et al., 2016). After being intravenously injected with tetrandrine (22.5 mg/kg), New Zealand white rabbits with ischemia-reperfusion injury of the spinal cord showed a notable repair of the integrity of the blood-spinal cord barrier, related to that tetrandrine could change the BCL-2/Bax ratio and reduce the production of pro-inflammatory factors (Pu et al., 2020).

5.1.11 Lycopene

Lycopene ($C_{40}H_{56}$), an open-chain unsaturated structure, is the most important carotenoid in human plasma. Tomatoes, watermelons and pink grapefruits, are all rich sources of lycopene (Grabowska et al., 2019). As a functional pigment, lycopene has a variety of biological effects, among which the antioxidant effect has received extensive attention.

In recent years, numerous studies have found that lycopene could inhibit the production of MDA, and effectively resist ROS-mediated lipid peroxidation, thereby reducing the secondary damage of free radicals to spinal blood vessels and nerve cells. Animal experiments showed that lycopene also had an antioxidant effect on mitochondrial dysfunction in SCI rats. The experimental data showed that the mtDNA content and function-related genes-cytochrome b and mitochondrial organism's function-Tfam of the SCI group significantly decreased. However, these changes were significantly hyperpolarized after intraperitoneally injecting lycopene (Hu et al., 2017). In addition, the outstanding effects of lycopene were directly proportional to the use time.

5.1.12 Curcumin

Curcumin ($C_{21}H_{20}O_6$) is a natural polyphenol compound, which is extracted from traditional Chinese medicine *Curcuma longa* L. [Zingiberaceae; Curcumae Longae Rhizoma]. Studies have found that curcumin's properties of anti-inflammatory, anti-glial cells, and antitumor activity (Vollono et al., 2019) (Barua and Buragohain, 2021).

In recent years, research results inferred that curcumin may play a therapeutic effect in SCI. In an animal experiment (Cemil et al., 2010), researchers applied curcumin (200 mg/kg/d intravenously for 1 day) to treat aneurysm clamp SCI and detected enzyme changes in the tissue. Their BBB score confirmed the recovery of nerve function after administrating with curcumin. Lin and his colleagues (Lin et al., 2011) established the spinal cord hemisection injury model and observed that curcumin (40 mg/kg/d intravenously for 6 days) could improve the motor function of SCI rats. The mechanism may be related to that curcumin increased the SOD content in spinal cord tissue, thereby promoting the production of GSH in astrocytes, improving mitochondrial dysfunction and lipid peroxidation, along with protecting the integrity of mitochondrial membranes.

5.2 Therapeutic intervention with Chinese botanical drugs

5.2.1 Salvia miltiorrhiza Bunge

As one of the most famous Chinese botanical drugs, Danshen, namely *Salvia miltiorrhiza* Bunge [Lamiaceae; Salviae Miltiorrhizae Radix et Rhizome] has the effects of promoting blood circulation, removing blood stasis, and reducing pain in TCM theory. Danshen has plenty of components, majorly including hydrophilic depside derivatives (e.g., danishes, salvianolic acids A–C, E–G, caffeic acid, and ferulic acid) and lipophilic diterpenoids (e.g., tanshinones I, IIA, andIIB, tanshinoneA, and tanshindiols A and B).

Recently, studies found that many components of Danshen could play a critical antioxidant role in improving SCI. Dihydrotanshinone I (DI) could alleviate the pathological damage to the spinal cord and promote neuronal functional recovery by suppressing iNOS, and total oxidant status levels, while improving the (total antioxidant status) TAS level. Moreover, the experiment revealed that the HMGB1/TLR4/NOX4 pathway may participate in the effects of DI on SCI (Yu and Qian, 2020). Intraperitoneal administration with tanshinone IIA (TIIA) inhibited OS by significantly rescuing the activity of SOD and decreasing the MDA. Notably, TIIA had strong analgesic actions *via* inhibiting MAPKs pathways to depress the activation of microglial and immune responses (Cao et al., 2015). Salvianolic acid B(SalB) In the SCI rat models, groups administered with SalB markedly preserved the activities of SOD and CAT, playing an antioxidant role. (Fu et al., 2014).

5.2.2 Cistanche deserticola ma

Cistanche deserticola Ma [Orobanchaceae; Cistanches herba] is a commonly used drug for tonifying yang qi and blood, and moistening the intestines in TCM theory. Modern medicine has proved that *Cistanche deserticola* is effective for cardiovascular and cerebrovascular diseases (Wang et al., 2020). A considerable number of components of *Cistanche deserticola* were shown to be antioxidants, including total glycosides (TGs, phenylethanoid glycosides, and other glycosides) and oligosaccharides.

It was reported that oligosaccharides from *Cistanche deserticola* significantly altered LP, GSH, superoxide dismutase, acetylcholine esterase, catalase, nitric acid, acetylcholine esterase, and ROS in the SCI rats. Extract supplementation of oligosaccharides reduced mRNA expression levels of iNOS, p53, IL-6, TNF-α and cyclooxygenase-2 more than 20%, showing effective effects against inflammation, apoptosis, and OS (Zhang et al., 2019). Moreover, according to the experimental results of Wang et al. (2020) TGs could significantly decrease MDA levels, while increasing antioxidant activities, such as SOD, GSH-Px, and CAT, *via* remarkably facilitating Nrf-2 nuclear translocation. Additionally, phenylethanoid glycosides, an extract of *Cistanche deserticola* also had the ability to enhance SOD activity and decreasing MDA content (Xuan and Liu, 2008).

5.3 Therapeutic intervention with traditional formulas.

5.3.1 JisuiKang

JSK, a TCM formula derived from classic prescriptions Buyang Huanwu Decoction, is composed of *Plantago asiatica* L. [Plantaginaceae; Plantaginis Semen] 15 g, *Paeonia lactiflora* Pall. [Paeoniaceae; Paeoniae Radix Rubra] 12 g, *Ligusticum*

chuanxiong Hort. [Apiaceae; Chuanxiong Rhizoma] 10 g, *Rheum palmatum* L. [Polygonaceae; Rhei Radix et Rhizoma] 10 g, *Angelica sinensis* (Oliv.) Diels [Apiaceae; Angelicae Sinensis Radix] 12 g, Salvia miltiorrhiza Bunge [Lamiaceae; Salviae Miltiorrhizae Radix et Rhizome] 20 g, *Poria cocos* (Schw.) Wolf [Polyporaceae; Poria] 10 g, *Magnolia officinalis* Rehd. et Wils. [Magnoliaceae; Magnoliae Officinalis Cortex] 10 g; *Astragalus mongholicus* Bunge [Fabaceae; Astragali Radix] 30 g, *Cistanche deserticola* Ma [Orobanchaceae; Cistanches herba] 10 g, *Eupolyphaga sinensis* Walker [Corydidae; Eupolyphaga Steleophaga] 10 g, *Scolopendra subspinipes mutilans* L. Koch [Scolopendridae; Scolopendra] 10 g, *Epimedium brevicornu* Maxim. [Berberidaceae; Epimedii Folium] 10 g, *Alpinia oxyphylla* Miq. [Zingiberaceae; Alipiniae Oxyphyllae Fructus] 10 g, *Alisma orientale* (Sam.) Juzep. [Alismataceae; Alismatis Rhizoma] 10 g, *Citrus aurantium* L. [Rutaceae; Aurantii Fructus Immaturus] 10 g. Many clinical tests on SCI patients have demonstrated that JSK has satisfactory clinical efficacy (Guo et al., 2017). JSK could improve the motor function of SCI rats by protecting the microstructure of neurons, such as mitochondria, dendritic spine, and endoplasmic reticulum. Moreover, JSK inhibited the expression of the Nogo receptor (NgR) in neurons and reduced the activation of the NgR/RhoA/ROCK signal pathway to improve the motor function of SCI rats. These effects indicated the clinical values of JSK as a potential nerve regeneration agent (Wu et al., 2020).

As for the aspects of antioxidation, JSK could inhibit the expression of NOS and decrease the content of NO and MDA, while improving the activity of SOD. Thus, JSK directly inhibited the process of LP after SCI, as well as weakened the secondary degeneration and necrosis of the spinal cord caused by free radicals. On the other hand, JSK could gradually enhance the activity of endogenous antioxidants and enhance the scavenging effects of free radicals (Zhou et al., 2009). Moreover, in the clinical trial including 84 SCI patients, Wang et al. (2008) demonstrated that JSK treatment had significantly beneficial effects in improving kinetic score, grades of spinal injury and effectiveness of the treatment ($p < 0.05$). Clinical trial including 68 SCI patients demonstrated that the effective rate of JSK treatment was 94.3%, which may be related to the inhibited expressions of GFAP and CSPG proteins (Shao, 2020).

5.3.2 Xuefuzhuyu decoction

Originated in Qing Dynasty, XFZYD is considered one of the most significant decoctions for promoting blood circulation and dissolving stasis to treat cardiovascular and cerebrovascular diseases. The abundant meta-analysis, clinical trials, and animal experiments showed that XFZYD had effects on treating hyperlipidemia (Liao et al., 2014), coronary heart disease (Liao et al., 2014), liver fibrosis (Zhou et al., 2014), and so on. Composed of 11 kinds of traditional botanical drugs, including *Angelica sinensis* (Oliv.) Diels [Apiaceae; Angelicae Sinensis Radix] 9 g, *Rehmannia glutinosa* Libosch. [Orobanchaceae; Rehmanniae Radix] 9 g, *Prunus persica* (L.) Batsch [Rosaceae; Persicae Semen] 12 g, *Citrus aurantium* L. [Rutaceae; Aurantii Fructus] 6 g, Paeonia lactiflora Pall. [Paeoniaceae; Paeoniae Radix Rubra] 6 g, *Carthamus tinctorius* L. [Asteraceae; Carthami Flos] 9 g, *Ligusticum chuanxiong* Hort. [Apiaceae; Chuanxiong Rhizoma] 5 g, *Bupleurum chinense* DC. [Apiaceae; Bupleuri Radix] 3 g, *Glycyrrhiza uralensis* Fisch. [Fabaceae; Glycyrrhizae Radix et Rhizoma] 6 g, *Platycodon grandiflorum* (Jacq.) A. DC. [Campanulaceae; Platycodonis Radix] 5 g, *Achyranthes bidentata* Blume [Amaranthaceae; Achyranthis Bidentatae Radix] 9 g, XFZYD was found to be beneficial for the treatment of SCI by attenuating OS.

XFZUD could promote the microcirculation reperfusion of spinal cord stasis, reduce the content of MDA in the spinal cord and promote the relief of spinal cord edema, so as to protect the injured spinal cord (Liu et al., 2006). Meanwhile, a current study showed that the content of SOD in XFZYD containing serum group was significantly higher than that in the injury control group and blank serum group (Liu et al., 2017). Besides, the level of SOD in the XFZYD group was similar to that in the neurotrophic factor protection (NFP) group, and this similitude also existed in the cell survival rate of these two groups (XFZYD group = 0.529 ± 0.010, NFP group = 0.548 ± 0.056) (Liu et al., 2017).

6 Conclusion

The complicated pathophysiologic mechanisms contained in SCI lead to the existing circumstances that fully restorative treatments of SCI do not exist. Among the various pathophysiologic mechanisms, OS plays a vital role in secondary injury, triggering a series of free-radical-mediated damages, including damages to biological macromolecules, ion imbalances, and mitochondrial dysfunctions. Thus, lessening OS may become an effective therapeutic strategy for SCI.

From classical TCM theory, the mentioned active herbal extracts, metabolites, traditional botanical drugs, and formulas can treat SCI *via* invigorating Qi, activating blood circulation, and removing blood stasis, which is in line with our above-mentioned TCM treatment principles for SCI. On the other hand, from the modern perspective, the mentioned TCM intervene in SCI by suppressing M1, enhancing SOD activity, decreasing MDA levels, promoting mitochondrial functions, and other pathways to attenuate the impacts of OS on SCI. In the treatment of SCI, traditional botanical drugs and formulas used for thousands of years, have the advantages of synergistic effect and multitarget action, which are more in line with the medication law of TCM theory. However, "Drug-Drug Interaction" (DDI) occurs in the traditional botanical drugs and formulas owing to their numerous compounds, which

may cause the complication of predicting and preventing adverse reactions. On the contrary, active herbal extracts and metabolites, new concepts proposed in modern medicine compared to traditional botanical drugs and formulas, have the superiority of simple composition, direct targeting, high safety, and clear effects, avoiding the problems of adverse reactions. Therefore, active herbal extracts and metabolites with scavenging capacity may be more suitable to be the supplementary treatment to improve SCI, particularly resveratrol and quercetin.

However, the investigations on the application of TCM in SCI are generally published in low-impact journals, suggesting that this field of study is still in the initial stages. Additionally, promising results have been widely verified in animal models, instead of the implementation in human clinical applications, which makes us more aware of the obstacles and limitations of TCM in SCI. Therefore, in-depth studies in this study are extremely necessary. Accordingly, we make the following three recommendations and perspectives for subsequent research in this area: 1) to comprehensively understand traditional botanical drugs and formulas, more clinical investigations need to be done, including underlying possible therapeutic mechanisms, the best route of administration, dosage, and timing. 2) combine the active herbal extracts and metabolites with emerging nanotechnology or modern tissue scaffold therapies, improve the effect of nerve function repair and reconstruction after SCI. 3) in-depth research on the traditional theory of TCM and the mechanism of antioxidants in TCM is needed to reveal the modern mechanism of the traditional efficacy of benefiting qi in TCM theory, thereby identifying appropriate treatments for SCI within the TCM treatment protocol.

Author contributions

ZH and JW conceived the presented idea. JT was responsible for the planning and administration of the topic of this article. ZH took the lead in drafting the manuscript with input from all authors. CL, JW, and ZW collected the literatures and analyzed them. HZ and JH interpreted results from a clinical point of view. All authors read and approved the final manuscript.

Funding

This work was funded by The Second Batch of Scientific Research Projects for the Business Construction of the National Traditional Chinese Medicine Clinical Research Base (NO. JDZX2015268). Relevant picture materials are from Figdraw. The free ID is 533420148.

Conflict of interest

The authors declare that the research was conducted in the absence of any commercial or financial relationships that could be construed as a potential conflict of interest.

Publisher's note

Supplementary material

The Supplementary Material for this article can be found online at: https://www.frontiersin.org/articles/10.3389/fphar.2022.976757/full#supplementary-material

References

Abdulkareem Aljumaily, S. A., Demir, M., Elbe, H., Yigitturk, G., Bicer, Y., and Altinoz, E. (2021). Antioxidant, anti-inflammatory, and anti-apoptotic effects of crocin against doxorubicin-induced myocardial toxicity in rats. *Environ. Sci. Pollut. Res. Int.* 28, 65802–65813.

Alkreathy, H. M., Alghamdi, M. K., and Esmat, A. (2020). Tetramethylpyrazine ameliorates indomethacin-induced gastric ulcer in rats: Impact on oxidative, inflammatory, and angiogenic machineries. *Saudi Pharm. J.* 28, 916–926. doi:10.1016/j.jsps.2020.06.012

Anjum, A., Yazid, M. D., Fauzi Daud, M., Idris, J., Ng, A. M. H., Selvi Naicker, A., et al. (2020). Spinal cord injury: Pathophysiology, multimolecular interactions, and underlying recovery mechanisms. *Int. J. Mol. Sci.* 21, E7533. doi:10.3390/ijms21207533

Anwar, M. A., Al Shehabi, T. S., and Eid, A. H. (2016). Inflammogenesis of secondary spinal cord injury. *Front. Cell. Neurosci.* 10, 98. doi:10.3389/fncel.2016.00098

Baharvand, Z., Nabiuni, M., Tahmaseb, M., Amini, E., and Pandamooz, S. (2020). Investigating the synergic effects of valproic acid and crocin on bdnf and gdnf expression in epidermal neural crest stem cells. *Acta Neurobiol. Exp. (Wars).* 80, 38–46. doi:10.21307/ane-2020-004

Bao, G., Li, C., Qi, L., Wang, N., and He, B. (2016). Tetrandrine protects against oxygen-glucose-serum deprivation/reoxygenation-induced injury via pi3k/akt/nf-?b signaling pathway in rat spinal cord astrocytes. *Biomed. Pharmacother.* 84, 925–930. doi:10.1016/j.biopha.2016.10.007

Barua, N., and Buragohain, A. K. (2021). Therapeutic potential of curcumin as an antimycobacterial agent. *Biomolecules* 11, 1278. doi:10.3390/biom11091278

Cadenas, S. (2018). Mitochondrial uncoupling, ros generation and cardioprotection. *Biochim. Biophys. Acta. Bioenerg.* 1859, 940–950. doi:10.1016/j.bbabio.2018.05.019

Cao, F. L., Xu, M., Wang, Y., Gong, K. R., and Zhang, J. T. (2015). Tanshinone iia attenuates neuropathic pain via inhibiting glial activation and immune response. *Pharmacol. Biochem. Behav.* 128, 1–7. doi:10.1016/j.pbb.2014.11.004

Cao, Y., Lv, G., Wang, Y. S., Fan, Z. K., Bi, Y. L., Zhao, L., et al. (2013). Mitochondrial fusion and fission after spinal sacord injury in rats. *Brain Res.* 1522, 59–66. doi:10.1016/j.brainres.2013.05.033

Cemil, B., Topuz, K., Demircan, M. N., Kurt, G., Tun, K., Kutlay, M., et al. (2010). Curcumin improves early functional results after experimental spinal cord injury. *Acta Neurochir.* 152, 1583–1590. doi:10.1007/s00701-010-0702-x

Chen, W., Zhao, Z., Zhao, S., Zhang, L., and Song, Q. (2020). Resveratrol and puerarin loaded polymeric nanoparticles to enhance the chemotherapeutic efficacy in spinal cord injury. *Biomed. Microdevices* 22, 69. doi:10.1007/s10544-020-00521-4

Çiftçi, U., Delen, E., Vural, M., Uysal, O., Turgut Coşan, D., Baydemir, C., et al. (2016). Efficiacy of resveratrol and quercetin after experimental spinal cord injury. *Ulus. Travma Acil Cerrahi Derg.* 22, 423–431. doi:10.5505/tjtes.2016.44575

Colica, C., Di Renzo, L., Aiello, V., De Lorenzo, A., and Abenavoli, L. (2018). Rosmarinic acid as potential anti-inflammatory agent. *Rev. Recent Clin. Trials* 13, 240–242. doi:10.2174/1574887113041809110958 18

Cuiqiong, W., Chao, X., Xinling, F., and Yinyan, J. (2020). Schisandrin B suppresses liver fibrosis in rats by targeting mir-101-5p through the tgf-B signaling pathway. *Artif. Cells Nanomed. Biotechnol.* 48, 473–478. doi:10.1080/21691401.2020.1717507

Ding, G., Zhao, J., and Jiang, D. (2016). Allicin inhibits oxidative stress-induced mitochondrial dysfunction and apoptosis by promoting pi3k/akt and creb/erk signaling in osteoblast cells. *Exp. Ther. Med.* 11, 2553–2560. doi:10.3892/etm.2016.3179

Du, F., Wang, X., Shang, B., Fang, J., Xi, Y., Li, A., et al. (2016). Gastrodin ameliorates spinal cord injury via antioxidant and anti-inflammatory effects. *Acta Biochim. Pol.* 63, 589–593. doi:10.18388/abp.2016_1272

Eckert, M. J., and Martin, M. J. (2017). Trauma: Spinal cord injury. *Surg. Clin. North Am.* 97, 1031–1045. doi:10.1016/j.suc.2017.06.008

Eli, I., Lerner, D. P., and Ghogawala, Z. (2021). Acute traumatic spinal cord injury. *Neurol. Clin.* 39, 471–488. doi:10.1016/j.ncl.2021.02.004

Every, A. E., and Russu, I. M. (2013). Opening dynamics of 8-oxoguanine in dna. *J. Mol. Recognit.* 26, 175–180. doi:10.1002/jmr.2262

Fagot, D., Pham, D. M., Laboureau, J., Planel, E., Guerin, L., Nègre, C., et al. (2018). Crocin, A natural molecule with potentially beneficial effects against skin ageing. *Int. J. Cosmet. Sci.* 40, 388–400. doi:10.1111/ics.12472

Fan, B., Wei, Z., Yao, X., Shi, G., Cheng, X., Zhou, X., et al. (2018). Microenvironment imbalance of spinal cord injury. *Cell Transpl.* 27, 853–866. doi:10.1177/0963689718755778

Fan, L., Wang, K., Shi, Z., Die, J., Wang, C., and Dang, X. (2011). Tetramethylpyrazine protects spinal cord and reduces inflammation in A rat model of spinal cord ischemia-reperfusion injury. *J. Vasc. Surg.* 54, 192–200. doi:10.1016/j.jvs.2010.12.030

Fang, H., Zhang, J. C., Yang, M., Li, H. F., Zhang, J. P., Zhang, F. X., et al. (2016). Perfusion of gastrodin in abdominal aorta for alleviating spinal cord ischemia reperfusion injury. *Asian pac. J. Trop. Med.* 9, 688–693. doi:10.1016/j.apjtm.2016.05.007

Fatima, G., Sharma, V. P., Das, S. K., and Mahdi, A. A. (2015). Oxidative stress and antioxidative parameters in patients with spinal cord injury: Implications in the pathogenesis of disease. *Spinal Cord.* 53, 3–6. doi:10.1038/sc.2014.178

Firgany, A. E. L., and Sarhan, N. R. (2020). Quercetin mitigates monosodium glutamate-induced excitotoxicity of the spinal cord motoneurons in aged rats via P38 mapk inhibition. *Acta Histochem.* 122, 151554. doi:10.1016/j.acthis.2020.151554

Fu, J., Fan, H. B., Guo, Z., Wang, Z., Li, X. D., Li, J., et al. (2014). Salvianolic acid B attenuates spinal cord ischemia-reperfusion-induced neuronal injury and oxidative stress by activating the extracellular signal-regulated kinase pathway in rats. *J. Surg. Res.* 188, 222–230. doi:10.1016/j.jss.2013.11.1118

Fu, S., Lv, R., Wang, L., Hou, H., Liu, H., and Shao, S. (2018). Resveratrol, an antioxidant, protects spinal cord injury in rats by suppressing mapk pathway. *Saudi J. Biol. Sci.* 25, 259–266. doi:10.1016/j.sjbs.2016.10.019

Garcia, V. B., Abbinanti, M. D., Harris-Warrick, R. M., and Schulz, D. J. (2018). Effects of chronic spinal cord injury on relationships among ion channel and receptor mrnas in mouse lumbar spinal cord. *Neuroscience* 393, 42–60. doi:10.1016/j.neuroscience.2018.09.034

Gedde, M. H., Lilleberg, H. S., Assmus, J., Gilhus, N. E., and Rekand, T. (2019). Traumatic vs non-traumatic spinal cord injury: A comparison of primary rehabilitation outcomes and complications during hospitalization. *J. Spinal Cord. Med.* 42, 695–701. doi:10.1080/10790268.2019.1598698

Golpich, M., Amini, E., Mohamed, Z., Azman Ali, R., Mohamed Ibrahim, N., and Ahmadiani, A. (2017). Mitochondrial dysfunction and biogenesis in neurodegenerative diseases: Pathogenesis and treatment. *CNS Neurosci. Ther.* 23, 5–22. doi:10.1111/cns.12655

Grabowska, M., Wawrzyniak, D., Rolle, K., Chomczynski, P., Oziewicz, S., Jurga, S., et al. (2019). Let food Be your medicine: Nutraceutical properties of lycopene. *Food Funct.* 10, 3090–3102. doi:10.1039/c9fo00580c

Guo, Y., Ma, Y., Pan, Y. L., Zheng, S. Y., Wang, J. W., and Huang, G. C. (2017). Jisuikang, A Chinese herbal formula, increases neurotrophic factor expression and promotes the recovery of neurological function after spinal cord injury. *Neural Regen. Res.* 12, 1519–1528. doi:10.4103/1673-5374.215264

Gurcan, O., Gurcat, A. G., Kazanci, A., Senturk, S., Bodur, E., Karaca, E. U., et al. (2017). Effect of asiatic acid on the treatment of spinal cord injury: An experimental study in rats. *Turk. Neurosurg.* 27, 259–264. doi:10.5137/1019-5149.JTN.15747-15.2

Hall, E. D., Vaishnav, R. A., and Mustafa, A. G. (2010). Antioxidant therapies for traumatic brain injury. *Neurotherapeutics* 7, 51–61. doi:10.1016/j.nurt.2009.10.021

Hall, E. D., Wang, J. A., Bosken, J. M., and Singh, I. N. (2016). Lipid peroxidation in brain or spinal cord mitochondria after injury. *J. Bioenerg. Biomembr.* 48, 169–174. doi:10.1007/s10863-015-9600-5

Hamann, K., and Shi, R. (2009). Acrolein scavenging: A potential novel mechanism of attenuating oxidative stress following spinal cord injury. *J. Neurochem.* 111, 1348–1356. doi:10.1111/j.1471-4159.2009.06395.x

Hawkins, C. L., and Davies, M. J. (2019). Detection, identification, and quantification of oxidative protein modifications. *J. Biol. Chem.* 294, 19683–19708. doi:10.1074/jbc.REV119.006217

Hu, W., Wang, H. B., Liu, Z. F., Liu, Y. L., Wang, R., Luo, X., et al. (2017). Neuroprotective effects of lycopene in spinal cord injury in rats via antioxidative and anti-apoptotic pathway. *Neurosci. Lett.* 642, 107–112. doi:10.1016/j.neulet.2017.02.004

Jiang, W., Li, M., He, F., Bian, Z., He, Q., Wang, X., et al. (2016). Neuroprotective effect of asiatic acid against spinal cord injury in rats. *Life Sci.* 157, 45–51. doi:10.1016/j.lfs.2016.05.004

Kang, S., Piao, Y., Kang, Y. C., Lim, S., and Pak, Y. K. (2020). Qi-activating quercetin alleviates mitochondrial dysfunction and neuroinflammation *in vivo* and *in vitro*. *Arch. Pharm. Res.* 43, 553–566. doi:10.1007/s12272-020-01238-x

Karami, M., Bathaie, S. Z., Tiraihi, T., Habibi-Rezaei, M., Arabkheradmand, J., and Faghihzadeh, S. (2013). Crocin improved locomotor function and mechanical behavior in the rat model of contused spinal cord injury through decreasing calcitonin gene related peptide (cgrp). *Phytomedicine* 21, 62–67. doi:10.1016/j.phymed.2013.07.013

Katoh, H., Yokota, K., and Fehlings, M. G. (2019). Regeneration of spinal cord connectivity through stem cell transplantation and biomaterial scaffolds. *Front. Cell. Neurosci.* 13, 248. doi:10.3389/fncel.2019.00248

Kroner, A., Greenhalgh, A. D., Zarruk, J. G., Passos Dos Santos, R., Gaestel, M., and David, S. (2014). Tnf and increased intracellular iron alter macrophage polarization to A detrimental M1 phenotype in the injured spinal cord. *Neuron* 83, 1098–1116. doi:10.1016/j.neuron.2014.07.027

Li, D., Liang, H., Li, Y., Zhang, J., Qiao, L., and Luo, H. (2021). Allicin alleviates lead-induced bone loss by preventing oxidative stress and osteoclastogenesis via sirt1/foxo1 pathway in mice. *Biol. Trace Elem. Res.* 199, 237–243. doi:10.1007/s12011-020-02136-5

Liao, J., Tian, J., Li, T., Song, W., Zhao, W., and Du, J. (2014). Xuefuzhuyu decoction for hyperlipidemia: A systematic review and meta-analysis of randomized clinical trails. *J. Tradit. Chin. Med.* 34, 411–418. doi:10.1016/s0254-6272(15)30040-6

Lin, M. S., Lee, Y. H., Chiu, W. T., and Hung, K. S. (2011). Curcumin provides neuroprotection after spinal cord injury. *J. Surg. Res.* 166, 280–289. doi:10.1016/j.jss.2009.07.001

Lin, Y., Yao, J., Wu, M., Ying, X., Ding, M., Wei, Y., et al. (2020). Erratum to "tetrandrine ameliorates airway remodeling of chronic asthma by interfering tgf-ß1/nrf-2/Ho-1 signaling pathway-mediated oxidative stress. *Can. Respir. J.* 2020, 6958283. doi:10.1155/2020/6958283

Lin, Y., Yao, J., Wu, M., Ying, X., Ding, M., Wei, Y., et al. (2019). Tetrandrine ameliorates airway remodeling of chronic asthma by interfering tgf-ß1/nrf-2/Ho-1 signaling pathway-mediated oxidative stress. *Can. Respir. J.* 2019, 7930396. doi:10.1155/2019/7930396

Liu, D. K., Wang, G., Zhao, G., and Chi, X. F. (2017). *Protective effect of xuefu zhuyu serum on anoxic injury of dorsal root neurons in rats*, 189–191.

Liu, R. Z., Pan, H. S., Tang, X. J., Peng, J., and Bao, J. (2006). Effect of xuefu zhuyu decoction on neurons and vascular perfusion in rabbits after decompression of acute cervical spine cord damage in an early time. *Chin. J. Of Clin. Rehabilitation* 10.

Liu, S. G., Ren, P. Y., Wang, G. Y., Yao, S. X., and He, X. J. (2015). Allicin protects spinal cord neurons from glutamate-induced oxidative stress through regulating the heat shock protein 70/inducible nitric oxide synthase pathway. *Food Funct.* 6, 321–330. doi:10.1039/c4fo00761a

Liu, Y., Gao, J. L., Peng, M., Meng, H. Y., Ma, H. B., Cai, P. P., et al. (2018). A review on central nervous system effects of gastrodin. *Front. Pharmacol.* 9, 24. doi:10.3389/fphar.2018.00024

Lowry, C. A., Golod, M. E., Andrew, R. D., and Bennett, B. M. (2020). Expression of neuronal Na(+)/K(+)-Atpase alpha subunit isoforms in the mouse brain following genetically programmed or behaviourally-induced oxidative stress. *Neuroscience* 442, 202–215. doi:10.1016/j.neuroscience.2020.07.009

Lv, R., Mao, N., Wu, J., Lu, C., Ding, M., Gu, X., et al. (2015). Neuroprotective effect of allicin in A rat model of acute spinal cord injury. *Life Sci.* 143, 114–123. doi:10.1016/j.lfs.2015.11.001

Ma, Z., Lu, Y., Yang, F., Li, S., He, X., Gao, Y., et al. (2020). Rosmarinic acid exerts a neuroprotective effect on spinal cord injury by suppressing oxidative stress and inflammation via modulating the Nrf2/HO-1 and TLR4/NF-κB pathways. *Toxicol. Appl. Pharmacol.* 397, 115014. doi:10.1016/j.taap.2020.115014

Piao, F., Li, S., Li, Q., Ye, J., and Liu, S. (2011). Abnormal expression of 8-nitroguanine in the brain of mice exposed to arsenic subchronically. *Ind. Health* 49, 151–157. doi:10.2486/indhealth.ms1058

Pu, X. W., Wang, L. H., Lu, T. S., Yao, S. D., Yang, J. W., and Luo, C. S. (2020). Effects of tetrandrine pretreatment on spinal cord ischemia-reperfusion injury in rabbits. *Int. J. Of Clin. Exp. Med.* 13, 7499–7508.

Rao, S., Lin, Y., Du, Y., He, L., Huang, G., Chen, B., et al. (2019). Designing multifunctionalized Selenium nanoparticles to reverse oxidative stress-induced spinal cord injury by attenuating ros overproduction and mitochondria dysfunction. *J. Mat. Chem. B* 7, 2648–2656. doi:10.1039/c8tb02520g

Recalde, M. D., Miguel, C. A., Noya-Riobó, M. V., González, S. L., Villar, M. J., and Coronel, M. F. (2020). Resveratrol exerts anti-oxidant and anti-inflammatory actions and prevents oxaliplatin-induced mechanical and thermal allodynia. *Brain Res.* 1748, 147079. doi:10.1016/j.brainres.2020.147079

Reyes-Farias, M., and Carrasco-Pozo, C. (2019). The anti-cancer effect of quercetin: Molecular implications in cancer metabolism. *Int. J. Mol. Sci.* 20, E3177. doi:10.3390/ijms20133177

Savikj, M., Kostovski, E., Lundell, L. S., Iversen, P. O., Massart, J., and Widegren, U. (2019). Altered oxidative stress and antioxidant defence in skeletal muscle during the first year following spinal cord injury. *Physiol. Rep.* 7, E14218. doi:10.14814/phy2.14218

Shao, Y. (2020). "Clinical observation of "jisuikang," in *Treating spinal cord injury and experimental study on promoting nerve regeneration after spinal cord injury* (Doctor: Nanjing University Of Traditional Chinese Medicine).

Singh, A., Kukreti, R., Saso, L., and Kukreti, S. (2019). Oxidative stress: Role and response of short guanine tracts at genomic locations. *Int. J. Mol. Sci.* 20, E4258. doi:10.3390/ijms20174258

Song, Y., Liu, J., Zhang, F., Zhang, J., Shi, T., and Zeng, Z. (2013). Antioxidant effect of quercetin against acute spinal cord injury in rats and its correlation with the P38mapk/inos signaling pathway. *Life Sci.* 92, 1215–1221. doi:10.1016/j.lfs.2013.05.007

Sullivan, P. G., Krishnamurthy, S., Patel, S. P., Pandya, J. D., and Rabchevsky, A. G. (2007). Temporal characterization of mitochondrial bioenergetics after spinal cord injury. *J. Neurotrauma* 24, 991–999. doi:10.1089/neu.2006.0242

Tang, Y., and Le, W. (2016). Differential roles of M1 and M2 microglia in neurodegenerative diseases. *Mol. Neurobiol.* 53, 1181–1194. doi:10.1007/s12035-014-9070-5

Terraf, P., Kouhsari, S. M., Ai, J., and Babaloo, H. (2017). Tissue-engineered regeneration of hemisected spinal cord using human endometrial stem cells, poly E-caprolactone scaffolds, and crocin as A neuroprotective agent. *Mol. Neurobiol.* 54, 5657–5667. doi:10.1007/s12035-016-0089-7

Tian, J., Huang, Y., Wu, T., Huang, H. D., Ko, K. M., Zhu, B. T., et al. (2021). The use of Chinese yang/qi-invigorating tonic botanical drugs/herbal formulations in ameliorating chronic kidney disease by enhancing mitochondrial function. *Front. Pharmacol.* 12, 622498. doi:10.3389/fphar.2021.622498

Turtle, J. D., Henwood, M. K., Strain, M. M., Huang, Y. J., Miranda, R. C., and Grau, J. W. (2019). Engaging pain fibers after A spinal cord injury fosters hemorrhage and expands the area of secondary injury. *Exp. Neurol.* 311, 115–124. doi:10.1016/j.expneurol.2018.09.018

Valdez, L. B., Alvarez, S., Arnaiz, S. L., Schopfer, F., Carreras, M. C., Poderoso, J. J., et al. (2000). Reactions of peroxynitrite in the mitochondrial matrix. *Free Radic. Biol. Med.* 29, 349–356. doi:10.1016/s0891-5849(00)00301-4

Vanzulli, I., and Butt, A. M. (2015). Mglur5 protect astrocytes from ischemic damage in postnatal cns white matter. *Cell Calcium* 58, 423–430. doi:10.1016/j.ceca.2015.06.010

Vollono, L., Falconi, M., Gaziano, R., Iacovelli, F., Dika, E., Terracciano, C., et al. (2019). Potential of curcumin in skin disorders. *Nutrients* 11, E2169. doi:10.3390/nu11092169

Von Leden, R. E., Yauger, Y. J., Khayrullina, G., and Byrnes, K. R. (2017). Central nervous system injury and nicotinamide adenine dinucleotide phosphate oxidase: Oxidative stress and therapeutic targets. *J. Neurotrauma* 34, 755–764. doi:10.1089/neu.2016.4486

Wang, C., Zhang, L., Ndong, J. C., Hettinghouse, A., Sun, G., Chen, C., et al. (2019). Progranulin deficiency exacerbates spinal cord injury by promoting neuroinflammation and cell apoptosis in mice. *J. Neuroinflammation* 16, 238. doi:10.1186/s12974-019-1630-1

Wang, F., Li, R., Tu, P., Chen, J., Zeng, K., and Jiang, Y. (2020). Total glycosides of Cistanche deserticola promote neurological function recovery by inducing neurovascular regeneration via nrf-2/keap-1 pathway in mcao/R rats. *Front. Pharmacol.* 11, 236. doi:10.3389/fphar.2020.00236

Wang, H. D., Shi, Y. M., Li, L., Guo, J. D., Zhang, Y. P., and Hou, S. X. (2013). Treatment with resveratrol attenuates sublesional bone loss in spinal cord-injured rats. *Br. J. Pharmacol.* 170, 796–806. doi:10.1111/bph.12301

Wang, J. W., Wu, M., and Huang, G. C. (2008). Effect of jisuikang on kinetic dysfunction in patients after spinal injury. *Chin. J. Integr. Med.* 14, 190–193. doi:10.1007/s11655-008-9006-x

Wang, S., and Ren, D. (2016). Allicin protects traumatic spinal cord injury through regulating the hsp70/akt/inos pathway in mice. *Mol. Med. Rep.* 14, 3086–3092. doi:10.3892/mmr.2016.5651

Wong, H. S., and Ko, K. M. (2013). Herba Cistanches stimulates cellular glutathione redox cycling by reactive oxygen species generated from mitochondrial respiration in H9c2 cardiomyocytes. *Pharm. Biol.* 51, 64–73. doi:10.3109/13880209.2012.710242

Wu, C., Zhou, Y., Tu, P., Yang, G., Zheng, S., Pan, Y., et al. (2020). Jisuikang promotes the repair of spinal cord injury in rats by regulating ngr/rhoa/rock signal pathway. *Evid. Based. Complement. Altern. Med.* 2020, 9542359. doi:10.1155/2020/9542359

Wu, D., Zheng, C., Wu, J., Xue, J., Huang, R., Wu, D., et al. (2017). The pathologic mechanisms underlying lumbar distraction spinal cord injury in rabbits. *Spine J.* 17, 1665–1673. doi:10.1016/j.spinee.2017.05.024

Xiao, M., Zhong, H., Xia, L., Tao, Y., and Yin, H. (2017). Pathophysiology of mitochondrial lipid oxidation: Role of 4-hydroxynonenal (4-hne) and other bioactive lipids in mitochondria. *Free Radic. Biol. Med.* 111, 316–327. doi:10.1016/j.freeradbiomed.2017.04.363

Xin, D. Q., Hu, Z. M., Huo, H. J., Yang, X. J., Han, D., Xing, W. H., et al. (2017). Schisandrin B attenuates the inflammatory response, oxidative stress and apoptosis induced by traumatic spinal cord injury via inhibition of P53 signaling in adult rats. *Mol. Med. Rep.* 16, 533–538. doi:10.3892/mmr.2017.6622

Xiong, Y., Rabchevsky, A. G., and Hall, E. D. (2007). Role of peroxynitrite in secondary oxidative damage after spinal cord injury. *J. Neurochem.* 100, 639–649. doi:10.1111/j.1471-4159.2006.04312.x

Xuan, G. D., and Liu, C. Q. (2008). Research on the effect of phenylethanoid glycosides (peg) of the Cistanche deserticola on anti-aging in aged mice induced by D-galactose. *Zhong Yao Cai* 31, 1385–1388.

Yang, J., Song, X., Feng, Y., Liu, N., Fu, Z., Wu, J., et al. (2020). Natural ingredients-derived antioxidants attenuate H(2)O(2)-induced oxidative stress and have chondroprotective effects on human osteoarthritic chondrocytes via keap1/nrf2 pathway. *Free Radic. Biol. Med.* 152, 854–864. doi:10.1016/j.freeradbiomed.2020.01.185

Yang, Y., Liu, F., Tang, M., Yuan, M., Hu, A., Zhan, Z., et al. (2016). Macrophage polarization in experimental and clinical choroidal neovascularization. *Sci. Rep.* 6, 30933. doi:10.1038/srep30933

Yong, R. L., Dong, J. Z., Zhang, L., and Wu, L. (2020). Effects of electroacupuncture at "Zusanli"(St36) on ultrastructure and mitochondrial dynamics of skeletal muscle in rats with spleen qi deficiency syndrome. *Zhen Ci Yan Jiu* 45, 15–20. doi:10.13702/j.1000-0607.1903376

Yu, D. S., Lv, G., Mei, X. F., Cao, Y., Wang, Y. F., Wang, Y. S., et al. (2015). Mir-200c regulates ros-induced apoptosis in murine bv-2 cells by targeting fap-1. *Spinal Cord.* 53, 182–189. doi:10.1038/sc.2014.185

Yu, L., and Qian, J. (2020). Dihydrotanshinone I alleviates spinal cord injury via suppressing inflammatory response, oxidative stress and apoptosis in rats. *Med. Sci. Monit.* 26, E920738. doi:10.12659/MSM.920738

Zhang, H., Wang, P., Xue, Y., Liu, L., Li, Z., and Liu, Y. (2018). Allicin ameliorates cognitive impairment in app/ps1 mice via suppressing oxidative stress by blocking jnk signaling pathways. *Tissue Cell* 50, 89–95. doi:10.1016/j.tice.2017.11.002

Zhang, H., Xiang, Z., Duan, X., Jiang, J. L., Xing, Y. M., Zhu, C., et al. (2019). Antitumor and anti-inflammatory effects of oligosaccharides from Cistanche deserticola extract on spinal cord injury. *Int. J. Biol. Macromol.* 124, 360–367. doi:10.1016/j.ijbiomac.2018.11.132

Zhang, W., Sun, Z., and Meng, F. (2017). Schisandrin B ameliorates myocardial ischemia/reperfusion injury through attenuation of endoplasmic reticulum stress-induced apoptosis. *Inflammation* 40, 1903–1911. doi:10.1007/s10753-017-0631-4

Zhou, J. Z., Ma, Y., Yin, S. J., and Sun, S. J. (2009). *Experiment study of jisuikang on treatment of rat after spinal cord injury*. Nanchang: Journal Of Jiangxi University Of Traditional Chinese Medicine, 21. doi:10.3969/j.issn.1005-9431.2009.02.030

Zhou, Y. N., Sun, M. Y., Mu, Y. P., Yang, T., Ning, B. B., Ren, S., et al. (2014). Xuefuzhuyu decoction inhibition of angiogenesis attenuates liver fibrosis induced by CCl_4 in mice. *J. Ethnopharmacol.* 153, 659–666. doi:10.1016/j.jep.2014.03.019

Zrzavy, T., Schwaiger, C., Wimmer, I., Berger, T., Bauer, J., Butovsky, O., et al. (2021). Acute and non-resolving inflammation associate with oxidative injury after human spinal cord injury. *Brain.* 144, 144–161. doi:10.1093/brain/awaa360

Glossary

3- NT 3-nitrotyrosine
4- HNE 4-hydroxynonenal
AA asiatic acid
ATF2 activating transcription factor 2
ATP adenosine triphosphate
ATRA all-trans retinoic acid
BBB Basso-Beattie-Bresnahan
BSCB blood-spinal cord barrier
CA Carnosic acid
DDI Drug-Drug Interaction
EGb Ginkgo biloba extract
EGCG Epigallocatechin gallate
FAP-1 Fas-associated phosphatase-1
GSH-Px glutathione peroxidase
IRI ischemia-reperfusion injury
iROS intracellular reactive oxygen species
JSK JisuiKang
LP lipid peroxidation
MAPK mitogen-activated protein kinase
MDA malondialdehyde
NO nitric oxide
OS oxidative stress
PON peroxynitrite
Q- PCR Quantitative real-time polymerase chain reaction
RA Rosmarinic acid
RNS reactive nitrogen species
ROS reactive oxygen species
Sch B Schisandrin B
SCI Spinal cord injury
SeNPs Selenium nanoparticles
T- AOC total antioxidant capacity
TCM traditional Chinese medicine
TMP Tetramethylpyrazine
XFZYD Xuefuzhuyu Decoction

frontiers | Frontiers in Pharmacology

TYPE Original Research
PUBLISHED 12 October 2022
DOI 10.3389/fphar.2022.968664

OPEN ACCESS

EDITED BY
Dnyaneshwar Umrao Bawankule,
Council of Scientific and Industrial Research (CSIR), India

REVIEWED BY
Christian Agyare,
Kwame Nkrumah University of Science and Technology, Ghana
Papiya Mitra Mazumder,
Birla Institute of Technology, India

*CORRESPONDENCE
Ahmad Nazrun Shuid,
anazrun@yahoo.com

SPECIALTY SECTION
This article was submitted to Ethnopharmacology, a section of the journal Frontiers in Pharmacology

RECEIVED 14 June 2022
ACCEPTED 26 September 2022
PUBLISHED 12 October 2022

CITATION
Ibrahim N'I, Mohamed IN, Mohamed N, Mohd Ramli ES and Shuid AN (2022), The effects of aqueous extract of Labisia Pumila (Blume) Fern.-Vill. Var. Alata on wound contraction, hydroxyproline content and histological assessments in superficial partial thickness of second-degree burn model.
Front. Pharmacol. 13:968664.
doi: 10.3389/fphar.2022.968664

The effects of aqueous extract of *Labisia Pumila (Blume) Fern.-Vill. Var. Alata* on wound contraction, hydroxyproline content and histological assessments in superficial partial thickness of second-degree burn model

Nurul 'Izzah Ibrahim[1], Isa Naina Mohamed[1], Norazlina Mohamed[1], Elvy Suhana Mohd Ramli[2] and Ahmad Nazrun Shuid[3]*

[1]Department of Pharmacology, Faculty of Medicine, Universiti Kebangsaan Malaysia Medical Centre, Kuala Lumpur, Malaysia, [2]Department of Anatomy, Faculty of Medicine, Universiti Kebangsaan Malaysia Medical Centre, , Kuala Lumpur, Malaysia, [3]Department of Pharmacology, Faculty of Medicine, Universiti Teknologi MARA, Sungai Buloh Campus, Jalan Hospital, Sungai Buloh, Selangor, Malaysia

Background: Burns are considered a critical care problem in emergency medicine, resulting in physical, psychological, and chronic disabilities. Silver sulfadiazine is the gold standard in topical burn treatment but was associated with toxicity to keratinocytes and fibroblasts, which may delay wound healing. In discovering potential alternative treatments for burn wound healing, this study was performed to determine the effect of *Labisia Pumila (Blume) Fern.-Vill. Var. Alata* (LPVa) extract on thermal-burn wounds in rats.

Methods: A total of 50 *Sprague-Dawley* male rats were categorized into five groups. There were three control groups; normal control (left untreated), negative control (given ointment base) and positive control (given silver sulfadiazine). Meanwhile, the two intervention groups were given with 2% LPVa leaf and root extracts, respectively. Burn wounds were inflicted on the loin region of the rat by applying a heated steel rod at 80°C for 10 s. On days 3, 7, 14, and 21, wounds were measured macroscopically using a digital calliper and one animals of each group were sacrificed, and the wounded skin were excised for histomorphological assessments. The wounds were excised for hydroxyproline content on Day 14 of treatment.

Abbreviations: ABTS, 2,29-azino-bis (3-ethylbenzothiazoline-6-sulfonic acid); AUC, area under the curve; Col I, Collagen type I; Col III, Collagen type III; DPPH, 2,2-diphenyl-1-picrylhydrazyl; Fib, Fibroblast; H&E, hematoxylin & eosin; IHC, Immunohistochemistry; LF, Leaf; LP, Labisia pumila; LPVa, Labisia pumila var alata; NG, negative control group; RNS, reactive nitrogen species; ROS, reactive oxygen species; PS, positive control group; RT, Root; SEM, Standard Error Mean; SERMs, selective estrogen receptor modulators; SSD, silver sulfadiazine; TRI, Masson's Trichrome.

Result: For wound contraction percentage, both the leaf and root extracts of LPVa showed a significant reduction in burn wound size on Day 7 onwards, when compared to other groups. For hydroxyproline content, only the leaf extract of LPVa produced significantly higher content compared to both negative and normal control groups. In terms of histological examination, the leaf extract group demonstrated a superior healing effect than the root extract group.

Conclusion: Both leaf and root extracts of LPVa could promote wound healing in the thermal-burn wound rat model, with leaf extract being superior to root extract.

KEYWORDS

labisia pumila, antioxidant, burn wound healing, hydroxyproline, histomorphology

Introduction

Burns are a critical care problem requiring specialised care focusing on stabilising the patient, preventing infection, and optimizing functional recovery (Rowan et al., 2015). Burns can be defined as tissue lesions that occur as a result of exposure to thermal origin such as flames, hot surface and liquids, extreme cold, chemicals, radiation or friction (Tavares Pereira et al., 2012). Burns are categorised according to the severity of lesion into first, second and third-degree of burns. For the first-degree burn, it is restricted to the epidermal layer that results into redness and require simple first-aid procedures with over-the-counter pain relievers. Second-degree burn or also known as partial-thickness burns are subdivided into two categories: superficial and deep. As for the superficial partial thickness, the burn may reach the epidermis and superficial dermis, causing hypersensitivity and pain. Deep partial-thickness burn occurs when it reaches the deepest layer of the dermis, resulting in reduced sensitivity with red and/or white colouration of the tissue. Finally, the third-degree burn or also known as full-thickness burn involves the subcutaneous layer, without sensitivity and white in colour (Lanham et al., 2020).

Burn wound healing is a complex process that can be divided into three overlapping phases: inflammatory, proliferative and remodelling phases. During the inflammatory phase, neutrophils and monocytes arrive at the injury site *via* localized vasodilation and fluid extravasation (Tiwari, 2012). The inflammation prevents wound infection, degrades necrotic tissue and activate signals required for wound repair (Reinke and Sorg, 2012). The next overlapping phase is known as the proliferative phase, which is characterized by activation of keratinocyte and fibroblast by cytokines and growth factors (Werner et al., 2007). During this phase, keratinocytes, the dominant cell types in epidermis layer will migrate over the wound to aid in closure and restoration of a vascular network that results into maturation of epidermis and scar. The communication between stromal, endothelial and immune cells may define the healing course of the wound such as closure and revascularization (Pastar et al., 2014).

The healing of burn-wound lesions involves tissue inflammation, oedema, and hypertrophic scars (Rowan et al., 2015). Hence, the type of topical agent or coverage for treating burns should be selected based on assessment of lesion characteristics and evidence reported by specific literatures. Topical agents used for treating burn wounds should have properties such as antimicrobial activity, good compliance and cheap. They should also be less toxic, produce less hypersensitivity reactions and able to shorten the healing time (Tavares Pereira et al., 2012).

Silver sulfadiazine is the gold standard for topical burn treatment. It improves the survival of patients with major burns and minimizes the incidence of burn wound sepsis, a leading cause of mortality and morbidity in burn patients (Church et al., 2006). It is composed of sodium sulfadiazine and silver nitrate, whereby the silver ion attaches to the nucleic acid of the microorganisms, releasing the sulfadiazine. The sulfadiazine produced from the reaction will then disrupt the metabolism of the microbe (Lansdown, 2002b). However, the silver constituent in the silver sulfadiazine has been demonstrated to interact with structural proteins and preferentially bind to DNA nucleic acid bases to inhibit replication of the cells in the skin (Lansdown, 2002a; 2002b). Due to this reaction, silver is toxic to keratinocytes and fibroblasts, which may cause delay in burn wound healing if applied continuously to the healing tissue areas (Nešporová et al., 2020). Thus, an alternative treatment that could promote burn wound healing effectively but less toxic needs to be developed. The treatment of burn wounds has evolved over several decades through clinical and preclinical research. Significant advancements have been made in treatment of burn wound, including the testing of unique pharmacological interventions such as herbal plant extracts.

Labisia pumila (Blume) Fern.-Vill. (Primulaceae) (LP) or locally known as 'Kacip Fatimah' is one of the herbal plants in the *Myrsinaceae* family, characterized by lanceolate leaves with a creeping stem and long roots (Jamal et al., 2003). The plant is commonly found in the South East Asian region, including

Malaysia, Indonesia, Thailand, and China (Stone, 1989). LP is a jungle species and difficult to cultivate *ex situ*, which requires adaptation to the agricultural environment before it can survive and grow optimally. Therefore, LP does not associate with seasonal collection of the plants. In Malaysia, for instance, the plant raw materials come directly from the jungle or are imported from neighbouring countries. (Rosnani et al., 2019). LP is a well-known and widely used herbal remedy by women for general well-being and specifically to facilitate and expedite recovery after childbirth. This includes expediting healing of childbirth wounds. Its pharmacological effects on women's health may be related to its phytoestrogen properties, having similar chemical structure to estrogen (Jamal et al., 2003). Phytoestrogens are regarded as the naturally occurring selective estrogen receptor modulators (SERMs) and possess potential effect in providing a natural estrogen replacement especially to postmenopausal women. Phytoestrogens demonstrated protection against oxidative stress, an imbalanced condition between ROS and antioxidant defence mechanism (Liu et al., 2020). There are three known varieties of LP which are var. *pumila,* var. *alata*, and var. *lanceolata* (Karimi et al., 2013). The var. *alata* and var. *pumila* variants were more commonly used as medicinal plants than var. *lanceolata* (Abdul Kadir et al., 2012). Several studies have demonstrated that LP extracts possess medicinal properties such as antifungal, anti-inflammatory, cytotoxicity (Karimi et al., 2013), anticancer, antioxidant and anti-osteoporosis (Nadia et al., 2012). However, there are limited studies on LP effects on skin tissue. In a previous study by Choi et al. (2010), LP extract demonstrated protection of skin against photoaging induced by ultraviolet irradiation (Choi et al., 2010). Meanwhile, a study by Ahmad et al. (2018) reported that LP extract promoted minor wound healing in ovariectomized rat model (Ahmad et al., 2018). However, the effects of LP on burn wound healing have not been studied yet. To the best of our knowledge, this is the first study aimed to determine the potential of LP var alata in promoting burn wound healing.

Materials and methods

Preparation of *Labisia Pumila* extracts and combination with ointment

Standardised methods were used to obtain aqueous extracts of leaf and roots of *Labisia pumila var. alata* (Jamal et al., 2003). Briefly, the extraction was performed with water by successive maceration at room temperature for a week, followed by filtration. The filtration process was repeated several times. The filtrate obtained after filtration were concentrated by evaporation using a rotary evaporator (Buchi Rotavapor R-100, Switzerland) at temperatures of 35°C until dryness to maximize the proportion of desired bioactive fractions contained in each of the extract. The filtrate was then freeze-dried to obtain the powdered form. The process of extraction, filtration and concentration were repeated several times until maximum yield of aqueous extracts has been reached.

The LP leaf and root aqueous extracts were combined with cetomacrogol emulsifying ointment (Hovid Berhad, Malaysia), which is a type of paraffin used as a vehicle in these topically-applied preparations to the rats. This emulsifying ointment was chosen as a vehicle as it is chemically inert and inactive to the skin (Ahmad et al., 2021). A 2.0% dose concentration was chosen for both the leaf and root extracts as previously established by Ahmad et al. (2018) using LP extracts on minor wound healing (Ahmad et al., 2018). The extracts were crushed using a pestle and mortar to obtain fine powder which have faster absorption rates and better uniformity when mixed with emulsifying ointment. In brief, the emulsifying ointment and extract powder were put together onto a clean glass plate and mixed thoroughly with a spatula to ensure uniformity. The extract appeared dissolved during the mixing process, which confirmed its compatibility with the ointment.

Animals

Fifty male Sprague-Dawley rats aged 4–5 months and weighing 250 ± 50 g were obtained from the Universiti Kebangsaan Malaysia Laboratory Animal Research Unit. All rats were housed in individually ventilated cages at temperature-controlled (25 ± 1°C) environment under natural day/night cycle. They were fed with standard laboratory food pellets and given water *ad libitum*. All animal experiments were approved by Universiti Kebangsaan Malaysia Animal Ethical Committee (FAR/PP/2018/NAZRUN/25-JULY/935-AUG-2018-MAR-2019).

Burn wound model and treatments

The rats were acclimatized to laboratory conditions for 1 week prior to the experiment. Initially, the rats were anesthetized with intraperitoneal injection of Ketamine and Xylazil at 1:1 ratio before inducing burn wound. The dorsal regions of the rats were shaven with an electric shaver and sterilized with 70% alcohol. Prior to burn-wound infliction, the rats were injected intramuscularly with tramadol (12.5 mg/kg body weight) for pain control. Burn infliction techniques were performed accordingly to the methods by Cai et al. (2014) with slight modification (Cai et al., 2014). Burn wounds were created at dorsum of the rats using a 100 g cylindrical stainless-steel rod (1 cm diameter), which was heated to 80°C in boiling water. Temperature was monitored using a thermocouple thermometer (Figure 1A). The area for burn infliction was limited to the loin region of the rat. Four points were marked for burn wound sites at the loin with 2 cm apart side to side and 4 cm up and down. Then, the skin was

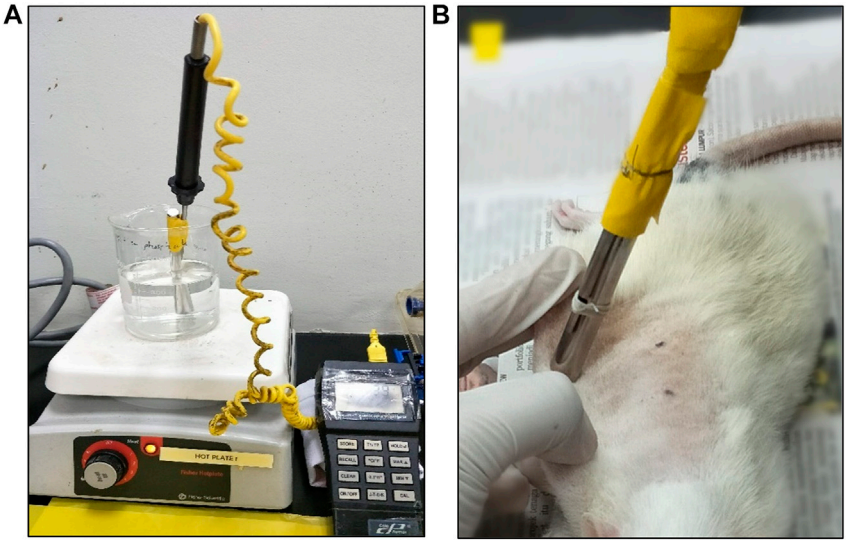

FIGURE 1
(A) Configuration of thermocouple thermometer and boiling water. **(B)** Experimental burn wound infliction performed on a rat.

pulled upwards, away from the underlying viscera, creating a flat surface (Figure 1B). The rod was left rested on its own weight for 10 s at the four different sites on each rat. Treatments were given topically to the rats, which were categorized into five groups, each containing 10 rats. As for the control groups, the wounds were left untreated for normal control (NM) group, treated with emulsifying ointment for negative control (NG) group and treated with silver sulfadiazine for positive control (PS) group. For the two intervention groups, the wounds were treated with LPVa leaf (LF) and root (RT) extracts, respectively. Treatments were performed for 3 weeks on daily basis.

Macroscopic evaluation of burn wounds

Following the burn infliction, macroscopic changes of burn wounds were evaluated at day 0 post burn and subsequently at days 3, 7, 14, and 21 post burn. Photographs were taken with digital camera (SONY DSC-RX100M2, 15x) until complete closure of wound. The images were scored blindly by anatomical expert using a macroscopic scoring tool for burns as described by Schlager et al. (2000)(Schlager et al., 2000) (Table 1).

TABLE 1 Macroscopic scoring system used for burns. Source: Schlager et al. (2000).

Variable	Scoring		
	0	1	2
Redness	None	Slightly red	Completely red
Edema	None	Minimal edema	Clearly distinctive

Measurement of wound area

Wounds were observed and measured at day 0, 3, 7, 14, and 21 by using a digital caliper (General Ultratech, New York, NY). Woud contraction will be expressed as reduction in percentage of the original wound size (Figure 2).

Determination of the hydroxyproline content

On the 14th day, one rat from each group was euthanized using ketamine and xylazil (overdose) to excise the wound tissue for determination of hydroxyproline content. The protein content of the wound tissue was estimated using the techniques described by Neuman and Logan (1950) (Neuman and Logan, 1950). Wound tissue were excised and stored at −70°C until ready for processing. For the procedure, 80–100 mg of tissues were weighed and minced to small pieces and were put in test tubes. Tissues were hydrolysed by adding 6 mol/L HCl to each test tubes and placed in boiling water bath for 5 h. Then, the pH of the

$$\text{Wound contraction percentage} = \frac{\text{Wound diameter on day 0} - \text{Wound diameter on respective day}}{\text{Wound diameter on day 0}} \times 100$$

FIGURE 2
Formula for calculating reduction in percentage of the original wound size.

hydrolysate was adjusted between 6.0 and 6.8 by testing with pH indicator paper. Distilled water was added into each test tubes to a final volume of 10 ml and they were mixed thoroughly. Approximately 3–4 ml of diluted test solution was taken and added with 20–30 mg of activated carbon. The solution was mixed thoroughly and centrifuged at 3,500 rpm for 10 min. For detection, 1 ml of the test solution was taken and prepared according to the manual given in the test kit. Blank and standard tubes were also prepared accordingly. After mixing the solution thoroughly, the mixture was incubated at 60°C in water bath for 15 min and centrifuged at 3,500 rpm for 10 min. Supernatants were taken and measured using ELISA plate reader at 550 nm wavelength.

Histomorphological analysis

Three types of staining methods were used for histomorphological analysis; 1) Hematoxylin & eosin (H&E), 2) Masson's Trichrome (TRI), and 3) Immunohistochemistry (IHC). Wound bed biopsies were excised at days 3, 7, 14 and 21 post-wounding. The tissue samples were fixed in 10% buffered formalin, processed and embedded in paraffin to prepare tissue blocks. Then, the tissue blocks were sectioned for 5 µm (H&E, TRI) and 3 µm (IHC). All sections were deparafinized and rehydrated conventionally prior to staining. For H&E and Masson's trichome, the sections were stained with their respective staining kits. For further investigation, immunohistochemistry was performed to visualize distribution and localization of specific antigen or cellular components responsible for wound healing. In this study, three antibodies were used: Collagen I, Collagen III, and fibroblast. Following deparaffinization and dehydration processes, the sections undergone antigen retrieval process using citrate-based solution in microwave for 10 min and blocking process in 0.3% H_2O_2 in methanol for 30 min. Subsequently, the sections were incubated with normal serum for 20 min and were incubated with primary antibody diluted in buffer at 4°C. The sections were then incubated for 1 hour with diluted biotinylated secondary antibody and incubated for 30 min with Vectastain ABC reagent. In between of each incubations, the sections were washed in buffer for 5 min. Following the incubation with Vectastain, the antibody binding sites were visualized by incubation with DAB signal stain kit for 15 min and counterstained with Haematoxylin for 2 min.

All the tissue sections were then subjected to clearing and mounting processes. The slides were observed under microscope (Olympus BX3-25ND6, Japan) and photomicrographs were taken at ×20 magnification for two parts; dermis and hypodermis. The stained tissue sections were scored blindly by histological experts using the modified 0 to three numerical scale as described by Abramov et al. (2007) (Table 2) (Abramov et al., 2007). Any difference in scoring was discussed to a consensus.

Data analysis

All the quantitative data were analysed using SPSS version 23. Data were presented as Mean ± Standard Error Mean (SEM). Normality test was performed using Kolmogorov-Smirnov test. One-way ANOVA was conducted followed by Post Hoc Tukey's test to determine statistical significance. p values < 0.05 were considered significant. GraphPad Prism software version 9.0 (GraphPad Software, San Diego, California United States) was used to estimate the area under the curve (AUC) with a 95% confidence interval. The AUC was calculated from the wound contraction percentage *versus* time profiles, which was determined by the area normalized to the baseline for the 21-day period (Gagnon and Peterson, 1998).

Results

Macroscopic view of wounds

Macroscopic changes over time for Day 0, 3, 7, 14, and 21 for superficial partial thickness of second-degree burn wounds were shown in Figure 3. In general, immediately after the burn induction, all wounds were non-uniformly round and white in color. Macroscopically, no difference was observed between all the groups following the burn induction, which was reflected by the similar score (score 0) for macroscopic evaluation at day 0 (Table 3). On Day 3, the edemas were more prominent compared to the Day 0, with the score 1 (minimal edema), and the wounds were slightly red

TABLE 2 Scoring system for Hematoxylin & Eosin, Masson's Trichome and immunohistochemistry staining. Source: (Abramov et al., 2007).

	Variable	Scoring			
		0	1	2	3
H&E	Reepithelization	None	Partial	Complete but immature or thin	Complete and mature
	Fibroblast proliferation	None	Scant	Moderate	Abundant
	Inflammation cell infiltration	None	Scant	Moderate	Abundant
	Neo- vascularization	None	<5 vessels/HPF	6–10 vessels/HPF	>10 vessels/HPF
	Granulation tissue formation	Immature	Mild maturation	Moderate maturation	Fully matured
Masson's Trichome	Collagen	None	Scant	Moderate	Abundant
Immunohistochemistry	Collagen I	None	Scant	Moderate	Abundant
	Collagen 111	None	Scant	Moderate	Abundant
	Fibroblast	None	Scant	Moderate	Abundant

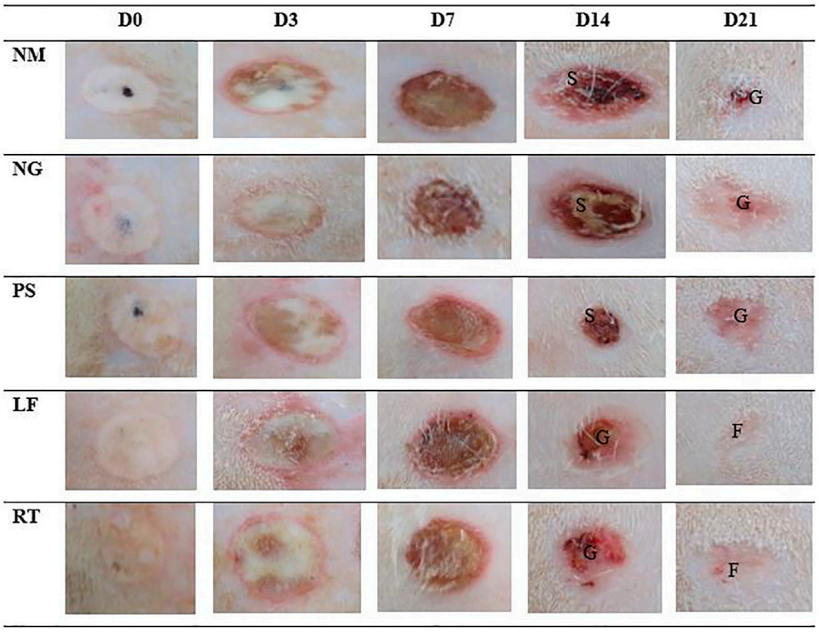

FIGURE 3
Macroscopic view of five representative male rats from each group at day 0, 3, 7, 14 and 21. S: Scab; G: Granulation tissue; F: Fibrous tissue. NM: normal control group, NG: negative control group, PS: positive control group, LF: LPVa leaf-treated group, RT: LPVa root-treated group.

with score 1 in all groups. On Day 7, the scabs on the wounds gradually appeared drier and smaller in all the groups, indicated by the score 2 (completely red) in the macroscopic evaluation. While for edema, all groups showed similar score of 2 (clearly distinctive). On Day 14, all control groups demonstrated that the scabs were still present as dark red in color and still attached to the wounds, which represented by the score 2 (completely red) for macroscopic evaluation. Meanwhile, for LF and RT groups, the scabs were mild red in color, or the scabs had dropped off, which represented by the score 0 (none) and 1 (slightly red). On Day 21, the wounds appeared to have almost disappeared in LF and RT groups, with whitish appearance (fibrous tissue) and represented by the score 0 (no redness) in the macroscopic evaluation. Meanwhile, for all control groups, the wounds were still present with pinkish appearance, which indicated granulation tissue and represented by the score 1 (slightly red) for macroscopic examination.

TABLE 3 Scoring from macroscopic evaluation at Day 0, 3, 7, 14, and 21. Please refer Table 1 for the scoring system.

Groups	Redness					Edema				
	DO	D3	D7	D14	D21	DO	D3	D7	D14	D21
NM	0	1	2	2	1	0	1	2	2	0
NG	0	1	2	2	1	0	1	2	2	0
PS	0	1	2	2	1	0	1	2	2	0
LF	0	1	2	1	0	0	1	2	0	0
RT	0	1	2	1	0	0	1	2	1	0

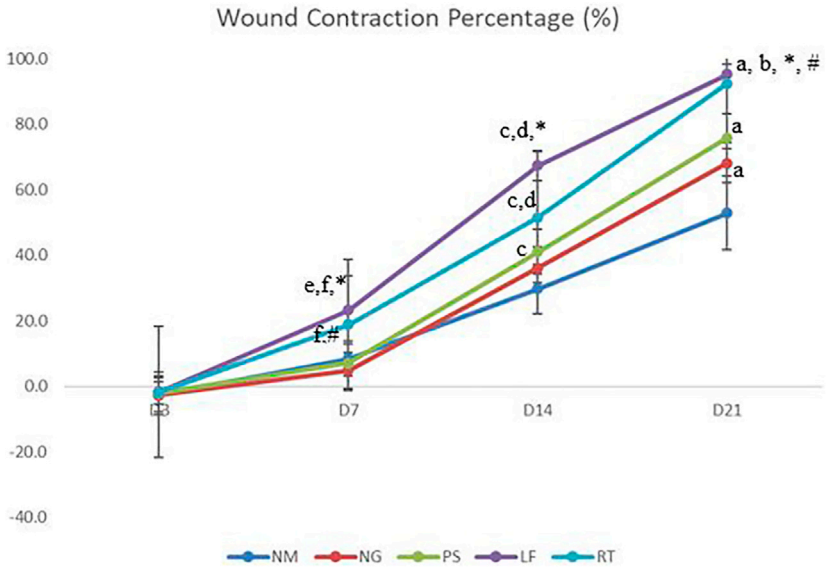

FIGURE 4
The percentage of wound contraction. NM: normal control group, NG: negative control group, PS: positive control group, LF: LPVa leaf-treated group, RT: LPVa root-treated group. Data were expressed as mean ± SD. Statistically significant results were indicated as **(A)** $p \leq 0.05$ compared to NM group, **(B)** $p \leq 0.05$ between NG group, **(C)** $p \leq 0.05$ compared to NM group, **(D)** $p \leq 0.05$ compared to NG group, **(E)** $p \leq 0.05$ compared to NM group, **(F)** $p \leq 0.05$ compared to NG group, *$p \leq 0.05$ compared to LF and PS groups, #$p \leq 0.05$ compared to RT and PS groups.

Wound contraction percentage

On Day 3, all the groups did not show any significant value and demonstrated mildly negative percentage of wound contraction (Figure 4). At Day 7 and 14 of the wound healing, leaf extract group have shown significantly higher percentage of wound contraction when compared to normal, negative and positive control groups. On Day 7, root extract group have shown significantly higher percentage of wound contraction when compared to negative and positive control groups. Meanwhile, on day 14, root extract group have shown significantly higher percentage of wound contraction when compared to negative and normal control groups. Additionally, on Day 14, positive control group had shown significantly higher wound contraction percentage compared to normal control group. For Day 21 of the wound healing, leaf extract and root extract, as well as positive control groups have shown significantly higher wound reduction percentage when compared to normal control group. Most of the wounds were almost healed on Day 21 with leaf and root extract have the highest range of wound percentage (90%–95%).

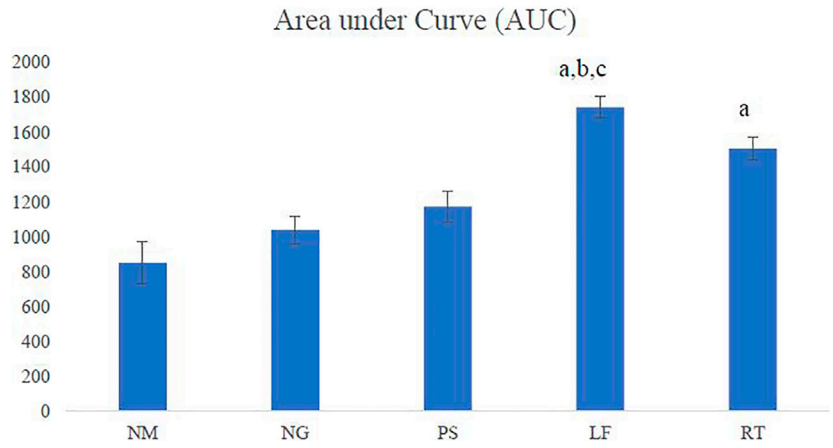

FIGURE 5
Area under the curve (AUC). NM: normal control group, NG: negative control group, PS: positive control group, LF: LPVa leaf-treated group, RT: LPVa root-treated group. Data were expressed as AUC±SEM. Statistically significant results were indicated as **(A)** $p \leq 0.05$ compared to NM group, **(B)** $p \leq 0.05$ between NG group, **(C)** $p \leq 0.05$ compared to PS group.

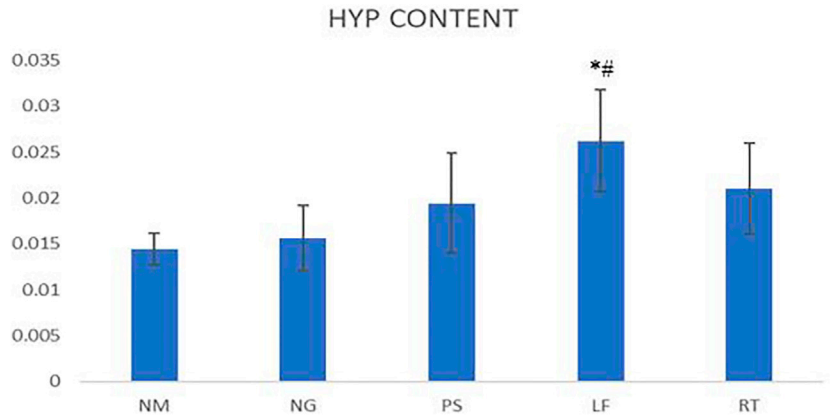

FIGURE 6
Hydroxyproline contents for wounds Statistically significant difference were indicated as $^{*}p \leq 0.05$ between NM group and $^{\#}p \leq 0.05$ between NG group. NM: normal control group, NG: negative control group, PS: positive control group, LF: LPVa leaf-treated group, RT: LPVa root-treated group.

Area under the curve

The LF group demonstrated the highest AUC among all the groups and showed significant difference when compared to normal (NM), negative (NG) and positive (PS) control groups. The RT group showed significant difference when compared to the NM group (Figure 5).

Hydroxyproline content

On day 14, the hydroxyproline content of LF group demonstrated significant difference when compared to NM and NG groups. For the PS and RT groups, the hydroxyproline content were increased but did not reach significant value (Figure 6).

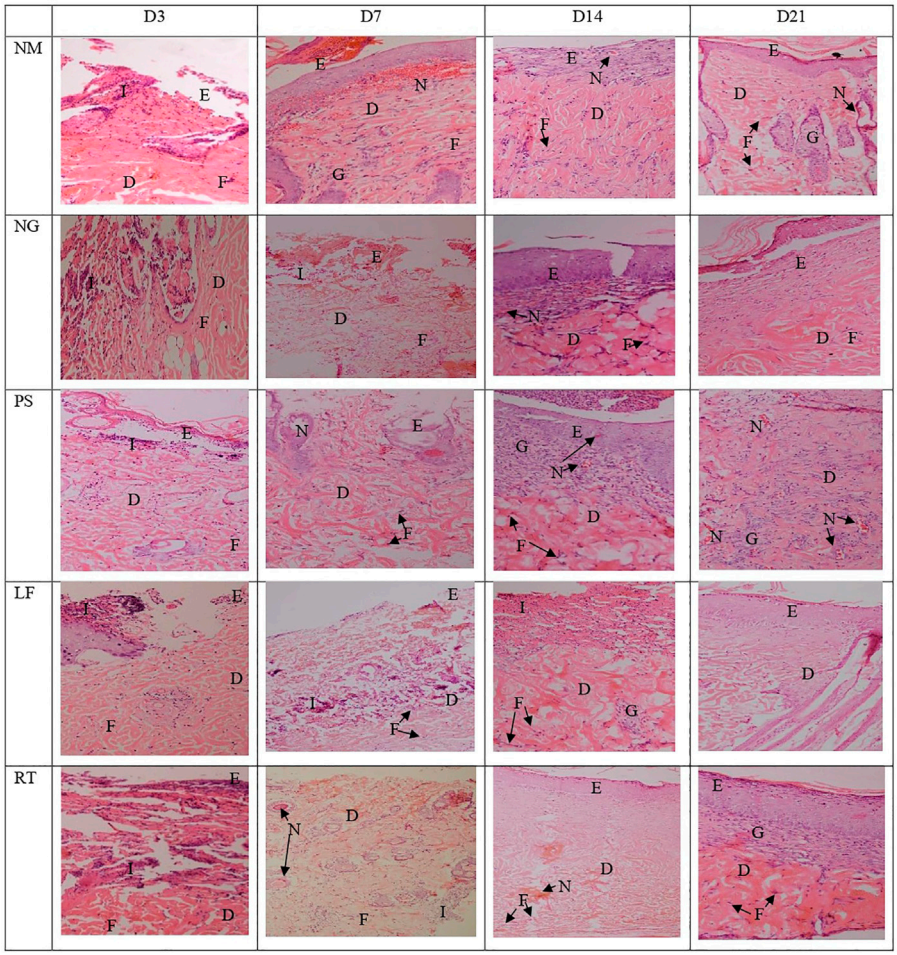

FIGURE 7
Histopathological view of the burn wounds at Day 3, 7, 14 and 21. Stained with H&E, at ×200 magnification. At day 3, a complete destruction of epidermis layer and partial destruction of dermis layer were observed in all groups, with moderate inflammatory cells and scant fibroblast cells. At Day 21, the re-epithelization in most groups were improved, with abundant fibroblast proliferation, neo-vascularization, and granulation tissue infiltration. E: Epidermis; D: Dermis; I: Inflammatory cells; F: Fibroblast cells, G: Granulation tissue; N: Neovascularization. NM: normal control group, NG: negative control group, PS: positive control group, LF: LPVa leaf-treated group, RT: LPVa root-treated group.

Histomorphology assessments

Histopathological view of the burn wounds for all the five groups stained with haematoxylin and Eosin (H&E) were shown in Figure 7. At Day 3, all the groups demonstrated complete destruction of epidermis layer and partial destruction of dermis layer, which indicated superficial partial thickness of second-degree burn. This was also reflected by the zero score for re-epithelization in all groups, except for RT group (Table 4). At Day 21, the re-epithelization in all the groups had improved to score 3, except for RT group which scored 1. All the groups showed scant amount of fibroblast proliferation initially at Day 3, which progressed to abundant amount at Day 21, except for RT group. At Day 7, both the NM and NG groups were still scored as scant (score 1). In terms of inflammation cell infiltration, all the groups demonstrated improvement from Day 3 to Day 21, except for the RT group. Similar patterns were observed for neo-vascularization and granulation tissue formation.

Histopathological views of the burn wounds for all the five groups stained with Masson's trichome were shown in Figure 8. Complete destruction of epidermis and partial destruction of dermis were demonstrated at Day 3 post-wounding for all the groups, confirming the success of burn induction in the rat model. In terms of histological scoring, collagen deposition of all the groups for each time points showed similar score of 3, denoting abundant collagen deposition. Therefore, collagen types were differentiated by immunohistochemistry staining (Figure 9). At Day 3, all the groups demonstrated moderate amount of collagen I, except for NM group, which denoted scant amount of collagen I (Table 5). The LF and RT groups showed moderate amount of collagen I from Day

TABLE 4 Scoring from histological observations (H&E) of the burn wounds at Day 3, 7, 14 and 21. Please refer Table 2 for the scoring system.

Groups	Reepithelization				Fibroblast proliferation				Inflammation cell infiltration				Neo-vascularization				Granulation tissue formation			
	D3	D7	D14	D21	D3	D7	D14	D21	D3	D7	D14	D21	D3	D7	D14	D21	D3	D7	D14	D21
NM	0	2	2	3	1	2	2	3	1	2	2	3	1	2	2	3	0	2	2	3
NG	0	0	2	3	1	1	2	3	1	1	2	3	0	1	2	3	0	0	2	3
PS	0	0	2	3	1	1	2	3	1	2	2	3	3	1	2	3	0	0	2	3
LF	0	1	2	3	1	2	2	3	2	3	2	3	3	1	2	3	0	1	3	3
RT	0	1	3	3	1	2	2	3	2	2	2	3	1	1	2	3	0	1	3	3

NM: normal control group, NG: negative control group, PS: positive control group, LF: LPVa, leaf-treated group, RT: LPVa, root-treated group.

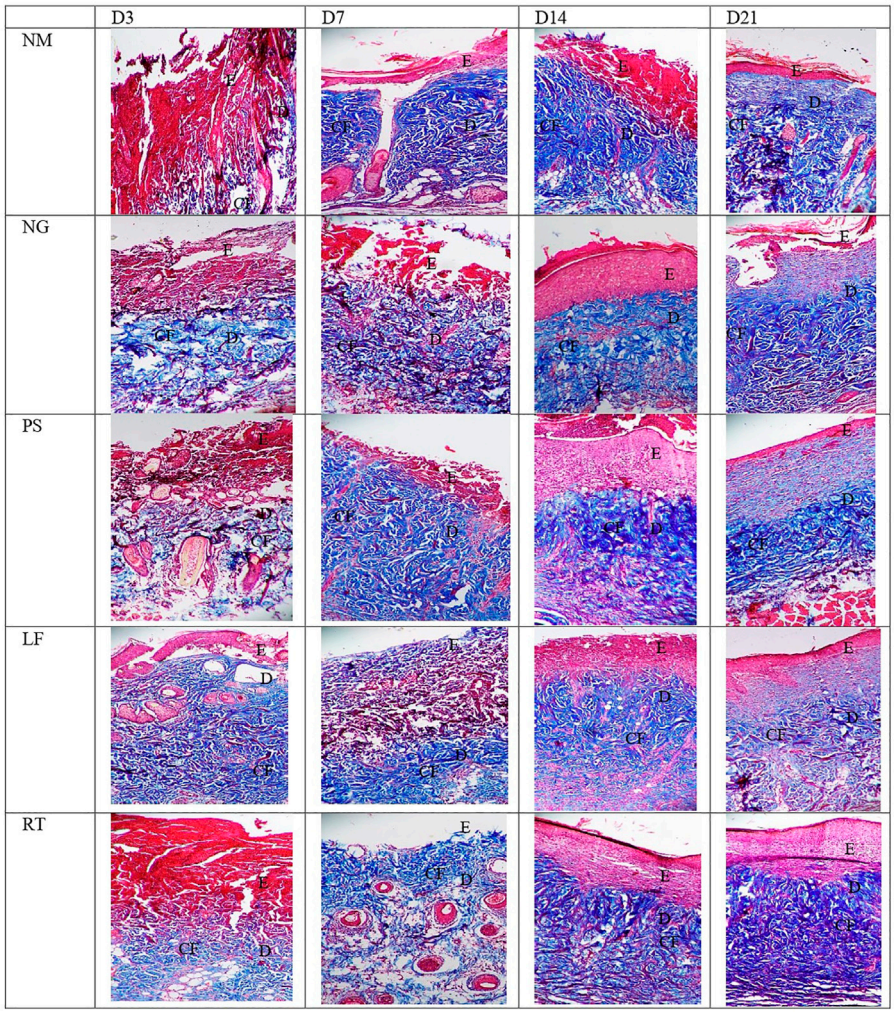

FIGURE 8
Histopathological view of the burn wounds at Day 3, 7, 14 and 21. Stained with Masson's trichome staining, at ×200 magnification. Collagen fibers were stained blue, cytoplasm and erythrocyte were stained red, and nuclei were stained bluish brown. Collagen deposition of all groups were abundant, from day 3 to day 21. E: epidermis; D: Dermis; CF: collagen fibers. NM: normal control group, NG: negative control group, PS: positive control group, LF: LPVa leaf-treated group, RT: LPVa root-treated group.

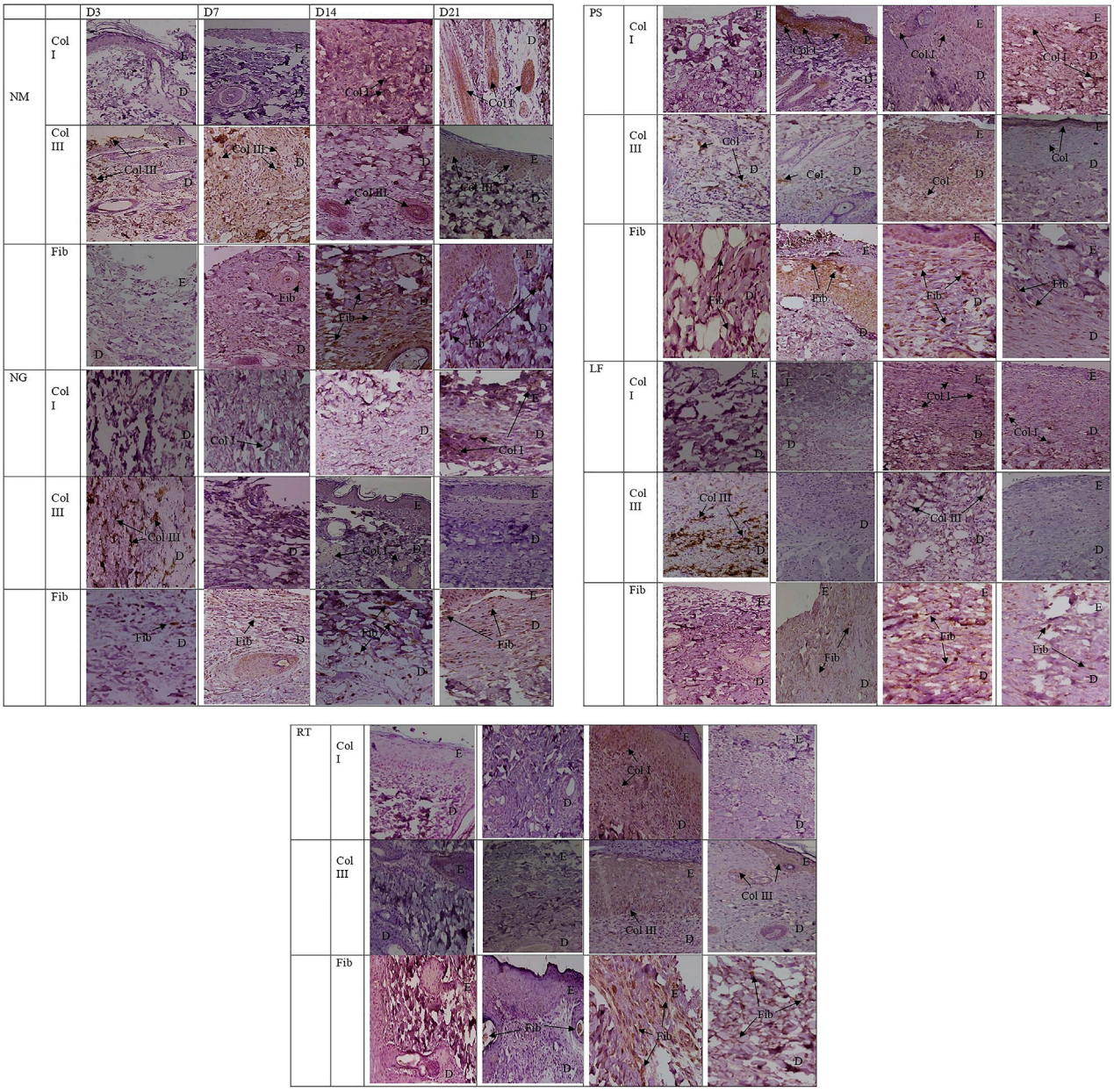

FIGURE 9
Histopathological view of the burn wounds at Day 3, 7, 14 and 21. Immunohistochemistry staining for collagen I, collagen III and fibroblast, at ×200 magnification. Light brown staining represents positive immunostaining. In most of the groups, collagen III was scant or moderate at day 3, while collagen I were abudant at day 21. Fibroblast were scant at day 3 and were improved to moderate and abundant in most of the groups at day 21. E: epidermis; D: Dermis, Fib: Fibroblast; Col I: Collagen type I, Col III: Collagen type III. NM: normal control group, NG: negative control group, PS: positive control group, LF: LPVa leaf-treated group, RT: LPVa root-treated group.

7 to Day 28. Meanwhile, for the other type of collagen, known as collagen III, only the LF group showed moderate amount and RT group scored zero at Day 3. For all the control groups (NM, NG and PS), scant amount of collagen III was noted. However, for RT group, moderate collagen III was noted at Day 14 and Day 21. While, LF group showed scant amount of collagen III since Day 7. Histopathological view of burn wounds using immunohistochemistry staining was also performed for fibroblast (Figure 9). As expected, fibroblasts for all the groups were scant at Day 3 and were subsequently more abundant except for RT root, which paralleled to the H&E staining findings (Table 4).

TABLE 5 Scoring for Masson's trichome staining (collagen deposition) and immunohistochemistry staining (fibroblast, collagen I and III) of the burn wounds at Day 3, 7, 14, and 21.

Groups	Fibroblast				Collagen I				Collagen III				Collagen deposition			
	Immunohistochemistry				Immunohistochemistry				Immunohistochemistry				Masson's trichom			
	D3	D7	D14	D21	D3	D7	D14	D21	D3	D7	D14	D21	D3	D7	D14	D21
NM	1	2	3	2	1	2	3	3	1	2	1	1	3	3	3	3
NG	1	2	2	2	2	2	2	3	1	1	1	0	3	3	3	3
PS	1	2	3	2	2	2	2	3	1	1	3	2	3	3	3	3
LF	1	2	2	2	2	2	3	2	2	1	1	1	3	3	3	3
RT	1	1	3	3	2	2	2	2	0	0	2	2	3	3	3	3

NM: normal control group, NG: negative control group, PS: positive control group, LF: LPVa, leaf-treated group, RT: LPVa, root-treated group.

Discussions

Oxidative stress plays an important role in burn wound conversion, in which the zone of stasis cannot be rescued and progresses to necrosis. Reduction in oxidative stress may halt or arrest burn injury progression into deeper tissue (Wardhana and Halim, 2020). Burn wound is also associated with release of mediators such as reactive oxygen species (ROS) and reactive nitrogen species (RNS) which ultimately contribute to local and distant pathophysiological events observed in burn cases. Treatments with antioxidant therapy could be useful to minimize injury in burned patients (Parihar et al., 2008). Xi et al. (2018) reported that LPVa leaves contained various flavonoids such as catechins, rutin, naringin, and myricetin. These compounds have been identified as natural antioxidants that may reduce oxidative stress within the human body. These flavonoids exhibited high 2,2-diphenyl-1-picrylhydrazyl (DPPH) and 2,2′-azino-bis (3-ethylbenzothiazoline-6-sulfonic acid) (ABTS) radical scavenging abilities (Xi et al., 2018). These high radical scavenging abilities may contribute to the antioxidant activity on burn injury and promote formation of scabs and wound contraction, when treated with LPVa leaf extracts. This is in parallel with our findings on wound contraction percentage and the area under the curve, where LPVa leaf extract demonstrated significantly higher value compared to normal control, negative control and positive control rat groups.

The LPVa root extract was as effective as the leaf extract in terms of wound contraction percentage and area under the curve. According to Karimi et al. (2013), the root extract of LPVa contains saponin (Karimi et al., 2013), a bioactive compound that possess beneficial properties related to wound healing including anti-inflammatory, antimicrobial and antioxidant activities (Rao and Gurfinkel, 2000). Similarly, curcumin, a natural polyphenolic molecule extracted from the rhizome of Curcuma longa, also possess anti-inflammatory, antibacterial and antioxidant properties and it demonstrated wound healing properties (Ibrahim and Wong, 2018; Alven and Nqoro, 2020). Curcumin was involved in various stages of the healing process including wound contractions, granulation tissue formation, collagen deposition and tissue remodelling (Zhao et al., 2019). Therefore, the wound contraction ability of LPVa root extract might be due to the saponin content, exerting beneficial effects on wound healing. Karimi et al. (2013) reported that LPVa root also contained kaempferol and myricetin, which are both flavonoids and strong antioxidants (Karimi et al., 2011).

Both leaf and root extracts of LPVa were as effective as silver sulfadiazine, which is the standard burn wound treatment and positive control in this study. As expected, silver sulfadiazine had shown significant wound contraction percentage when compared to normal control at Day 14 and Day 21, but was not significant at early phase of healing (day 7). The silver component is effective in eliminating pathogens *via* direct interactions with bacterial cell membranes, DNA, enzymes and proteins (Zhu et al., 2014). This antimicrobial activity of silver-containing formulation depends on the surrounding environment that drives the release of Ag^{+} ions and other formulations such as sorbents, biologically active compounds and biomolecules (Nešporová et al., 2020). However, silver sulfadiazine failed to produce significant wound contraction percentage from Day 7, as demonstrated by both root and leaf extracts, as well as normal and negative controls. This may have shown that the silver sulfadiazine had delayed wound healing during the early phase of healing process. This could be attributed by a slow progression of silver sulfadiazine in re-epithelization (Aziz et al., 2012), which lead to impaired wound healing at the early stage. Re-epithelialization is an important process to cover damaged epithelial surface as barrier breach offers an entry for wound infection (Pastar et al., 2014). Additionally, repeated usage of silver sulfadiazine has been associated with the formation of pseudoeschar over the affected area which may prevent adequate assessment of the burn wound. In some cases, mechanical debridement is required

to remove the pseudoeschar, which is often painful (Lo et al., 2008). Moreover, the insignificant wound contraction percentage of silver sulfadiazine could have been attributed to silver constituent that impair healing during the early phase. The silver constituents have preference to bind to DNA nucleic acid bases and may inhibit replication of the cells during wound healing (Lansdown, 2002a; Lansdown, 2002b). Contradictorily, it was found that LPVa extracts were non-cytotoxic as observed in an *in vitro* cytotoxicity study on L292 rat's fibroblast cell. Moreover, a repeated dose of LPVa extracts for 28-days in an *in vivo* dermal toxicity study had shown a non-observed adverse effect level (NOAEL) of up to 1,000 mg/kg, indicating that the LPVa extract is safe for skin application with appropriate concentration (Ali, 2014). Additionally, LPVa had also demonstrated protection on human skin keratinocytes from photoaging induced by ultraviolet irradiation (Choi et al., 2010). Therefore, these studies demonstrated that LPVa extracts were not toxic but provide protective effects on skin. Macroscopically on Day 14, burn wounds treated with SSD, LPVa leaf and root extracts showed better healing compared to normal and negative controls. As for the normal and negative controls, the crusts were still attached to the wound on the day 14. After the crust has fallen off, granulation tissue characterized by pinkish coloration could be observed. The granulation tissue will slowly be replaced by fibrous tissue, which appeared whitish on the wound. The negative control group showed that at Day 21, the wounds were still pinkish (indicating granulation tissue) compared to LPVa leaf and root treatment groups that appeared more whitish (indicating fibrous tissue).

Hydroxyproline which is a basic constituent of collagen is a good marker for wound healing assessment. It is one of the most abundant amino acids in collagen and its concentration indicates the concentration of collagen. High concentration of hydroxyproline symbolises faster rate of wound healing (Dwivedi et al., 2016). In this study, positive control, LPVA leaf and root groups have shown increased hydroxyproline content that might reflect increased cellular proliferation and increased collagen synthesis. Among these three groups, the LPVa leaf group showed significantly higher hydroxyproline concentration compared to normal and negative control groups. This result was supported by Chua et al. (2011), which reported that LPVa leaves contain various flavonoids (quercetin, myricetin and kaempferol) and phenolic acids (salicylic acid, vanillic acid, gallic acid, coumaric acid, caffeic acid and chlorogenic acid) (Chua et al., 2011) that could promote collagen synthesis (Chua et al., 2012). Collagen deposition is important for wound strength, cell shape and differentiation (Schultz GS and Moldawer, 2011). Additionally, Karimi et al. (2011) reported that LPVa leaf extract has superior antimicrobial effect (Karimi et al., 2011) which might contribute to the better collagen content. In a previous study by Liang et al. (2019), antibacterial hydrogel dressings applied on mouse full-thickness wound model have improved the granulation tissue thickness and collagen deposition, which also suggests that the antibacterial effect could promote collagen content (Liang et al., 2019).

Histological analyses of all staining used in this study revealed complete destruction of epidermis and partial destruction of dermis for all the groups, observed at Day 3 after wound induction. These characteristics confirmed second-degree or superficial partial thickness of burn wound (Lanham et al., 2020). Involvement of superficial dermis produces the red and wet appearance of wound with blisters. The healing process typically lasted for 3 weeks with minimal scarring (Tolles, 2018), which could be observed by the histological analysis of H&E staining. All the groups received the highest score of three for all the H&E histological scoring at Day 21, indicating that the wounds have completely healed.

As for the scoring of Masson's trichome staining, all the groups received the highest score of 3, indicating the presence of complete and mature collagen in the wounds of all the groups. Most collagens found in the skin are type I and III, that plays an important role of attracting fibroblast and keratinocytes to the wound (Barbul et al., 2015). The dermis layer of skin could be divided into two layers: papillary and reticular. Papillary is superficial and is structured by flowing connective tissue including reticular, elastic, and non-organized collagen (mostly type III) fibers and capillaries. Meanwhile, reticular is deep and represented by compact connective tissue, which has crosslinked elastic and well-organized collagen fibers (type I and III) and large blood vessels (Arda et al., 2014). In the recent study, the collagen deposition observed in the Masson's trichome were further differentiated into collagen I and collagen III by immunohistochemistry staining.

Collagen III is the type of collagen synthesized during the early stages of wound healing and is progressively replaced by the dominant skin collagen (collagen I) (Mathew-Steiner et al., 2021). This condition was parallel to our study where at day 21, all three control groups (normal, negative and positive controls) were scored at 3, indicating complete and mature collagen I. However, for both treatment groups (LPVa leaf and root), the scoring was 2, indicating complete but immature or thin collagen I. Both LPVa leaf and root groups have shown complete but immature or thin collagen A except for Day 14 of LPVa leaf group. This might indicate that leaf extract was better at promoting skin collagen synthesis. This was in agreement with the findings by Choi et al. (2010), which reported that LP extract was able to restore skin pro-collagen of human dermal fibroblast cell line that has been destroyed by ultraviolet radiation (Choi et al., 2010).

Fibroblast is the cell responsible for the production of extracellular matrix and collagen, and therefore plays an important role during tissue repair. The migration and proliferation of fibroblast to the wounded area may initiate proliferative phase of repair which subsequently promote effective wound healing and wound contraction. Based on the H & E staining of this study, the LPVa

leaf group demonstrated complete and mature fibroblasts at Day 21 compared to the LPVa root group. The superior effect of leaf extract for fibroblast proliferation was in parallel to the hydroxyproline concentration measurements. In fact, fibroblasts in wound healing areas may proliferate and are encircled by collagen fibrils. The new growth-initiating factor for fibroblasts are present and may attach to collagen fibrils at the wound healing site, generating peptides of collagen including prolyl-hydroxyproline (Sato et al., 2020). The prolyl-hydroxyproline which is the main food-derived collagen peptides present in human blood plasma may contribute to chemotactic action on fibroblasts, peripheral blood neutrophils, and monocytes, which are responsible for wound healing and inflammation (Shigemura et al., 2009; Asai et al., 2019). Therefore, the superior effect of leaf extract for fibroblast proliferation may subsequently contribute to the increased amount of hydroxyproline.

Conclusion

Both leaf and root extracts of LPVa could promote the healing of thermal-burn wounds, with leaf extract being more superior in terms of the hydroxyproline content and histological analysis (Haematoxylin & Eosin and immunohistochemistry). Further studies related with molecular aspects should be performed to determine the mechanism of wound healing by LPVa leaf.

Data availability statement

The original contributions presented in the study are included in the article/Supplementary Material, further inquiries can be directed to the corresponding author.

Ethics statement

The animal study was reviewed and approved by Universiti Kebangsaan Malaysia Animal Ethical Committee.

Author contributions

NI performed the experiments and data analysis, designed, and wrote the manuscript. EM performed the anatomical and histological evaluation, NM reviewed the manuscript and critically revised the manuscript. AS and IM conceptualized the research, acquired the funding, and reviewed and critically revised the manuscript. All authors read and approved the final manuscript.

Funding

This research was funded by Universiti Kebangsaan Malaysia (UKM), grant number MI-2017-005.

Acknowledgments

The authors would also like to thank the Pharmacology staffs especially Madam Juliana Abdul Hamid and Fadhlullah Zuhair Japar Sidik.

Conflict of interest

The authors declare that the research was conducted in the absence of any commercial or financial relationships that could be construed as a potential conflict of interest.

Publisher's note

References

Abdul Kadir, A., Nik Hussain, N. H., Wan Bebakar, W. M., Mohd, D. M., Wan Mohammad, W. M. Z., Hassan, I. I., et al. (2012). The effect of labisia pumila var. alata on postmenopausal women: A pilot study. *Evid. Based. Complement. Altern. Med.* 2012, 216525. doi:10.1155/2012/216525

Abramov, Y., Golden, B., Sullivan, M., Botros, S. M., Miller, J. J., Alshahrour, A., et al. (2007). Histologic characterization of vaginal vs. abdominal surgical wound healing in a rabbit model. *Wound Repair Regen.* 15 (1), 80–86. doi:10.1111/j.1524-475X.2006.00188.x

Ahmad, S. U., Binti Aladdin, N. A., Jamal, J. A., Shuid, A. N., and Mohamed, I. N. (2021). Evaluation of wound-healing and antioxidant effects of marantodes pumilum (blume) kuntze in an excision wound model. *Molecules* 26 (1), 228. doi:10.3390/molecules26010228

Ahmad, S. U., Shuid, A., and Mohamed, I. (2018). Labisia pumila improves wound healing process in ovariectomized rat model. *Bangladesh J. Pharmacol.* 13, 106. doi:10.3329/bjp.v13i1.34473

Ali, N. (2014). "The dermatoxicological profile of labisia pumila extract for cosmetic application," (Malaysia: Universiti Teknologi Malaysia). Master of Engineering (Bioprocess).

Alven, S., Nqoro, X., and Aderibigbe, B. A. (2020). Polymer-based materials loaded with curcumin for wound healing applications. *Polymers* 12 (10), E2286. doi:10.3390/polym12102286

Arda, O., Göksügür, N., and Tüzün, Y. (2014). Basic histological structure and functions of facial skin. *Clin. Dermatol.* 32 (1), 3–13. doi:10.1016/j.clindermatol.2013.05.021

Asai, T., Oikawa, Y., Inoue, N., and Sato, K. (2019). Food-derived collagen peptides, prolyl-hydroxyproline (Pro-Hyp), and hydroxyprolyl-Glycine (Hyp-Gly) enhance growth of primary cultured mouse skin fibroblast using fetal bovine serum free from hydroxyprolyl peptide. *Int. J. Mol. Sci.* 21, 229. doi:10.3390/ijms21010229

Aziz, Z., Abu, S. F., and Chong, N. J. (2012). A systematic review of silver-containing dressings and topical silver agents (used with dressings) for burn wounds. *Burns* 38 (3), 307–318. doi:10.1016/j.burns.2011.09.020

Barbul, A., Efron, D. T., and Kavalukas, S. L. (2015). "Wound healing," in *Schwartz's Principles of Surgery, 10e*. Editors F. C. Brunicardi, D. K. Andersen, T. R. Billiar, D. L. Dunn, J. G. Hunter, J. B. Matthews, et al. (New York, NY: McGraw-Hill Education).

Cai, E. Z., Ang, C. H., Raju, A., Tan, K. B., Hing, E. C. H., Loo, Y., et al. (2014). Creation of consistent burn wounds: A rat model. *Arch. Plast. Surg.* 41 (4), 317–324. doi:10.5999/aps.2014.41.4.317

Choi, H. K., Kim, D. H., Kim, J. W., Ngadiran, S., Sarmidi, M. R., and Park, C. S. (2010). Labisia pumila extract protects skin cells from photoaging caused by UVB irradiation. *J. Biosci. Bioeng.* 109 (3), 291–296. doi:10.1016/j.jbiosc.2009.08.478

Chua, L. S., Abdul latiff, N., Lee, S., Lee, C. T., Sarmidi, M., and Aziz, R. (2011). Flavonoids and phenolic acids from labisia pumila (kacip fatimah). *Food Chem.* 127, 1186–1192. doi:10.1016/j.foodchem.2011.01.122

Chua, L. S., Lee, S. Y., Abdullah, N., and Sarmidi, M. R. (2012). Review on Labisia pumila (Kacip Fatimah): Bioactive phytochemicals and skin collagen synthesis promoting herb. *Fitoterapia* 83 (8), 1322–1335. doi:10.1016/j.fitote.2012.04.002

Church, D., Elsayed, S., Reid, O., Winston, B., and Lindsay, R. (2006). Burn wound infections. *Clin. Microbiol. Rev.* 19 (2), 403–434. doi:10.1128/CMR.19.2.403-434.2006

Dwivedi, D., Dwivedi, M., Malviya, S., and Singh, V. (2016). Evaluation of wound healing, anti-microbial and antioxidant potential of Pongamia pinnata in wistar rats. *J. Tradit. Complement. Med.* 7 (1), 79–85. doi:10.1016/j.jtcme.2015.12.002

Gagnon, R. C., and Peterson, J. J. (1998). Estimation of confidence intervals for area under the curve from destructively obtained pharmacokinetic data. *J. Pharmacokinet. Biopharm.* 26 (1), 87–102. doi:10.1023/a:1023228925137

Ibrahim, N., Wong, S. K., Mohamed, I. N., Mohamed, N., Chin, K. Y., Ima-Nirwana, S., et al. (2018). Wound healing properties of selected natural products. *Int. J. Environ. Res. Public Health* 15 (11), E2360. doi:10.3390/ijerph15112360

Jamal, J. A., Houghton, P. J., Milligan, S. R., and Jantan, I. (2003). The oestrogenis and cytotoxic effects of the extracts of labisia pumila var. alata and labisia pumila var. pumila *in vitro*. *Sains Kesihat.* 1, 53–60.

Karimi, E., Jaafar, H. Z., and Ahmad, S. (2011). Phytochemical analysis and antimicrobial activities of methanolic extracts of leaf, stem and root from different varieties of Labisa pumila Benth. *Mol. (Basel, Switz.* 16 (6), 4438–4450. doi:10.3390/molecules16064438

Karimi, E., Jaafar, H. Z. E., and Ahmad, S. (2013). Antifungal, anti-inflammatory and cytotoxicity activities of three varieties of labisia pumila benth: From microwave obtained extracts. *BMC Complement. Altern. Med.* 13 (1), 20. doi:10.1186/1472-6882-13-20

Lanham, J. S., Nelson, N. K., Hendren, B., and Jordan, T. S. (2020). Outpatient burn care: Prevention and treatment. *Am. Fam. Physician* 101 (8), 463–470.

Lansdown, A. B. (2002a). Silver. 2: Toxicity in mammals and how its products aid wound repair. *J. Wound Care* 11 (5), 173–177. doi:10.12968/jowc.2002.11.5.26398

Lansdown, A. B. (2002b). Silver. I: Its antibacterial properties and mechanism of action. *J. Wound Care* 11 (4), 125–130. doi:10.12968/jowc.2002.11.4.26389

Liang, Y., Zhao, X., Hu, T., Chen, B., Yin, Z., Ma, P. X., et al. (2019). Adhesive hemostatic conducting injectable composite hydrogels with sustained drug release and photothermal antibacterial activity to promote full-thickness skin regeneration during wound healing. *Small* 15 (12), 1900046. doi:10.1002/smll.201900046

Liu, T., Li, N., Yan, Y. Q., Liu, Y., Xiong, K., Liu, Y., et al. (2020). Recent advances in the anti-aging effects of phytoestrogens on collagen, water content, and oxidative stress. *Phytother. Res.* 34 (3), 435–447. doi:10.1002/ptr.6538

Lo, S. F., Hayter, M., Chang, C. J., Hu, W. Y., and Lee, L. L. (2008). A systematic review of silver-releasing dressings in the management of infected chronic wounds. *J. Clin. Nurs.* 17 (15), 1973–1985. doi:10.1111/j.1365-2702.2007.02264.x

Mathew-Steiner, S. S., Roy, S., and Sen, C. K. (2021). Collagen in wound healing. *Bioeng. (Basel)* 8 (5), 63. doi:10.3390/bioengineering8050063

Nadia, M. E., Nazrun, A. S., Norazlina, M., Isa, N. M., Norliza, M., and Ima Nirwana, S. (2012). The anti-inflammatory, phytoestrogenic, and antioxidative role of labisia pumila in prevention of postmenopausal osteoporosis. *Adv. Pharmacol. Sci.* 2012, 706905. doi:10.1155/2012/706905

Nešporová, K., Pavlík, V., Šafránková, B., Vágnerová, H., Odráška, P., Žídek, O., et al. (2020). Effects of wound dressings containing silver on skin and immune cells. *Sci. Rep.* 10 (1), 15216. doi:10.1038/s41598-020-72249-3

Neuman, R. E., and Logan, M. A. (1950). The determination of hydroxyproline. *J. Biol. Chem.* 184 (1), 299–306. doi:10.1016/s0021-9258(19)51149-8

Parihar, A., Parihar, M. S., Milner, S., and Bhat, S. (2008). Oxidative stress and anti-oxidative mobilization in burn injury. *Burns* 34 (1), 6–17. doi:10.1016/j.burns.2007.04.009

Pastar, I., Stojadinovic, O., Yin, N. C., Ramirez, H., Nusbaum, A. G., Sawaya, A., et al. (2014). Epithelialization in wound healing: A comprehensive review. *Adv. Wound Care* 3 (7), 445–464. doi:10.1089/wound.2013.0473

Rao, A. V., and Gurfinkel, D. M. (2000). The bioactivity of saponins: Triterpenoid and steroidal glycosides. *Drug Metabol. Drug Interact.* 17 (1-4), 211–235. doi:10.1515/dmdi.2000.17.1-4.211

Reinke, J. M., and Sorg, H. (2012). Wound repair and regeneration. *Eur. Surg. Res.* 49 (1), 35–43. doi:10.1159/000339613

Rosnani, A. G., Zaki, W. M. W., Shukri, M. A. M., Razali, M., Herman, S. E., and Fauzi, M. S. A. (2019). The effect of kacip fatimah (Marantodes pumilum) plant density under semi-controlled environment for high production of biomass and bioactive content. *J. Trop. Agric. Fd. Sc.* 47 (2), 55–64.

Rowan, M. P., Cancio, L. C., Elster, E. A., Burmeister, D. M., Rose, L. F., Natesan, S., et al. (2015). Burn wound healing and treatment: Review and advancements. *Crit. Care* 19, 243. doi:10.1186/s13054-015-0961-2

Sato, K., Asai, T. T., and Jimi, S. (2020). Collagen-derived di-peptide, prolylhydroxyproline (Pro-Hyp): A new low molecular weight growth-initiating factor for specific fibroblasts associated with wound healing. *Front. Cell Dev. Biol.* 8, 548975. doi:10.3389/fcell.2020.548975

Schlager, A., Kronberger, P., Petschke, F., and Ulmer, H. (2000). Low-power laser light in the healing of burns: A comparison between two different wavelengths (635 nm and 690 nm) and a placebo group. *Lasers Surg. Med.* 27 (1), 39–42. doi:10.1002/1096-9101(2000)27:1<39:aid-lsm5>3.0.co;2-4

Schultz Gs, C. G., Moldawer, L., et al. (2011). "Principles of wound healing," in *Mechanisms of vascular disease: A reference book for vascular specialists*. Editors R. Fitridge and M. Thompson (Adelaide (AU): University of Adelaide Press), 23. Internet.

Shigemura, Y., Iwai, K., Morimatsu, F., Iwamoto, T., Mori, T., Oda, C., et al. (2009). Effect of Prolyl-hydroxyproline (Pro-Hyp), a food-derived collagen peptide in human blood, on growth of fibroblasts from mouse skin. *J. Agric. Food Chem.* 57 (2), 444–449. doi:10.1021/jf802785h

Stone, B. C. (1989). "New and noteworthy malesian Myrsinaceae, III. On the genus Ardisia sw. in borneo," in *Proceedings of the academy of natural sciences of philadelphia* (Philadelphia, USA: Academy Of Natural Sciences), 263–306.

Tavares Pereira, D., Lima-Ribeiro, M. H. M., de Pontes-Filho, N. T., Carneiro-Leão, A. M., and Correia, M. T. (2012). Development of animal model for studying deep second-degree thermal burns. *J. Biomed. Biotechnol.* 2012, 460841. doi:10.1155/2012/460841

Tiwari, V. K. (2012). Burn wound: How it differs from other wounds? *Indian J. Plast. Surg.* 45 (2), 364–373. doi:10.4103/0970-0358.101319

Tolles, J. (2018). Emergency department management of patients with thermal burns. *Emerg. Med. Pract.* 20 (2), 1–24.

Wardhana, A., and Halim, J. (2020). Antioxidants reduce tissue necrosis in the zone of stasis: Review of burn wound conversion. *J. Plast. Rekons.* 7, 18–28. doi:10.14228/jpr.v7i1.292

Werner, S., Krieg, T., and Smola, H. (2007). Keratinocyte-fibroblast interactions in wound healing. *J. Invest. Dermatol.* 127 (5), 998–1008. doi:10.1038/sj.jid.5700786

Xi, H. R., Wu, H., Lai, F. R., Ma, J. J., Liu, H. F., and Chen, W. B. (2018). Composition and antioxidant activity of flavonoids from kacip fatimah. *Mod. Food Sci. Technol.* 34, 52–56. doi:10.13982/j.mfst.1673-9078.2018.8.008

Zhao, Y., Dai, C., Wang, Z., Chen, W., Liu, J., Zhuo, R., et al. (2019). A novel curcumin-loaded composite dressing facilitates wound healing due to its natural antioxidant effect. *Drug Des. devel. Ther.* 13, 3269–3280. doi:10.2147/DDDT.S219224

Zhu, X., Radovic-Moreno, A. F., Wu, J., Langer, R., and Shi, J. (2014). Nanomedicine in the management of microbial infection - overview and perspectives. *Nano today* 9 (4), 478–498. doi:10.1016/j.nantod.2014.06.003

frontiers | Frontiers in Pharmacology

TYPE Original Research
PUBLISHED 12 January 2023
DOI 10.3389/fphar.2022.971443

OPEN ACCESS

EDITED BY
Ahmad Nazrun Shuid,
MARA University of Technology, Malaysia

REVIEWED BY
K. M. Sakthivel,
PSG College of Arts and Science, India
Mohamed Aly Morsy,
King Faisal University, Saudi Arabia
Pouya Hassandarvish,
University of Malaya, Malaysia
Ahmad Naqib Shuid,
Universiti Sains Malaysia (USM), Malaysia

*CORRESPONDENCE
Mohd Fahami Nur Azlina,
nurazlinamf@ukm.edu.my

SPECIALTY SECTION
This article was submitted to Ethnopharmacology, a section of the journal Frontiers in Pharmacology

RECEIVED 17 June 2022
ACCEPTED 29 December 2022
PUBLISHED 12 January 2023

CITATION
Akmal MN, Abdel Aziz I and Nur Azlina MF (2023), *Piper sarmentosum* Roxb. methanolic extract prevents stress-induced gastric ulcer by modulating oxidative stress and inflammation. *Front. Pharmacol.* 13:971443. doi: 10.3389/fphar.2022.971443

Piper sarmentosum Roxb. methanolic extract prevents stress-induced gastric ulcer by modulating oxidative stress and inflammation

Muhamad Nurul Akmal[1], Ibrahim Abdel Aziz[2] and Mohd Fahami Nur Azlina[1]*

[1]Department of Pharmacology, Faculty of Medicine, UKM Medical Centre, Universiti Kebangsaan Malaysia, Kuala Lumpur, Malaysia, [2]Department of Pharmacology and Toxicology, Faculty of Medicine, Umm Al-Qura University, Makkah, Saudi Arabia

This study investigated the gastroprotective effect of *Piper sarmentosum* (PS) on stress-induced gastric ulcers in rats by measuring its effect on oxidative stress, gastric mucosal nitric oxide (NO), and inflammatory biomarkers. Twenty-eight male Wistar rats were randomly divided into four groups; two control groups (non-stress and stress) and two treated groups supplemented with either methanolic PS extract (500 mg/kg body weight) or omeprazole (OMZ; 20 mg/kg) orally. After 28 days of treatment, the stress control, PS, and OMZ groups were subjected to water-immersion restrain stress (WIRS) for 3.5 h. Gastric tissue malondialdehyde (MDA), NO, superoxide dismutase (SOD), inducible NO synthase (iNOS), SOD mRNA, tumor necrosis factor (TNF)-α, interleukin (IL)-1β, and IL-6 levels were measured. WIRS significantly increased gastric MDA, NO, and pro-inflammatory cytokine levels compared to the non-stressed control group. PS and omeprazole supplementation significantly reduced WIRS-exposure-induced gastric ulcers and MDA, iNOS, and IL-1β levels. However, only PS reduced NO, TNF-α, and IL-6 levels, which were upregulated in this ulcer model. In conclusion, the gastroprotection afforded by PS is possibly mediated by gastric mucosal NO normalization through reduced iNOS expression and attenuation of inflammatory cytokines. PS showed a greater protective effect than omeprazole in reducing gastric lesions and NO, TNF-α, and IL-6 levels, and iNOS expression.

KEYWORDS

***Piper sarmentosum*, malondialdehyde, gastric ulcer, nitric oxide, iNOS, IL-1β, TNF-α, IL-6**

Abbreviations: 4-HNE, 4-hydroxynonenal; eNOS, endothelial NO synthase; FRIM, Forest Research Institute Malaysia; H_2O_2, hydrogen peroxide; iNOS, inducible NO synthase; IL-1β, interleukin-1β; MDA, malondialdehyde; NO, nitric oxide; NSAIDS, non-steroidal anti-inflammatory drugs; $O_2^{\bullet-}$, radical anions; OMZ, omeprazole; PS, *Piper sarmentosum*; SAPE, streptavidin phycoerythrin; SOD, superoxide dismutase; SOD, superoxide dismutase enzyme; TNF-α, tumor necrosis factor-α; UKMAEC, University Kebangsaan Malaysia Animal Ethics Committee; WIRS, water-immersion restraint stress.

1 Introduction

Upper gastrointestinal bleeding is associated with significant morbidity and mortality. Bleeding peptic ulcers remain the most common cause of acute non-variceal upper gastrointestinal bleeding. This condition is often associated with non-steroidal anti-inflammatory drug use (Atchison et al., 2013), *Helicobacter pylori* infection (Wang et al., 2014), and stress (Nur Azlina et al., 2013; Kudryavtsev et al., 2014). Stress ulcer syndrome can cause mucosal erosions and superficial hemorrhages in critically ill patients or individuals under extreme physiologic stress. The ulcers frequently emerge due to major stressful events, including surgery, trauma, shock, sepsis, and burns. This study used water-immersion restraint stress (WIRS), an established method to induce gastric lesions in rats (Konturek et al., 2008; Kwiecien et al., 2012; Raja Kumar et al., 2019), to create a stress model that mimics stress ulcers in human patients.

Stress is associated with increased oxidative stress due to increased free radical formation. Kwiecien et al. (2012) found that WIRS causes acute inflammatory responses, with interleukin (IL)-1 and tumor necrosis factor-alpha (TNF-α) acting as the primary pro-inflammatory cytokines induced by neutrophil infiltration into the gastric mucosa. Neutrophils produce superoxide anions ($O_2^{\bullet-}$) that react with cellular membrane lipids, resulting in lipid peroxidation. Malondialdehyde (MDA) and 4-hydroxynonenal are examples of lipid peroxidation end-products (Khoubnasabjafari et al., 2015). Stress will also produce high nitric oxide (NO) levels. NO is catalyzed by inducible NO synthase (iNOS) and acts as a potent cytotoxic oxidant (Lanas, 2008; Nimse and Pal, 2015). Stress also decreases superoxide dismutase (SOD) activity in gastric mucosa, impairing its antioxidative defense mechanism (Kwiecień et al., 2002; Nur Azlina et al., 2013; Patlevič et al., 2016).

Piper (P.) sarmentosum Roxb. belongs to the Piperaceae family. It is an about 20 cm tall herb that grows wild in the forest and is commonly found in Southeast Asia (e.g., Malaysia, Cambodia, Philippines, Thailand, and Myanmar). *P. sarmentosum* is a traditional medicinal plant whose leaves are usually eaten raw as *ulam*. For centuries, it has been used to treat wind-cold cough, fever, postpartum foot edema, stomachache, toothache, diabetes, and traumatic injury (Sun et al., 2020). *P. sarmentosum* has anti-inflammatory (Zakaria et al., 2010; Azlina et al., 2019; Salehi et al., 2019) and anti-atherosclerotic (Amran et al., 2010) properties. Methanolic *P. sarmentosum* extract has been shown to have antioxidative activity due to the natural antioxidant superoxide scavenger, naringenin (Subramaniam et al., 2003; Chanwitheesuk et al., 2005). Therefore, this study investigated the protective effects of methanolic *P. sarmentosum* extract against gastric mucosa injury as an alternative to other antioxidants. We used omeprazole as a positive control since it is one of the most widely prescribed drugs to treat gastric ulcers (Hajrezaie et al., 2012; Ketuly et al., 2013).

2 Materials and methods

2.1 Plant materials

Fresh *P. sarmentosum* leaves were collected from the Forest Research Institute Malaysia (FRIM) reserve forest at Kepong, Selangor, Malaysia, and identified by FRIM's Medicinal Plant Division. A voucher specimen (FRI 45870) was deposited at FRIM's Medicinal Plant Division.

2.2 Preparation of methanolic *P. sarmentosum* extract

The methanolic extraction procedure was performed at the FRIM laboratory. The leaves were cleaned with tap water and dried at room temperature before being finely chopped. Next, 250 g of leaves were extracted in 2.5 L of methanol. This mixture was heated to 40°C–60°C using a Soxhlet to evapourate the methanol (Sawangjaroen et al., 2004). The paste material produced was kept at 4°C until required. The percentage yield from the crude dried extract was around 10%. The plant extract was analyzed using liquid chromatography-mass spectrometry at the Universiti Kebangsaan Malaysia's (UKM) Research and Instrumentation Management Center. The active chemical and purity results have been previously reported (Bactiar and Fahami, 2019). Methanol *P. sarmentosum* leaf extracts yielded fifteen compounds extracted and characterized by spectroscopic methods, including didymin, naringenin, methyl piperate, quercetin, beta asarone, brachyamide, amurensin, piperitol, guineensine, hesperidin, rutin, malvidin, and difucol (Table 1). The term *P. sarmentosum* in this study refers to *P. sarmentosum* methanolic extract.

2.3 Experimental design

Twenty-eight male *Sprague Dawley* rats (obtained from the Animal Unit, Faculty of Medicine, UKM) were divided into four groups: non-stress control, stress control, *P. sarmentosum*-treated, and omeprazole-treated. The non-stress and stress control groups were administered vitamin E-free palm oil *via* oral gavage. Omeprazole and *P. sarmentosum* were diluted in vitamin E-free palm oil as a vehicle. Omeprazole (20 mg/kg body weight) and *P. sarmentosum* extract (500 mg/kg body weight) were administered *via* oral gavage. This *P. sarmentosum* dose was chosen based on our previous study showing a protective *P. sarmentosum* methanolic extract effect on stress-induced gastric lesions (Azlina et al., 2019). Throughout the feeding period, all rats were habituated to handling to reduce their stress-related disturbances. After 28 days, the rats in the stress control, omeprazole-treated, and *P. sarmentosum*-treated groups were exposed to WIRS for 3.5 h. The rats in the non-stress control group were not subjected to any stress. The rats were restrained in a plastic restrainer before being placed individually in a beaker containing room-temperature tap water. The water level was adjusted to the rat's neck level (Azlina et al., 2015). Then, the rats were sacrificed, and their stomach was isolated to measure gastric lesion index, gastric MDA content, NO level, iNOS mRNA level, SOD activity, SOD mRNA levels, TNF-α, IL-1β, and IL-6 levels. This study was approved by the UKM Animal Ethics Committee (354/2011).

2.4 Parameters measurements

2.4.1 Gastric lesion

Gastric lesions were measured using an image analyzer at ×3 magnification. The lesion length in mm was measured at the

TABLE 1 Isolated compound from methanol *P. sarmentosum* leaf extracts.

No	Name of compound	Formula	Molecular weight	Molecular structure
1	Didymin	$C_{28}H_{34}O_{14}$	594.6	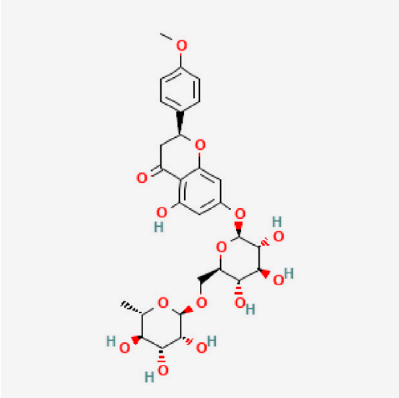 PubChem Identifier: CID 16760075 URL: https://pubchem.ncbi.nlm.nih.gov/compound/16760075#section=2D-Structure
2	Naringenin	$C_{15}H_{12}O_5$	272.25	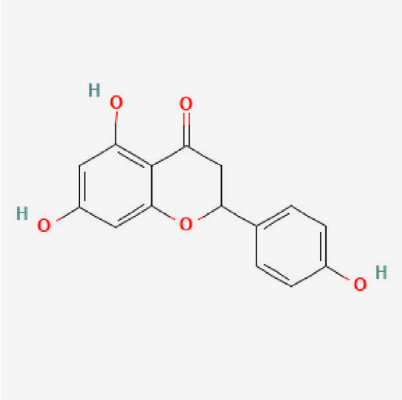 PubChem Identifier: CID 932 URL: https://pubchem.ncbi.nlm.nih.gov/compound/932#section=2D-Structure
3	Methyl piperate	$C_{13}H_{12}O_4$	232.23	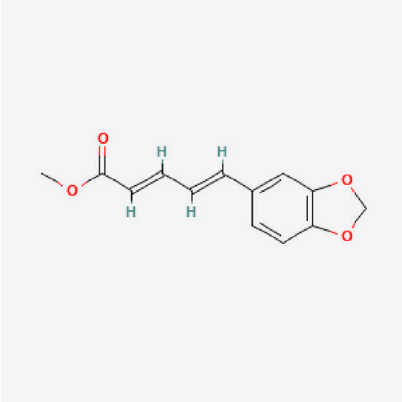 PubChem Identifier: CID 9921021 URL: https://pubchem.ncbi.nlm.nih.gov/compound/9921021#section=2D-Structure

(Continued on following page)

TABLE 1 (*Continued*) Isolated compound from methanol *P. sarmentosum* leaf extracts.

No	Name of compound	Formula	Molecular weight	Molecular structure
4	Quercetin	$C_{15}H_{10}O_7$	302.23	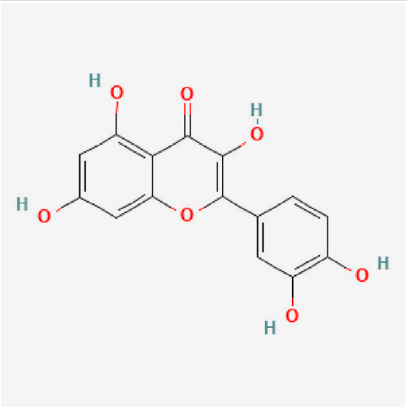 PubChem Identifier: CID 5280343 URL: https://pubchem.ncbi.nlm.nih.gov/compound/5280343#section=2D-Structure
5	Beta-Asarone	$C_{12}H_{16}O_3$	208.25	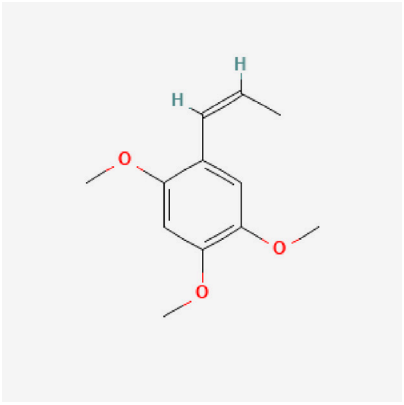 PubChem Identifier: CID 5281758 URL: https://pubchem.ncbi.nlm.nih.gov/compound/5281758#section=2D-Structure
6	Brachyamide B	$C_{20}H_{25}NO_3$	327.4	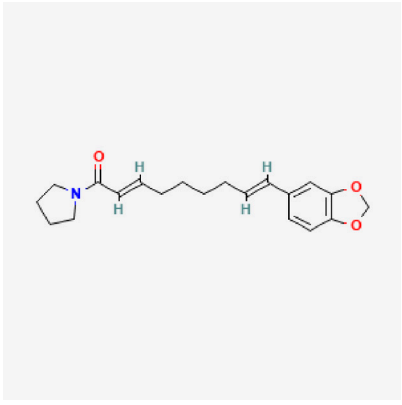 PubChem Identifier: CID 14162526 URL: https://pubchem.ncbi.nlm.nih.gov/compound/14162526#section=2D-Structure

(Continued on following page)

TABLE 1 (*Continued*) Isolated compound from methanol *P. sarmentosum* leaf extracts.

No	Name of compound	Formula	Molecular weight	Molecular structure
7	Amurensin	$C_{26}H_{30}O_{12}$	534.5	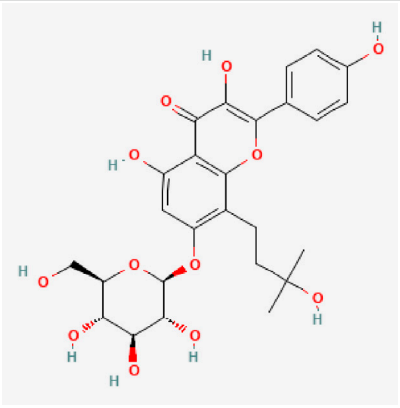 PubChem Identifier: CID 5318156 URL: https://pubchem.ncbi.nlm.nih.gov/compound/5318156#section=2D-Structure
8	Piperitol	$C_{20}H_{20}O_6$	356.4	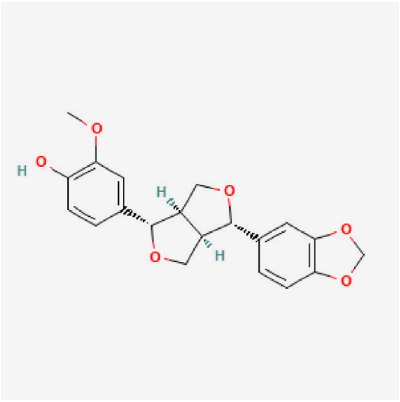 PubChem Identifier: CID 10247670 URL: https://pubchem.ncbi.nlm.nih.gov/compound/10247670#section=2D-Structure
9	Guineensine	$C_{24}H_{33}NO_3$	383.5	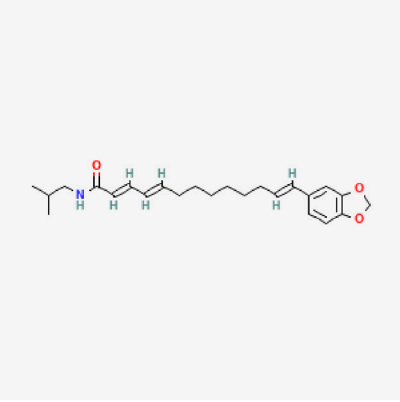 PubChem Identifier: CID 6442405 URL: https://pubchem.ncbi.nlm.nih.gov/compound/6442405#section=2D-Structure

(Continued on following page)

TABLE 1 (*Continued*) Isolated compound from methanol *P. sarmentosum* leaf extracts.

No	Name of compound	Formula	Molecular weight	Molecular structure
10	Hesperidin	$C_{28}H_{34}O_{15}$	610.6	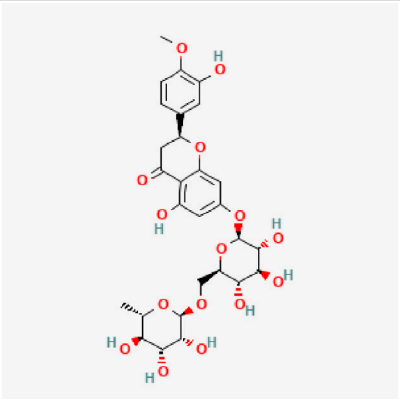 PubChem Identifier: CID 10621 URL: https://pubchem.ncbi.nlm.nih.gov/compound/10621#section=2D-Structure
11	Rutin	$C_{27}H_{30}O_{16}$	610.5	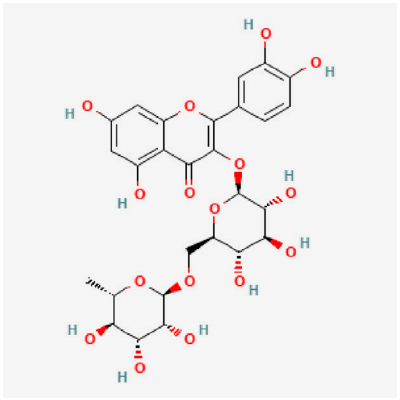 PubChem Identifier: CID 5280805 URL: https://pubchem.ncbi.nlm.nih.gov/compound/5280805#section=2D-Structure
12	Malvidin	$C_{17}H_{15}O_7^+$	331.30	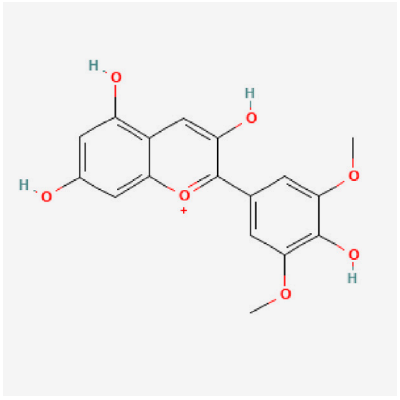 PubChem Identifier: CID 159287 URL: https://pubchem.ncbi.nlm.nih.gov/compound/159287#section=2D-Structure

(Continued on following page)

TABLE 1 (*Continued*) Isolated compound from methanol *P. sarmentosum* leaf extracts.

No	Name of compound	Formula	Molecular weight	Molecular structure
13	Difucol	$C_{12}H_{10}O_6$	250.20	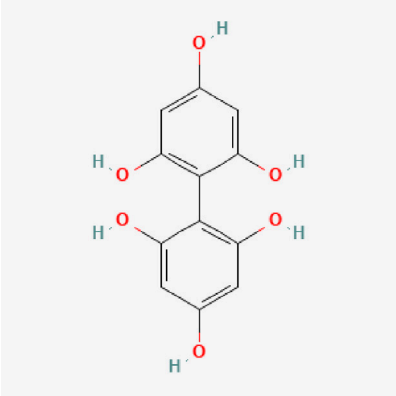 PubChem Identifier: CID 433697 URL: https://pubchem.ncbi.nlm.nih.gov/compound/433697#section=2D-Structure

lesion's greatest diameter. Each five petechial was equal to a 1 mm lesion. Lesion length was expressed as the lesion index according to a previously described method (Ibrahim et al., 2012).

2.4.2 Gastric MDA levels

Gastric MDA levels were measured using a previously described method (Ledwoz et al., 1986). Briefly, 2.5 mL of a trichloroacetic acid (1.22 mol/L) and hydrochloric acid (.6 mol/L) solution was added to .5 mL of the sample and incubated at room temperature for 15 min. Next, .05 mL of sodium hydroxide was added, and the sample was incubated at 100°C for 30 min before being cooled to room temperature. Then, 4 mL of n-butanol was added, and the sample was vigorously vortex for 3 min. Finally, the sample was centrifuged at 3,000 rpm for 10 min, and the absorbance of the upper layer at 535 nm was measured using a spectrophotometer.

2.4.3 Gastric SOD levels

SOD levels in gastric tissue were measured using Cayman's SOD Assay Kit (70600; Ann Arbor, MI, United States). This kit uses a tetrazolium salt to detect $O_2^{\bullet-}$ generated by xanthine oxidase.

2.4.4 NO levels

NO levels in gastric tissue were measured using the Quantichrome NO Assay Kit (D2NO-100; BioAssay Systems; Hayward, CA, United States). NO was oxidized to nitrate and nitrite. Total nitrate and nitrites levels were quantified based on the absorbance at 540 nm measured using an ELISA reader.

2.4.5 SOD and iNOS mRNA levels

SOD and iNOS mRNA levels were measured using the QuantiGene Plex Assay Lit (Genospectra; Fremont, CA, United States). Tissue lysate was added to a well containing a gene-specific probe set and then hybridized overnight at 53°C. Next, wells were washed twice with bDNA wash buffer before being incubated at 46°C with an amplifier and then an alkaline phosphatase-linked label probe, with a wash step in between. Finally, streptavidin phycoerythrin was added, producing a luminescent signal proportional to the target RNA amount that was measured using a Luminex machine (Zhang et al., 2005).

2.4.6 TNF-α, IL-1β, and IL-6 protein quantification assays

TNF-α, IL-1β, and IL-6 levels in gastric tissue were measured using Panomics' Procarta Cytokine Assay Kit (Affymetrix; Santa Clara, CA, United States) and a Luminex 200 analyzer (Luminex Corporation; Darmstadt, Germany). Procarta Protein Assays use xMAP technology (multi-analyte profiling beads) to enable simultaneous quantitation of multiple protein targets. The xMAP system combines a flow cytometer, fluorescent-dyed microspheres (beads), lasers, and digital signal processing to effectively multiplex up to 100 different assays within a single sample.

2.5 Statistical analysis

Statistical analyses were performed using SPSS v.23 (SPSS Inc., Chicago, IL, United States). The normality of each variable's distribution was assessed using the Shapiro–Wilk test. All results are expressed as the mean ± standard error of the mean (SEM). The significance ($p < .05$) of differences between groups was assessed with an analysis of variance followed by Tukey's *post hoc* test.

3 Results

3.1 Gastric lesions

No lesions were observed in the stomachs of rats in the non-stressed control group. Rats exposed to WIRS for 3.5 h developed gastric lesions at the glandular part of the stomach (Figure 1). Supplementation with *P. sarmentosum* or omeprazole significantly lowered gastric lesion scores ($p = .002$ and $p = .026$, respectively; Figure 2). Moreover, *P. sarmentosum* reduced stomach lesions significantly more than omeprazole ($p = .002$; Figure 2).

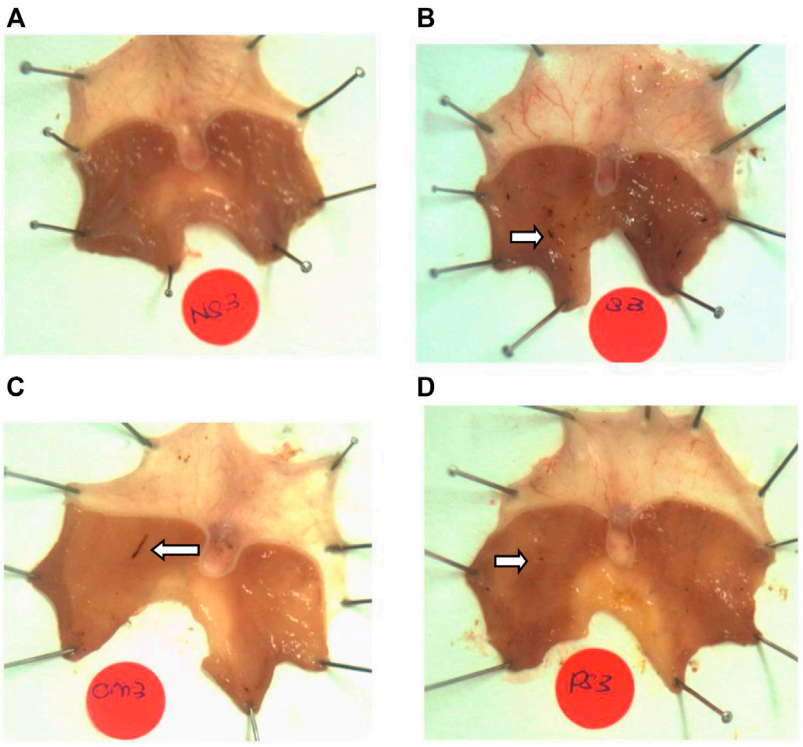

FIGURE 1
Macroscopic observation of gastric lesions in **(A)** normal rats (no lesions), **(B)** rats exposed to WIRS for 3.5 h (developed lesions), **(C)** omeprazole-treated, and **(D)** *P. sarmentosum*-treated. Arrows indicate gastric lesions.

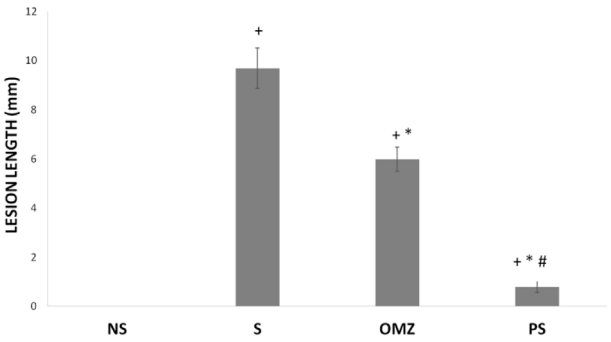

FIGURE 2
Effects of *P. sarmentosum* (500 mg/kg; PS) and omeprazole (20 mg/kg; OMZ) on gastric lesion length (in mm) in rats exposed to WIRS. Bars represent mean ± SEM ($n = 7$). Key: +, $p < .05$ compared to the non-stress (NS) control group; *, $p < .05$ compared to the stress (S) control group; #, $p < .05$ compared to the OMZ-treated group.

3.2 Antioxidant levels

Gastric MDA content was significantly higher in stress-exposed rats than in non-stressed rats ($p = .001$; Table 2). *P. sarmentosum* and omeprazole supplementation attenuated the stress-induced increase in MDA levels, maintaining them at similar levels to non-stress rats. *P. sarmentosum* and omeprazole showed comparable effects on WIRS-induced gastric MDA levels. In addition, WIRS exposure significantly reduced gastric SOD activity ($p = .002$). However, *P. sarmentosum* and omeprazole supplementation did not attenuate the reduction in SOD activity in stress-exposed rats.

SOD mRNA levels were significantly lower in non-stressed rats than in stress-exposed rats. In addition, SOD mRNA levels were significantly lower in stress-exposed rats treated with *P. sarmentosum* or omeprazole than in untreated stress-exposed rats (Figure 3).

3.3 NO and iNOS mRNA levels

NO levels were significantly higher in stress-exposed rats than in non-stressed rats ($p = .036$). *P. sarmentosum* but not omeprazole supplementation significantly attenuated the increase in NO levels ($p = .026$; Table 2). In addition, iNOS mRNA levels were significantly higher in stress-exposed rats than in non-stressed rats (Figure 4). However, *P. sarmentosum* and omeprazole supplementation significantly attenuated the stress-induced elevation in gastric iNOS mRNA levels. Moreover, iNOS mRNA levels were significantly lower with *P. sarmentosum* than with omeprazole supplementation.

3.4 Cytokines

Gastric TNF-α levels were significantly higher (~2-fold) in stress-exposed rats than in non-stressed rats ($p = .001$; Figure 5A). *P. sarmentosum* supplementation significantly attenuated the increase

TABLE 2 The effect of *P. sarmentosum* and omeprazole on MDA and NO levels and SOD activity in rats exposed to WIRS for 3.5 h.

Treatment	MDA content (mmol/tissue)	SOD activity (U/mg)	NO level (μM)
Non-stress control	1.725*	.6371	10.944
Stress control	4.656	.1173^{+}	15.5^{+}
Omeprazole	2.217*	.213^{+}	14.207^{+}
Piper sarmentosum	2.903*	.0882^{+}	10.676*

+ vs. non-stress control ($p < .05$), * vs. stress control ($p < .05$), # vs. omeprazole ($p < .05$).

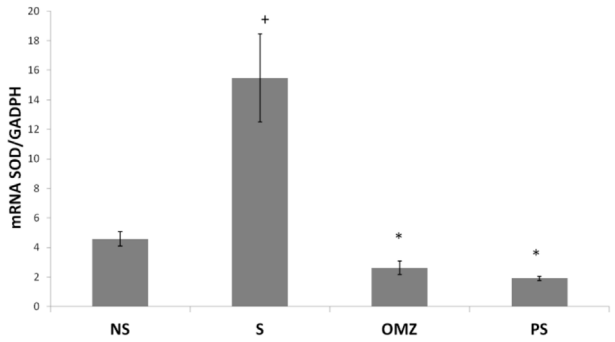

FIGURE 3
Effects of *P. sarmentosum* (500 mg/kg; PS) and omeprazole (20 mg/kg; OMZ) on gastric *Sod* mRNA levels in rats exposed to WIRS for 3.5 h. Bars represent mean ± SEM ($n = 7$). Key: +, $p < .05$ compared to the non-stress (NS) control group; *, $p < .05$ compared to the stress (S) control group; #, $p < .05$ compared to the omeprazole-treated group.

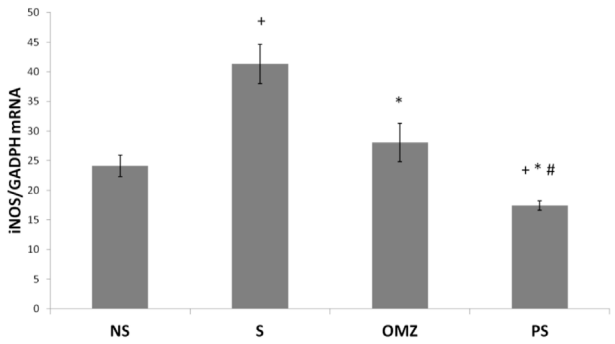

FIGURE 4
Effects of *P. sarmentosum* (500 mg/kg; PS) and omeprazole (20 mg/kg; OMZ) on gastric iNOS mRNA levels in rats exposed to WIRS for 3.5 h. Bars represent mean ± SEM ($n = 7$). Key: +, $p < .05$ compared to the non-stress (NS) control group; *, $p < .05$ compared to the stress (S) control group; #, $p < .05$ compared to the omeprazole-treated group.

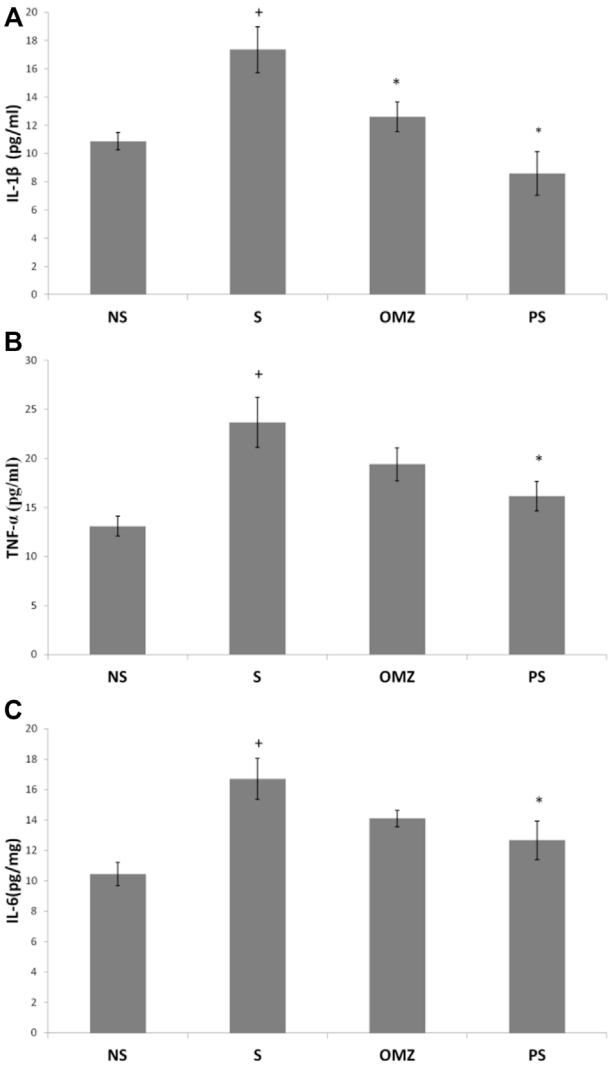

FIGURE 5
Effects of *P. sarmentosum* (500 mg/kg; PS) and omeprazole (20 mg/kg; OMZ) on gastric **(A)** TNF-α, **(B)** IL-1β, and **(C)** IL-6 protein levels in rats exposed to WIRS for 3.5 h. Bars represent mean ± SEM ($n = 7$). Key: +, $p < .05$ compared to the non-stress (NS) control group; *, $p < .05$ compared to the stress (S) control group; #, $p < .05$ compared to the omeprazole-treated group.

in TNF-α levels in stress-exposed rats ($p = .026$). However, omeprazole supplementation did not affect TNF-α levels.

In addition, gastric IL-1β levels were significantly increased in stress-exposed rats than in non-stressed rats ($p = .004$; Figure 5B). However, *P. sarmentosum* ($p = 1.0 \times 10^{-4}$) and omeprazole ($p = .043$) supplementation significantly attenuated the increase in IL1-β levels in stress-exposed rats. Gastric IL-1β levels did not differ significantly between stress-exposed rats given *P. sarmentosum* and omeprazole supplements, suggesting they have comparable beneficial effects.

Gastric IL-6 levels were significantly increased in stress-exposed rats than in non-stressed rats ($p = .004$; Figure 5C). *P. sarmentosum*

supplementation significantly attenuated the increase in gastric IL-6 levels in stress-exposed rats (p = .044). However, omeprazole supplementation did not restore gastric tissue IL-6 levels to their non-stressed values (p = .043).

4 Discussion

Our findings showed that rats exposed to WIRS for 3.5 h developed gastric lesions at the glandular part of the stomach, consistent with previous studies (Konturek et al., 2008; Kwiecien et al., 2012; Azlina et al., 2017). This study showed that *P. sarmentosum* could protect gastric mucosa against stress-induced injury, supporting this plant's use as a preventive treatment against gastric mucosa injury. *P. sarmentosum* supplementation provided better protection against stress-induced gastric ulcers than omeprazole. Omeprazole is an established gastric ulcer treatment used in numerous studies to provide gastroprotective effects (Hajrezaie et al., 2012; Sidahmed et al., 2013). However, this study showed that pretreatment with *P. sarmentosum* provided better protection in reducing gastric mucosal lesions than omeprazole. Our assessment of gastric lesions was based on measuring their greatest diameter and averaging their total length.

Chan et al. (2019) described *P. sarmentosum*'s ability to inhibit pro-inflammatory cytokines such IL-1β, TNF-α, and Il-6. Omeprazole affects cytokines differently from *P. sarmentosum,* decreasing IL-1β levels but increasing IL-6 and TNF-α levels compared to the non-stress control group. While studies in *H. pylori*-infected humans have shown omeprazole to positively affect pro-inflammatory cytokines (Kountouras et al., 2000), our rat-based study did not show similar effects. In addition, IL-1β significantly increased intercellular adhesion molecule 1 expression (Watanabe et al., 2001) and leucocyte infiltration in the scarred mucosa's superficial region before ulcer recurrence (Watanabe et al., 1997). They discovered that inhibiting gastric acid sufficiently with omeprazole prevented both ulcer recurrence and responses, indicating that acid may enhance gastric mucosal inflammation in response to IL-1β stimulation, resulting in gastric ulcers. Metabolic pathway analysis indicated that *P. sarmentosum* exerts anti-inflammatory activity mainly by affecting tryptophan metabolism (Wang et al., 2020). Its metabolic product, melatonin, has anti-inflammatory properties by inhibiting the activation of nuclear factor kappa-light-chain-enhancer of activated B cells (Wang et al., 2020). These findings are consistent with our results showing *P. sarmentosum*'s anti-inflammatory activity on the inflammatory signaling pathway by downregulating IL-1β, IL-6, and TNF-α.

The enhanced expression and release of IL-1β, IL-6, and TNF-α could also contribute to increased reactive oxygen species production in the gastric mucosa. Lipid peroxidation arises in biological systems due to the oxidation of unsaturated, mostly polyunsaturated, lipids, leading to the formation of free radicals and lipid peroxides that are harmful to viable tissues. Lipid peroxides quickly decompose to produce many compounds. One common byproduct of that process is MDA. MDA is present in serum, plasma, and tissues because of lipid peroxidation. It is the most reported analyte for estimating lipid peroxidation and oxidative stress (Del Rio et al., 2005; Rappaport, 2006). Our results indicate that MDA levels are significantly higher in stress-exposed rats. This study confirms the involvement of free radicals in the pathogenesis of stress-induced gastric injuries. This finding is consistent with other studies showing the importance of lipid peroxidation in causing injuries to the gastric mucosa (Kamisah et al., 2011; Nur Azlina et al., 2013).

Antioxidants have been shown to protect against gastric mucosa injury (Nur Azlina et al., 2009; Ibrahim et al., 2012; Azlina et al., 2015). This study showed that *P. sarmentosum* significantly reduced MDA levels compared to stress control rats, which probably reduced gastric injury by retarding the lipid peroxidation process. *P. sarmentosum* has higher antioxidant activity than other traditional plants (Chanwitheesuk et al., 2005). This plant also contains a natural antioxidant (naringenin, didymin, methyl piperate, quercetin, beta asarone, brachyamide, amurensin, piperitol, guineensine, hesperidin, rutin, malvidin, and difucol) (Subramaniam et al., 2003; Bactiar and Fahami, 2019; Raja Kumar et al., 2019), which might contribute to *P. sarmentosum*'s ability to reduce MDA. Our findings also showed no differences between *P. sarmentosum* and omeprazole in reducing gastric MDA levels, suggesting they have similar radical scavenging abilities. Omeprazole was previously shown to confer dose-dependent protection against ethanol (Sener et al., 2004) and stress-induced (Azlina et al., 2015) acute gastric mucosal injury by inhibiting lipid peroxidation.

Several reactive oxygen species scavenging systems, including SOD, glutathione peroxidases, and catalases, prevent their destructive action. SOD catalyzes the dismutation of O_2-into less noxious hydrogen peroxide, which is further degraded by catalases or glutathione peroxidases. This study found that stress exposure led to lipid peroxide production, indicated by increased gastric tissue MDA levels and SOD mRNA levels. This effect could be due to the normal physiological response upregulating SOD expression due to impaired antioxidative enzymes. Dinu et al. (2009) found reduced SOD activity in the gastric mucosa due to stress, increasing lipid peroxidation. *P. sarmentosum* and omeprazole supplementation did not increase SOD expression and enzyme activity, suggesting that they do not affect SOD activity. Reduced MDA levels and lesion occurrences in the *P. sarmentosum*-supplemented group indicate that it acts as an antioxidant (Subramaniam et al., 2003), potentially reflecting its naringenin content, a natural antioxidant superoxide scavenger (Bactiar and Fahami, 2019; Raja Kumar et al., 2019). Antioxidant agents have been shown to be effective in treating gastric ulcers (Kudryavtsev et al., 2014).

NO exerts either protective or destructive effects depending on the extent of its production. While NO produced by endothelial NO synthase plays an important role in gastric ulcer formation and healing, NO produced by iNOS only participates in ulcer formation. This study has shown that iNOS mRNA levels were significantly higher in stress-exposed rats than in non-stressed control rats, with a concomitant increase in NO levels in the stress-exposed rats. This change is mainly due to excessive iNOS NO production in inflammatory cells, inducing oxidative tissue stress and promoting mucosal damage (Cho, 2001; Mittal et al., 2014). Nitrite levels were significantly elevated, potentially due to iNOS stimulation, which reacts with superoxide to form peroxynitrite, a potent cytotoxic oxidant causing gastric tissue damage (Lanas, 2008; Azlina et al., 2015). *P. sarmentosum* supplementation significantly reduced stress-induced increases in NO levels and iNOS expression. It also reduced iNOS expression to a significantly greater extent than

omeprazole. Therefore, its beneficial effects are likely due to its ability to decrease gastric iNOS expression and NO levels, reducing gastric mucosal damage.

5 Conclusion

Our findings provide evidence that oral *P. sarmentosum* supplementation confers protection against stress-induced gastric lesions, possibly *via* its antioxidant mechanism, reducing pro-inflammatory cytokines, and its effects on NO through reduced iNOS expression. *P. sarmentosum* extract showed a better protective effect than omeprazole in reducing gastric lesions; TNF-α, IL-6, NO levels; and iNOS expression. Therefore, it is a potential therapeutic agent for gastric ulcers with similar pathologies.

Data availability statement

The original contributions presented in the study are included in the article/supplementary material, further inquiries can be directed to the corresponding author.

Ethics statement

The animal study was reviewed and approved by the Animal research of Universiti Kebangsaan Malaysia (FAR/PP/2016/AZLINA/28-SEPT./354-OCT.2016-OCT.-2019).

Author contributions

MN and MA had full access to all the data in the study and take responsibility for the integrity of the data and the accuracy of the data analysis. Study concept and design: MN, IA, and MA. MA and MN performed the research and wrote the manuscript. All authors approved the final manuscript.

Funding

This research was funded by Ministry of Education, Malaysia, grant number FGRS/1/2016/SKK08/UKM/02/5 and by Universiti Kebangsaan Malaysia, grant number UKM-DLP-066 and FF-2018-422.

Acknowledgments

We also thank to Mr Muhamad Arizi Aziz, Mrs Nurfarhana Mohd Fozi, Ms Hafizah Abas, Mrs Juliana Abdul Abdul Hamid and Fadhlullah Zuhair Japar Sidik for their technical help.

Conflict of interest

The authors declare that the research was conducted in the absence of any commercial or financial relationships that could be construed as a potential conflict of interest.

Publisher's note

All claims expressed in this article are solely those of the authors and do not necessarily represent those of their affiliated organizations, or those of the publisher, the editors and the reviewers. Any product that may be evaluated in this article, or claim that may be made by its manufacturer, is not guaranteed or endorsed by the publisher.

References

Amran, A. A., Zakaria, Z., Othman, F., Das, S., Raj, S., and Nordin, N. A. M. M. (2010). Aqueous extract of Piper sarmentosum decreases atherosclerotic lesions in high cholesterolemic experimental rabbits. *Lipids Health Dis.* 9 (1), 44–46. doi:10.1186/1476-511X-9-44

Atchison, J. W., Herndon, C. M., and Rusie, E. (2013). NSAIDs for musculoskeletal pain management:current perspectives and novel strategies to improve safety. *J. Manag. Care Pharm. JMCP* 19 (9), 1–19. doi:10.18553/jmcp.2013.19.s9.1

Azlina, M. F. N., Kamisah, Y., Chua, K. H., Ibrahim, I. A. A., and Qodriyah, H. M. S. (2015). Preventive effects of tocotrienol on stress-induced gastric mucosal lesions and its relation to oxidative and inflammatory biomarkers. *PLoS ONE* 10 (10), 01393488–e139414. doi:10.1371/journal.pone.0139348

Azlina, M. F. N., Qodriyah, H. M. S., Akmal, M. N., Ibrahim, I. A. A., and Kamisah, Y. (2019). *In vivo* effect of Piper sarmentosum methanolic extract on stress-induced gastric ulcers in rats. *Archives Med. Sci.* 15 (1), 223–231. doi:10.5114/aoms.2016.63156

Azlina, M. F. N., Qodriyah, H. M. S., Chua, K. H., and Kamisah, Y. (2017). Comparison between tocotrienol and omeprazole on gastric growth factors in stress-exposed rats. *World J. Gastroenterology* 23 (32), 5887–5894. doi:10.3748/wjg.v23.i32.5887

Bactiar, C. F., and Fahami, N. A. M. (2019). LC-MS analysis of phytocomponents in the methanol extract of piper sarmentosum leaves. *Pharmacogn. J.* 11 (5), 1071–1076. doi:10.5530/pj.2019.11.167

Chan, E. W. L., Yeo, E. T. Y., Wong, K. W. L., See, M. L., Wong, K. Y., and Gan, S. Y. (2019). Piper sarmentosum Roxb. Root extracts confer neuroprotection by attenuating beta amyloid-induced pro-inflammatory cytokines released from microglial cells. *Curr. Alzheimer Res.* 16 (3), 251–260. doi:10.2174/1567205016666190228124630

Chanwitheesuk, A., Teerawutgulrag, A., and Rakariyatham, N. (2005). Screening of antioxidant activity and antioxidant compounds of some edible plants of Thailand. *Food Chem.* 92 (3), 491–497. doi:10.1016/j.foodchem.2004.07.035

Cho, C. H. (2001). Current roles of nitric oxide in gastrointestinal disorders. *J. Physiology Paris* 95 (1–6), 253–256. doi:10.1016/S0928-4257(01)00034-1

Del Rio, D., Stewart, A. J., and Pellegrini, N. (2005). A review of recent studies on malondialdehyde as toxic molecule and biological marker of oxidative stress. *Nutr. Metabolism Cardiovasc. Dis.* 15 (4), 316–328. doi:10.1016/j.numecd.2005.05.003

Dinu, C., Diaconescu, C., and Avram, N. (2009). Gastric mucosa injury associated with oxidative stress. *Lucr. Stiintife Med. Veterinaara* XLII (2), 369–374.

Hajrezaie, M., Golbabapour, S., Hassandarvish, P., Gwaram, N. S., Hadi, A., Mohd Ali, H., et al. (2012). Acute toxicity and gastroprotection studies of a new schiff base derived copper (II) complex against ethanol-induced acute gastric lesions in rats. *PLoS ONE* 7 (12), e51537. doi:10.1371/journal.pone.0051537

Ibrahim, I. A. A., Kamisah, Y., Nafeeza, M. I., and Nur Azlina, M. F. (2012). The effects of palm vitamin E on stress hormone levels and gastric lesions in stress-induced rats. *Archives Med. Sci.* 8 (1), 22–29. doi:10.5114/aoms.2012.27276

Kamisah, Y., Ibrahim, A. A. I., Nafeeza, M. I., and Nur-Azlina, M. F. (2011). Palm tocotrienol-rich fraction supplementation suppressed stress-induced gastric oxidative stress in rats. *J. Appl. Pharm. Sci.* 1 (10), 118–122.

Ketuly, A., Hadi, K. A., Golbabapour, S., Hajrezaie, M., Hassandarvish, P., Ali, H. M., et al. (2013). Acute toxicity and gastroprotection studies with a newly synthesized steroid. *PLoS ONE* 8 (3), e59296–e59299. doi:10.1371/journal.pone.0059296

Khoubnasabjafari, M., Ansarin, K., and Jouyban, A. (2015). Reliability of malondialdehyde as a biomarker of oxidative stress in psychological disorders. *BioImpacts* 5 (3), 123–127. doi:10.15171/bi.2015.20

Konturek, S. J., Brzozowski, T., Konturek, P. C., Zwirska-Korczala, K., and Reiter, R. J. (2008). Day/night differences in stress-induced gastric lesions in rats with an intact pineal

gland or after pinealectomy. *J. Pineal Res.* 44 (4), 408–415. doi:10.1111/j.1600-079X.2007.00543.x

Kountouras, J., Boura, P., and Lygidakis, N. (2000). Omeprazole and regulation of cytokine profile in Helicobacter pylori-infected patients with duodenal ulcer disease. *Hepatogastroenterology* 47 (35), 1301–1304.

Kudryavtsev, K. V., Markevich, A. O., Virchenko, O. V., Falalyeyeva, T. M., Beregova, T. V., Ostapchenko, L. I., et al. (2014). Pharmacological correction of stress-induced gastric ulceration by novel small-molecule agents with antioxidant profile. *Sci. World J.* 2014, 217039. doi:10.1155/2014/217039

Kwiecień, S., Brzozowski, T., and Konturek, S. J. (2002). Effects of reactive oxygen species action on gastric mucosa in various models of mucosal injury. *J. Physiology Pharmacol.* 53 (1), 39–50.

Kwiecien, S., Ptak-Belowska, A., Krzysiek-Maczka, G., Targosz, A., Jasnos, K., Magierowski, M., et al. (2012). Asymmetric dimethylarginine, an endogenous inhibitor of nitric oxide synthase, interacts with gastric oxidative metabolism and enhances stress-induced gastric lesions. *J. Physiology Pharmacol.* 63 (5), 515–524.

Lanas, A. (2008). Role of nitric oxide in the gastrointestinal tract. *Arthritis Res. Ther.* 10 (2), S4–S7. doi:10.1186/ar2465

Ledwoz, A., Michalak, J., Stępień, A., Kądziołka, A., Stepien, A., et al. (1986). The relationship between plasma triglycerides, cholesterol, total lipids and lipid peroxidation products during human atherosclerosis. *Clin. Chim. Acta* 155 (3), 275–283. doi:10.1016/0009-8981(86)90247-0

Mittal, M., Siddiqui, M. R., Tran, K., Reddy, S. P., and Malik, A. B. (2014). Reactive oxygen species in inflammation and tissue injury. *Antioxidants Redox Signal.* 20 (7), 1126–1167. doi:10.1089/ars.2012.5149

Nimse, S. B., and Pal, D. (2015). Free radicals, natural antioxidants, and their reaction mechanisms. *RSC Adv.* 5 (35), 27986–28006. doi:10.1039/c4ra13315c

Nur Azlina, M. F., Kamisah, Y., Chua, K. H., and Qodriyah, H. M. S. (2013). Tocotrienol attenuates stress-induced gastric lesions via activation of prostaglandin and upregulation of COX-1 mRNA. *Evidence-Based Complementary Altern. Med.* 2013, 804796. doi:10.1155/2013/804796

Nur Azlina, M. F., Rubaizah, K., Siti Muliana, M., and Nafeeza, M. I. (2009). Modulation of restraint induced gastric oxidative changes in rats by tocotrienol and tocopherol. *Int. J. Pharmacol.* 5, 58–64. doi:10.3923/ijp.2009.58.64

Patlevič, P., Vašková, J., Švorc, P., Vaško, L., and Švorc, P. (2016). Reactive oxygen species and antioxidant defense in human gastrointestinal diseases. *Integr. Med. Res.* 5 (4), 250–258. doi:10.1016/j.imr.2016.07.004

Raja Kumar, S., Mohd Ramli, E. S., Abdul Nasir, N. A., Ismail, N. H. M., and Mohd Fahami, N. A. (2019). Preventive effect of naringin on metabolic syndrome and its mechanism of action: A systematic review. *Evidence-Based Complementary Altern. Med.* 2019, 9752826. doi:10.1155/2019/9752826

Rappaport, Z. H. (2006). Robotics and artificial intelligence: Jewish ethical perspectives. *Acta Neurochir. Suppl.* 98, 9–12. doi:10.1007/978-3-211-33303-7_2

Salehi, B., Zakaria, Z. A., Gyawali, R., Ibrahim, S. A., Rajkovic, J., Shinwari, Z. K., et al. (2019). Piper species: A comprehensive review on their phytochemistry, biological activities and applications. *Molecules* 24 (7), 1364. doi:10.3390/molecules24071364

Sawangjaroen, N., Sawangjaroen, K., and Poonpanang, P. (2004). Effects of Piper longum fruit, Piper sarmentosum root and Quercus infectoria nut gall on caecal amoebiasis in mice. *J. Ethnopharmacol.* 91 (2–3), 357–360. doi:10.1016/j.jep.2004.01.014

Sener, G., Paskaloglu, K., and Ayanoglu-Dülger, G. (2004). Protective effect of increasing doses of famotidine, omeprazole, lansoprazole, and melatonin against ethanol-induced gastric damage in rats. *Indian J. Pharmacol.* 36 (3), 171–174.

Sidahmed, H. M. A., Abdelwahab, S. I., Mohan, S., Abdulla, M. A., Mohamed Elhassan Taha, M., Hashim, N. M., et al. (2013). α -mangostin from cratoxylum arborescens (vahl) blume demonstrates anti-ulcerogenic property: A mechanistic study. *Evidence-Based Complementary Altern. Med.* 2013, 450840. doi:10.1155/2013/450840

Subramaniam, V., Adenan, M. I., Ahmad, A. R., and Sahdan, R. (2003). Natural antioxidants: Piper sarmentosum (kadok) and Morinda elliptica (mengkudu). *Malays. J. Nutr.* 9 (1), 41–51.

Sun, X., Chen, W., Dai, W., Xin, H., Rahmand, K., Wang, Y., et al. (2020). Piper sarmentosum Roxb: A review on its botany, traditional uses, phytochemistry, and pharmacological activities. *J. Ethnopharmacol.* 263, 112897. doi:10.1016/j.jep.2020.112897

Wang, D., Zhou, L., Hanlin, Z., and Hou, G. (2020). Piper sarmentosum extract alleviates inflammatory responses and improves barrier function in porcine intestinal epithelial (IPEC-J2) cells induced by lipopolysaccharide (LPS). *J. Ethnopharmacol.* doi:10.21203/rs.3.rs-17917/v1

Wang, F., Meng, W., Wang, B., and Qiao, L. (2014). Helicobacter pylori-induced gastric inflammation and gastric cancer. *Cancer Lett.* 345 (2), 196–202. doi:10.1016/j.canlet.2013.08.016

Watanabe, T., Arakawa, T., Fukuda, T., Higuchi, K., and Kobayashi, K. (1997). Role of neutrophils in a rat model of gastric ulcer recurrence caused by interleukin-1 beta. *Am. J. Pathology* 150 (3), 971–979.

Watanabe, T., Higuchi, K., Tominaga, K., Fujiwara, Y., and Arakawa, T. (2001). Acid regulates inflammatory response in a rat model of induction of gastric ulcer recurrence by interleukin 1beta. *Gut* 48 (6), 774–781. doi:10.1136/gut.48.6.774

Zakaria, Z. A., Patahuddin, H., Mohamad, A. S., Israf, D. A., and Sulaiman, M. R. (2010). *In vivo* anti-nociceptive and anti-inflammatory activities of the aqueous extract of the leaves of Piper sarmentosum. *J. Ethnopharmacol.* 128 (1), 42–48. doi:10.1016/j.jep.2009.12.021

Zhang, A., Pastor, L., Nguyen, Q., Luo, Y., Yang, W., Flagella, M., et al. (2005). Small interfering RNA and gene expression analysis using a multiplex branched DNA assay without RNA purification. *J. Biomol. Screen.* 10 (6), 549–556. doi:10.1177/1087057105277414

frontiers | Frontiers in Pharmacology

TYPE Original Research
PUBLISHED 08 February 2023
DOI 10.3389/fphar.2023.1006265

OPEN ACCESS

EDITED BY
Ahmad Nazrun Shuid,
MARA University of Technology, Malaysia

REVIEWED BY
Chinedum Ogbonnaya Eleazu,
Alex Ekwueme Federal University, Ndufu-Alike, Ikwo (AE-FUNAI), Nigeria
Yuhaniza Kamsani,
MARA University of Technology, Malaysia

*CORRESPONDENCE
Suzana Makpol,
suzanamakpol@ppukm.ukm.edu.my

SPECIALTY SECTION
This article was submitted to Ethnopharmacology, a section of the journal Frontiers in Pharmacology

RECEIVED 29 July 2022
ACCEPTED 16 January 2023
PUBLISHED 08 February 2023

CITATION
Razak AM, Zakaria SNA, Abdul Sani NF, Ab Rani N, Hakimi NH, Mohd Said M, Tan JK, Gan HK, Mad Nordin MF and Makpol S (2023), A subcritical water extract of soil grown *Zingiber officinale* Roscoe: Comparative analysis of antioxidant and anti-inflammatory effects and evaluation of bioactive metabolites.
Front. Pharmacol. 14:1006265.
doi: 10.3389/fphar.2023.1006265

A subcritical water extract of soil grown *Zingiber officinale* Roscoe: Comparative analysis of antioxidant and anti-inflammatory effects and evaluation of bioactive metabolites

Azraul Mumtazah Razak[1,2], Siti Nor Asyikin Zakaria[1], Nur Fathiah Abdul Sani[1], Nazirah Ab Rani[1], Nur Haleeda Hakimi[1], Mazlina Mohd Said[3], Jen Kit Tan[1], Han Kwang Gan[4], Mariam Firdhaus Mad Nordin[5] and Suzana Makpol[1]*

[1]Department of Biochemistry, Faculty of Medicine, Universiti Kebangsaan Malaysia, Kuala Lumpur, Malaysia, [2]Faculty of Health Sciences, University College of MAIWP International, Kuala Lumpur, Malaysia, [3]Centre of Drug and Herbal Research, Faculty of Pharmacy, Universiti Kebangsaan Malaysia, Kuala Lumpur, Malaysia, [4]Millercle Resources Sdn Bhd, Klang, Malaysia, [5]AM Zaideen Ventures Sdn Bhd, Kuala Lumpur, Malaysia

Introduction: Ginger (*Zingiber officinale* Roscoe) can scavenge free radicals, which cause oxidative damage and inflamm-ageing. This study aimed to evaluate the antioxidant and anti-inflammatory effects of soil ginger's sub-critical water extracts (SWE) on different ages of Sprague Dawley (SD) rats. The antioxidant properties and yield of SWE of soil- and soilless-grown ginger (soil ginger and soilless ginger will be used throughout the passage) were compared and evaluated.

Methods: Three (young), nine (adult), and twenty-one (old) months old SD rats were subjected to oral gavage treatments with either distilled water or the SWE of soil ginger at a concentration of 200 mg/kg body weight (BW) for three months.

Results: Soil ginger was found to yield 46% more extract than soilless ginger. While [6]-shogaol was more prevalent in soilless ginger, and [6]-gingerol concentration was higher in soil ginger ($p < 0.05$). Interestingly, soil ginger exhibited higher antioxidant activities than soilless ginger by using 2,2-diphenyl-1-(2,4,6-trinitrophenyl) hydrazyl (DPPH) and ferric reducing antioxidant power (FRAP) assay. With ginger treatment, a reduced levels of tumour necrosis factor-α (TNF-α) and C-reactive protein (CRP) but not interleukin-6 (IL-6) were observed in young rats. In all ages of SD rats, ginger treatment boosted catalase activity while lowering malondialdehyde (MDA). Reduction of urine 15-isoprostane F_{2t} in young rats, creatine kinase-MM (CK-MM) in adult and old rats and lipid peroxidation (LPO) in young and adult rats were also observed.

Discussion: The findings confirmed that the SWE of both soil and soilless grown ginger possessed antioxidant activities. Soil ginger produced a higher yield of extracts with a more prominent antioxidant activity. The SWE of soil ginger treatment on the different ages of SD rats ameliorates oxidative stress and inflammation responses. This could serve as the basis for developing a nutraceutical that can be used as a therapeutic intervention for ageing-related diseases.

KEYWORDS

Zingiber officinale Roscoe, antioxidant, anti-inflammatory, anti-ageing, sub-critical water extraction

1 Introduction

Ginger is a Zingiberaceae perennial plant. It has been harvested for countless generations as a spice and use in herbal remedies (Mohd et al., 2012). Ginger can be collected whether it is young (between three and 4 months old) or mature (8–10 months) (Marsh et al., 2021). Nutritional support for the growth of a plant is provided by soil (Fussy and Papenbrock, 2022). The conventional method of ginger cultivation is soil-bound, using a shifting cultivation technique. This technique mainly produces land corrosion in the highlands, and it takes 6 years to resolve the issue of soil infertility before replanting can be done (Shuhaimi et al., 2016). Consequently, a different approach to solving this issue is to grow ginger using the soilless culture system. By growing ginger without soil, soilborne ailments like *Fusarium oxysporum, Pseudomonas solanacearum* that might infect the plant root, and leaf spot illnesses, can be avoided. The availability of water and nutrients for the plant may be significantly influenced by the substrate, which may also impact on the metabolic processes involved in synthesing the bioactive chemicals. This technique uses substrates of rock wool, perlite, vermiculite and peat (Mohd et al., 2015).

Several bioactive compounds are present in ginger. They include terpenes (Halimin et al., 2022) and phenolic substances such as gingerols, shogaols, and paradols. The combinations of [6]-gingerol, [6]-shogaol, [10]-gingerol, gingerdiones, gingerdiols, paradols, [6]-dehydrogingerols, [5]-acetoxy-6-gingerol, [3,5]-diacetoxy-[6]-gingerdiol, and [12]-gingerol are responsible for its recognised biological activity (Zammel et al., 2021; Arcusa et al., 2022). The two most potent active ingredients are [6]-shogaol and [6]-gingerol (Mao et al., 2019; Aghamohammadi et al., 2020; Zammel et al., 2021). Studies on ginger rhizomes have revealed that it exhibits a wide range of bioactivities including neuroprotective (Sapkota et al., 2019), hepatoprotective (Bekkouch et al., 2022), gastroprotective effects (Ebrahimzadeh Attari et al., 2019), photoprotective effect (Nobile et al., 2016), antimicrobial (Abdullahi et al., 2020), anti-obesity (Seo et al., 2021), anticancer (Osman et al., 2021), anti-inflammatory (Askari et al., 2020) and antioxidant properties (Hur et al., 2020).

A state known as “oxidative stress”, which is defined as “an imbalance between reactive species (RS), reactive oxygen species (ROS), and antioxidant reserve”, is linked to ageing and chronic disease (Mao et al., 2019). Alterations in DNA transcription and a reduction in the ability to repair DNA could result from oxidative damage to macromolecules such as lipids, proteins and DNA. Oxidative stress and high concentration of polyunsaturated fatty acids (PUFAs) in cellular or organelle membranes induce lipid peroxidation which results in the release of α - and β-unsaturated reactive aldehydes (Taso et al., 2019) such as malondialdehyde (MDA), 4-hydroxy-2-noneal (HNE), and acrolein, which are the most reactive (Mas-Bargues et al., 2021). When ROS oxidize membrane phospholipids, lipid hydroperoxide (LPO) molecules are produced within the cell membrane (Thimraj et al., 2018). These aldehydes can bond covalently with biological components. Besides, the oxidation of arachidonic acid and docosahexaenoic acid (DHA) also produces lipid peroxidation products such as isoprostanes (IsoPs) and neuroprostanes (neuroPs) (Taso et al., 2019). They also cause an increase in nitric oxide (NO) which subsequently leads to a considerable drop in the blood levels of endogenous antioxidants such as glutathione (GSH), superoxide dismutase (SOD) and catalase (CAT) (Nandi et al., 2019).

The imbalance of the normal redox state exponentially develops with age and is accompanied by a remarkable decrease in the cell repair system. Inflammageing, a modest, low-grade chronic inflammatory condition, has been reported to contribute to ageing (Sanada et al., 2018) with an elevation of proinflammatory cytokines, chemokines, and adipokines interleukin-1ß (IL-1ß), interleukin-6 (IL-6), tumour necrosis factor-α (TNF-α), and monocyte chemoattractant protein-1 chemokine (C-C motif ligand 2, CCL2) as the most important characteristics (Jalali et al., 2020). In healthy individuals, initial defence against pathogens and the injury-repair cycle depends on inflammation (Petersen and Smith, 2016). These inflammatory mediators may persist excessively for a long time, leading to chronic inflammation. Chronic inflammatory diseases can cause persistently high C-reactive protein (CRP) values (Sproston and Ashworth, 2018). The aberrant release of TNF-α causes psoriasis, psoriatic arthritis, and non-infectious uveitis (NIU) (Zhou et al., 2020; Jang et al., 2021). As ageing is the primary risk factor for most neurodegenerative diseases in humans (Hou et al., 2019), age-related disorders may be delayed, if not prevented, by therapies that use phytochemicals to target the ageing process. Since the antioxidant properties of plants could stem from their polyphenolic compounds, it is crucial to assess the polyphenolic contents of these plants, which could be extracted using various techniques.

Various extraction techniques which incorporated inorganic solvents can be used in the plant extraction process (Dias et al., 2021). The use of these solvents during the extraction and downstream processing of medicinal herbs is constrained as many organic solvents can be toxic to humans, depending on the level of exposure. It is almost impossible to remove the residual solvents completely from liquid and dried herbal extracts (Truong et al., 2019). Subcritical-water extraction, an eco-friendly process uses only water to extract phytochemical components and can concentrate less-polar chemicals quickly (Ko et al., 2020). Hence, this study aimed to evaluate the antioxidant and anti-inflammatory effects of the sub-critical water extracts of soil ginger on different ages of Sprague Dawley (SD) rats. We also assessed and compared the antioxidant properties and yield of SWE of soil- and soilless-produced ginger.

2 Materials and methods

2.1 Plant materials

Thirty kilograms of fresh rhizomes of young soil grown ginger and 30 kg of fresh rhizomes of young soilless grown ginger aged 150 days were supplied by Millercle Resources Sdn. Bhd. The soilless ginger grows in 100% cocopeat. The voucher specimens were identified and deposited at the Universiti Kebangsaan Malaysia's Herbarium (UKMB), Bangi (ID016/2021).

2.2 Extraction

Unpeeled ginger rhizomes were washed and grinded to increase the surface area by 1:3 solid-to-liquid ratio. The extraction was performed in 70 L subcritical water extraction at the optimum temperature and pressure of 120°C and 10 bar, respectively. The processing time of 5, 10, 15 and 20 min were used with a solvent-to-solid ratio of 28/2 $mLmg^{-1}$. The subcritical water extraction was performed by inserting the grounded ginger (weight varied based on the solvent-to-solid ratio for each run) into a sample holder placed in the extraction vessel and filled with distilled water (2.5 L). A fitting cover was installed on top of the extraction vessel to prevent pressure loss during the extraction process. Nitrogen gas was used to purge the oxygen present in the solution. The required pressure was maintained until the experiment was completed. Finally, the extracts were streamed into the cooling vessels to be collected for analysis and further drying.

2.3 Chromatographic analysis

Two selected chemical markers for the extract, [6]-gingerol and [6]-shogaol were identified and quantified using HPLC (Waters Alliance 2,695, United States) equipped with a PhotoDiode Array Detector (Waters 2,996, United States) Table 1 and the Empower Chromatography Data System for data processing. Analysis method were adapted from Mohd Sahardi et al. (2021) and optimized to the following parameters:

The extraction yield was calculated using the equation below:

TABLE 1 HPLC parameters for chromatographic analysis.

HPLC Parameters	Condition
Column	C_{18} reversed-phase column
Mobile phase	As the mobile phases A and B, respectively, we utilized water and 100% acetonitrile (Merck, Germany). The active components of ginger were separated as follows: the volumetric ratio was 70:30 from 0 to 15 min; 5.0:95 from 15 to 16 min; 5.0:95 from 16 to 17 min; and 70:30 from 17 to 20 min.
Flow rate	0.4 mL/min
Detector	Photodiode array (PDA) at 282 nm

$$Extraction\ yield\ (\%\ yield) = (W1{*}100)/W2$$

*W1 is the weight of the extract
*W2 is the weight of the plant powder

2.4 Preparation of controls for ferric reducing antioxidant power (FRAP) and 2,2-diphenyl-1-picrylhydrazyl (DPPH) assays

Tocotrienol-rich fraction (TRF) purchased from Sime Darby Sdn. Bhd., Selangor, Malaysia (TRF Gold Tri E 50) and Vitamin C (L-ascorbic acid 99%, Sigma, United States) were used as controls for the DPPH assay. Each ginger extract and control were weighed and diluted with either 100% ethanol or 95% ethanol and ultrapure water based on its solubility characteristics to create 10 mg/mL of the stock solutions.

2.5 DPPH free radical scavenging activity

The free radical scavenging activity of ginger extracts was measured using DPPH. Briefly, 40 mL of acetate buffer and 60 mL of methanol (both from Merck, Germany) were combined to make the stock solution of 1,1-diphenyl-2-picryl-hydrazyl (Sigma, United States) (pH 5.5). The appropriate diluents were used to dilute a series of final concentrations of the ginger extracts and the controls to 0, 10, 20, 50, 100, 200, 500, and 1,000 μg/mL. Then, a vortex was used to combine .75 mL of the diluted extract or control with 1.5 mL of .009 $mgmL^{-1}$ DPPH in methanol. Following the incubation, the mixture was let to stand at room temperature for 10 min. The absorbance was determined at a wavelength of 517 nm by EnSpire Multimode Plate Reader (Perkin Elmer, Singapore). Methanol served as a standard (Ac). The inhibition percentage was calculated using the formula below (Garcia et al., 2012):

$$Inhibition = \frac{Ac - As}{Ac}\ x\ 100$$

2.6 FRAP assay

Two point 5 mL of TPTZ 2,4,6-tri (2-pyridyl-1,3,5-triazine) (Sigma, United States), 2.5 mL of ferric chloride hexahydrate (FeCl3.6H2O) solution (20 mM) (Merck, United States), and 2.5 mL of acetate buffer (300 mM; pH 3.6) (Merck, Germany) were mixed in a ratio of 1:1:30 to create the FRAP reagent. Then, 1.2 mL of the FRAP reagent were added to the ginger extract and control solution to make a final concentration of 0, 10, 20, 50, 100, 200, 500, or 1,000 μgmL^{-1}. The mixtures were incubated for 10 min and absorbance were recorded at 593 nm by EnSpire Multimode Plate Reader (Perkin Elmer, Singapore). The sample's antioxidant capacity was assessed using a standard curve of ferrous sulfate ($FeSO_47H_2O$) (Sigma, United States).

2.7 Animal model

The Sprague Dawley (SD) rats were purchased from the Universiti Kebangsaan Malaysia Laboratory Animal Resource Unit (LARU). Throughout the study, the rats were housed in animal care

facilities with a 12-h light/dark cycle and a temperature of 24°C. Rats also had unrestricted access to water and rat pellets (Gold Coin, Malaysia). The rat pellet has an approximate nitrogen-free extract content of 49%, a minimum crude protein content of 22%, a maximum crude fiber content of 5%, a minimum crude fat content of 3.0%, a maximum moisture content of 13%, and a minimum ash content of 8%. The bedding for the rats was Kenaff (Muhaaz Enterprise, Terengganu, Malaysia) and was changed twice a week. Animals were separated into three groups: 18 male young SD rats aged 3 months, 18 male adults aged 9 months, and 18 old males aged 21 months (Makpol et al., 2020). Each group was further divided into two groups, with Group 1 receiving 1 mL of distilled water as the control (n = 8) and Group 2 receiving 200 mg/kg/day of soil *Z. officinale* Roscoe extract (n = 10) daily for 3 months. Prior to receiving therapy, each rat was kept in a cage for a week in a Sealsafe® Plus Rat IVC Green Line (TECHNIPLAST, Varese, Italy) for acclimatization. For each test carried out, the animals were tested according to their groupings, commencing with Group 1 and moving on to Group 2. The Universiti Kebangsaan Malaysia Animal Ethics Committee approved the experimental plan (UKMAEC Approval Number: BIOK/PP/2018/SUZANA/14-MAY/924-JUNE-2018-MAY-2020). Figure 1 shows the experimental design for this research. The animal numbers were selected based on a previous study (Makpol et al., 2020).

2.8 Urine collection

One milliliter of rat's urine was collected *via* spontaneous urination into a clear plastic bag on day 0 and day 90 of treatment using a pipette tip. Prior to analysis, the urine was stored in a freezer set at −80°C.

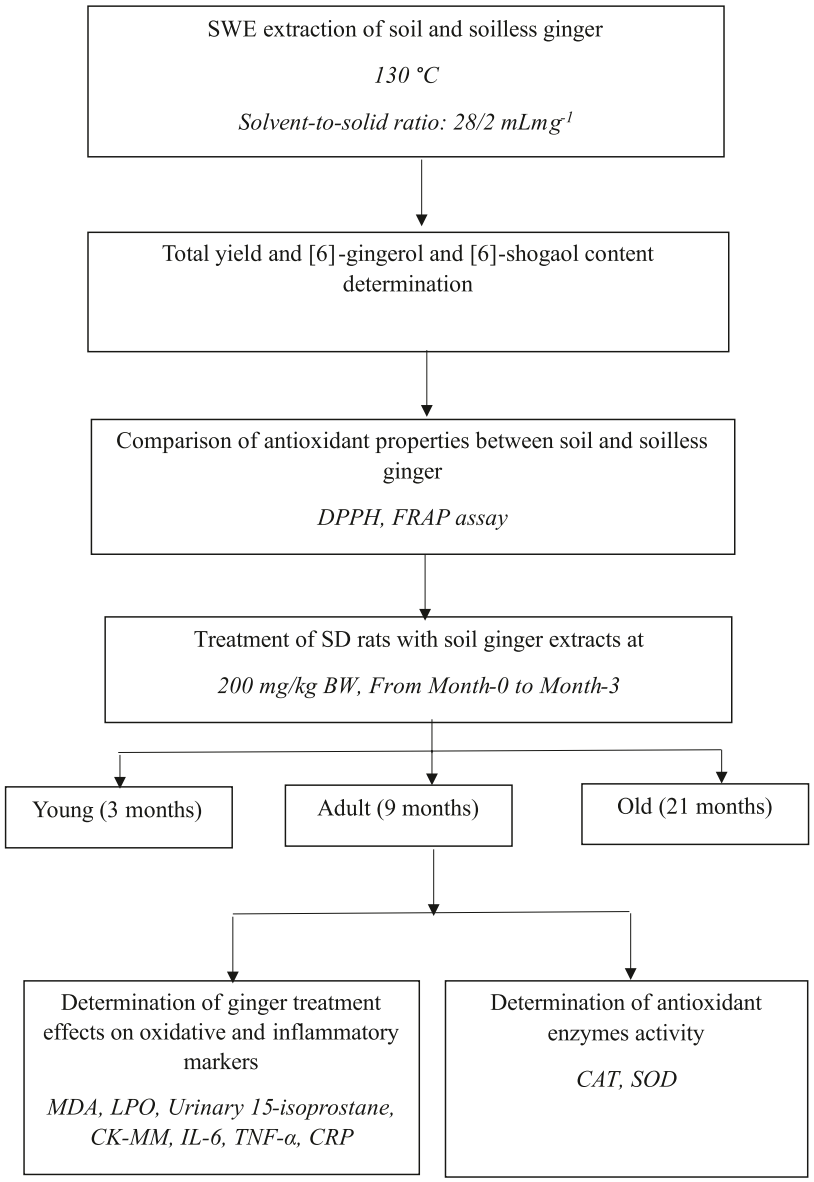

FIGURE 1
Diagram showing the experimental process and the study's objectives.

2.9 Blood collection

Blood was withdrawn from each rat through the orbital sinus collection technique on day 0 and day 90 of treatment. After centrifuging the collected blood in the EDTA tube at 3,000 rpm for 10 min at 4°C, the plasma was stored in a—80°C freezer until analysis.

2.10 Euthanisation of animals

KTX agents with a mixture of ketamine, xylazine, and zoletil-50 (tiletamine and zolazepam) were used as anesthetics in this study due to their effectiveness, speed, minimal discomfort, anxiety, and distress. The KTX agents were injected intraperitoneally at a dose of 0.1 mL/250 g of body weight (BW). They were sacrificed by decapitation.

2.11 Collection of organs

On day 90, all rats were fasted overnight before being euthanized for necropsy analysis. Gastrocnemius muscles were obtained from the rats. The organs were cleaned in 90% normal saline to remove any adhering tissue before weighing. The organ weight was measured as soon as possible to prevent drying, and it's relative to the animals' body weight (BW) was analyzed.

2.12 MDA analysis

Analysis of MDA in rat plasma was conducted in accordance with a previous study (Hamezah et al., 2017). The reagent was prepared through mixing of 5 mM DNPH (2,4-dinitrophenyl benzine) (Sigma Aldrich, St. Louis, MO, United States), 2 M HCl (hydrochloric acid) (Sigma Aldrich, St. Louis, MO, United States), 35% perchloric acid ($HClO_4$) (Merck, Germany), 1% sulfuric acid (H_2SO_4) and 1.3 M NaOH (natrium hydroxide, Merck, Germany). 12.5 µL TEP (1,1,3,3-tetraethoxypropane) (Sigma Aldrich, St. Louis, MO, United States) and 50 mL 1% sulfuric acid were combined and incubated overnight at 4 °C to produce mega stock solution (1 mM stock solution). For working standard (100 uM), 500 µL TEP (Mega stock) was added to 4.5 mL mili Q water. 380 mL acetonitrile (HPLC Grade, Merck, Germany), 620 mL mili Q and 2 mL of acetic acid (Merck, Germany) were used as the mobile phase. This mixture was filtered by a .45 µm filter membrane using a vacuum pump and sonicated for 20 min to de-gas. A series of standard concentrations (Table 2) was prepared. Briefly, 50 µL standard/sample was added to 200 µL 1.3 M NaOH. This mixture was incubated in a 60°C water bath for 1 h for alkaline hydrolysis of protein-bound followed by 5 min of a cooling period in ice. Thirty-five percent perchloric acid was added and further centrifuged at 10,000 g, 10 min, and 4°C to precipitate the protein. Three hundred microliter supernatant was transferred and added with 12.5 µL, 5 mM DNPH. This mixture was incubated at room temperature for 30 min. Standard/sample was filtered (size .45 µm) and transferred into an insert in the vial.

Five microliter of sample was injected onto the UPLC system (Waters Alliance 2,695, United States) equipped with PhotoDiode Array Detector (Waters 2,996, United States). The reverse-phase Acquity UPLC® BEH C18, 1.7 m, 2.1 mm 50 mm column was part of the UPLC system. Photodiode array detection was set at a wavelength of 310 nm and a programmed solvent delivery system with a flow rate of 0.4 mL/min (Waters Corporation, Milford, MA, United States). By contrasting the retention period of the sample with the established standard, plasma MDA was determined. The sample's MDA had a 2.6-min retention period, which permitted an entire chromatographic run every 5 minutes. The peak area of the external standards was used to compute the MDA concentrations, and the results from the calibration curves were expressed in nmol/mL. Each sample was analyzed simultaneously.

TABLE 2 Standard concentration for MDA analysis.

MDA (µM)	Mili Q H_20 (µL)	Working standard
10	900	100
20	800	200
30	700	300
40	600	400
50	500	500

2.13 Antioxidant enzyme activity

The activities of the antioxidant enzymes catalase (CAT) and superoxide dismutase (SOD) in rat plasma were assessed using Catalase Assay kit (Cayman, Ann Arbor, MI, United States) and Superoxide Dismutase Assay Kit (Cayman, Ann Arbor, MI, United States), by referring to the kits' manuals. The absorbance was measured at wavelengths of 540 nm for CAT and 440–460 nm for SOD by EnSpire Multimode Plate Reader (Perkin Elmer, Singapore). The results were presented as µmol/min/mL and U/mL for CAT and SOD activity, respectively. A bsorbance was measured at wavelengths of 540 nm for CAT and 440–460 nm for SOD. The results were presented as µmol/min/mL for CAT activity. SOD activity was shown as U/mL.

2.14 Analysis of urinary oxidative stress

Urine samples from each rat were tested for 15-isoprostane F_{2t} activity using a urinary isoprostane ELISA kit (Oxford Biomedical Research, Oxford, United States) according to the manufacturer's instruction. The sample was prepared by adding 100 L of urine to an anti-15-isoprostane F_{2t}-coated well plate following dilution with glucuronidase. The 15-isoprostane F_{2t} horseradish peroxidase (HRP) conjugate and tetramethylbenzidine (TMB) substrate were then added to the mixture. An EnSpire Multimode Plate Reader (Perkin Elmer, Singapore) quantified the produced colour as the absorbance at 650 nm. Based on the data collected and the standard curve produced using the given standard solution, the isoprostane concentration (ng/mL) of each sample was calculated.

2.15 Analysis of creatine kinase-MM (CK-MM)

CK-MM activity was assessed using a Rat CK-MM ELISA Kit (Life Diagnostics Inc., West Chester, PA, United States) in accordance with the manufacturer's instructions. The sample was prepared by diluting a total of 25 L of plasma with a diluent before being transferred to microtiter

plates that were coated with an anti-rat CK-MM antibody. Then, TMB reagent was added to each well and lastly, enzyme conjugates. After adding the stop solution to halt the reaction, the plates were gently shaken so that their absorbance could be measured at 450 nm using an EnSpire Multimode Plate Reader (Perkin Elmer, Singapore). Based on the results, each sample's CKMM concentration (ng/mL) was determined using the standard curve that was plotted using the supplied standard solution.

2.16 Analysis of skeletal muscle oxidative stress

Lipid peroxidation marker, and lipid hydroperoxides were analyzed using Lipid Hydroperoxide (LPO) assay kit (Cayman Chemical, Ann Harbor, MI, United States), in accordance with the manufacturer's instructions. To prevent batch-to-batch variability, all samples for each lipid peroxidation marker were examined in the same batch. In summary, 100 mg of gastrocnemius muscle was homogenized using PBS buffer containing .5 M BHT. After adding the R2 reagent, clear supernatant homogenates were generated, which were then combined with the diluted R1 reagent. Through redox interactions with ferrous ions and thiocyanate as the chromogen, this kit directly assessed the lipid hydroperoxide radicals. Three duplicates of each sample were plated. By using an EnSpire Multimode Plate Reader (Perkin Elmer, Singapore) at 500 nm, the supernatant absorbance was measured. The data were computed to determine the concentration of each sample using a standard curve from the provided standard solution. By adjusting each sample's spectrophotometrically measured absorbance (500 nm) to μM using a hydroperoxide concentration standard curve, the average lipid hydroperoxide concentration for each sample was determined using this calculation:

Hydroperoxide concentration in sample (μM):

$$\frac{Hydroperoxide\ values\ of\ the\ sample\ tubes\ (HPST)}{Volume\ of\ extract\ used\ for\ the\ assay\ (VE)} \text{ X } \frac{1\ mL}{Volume\ of\ the\ original\ sample\ used\ for\ extraction\ (SV)}$$

2.17 Measurement of inflammatory biomarkers

By using an ELISA kit from Elabscience Biotechnology (United States), the levels of inflammatory biomarkers including IL-6 (E-EL-R0015), TNF-α (E-EL-R0019), and CRP (E-EL-R3002) were assessed in a 96-well plate. In order to get the plasma, the blood was collected into heparin tubes and separated for 15 min at 1,000 g at 4°C. The 96-well plate was then filled with the plasma, which was then incubated for 90 min at 37°C. Utilizing the EnSpire Multimode Plate Reader (Perkin Elmer, Singapore), the absorbance of IL-6, TNF-α, and CRP was measured at 450 nm and compared to the standard curve.

2.18 Statistical analysis

The results of each experiment were recorded as mean ± standard deviation, with each experiment carried out in triplicate. One-way or two-way ANOVA was used to analyze the significant differences, and multiple comparisons were performed using the Bonferroni or Tukey test *post hoc* test. Levene's test was used to test the homogeneity of the variances. Old rats and young rats were compared using Student's t-tests. $P < .05$ was considered as a significant difference in the analysis, which was conducted using SPSS software version 28.

3 Results

3.1 Determination of total yield of dry extract

Thirty kilograms of soilless ginger yielded 440 g (1.46%) of ginger extract while 950 g (3.17%) of ginger extract was yielded from soil ginger (Figures 2A, B).

3.2 Total amount of phenolic compounds, [6]-Gingerol and [6]-Shogaol (μg/mL)

In comparison to soilless ginger, the total amount of [6]-gingerol was significantly higher in soil ginger extract at 5, 10, 15, and 20 min of extraction ($p < .05$) (Figure 3A). On the other hand, the total amount of [6]-shogaol was higher in 5 min and 10 min of extraction time compared to soilless ginger ($p < .05$). Contrarily, compared to soil ginger, the amount

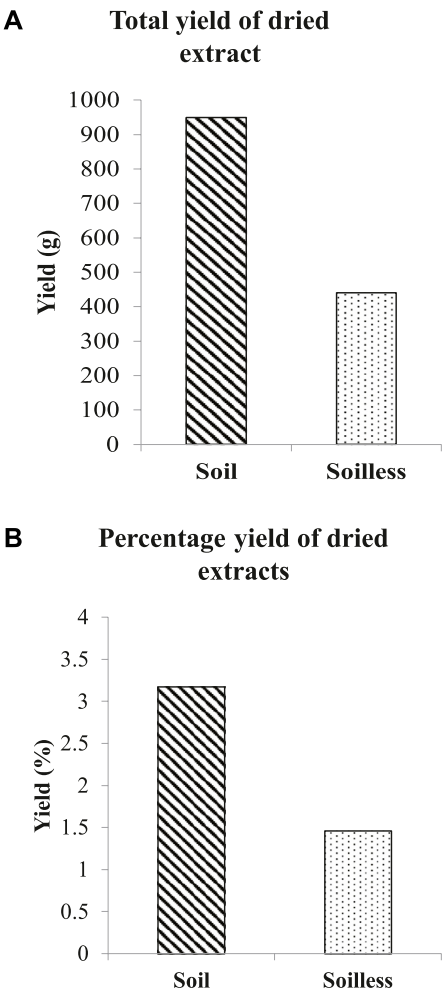

FIGURE 2
Total yield of dried extracts of soil and soilless ginger in g **(A)** and % **(B)**.

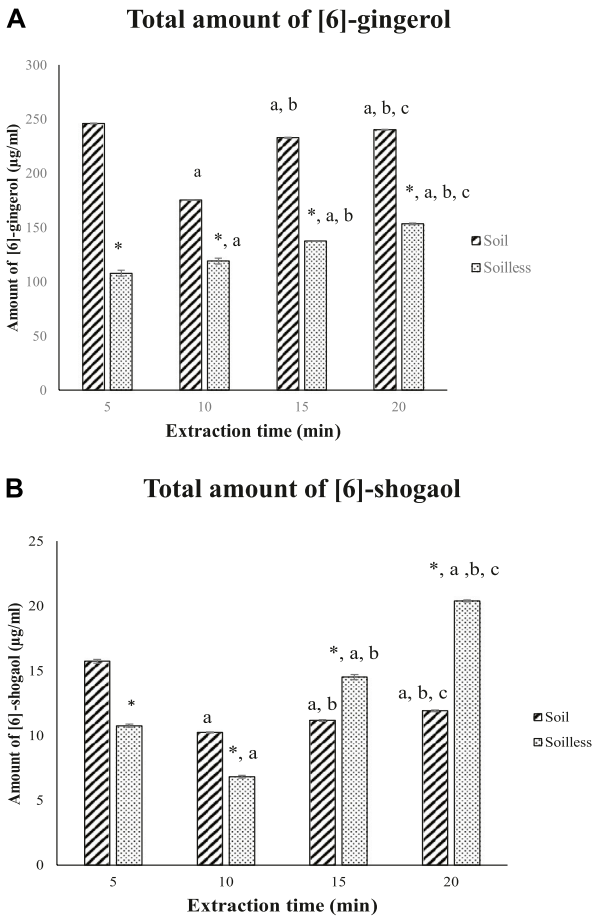

FIGURE 3
Total amount of [6]-gingerol **(A)** and [6]-shogaol **(B)** (µg/mL) for both soil and soilless ginger. Data presented as mean ± SD (n = 6), *$p < .05$ indicates a significant difference from the soil at the corresponding extraction time [a]$p < .05$ indicates a significant difference from the extraction time of 5 min; [b]$p<.05$ indicates a significant difference from the extraction time of 10 min; And [c]$p < .05$ indicates a significant difference from the extraction time of 15 min

of [6]-shogaol in soilless ginger was significantly increased with increasing extraction time (15 min and 20 min) ($p < .05$) (Figure 3B).

3.3 Total percentage of phenolic compounds, [6]-Gingerol and [6]-Shogaol (%)

The total percentage of [6]-gingerol was significantly higher in soil ginger extract at 5, 15 and 20 min of extraction time compared to soilless ginger at respective extraction times. No significant difference in the percentage of [6]-gingerol was observed at 10 min of extraction time between soil and soilless ginger although the percentage of [6]-gingerol increased significantly during this interval compared to 5 min of extraction time ($p < .05$) (Figure 4A). In contrast, the percentage of [6]-shogaol was significantly higher in soilless ginger at 5, 15 and 20 min of extraction time ($p < .05$, Figure 4B) compared to soil ginger.

3.4 DPPH radical scavenging activity

By using DPPH assay, soil ginger at 5 min of extraction time (B5) with a concentration of 1,000 µg/mL exhibited higher antioxidant activities than soilless ginger at 5 min and 20 min of extraction times (A5, A20) with similar concentrations (Table 3; Figure 5).

3.5 FRAP activities

Soil ginger with a concentration of 1,000 µg/mL at all extraction times (B5, B10, B15 B20) exhibited higher antioxidant activities than the soilless ginger at similar concentrations and respective extraction times (A5, A10, A15, A20) with the highest activity was by soil ginger at 20 min of extraction time (B20) (Table 4; Figure 6).

3.6 Level of oxidative stress markers in the tissue, plasma, and urine

When compared to the young control rats at month 0, the plasma level of CKMM was significantly higher in the older rats ($p < .05$) (Figure 7A). At month 3, adult and elderly rats were shown to have similar increases in plasma CKMM compared to their respective control groups ($p < .05$). In comparison to the

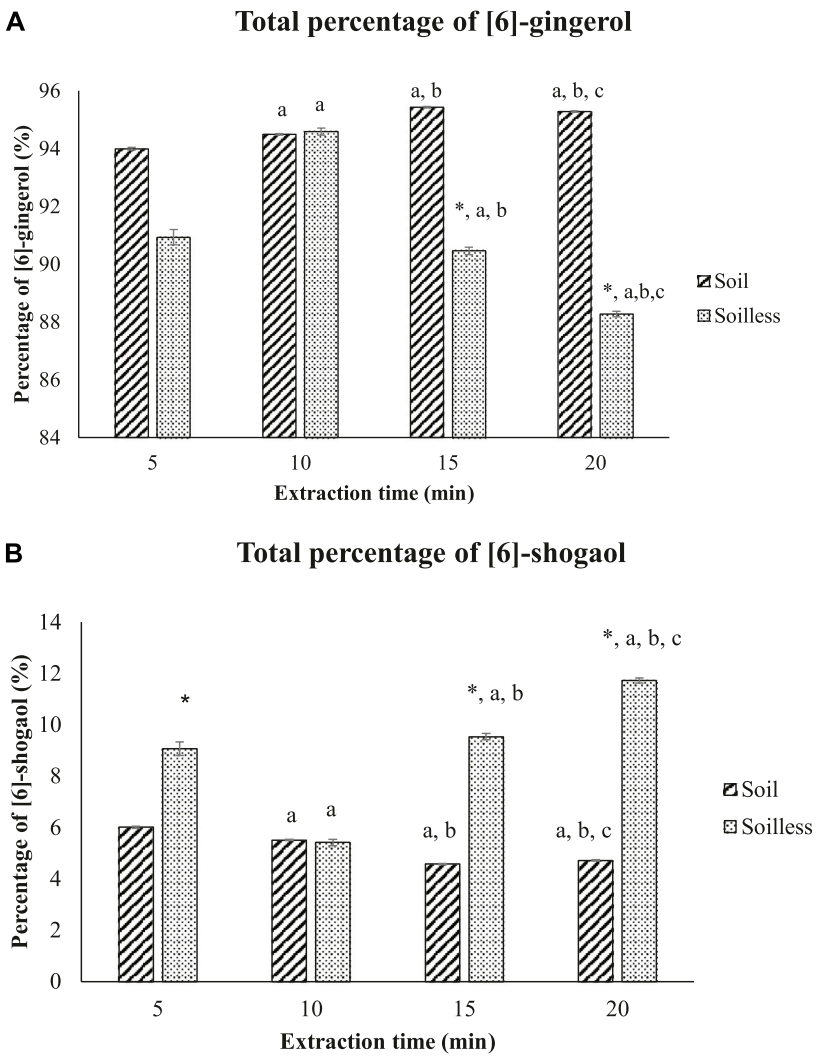

FIGURE 4
Percentage of [6]-gingerol **(A)** and [6]-shogaol **(B)** in both soil and soilless ginger. Data presented as mean ± SD (n = 6), *$p < .05$ indicates a significant difference from the soil at the indicated extraction time; [a]$p < .05$ indicates a significant difference from the extraction time of 5 min; [b] $p < .05$ indicates a significant difference from the extraction time of 10 min; [c]$p<.05$ indicates a significant difference from the extraction time of 15 min.

untreated adult and old rats at month 0, ginger administration significantly reduced plasma CKMM in both groups at month 3 ($p < .05$). For LPO, when compared to young control rats, lipid hydroxyperoxide was significantly higher in adult control rats ($p < .05$). When compared to the untreated groups, ginger treatment significantly decreased LPO levels in both young and adult rats ($p < .05$). As opposed to their untreated aged group, ginger therapy dramatically raises the LPO level in old rat groups. ($p < .05$) (Figure 7B). We observed a stable MDA level in all control rats. When compared to the untreated young and old rats at month 0, ginger treatment dramatically lowered the MDA levels in both young and old rats at 3 months of treatment. ($p < .05$) (Figure 7C). At month 0 compared to their controls, the urine 15-isoprostane F2t levels were significantly higher in the adult and old groups. Compared to the untreated groups at month 0, ginger treatment significantly reduced the concentration of 15-isoprostane F_{2t} in both young and old rat groups at month 3 ($p < .05$, Figure 7D).

3.7 Level of antioxidant enzymes

When compared to young control rats, there was a substantial decline in T-SOD activity ($p < .05$) in old rats. On the other hand, neither the ginger intervention nor the control significantly changed the SOD activity in young or adult rats (Figure 8A) after 3 months of treatment. In terms of catalase activity, when compared to young control rats, the catalase activity in old rats was significantly reduced ($p < .05$). Interestingly, rats of all ages treated with ginger had significantly higher catalase activity than the untreated rats ($p < .05$, Figure 8B).

3.8 Level of plasma pro-inflammatory biomarkers

When compared to young control rats at 0 months, adult control and baseline untreated adult rats had significantly higher plasma IL-6 concentrations ($p < .05$, Figure 9A). For the whole course of treatment,

TABLE 3 DPPH radical scavenging activity in both soil and soilless ginger. Data presented as mean ± SD (n = 3).

Concentration µg/mL	% DPPH radical scavenging activity assay							
	0	10	20	50	100	200	500	1,000
Vit C	.00 ± 0	43.35 ± 7.8	82.22 ± 9.8	87.86 ± 0.4	88.20 ± 1.0	88.12 ± 0.4	86.06 ± 1.0	85.76 ± 1.6
TRF	.00 ± 0	33.75 ± 8.7	54.95 ± 25.8	82.95 ± 5.0	87.84 ± 4.0	90.51 ± 2.2	89.40 ± 2.0	89.68 ± 1.5
A5	.00 ± 0	.00 ± 3.6	3.86 ± 2.1	11.77 ± 2.4*#	20.48 ± 2.1	35.64 ± 1.0	57.79 ± 6.4	50.90 ± 4.1*#
A10	.00 ± 0	.00 ± 0.7	4.38 ± 3.8	8.92 ± 2.6	15.06 ± 4.0	26.70 ± 3.6	46.86 ± 9.3	67.19 ± 6.3
A15	.00 ± 0	.00 ± 0.7	.00 ± 3.4	6.69 ± 2.5	17.54 ± 2.5	26.18 ± 7.1	55.73 ± 4.8	61.18 ± 1.5
A20	0.00 ± 0	0.00 ± 4.45	3.67 ± 0.4	8.44 ± 3.36	13.29 ± 2.66	25.02 ± 2.45	52.66 ± 3.96	52.02 ± 1.75*#
B5	.00 ± 0	.00 ± 3.64	.00 ± 5.98	1.11 ± 0.91*#a	14.02 ± 12.45	25.96 ± 9.71	55.37 ± 2.18	71.46 ± 2.44*#ac
B10	0.00 ± 0	0.00 ± 22.3	0.00 ± 28.4	4.57 ± 1.96	6.71 ± 1.16	19.93 ± 3.67	47.15 ± 18.9	68.36 ± 10.4*#b
B15	.00 ± 0	.00 ± 0.37	.00 ± 2.58	6.31 ± 4.81	11.84 ± 5.87	26.68 ± 13.94	53.72 ± 5.06	69.98 ± 2.75
B20	.00 ± 0	.00 ± 1.76	4.28 ± 1.91	8.42 ± 2.46	19.86 ± 13.9	31.62 ± 12.4	54.90 ± 11.47	66.16 ± 12.9

*A5, A10, A15 and A20 denote soilless ginger groups. B5, B10, B15, B20 denote soil ginger groups, *p < .05 significantly different compared to Vit C, #p < 005 significantly different compared to TRF, ap<.05 significantly different compared to soilless ginger at similar concentration, bp<.05 significantly different compared to A5 at similar concentration, cp<.05 significantly different compared to A20 at similar concentration.*

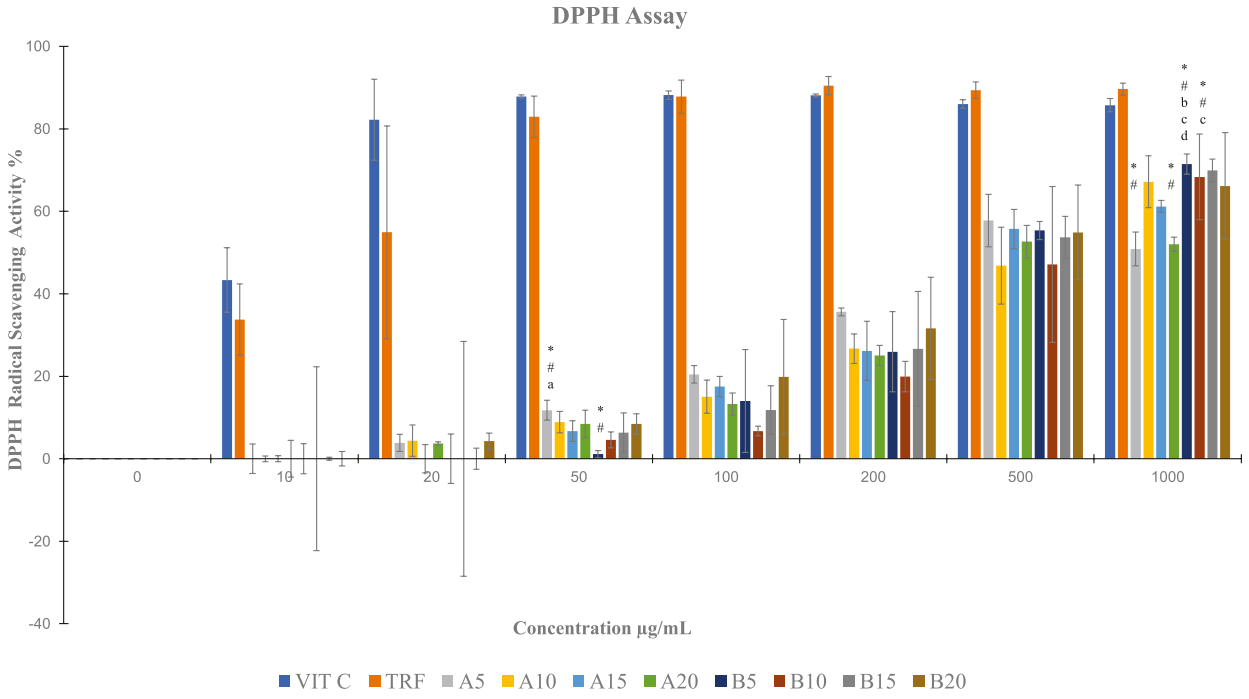

FIGURE 5
DPPH radical scavenging activity in both soil and soilless ginger. Data presented as mean ± SD (n = 3). A5, A10, A15 and A20 denote soilless ginger groups. B5, B10, B15, B20 denote soil ginger groups, *p < .05 significantly different from Vit C, #p < 005 significantly different from TRF, [a]p <.05 significantly different from soil ginger at the same extraction time, [b]p <.05 significantly different from soilless ginger at the same extraction time, [c]p <.05 significantly different from A5 at the same extraction time, and [d]p <0.05 significantly different from A20 at the same extraction time.

there were no significant changes in plasma IL-6 concentration between young, adult and old rats. For TNF-α, when compared to the young control at 0-month and 1.5-month intervals, the young control's plasma TNF-α level at 3 months was significantly decreased. Although the ginger treatment did not significantly reduce TNF-α concentration at months 0 and 3, it did significantly reduce TNF-α concentration in young, treated rats at intervals of 1.5 months when compared to the untreated group (p < .05, Figure 9B). On the other

TABLE 4 FRAP activities of soil and soilless ginger and controls. Data presented as mean ± SD (n = 6).

Mean FRAP value, μM								
Concentration μg/mL	0	10	20	50	100	200	500	1000
TRF	0.00 ± 0	38.81 ± 7.23	152.52 ± 16.64	187.33 ± 19.28	364.37 ± 24.50	783.63 ± 16.97	1083.63 ±13.58	1311.04 ± 18.10
VIT C	0.00 ± 0	82.52 ± 9.32	208.81 ± 18.90	269.93 ± 16.86	364.37 ± 12.49	562.15 ± 19.13	941.41 ± 20.53	1386.59 ± 24.70
A5	0.00 ± 0	0.00 ± 8.7	36.08 ± 4.33^{abf}	96.36 ± 11.68^{abfh}	138.31 ± 12.29	159.42 ± 28.66	206.36 ± 13.57	345.53 ± 11.25
A10	0.00 ± 0	0.00 ± 17.29	45.25 ± 18.28	88.86 ± 6.99^{abf}	136.64 ± 9.94	170.25 ± 3.63	236.08 ± 28.00	329.14 ± 4.59
A15	0.00 ± 0	0.00 ± 20.97	25.63 ± 17.01	66.00 ± 19.75	168.22 ± 15.40	209.33 ± 12.62	257.85 ± 7.06	309.70 ± 5.25
A20	0.00 ± 0	0.00 ± 7.56	12.67 ± 2.94	46.00 ± 4.44^{abd}	118.96 ± 19.76	205.63 ± 10.26	259.70 ± 6.32	308.96 ± 8.63
B5	0.00 ± 0	0.00 ±14.82	45.81 ± 5.91	80.25 ± 6.82	238.86 ±14.35^{abcdef}	436.36 ± 5.36^{abcdefij}	548.86 ± 16.86^{abcdefhij}	561.36 ± 8.22^{abcdefij}
B10	0.00 ± 0	0.00 ± 2.55	28.31 ± 8.01	54.97 ±6.68	258.31 ± 17.17^{abcdefij}	387.47 ± 12.54^{abcdefgij}	488.31 ± 17.68^{abcdef}	565.53 ± 19.41^{abcdef}
B15	0.00 ± 0	0.00 ± 30.75	22.67 ± 3.33	61.56 ± 20.16	174.89 ± 15.03	269.89 ± 14.37^{abcdfgh}	364.33 ±10.93^{abcefgh}	647.67 ± 8.82^{abcdefg}
B20	0.00 ± 0	0.00 ± 17.66	18.78 ± 5.09	72.11 ± 16.02	167.67 ± 9.28	247.11 ± 14.37^{abdgh}	442.67 ± 18.56^{abcdefg}	663.22 ± 2.55^{abcdefg}

A5, A10, A15 and A20 denote soilless ginger groups. B5, B10, B15, B20 denote soil ginger groups.
[a]$p<0.05$ significantly different compared to TRF,
[b]$p<0.05$ significantly different compared to Vit C,
[c]$p<0.05$ significantly different compared to A5,
[d]$p<0.05$ significantly different compared to A10,
[e]$p<0.05$ significantly different compared to A15,
[f]$p<0.05$ significantly different compared to A20,
[g]$p<0.05$ significantly different compared to B5,
[h]$p<0.05$ significantly different compared to B10,
[i]$p<0.05$ significantly different compared to B15,
[j]$p<0.05$ significantly different compared to B20.

10.3389/fphar.2023.1006265

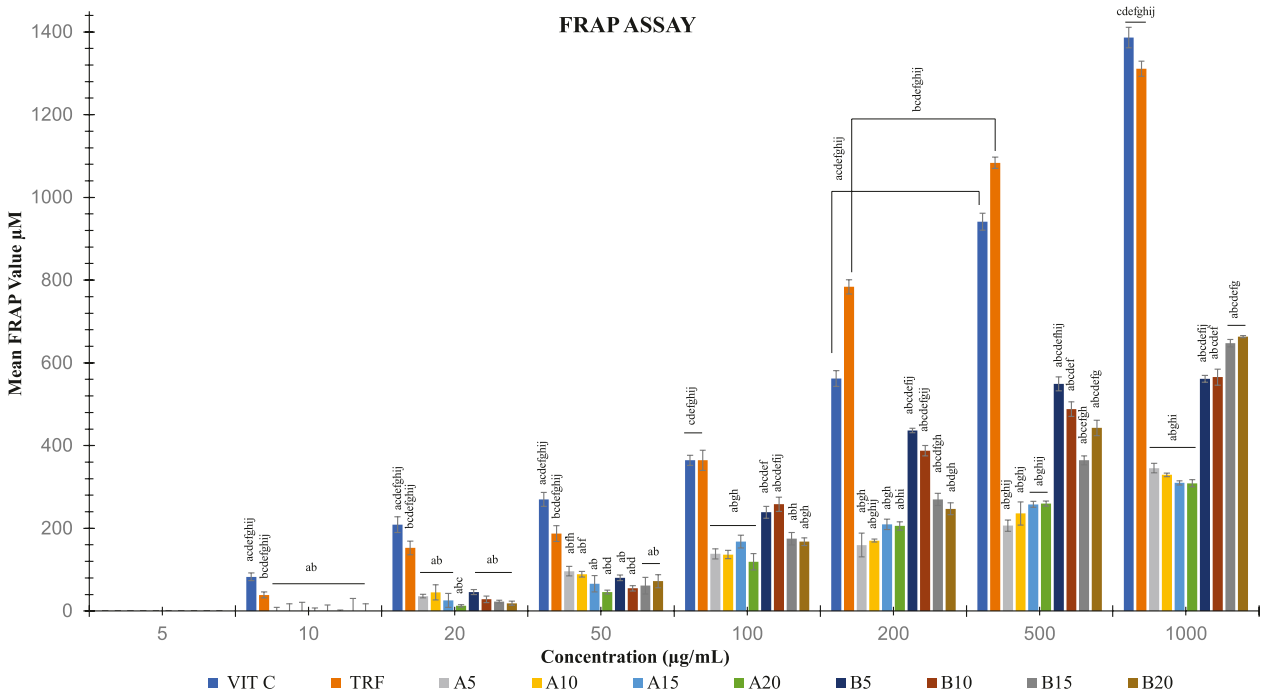

FIGURE 6
FRAP activities in both soil and soilless ginger. The data is shown as mean SD (n = 6). A5, A10, A15 and A20 denote soilless ginger groups. B5, B10, B15, B20 denote soil ginger groups. [a]p<0.05 is significantly different from TRF, [b]p<0.05 is significantly different from Vit C, [c]p<0.05 is significantly different from A5, [d]p<0.05 is significantly different from A10, [e]p<0.05 is significantly different from A15, [f]p<0.05 is significantly different from A20, and [g]p<0.05 is significantly different from B5, [h]p<0.05 is significantly different from B10, [i]p<0.05 is significantly different from B15 and [j]p<0.05 is significantly different from B20.

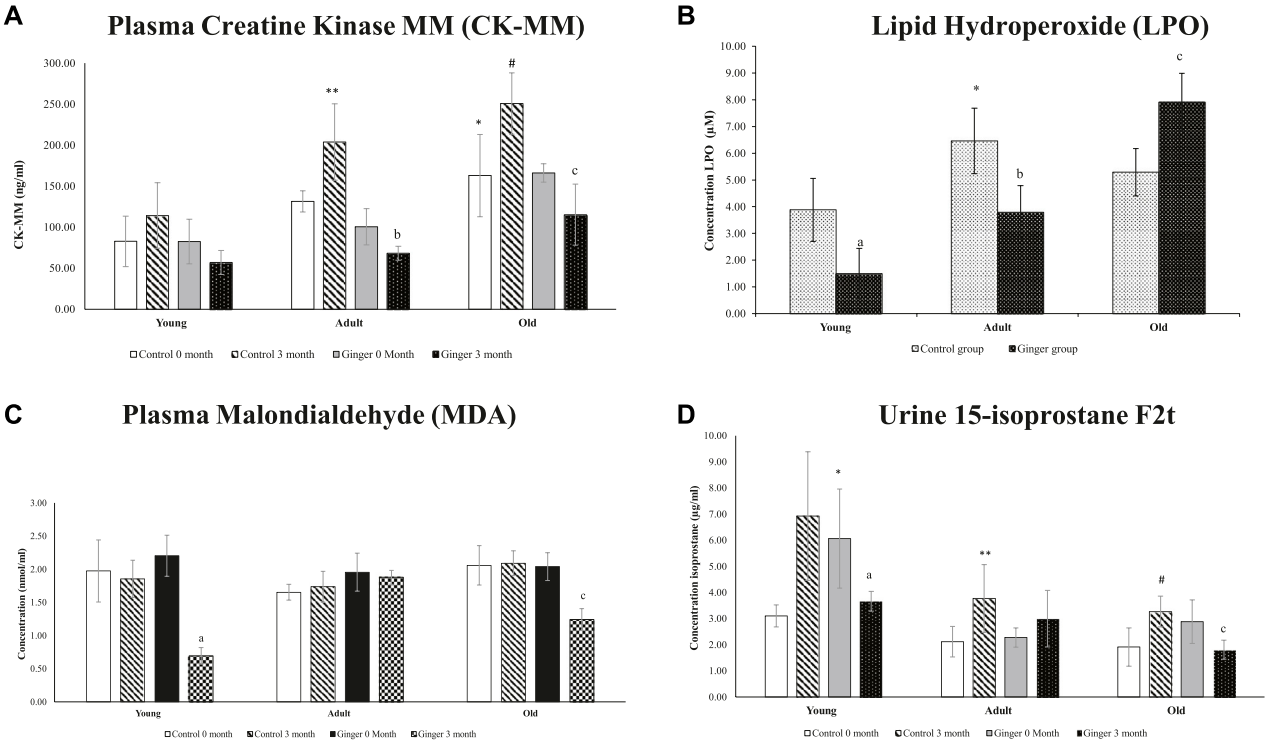

FIGURE 7
Plasma Creatine Kinase MM (CK-MM) **(A)**, lipid hydroxyperoxide **(B)**, plasma malondialdehyde (MDA) **(C)** and urine 15-isoprostane F2t **(D)** concentrations in young, adult, and old rats. The data were presented as mean ± SD, *p < .05 significantly different compared to young control rats at 0 month, **p < .05 significantly different compared to adult control rats at 0 month. #p < .05 significantly different compared to old control rats at 0 month, [a]p<.05 significantly different compared to young ginger rats at 0 month, [b]p<.05 significantly different compared to adult ginger rats at 0-month, [c]p<.05 significantly different compared to old ginger rats on at 0 month.

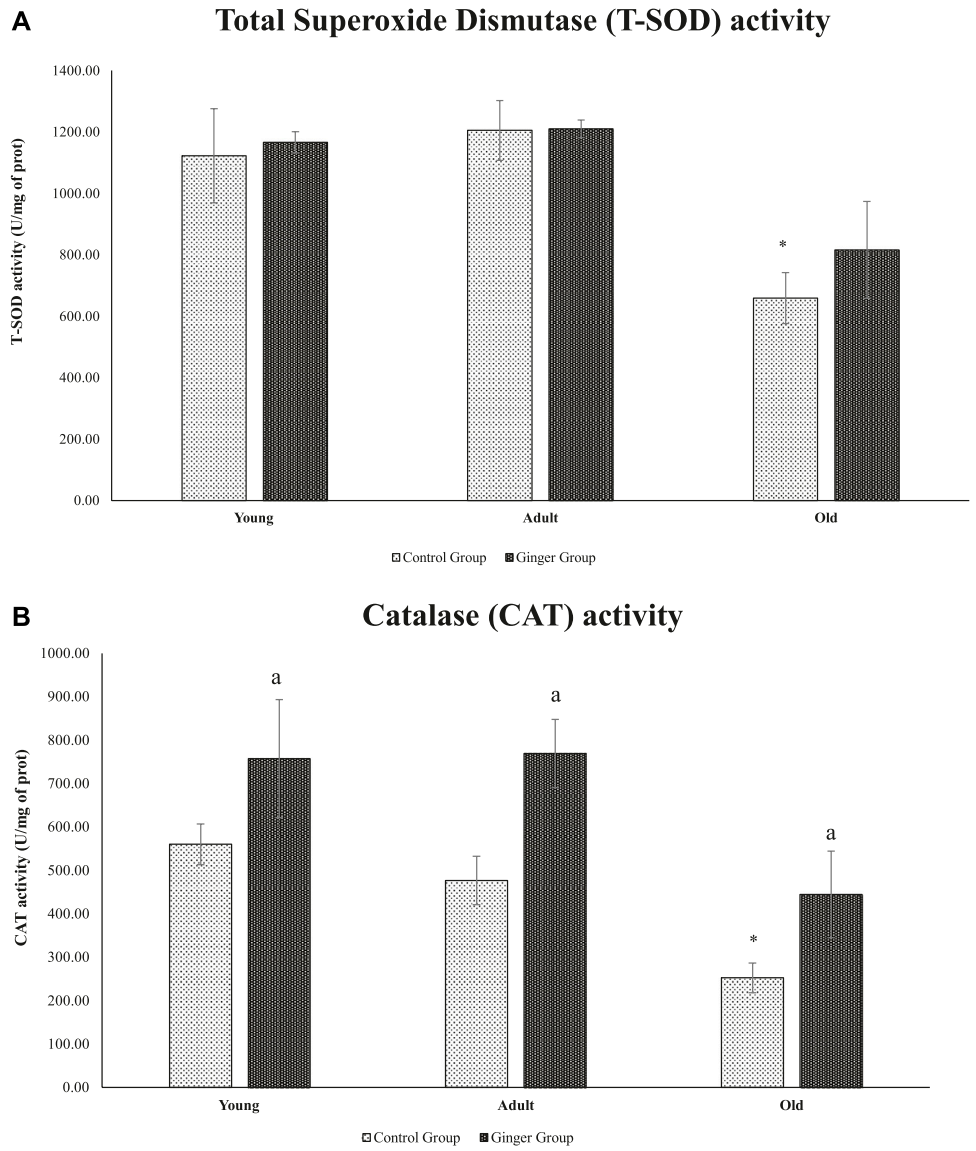

FIGURE 8
Age-related differences in T-SOD activity **(A)** and catalase activity of young, adult, and old rats **(B)**. The data was presented as mean ± SD, *p < .05 significantly different compared to young control rats, ^{a}p<.05 significantly different compared to untreated rats at respective months.

hand, young control groups' plasma CRP levels remained constant at all intervals during the entire course of treatment. However, compared to the untreated group, the young rats treated with ginger extract for 3 months with ginger extract had lower plasma CRP levels (p < .05, Figure 9C).

4 Discussion

The use of natural sources of bioactive chemicals as nutraceuticals to support human health has drawn a lot of interest lately. The natural source of phenolic component used in this study was *Zingiber officinale* Roscoe. We used water for extraction since a number of scientific studies revealed that extraction technologies that primarily use organic solvents may leave an unwelcome hazardous residue in the finished product (Soquetta et al., 2018; Chaves et al., 2020; Carpentieri et al., 2021). Organic volatile solvents such as acetone, chloroform, ethyl ether, ethanol, dichloromethane, ethyl acetate, hexane, benzene, and toluene are highly toxic, human carcinogens, environmental hazards, non-genotoxic animal carcinogens. Accumulation and metabolism of the volatile solvent residue can generate highly toxic metabolites which bind covalently to some macromolecules and produce toxic effects (Opuni et al., 2021). Due to their high solubility in fat, the unmetabolized residual solvents accumulate in fatty tissues such as those of the nervous system which may cause neurotoxicity (Joshi and Adhikari, 2019).

Our results showed that soil ginger possessed a higher extraction yield than soilless ginger. Similar to this, a prior study found that soil-grown lettuce produced more and had leaves with a greater nitrate content than soilless lettuce (Fussy and Papenbrock, 2022). Nitrates in the soil are a primary source of nitrogen which is essential for plant

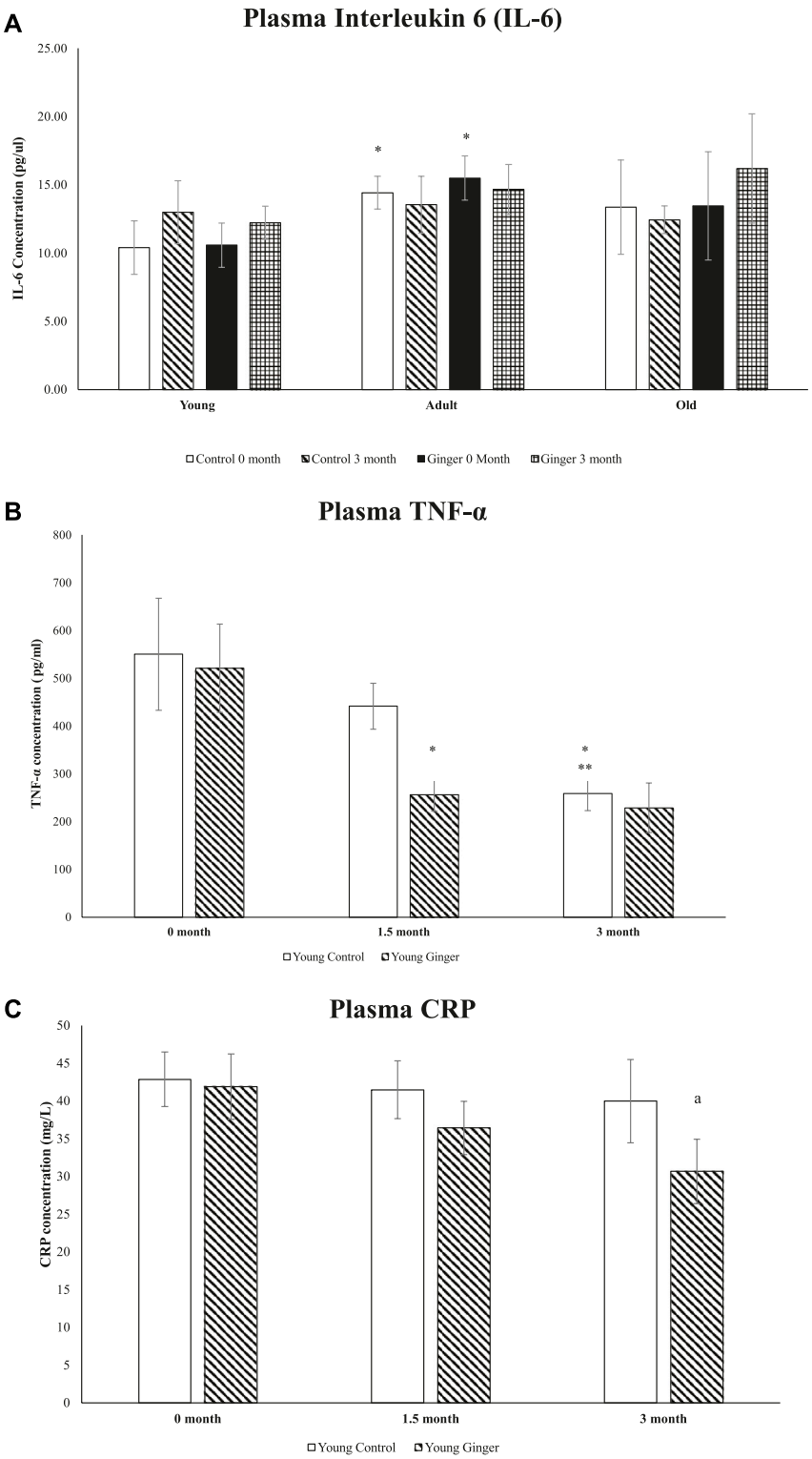

FIGURE 9
Plasma interleukin 6 (IL-6) levels in young, adult, and old rats (A), plasma levels of TNF-α **(B)** and CRP (C) in young rats. The data were presented as mean ± SD. *$p < 0.05$ significantly different compared to young control rat at 0 month, **$p < 0.05$ significantly different compared to young control rat at 1.5 months, [a]$p<0.05$ significantly different compared to untreated rats at respective months.

growth. Fresh ginger typically contains between 85 and 95 percent water, making them vulnerable to microbial deterioration and chemical degradation (An et al., 2016). Volatile compounds make up 97 percent of the *Zingiber officinale* rhizome's constituents in essential oils (Ghasemzadeh et al., 2018). The primary source for ginger's bioactivities came from its rhizomes which consist of non-

volatile substances (oleoresins). A previous study reported the most significant categories among these are gingerols, shogaols, and paradols (Arcusa et al., 2022).

According to the outcomes of the ultrahigh-performance liquid chromatography (UHPLC), the active components in our extract were discovered to be [6]-gingerol and [6]-shogaol (0.6% w/w). The main polyphenols in fresh ginger are [6]-gingerols, however with heat treatment or prolonged storage, gingerols can change into their corresponding [6]-shogaols (An et al., 2016). Among the factors influencing this transformation are acidity, temperature, and the length of the extraction (Ghasemzadeh et al., 2018). When [6]-gingerols are converted into [6]-shogaols, it takes place in an acidic aquatic environment (Ghasemzadeh et al., 2018). The acidic solutions facilitate the dehydration of 6-gingerol to produce 6-shogaol. In aqueous solutions, these acids form different anions which can catalyze the conversion of gingerols to the corresponding shogaols. In line with this, we observed an increased level of [6]-shogaols with increased of extraction time in soilless ginger. A similar increase in other extracted phytochemicals was observed using soilless culture compared to soil-based plants (Verdoliva et al., 2021). Crop production and quality in soil and soilless systems depend on how well the plant absorbs nutrients from the growing medium, which is impacted by the number of nutrients present in the medium, the sources of the nutrients, or interactions between the different nutrients (Sambo et al., 2019). Active components in the material, which may disintegrate at high temperatures, can be preserved by drying them at a low temperature. However, it has been recommended that ginger be heated to increase its curative properties (Jung et al., 2018).

An earlier investigation revealed that ginger's total phenolic content was linearly correlated with antioxidant activity (Ghasemzadeh et al., 2018). Prior work found that providing ginger to old animals successfully reduced DNA oxidative damage (Makpol et al., 2020). We supported this observation with our DPPH scavenging activity assays and FRAP activity assays. The organic nitrogen free radical known as the DPPH free radical has a deep purple colour which turned yellow during the test. Antioxidants contained in the ginger extract donate hydrogen in order to scavenge the DPPH free radical in the DPPH assay, which helped to create the non-radical form of DPPH (Mohd Sahardi et al., 2021). In FRAP assay, the identified antioxidant property changed the ferrous ion (Fe^{2+}) from the ferric ion (Fe^{3+}), causing a blue complex (Fe^{2+}/TPTZ) to form (Spiegel et al., 2020). This is because antioxidants are reducing agents, which means they can aid in the reduction process by providing one electron or one hydrogen. In comparison to soilless ginger, we observed an increase in FRAP and DPPH radical scavenging activity with higher ginger extract concentrations and longer extraction periods. This increased antioxidant power can be due to the soil ginger's higher yield of total [6]-gingerols and [6]-shogaols, which resulted in a higher presence of total α, and β-unsaturated ketones moieties than in soilless ginger. In comparison to *Moringa oleifera*, Kelulut honey (Mohd Sahardi et al., 2021), and other spices extracts (Abdul Qadir et al., 2017), ginger showed stronger antioxidant activity.

ROS are continuously produced *via* cell metabolism in trace amounts. However, excessive ROS production damages macromolecules and harms cells. Biomembranes can be destroyed by polyunsaturated fatty acids (PUFAs) that are esterified in membranes or store lipids due to ROS-induced peroxidation. It is produced from the peroxidation of arachidonic acid by free radicals without the aid of cyclooxygenase enzymes (Soffler et al., 2010). Ginger might reduce oxidative stress in ageing and diseased animal models. The increase in lipid peroxidation (LPO) that we saw in aged animals was also observed in pathological rat brains as reported by Sharma and Singh (2012). This study proposed that ginger ameliorated the condition, with a higher level of antioxidant enzyme activities including catalase observed, similar to our findings (Sharma and Singh, 2012). Numerous age-related disorders are linked to older individuals' higher levels of lipid peroxide and malondialdehyde (MDA) end products and lower levels of antioxidants (Ali et al., 2022). LPO has been linked to the onset and progression of atherosclerotic illnesses, heart failure, and other cardiovascular disorders, according to several studies (Gianazza et al., 2020; Miyazawa, 2021). Measuring urine F_{2t} isoprostanes is one of the most accurate indicators of oxidative stress in living organisms (Guerreiro et al., 2015). Although they are stable, they have distinct half-lives in the blood (minutes) and urine (hours) (Turnbull et al., 2017).

In practically all organs, including skeletal muscle, oxidative damage increases with ageing. Aged rats have been demonstrated to develop sarcopenia phenotype as a result of macromolecule oxidative damage (Makpol et al., 2020). The signaling pathways that control the protein synthesis and proteolysis in muscle have been reported to be impacted by the imbalance of the redox state (Di Filippo et al., 2016). Because of this, oxidative stress indicators for ageing such as creatine kinase (CK) have been utilized. Creatinine, a breakdown product of the muscle's creatine phosphate has been used as a measure of age-related decline in muscle mass. There are three isoenzymes of creatine kinase (CK), known as creatine phosphokinase: CK1, CK2, and CK3. Skeletal muscle contains the isoenzyme CK3, which comprises MM subunits (Mourad, 2021). The CK-MM released into the bloodstream reflects the integrity, stability, and function of the plasma membrane as well as the manifestation of mechanical and metabolic abnormalities inside the sarcomere of skeletal muscle (Kumar and Gill, 2018).

In this investigation, urine isoprostane F_{2t}, LPO, and MDA levels were significantly higher in untreated old rats. However, in both young and old rats, CK-MM, LPO, and MDA levels were shown to be significantly lower after ginger administration. The antioxidant qualities of ginger may account for this finding. According to other *in-vivo* research, ginger's active ingredients can boost antioxidant defense mechanisms including glutathione peroxidase and glutathione S-transferase, as well as lower the levels of malondialdehyde (MDA) and hepatic steatosis (Rahimlou et al., 2016). Through the activation of nuclear factor erythroid 2 (NFE2)-related factor 2 (Nrf2) and the expression of various antioxidant enzymes, ginger supplementation strengthens the antioxidant defense system and may therefore balance the redox state manifested by decrease in lipid peroxidation products.

We looked at the effects of ginger extract on the activity of antioxidant enzymes such as superoxide dismutase (SOD) and catalase to determine whether the Nrf2-inducing action of the ginger extract is connected to its capacity to induce endogenous antioxidant enzymes (CAT). SOD and CAT, a hemoprotein that lowers H_2O_2 and protects tissue from highly reactive OH• radicals catalyze the dismutation of superoxide radicals. They are regarded as major enzymes because they directly eliminate reactive oxygen species and guard cytosolic and membrane components from free radical damage. In young, adult, and old ginger-treated rats, ginger increased catalase's catalytic activity, while we noticed decreased SOD activity in the old rats. This was consistent with earlier research that reported ginger extract has potent antioxidant activities and can serve a similar

purpose as antioxidant enzymes including catalase (CAT), glutathione peroxidase (GPx), and superoxide dismutase (SOD) (Rostamkhani et al., 2022). Ginger's anti-inflammatory characteristics benefited type 2 diabetics with insulin resistance by improving glucose tolerance and uptake in the body, which led to a reduction in insulin resistance (Pakan et al., 2021). Previous research had also suggested that [6]-shogaol modified KEAP1, a redox sensor and prevented Nrf2 from being degraded by proteasomes. Under dormant conditions, the Nrf2 is associated with its Kelch-like ECH-associated protein 1 (KEAP1) by forming the Nrf2-KEAP1 complex. Different alterations in KEAP1 structure induced by ROS lead to its dissociation from this complex and activation of Nrf2. The expression of Nrf2 target genes rises as a result of Nrf2 being translocated into the nucleus. GSH and glutathione levels rise as a result, and ROS levels drop (Mao et al., 2019). By altering proteins and genes, the extra ROS created has the potential to start and advance inflammatory disease pathways.

Immune cells produce a variety of cytokines and chemokines during inflammation in order to draw additional immune cells to the area of oxidative stress or infection (Chatterjee, 2016). In this work, we explored the potential effects of ginger supplementation (200 mg/day) on reducing proinflammatory biomarkers in rats. TNF-α, IL-6, and CRP were the three plasma proinflammatory biomarkers that were chosen as inflammatory state indicators. Interleukin-6 (IL-6) is known as the cytokine of the gerontologist (Rea et al., 2018). Our findings demonstrated that adult rats had levels of IL-6 that were noticeably higher than those of young rats. In addition to being able to create particular cellular and humoral immune responses, such as end-stage B cell differentiation, immunoglobulin production, and T cell activation. IL-6 also plays a significant role in the transition between acute and chronic inflammation (Yousif et al., 2021). Through local leukocyte recruitment, death, and migration, it stimulates an immunological response that can quickly eradicate the harmful substance (Choy and Rose-John, 2017). Age-related mild increases in circulating IL-6 levels are known, and their excessive presence in blood serum is a risk factor and potential biomarker for a variety of inflammatory disorders (Pogue et al., 2017). The results of our study's IL-6 measurements agreed with those of Song et al. (2021). It demonstrated a general decrease in IL-6 levels following ginger supplementation, though it was not statistically significant (Song et al., 2021). It is likely that the ginger dosage and/or supplementation period were not sufficient to significantly reduce the inflammatory cytokines.

TNF-α and IL-6 may be in a connection that is susceptible to negative feedback. These biomarkers have a direct correlation, whereby an increase in one causes a decrease in the other and *vice versa*, according to a study conducted on mice (Yimin and Kohanawa, 2006). It is still unknown how exactly this interaction works and how TNF-α and IL-6 play different roles. In this study, treatment with ginger significantly lowered plasma levels of TNF-α at 1.5 months and CRP at 3 months in young rats, supporting this observation. A previous study reported lower mRNA expression of TNF-α in the soleus muscle of physically active mice following supplementation of black ginger extract for 4 weeks (Toda et al., 2016). It is possible that ginger's anti-inflammatory properties could improve a person's health acutely. This validates earlier research's findings that ginger supplementation may be able to prevent the COX-2 inflammatory pathway, which raises oxidative stress and unfavorable cytokine inflammation (Fajrin et al., 2021). In addition to decreasing NF-κB activity, [6]-gingerol also inhibits the production of TNF-α, cyclooxygenase 2, and the by-products it generates, such as PGE2. As a result, acute-phase proteins like CRP are blocked in this process, which is consistent with the findings reported previously (Mazidi et al., 2016). Randomized clinical trials corroborated ginger's action in TNF-α reduction (Rahimlou et al., 2016). Our findings support the claims made by other researchers that the consumption of ginger significantly lowers serum of CRP and TNF-α but not IL-6 (Jalali et al., 2020; Morvaridzadeh et al., 2020). Thus, we propose ginger as a nutraceutical agent in controlling inflammatory disorders due to its clinically substantial lowering CRP and TNF-α levels activities.

5 Conclusion

High biological activity in the soil and soilless ginger extracts is possible with sub-critical water extraction without hazardous solvents. Based on the current study's findings, we confirmed that the SWE of both soil and soilless ginger possessed comparable antioxidant properties.

6 Recommendation

Further study is required to assess TNF-α and CRP levels in old rats since we did not measure them in this study design. However, soil ginger produced a higher yield of extracts with a more prominent antioxidant activity. The SWE of soil ginger treatment on the different ages of SD rats ameliorates oxidative stress and inflammation responses. This could serve as the basis for developing a nutraceutical agent that can be used as a therapeutic intervention for ageing-related diseases while minimizing the dangers associated with toxicological waste that will affect the environment in addition to being safe for human health. More data will be required from future research in order to establish clinical results, efficacy, and safety in a clinical context, as well as to understand the pathway modification of these polyphenols in reducing oxidative stress and their inflammatory response.

Data availability statement

The raw data supporting the conclusion of this article will be made available by the authors, without undue reservation.

Ethics statement

The experimental plan involving animals were reviewed and approved by Universiti Kebangsaan Malaysia Animal Ethics Committee (UKMAEC Approval Number: BIOK/PP/2018/SUZANA/14-MAY/924-JUNE-2018-MAY-2020).

Author contributions

MMS, JKT, HKG, and MFMN have engaged in the research and in the collecting of data; NFAS, SNAZ, NAR, NHH, and AMR

performed experiments and processed data with equal contributions; AMR and SM drafted and revised the paper. SM designed this study.

Funding

The Ministry of Higher Education (PRGS/1/2021/SKK0/UKM/01/1) provided funding for this study.

Acknowledgments

The Department of Biochemistry, Faculty of Medicine, Universiti Kebangsaan Malaysia researchers and staff members contributed to this study, and the authors are grateful for their assistance.

Conflict of interest

Author HKG was employed by company Millercle Resources Sdn Bhd. Author MFMN was employed by company AM Zaideen Ventures Sdn Bhd.

The remaining authors declare that the research was conducted in the absence of any commercial or financial relationships that could be construed as a potential conflict of interest.

Publisher's note

References

Abdul Qadir, M., Shahzadi, S. K., Bashir, A., Munir, A., and Shahzad, S. (2017). Evaluation of phenolic compounds and antioxidant and antimicrobial activities of some common herbs. *Int. J. Anal. Chem.* 2017, 3475738. doi:10.1155/2017/3475738

Abdullahi, A., Khairulmazmi, A., Yasmeen, S., Ismail, I. S., Norhayu, A., Sulaiman, M. R., et al. (2020). Phytochemical profiling and antimicrobial activity of ginger (Zingiber officinale) essential oils against important phytopathogens. *Arabian J. Chem.* 13 (11), 8012–8025. doi:10.1016/j.arabjc.2020.09.031

Aghamohammadi, D., Dolatkhah, N., Shakouri, S. K., Hermann, P., and Eslamian, F. (2020). Ginger (zingiber officinale) and turmeric (curcuma longa L.) supplementation effects on quality of life, body composition, bone mineral density and osteoporosis related biomarkers and micro-RNAs in women with postmenopausal osteoporosis: A study protocol for a randomized controlled clinical trial. *J. Complement. Integr. Med.* 18 (1), 131–137. doi:10.1515/jcim-2020-0017

Ali, J., Aziz, M. A., Rashid, M. M. O., Basher, M. A., and Islam, M. S. (2022). Propagation of age-related diseases due to the changes of lipid peroxide and antioxidant levels in elderly people: A narrative review. *Health Sci. Rep.* 5 (3), e650. doi:10.1002/hsr2.650

An, K., Zhao, D., Wang, Z., Wu, J., Xu, Y., and Xiao, G. (2016). Comparison of different drying methods on Chinese ginger (Zingiber officinale Roscoe): Changes in volatiles, chemical profile, antioxidant properties, and microstructure. *Food Chem.* 197, 1292–1300. doi:10.1016/j.foodchem.2015.11.033

Arcusa, R., Villaño, D., Marhuenda, J., Cano, M., Cerdà, B., and Zafrilla, P. (2022). Potential role of ginger (zingiber officinale roscoe) in the prevention of neurodegenerative diseases. *Front. Nutr.* 9, 809621. doi:10.3389/fnut.2022.809621

Askari, G., Aghajani, M., Salehi, M., Najafgholizadeh, A., Keshavarzpour, Z., Fadel, A., et al. (2020). The effects of ginger supplementation on biomarkers of inflammation and oxidative stress in adults: A systematic review and meta-analysis of randomized controlled trials. *J. Herb. Med.* 22, 100364. doi:10.1016/j.hermed.2020.100364

Bekkouch, O., Dalli, M., Harnafi, M., Touiss, I., Mokhtari, I., Assri, S. E., et al. (2022). Ginger (zingiber officinale roscoe), lemon (citrus limon L.) juices as preventive agents from chronic liver damage induced by CCl4: A biochemical and histological study. *Antioxidants* 11 (2), 390. doi:10.3390/antiox11020390

Carpentieri, S., Soltanipour, F., Ferrari, G., Pataro, G., and Donsì, F. (2021). Emerging green techniques for the extraction of antioxidants from agri-food by-products as promising ingredients for the food industry. *Antioxidants* 10 (9), 1417. doi:10.3390/antiox10091417

Chatterjee, S. (2016). "Chapter two - oxidative stress, inflammation, and disease," in *Oxidative stress and biomaterials*. Editors T. Dziubla and D. A. Butterfield (Cambridge: Academic Press), 35–58. doi:10.1016/b978-0-12-803269-5.00002-4

Chaves, J. O., de Souza, M. C., da Silva, L. C., Lachos-Perez, D., Torres-Mayanga, P. C., Machado, A. P. d. F., et al. (2020). Extraction of flavonoids from natural sources using modern techniques. *Front. Chem.* 8, 507887. doi:10.3389/fchem.2020.507887

Choy, E., and Rose-John, S. (2017). Interleukin-6 as a multifunctional regulator: Inflammation, immune response, and fibrosis. *J. Scleroderma Relat. Disord.* 2, S1–S5. doi:10.5301/jsrd.5000265

Di Filippo, E. S., Mancinelli, R., Pietrangelo, T., La Rovere, R. M., Quattrocelli, M., Sampaolesi, M., et al. (2016). Myomir dysregulation and reactive oxygen species in aged human satellite cells. *Biochem. Biophys. Res. Commun.* 473 (2), 462–470. doi:10.1016/j.bbrc.2016.03.030

Dias, A. L. B., de Aguiar, A. C., and Rostagno, M. A. (2021). Extraction of natural products using supercritical fluids and pressurized liquids assisted by ultrasound: Current status and trends. *Ultrason. Sonochemistry* 74, 105584. doi:10.1016/j.ultsonch.2021.105584

Ebrahimzadeh Attari, V., Somi, M. H., Asghari Jafarabadi, M., Ostadrahimi, A., Moaddab, S.-Y., and Lotfi, N. (2019). The gastro-protective effect of ginger (zingiber officinale roscoe) in *Helicobacter pylori* positive functional dyspepsia. *Adv. Pharm. Bull.* 9 (2), 321–324. doi:10.15171/apb.2019.038

Fajrin, F. A., Hidayanti, E. D., Khoiroh, N. L., Sulistyaningrum, G., Imandasari, N., Afifah, A., et al. (2021). Red ginger oil affects COX-2 and NMDAR expression during inflammatory- or neuropathy-induced chronic pain in mice. *Jundishapur J. Nat. Pharm. Prod.* 16 (4). doi:10.5812/jjnpp.112353

Fussy, A., and Papenbrock, J. (2022). An overview of soil and soilless cultivation techniques—chances, challenges and the neglected question of sustainability. *Plants* 11, 1153. doi:10.3390/plants11091153

Garcia, E. J., Oldoni, T. L., Alencar, S. M., Reis, A., Loguercio, A. D., and Grande, R. H. (2012). Antioxidant activity by DPPH assay of potential solutions to be applied on bleached teeth. *Braz Dent. J.* 23 (1), 22–27. doi:10.1590/s0103-64402012000100004

Ghasemzadeh, A., Jaafar, H., Baghdadi, A., and Tayebi-Meigooni, A. (2018). Formation of 6-8- and 10-shogaol in ginger through application of different drying methods: Altered antioxidant and antimicrobial activity. *Molecules* 23 (7), 1646. doi:10.3390/molecules23071646

Gianazza, E., Brioschi, M., Martinez Fernandez, A., Casalnuovo, F., Altomare, A., Aldini, G., et al. (2020). Lipid peroxidation in atherosclerotic cardiovascular diseases. *Antioxidants Redox Signal.* 34 (1), 49–98. doi:10.1089/ars.2019.7955

Guerreiro, G., Mescka, C. P., Sitta, A., Donida, B., Marchetti, D., Hammerschmidt, T., et al. (2015). Urinary biomarkers of oxidative damage in maple syrup urine disease: The L-carnitine role. *Int. J. Dev. Neurosci.* 42, 10–14. doi:10.1016/j.ijdevneu.2015.02.003

Halimin, N. M. S., Abdullah, M. O., Wahab, N. A., Junin, R., Husaini, A. A. S. A., and Agi, A. (2022). Oil extracts from fresh and dried Iban ginger. *Chin. J. Anal. Chem.* 50 (8), 100119. doi:10.1016/j.cjac.2022.100119

Hamezah, H. S., Durani, L. W., Ibrahim, N. F., Yanagisawa, D., Kato, T., Shiino, A., et al. (2017). Volumetric changes in the aging rat brain and its impact on cognitive and locomotor functions. *Exp. Gerontol.* 99, 69–79. doi:10.1016/j.exger.2017.09.008

Hou, Y., Dan, X., Babbar, M., Wei, Y., Hasselbalch, S., Croteau, D., et al. (2019). Ageing as a risk factor for neurodegenerative disease. *Nat. Rev. Neurol.* 15, 565–581. doi:10.1038/s41582-019-0244-7

Hur, J., Lee, Y., Lee, C. J., Park, H.-Y., and Choi, S. Y. (2020). 6-shogaol suppresses oxidative damage in L6 muscle cells. *Appl. Biol. Chem.* 63 (1), 57. doi:10.1186/s13765-020-00544-8

Jalali, M., Mahmoodi, M., Moosavian, S. P., Jalali, R., Ferns, G., Mosallanezhad, A., et al. (2020). The effects of ginger supplementation on markers of inflammatory and oxidative stress: A systematic review and meta-analysis of clinical trials. *Phytotherapy Res.* 34 (8), 1723–1733. doi:10.1002/ptr.6638

Jang, D. I., Lee, A. H., Shin, H. Y., Song, H. R., Park, J. H., Kang, T. B., et al. (2021). The role of tumor necrosis factor alpha (TNF-α) in autoimmune disease and current TNF-α inhibitors in therapeutics. *Int. J. Mol. Sci.* 22 (5), 2719. doi:10.3390/ijms22052719

Joshi, D. R., and Adhikari, N. (2019). An overview on common organic solvents and their toxicity. *J. Pharm. Res. Int.* 28 (3), 1–18. doi:10.9734/jpri/2019/v28i330203

Jung, M. Y., Lee, M. K., Park, H. J., Oh, E.-B., Shin, J. Y., Park, J. S., et al. (2018). Heat-induced conversion of gingerols to shogaols in ginger as affected by heat type (dry or moist heat), sample type (fresh or dried), temperature and time. *Food Sci. Biotechnol.* 27 (3), 687–693. doi:10.1007/s10068-017-0301-1

Kumar, V., and Gill, K. D. (2018). "To measure activity of creatine kinase in serum," in *Basic concepts in clinical Biochemistry: A practical guide*. Editors V. Kumar and K. D. Gill (Singapore: Springer Singapore), 131–133. doi:10.1007/978-981-10-8186-6_33

Ko, M.-Y., Nam, H.-H., and Chung, M.-S. (2020). Subcritical water extraction of bioactive compounds from *Orostachys japonicus* A. Berger (Crassulaceae). *Sci. Rep.* 10 (1), 10890. doi:10.1038/s41598-020-67508-2

Makpol, S., Abdul Sani, N. F., Hakimi, N. H., Ab Rani, N., Zakaria, S. N. A., Abd Rasid, A. F., et al. (2020). Zingiber officinale roscoe prevents DNA damage and improves muscle performance and bone integrity in old Sprague Dawley rats. *Evidence-Based Complementary Altern. Med.* 2020, 1–18. doi:10.1155/2020/3823780

Mao, Q. Q., Xu, X. Y., Cao, S. Y., Gan, R. Y., Corke, H., Beta, T., et al. (2019). Bioactive compounds and bioactivities of ginger (zingiber officinale roscoe). *Foods* 8 (6), 185. doi:10.3390/foods8060185

Marsh, L., Hashem, F., and Smith, B. (2021). Organic ginger (<i>Zingiber officinale</i> rosc.) development in a short temperate growing season: Effect of seedling transplant type and mycorrhiza application. *Am. J. Plant Sci.* 12 (03), 315–328. doi:10.4236/ajps.2021.123020

Mas-Bargues, C., Escrivá, C., Dromant, M., Borrás, C., and Viña, J. (2021). Lipid peroxidation as measured by chromatographic determination of malondialdehyde. Human plasma reference values in health and disease. *Archives Biochem. Biophysics* 709, 108941. doi:10.1016/j.abb.2021.108941

Mazidi, M., Gao, H.-K., Rezaie, P., and Ferns, G. A. (2016). The effect of ginger supplementation on serum C-reactive protein, lipid profile and glycaemia: A systematic review and meta-analysis. *Food Nutr. Res.* 60, 32613. doi:10.3402/fnr.v60.32613

Miyazawa, T. (2021). Lipid hydroperoxides in nutrition, health, and diseases. *Proc. Jpn. Acad. Ser. B, Phys. Biol. Sci.* 97 (4), 161–196. doi:10.2183/pjab.97.010

Mohd Sahardi, N. F. N., Jaafar, F., Zakaria, S. N. A., Tan, J. K., Mad Nordin, M. F., and Makpol, S. (2021). Comparison of the antioxidant activity of Malaysian ginger (zingiber officinale roscoe) extracts with that of selected natural products and its effect on the viability of myoblast cells in culture. *Sains Malays.* 50 (5), 1445–1456. doi:10.17576/jsm-2021-5005-23

Mohd, Y. S., Manas, M. A., Jaafar sidik, N., Ahmad, R., and Yaacob, A. (2015). Effects of organic substrates on growth and yield of ginger cultivated using soilless culture. 44, 63–68. http://journalarticle.ukm.my/10346/1/44_1_12.pdf.

Mohd, Y. S., Manas, M. A., Shahid, M., and Darus, K. (2012). Effects of substrates on growth and yield of ginger cultivated using soilless culture. *J. Trop. Agric. Food Sci.* 40 (2), 159–168. http://jtafs.mardi.gov.my/jtafs/40-2/Soilless%20culture.pdf.

Morvaridzadeh, M., Fazelian, S., Agah, S., Khazdouz, M., Rahimlou, M., Agh, F., et al. (2020). Effect of ginger (zingiber officinale) on inflammatory markers: A systematic review and meta-analysis of randomized controlled trials. *Cytokine* 135, 155224. doi:10.1016/j.cyto.2020.155224

Mourad, B. H. (2021). Prevalence of work-related musculoskeletal disorders among Egyptian printing workers evidenced by using serum biomarkers of inflammation, oxidative stress, muscle injury, and collagen type I turnover. *Toxicol. Ind. Health* 37 (1), 748233720977399–22. doi:10.1177/0748233720977399

Nandi, A., Yan, L.-J., Jana, C. K., and Das, N. (2019). Role of catalase in oxidative stress- and age-associated degenerative diseases. *Oxidative Med. Cell. Longev.* 2019, 9613090. doi:10.1155/2019/9613090

Nobile, V., Michelotti, A., Cestone, E., Caturla, N., Castillo, J., Benavente-García, O., et al. (2016). Skin photoprotective and antiageing effects of a combination of rosemary (Rosmarinus officinalis) and grapefruit (Citrus paradisi) polyphenols. *Food Nutr. Res.* 60, 31871. doi:10.3402/fnr.v60.31871

Opuni, K. F. M., Togoh, G., Frimpong-Manso, S., Adu-Amoah, D., Alkanji, O., and Boateng, K. P. (2021). Monitoring of residual solvent contamination in herbal medicinal products in Ghana: A pilot study. *Sci. Afr.* 13, e00825. doi:10.1016/j.sciaf.2021.e00825

Osman, A. M. E., Taj Eldin, I. M., Elhag, A. M., Elhassan, M. M. A., and Ahmed, E. M. M. (2021). *In-vitro* anticancer and cytotoxic activity of ginger extract on human breast cell lines. *Khartoum J. Pharm. Sci.* 1 (1). doi:10.53332/kjps.v1i1.39

Pakan, P., Lidia, K., and Riwu, M. (2021). Investigation of ginger (Zingiber officinale) aqueous extract as an anti-diabetic *in vitro*. *IOP Conf. Ser. Earth Environ. Sci.* 913 (1), 012108. doi:10.1088/1755-1315/913/1/012108

Petersen, K. S., and Smith, C. (2016). Ageing-associated oxidative stress and inflammation are alleviated by products from grapes. *Oxid. Med. Cell Longev.* 2016, 6236309. doi:10.1155/2016/6236309

Pogue, A. I., Jaber, V., Zhao, Y., and Lukiw, W. J. (2017). Systemic inflammation in C57bl/6J mice receiving dietary aluminum sulfate; up-regulation of the pro-inflammatory cytokines IL-6 and TNFα, C-reactive protein (CRP) and miRNA-146a in blood serum. *J. Alzheimers Dis. Park.* 7 (6), 403. doi:10.4172/2161-0460.1000403

Rahimlou, M., Yari, Z., Hekmatdoost, A., Alavian, S. M., and Keshavarz, S. A. (2016). Ginger supplementation in nonalcoholic fatty liver disease: A randomized, double-blind, placebo-controlled pilot study. *Hepat. Mon.* 16 (1), e34897. doi:10.5812/hepatmon.34897

Rea, I. M., Gibson, D. S., McGilligan, V., McNerlan, S. E., Alexander, H. D., and Ross, O. A. (2018). Age and age-related diseases: Role of inflammation triggers and cytokines. *Front. Immunol.* 9, 586. doi:10.3389/fimmu.2018.00586

Rostamkhani, H., Faghfouri, A. H., Veisi, P., Rahmani, A., Noshadi, N., and Ghoreishi, Z. (2022). The protective antioxidant activity of ginger extracts (zingiber officinale) in acute kidney injury: A systematic review and meta-analysis of animal studies. *J. Funct. Foods* 94, 105111. doi:10.1016/j.jff.2022.105111

Sanada, F., Taniyama, Y., Muratsu, J., Otsu, R., Shimizu, H., Rakugi, H., et al. (2018). Source of chronic inflammation in aging. *Front. Cardiovasc. Med.* 5, 12. doi:10.3389/fcvm.2018.00012

Sambo, P., Nicoletto, C., Giro, A., Pii, Y., Valentinuzzi, F., Mimmo, T., et al. (2019). Hydroponic solutions for soilless production systems: Issues and opportunities in a smart agriculture perspective. *Front. Plant Sci.* 10, 923. doi:10.3389/fpls.2019.00923

Sapkota, A., Park, S. J., and Choi, J. W. (2019). Neuroprotective effects of 6-shogaol and its metabolite, 6-paradol, in a mouse model of multiple sclerosis. *Biomol. Ther.* 27 (2), 152–159. doi:10.4062/biomolther.2018.089

Seo, S. H., Fang, F., and Kang, I. (2021). Ginger (zingiber officinale) attenuates obesity and adipose tissue remodeling in high-fat diet-fed C57bl/6 mice. *Int. J. Environ. Res. Public Health* 18 (2), 631. doi:10.3390/ijerph18020631

Sharma, P., and Singh, R. (2012). Dichlorvos and lindane induced oxidative stress in rat brain: Protective effects of ginger. *Pharmacogn. Res.* 4 (1), 27–32. doi:10.4103/0974-8490.91031

Shuhaimi, M., Mohamad, A., and Adzemi, M. (2016). Effects of seed rhizome size on growth and yield of ginger cultivated using fertigation system. *J. Trop. Agric. Food S. C.* 44 (2), 211–218. http://jtafs.mardi.gov.my/jtafs/44-2/ginger.pdf.

Soffler, C., Campbell, V. L., and Hassel, D. M. (2010). Measurement of urinary F2-isoprostanes as markers of *in vivo* lipid peroxidation: A comparison of enzyme immunoassays with gas chromatography–mass spectrometry in domestic animal species. *J. Veterinary Diagnostic Investigation* 22 (2), 200–209. doi:10.1177/104063871002200205

Song, M.-Y., Lee, D.-Y., Park, S.-Y., Seo, S.-A., Hwang, J.-S., Heo, S.-H., et al. (2021). Steamed ginger extract exerts anti-inflammatory effects in Helicobacter pylori-infected gastric epithelial cells through inhibition of NF-κB. *J. cancer Prev.* 26 (4), 289–297. doi:10.15430/JCP.2021.26.4.289

Soquetta, M. B., Terra, L. d. M., and Bastos, C. P. (2018). Green technologies for the extraction of bioactive compounds in fruits and vegetables. *CyTA - J. Food* 16 (1), 400–412. doi:10.1080/19476337.2017.1411978

Spiegel, M., Kapusta, K., Kołodziejczyk, W., Saloni, J., Żbikowska, B., Hill, G. A., et al. (2020). Antioxidant activity of selected phenolic acids-ferric reducing antioxidant power assay and QSAR analysis of the structural features. *Molecules* 25 (13), 3088. doi:10.3390/molecules25133088

Sproston, N. R., and Ashworth, J. J. (2018). Role of C-reactive protein at sites of inflammation and infection. *Front. Immunol.* 9, 754. doi:10.3389/fimmu.2018.00754

Taso, O. V., Philippou, A., Moustogiannis, A., Zevolis, E., and Koutsilieris, M. (2019). Lipid peroxidation products and their role in neurodegenerative diseases. *Ann. Res. Hosp.* 3, 2. doi:10.21037/arh.2018.12.02

Thimraj, T. A., George, L., Asrafuzzaman, S., Upadhyay, S., and Ganguly, K. (2018). "Chapter 7 - oxidative signaling in chronic obstructive airway diseases," in *Immunity and inflammation in health and disease*. Editors S. Chatterjee, W. Jungraithmayr, and D. Bagchi (Cambridge: Academic Press), 79–98. doi:10.1016/b978-0-12-805417-8.00007-x

Toda, K., Hitoe, S., Takeda, S., and Shimoda, H. (2016). Black ginger extract increases physical fitness performance and muscular endurance by improving inflammation and energy metabolism. *Heliyon* 2 (5), e00115. doi:10.1016/j.heliyon.2016.e00115

Truong, D.-H., Nguyen, D. H., Ta, N. T. A., Bui, A. V., Do, T. H., and Nguyen, H. C. (2019). Evaluation of the use of different solvents for phytochemical constituents, antioxidants, and *in vitro* anti-inflammatory activities of *Severinia buxifolia*. *J. Food Qual.* 2019, 8178294. doi:10.1155/2019/8178294

Turnbull, C. D., Akoumianakis, I., Antoniades, C., and Stradling, J. R. (2017). Overnight urinary isoprostanes as a marker of oxidative stress in obstructive sleep apnoea. *Eur. Respir. J.* 49 (2), 1601787. doi:10.1183/13993003.01787-2016

Verdoliva, S. G., Gwyn-Jones, D., Detheridge, A., and Robson, P. (2021). Controlled comparisons between soil and hydroponic systems reveal increased water use efficiency and higher lycopene and β-carotene contents in hydroponically grown tomatoes. *Sci. Hortic.* 279, 109896. doi:10.1016/j.scienta.2021.109896

Yimin and Kohanawa, M. (2006). A regulatory effect of the balance between TNF-alpha and IL-6 in the granulomatous and inflammatory response to Rhodococcus aurantiacus infection in mice. *J. Immunol.* 177 (1), 642–650. doi:10.4049/jimmunol.177.1.642

Yousif, A. S., Ronsard, L., Shah, P., Omatsu, T., Sangesland, M., Bracamonte Moreno, T., et al. (2021). The persistence of interleukin-6 is regulated by a blood buffer system derived from dendritic cells. *Immunity* 54 (2), 235–246.e5. doi:10.1016/j.immuni.2020.12.001

Zammel, N., Saeed, M., Bouali, N., Elkahoui, S., Alam, J. M., Rebai, T., et al. (2021). Antioxidant and anti-inflammatory effects of zingiber officinale roscoe and allium subhirsutum: *In silico*, biochemical and histological study. *Foods* 10 (6), 1383. doi:10.3390/foods10061383

Zhou, M., Xu, R., Kaelber, D. C., and Gurney, M. E. (2020). Tumor Necrosis Factor (TNF) blocking agents are associated with lower risk for Alzheimer's disease in patients with rheumatoid arthritis and psoriasis. *PLoS One* 15 (3), e0229819. doi:10.1371/journal.pone.0229819

frontiers | Frontiers in Pharmacology

TYPE Review
PUBLISHED 23 February 2023
DOI 10.3389/fphar.2023.1120457

OPEN ACCESS

EDITED BY
Wei Peng,
Chengdu University of Traditional Chinese Medicine, China

REVIEWED BY
Yaoting Ji,
Wuhan University, China
Vijay Kumar Chava,
NDC, India

*CORRESPONDENCE
Ahmad Nazrun Shuid,
anazrun@uitm.edu.my

SPECIALTY SECTION
This article was submitted to Ethnopharmacology, a section of the journal Frontiers in Pharmacology

RECEIVED 10 December 2022
ACCEPTED 10 February 2023
PUBLISHED 23 February 2023

CITATION
Jayusman PA, Nasruddin NS, Baharin B, Ibrahim N'I, Ahmad Hairi H and Shuid AN (2023), Overview on postmenopausal osteoporosis and periodontitis: The therapeutic potential of phytoestrogens against alveolar bone loss.
Front. Pharmacol. 14:1120457.
doi: 10.3389/fphar.2023.1120457

Overview on postmenopausal osteoporosis and periodontitis: The therapeutic potential of phytoestrogens against alveolar bone loss

Putri Ayu Jayusman[1], Nurrul Shaqinah Nasruddin[1], Badiah Baharin[2], Nurul 'Izzah Ibrahim[3], Haryati Ahmad Hairi[4] and Ahmad Nazrun Shuid[5]*

[1]Department of Craniofacial Diagnostics and Biosciences, Faculty of Dentistry, Universiti Kebangsaan Malaysia, Kuala Lumpur, Malaysia, [2]Unit of Periodontology, Department of Restorative Dentistry, Faculty of Dentistry, Universiti Kebangsaan Malaysia, Kuala Lumpur, Malaysia, [3]Department of Pharmacology, Faculty of Medicine, Universiti Kebangsaan Malaysia Medical Centre, Kuala Lumpur, Malaysia, [4]Department of Biochemistry, Faculty of Medicine, Manipal University College, Melaka, Malaysia, [5]Department of Pharmacology, Faculty of Medicine, Universiti Teknologi MARA, Sungai Buloh Campus, Jalan Hospital, Sungai Buloh, Selangor, Malaysia

Osteoporosis and periodontitis are two major chronic diseases of postmenopausal women. The association between these two diseases are evident through systemic bone loss and alveolar bone loss. Both postmenopausal osteoporosis and periodontitis impose a considerable personal and socioeconomic burden. Biphosphonate and hormone replacement therapy are effective in preventing bone loss in postmenopausal osteoporosis and periodontitis, but they are coupled with severe adverse effects. Phytoestrogens are plant-based estrogen-like compounds, which have been used for the treatment of menopause-related symptoms. In the last decades, numerous preclinical and clinical studies have been carried out to evaluate the therapeutic effects of phytoestrogens including bone health. The aim of this article is to give an overview of the bidirectional interrelationship between postmenopausal osteoporosis and periodontitis, summarize the skeletal effects of phytoestrogens and report the most studied phytoestrogens with promising alveolar bone protective effect in postmenopausal osteoporosis model, with and without experimental periodontitis. To date, there are limited studies on the effects of phytoestrogens on alveolar bone in postmenopausal osteoporosis. Phytoestrogens may have exerted their bone protective effect by inhibiting bone resorption and enhancing bone formation. With the reported findings on the protective effects of phytoestrogens on bone, well-designed trials are needed to better investigate their therapeutic effects. The compilation of outcomes presented in this review may provide an overview of the recent research findings in this field and direct further *in vivo* and clinical studies in the future.

KEYWORDS

periodontitis, postmenopausal osteoporosis, alveolar bone loss, phytoestrogens, estrogen deficiency

1 Introduction

- Osteoporosis is an age-related bone disease characterized by low bone mass and deterioration of bone tissue micro-architecture resulting in increased bone fragility and susceptibility to fracture (Sözen et al., 2017). It is an emerging geriatric condition in developing nations. It affects men and women of all races, but the prevalence of osteoporosis is higher among women compared to men (Clynes et al., 2020). The global increase in life expectancy, being 74 years for women has lead them to suffer from many debilitating diseases such as osteoporosis (Manyonda et al., 2020).
- The alveolar bone is the thick ridge of bone located on the jaw bones. It contains the tooth sockets which hold the teeth. Anatomically, these human bones are called the maxilla and mandible. Alveolar bone loss is one of the hallmarks of periodontitis. It causes weakening of the supporting structures of the teeth and predisposes to tooth mobility and loss. Postmenopausal osteoporosis is closely related to the development of periodontitis (Contaldo et al., 2020). Periodontitis, the sixth most prevalent disease worldwide, is multifactorial inflammatory disease mediated by host response and dysbiotic plaque biofilms, resulting in periodontal tissue destruction, alveolar bone loss and eventually tooth loss (Tonetti et al., 2017; Papapanou et al., 2018).
- Both osteoporosis and periodontitis are prevalent inflammation-associated bone disorders that have common features of bone resorption, being silent and asymptomatic (Mashalkar et al., 2018; Ayed et al., 2019). These diseases remain a major public health problem particularly in the aging population (Yu & Wang, 2022). It is projected that osteoporosis and periodontitis cases will increase as the population advances in age and is predicted to cause great health challenges (Wang and McClauley, 2016). As periodontitis leads to alveolar bone loss, tooth loss, edentulism and masticatory dysfunction, it could indirectly affect nutrition, impair quality of life and self-esteem of the affected individuals (Chang et al., 2020). Postmenopausal osteoporosis and periodontitis may impose huge socioeconomic impacts and healthcare costs (Brandão et al., 2012; Mohd-Dom et al., 2014; Mohd Dom et al., 2016). Both diseases share a number of risk factors such as age, smoking, alcohol consumption and diabetes, and common features of bone resorption that might require mutual concomitant management (Wang & McCauley, 2016).
- Anti-resorptive drugs such as biphosphonates are the commonly used pharmacological agents for the treatment of osteoporosis. Zoledronate is a long-acting bisphosphonate and most potent anti-resorptive drug that has been reported in the literature to have a positive effect on bone density in patients with osteoporosis. Apart from that, zoledronate could also improve periodontal disease and prevent tooth loss (Taguchi et al., 2019). Postmenopausal women on hormone replacement therapy (HRT) were found to have better natural teeth retention than those not receiving HRT (Han et al., 2016). However, the use of these treatment modalities is associated with unwanted side effects. Anti-resorptive agent biphosphonate may lead to renal toxicity, acute-phase reactions, gastro-intestinal toxicity, and osteonecrosis of the jaw (Ralston, 2015). The use of HRT is also associated with side effects and risks, including stroke, thromboembolism, vascular diseases and breast cancer. It was reported that to avoid the HRT adverse effects, women nowadays are shifting to herbal medicine, particularly for the prevention and treatment of menopause related symptoms (Gerbarg & Brown, 2016; Djapardy and Panay. 2022). The search of natural substances with promising results for the treatment of postmenopausal osteoporosis and periodontitis therefore is highly desirable.
- In this regard, phytomedicine or plant-based medicine with therapeutic and healing properties have gain scientific and clinical interest. Phytoestrogens are naturally occurring non-steroidal polyphenolic compounds that have structural and biological similarity to 17-β-estradiol, the main female sex hormone. Even though the affinity is lesser than that of endogenous estrogens, phytoestrogens can bind to estrogen receptors (ER) and exert anti-estrogenic or pro-estrogenic effects (Rowe and Barber, 2021). Most of phytoestrogens are also antioxidant and anti-inflammatory agents and these properties contribute to their distinguished therapeutic health effects Kładna et al., 2016. A growing body of evidence supported their therapeutic potential in preventing and treating several dysfunctions and diseases related to aging including menopausal symptoms and osteoporosis (Sirotkin & Harrath, 2014). In fact, phytoestrogens are used as a dietary supplement and as an alternative to HRT as they are believed to be safe and effective. Such properties turn these substances into promising targets for development as adjunctive preventive and therapeutic strategies for postmenopausal osteoporosis and periodontitis. In this review, we summarized the effects of the most studied phytoestrogens on bone health and screened phytoestrogens with the most promising alveolar bone protective effect in postmenopausal osteoporosis model with and without experimental periodontitis. This review may provide important insights for further *in vivo* and clinical studies of postmenopausal osteoporosis and periodontitis.

2 Association between postmenopausal osteoporosis and periodontitis

The association between postmenopausal osteoporosis and periodontitis has been reported extensively in epidemiologic and experimental studies (Luo et al., 2014; Juluri et al., 2015; Ayed et al., 2019). Though the mechanism of periodontitis in postmenopausal women has not been fully elucidated, an explicit understanding on the mechanistic link between the two diseases and their interplay is important for the prevention and management of these disorders, particularly in the elderly. The pathogenesis of postmenopausal osteoporosis involved the activation of systemic inflammation and dysregulation of immune response (Al-Daghri et al., 2017;

Fang et al., 2022). Healthy bone continuously remodels through osteoblast-mediated bone formation and osteoclast-mediated bone resorption until the fourth to sixth decade of life when resorption exceeded the formation, causing a continuous loss of bone mass and a progressive decline in bone mineral density (BMD) (Kirk et al., 2020; Munoz et al., 2020). The cessation of ovarian function at menopause is one of the main causes of osteoporosis (Wu et al., 2021). Withdrawal of the protective effect of estrogen and immune cells alteration contribute to ongoing bone destruction in postmenopausal osteoporosis (Fischer and Haffner-Luntzer, 2022). The crosstalk between the immune system and the bone has been reported in the literature since the past decades (Takayanagi et al., 2000). Various immune cells interact with bone cells, the osteoblasts and osteoclasts, through cell-cell direct contact or *via* paracrine mechanisms (Fischer and Haffner-Luntzer, 2022). Immune cells including subtypes of T lymphocytes, B lymphocytes, macrophages, neutrophils and mast cells influence bone cells *via* factors including inflammatory cytokines, the interleukin (IL)-6 and tumor necrosis factor -α (TNF-α), osteoprotegerin/receptor activator of nuclear factor kappa-β ligand (OPG/RANKL) and other mediators, by increasing osteoblast apoptosis and stimulating osteoclastogenesis, thereby triggering bone loss during postmenopausal osteoporosis (Du et al., 2018; Zhang et al., 2020; Fischer and Haffner-Luntzer, 2022).

Bacterial dental plaque or biofilm is the primary etiological factor that dissociate periodontitis from osteoporosis. Though the pathogenesis and progression of periodontitis is primarily dependent on host interaction with the dysbiotic biofilm, the subsequent exacerbation of inflammatory response and its influence on bone homeostasis play crucial roles in both osteoporosis and periodontitis (Yu & Wang, 2022). Inflammatory response, the recruitment of polymorphonuclear neutrophils in particular, is the first line of defense against the invading periodontal pathogens in subgingival dental biofilm that is intended to eliminate the initial cause of tissue injury. As inflammation involve the activation of immune cells in the innate and adaptive immunity, the interplay between microbes and immune components initiate and propagate periodontal inflammation (Hajishengallis, 2014). The activation of lymphocyte and amplification of local inflammatory signaling cascade could stimulate RANKL signal, promoting osteoclastogenesis and inhibiting osteoblast lineage cells, thereby causing an uncoupling of bone remodeling process (Kawai et al., 2006; Pacios et al., 2015). These events are thought to be responsible for bone resorptive lesion and periodontal bone loss in periodontitis.

As described above, it is known that osteoporosis and periodontitis are closely related with inflammation and aging. Apart from inflammation, oxidative stress, is another major causative factor implicated in the pathogenesis and progression of these diseases. During aging, the accumulation of intracellular reactive oxygen species (ROS) and depletion of antioxidant enzymes lead to the elevation of oxidative stress in skeletal system (Manolagas, 2010). Excessive production of ROS, which is also responsible for elevation of immune cytokines could trigger the increase in osteoclastogenesis and osteoblast apoptosis as well as decrease in osteoblastogenesis. A population-based study suggested an interplay between oxidative stress and bone resorption that possibly underlies the development of postmenopausal osteoporosis (Cervellati et al., 2014). Menopause-related estrogen withdrawal increase the risk of postmenopausal osteoporosis basically by making the bone more vulnerable to oxidative injury. The theory that oxidative stress affects BMD was also supported by numerous clinical studies. Oxidant and antioxidant status imbalance in postmenopausal osteoporosis could affect the osteoclastic and osteoblastic activity. With regards to its involvement in periodontitis, oxidative stress has been linked to periodontal tissue destruction. ROS initially act as an antimicrobial defense system by killing the invaded pathogenic microorganism triggered by the infiltration of polymorphonuclear neutrophil (Wang, 2015). The generation of ROS is also considered as a "double-edge" sword as it helps to kill invading pathogen and it can be cytotoxic to host cells when the inflammatory response is exaggerated. Overproduction of ROS within the affected tissues leads to oxidant-antioxidant imbalance which then results in oxidative stress and pathological changes and consequently cause destruction of host tissues (Sczepanik et al., 2020). Hence, ROS is responsible for destruction of periodontal tissues and tooth loss in periodontitis. Due to these facts, periodontitis is also referred to as an inflammatory disease of oxidative stress.

The evolution of classification and diagnostic criteria for osteoporosis and periodontitis have been described and reported in the literature. Osteoporosis is determined by the measurement of BMD, expressed in terms of the number of standard deviations (SD) from the mean BMD of healthy individuals that matched to age and sex (Z-score), and the number of SD from the mean BMD of healthy young sex-matched individuals (T-score). According to WHO criteria, osteoporosis is present when BMD lies 2.5 SD or more below the BMD of young healthy women. Meanwhile, osteopenia or low bone mass is defined as BMD levels between one SD and 2.5 SD below the normal BMD (Lorentzon & Cummings, 2015). The most widely recognized tools used to measure BMD is dual energy x-ray absorptiometry (DXA). This technique is a standard non-invasive diagnosis approach that is reliably used worldwide to identify patients with low BMD due to its high precision and resolution but low radiation and cost. Additionally, quantitative ultrasound (QUS) methods have been used in the diagnosis and follow-up treatment in osteoporosis. Advances in computed tomography (CT) and magnetic resonance imaging (MRI) are promising in clinical and research settings in terms of capturing bone microarchitecture and also characterizing processes at the molecular level (Oei et al., 2016).

The diagnosis of periodontitis is primarily based on clinical evaluation whereby radiographs are used to confirm the clinical manifestation. The patient is considered to have periodontitis when there are at least four teeth with 4 mm probing depth in one or more sites, clinical attachment loss (CAL) up to 3 mm at the same site and presence of bleeding on probing (Ayed et al., 2019). The American Academy of Periodontology and the European Federation of Periodontology has modified the definition and classification framework for periodontitis based on staging and grading system (Tonetti et al., 2017). The staging refers to the severity and extent of periodontitis at present while grading refers to the rate of its progression. In clinical setting, the periodontal health can be evaluated by the measurement of CAL using probing pocket depths (PPD) and gingival recession but the reliability of this method is limited in terms of probing force, angulation,

placement and tip diameter (Trombelli et al., 2018). Radiographic bone loss (RBL) should be used in cases if the CAL is unavailable (Tonetti et al., 2017). Loss of alveolar crestal height (ACH), oral hygiene simplified (OHI-S) and sites with bleeding on probing (BOP) percentage are among other important clinical parameters in the evaluation of periodontal status (Qi et al., 2021). Apart from that, identification of cavities and periodontal lesions, maxillary sinusitis and other lesions in the oral and maxillofacial field as well as osteoporosis can be done with the use of computer-aided diagnosis (CAD) (Wang and McCauley. 2016).

Tooth loss, periodontal disease, ill-fitting or loose dentures and severe bone loss around the teeth, are among the early indicators of osteoporosis detected in the oral cavity (Ayed et al., 2019). In the clinical setting, patients at risk can be identified by a dentist from medical history, clinical examination and radiographic findings while patient's osteoporosis status can be obtained by further determination of BMD together with the evaluation of dental radiography. Knowledge on the relationship between postmenopausal osteoporosis and periodontitis, as well as sufficient clinical and radiographic information would enable dentists to play their role in early diagnosis and screening of osteoporosis in postmenopausal women. Regardless of gender, patients with osteoporosis may have two-fold increase in the risk of periodontitis. Though osteoporosis is not an etiologic factor in periodontal disease, osteoporotic women presented a higher risk and greater severity of periodontitis than men (Pepelassi et al., 2012; Manjunath et al., 2019). This association suggested that patients with osteoporosis should be evaluated for periodontal health and *vice versa*. Efforts towards the prevention of periodontal disease in patients at risk of osteoporosis particularly in postmenopausal women would be enviable. Although the mechanisms underlying this association has not been not fully elucidated, information collected from the literature strongly explained the association.

3 Estrogen deficiency and inflammatory response in alveolar bone loss

Estrogen is a steroid hormone that is not only responsible for female sexual characteristics development but also has other non-reproductive physiological roles. It is one of the key regulators of bone metabolism with significant influence on skeletal growth and homeostasis in both women and men. Estrogens act directly on osteoblasts, osteocytes, immune cells and other cells *via* the ER found on these bone cells (Bord et al., 2001; Braidman et al., 2001; Crusodé-Souza et al., 2009). In general, ER signaling pathway activation stimulated differentiation of osteoblast and suppressed osteoclastic activity (Manolagas, 2000). Estrogen also prevented apoptosis of osteocytes and its anti-apoptotic effect is related to their autophagy regulation in osteocytes (Florencio-Silva et al., 2018). Estrogen deficiency increased osteoclastogenesis, prolonged osteoclast lifespan and increased the rate of bone turnover, causing accelerated resorption than formation (Manolagas, 2000; Manolagas et al., 2013). A recent study showed that estrogen deficiency decreased autophagy and increased apoptosis in alveolar process osteocytes, whereby estrogen replacement enhanced osteocyte viability simply by inhibiting apoptosis and maintaining autophagy in these cells (Florencio-Silva et al., 2018).

Apart from its direct effects on bone cells, research has revealed estrogen regulated bone hemostasis through its influence on the immune system and on oxidative stress. In essence, the proinflammatory cytokines, IL-1, IL-6, TNF-α, granulocyte macrophage colony-stimulating factor, macrophage colony-stimulating factor (M-CSF), and prostaglandin-E_2 (PGE_2) played a significant role in bone metabolism by increasing bone resorption (Riggs, 2000). These proinflammatory cytokines particularly IL-1, IL-6 and TNF-α were considered as osteoclastogenic bone resorption-inducing cytokines (Scheidt-Nave et al., 2001). Activation of inflammatory cascades due to estrogen deficiency led to increased production of M-CSF and RANKL. The binding of M-CSF to its receptor stimulated the proliferation of osteoclast and the survival of its precursors as well as mature osteoclasts. The binding of RANKL to RANK receptors stimulated differentiation and activity of osteoclast and prevented their apoptosis (Feng et al., 2019). In osteoporotic patients, the increased in systemic levels of IL-6 could predict BMD change and fracture rate (Barbour et al., 2014). A significant elevation in IL-6 as well as TNF-α were also observed in ovariectomized (OVX) animals compared to the SHAM group (Eminov et al., 2018; Delgobo et al., 2019). Apart from the increase in IL-6 expression, OVX rats also showed increased RANKL and to a lesser extent, OPG expression. OVX rat is a suitable model for studying postmenopausal bone loss as it mimics the decline in endogenous estrogen production by the ovaries during menopause (Johnston & Ward, 2015). This model resembles deterioration of bone tissue in the hip and spine in postmenopausal osteoporosis and hence it can also be used to study mineral and structural changes in alveolar bone.

Alveolar bone loss due to periodontitis is a frequent complication in postmenopausal women suffering from osteoporosis due to estrogen deficiency (Tanaka et al., 2020). As described earlier, changes in hormone level particularly estrogen have impact on systemic bone homeostasis and inflammatory response. Following menopause, estrogen levels in the circulation fall drastically as the production by the ovaries cease. Estrogen reduced osteoclast activity and prevented apoptosis of osteocytes, and for that reason rapid decline in estrogen may lead to systemic bone loss due to disruption of bone homeostasis (Grover et al., 2014). Other than bones, estrogen receptors can also be found in the oral mucosa, gingiva and salivary glands. ER-β is the predominant ER present in the gingival epithelium (Valimaa et al., 2004). Therefore, hormone fluctuations may also contribute to changes in the oral cavity and acceleration of inflammatory response (Jafri et al., 2015). Upregulation of immune cells and osteoclasts due to estrogen deficiency eventually result in a greater production of bone-resorbing cytokines. The increase in inflammatory cytokines and other factors in the circulation may not only have impact on systemic bone remodeling but also may locally compromise the tissue response to periodontal disease (Golub et al., 2006).

Estrogen deficiency in postmenopausal women or in experimental OVX rodents has been markedly linked to alterations in trabecular and cortical bone including the alveolar bone of mandible (Johnston & Ward, 2015; Jonasson et al., 2018). Studies also showed that estrogen deficiency aggravates the severity of experimental periodontitis (Anbinder et al., 2016). Clinically, postmenopausal women with osteoporosis and concurrent periodontitis have been found to exhibit an exaggerated response

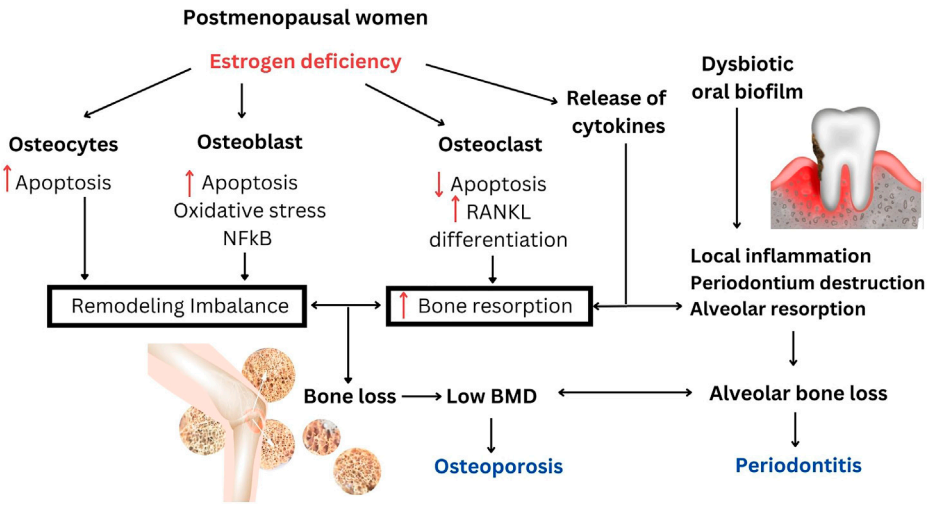

FIGURE 1
The impact of estrogen deficiency and the association between postmenopausal osteoporosis and periodontitis. Estrogen deficiency is responsible for the increase in systemic bone resorption and remodeling imbalance that would also accelerate the increase in alveolar bone resorption. Loss of BMD in postmenopausal osteoporosis may be responsible for increasing alveolar bone loss in periodontitis. Local inflammation in periodontitis may activate systemic osteoclastogenic cytokines and further aggravates bone loss.

to dental plaque, higher periodontal attachment loss and a significant reduction of alveolar bone compared to healthy women (Singh et al., 2014). These changes are evident through the assessment of periodontal health such as increased gingival bleeding and periodontal pocket depth, decreased BMD of the alveolar crestal and subcrestal bone, loss of dentoalveolar bone height, or loss of clincial attachment and tooth (Marjanovic et al., 2013; Jang et al., 2015; Juluri et al., 2015; Savić Pavičin et al., 2017).

It was hypothesized that osteoporosis could accelerate alveolar bone resorption and bone loss in periodontitis because the loss of alveolar BMD allowed deeper bacterial penetration into the enlarged periodontal space. In response to local inflammation, alveolar resorption could be further amplified and accelerated as focal infection of the periodontium may also release inflammatory cytokines into the system (Barbato et al., 2015). Additionally, overexpression of proinflammatory cytokines with osteoclastic activity occured in both osteoporosis and periodontitis (Barbato et al., 2015; Inchingolo et al., 2020). The impact of estrogen deficiency and the association between postmenopausal osteoporosis and periodontitis are shown in the schematic diagram (Figure 1).

4 Therapeutic potential of phytoestrogens

Phytoestrogens are generally divided into four major groups: isoflavones, stilbenes, coumestans and lignans. Isoflavones are the most widely used and studied phytoestrogens. They are found primarily in soybeans and other legumes, which constitute the major dietary source of phytoestrogens in Asian communities (Rowe & Baber, 2021). Genistein and daidzein are the two well-characterized isoflavones that have also been shown to have estrogenic potential. Resveratrol is the most common and the main dietary source of phytoestrogenic stilbenes. Its estrogenic activity is dependent on the two isomers, cis and trans. Trans has been reported to have higher estrogenic activity (Desmawati & Sulastri, 2019). Coumestans are biosynthetically related to isoflavones but only a small number of coumestans have shown estrogenic activity (Poluzzi et al., 2014). Lignans, the major dietary source in Western diets, are mostly derived from fruit, vegetables, legumes and whole grains. Lignan dimers that are not estrogenic themselves can be converted by gut microflora to mammalian lignans, the enterodiol and enterolactone which are estrogenic (Cornwell et al., 2004).

Phytoestrogens have been extensively studied for their potential role to prevent and treat diseases related to aging such as menopausal symptoms and skin aging, cardiovascular, neurodegenerative, immune and metabolic diseases and cancer. Recent systematic review and meta-analysis reported that consumption of low doses of phytoestrogen (25 mg/d ≤ dose ≤100 mg/d) for a long-term duration were effective in relieving depression symptoms in postmenopausal women (Li et al., 2021). Some reported adverse effect associated to phytoestrogens in menopausal women however are not yet clear and required more supportive evidence from high-quality randomized control trial (RCT) studies. Animal studies showed that high-dose administration of phytoestrogens (equol and *puerarian mirica*) modulated female reproductive system by enhancing the levels of serum luteinizing hormone and reducing urinary follicular stimulating hormone in ovariectomized rats and cynomolgus monkeys respectively (Rachoń et al., 2007; Trisomboon et al., 2007). Exogenous estrogen-like molecules could promote reproductive function and it also could possibly destroy reproductive processes (Sirotkin & Harrath, 2014). Nevertheless,

no adverse effects of phytoestrogens on human reproduction has been reported yet. In a RCT, supplemention of 100 mg isoflavones-rich, concentrated soy extract daily to postmenopausal women for 6 months has improved their skin health by increasing epithelial thickness, number of elastic and collagen fibres (Accorsi-Neto et al., 2009).

Soy genistein has been proposed to have a promising therapeutic effect for metabolism improvement and treatment of metabolic disorder (Behloul & Wu, 2013). In an RCT, 250 mg per day of genistein administered to non-alcoholic fatty liver patients for 2 months demonstrated reduction in insulin levels, indicating the ability of phytoestrogen to modulate human endocrine system (Amanat et al., 2018). Supplementation of soy protein with 66 mg isoflavones for 6 months has been found to significantly improve cardiovascular disease risk markers in women during the early menopause (Sathyapalan et al., 2018). A meta-analysis of epidemiological studies has found that the intake of soy isoflavones by pre- and post-menopausal women in Asian countries could lower the risk of breast cancer (Chen et al., 2014). Several other studies have shown the potential effect of phytoestrogen consumption in reducing the risks of lung cancer (Shimazu et al., 2011), stomach cancer (Ko et al., 2013), prostate cancer (He et al. 2015; Hwang et al., 2009), endometrial and ovarian cancer (Bandera et al., 2009; Qu et al., 2014).

The therapeutic potential described above indicated that phytoestrogens possess beneficial effect on the health of various organs and systems at different doses. Though the main mechanism of action of phytoestrogens is due to ER binding, their antioxidant, anti-inflammatory and other properties could also contribute to their pro-health effects. For example, the interaction of phytoestrogens with ER as well as their antioxidant properties might contribute to its neuroprotective effects (Gorzkiewicz et al., 2021). Several studies showed that different forms of soybean including soy isoflavones have antibacterial activity against oral microbes (Lee & Kim, 2006; Wang et al., 2010; Laodheerasiri and Horana Pathirage, 2017; Choo et al., 2020; How et al., 2020). Antimicrobial activity of phytoestrogens may be useful for the treatment and prevention of periodontal disease as periodontitis is known to have bacterial cause. Dental plaque and polymicrobial infections play a pivotal role in the initiation of periodontitis. For this reason, elimination or controlling the bacteria could be a beneficial approach in managing periodontal diseases.

5 Phytoestrogens and bone

In view of its role as the key regulator of bone metabolism, it has been hypothesized that phytoestrogens exerted bone health effects through their estrogenic potential, usually by binding to estrogen receptors (Chiang and Pan. 2013). As described earlier, soy isoflavones is one of the most widely studied phytoestrogens and they have received considerable attention in the management of postmenopausal bone loss. In the last decades, numerous clinical studies have been conducted in a wide range of populations including Western and Asian counterparts using different types of isoflavones preparations. Observational studies showed that women who consume higher amounts of soy foods have lower risk of postmenopausal fracture (Setchell & Lydeking-Olsen, 2003; Messina et al., 2004; McCarty, 2006) and as a consequent many clinical trials have attempted to evaluate the protective role of soy isoflavones on bone health (Lagari & Levis, 2013). Reported findings on the skeletal effects of isoflavones from clinical trials however are inconsistent due to the variation of study design and length of intervention, study population, dose and types of isoflavones preparation. The inconclusive results from human clinical trials are generally contributed by their heterogeneity and poor quality (Rowe & Baber, 2021).

A systematic review of RCT in 2016 compiled 23 eligible studies that ranged from 7 weeks to 3 years of interventions, which mainly assessed the effectiveness of phytoestrogens intervention through the measurement of whole body or regional BMD or bone mineral content, T-scores and bone metabolism biomarkers during the menopause transition (Abdi et al., 2016). Though there were controversial reports about changes in BMD, different types of soy isoflavones extracts (including genistein and daidzein), dietary products containing different amounts of phytoestrogens and red clover extract may have beneficial effects on bone health in postmenopausal women. A recent meta-analysis and systemic review of RCT concluded that isoflavones could be beneficial in preserving BMD and reducing bone resorption in premenopausal and postmenopausal women (Lambert et al., 2017). This could be linked to the effect of phytoestrogens principally as antiresorptive agents rather than their potential in bone formation. The use of isoflavones aglycones with well-controlled, standardized and defined isoflavones interventions revealed greater efficacy in treating BMD loss in estrogen-deficient women compared to glycosides and less well-defined isoflavones formulation. One year intake of novel red clover extract rich in isoflavones aglycones and probiotics has been found to potently attenuated BMD loss and improved bone turnover in postmenopausal osteopenic women (Lambert et al., 2017).

Although human clinical trials are inconsistent and some reported negative findings, numerous *in vitro* and animal studies on phytoestrogens revealed encouraging bone sparing effects. Phytoestrogen could promote osteogenesis by specifically targeting osteoblast and osteoclast. The administration of phytoestrogens such as isoflavones and flavonoids promoted bone formation, which stimulate the expression of osteogenic markers such as Runx2, ALP, osteocalcin, type 1 collagen (COL-1), osteopontin, and morphogenetic protein-2 (BMP-2) for osteoblast differentiation and bone matrix mineralization (Ramesh et al., 2021; Ortiz et al., 2022; Sekaran et al., 2022). Additionally, by virtue of its similar structure to 17β-estradiol in conformational binding to estrogen receptors, phytoestrogen has capability to reciprocally affect osteogenic *versus* adipogenic differentiation of mesenchymal stem cells (MSCs) in a dose dependent manner. For instance, phytoestrogen stimulated osteoblast differentiation from MSCs *via* the activation of important signalling pathways such as Smad, Wnt/β-catenin and Sirt1 pathways (Schilling et al., 2014; Gorabi et al., 2019; Khezri et al., 2021; Wang et al., 2021). Concomitantly, there is evidence that phytoestrogen suppressed the adipogenic differentiation signalling pathway including PPAR and C/EBP pathways in a dose dependent manner (Schilling et al., 2014; Ahmed 2014).

TABLE 1 Summary findings on the therapeutic potential of phytoestrogens against alveolar bone loss.

Phytoestrogen	Summary findings	Author
Soy Isoflavones	Soy isoflavones increased the expression of tight junction proteins, and reduced IL-17 level and alveolar bone loss, alleviating periodontitis in ovariectomised rats	Liu et al. (2022)
Diosgenin	Diosgenin significantly reduced TNF-α and osteocalcin expression. Results from circRNA profile and the circRNA-miRNA-mRNA network demonstrated that the potential mechanism of diosgenin to inhibit osteoclastogenesis by regulating the expression of Wnt, PI3K, RANK/RANKL or osteoclastogenic cytokine pathways	Zhang et al. (2020)
Diosgenin	Diosgenin significantly reduced the level of TRAP and increased the level of ALP. Diosgenin promoted the bone formation process by increasing Smad4, Smad8, and beta-catenin/Tcf, osterix, ALP and OPN and inhibited two potent stimulators of osteoclastogenesis TNF-α and IL-1 β and their receptors, IL-1R and TNF-R1. mRNA expression of TRAP in alveolar bone was shown to be downregulated after a 12-week diosgenin treatment	Zhang et al. (2018)
Genistein	Histological and μCT analyses demonstrated that genistein administration decreased distance between the CEJ and the apex of the alveolar bones. Genistein significantly reduced the level of TRAP, COX-2 and ICAM expression in the inflamed region of mice with periodontitis	Bhattarai et al. (2017)
Genistein	Genistein administration prevented alveolar bone loss significantly induced by ligature placement (about 74%). Genistein administration also increased microstructural parameters of trabecular bone, including Tb.Th, Tb.Sp, bone BMD and structure model index	Choi et al., 2016

IL, interleukin; TNF-α, tumor necrosis factor; RANKL, receptor activator of nuclear factor kappa-ligand; OPN, osteopontin; ALP, alanine phosphatase; TRAP, tartrate-resistant acid phosphatase; μCT, micro-computed tomography; COX-2, clyclooxygenase; ICAM, intercellular adhesion molecule; Tb.Th, trabecular thickness; Tb.Sp, trabecular separation; BMD, bone mineral density; SMI, structure model index; BMD, bone mineral density.

In addition, the process of bone resorption and formation are closely coupled through the RANKL/OPG system. The integrity of the skeleton is maintained through bone formation followed by a balanced cycle of bone resorption (Narducci et al., 2011; Sharma et al., 2022). Intriguingly, phytoestrogen was able to regulate the RANKL/OPG system, thereby playing an important role in the pathogenesis of osteoporosis (Ni et al., 2023; Hooshiar et al., 2022; Zakłos-Szyda et al., 2020). Furthermore, phytoestrogen exerted antiresorptive activities by suppressing the expression of osteoclast differentiation markers such as matrix metalloproteinase 9 (MMP9), cathepsin-K and tartrate-resistant acid phosphatase (TRAP) *via* downregulating the activation of NF-κB and MAPK signaling pathways (Xu et al., 2022; Tanaka et al., 2020). These findings demonstrated that phytoestrogen treatments could inhibit osteoclast activation and therefore have therapeutic potential for osteoporosis.

The primary endpoints that generally measured following hormone ablation in *in vivo* studies include, trabecular bone and/or cortical bone mass, BMD and mechanical strength. Changes in bone turnover markers and uterine weight were also measured. Phytoestrogens significantly increased both trabecular and/or cortical bone volume in OVX-induced bone loss with no uterotrophic effect in animal models (Inchingolo et al., 2020; Long et al., 2022). Phytoestrogen was also shown to significantly decreased urinary excretion of deoxypyridinoline (DPD), which is one of the bone resorption markers (Li et al., 2021; Song et al., 2016). Furthermore, phytoestrogen exerted antioxidant effects as shown by the increased expression of antioxidant enzymes such as superoxide dismutase (SOD) and gluthathione (GSH), that serve to scavenge the excess free radicals. This antioxidative effect of phytoestrogens also inhibit osteoclast differentiation (Oršolić et al., 2022). Overall, findings from *in vivo* studies are in line with *in vitro* studies, which demonstrated the bone-conserving effects of phytoestrogens in reducing bone loss due to estrogen deficiency.

5.1 Effects of phytoestrogens on alveolar bone loss

Being a systemic disease, the manifestation of bone loss in osteoporosis is not only evident in vertebrae and appendicular skeleton but also in alveolar bone (Muslita et al., 2012). For this reason, osteoporosis is expected to accelerate alveolar bone resorption caused by periodontitis (Guiglia et al., 2013). Additionally, osteoporosis results in an increase in certain inflammatory cytokines which are also affected in the progression of periodontitis. Oxidative stress is also an indicator of periodontitis development, which is evident by the accumulation of ROS (Kanzaki et al., 2017). Studies on the potential skeletal effects of phytoestrogens in postmenopausal osteoporosis at the preclinical (*in vitro* and in animal models) and clinical level have been substantially reported in the literature. To the best of our knowledge, studies on the effect of phytoestrogens on postmenopausal osteoporosis with periodontal disease in human are still lacking. Nonetheless, several animal studies have been carried out recently to evaluate the protective effects of phytoestrogens against alveolar bone loss in postmenopausal osteoporosis with or without experimental periodontitis.

Table 1 summarizes the effect of phytoestrogens against alveolar bone loss. In a recently published study, oral administration of soy isoflavones was found to alleviate experimental periodontitis in estrogen-deficient rats as revealed by the increased expression of tight junction proteins in the gingiva, reduced proinflammatory cytokines, IL-17 and ROS levels (Liu et al., 2022). Attenuation of alveolar bone loss was observed through micro-CT and histologic observation. Experimental periodontitis in OVX rats was established by silk ligature and inoculation with *Porphyromonas gingivalis,* a Gram-negative anaerobe, which is one of the well-characterized periodontal pathogens involved in periodontitis. *P. gingivalis* possibly modulate the immune response through the

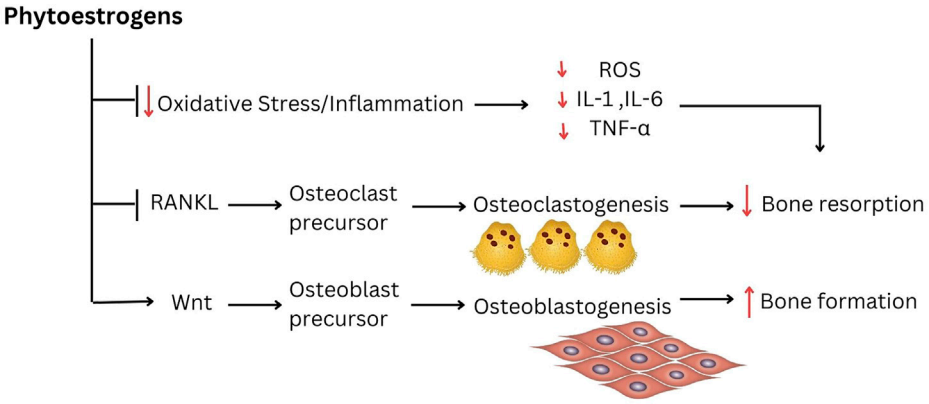

FIGURE 2
The possible molecular mechanism underlying the protection against alveolar bone loss by phytoestrogens.

inactivation of certain cytokines (Baek et al., 2015). An *in vitro P. gingivalis* infection model was also used to determine whether grainyhead-like 2 (GRHL2), the epithelial transcription factor and ER-binding partner (He et al., 2020) is required by soy isoflavones to enhance the oral epithelial barrier. It was found that the enhancement of oral gingival epithelial barrier function by soy isoflavones treatment was partially dependent on GRHL2 (Liu et al., 2022).

Earlier studies showed that genistein, a major subclass of isoflavones found in soybean was protective against periodontitis-induced alveolar bone loss (Choi et al., 2016; Bhattarai et al., 2017). Genistein was found to significantly attenuated *Prevotella intermedia* LPS-induced production of inducible nitric oxide synthase (iNOS) and IL-6 coupled with the decreased in their mRNA expression in RAW264.7 cells. In experimental animal, alveolar bone height and bone volume fraction were decreased and microstructural parameters of trabecular bone were improved with administration of genistein (Choi et al., 2016). These findings were in line with a study by Bhattarai et al. (2017) that also showed a reduction in LPS-induced alveolar bone loss with genistein administration. Additionally, genistein significantly prevented osteoclast differentiation by suppressing the expression of osteoclast-specific molecules in NFκB ligand- or LPS-stimulated macrophages. Apart from its inhibitory effect on osteoclast activation, the protection against LPS-mediated stresses by genistein was indicated by the reduction of mitochondrial impairment and ROS accumulation, which lead to the reduction of periodontal damage. The reported antioxidant and anti-osteoclastic potential of phytoestrogen genistein might be protective against alveolar bone loss in postmenopausal osteoporosis condition.

A study done by Zhang et al. (2018) has found that 12-week oral treatment with diosgenin, a natural steroidal saponin and a phytoestrogen, suppressed alveolar bone loss in OVX rats by promoting bone formation. Though the effects of estradiol valerate on alveolar bone volume was greater than diosgenin, both treatments showed reduced alveolar bone loss compared to OVX rats as indicated by 3-D bone microstructure analysis and histological observation. The protective role of diosgenin on bone loss was also described earlier in the peripheral skeletal of OVX rats (Zhang et al., 2014; Folwarczna et al., 2016). The bone protective effect of diosgenin might be associated with the modulation of RANKL/OPG ratio (Zhang et al., 2014). As with other phytoestrogens, diosgenin may be one of the sparse compounds that have the potential to increase bone formation and inhibit bone resorption. In this study, lncRNA and mRNA profiles were evaluated using a microarray to confirm the anti-osteoporotic effects of diosgenin on alveolar bone. Diosgenin may have exerted this effect by increasing the Wnt and BMPs pathways, the two recognized signaling pathways that regulate the osteogenic differentiation of mesenchymal stem cells or preosteoblasts (Lin and Hankenson, 2011; Marcellini et al., 2012). This finding was further supported by another study by Zhang et al. (2020). The study revealed that anti-bone loss action of diosgenin on alveolar bone was attributed by the regulation of important molecules expression in the Wnt, P13K, RANK/RANKL or osteoclastogenic cytokine pathways. The possible molecular mechanisms underlying the protection against alveolar bone loss by phytoestrogens are summarized in Figure 2.

6 Conclusion

Association between postmenopausal osteoporosis and periodontitis has long been postulated though its causal relationship is yet to be determined. *In vitro* and animal studies have demonstrated phytoestrogens favorable effects on skeletal health. Phytoestrogens may exert their bone protective effect by inhibiting bone resorption and promoting bone formation. Phytoestrogens mainly isoflavones, may offer protection against alveolar bone loss in postmenopausal osteoporosis condition. Well-designed clinical trials are needed to determine the therapeutic potential of phytoestrogen on skeletal health particularly in postmenopausal women. Phytoestrogens can be potentially developed as adjunctive preventive and therapeutic cost-effective strategies in the treatment and prevention of bone loss in postmenopausal osteoporosis with periodontitis.

Author contributions

PJ and AS contributed toward conceptualization, planning and writing the paper. PJ and HA took the lead in drafting and writing the manuscript. AS and BB revise the manuscript for important intellectual content. NN and NI contributed toward conceptualization and editing of the manuscript. All authors read and approved the final manuscript.

Acknowledgments

We thank Universiti Kebangsaan Malaysia, Universiti Teknologi MARA and Manipal University College Malaysia for the support in completing this project.

Conflict of interest

The authors declare that the research was conducted in the absence of any commercial or financial relationships that could be construed as a potential conflict of interest.

Publisher's note

All claims expressed in this article are solely those of the authors and do not necessarily represent those of their affiliated organizations, or those of the publisher, the editors and the reviewers. Any product that may be evaluated in this article, or claim that may be made by its manufacturer, is not guaranteed or endorsed by the publisher.

References

Abdi, F., Alimoradi, Z., Haqi, P., and Mahdizad, F. (2016). Effects of phytoestrogens on bone mineral density during the menopause transition: A systematic review of randomized, controlled trials. *Climacteric* 19 (6), 535–545. doi:10.1080/13697137.2016.1238451

Accorsi-Neto, A., Haidar, M., Simões, R., Simões, M., Soares, J., Jr, and Baracat, E. (2009). Effects of isoflavones on the skin of postmenopausal women:a pilot study. *Clinics* 64 (6), 505–510. doi:10.1590/s1807-59322009000600004

Ahmed, B. (2014). Combinations of genistein, EGCG and/or resveratrol synergistically inhibit pre-adipocyte differentiation by suppressing PPAR-γ/C/EBP-α pathway (Doctoral dissertation, Tennessee State University)

Al-Daghri, N. M., Aziz, I., Yakout, S., Aljohani, N. J., Al-Saleh, Y., Amer, O. E., et al. (2017). Inflammation as a contributing factor among postmenopausal Saudi women with osteoporosis. *Medicine* 96 (4), e5780. doi:10.1097/MD.0000000000005780

Amanat, S., Eftekhari, M. S., Fararouei, M., BagheriLankarani, K. B., and Massoumi, S. J. (2018). Genistein supplementation improves insulin resistance and inflammatory state in non-alcoholic fatty liver patients: A randomized, controlled trial. *Clin. Nutr.* 37 (4), 1210–1215. doi:10.1016/j.clnu.2017.05.028

Anbinder, A. L., Moraes, R. M., Lima, G. M., Oliveira, F. E., Campos, D. R., Rossoni, R. D., et al. (2016). Periodontal disease exacerbates systemic ovariectomy-induced bone loss in mice. *Bone* 83, 241–247. doi:10.1016/j.bone.2015.11.014

Ayed, M. S., Alsharif, A. F., Divakar, D. D., Jhugroo, C., Alosaimi, B., and Mustafa, M. (2019). Evaluating the possible association between systemic osteoporosis and periodontal disease progression in postmenopausal women. *Disease-a-month.* 65 (6), 193–215. doi:10.1016/j.disamonth.2018.11.001

Baek, K. J., Ji, S., Kim, Y. C., and Choi, Y. (2015). Association of the invasion ability of Porphyromonas gingivalis with the severity of periodontitis. *Virulence* 6 (3), 274–281. doi:10.1080/21505594.2014.1000764

Bandera, E. V., Williams, M. G., Sima, C., Bayuga, S., Pulick, K., Wilcox, H., et al. (2009). Phytoestrogen consumption and endometrial cancer risk: A population-based case–control study in New Jersey. *Cancer Causes Control* 20, 1117–1127. doi:10.1007/s10552-009-9336-9

Barbato, L., Francioni, E., Bianchi, M., Mascitelli, E., Marco, L. B., and Tonelli, D. P. (2015). Periodontitis and bone metabolism. *Clin. Cases Min. Bone Metab.* 12 (2), 174–177. doi:10.11138/ccmbm/2015.12.2.174

Barbour, K. E., Lui, L. Y., Ensrud, K. E., Hillier, T. A., LeBlanc, E. S., Ing, S. W., et al. (2014). Inflammatory markers and risk of hip fracture in older white women: The study of osteoporotic fractures. *J. Bone Min. Res.* 29 (9), 2057–2064. doi:10.1002/jbmr.2245

Behloul, N., and Wu, G. (2013). Genistein: A promising therapeutic agent for obesity and diabetes treatment. *Eur. J. Pharmacol.* 698 (1-3), 31–38. doi:10.1016/j.ejphar.2012.11.013

Bhattarai, G., Poudel, S. B., Kook, S. H., and Lee, J. C. (2017). Anti-inflammatory, anti-osteoclastic, and antioxidant activities of genistein protect against alveolar bone loss and periodontal tissue degradation in a mouse model of periodontitis. *J. Biomed. Mat. Res. Part A* 105 (9), 2510–2521. doi:10.1002/jbm.a.36109

Bord, S., Horner, A., Beavan, S., and Compston, J. (2001). Estrogen receptors α and β are differentially expressed in developing human bone. *J. Clin. Endocrinol. Metab.* 86 (5), 2309–2314. doi:10.1210/jcem.86.5.7513

Braidman, I. P., Hainey, L., Batra, G., Selby, P. L., Saunders, P. T., and Hoyland, J. A. (2001). Localization of estrogen receptor β protein expression in adult human bone. *J. Bone Min. Res.* 16 (2), 214–220. doi:10.1359/jbmr.2001.16.2.214

Brandão, C. M. R., Machado, G. P. D. M., and Acurcio, F. D. A. (2012). Análise farmacoeconômica das estratégias de tratamento da osteoporose em mulheres na pós-menopausa: uma revisão sistemática. *Rev. Bras. Reumatol.* 52, 924–937. doi:10.1590/s0482-50042012000600010

Cervellati, C., Bonaccorsi, G., Cremonini, E., Romani, A., Fila, E., Castaldini, M. C., et al. (2014). Oxidative stress and bone resorption interplay as a possible trigger for postmenopausal osteoporosis. *Biomed. Res. Int.* 2014, 569563. doi:10.1155/2014/569563

Chang, H. J., Lee, S. J., Yong, T. H., Shin, N. Y., Jang, B. G., Kim, J. E., et al. (2020). Deep learning hybrid method to automatically diagnose periodontal bone loss and stage periodontitis. *Sci. Rep.* 10 (1), 7531–7538. doi:10.1038/s41598-020-64509-z

Chen, M., Rao, Y., Zheng, Y., Wei, S., Li, Y., Guo, T., et al. (2014). Association between soy isoflavone intake and breast cancer risk for pre-and post-menopausal women: A meta-analysis of epidemiological studies. *PloS One* 9 (2), e89288. doi:10.1371/journal.pone.0089288

Chiang, S. S., and Pan, T. M. (2013). Beneficial effects of phytoestrogens and their metabolites produced by intestinal microflora on bone health. *Appl. Microbiol. Biotechnol.* 97 (4), 1489–1500. doi:10.1007/s00253-012-4675-y

Choi, E. Y., Bae, S. H., Ha, M. H., Choe, S. H., Hyeon, J. Y., Choi, J. I., et al. (2016). Genistein suppresses Prevotella intermedia lipopolysaccharide-induced inflammatory response in macrophages and attenuates alveolar bone loss in ligature-induced periodontitis. *Arch. Oral Biol.* 62, 70–79. doi:10.1016/j.archoralbio.2015.11.019

Choo, S. M., Yap, K. Y., Yap, W. H., and Ewe, J. A. (2020). Soy fermentation by orally isolated putative probiotic Streptococcus salivarius for healthy oral. *J. Int. Oral Health* 12 (1), 33. doi:10.4103/jioh.jioh_196_19

Clynes, M. A., Harvey, N. C., Curtis, E. M., Fuggle, N. R., Dennison, E. M., and Cooper, C. (2020). The epidemiology of osteoporosis. *Br. Med. Bull.* 133, 105–117. doi:10.1093/bmb/ldaa005

Contaldo, M., Itro, A., Lajolo, C., Gioco, G., Inchingolo, F., and Serpico, R. (2020). Overview on osteoporosis, periodontitis and oral dysbiosis: The emerging role of oral microbiota. *Appl. Sci.* 10 (17), 6000. doi:10.3390/app10176000

Cornwell, T., Cohick, W., and Raskin, I. (2004). Dietary phytoestrogens and health. *Phytochem* 65 (8), 995–1016. doi:10.1016/j.phytochem.2004.03.005

Cruzoé-Souza, M., Sasso-Cerri, E., and Cerri, P. S. (2009). Immunohistochemical detection of estrogen receptor β in alveolar bone cells of estradiol-treated female rats: Possible direct action of estrogen on osteoclast life span. *J. Anat.* 215 (6), 673–681. doi:10.1111/j.1469-7580.2009.01158.x

Delgobo, M., Agnes, J. P., Goncalves, R. M., Dos Santos, V. W., Parisotto, E. B., Zamoner, A., et al. (2019). N-acetylcysteine and alpha-lipoic acid improve antioxidant defenses and decrease oxidative stress, inflammation and serum lipid levels in ovariectomized rats via estrogen-independent mechanisms. *J. Nutr. Biochem.* 67, 190–200. doi:10.1016/j.jnutbio.2019.02.012

Desmawati, D., and Sulastri, D. (2019). Phytoestrogens and their health effect. *Open Access Maced. J. Med. Sci.* 7 (3), 495–499. doi:10.3889/oamjms.2019.044

Djapardy, V., and Panay, N. (2022). Alternative and non-hormonal treatments to symptoms of menopause. *Best. Pract. Res. Clin. Obstet. Gynaecol.* 81, 45–60. doi:10.1016/j.bpobgyn.2021.09.012

Du, D., Zhou, Z., Zhu, L., Hu, X., Lu, J., Shi, C., et al. (2018). TNF-α suppresses osteogenic differentiation of MSCs by accelerating P2Y2 receptor in estrogen-deficiency induced osteoporosis. *Bone* 117, 161–170. doi:10.1016/j.bone.2018.09.012

Eminov, E., Hortu, I., Akman, L., Erbas, O., Yavasoglu, A., and Cirpan, T. (2018). Exenatide preserves trabecular bone microarchitecture in experimental ovariectomized rat model. *Arch. Gynecol. Obstet.* 297 (6), 1587–1593. doi:10.1007/s00404-018-4776-7

Fang, H., Deng, Z., Liu, J., Chen, S., Deng, Z., and Li, W. (2022). The mechanism of bone remodeling after bone aging. *Clin. Interv. Aging.* 405, 405–415. doi:10.2147/CIA.S349604

Feng, W., Guo, J., and Li, M. (2019). RANKL-independent modulation of osteoclastogenesis. *J. Oral Biosci.* 61 (1), 16–21. doi:10.1016/j.job.2019.01.001

Fischer, V., and Haffner-Luntzer, M. (2022). Interaction between bone and immune cells: Implications for postmenopausal osteoporosis. *Seminars Cell and Dev.* Biol. 123, 14–21. doi:10.1016/j.semcdb.2021.05.014

Florencio-Silva, R., Sasso, G. R., Sasso-Cerri, E., Simões, M. J., and Cerri, P. S. (2018). Effects of estrogen status in osteocyte autophagy and its relation to osteocyte viability in alveolar process of ovariectomized rats. *Biomed. Pharmacother.* 98, 406–415. doi:10.1016/j.biopha.2017.12.08910.1016/j.biopha.2017.12.089

Folwarczna, J., Zych, M., Nowińska, B., Pytlik, M., Bialik, M., Jagusiak, A., et al. (2016). Effect of diosgenin, a steroidal sapogenin, on the rat skeletal system. *Acta Biochim. Pol.* 63 (2), 287–295. doi:10.18388/abp.2015_1095

Gerbarg, P. L., and Brown, R. P. (2016). Pause menopause with Rhodiola rosea, a natural selective estrogen receptor modulator. *Phytomedicine* 23 (7), 763–769. doi:10.1016/j.phymed.2015.11.013

Golub, L. M., Payne, J. B., Reinhardt, R. A., and Nieman, G. (2006). Can systemic diseases co-induce (not just exacerbate) periodontitis? A hypothetical "two-hit" model. *J. Dent. Res.* 85 (2), 102–105. doi:10.1177/154405910608500201

Gorabi, A. M., Kiaie, N., Hajighasemi, S., Jamialahmadi, T., Majeed, M., and Sahebkar, A. (2019). The effect of curcumin on the differentiation of mesenchymal stem cells into mesodermal lineage. *Molecules* 24 (22), 4029. doi:10.3390/molecules24224029

Gorzkiewicz, J., Bartosz, G., and Sadowska-Bartosz, I. (2021). The potential effects of phytoestrogens: The role in neuroprotection. *Molecules* 26 (10), 2954. doi:10.3390/molecules26102954

Grover, C. M., More, V. P., Singh, N., and Grover, S. (2014). Crosstalk between hormones and oral health in the mid-life of women: A comprehensive review. *J. Int. Soc. Prev. Community Dent.* 4, S5–S10. doi:10.4103/2231-0762.144559

Guiglia, R., Di-Fede, O., Lo-Russo, L., Sprini, D., Rini, G. B., and Campisi, G. (2013). Osteoporosis, jawbones and periodontal disease. *Med. Oral Patol. Oral Cir. Bucal* 18 (1), e93–e99. doi:10.4317/medoral.18298

Hajishengallis, G. (2014). Immunomicrobial pathogenesis of periodontitis: Keystones, pathobionts, and host response. *Trends Immunol.* 35 (1), 3–11. doi:10.1016/j.it.2013.09.001

Han, K., Ko, Y., Park, Y. G., and Park, J. B. (2016). Associations between the number of natural teeth in postmenopausal women and hormone replacement therapy. *Maturitas* 94, 125–130. doi:10.1016/j.maturitas.2016.10.005

He, J., Feng, C., Zhu, H., Wu, S., Jin, P., and Xu, T. (2020). Grainyhead-like 2 as a double-edged sword in development and cancer. *Am. J. Trans. Res.* 12 (2), 310–331.

He, J., Wang, S., Zhou, M., Yu, W., Zhang, Y., and He, X. (2015). Phytoestrogens and risk of prostate cancer: A meta-analysis of observational studies. *World J. Surg. Oncol.* 13 (1), 1–11. doi:10.1186/s12957-015-0648-9

How, Y. H., Ewe, J. A., Song, K. P., Kuan, C. H., Kuan, C. S., and Yeo, S. K. (2020). Soy fermentation by indigenous oral probiotic Streptococcus spp. and its antimicrobial activity against oral pathogens. *Int. Food Res. J.* 27 (2), 357–365.

Hooshiar, S. H., Tobeiha, M., and Jafarnejad, S. (2022). Soy Isoflavones and Bone Health: Focus on the RANKL/RANK/OPG Pathway. *BioMed Res. Int.*, 1–10. doi:10.1155/2022/8862278

Hwang, Y. W., Kim, S. Y., Jee, S. H., Kim, Y. N., and Nam, C. M. (2009). Soy food consumption and risk of prostate cancer: A meta-analysis of observational studies. *Nutr. Cancer.* 61 (5), 598–606. doi:10.1080/01635580902825639

Inchingolo, F., Martelli, F. S., Gargiulo Isacco, C., Borsani, E., Cantore, S., Corcioli, F., et al. (2020). Chronic periodontitis and immunity, towards the implementation of a personalized medicine: A translational research on gene single nucleotide polymorphisms (SNPs) linked to chronic oral dysbiosis in 96 caucasian patients. *Biomedicines* 8 (5), 115. doi:10.3390/biomedicines8050115

Jafri, Z., Bhardwaj, A., Sawai, M., and Sultan, N. (2015). Influence of female sex hormones on periodontium: A case series. *J. Nat. Sci. Biol. Med.* 6, S146–S149. doi:10.4103/0976-9668.166124

Jang, K. M., Cho, K. H., Lee, S. H., Han, S. B., Han, K. D., and Kim, Y. H. (2015). Tooth loss and bone mineral density in postmenopausal south Korean women: The 2008–2010 Korea national health and nutrition examination survey. *Maturitas* 82 (4), 360–364. doi:10.1016/j.maturitas.2015.07.016

Johnston, B. D., and Ward, W. E. (2015). The ovariectomized rat as a model for studying alveolar bone loss in postmenopausal women. *Biomed. Res. Int.* 2015, 635023. doi:10.1155/2015/635023

Jonasson, G., Skoglund, I., and Rythén, M. (2018). The rise and fall of the alveolar process: Dependency of teeth and metabolic aspects. *Arch. Oral Biol.* 96, 195–200. doi:10.1016/j.archoralbio.2018.09.016

Juluri, R., Prashanth, E., Gopalakrishnan, D., Kathariya, R., Devanoorkar, A., Viswanathan, V., et al. (2015). Association of postmenopausal osteoporosis and periodontal disease: A double-blind case-control study. *J. Int. Oral Health.* 7 (9), 119–123.

Kanzaki, H., Wada, S., Narimiya, T., Yamaguchi, Y., Katsumata, Y., Itohiya, K., et al. (2017). Pathways that regulate ROS scavenging enzymes, and their role in defense against tissue destruction in periodontitis. *Front. Physiol.* 8, 351. doi:10.3389/fphys.2017.00351

Kawai, T., Matsuyama, T., Hosokawa, Y., Makihira, S., Seki, M., Karimbux, N. Y., et al. (2006). B and T lymphocytes are the primary sources of RANKL in the bone resorptive lesion of periodontal disease. *Am. J. Pathol.* 169 (3), 987–998. doi:10.2353/ajpath.2006.060180

Khezri, K., Maleki Dizaj, S., Rahbar Saadat, Y., Sharifi, S., Shahi, S., Ahmadian, E., et al. (2021). Osteogenic differentiation of mesenchymal stem cells via curcumin-containing nanoscaffolds. *Stem Cells Int.* 2021, 1520052. doi:10.1155/2021/1520052

Kirk, B., Feehan, J., Lombardi, G., and Duque, G. (2020). Muscle, bone, and fat crosstalk: The biological role of myokines, osteokines, and adipokines. *Curr. Osteoporos. Rep.* 18 (4), 388–400. doi:10.1007/s11914-020-00599-y

Kładna, A., Berczy ´nski, P., Kruk, I., Piechowska, T., and Aboul-Enein, H. Y. (2016). Studies on the antioxidant properties of some phytoestrogens. *Luminescence* 31, 1201–1206. doi:10.1002/bio.3091

Ko, K. P., Park, S. K., Yang, J. J., Ma, S. H., Gwack, J., Shin, A., et al. (2013). Intake of soy products and other foods and gastric cancer risk: A prospective study. *J. Epidemiol.* 23 (5), 337–343. doi:10.2188/jea.JE20120232

Lagari, V. S., and Levis, S. (2013). Phytoestrogens in the prevention of postmenopausal bone loss. *J. Clin. Densitom.* 16 (4), 445–449. doi:10.1016/j.jocd.2013.08.011

Lambert, M. N. T., Hu, L. M., and Jeppesen, P. B. (2017). A systematic review and meta-analysis of the effects of isoflavone formulations against estrogen-deficient bone resorption in peri-and postmenopausal women. *Am. J. Clin. Nutr.* 106 (3), 801–811. doi:10.3945/ajcn.116.151464

Lambert, M. N. T., Thybo, C. B., Lykkeboe, S., Rasmussen, L. M., Frette, X., Christensen, L. P., et al. (2017). Combined bioavailable isoflavones and probiotics improve bone status and estrogen metabolism in postmenopausal osteopenic women: A randomized controlled trial. *Am. J. Clin. Nutr.* 106 (3), 909–920. doi:10.3945/ajcn.117.153353

Laodheerasiri, S., and Horana Pathirage, N. (2017). Antimicrobial activity of raw soybean, soybean flour and roasted soybean extracted by ethanol-hexane method. *Br. Food J.* 119 (10), 2277–2286. doi:10.1108/BFJ-10-2016-0499

Lee, S. L., and Kim, J. G. (2006). Anti-microbial activity of soybean extract against oral microbes. *J. Environ. Health Sci.* 32 (2), 192–197.

Li, J., Li, H., Yan, P., Guo, L., Li, J., Han, J., et al. (2021). Efficacy and safety of phytoestrogens in the treatment of perimenopausal and postmenopausal depressive disorders: A systematic review and meta-analysis. *Int. J. Clin. Pract.* 75 (10), e14360. doi:10.1111/ijcp.14360

Lin, G. L., and Hankenson, K. D. (2011). Integration of BMP, Wnt, and notch signaling pathways in osteoblast differentiation. *J. Cell. Biochem.* 112 (12), 3491–3501. doi:10.1002/jcb.23287

Liu, C., Zhang, S., Bai, H., Zhang, Y., Jiang, Y., Yang, Z., et al. (2022). Soy isoflavones alleviate periodontal destruction in ovariectomized rats. *J. Periodontal. Res.* 57 (3), 519–532. doi:10.1111/jre.12981

Long, L., Wang, X., Lei, Y., Guo, S., Wang, C., and Dai, W. (2022). Icariin: A Potential Alternative Against Osteoporosis. *Nat. Prod. Commun.* 17 (11), 1–15. doi:10.1177/1934578X221134881

Lorentzon, M., and Cummings, S. R. (2015). Osteoporosis: The evolution of a diagnosis. *J. Intern. Med.* 277 (6), 650–661. doi:10.1111/joim.12369

Luo, K., Ma, S., Guo, J., Huang, Y., Yan, F., and Xiao, Y. (2014). Association between postmenopausal osteoporosis and experimental periodontitis. *Biomed. Res. Int.* 2014, 316134. doi:10.1155/2014/316134

Manjunath, S. H., Rakhewar, P., Nahar, P., Tambe, V., Gabhane, M., and Kharde, A. (2019). Evaluation of the prevalence and severity of periodontal diseases between osteoporotic and nonosteoporotic subjects: A cross-sectional comparative study. *J. Contemp. Dent. Pract.* 20 (10), 1223–1228. doi:10.5005/jp-journals-10024-2717

Manolagas, S. C. (2000). Birth and death of bone cells: Basic regulatory mechanisms and implications for the pathogenesis and treatment of osteoporosis. *Endocr. Rev.* 21 (2), 115–137. doi:10.1210/edrv.21.2.0395

Manolagas, S. C. (2010). From estrogen-centric to aging and oxidative stress: A revised perspective of the pathogenesis of osteoporosis. *Endocr. Rev.* 31 (3), 266–300. doi:10.1210/er.2009-0024

Manolagas, S. C., O'brien, C. A., and Almeida, M. (2013). The role of estrogen and androgen receptors in bone health and disease. *Nat. Rev. Endocrinol.* 9 (12), 699–712. doi:10.1038/nrendo.2013.179

Manyonda, I., S Talaulikar, V., Pirhadi, R., and Onwude, J. (2020). Progestogens are the problem in hormone replacement therapy: Time to reappraise their use. *Post. Reprod. Health* 26 (1), 26–31. doi:10.1177/2053369119876490

Marcellini, S., Henriquez, J. P., and Bertin, A. (2012). Control of osteogenesis by the canonical Wnt and BMP pathways *in vivo*: Cooperation and antagonism between the canonical Wnt and BMP pathways as cells differentiate from osteochondroprogenitors to osteoblasts and osteocytes. *Bioessays* 34 (11), 953–962. doi:10.1002/bies.201200061

Marjanovic, E. J., Southern, H. N., Coates, P., Adams, J. E., Walsh, T., Horner, K., et al. (2013). Do patients with osteoporosis have an increased prevalence of periodontal disease? A cross-sectional study. *Osteoporos. Int.* 24 (7), 1973–1979. doi:10.1007/s00198-012-2246-9

Mashalkar, V. N., Suragimath, G., Zope, S. A., and Varma, S. A. (2018). A cross-sectional study to assess and correlate osteoporosis and periodontitis among postmenopausal women: A dual energy X-ray absorptiometry study. *J. Mid-life Health.* 9 (1), 2–7. doi:10.4103/jmh.JMH_39_17

McCarty, M. F. (2006). Isoflavones made simple–genistein's agonist activity for the beta-type estrogen receptor mediates their health benefits. *Med. Hypotheses.* 66 (6), 1093–1114. doi:10.1016/j.mehy.2004.11.046

Messina, M., Ho, S., and Alekel, D. L. (2004). Skeletal benefits of soy isoflavones: A review of the clinical trial and epidemiologic data. *Curr. Opin. Clin. Nutr. Metab. Care.* 7 (6), 649–658. doi:10.1097/00075197-200411000-00010

Mohd Dom, T. N., Ayob, R., Abd Muttalib, K., and Aljunid, S. M. (2016). National economic burden associated with management of periodontitis in Malaysia. *Int. J. Dent.* 2016, 1891074. doi:10.1155/2016/189107410.1155/2016/1891074

Mohd-Dom, T., Ayob, R., Mohd-Nur, A., Abdul-Manaf, M. R., Ishak, N., Abdul-Muttalib, K., et al. (2014). Cost analysis of periodontitis management in public sector specialist dental clinics. *BMC Oral Health* 14 (1), 56–10. doi:10.1186/1472-6831-14-5610.1186/1472-6831-14-56

Munoz, M., Robinson, K., and Shibli-Rahhal, A. (2020). Bone health and osteoporosis prevention and treatment. *Clin. Obstet. Gynecol.* 63 (4), 770–787. doi:10.1097/GRF.0000000000000572

Muslita, I., Lindawati, S. K., and Henni, K. (2012). Resorption level of edentulous alveolar bone in normal, osteopenia and osteoporosis postmenopausal women. *Int. J. Clin. Prev. Dent.* 8 (3), 141–146.

Narducci, P., Bareggi, R., and Nicolin, V. (2011). Receptor Activator for Nuclear Factor kappa B Ligand (RANKL) as an osteoimmune key regulator in bone physiology and pathology. *Acta histochem.* 113 (2), 73–81. doi:10.1016/j.acthis.2009.10.003

Ni, X., Wu, B., Li, S., Zhu, W., Xu, Z., Zhang, G., et al. (2023). Equol exerts a protective effect on postmenopausal osteoporosis by upregulating OPG/RANKL pathway. *Phytomedicine* 1, 108–154509. doi:10.1016/j.phymed.2022.154509

Oei, L., Koromani, F., Rivadeneira, F., Zillikens, M. C., and Oei, E. H. (2016). Quantitative imaging methods in osteoporosis. *Quant. Imaging Med. Surg.* 6 (6), 680–698. doi:10.21037/qims.2016.12.13

Oršolić, N., Nemrava, J., Jelec, Z., Kukolj, M., Odeh, D., and Jakopovic, B. (2022). Antioxidative and Anti-Inflammatory Activities of Chrysin and Naringenin in a Drug-Induced Bone Loss Model in Rats. *Int. J. Mol. Sci.* 23 (5), 2872–2895. doi:10.3390/ijms23052872

Ortiz, A. D., Fideles, S. O., Reis, C. H., Bellini, M. Z., Pereira, E. D., Pilon, J. P., et al. (2022). Therapeutic effects of citrus flavonoids neohesperidin, hesperidin and its aglycone, hesperetin on bone health. *Biomolecules* 12 (5), 626. doi:10.3390/biom12050626

Pacios, S., Xiao, W., Mattos, M., Lim, J., Tarapore, R. S., Alsadun, S., et al. (2015). Osteoblast lineage cells play an essential role in periodontal bone loss through activation of nuclear factor-kappa B. *Sci. Rep.* 5 (1), 1–12. doi:10.1038/srep16694

Papapanou, P. N., Sanz, M., Buduneli, N., Dietrich, T., Feres, M., Fine, D. H., et al. (2018). Periodontitis: Consensus report of workgroup 2 of the 2017 world workshop on the classification of periodontal and peri-implant diseases and conditions. *J. Periodontol.* 89, S173–S182. doi:10.1002/JPER.17-0721

Pepelassi, E., Nicopoulou-Karayianni, K., Archontopoulou, A. D., Mitsea, A., Kavadella, A., Tsiklakis, K., et al. (2012). The relationship between osteoporosis and periodontitis in women aged 45–70 years. *Oral Dis.* 18 (4), 353–359. doi:10.1111/j.1601-0825.2011.01881.x

Poluzzi, E., Piccinni, C., Raschi, E., Rampa, A., Recanatini, M., and De Ponti, F. (2014). Phytoestrogens in postmenopause: The state of the art from a chemical, pharmacological and regulatory perspective. *Curr. Med. Chem.* 21 (4), 417–436. doi:10.2174/09298673113206660297

Qi, J., Liu, E., Guo, Y. F., Hu, J. M., Liu, Y. T., Chen, G., et al. (2021). Association between periodontal disease and osteoporosis in postmenopausal women: A protocol for systematic review and meta-analysis. *BMJ Open* 11 (9), e049277. doi:10.1136/bmjopen-2021-049277

Qu, X. L., Fang, Y., Zhang, M., and Zhang, Y. Z. (2014). Phytoestrogen intake and risk of ovarian cancer: A meta-analysis of 10 observational studies. *Asian pac. J. Cancer Prev.* 15 (21), 9085–9091. doi:10.7314/apjcp.2014.15.21.9085

Rachoń, D., Vortherms, T., Seidlová-Wuttke, D., and Wuttke, W. (2007). Effects of dietary equol on the pituitary of the ovariectomized rats. *Horm. Metab. Res.* 39, 256–261. doi:10.1055/s-2007-973074

Ralston, S. (2015). Bisphosphonates for osteoporosis. *Med. Women*, 345–371.

Ramesh, P., Jagadeesan, R., Sekaran, S., Dhanasekaran, A., and Vimalraj, S. (2021). Flavonoids: Classification, function, and molecular mechanisms involved in bone remodelling. *Front. Endocrinol.* 12, 779638. doi:10.3389/fendo.2021.779638

Riggs, B. L. (2000). The mechanisms of estrogen regulation of bone resorption. *J. Clin. Investig.* 106 (10), 1203–1204. doi:10.1172/JCI11468

Rowe, I. J., and Baber, R. J. (2021). The effects of phytoestrogens on postmenopausal health. *Climacteric* 24 (1), 57–63. doi:10.1080/13697137.2020.1863356

Sathyapalan, T., Aye, M., Rigby, A. S., Thatcher, N. J., Dargham, S. R., Kilpatrick, E. S., et al. (2018). Soy isoflavones improve cardiovascular disease risk markers in women during the early menopause. *Nutr. Metab. Cardiovas. Dis.* 28 (7), 691–697. doi:10.1016/j.numecd.2018.03.007

Savić Pavičin, I., Dumančić, J., Jukić, T., and Badel, T. (2017). The relationship between periodontal disease, tooth loss and decreased skeletal bone mineral density in ageing women. *Gerodontology* 34 (4), 441–445. doi:10.1111/ger.12290

Scheidt-Nave, C., Bismar, H., Leidig-Bruckner, G., Woitge, H., Seibel, M. J., Ziegler, R., et al. (2001). Serum interleukin 6 is a major predictor of bone loss in women specific to the first decade past menopause. *J. Clin. Endocrinol. Metab.* 86 (5), 2032–2042. doi:10.1210/jcem.86.5.7445

Schilling, T., Ebert, R., Raaijmakers, N., Schütze, N., and Jakob, F. (2014). Effects of phytoestrogens and other plant-derived compounds on mesenchymal stem cells, bone maintenance and regeneration. *J. Steroid Biochem. Mol. Biol.* 139, 252–261. doi:10.1016/j.jsbmb.2012.12.006

Sczepanik, F. S. C., Grossi, M. L., Casati, M., Goldberg, M., Glogauer, M., Fine, N., et al. (2020). Periodontitis is an inflammatory disease of oxidative stress: We should treat it that way. *Periodontol* 84 (1), 45–68. doi:10.1111/prd.12342

Sekaran, S., Roy, A., and Thangavelu, L. (2022). Re-appraising the role of flavonols, flavones and flavonones on osteoblasts and osteoclasts-A review on its molecular mode of action. *Chem-Biol. Interact.* 355, 109831. doi:10.1016/j.cbi.2022.109831

Setchell, K. D., and Lydeking-Olsen, E. (2003). Dietary phytoestrogens and their effect on bone: Evidence from *in vitro* and *in vivo*, human observational, and dietary intervention studies. *Am. J. Clin. Nutr.* 78 (3), 593S–609S. doi:10.1093/ajcn/78.3.593S

Sharma, G., Sultana, A., Abdullah, K. M., Pothuraju, R., Nasser, M. W., Batra, S. K., et al. (2022). Epigenetic regulation of bone remodeling and bone metastasis. *Semin. Cell and Dev. Biol.* doi:10.1016/j.semcdb.2022.11.002

Shimazu, T., Inoue, M., Sasazuki, S., Iwasaki, M., Sawada, N., Yamaji, T., et al. (2011). Plasma isoflavones and the risk of lung cancer in women: A nested case–control study in Japan. *Cancer Epidemiol. Biomarkers Prev.* 20 (3), 419–427. doi:10.1158/1055-9965.EPI-10-1025

Singh, P., Gupta, N. D., Bey, A., and Khan, S. (2014). Salivary TNF-alpha: A potential marker of periodontal destruction. *J. Indian Soc. Periodontol.* 18 (3), 306–310. doi:10.4103/0972-124X.134566

Sirotkin, A. V., and Harrath, A. H. (2014). Phytoestrogens and their effects. *Eur. J. Pharmacol.* 741, 230–236. doi:10.1016/j.ejphar.2014.07.057

Song, S. H., Zhai, Y. K., Li, C. Q., Yu, Q., Lu, Y., and Zhang, Y. (2016). Effects of total flavonoids from Drynariae Rhizoma prevent bone loss in vivo and in vitro. *Bone Rep.* 5, 262–273. doi:10.1016/j.bonr.2016.09.001

Sözen, T., Özışık, L., and Başaran, N. Ç. (2017). An overview and management of osteoporosis. *Eur. J. Rheumatol.* 4 (1), 46–56. doi:10.5152/eurjrheum.2016.048

Taguchi, A., Shiraki, M., Tanaka, S., Ohshige, H., and Nakamura, T. (2019). Improved periodontal disease and prevention of tooth loss in osteoporosis patients receiving once-yearly zoledronic acid: A randomized clinical trial. *Menopause* 26 (11), 1277–1283. doi:10.1097/GME.0000000000001393

Takayanagi, H., Ogasawara, K., Hida, S., Chiba, T., Murata, S., Sato, K., et al. (2000). T-cell-mediated regulation of osteoclastogenesis by signalling cross-talk between RANKL and IFN-gamma. *Nature* 408 (6812), 600–605. doi:10.1038/35046102

Tanaka, R., Tanaka, T., Yeung, A. W. K., Taguchi, A., Katsumata, A., and Bornstein, M. M. (2020). Mandibular radiomorphometric indices and tooth loss as predictors for the risk of osteoporosis using panoramic radiographs. *Oral Health Prev. Dent.* 18 (1), 773–782. doi:10.3290/j.ohpd.a45081

Tonetti, M. S., Jepsen, S., Jin, L., and Otomo-Corgel, J. (2017). Impact of the global burden of periodontal diseases on health, nutrition and wellbeing of mankind: A call for global action. *J. Clin. Periodontol.* 44 (5), 456–462. doi:10.1111/jcpe.12732

Trisomboon, H., Malaivijitnond, S., Cherdshewasart, W., Watanabe, G., and Taya, K. (2007). Assessment of urinary gonadotropin and steroid hormone profiles of female cynomolgus monkeys after treatment with Pueraria mirifica. *J. Reprod. Dev.* 53, 395–403. doi:10.1262/jrd.18079

Trombelli, L., Farina, R., Silva, C. O., and Tatakis, D. N. (2018). Plaque-induced gingivitis: Case definition and diagnostic considerations. *J. Clin. Periodontol.* 45, S44–S67. doi:10.1111/jcpe.12939

Valimaa, H., Savolainen, S., Soukka, T., Silvoniemi, P., Makela, S., Kujari, H., et al. (2004). Estrogen receptor-beta is the predominant estrogen receptor subtype in human oral epithelium and salivary glands. *J. Endocrinol.* 180 (1), 55–62. doi:10.1677/joe.0.1800055

Wang, C. W. J., and McCauley, L. K. (2016). Osteoporosis and periodontitis. *Curr. Osteoporos. Rep.* 14 (6), 284–291. doi:10.1007/s11914-016-0330-3

Wang, G. P. (2015). Defining functional signatures of dysbiosis in periodontitis progression. *Genome Med.* 7 (1), 40–43. doi:10.1186/s13073-015-0165-z

Wang, Q., Wang, H., and Xie, M. (2010). Antibacterial mechanism of soybean isoflavone on *Staphylococcus aureus*. *Arch. Microbiol.* 192 (11), 893–898. doi:10.1007/s00203-010-0617-1

Wang, X., Zheng, A., Xin, X. Z., Peng, L. J., Wang, J., Cao, L. Y., et al. (2021). Osteogenic induction of low-dose ipriflavone on bone marrow mesenchymal stem cells extracted from osteoporosis rats. *Chin. J. Dent. Res.* 24, 153–158. doi:10.3290/j.cjdr.b1965039

Wu, D., Cline-Smith, A., Shashkova, E., Perla, A., Katyal, A., and Aurora, R. (2021). T-cell mediated inflammation in postmenopausal osteoporosis. *Front. Immunol.* 12, 687551. doi:10.3389/fimmu.2021.687551

Xu, Q., Cao, Z., Xu, J., Dai, M., Zhang, B., and Lai, Q. (2022). Effects and mechanisms of natural plant active compounds for the treatment of osteoclast-mediated bone destructive diseases. *J. Drug Target.* 30(4), 394-412. doi:10.1080/1061186X.2021.2013488

Yu, B., and Wang, C. Y. (2022). Osteoporosis and periodontal diseases–An update on their association and mechanistic links. *Periodontology* 89 (1), 99–113. doi:10.1111/prd.12422

Zakłos-Szyda, M., Budryn, G., Grzelczyk, J., Perez-Sanchez, H., and Zyzelewicz, D. (2020). Evaluation of Isoflavones as bone resorption inhibitors upon interactions with receptor activator of nuclear factor-κb ligand (RANKL). *Molecules.* 25(1), 206-225. doi:10.3390/molecules25010206

Zhang, W., Dang, K., Huai, Y., and Qian, A. (2020). Osteoimmunology: The regulatory roles of T lymphocytes in osteoporosis. *Front. Endocrinol.* 11, 465. doi:10.3389/fendo.2020.00465

Zhang, Z., Chen, Y., Xiang, L., Wang, Z., Xiao, G. G., and Ju, D. (2018). Diosgenin protects against alveolar bone loss in ovariectomized rats via regulating long non-coding RNAs. *Exp. Ther. Med.* 16 (5), 3939–3950. doi:10.3892/etm.2018.6681

Zhang, Z., Song, C., Fu, X., Liu, M., Li, Y., Pan, J., et al. (2014). High-dose diosgenin reduces bone loss in ovariectomized rats via attenuation of the RANKL/OPG ratio. *Int. J. Mol. Sci.* 15 (9), 17130–17147. doi:10.3390/ijms150917130

Zhang, Z., Yue, L., Wang, Y., Jiang, Y., Xiang, L., Cheng, Y., et al. (2020). A circRNA-miRNA-mRNA network plays a role in the protective effect of diosgenin on alveolar bone loss in ovariectomized rats. *BMC Complement. Med. Ther.* 20 (1), 1–16. doi:10.1186/s12906-020-03009-z

Frontiers in Pharmacology

Explores the interactions between chemicals and living beings

The most cited journal in its field, which advances access to pharmacological discoveries to prevent and treat human disease.

Discover the latest Research Topics

See more →

Frontiers

Avenue du Tribunal-Fédéral 34
1005 Lausanne, Switzerland
frontiersin.org

Contact us

+41 (0)21 510 17 00
frontiersin.org/about/contact